DESIGN and SYNTHESIS of NOVEL CYP51 INHIBITORS

A thesis submitted in accordance with the conditions governing candidates for the degree of Philosophiae Doctor in Cardiff University

by

Faizah Ahmed Saleh Binjubair

Supervisor: Prof. Claire Simons

April 2021

Cardiff School of Pharmacy and Pharmaceutical Science

Cardiff University

To my beloved father and mother, my supportive husband, and my lovely sons; Turki and Mohammed

Contents:

Chapter I (Introduction)

Chapter II (Series I)

Chapter VIII (References)

Chapter IV

Chapter V

Chapter VI

Chapter V

List of abbreviations

ABC	ATP-binding cassette
K_d	Binding affinity
C. albicans	*Candida albicans*
C. auris	*Candida auris*
CaCYP51	*Candida* lanosterol 14α-demethylase
CDC	Centers for Disease Control and Prevention
CLSI	Clinical and Laboratory Standards Institute
CL	Cutaneous leishmaniasis
CYP	Cytochrome P450
CPME	Cyclopentyl methyl ether
DND*i*	Drug for Neglected Diseases *initiative*
ExPASy	Expert Protein Analysis System
BD766	*N, N''*-(Furan-2,5-diylbis(3-isopropoxy-4,1-phenylene))dipicolinimidamide
GOF	Gain-of-function
FKS1	1,3-β-D-Glucan synthase
EC_{50}	Half maximum effect concentration
IC_{50}	Half maximum inhibitory concentration
HRMS	High resolution mass spectrometry
hCYP51	Human lanosterol 14α-demethylase
THP-1	Human monocytic leukaemia cell line
HOBt	Hydroxybenzotriazole
ICU	Intensive care unit
InMac	Intra-macrophage assay
IM	Intramuscular
IV	Intravenous
CYP51, ERG11	Lanosterol 14α-demethylase
L.	*Leishmania*
L. donovani	*Leishmania donovani*
L. infantum	*Leishmania infantum*
LiCYP51	*L. infantum* CYP51
MFS	Major facilitator superfamily
MIC	Minimum inhibitory concentration
MD	Molecular dynamic
MOE	Molecular Operating Environment
ML	Mucocutaneous leishmaniasis
pEC_{50}	Negative logarithm of the half maximum effect concentration
NADPH	Nicotinamide adenine dinucleotide phosphate
CPR	NADPH-cytochrome P450 reductase
PKDL	Post-kala-azar dermal leishmaniasis
PDB	Protein data bank

ProSA   Protein statistical analysis
RMSD   Root Mean Square Deviation
SAR   Structure-activity relationship
SRS   Substrate recognition sites
$SOCl_2$ Thionyl chloride
p-TsOH   *p*-Toluenesulfonic acid
$B(OMe)_3$ Trimethyl borate
TMSOI   Trimethylsulfoxonium iodide
PPh_3 Triphenylphosphine
$B(OCH_2CF_3)_3$ Tris(2,2,2-trifluoroethyl)borate
T.   *Trypanosoma*
VL   Visceral leishmaniasis
WHO   World Health Organization

List of amino acids and their abbreviations

Amino acid	3-letter abbreviation	1-letter abbreviation
Alanine	Ala	A
Arginine	Arg	R
Asparagine	Asn	N
Aspartic acid	Asp	D
Cysteine	Cys	C
Glutamic acid	Glu	E
Glutamine	Gln	Q
Glycine	Gly	G
Histidine	His	H
Isoleucine	Ile	I
Leucine	Leu	L
Lysine	Lys	K
Methionine	Met	M
Phenylalanine	Phe	F
Proline	Pro	P
Serine	Ser	S
Threonine	Thr	T
Tryptophan	Trp	W
Tyrosine	Tyr	Y
Valine	Val	V

List of paper, conference poster and workshop

1. Binjubair, F.A.; Parker, J.E.; Warrilow, A.G.; Puri, K.; Braidley, P.J.; Tatar, E.; Kelly, S.L.; Kelly, D.E.; Simons, C. Small molecule inhibitors targeting sterol 14α-demethylase (CYP51): synthesis, molecular modelling and evaluation against *Candida albicans*. *Chem. Med. Chem.* **2020**, *15*, 1294-1309. http://dx.doi.org/10.1002/cmdc.202000250

2. Binjubair, F.A.; Parker, J.E.; Warrilow, A.G.; Kelly, S.L.; Kelly, D.E.; Simons, C. Small molecule inhibitors targeting sterol 14α-demethylase (CYP51): synthesis, molecular modelling and evaluation against *Candida albicans*. Presented at ACS Spring National Meeting and Expo on Macromolecular Chemistry: The Second Century, Philadelphia, US, March 22-26, **2020**; Paper MEDI 305. https://doi.org/10.1021/scimeetings.0c02434

3. MOE - molecular modeling – workshops, 23rd - 24th February **2017**, Cambridge.

4. SCI-RSC Workshop on Computational Tools for Drug Discovery: Six Online Workshops from 6th May to 10th June **2020**.

Abstract

Fungal infections are a global issue affecting over 150 million people worldwide annually with 750,000 of these caused by invasive Candida infections. The outcomes of life-threatening systemic infections caused by *Candida albicans* are poor with mortality rates estimated to be between 46-75%. Azole drugs are the frontline treatment against fungal infections however resistance to current azole antifungals in *C. albicans* poses a threat to public health. Azole resistance can arise through several mechanisms with point mutations in sterol 14α-demethylase (CYP51) leading to amino acid substitutions a major contributor. The aim of this research is to design and synthesise novel azole inhibitors effective against wild type and fluconazole-resistance Candida strains. The development of potent and selective inhibitors from three azole series were investigated for CYP51 inhibitory activity, binding affinity, and minimum inhibitory concentration (MIC) against *C. albicans* strains biologically as well as computationally. The first series, short and extended novel imidazole/triazole derivatives were synthesised successfully. The short derivatives were more potent against the *C. albicans* strains (MIC 0.03 µg/mL) compared with the extended derivatives (MIC 1 µg/mL), while both series showed similar enzyme binding and inhibition (K_d low nM, IC_{50} submicromolar) and were comparable with the standards fluconazole and posaconazole. The short series had poor selectivity for CaCYP51 over the human homolog, while the selectivity of the extended series was higher (21.5-fold) than posaconazole (4.7-fold) based on K_d values, although posaconazole was more selective (615-fold) compared with the extended series (461-fold) based on IC_{50} values. Series two, 2-(arylphenyl)-*N*-(4-((4-arylphenyl)amido)benzyl)-3-(1*H*-1,2,4-triazol-1-yl)propanamides derivatives, were synthesised successfully. The novel inhibitors exhibited weak activity against *C. albicans* strains; however, a slight improvement in the IC_{50} was shown in chloro derivatives (IC_{50} 4.6 -1.3 µM). A series of *N*-(2-(arylphenyl)-2-hydroxy-3-(1*H*-1,2,4-triazol-1-yl)butanamide derivatives have been synthesised using an efficient synthetic route and shown to be potent against the *C. albicans* strains (MIC from <0.03 to 1 µg/mL) and potent inhibitors of CaCYP51 (IC_{50} 0.78 to 1.6 µM) compared with the standard fluconazole. All series were studied computationally using CaCYP51 crystal structure (PDB 5FSA) for molecular modelling and molecular dynamic simulations to determine optimal fit in the active site and binding interactions. Leishmania was also of interest as it has been identified by the WHO as a disease with unmet needs with an estimated 700,000 to one million new cases each year in the endemic regions such as East Africa, North Africa and West Asia. CYP5122A1 an orphan enzyme has been identified as a CYP enzyme specific to leishmania, which could provide a novel target in the treatment of leishmania infections. A CYP5122A1 homology model was developed, as no crystal structure is available, using a combination of homology modelling, molecular dynamics simulations, and molecular docking to understand the active site and the binding interaction of CYP5122A1 and selected ligands complexes. Docking results for CYP5122A1 showed amino acids Glu365, Thr366, Val440 in the haem binding pocket and Tyr175, Phe178, Pro441, Asp584 in the access channel, which could have an important role in the binding interactions with designed ligands. Furthermore, some of the novel compounds synthesised in this research were also tested against *Leishmania donovani* to investigate the inhibitory potential.

Chapter I

Introduction

1.1 Introduction

Fungal infections are a major problem that healthcare faces and that affect annually more than 150 million people worldwide, 750,000 of which are invasive infections by *Candida* species.[1] The mortality of fungal infections is estimated to be similar to that of tuberculosis with more than 1.6 million deaths and three times more than malaria annually.[2,3] Fungal infections range from superficial, oral and vulvovaginal thrush to life-threatening invasive candidiasis or candidemia. The most common fungal pathogens, which cause 90 % of serious fungal diseases, are Candida, Cryptococcus, Aspergillus and Pneumocystis species.[2,4,5] The fungal genus Candida includes over 20 different species that are known to be opportunistic pathogens to humans. The most common *Candida* species are *C. albicans*, *C. glabrata*, *C. parapsilosis*, *C. tropicalis* and *C. krusei*, which cause infection when certain circumstances arise. Each species involve variation on the infection site and geographical location.[6] Candida infections caused by *C. albicans* are distributed widely in the United States, Europe, and the Middle East,[6-9] whereas *C. auris*, which was first identified in Japan,[10] is currently a global health problem especially in the intensive care unit (ICU) patients owing to the difficulty in identification with standard laboratory methods, such as MicroScan, resulting in an unsuitable period of treatment causing multidrug resistance.[11] Furthermore, the invasive fungal infections caused by *Aspergillus* and *Cryptococcus* are spread globally with 33.1 % of annual mortality owing to invasive aspergillosis in the ICU. Cryptococcosis is ranked the third predominant disease in the immunocompromised patients.[12] Candida species are ranked the fourth most common pathogen causing invasive infections globally after bacterial pathogens.[4,13,14] Over the past several decades the mortality rates of candidiasis and candidemia has risen to between 46-75%.[1]

Candidiasis describes the fungal infections caused by Candida species, especially *C. albicans*.[1,2,4,6] Normally *C. albicans* is present in the human flora, on the skin and mucosal membranes without causing harmful effects; however, the overgrowth of this pathogen can lead to severe fungal infections.[15] Candidiasis can vary depending on the infected organ with *C. albicans* overgrowth resulting in infections such as thrush, vulvovaginal or oropharyngeal candidiasis.[1,16] However, the most severe and dangerous type of Candida infection is invasive candidiasis, which affects the blood (candidemia), heart, brain, bones or other parts of the body.[1,17] Immunocompromised patients, such as cancer patients, those with HIV/AIDS, people on broad-spectrum antibiotics, transplant patients and diabetics, are more susceptible to these infections in both developed and developing countries.[1,18] In England, Wales and Northern Ireland the total rate of candidemia was 3.6 per 100,000 population in

2017, an increase of 17% from 2013; and the most common species causing candidemia were *C. albicans*, *C. glabrata* and *C. parapsilosis*.[18] Furthermore, an estimated 2 million people annually contract oral candidiasis and a further 1.3 million oesophageal candidiasis.[2] Recurrent bouts of vulvovaginal candidiasis affect at least 75 million women annually,[19] indicating an unmet need for better treatments that could target the biosynthesis of the fungal cell wall, proteins or lipids.

1.2 Classification of antifungal agents

Antifungal agents can be classified into three main groups according to their targets in the fungal cell and these classes contain the five most currently used antifungal agents in the clinic, which include echinocandins, 5-fluorocytosine, polyenes, allylamines and azoles (Figure 1).
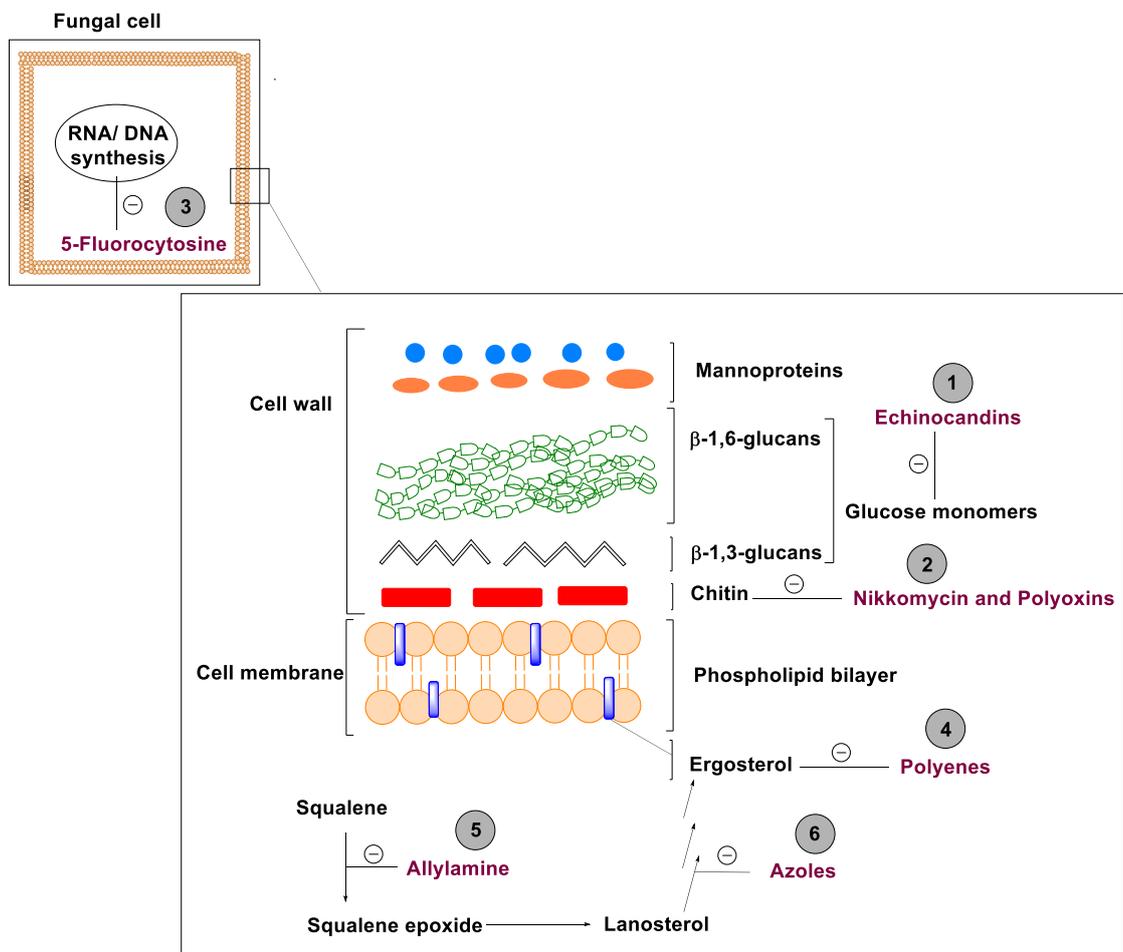
Figure 1. Antifungal agents targets. Echinocandins (1) inhibit β-(1,3)-glucan synthases thus damage the fungal cell wall, nikkomycin and polyoxins (2) interact with chitin synthase leading to fungal cell damage. 5-Fluorocytosine (3) inhibits RNA/DNA synthesis leading to the disruption of fungal growth. Polyenes (4) bind to ergosterol and disrupt the cell

membrane structure. Allylamine agents (5) inhibit squalene syntheses, which converts squalene to squalene epoxide. Azoles (6) block ergosterol biosynthesis by inhibiting 14α-demethylase that converts lanosterol to ergosterol leading to fungal cell death.

1.2.1 Fungal cell wall synthesis inhibitors

The fungal cell wall is a dynamic structure that allows the cell to interact with the surrounded environment but also protect the cell from any environmental stresses. The cell wall consists of glycoproteins (containing a glycosylphosphatidylinositol anchor) and polysaccharides, mainly chitin and glucan, which connect to form the complex network structure (Figure 1).[20,21]

1.2.1.1 Inhibitions of β-glucan synthesis

Glucans consists of D-glucose monomers attached by β-(1,3)-glucan or β-(1,6)-glucan linkages and is important component to maintain the integrity and the strength of the cell wall (Figure 1). The polysaccharide structure of β-(1,3)-glucan represents 50% of the cell wall, and the remaining components are chitin and glycoproteins.[22,23,24] The inhibition of glucan synthase disrupts the cell wall of the fungi leading to cell death.

Echinocandins contain a cyclic hexapeptide core with a lipophilic side-chain responsible for antifungal activity as it acts as an anchor to the fungal cell wall.[25] Echinocandins non-competitively target the fungal cell wall biosynthesis through inhibiting β-(1,3)-D-glucan synthase enzyme complexes, especially targeting FKS1, which is a catalytic subunit protein present in the cell wall that is regulated by a Rho GTPase subunit.[23,25] β-(1,3)-D-glucan synthase catalyses the formation of β-glucan, the natural component of the fungal cell wall.[22,23,26] Inhibition of β-(1,3)-D-glucan synthase leads to disturbance in the growing structure of the cell wall, resulting in a deficit in the fungal cell integrity.[23,25] Caspofungin, Micafungin and Anidulafungin (Figure 2) are clinically used broad-spectrum antifungal echinocandins that are active against invasive candidiasis; however, low bioavailability, intravenous administration and elevated hepatic enzyme levels limit their use.[22,26] The resistance of this class could be owing to the *FKS1* gene mutation in *C. albicans*.[25]

Caspofungin

Micafungin

Anidulafungin
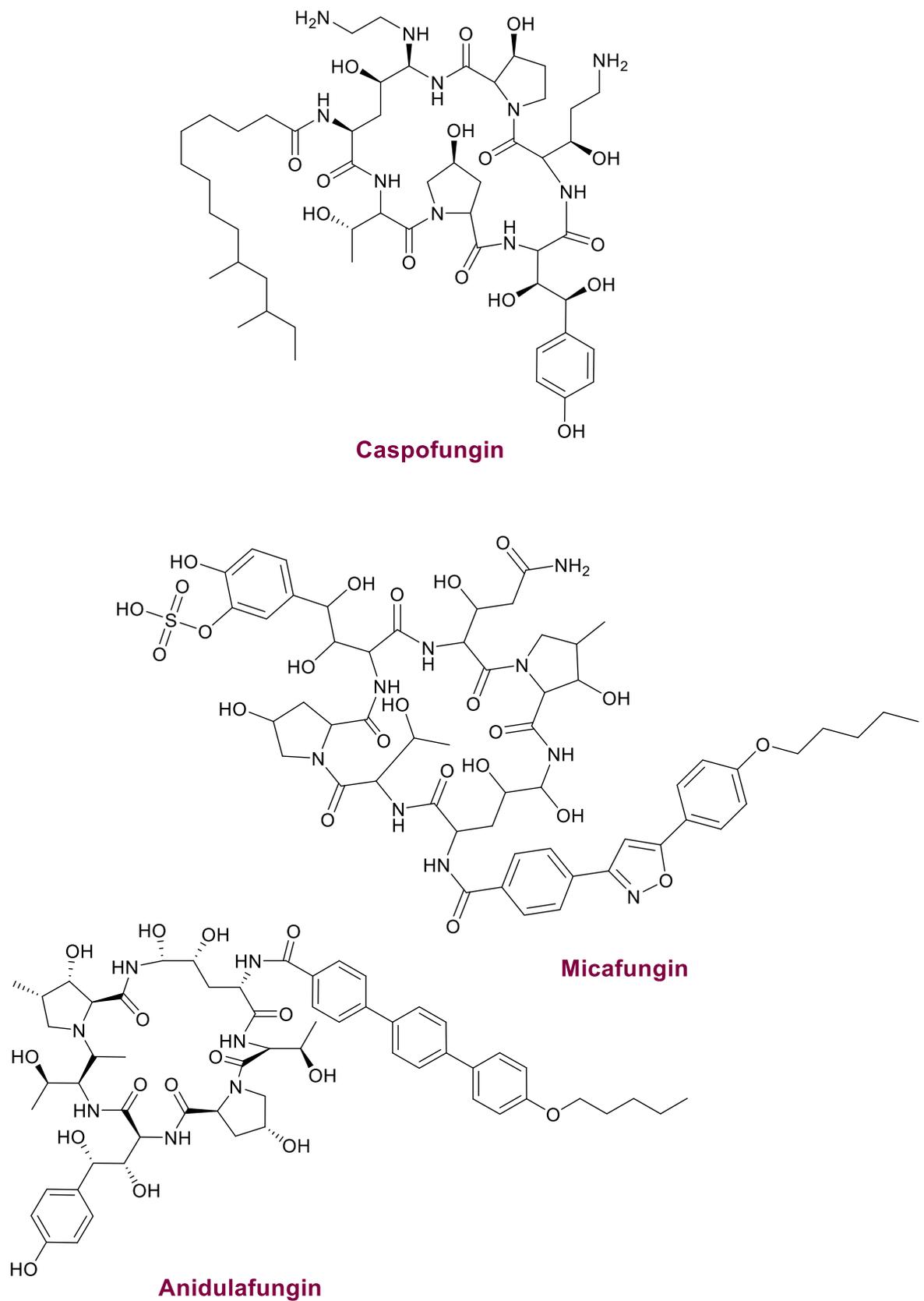
Figure 2. Echinocandin antifungal agents

1.2.1.2 Chitin synthesis inhibitions

Chitin, which is only 3 % of the constituents of the fungal cell wall, is composed of β-(1,4)-linked *N*-acetylglucosamine polymer units that are covalently linked to β-(1,3)-D-glucan to strengthen the cell wall (Figure 1).[26] Nikkomycin and Polyoxin (Figure 3) are chitin synthase inhibitors, which disrupt the structure of the fungal cell wall, and have very low activity against *C. albicans* and *C. tropicalis*; however, they are used against fungal infections caused by Aspergillus fumigatus as a combination therapy with Caspofungin.[22,26]

Nikkomycin   **Polyoxin**
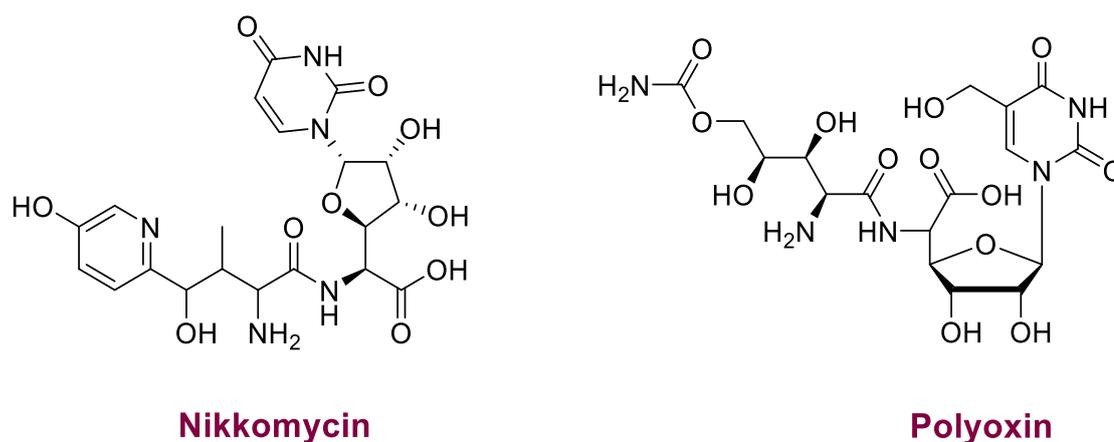
Figure 3. Nikkomycin and Polyoxin antifungal agents

1.2.2 Nucleic acid synthesis inhibitor

5-Fluorocytosine (Figure 4) is a pyrimidine analogue, which is converted to 5-fluorouracil by fungal cytosine deaminase after it enters the fungal cell via cytosine permeases.[22,25,26] 5-Fluorouracil can then be transformed to 5-fluorouridylic acid by UMP pyrophosphorylase, which is either incorporated into RNA after additional phosphorylation resulting in inhibition of protein synthesis or converted to 5-fluorodeoxyuridine monophosphate, which inhibits fungal DNA synthesis and nuclear division.[22,23,25] Therefore, 5-fluorocytosine interferes with RNA/DNA protein synthesis and pyrimidine metabolism leading to the disruption of fungal growth.[24,26] Resistance to 5-fluorocytosine develops rapidly therefore it is usually used in combination therapy with Amphotericin B in the clinic against *Candida* and *Cryptococcus* species.[22,23,26]
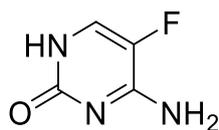
5-Fluorocytosine

Figure 4. 5-Fluorocytosine antifungal agent

1.2.3 Fungal ergosterol inhibitors

Ergosterol is the major component of the fungal cell membrane, which is responsible for the fluidity, permeability and integrity of the membrane.

Ergosterol biosynthesis

One of the essential sterols that plays a substantial role in fungal cell survival is ergosterol; therefore, ergosterol biosynthesis is an important target of antifungal agents. Sterols are essential lipids of most eukaryotic cells that play a major role in the composition of the cell membrane. Depending on their sources, natural sterols are represented by three predominant forms: cholesterol in animals and human, phytosterols in plants and ergosterol in fungi and protozoa.[27-29] This research is interested in ergosterol, an important constituent of membrane lipids in fungi and protozoa, which regulates the fluidity, permeability and thickness of the membrane.[27,29-31] The ergosterol biosynthetic pathway in *C. albicans* starts from squalene, a precursor of sterol biosynthesis, and after a long multistep synthesis produces the final sterol product, ergosterol.[27,28] One of the most essential cytochrome P450 (CYP) enzymes involved in the ergosterol biosynthesis pathway is lanosterol 14α-demethylase (CYP51), which is encoded by the *ERG11* gene (Figure 5).[32,33] The demethylated intermediates produced through the catalytic reaction of this enzyme are essential in the ergosterol biosynthesis pathway.

Squalene → Squalene epoxidase (*ERG1*) → Squalene epoxide → Lanosterol synthase (*ERG7*) → Lanosterol

Lanosterol → Lanosterol 14α-demethylase (*ERG11*, CYP51) → 4,4'-dimethyl-ergosta-8,14,24-trienol

4,4'-dimethyl-ergosta-8,14,24-trienol → C-14 Sterol reductase (*ERG24*) → 4,4'-dimethyl zymosterol

4,4'-dimethyl zymosterol → C-4 Sterol methyloxidase (*ERG25*) / C-4 Sterol decarboxylase (*ERG26)* / C-3 Sterol ketoreductase (*ERG27)* / C-24 Sterol methyl-transferase (*ERG6)* → Fecosterol

Fecosterol → C-8 Sterol isomerase (*ERG2)* / C-5 Sterol desaturase (*ERG3)* → Ergosta-5,7,24 (28)-trienol

Ergosta-5,7,24 (28)-trienol → C-22 Sterol desaturase (*ERG5)* / C-24 Sterol reductase (*ERG4)* → Ergosterol

Figure 5. Ergosterol biosynthesis pathway

1.2.3.1 Fungal membrane disruption

The main component of the fungal cell membrane is ergosterol (Figure 1 and 5). Polyenes are macrocyclic organic molecules known as macrolides, which act by forming a complex with ergosterol in the lipid bilayer producing pores owing to the amphoteric structure of this class. This complex disrupts the fungal cell membrane resulting in increased membrane permeability and finally death of the fungal cell.[22,26] Polyenes are fungicidal and have the broadest spectrum activity compared with any other antifungal agents available clinically.[22,25,26] Amphotericin B and Nystatin (Figure 6) are active against *Candida* species; Amphotericin B is administered intravenously and used in life-threatening fungal infections caused by *Candida* and *Aspergillus* whereas nystatin is used topically for cutaneous, vaginal and oesophageal candidiasis.[22,34] Polyene antifungal drugs have numerous side effects, which limit their use, including severe hepatotoxicity.[23] In recent years, research has focused on developing a different formulation of Amphotericin B to decrease the toxicity, such as encapsulation in liposomes or disc-like lipid complexes.[4,23]
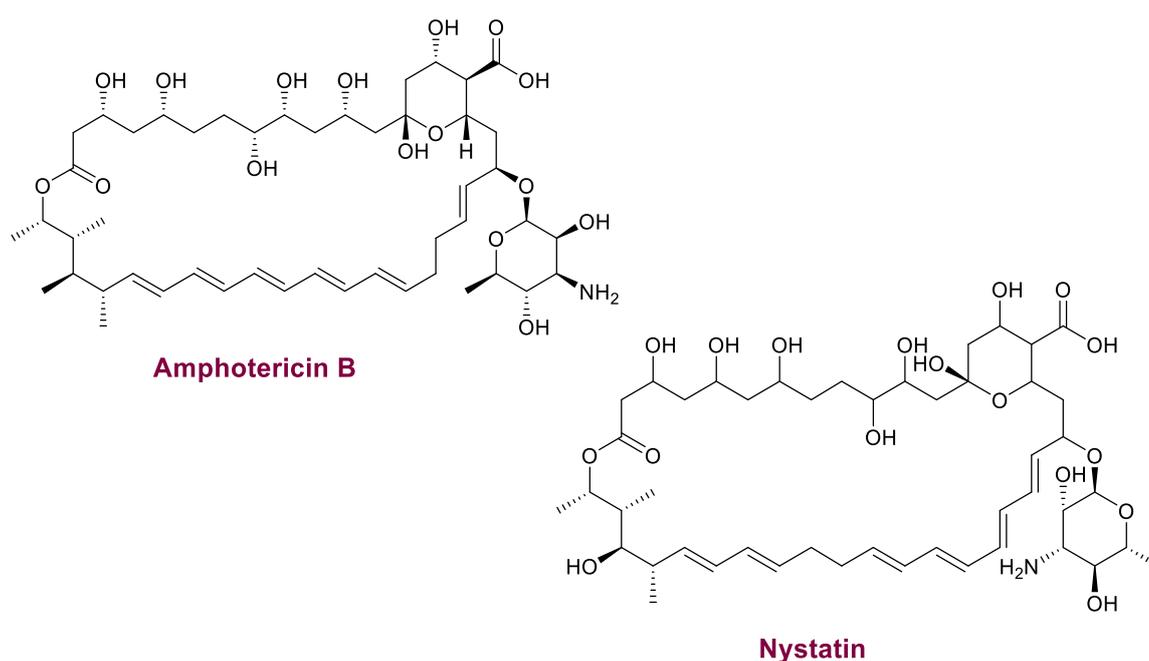
Figure 6. Polyene antifungal agents

1.2.3.2 Squalene epoxidase inhibitors

Squalene epoxidase is responsible for the conversion of squalene into 2,3-squalene epoxide, which is an early step in ergosterol biosynthesis (Figure 5). Allylamines act by inhibiting ergosterol biosynthesis through the inhibition of squalene epoxidase.[25,26]

Inhibition of squalene epoxide leads to disruption of cellular organisation (fungal cell death) owing to squalene accumulation resulting in an increase in cell permeability, rather than inhibition of ergosterol synthesis.[22,23,26] Allylamines are used mostly in nail and skin cutaneous infections.[22,23] Important members of this class are Naftifine and Terbinafine. Naftifine is used topically, whereas Terbinafine can be used topically and orally (Figure 7).[23,24]

Naftifine

Terbinafine
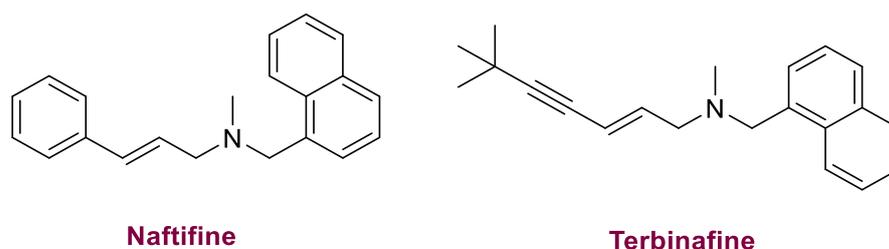
Figure 7. Allylamine antifungal agents

1.2.3.3 Fungal ergosterol synthesis inhibitors

Azoles are the largest class of antifungal drugs that inhibit ergosterol biosynthesis through inhibition of 14α-lanosterol demethylase (CYP51) leading to inhibition of fungal cell growth.[6,22,23,35] The most important functional group in all azoles is the 5-membered nitrogen containing azole ring e.g. imidazole, triazole or tetrazole ring, with the basic nitrogen atom forming an axial coordination bond with the haem iron of the enzyme.[35,36] In addition, replacing the imidazole ring with a triazole ring has been shown to enhance the selectivity of these agents to the fungal CYP51 enzyme,[25] and further replacement by a tetrazole ring shows more improvement in selectivity to fungal CYP51.[23] The antifungal drugs in this class include clotrimazole, itraconazole, fluconazole and others (Figure 8).[23,37] Fluconazole is the first-line agent for the treatment and also prophylaxis against invasive candidiasis with voriconazole and itraconazole as alternative options.[38,39] The use of posaconazole has been limited mainly for oropharyngeal or esophageal candidiasis and for prophylaxis in high-risk patients owing to its erratic bioavailability and unpredictable trough plasma concentration.[40] A new tetrazole-based drug candidate VT-1161 (oteseconazole) has been described and successfully completed Phase 2b clinical trials (Figure 8).[41,42]
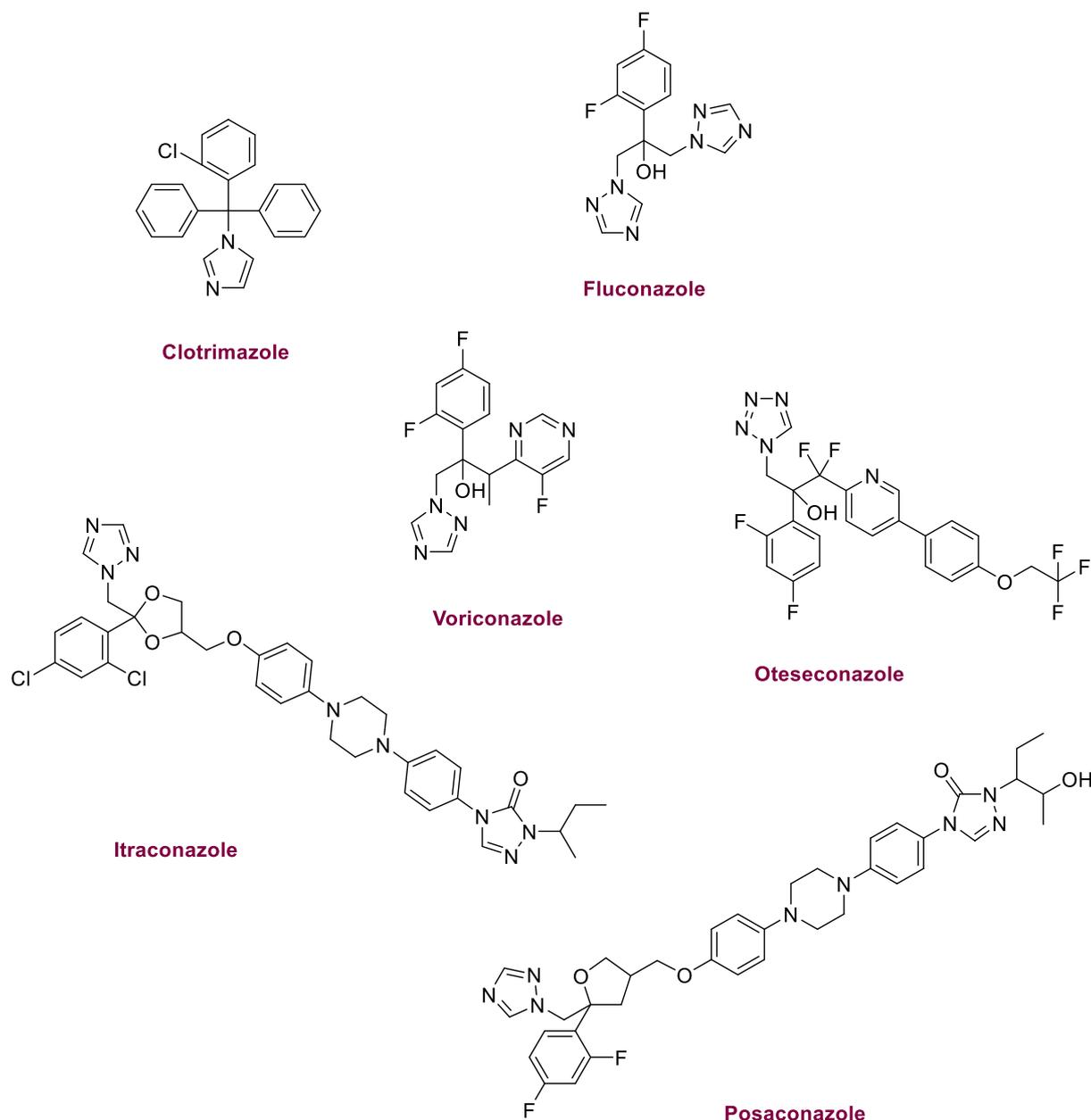
Figure 8. Azole antifungal agents

1.3 Sterol 14α-demethylase (CYP51)

Sterol 14α-demethylase (CYP51) is the most ancient CYP families found in all biological kingdoms.[43-46] CYP51 catalyses a unique three-step reaction of oxidative removal of the 14α-methyl group from the precursor lanosterol.[21,44,45] Furthermore, CYP51 plays an essential role in sterol biosynthesis in which the products produced in the pathway are crucial for the cell membrane integrity (Figure 9).[21,45,47,48]
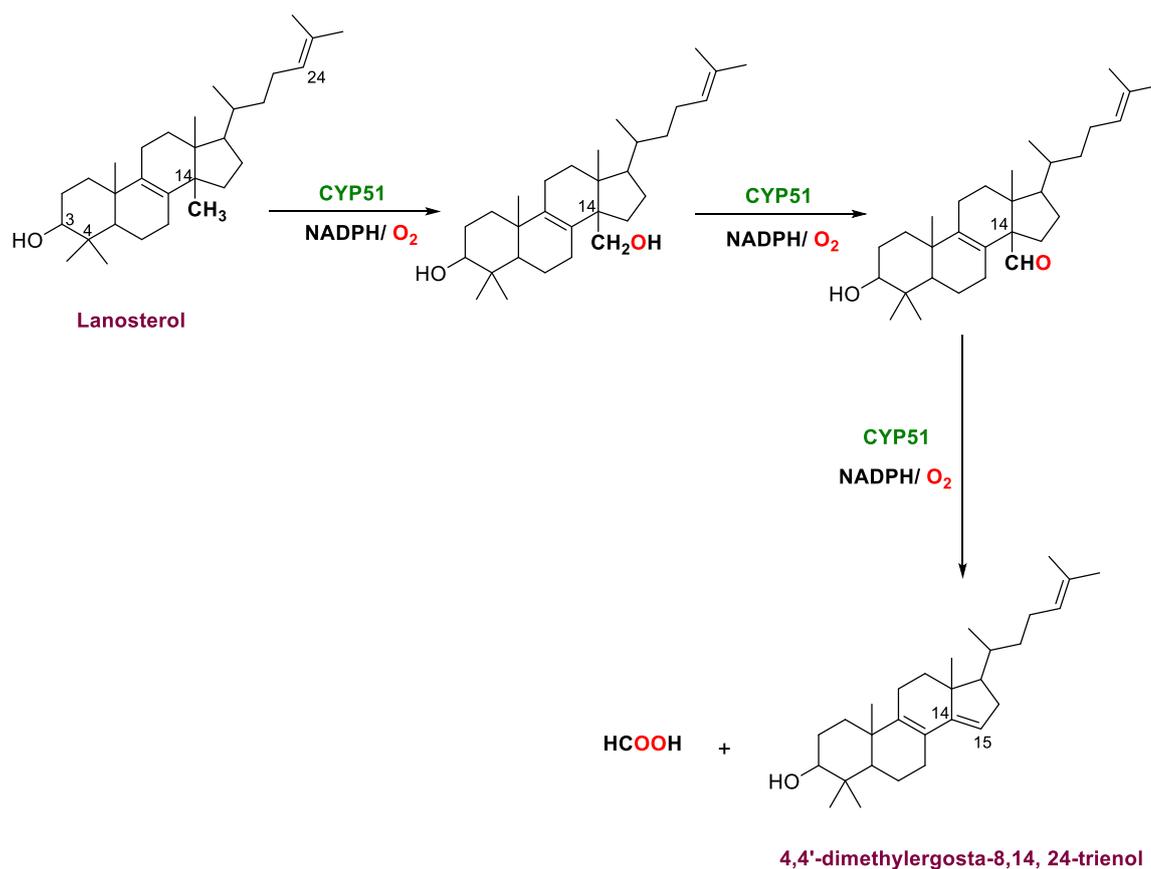
Figure 9. The reaction mechanism of 14α-demethylation of lanosterol catalysed by CYP51

CYP51 is essential for the survival of the fungal pathogens in the host cell and is, therefore, an important target enzyme in fungal infections. CYP51 is present in both human (hCYP51) and fungi; however, the amino acid sequence identity between them is less than 35 % which allows the development of a selective CaCYP51 inhibitor.[35,49] Inhibition of CaCYP51 results in accumulation of sterol intermediates without production of ergosterol, which is indispensable for fungal cell growth.[25,50] Azoles are by far the most common antifungal drugs in clinical use. Several factors allow the extensive use of azoles in treating fungal infections such as the broad-spectrum activity, low toxicity and tolerability by patients.[51,52] However, resistance to current azole antifungals in *C. albicans* is becoming progressively more serious, posing a threat to public health[51] and can be attributed to the prophylactic use of azole drugs and prolonged treatment regimens in the clinic as well as extensive agricultural use.[53-55]

1.4 Azole resistance

Figure 10. Resistance mechanisms of azole antifungals. (1) Alteration of CYP51 amino acid sequence leads to a decrease in the affinity of the azole to the target enzyme. Reduction of the effective azole concentration inside the cell by (2) overexpression (upregulation) of CYP51, (3) drug efflux transporters (ABC and MFS) or by (4) biofilm formation. (5) Metabolic bypass when mutation of ERG3 occurs

In the past three decades, the incidence of invasive fungal infections caused by *Candida* species has significantly increased particularly in the immunocompromised and the intensive care unit patients.[5,56,57] The first-line therapy for these fungal infections is azole antifungal agents owing to the safety profile and ease of administration.[51,52] However, prolonged treatment regiments and prophylaxis use of azole drugs in the clinic as well as the extensive use of azole antifungals in agricultural have led to an increase in the incidence of resistance for these agents, especially the mainstay treatment fluconazole.[57,58]

Antifungal azoles are fungistatic against *Candida* species, which mean they do not kill fungal cells but only arrest their growth, and act with the human immune system synergistically to excrete the microbial infection. However, with the immune deficiency in immunocompromised patients the ability to clear these cells that persist inside the host cells due to previous exposure to azole treatment or agricultural use; is significantly reduced, so they might form subclinical reservoirs for new infections by activating stress responses which could also result in resistance to azole antifungals.[33,59] With around 46,000 hospitalised patients infected annually owing to fluconazole resistant *C. albicans*, the Centers for Disease Control and Prevention (CDC) classified *C. albicans* as a serious pathogen.[1,31]

There are five different mechanisms responsible for azole resistance in *C. albicans* (Figure 10).[5,31,36,57]

1. **Alteration of the target site -** Mutations in the amino acid sequence of CaCYP51 that can result in reduced affinity of azoles to CaCYP51. Over 140 CaCYP51 mutations have been described with single, double, triple and more recently quadruple mutations identified from clinical isolates.[57,60] However, the majority occur in drug-sensitive strains and are therefore unlikely to contribute to azole resistance. CYP51 mutations associated with drug-resistant strains primarily occur in (1) the active site cavity (Y132H, Y132F, K143R, G307S and S405F), (2) those that interact with the haem or are present in the Cys-pocket, which may affect the redox potential of the haem (K143R, G464S and R467K), and (3) residues located on the β5-hairpin (Y447H, G448E, G448V and G450E) that may affect interaction with the electron partner NADPH-cytochrome P450 reductase (CPR) potentially affecting catalytic efficiency.[57,60-62] The catalytic tolerance to azole antifungals

especially fluconazole to CaCYP51 mutant strains was determined by measuring the concentration causing 50 % enzyme inhibition (IC_{50}, µM) as well as the minimum inhibitory concentration (MIC, µg/mL) compared with wild type CaCYP51.[51,57] The most serious CaCYP51 amino acid single mutants (K143R and G450E) showed a 2-4 fold increase in azole tolerance in both MIC and IC_{50} compared with the highest tolerance for the double mutants (Y132F+K143R, Y132H+K143R, Y132F+F145L and G307S+G450E) an 8-18 fold increase in azole tolerance was observed.[51,57,60]

2. **Up-regulation of target site** - The amount of CaCYP51 present intracellularly is increased owing to upregulation (overexpression) of the *ERG11* gene resulting in a reduction in the effectiveness of the azole antifungal agents.[4,31,51] This upregulation of the *ERG11* gene is established by transcription factor UPC2 that works only under stress conditions.[4,6] UPC2 is a zinc finger transcription factor responsible for overexpression of the *ERG11* gene.[4] The gain-of-function mutations (GOF mutations), which are located near UPC2 in the C-terminal, may contribute to the point mutation of UPC2 resulting in azole resistance.[5]

3. **Decreased effective drug concentrations** – Active transport efflux systems accomplish this mechanism of resistance. The overexpression of two efflux pump transporters Candida drug resistance (*CDR1* and *CDR2*) gene of the ATP-binding cassette (ABC) transporters and the *MDR* genes of the major facilitator superfamily (MFS) membrane transporters lead to a decrease in the intracellular concentration of azole drugs resulting in azole resistance.[4,5,26,51] ATP-binding cassette transporters use ATP hydrolysis to transport the drug (Figure 11) and the overexpression of these transporters was found to be related to cross-resistance in different azoles including fluconazole, itraconazole and ketoconazole.[4,31,63] However, "MFS transporters are transmembrane proteins, which use the electrochemical proton-motive force to mediate drug efflux"[4] and the overexpression of *MDR1* leads to azoles resistance as well.[5,31]
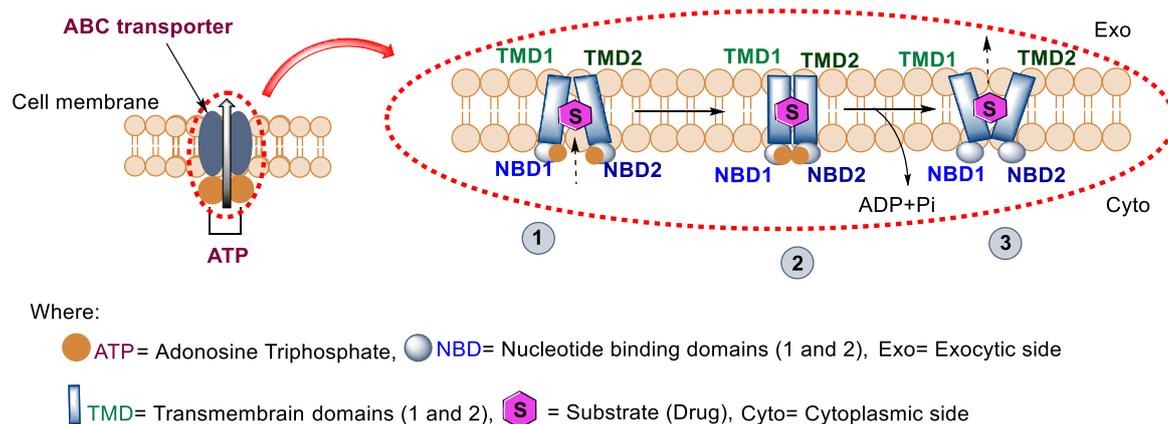
Figure 11. The structure of ABC transporters and the pathway of transported substrate. The ABC transporters contains two hydrophilic nucleotide binding domains (NBD1 and 2), which are located on the cytoplasmic side of the cell membrane, and two hydrophobic transmembrane domains (TMD1 and 2), all four domains are arranged in the order NBD1, TMD1, NBD2, TMD2. (1) The transporters have high affinity for the substrate, which penetrates the cavity between TMD1 and TMD2, and (2) ATP activates the binding in the ABC transporters. (3) The cavity then opens to release the substrate to the exocytic side of the membrane due to conformational changes resulting from ATP hydrolysis to adenosine diphosphate (ADP) and inorganic phosphate (Pi)

4. **Biofilm formation** – Fungal pathogens can form a biofilm that isolates the azole drugs extracellularly.[4] The sequestration by biofilm leads to a decrease in the intracellular concentration of azole drugs contributing to the azole resistance in *C. albicans*.[4,31] The biofilm consists of a dense network matrix composed of carbohydrate, polysaccharides and proteins acting as an isolator barrier for the azole antifungal agents.[4,23] The biofilm protects fungi against the antifungal agents, which increases the adherence to the mucosal cell surface of the human as well as to any substance such as catheters, which results in an increase resistance to these agents.[4,16]

5. **Bypass pathway production** - Secondary mutations in the ergosterol pathway, such as ERG3 null mutants, leads to an accumulation of 14α-methyl fecosterol, which is capable of supporting membrane function and fungal cell survival and bypasses the accumulation of 14α-methyl-ergosta-8,24(28)-dien-3β-6α-diol, a toxic metabolite, which causes cell death[4,6,51] (Figure 12).
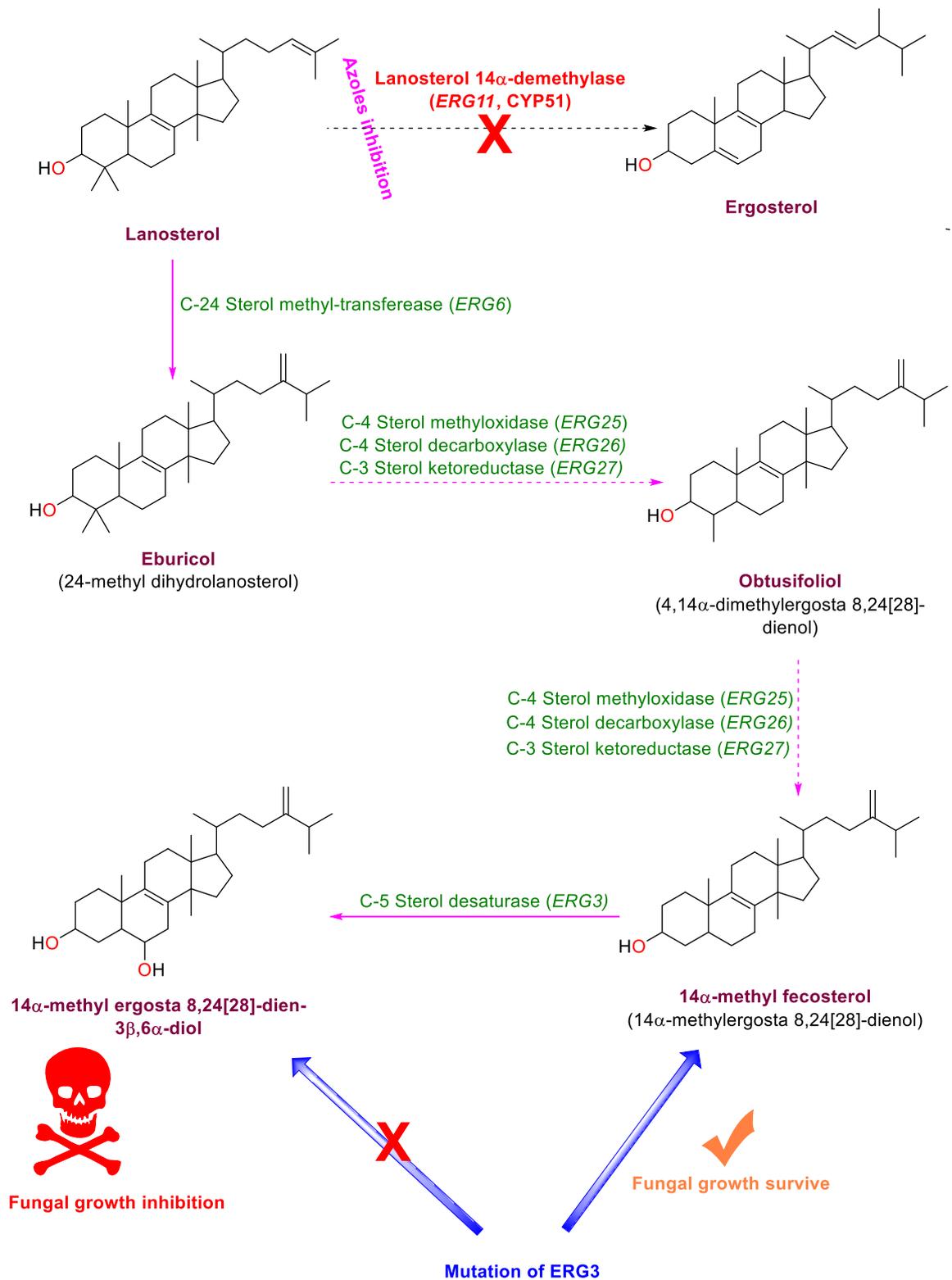
Figure 12. Mechanism of action of antifungal azole inhibitors and the mutation of ERG3. Inhibition of CYP51 with azoles lead to the accumulation of toxic methylated metabolite (14α-methyl ergosta 8,24[28]-dien-3β,6α-diol) that inhibits fungal cell growth, whereas the bypass pathway (ERG3 mutation) produces a survival metabolite (14α-methyl fecosterol) for the fungal cell; solid arrows: one enzymatic step, broken arrows: multiple enzymatic steps

The most widespread mechanism of azole-resistant clinical isolates in *C. albicans* is mutations of CaCYP51.[35,57,60] With the appearance of these resistance profiles to azole antifungals, the need for novel antifungal agents is required as well as alternative therapeutic approaches such as modifying gene expression, immunotherapy[64] as well as combination therapy with CYP51, which might improve the activity and reduce resistance.[31]

Some current studies include searching drugs libraries, repurposing of old drugs, (such as AR-12 which is an anticancer agent and has been reused to inhibit acetyl-CoA synthetase in some fungal infections and currently in animal studies),[23] and understanding cell metabolic pathways are new approaches to develop new antifungal agent.[34,65] Several new antifungal agents are in clinical trials (Figure 13) including agents that target fungal cell such as:

- F901318 targets dihydro-orotate dehydrogenase, which is an important enzyme for the fungal pyrimidine synthesis. F901318 is an inhibitor of the orotomide class and found to have a higher degree of affinity to the fungal enzyme compared with the host, and it is now under the Phase 2 study.[23,34,47]

- VT-1598, VT-1129 (quilseconazole) are analogues of VT-1161 (oteseconazole) and are tetrazole antifungal agents that inhibit fungal CYP51. The tetrazole antifungal agents have significant high selectivity to CaCYP51 rather than hCYP51 that might decrease toxicity. VT1598 is under investigation at the preclinical development stage, whereas VT1129 is in Phase 1 clinical trials and VT1161 is in a Phase 2b study in vulvovaginal candidiasis.[23,41,42]

Other new inhibitors targeting the fungal cell wall include:

- APX-001: a glycosylphosphatidylinositol inhibitor that inhibits the anchor cell proteins which help the fungal pathogen to invade the host cells and replicate. APX-001 is available in oral and IV formulations and has broad activity against different species; furthermore, it is in Phase 1 trials.[23,34,65]

- SCY-078: a triterpene drug that inhibits β-(1,3)-D-glucan synthase with a very different structure compared with the echinocandin antifungal agents. SCY-078 has broad-spectrum activity and is available in oral and IV formulations and is currently in Phase 2 clinical trials.[34,65]

- Rezafungin (CD101): a β-(1,3)-D-glucan synthase inhibitor with a modified ether ring structure that enhances the effectiveness and half-time life (81 h) compared with echinocandin agents (24 h) and is undergoing Phase 2 studies.[23,34]
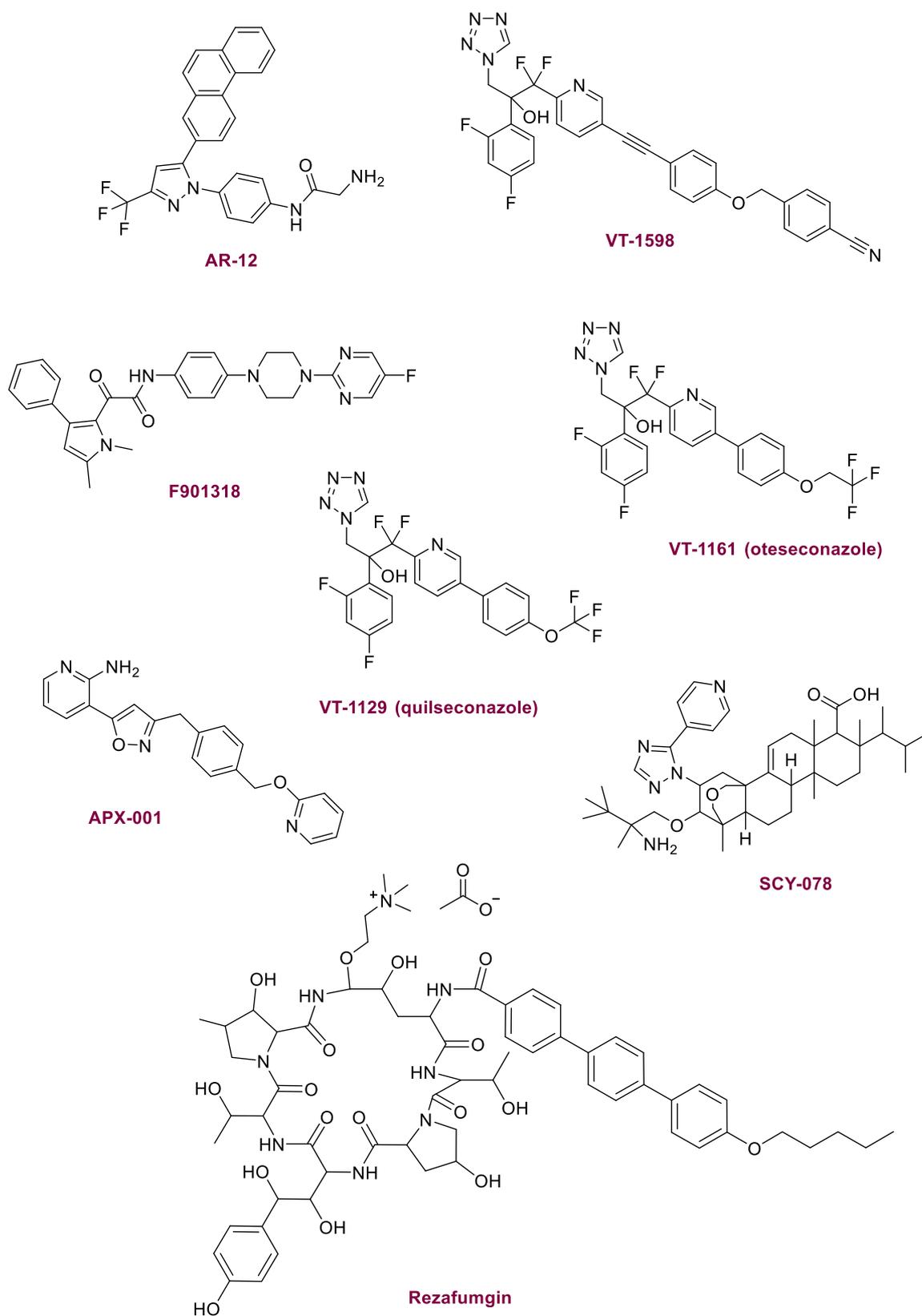
Figure 13. Antifungal agents undergoing Phase 1/2 clinical studies

1.5 Cytochrome P450 (CYP) enzymes

Cytochrome P450 (CYP) enzymes are a superfamily of haem-thiolate proteins discovered in the 1960s and found in all biological species.[56,58] In human, CYP enzymes can be found everywhere except red blood cells and skeletal muscles, however, they exist mainly in the hepatocytes.[66,67] The name cytochrome P450 was characterised as a coloured substance in the cell. This pigment shows an absorption band at a wavelength of 450 nm when reduced and bound to carbon monoxide.[13,66]

Fifty-seven human CYP genes have been identified and classified into 18 families and 44 subfamilies based on the amino acid sequence identity of the encoded proteins.[22,56,58,66,67] The nomenclature of CYP enzymes follows a systematic rule that provides information relating to enzyme sequence similarity:[13,66,68]

The name is given with a number-letter-number:

   a. Starts first with the symbol "CYP" for CYP450

   b. Followed by an Arabic number that indicates the family, which is based on ≥ 59 % amino acid similarity

   c. Then, a letter indicating the subfamily with 70% similarity in the amino acid sequence

   d. Finally, an Arabic number representing the individual gene

Moreover, when describing the gene, all letters and numbers should be written in italics, e.g. *CYP1A2*, whereas the non-italic (CYP1A2) represents the enzyme itself.[13,67,58]

CYP enzymes play vital roles in the biosynthesis and metabolism of endogenous compounds as well as the metabolism of foreign compounds such as drugs, steroids and carcinogens.[13,66,69] CYP enzymes are called monooxygenases since they convert an oxygen molecule into a very reactive oxygen species and then insert the oxygen atom into a substrate in order to make it polar and facilitate its mechanism.[69] Furthermore, CYP enzymes play a crucial role in the conversion of prodrugs into the active form, and they can also produce reactive, toxic metabolites.[13,66] Even though there are a large number of CYP enzymes in human, a small number of CYP enzymes found in families 1, 2 and 3 are involved in the majority of drug metabolic biotransformations, such as CYP1A2, CYP2D6 and CYP3A4.[13,66,67] These enzymes have interesting properties when metabolite drugs; a single CYP enzyme can metabolise a diverse range of drugs with different structures; on the other

hand, multiple CYP enzymes can metabolise a single drug at different sites, or multiple CYP enzymes could metabolise it with different catalytical rates at the same site.[13]

1.5.1 General structure of CYP

The CYP enzymes are haemoproteins that contain between 400-500 amino acid residues and a single iron-porphyrin complex (haem) in the active site that controls the spin state equilibrium during the catalytic cycle.[58,69-71] These enzymes are classified as CYP enzymes because of the conserved motif sequence of 10 amino acids Phe-X-X-Gly-X_b-X-X-Cys-X-Gly, where X_b is usually a basic amino acid that plays an indispensable role with the reductase partner, and this motif includes the conserved cysteine residue.[56,72] An additional feature is the formation of the fifth ligand between the haem iron and the sulfur atom of the conserved cysteine residue, while a water molecule acts as the sixth ligand during the enzyme rest state (low spin state) (Figure 14). The essential structure is stabilised by an absolute conserved (Glu-X-X-Arg) motif can be found on the proximal side of the haem.[69-71]
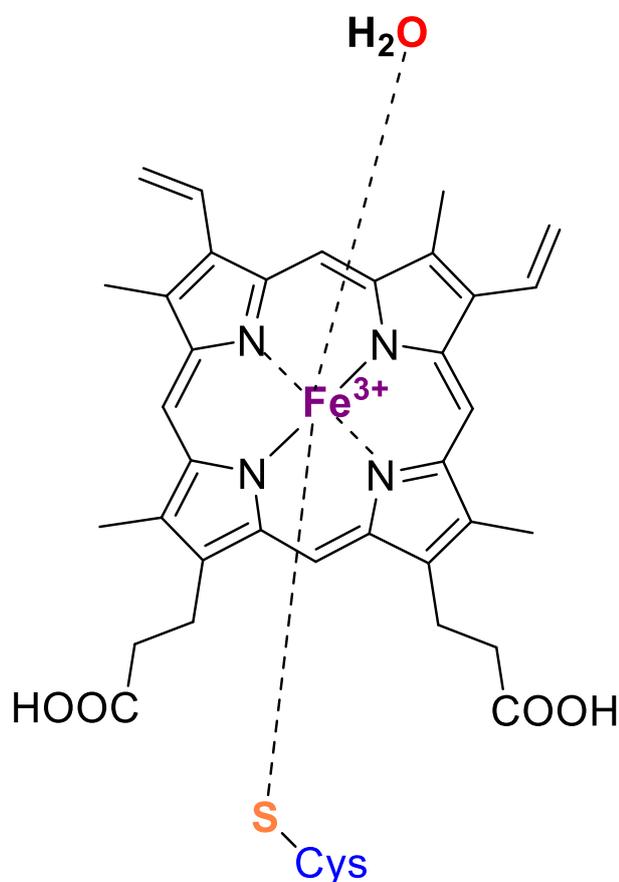
Figure 14. Structure of the CYP haem group

1.5.2 CYP catalytic cycle

The monooxygenase reaction mediated by CYP enzymes can be represented as follows:

$$RH + O_2 + 2e^- + 2H^+ \longrightarrow ROH + H_2O$$

These reactions require an oxygen molecule (O_2) and the substrate (**RH**) to produce the hydroxylated metabolite (**ROH**) and a water molecule (H_2O). To perform these monooxygenase reactions, the CYP enzyme needs two electrons and two protons (two reducing equivalents supplied by nicotinamide adenine dinucleotide phosphate (NADPH)) for each cycle to CYP via NADPH- cytochrome P450 reductase.[66,69,70,73,74]

The catalytic cycle of CYP starts with a water molecule bound to the ferric ion (Fe^{3+}), which is the resting state (Figure 15). When the substrate molecule enters the active site of the enzyme, it displaces the water molecule and forms a complex with ferric ion (Fe^{3+}), which leads the Fe^{3+} coordination number to change from six to five, leading to a slight increase in the reduction potential and allows the acceptance of electrons from NADPH-P450 reductase. The first addition of electrons causes the reduction of the ferric ion (Fe^{3+}) to the ferrous state (Fe^{2+}). Next binding of molecular oxygen results in the ferric peroxide complex (Fe^{3+}-O_2) and then a second electron enters the system to reduce the ferric peroxide complex and generate the ferric-peroxo anion (Fe^{3+}-O_2^{2-}). The ferric-peroxo anion complex is quickly protonated to generate the hydrogen peroxide intermediate (Fe^{3+}-H_2O_2), which initiates the formation of the hydroxylated substrate (Fe^{3+}-**ROH**) and water molecules by a free radical reaction. This free radical reaction could be produced by symmetrical cleavage of the H_2O_2 to form two hydroxyl radicals leading to the elimination of a water molecule and formation of the highly reactive oxoferryl species (Fe^{4+}=O), which then abstracts a proton from the substrate.

Iron-oxo
(very reactive intermediate)
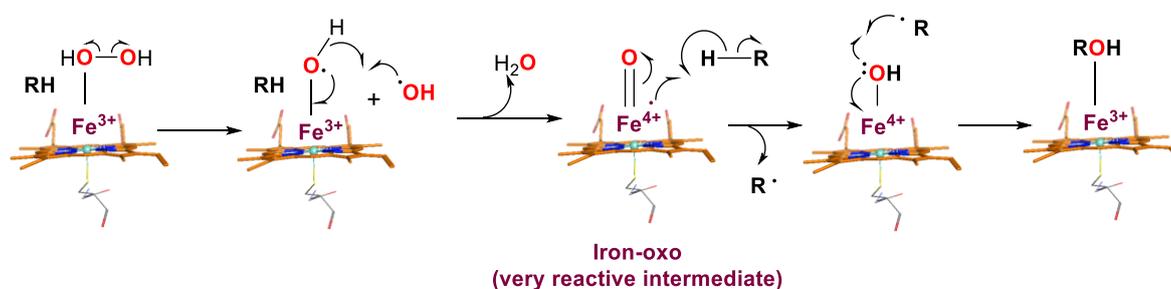
Finally, the hydroxylated substrate will dissociate from the enzyme reactive centre, and a water molecule will enter to return the enzyme to its resting state.[66,69,75]
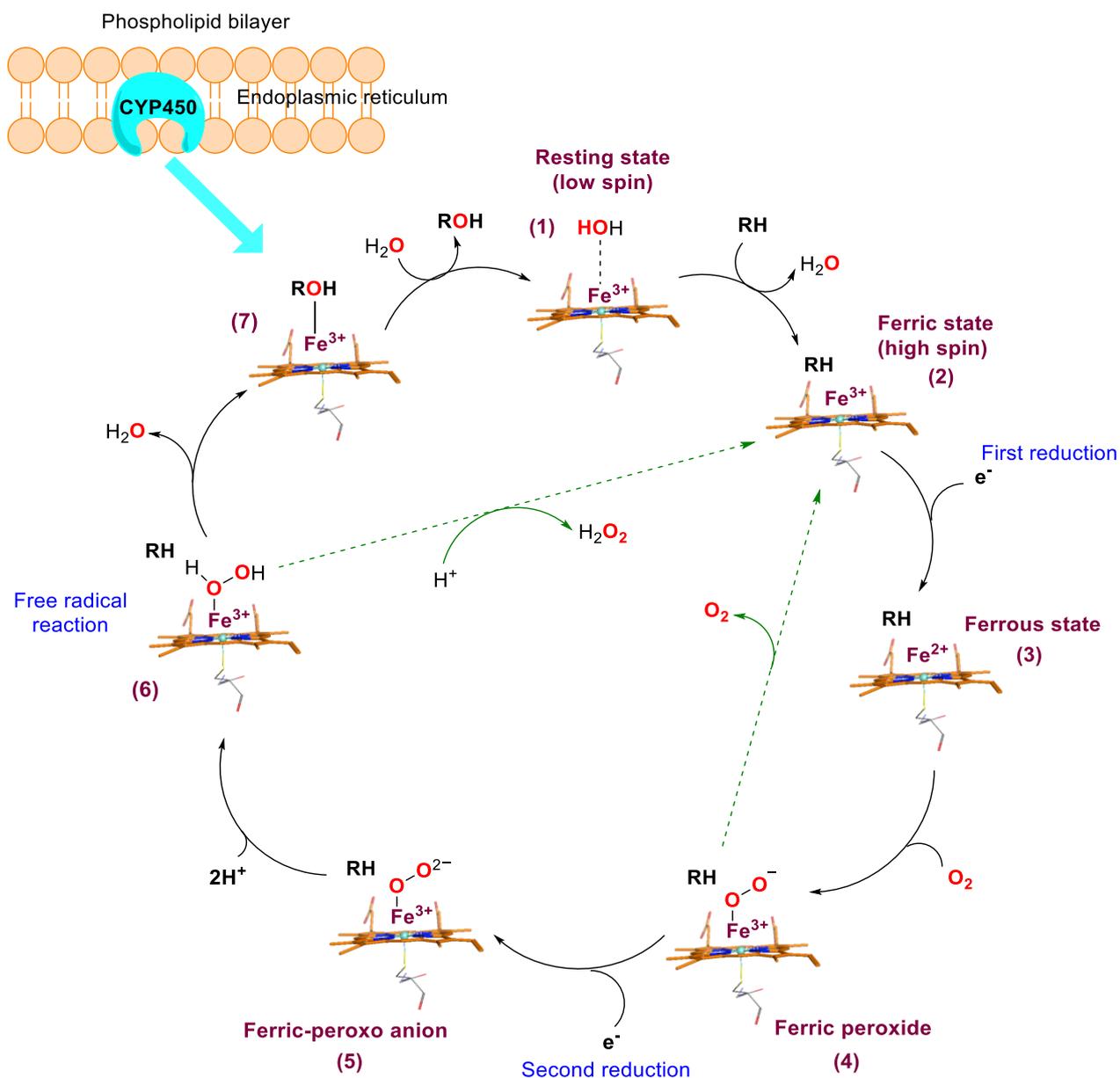
Figure 15. CYP catalytic cycle. Binding of the substrate to the active site of CYP enzymes displaces a water molecule with a change in the spin of Fe^{3+} from low spin (LS) state to high spin state (HS) causing an interaction with the redox component. The ferric CYP-substrate complex is reduced by electron transfer from NADPH via the electron transfer chain. This is followed by O_2 binding to form a stable ferric-peroxide (Fe^{3+}-O_2^-) complex that is reduced to the ferric-peroxo anion (Fe^{3+}-O_2^{2-}) by a second electron transfer from NADPH. Fe^{3+}-O_2^{2-} interactions with two protons from the surrounding solvent forms $(Fe-H_2O_2)^{3+}$ complex. Breakdown of the HO-OH bond radically eliminates H_2O and yields a hydroxylated product ($FeOH^{3+}$-R). Release of the product from the active site of the enzyme regenerates the un-complexed ferric CYP that can participate in the metabolism of other molecules

1.6 Aim and objectives

The global increase in the prevalence of invasive fungal infections makes it a dangerous community and hospital health disease.[1] Such infections are common in patients with immunodeficiencies, transplant surgery and prolonged use of antibiotics.[18] Azole antifungal agents act by inhibiting CYP51 that inhibits the fungal cell growth and are the most commonly used clinically and as prophylactic regimens for the treatment of these infections.[51,52] Nevertheless, the extensive use of these agents, particularly fluconazole, has resulted in the extensive development of resistance in *C. albicans*, which has become a severe problem for public health.[53-55] Thus, there is a great need for the development of new compounds that have broad-spectrum activity, high selectivity to CaCYP51 and activity against resistant strains.

Therefore, the current research aims to design, generate, and evaluate novel azole inhibitors with efficacy against wild type and fluconazole-resistant *Candida* strains. The novel designed azole antifungal agents should have several criteria to be useful clinically. The novel inhibitors need to specifically target the fungal enzyme (CaCYP51) rather than the human CYP51 (hCYP51), to avoid the inhibition of the sterol biosynthesis pathway in human and decrease the toxicity and drug-drug interactions that could occur.[25,51] As the similarity of the amino acid sequence between CaCYP51 and hCYP51 is relatively low (< 35%), CYP51 is a good target enzyme for treating *Candida* sp. infections. Furthermore, the novel inhibitors should be fungicidal and have broad-spectrum activity against different fungal species as well as be effective against resistant *C. albicans* strains resulting from CaCYP51 mutations.[51]

Designing agents that achieve the criteria mentioned above is a significant challenge. However understanding the binding and the occupation of the novel inhibitors within the CaCYP51 protein using computational studies, facilitated by the availability of the crystal structure of CaCYP51 co-crystallised with posaconazole (PDB: 5FSA)[35] in the protein data bank (PDB)[76,77], will assist in the design and computational investigations of these novel azole inhibitors.
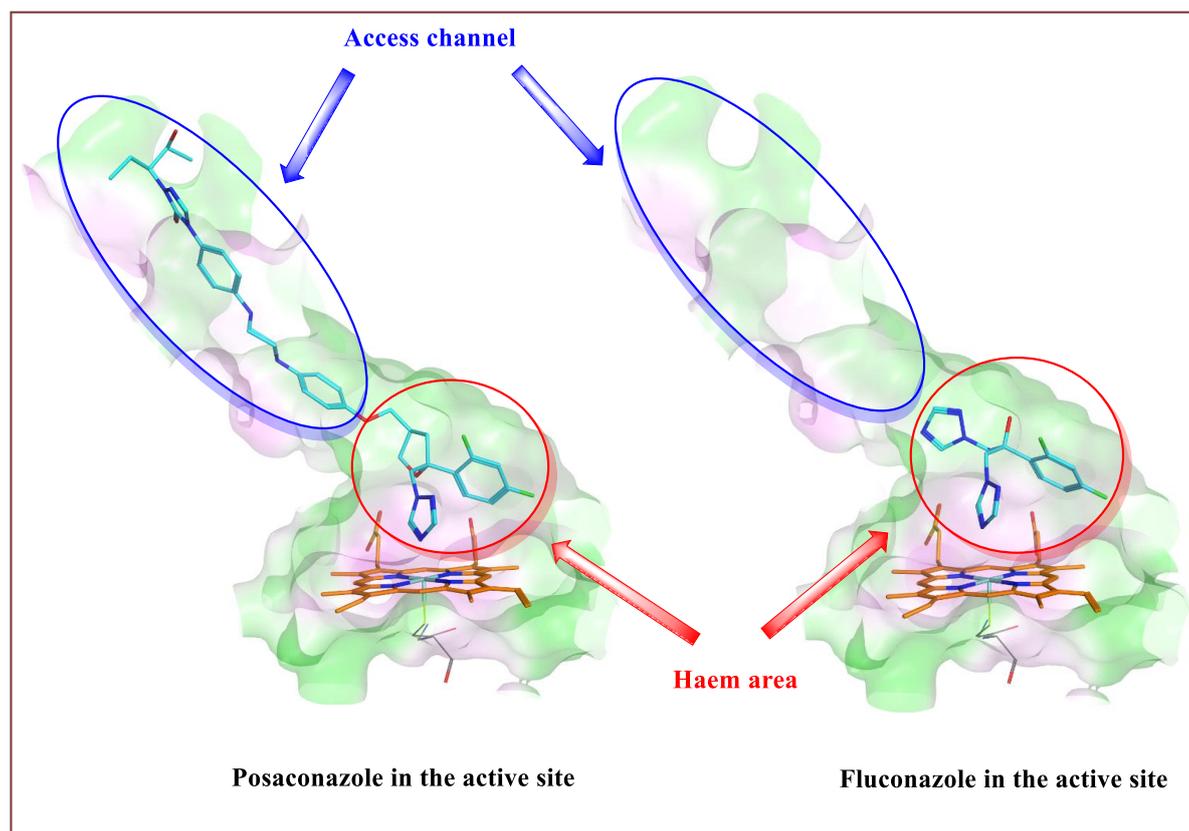
Figure 16. The occupancy of posaconazole and fluconazole in CaCYP51 protein

Based on the computational study investigation of occupancy and binding of fluconazole (the mainstay treatment) and posaconazole (co-crystallised structure) within CaCYP51 (PDB: 5FSA) active site (Figure 16), the design of novel inhibitors was determined. Recent studies demonstrate that the extended structures of antifungal agents, such as Oteseconazole, can form additional interactions with the amino acids within the substrate access channel, which increase the binding affinity and selective to CaCYP51, and importantly activity against azole-resistant strains.[57,60] As a result, the novel azole inhibitors will be designed as 'Y-shape' structures with a core amide scaffold, two short arms to occupy the haem binding site and the small hydrophobic pocket, while the long arm fills the long access channel of CaCYP51.
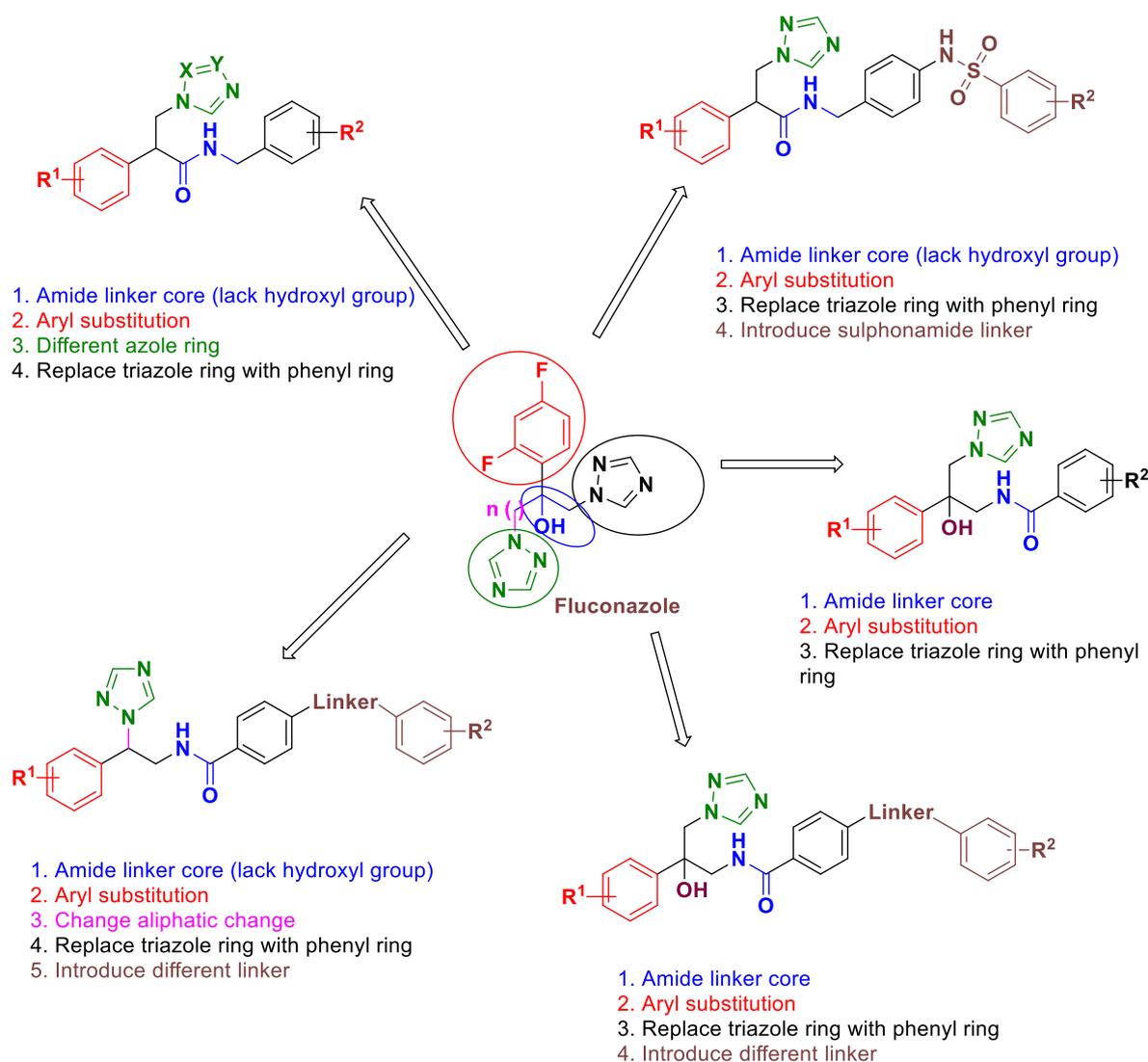
Figure 17. The possible suggested chemical modification of fluconazole

This research investigated some possible chemical modifications of the fluconazole as described in Figure 17, with amide linker scaffold and modification of the chain lengths either to the amide linker, azole ring and/or the side chain as well as different heterocyclic azole rings (Figure 17). One example of these modifications was to study the chain length attached to azole ring and how it affects the fit within the CaCYP51 protein computationally as well as biologically to determine the requirements of chain length for antifungal activity. In addition, all modifications resulting in new designs will be investigated biologically and computationally and correlation analysis performed to establish the important moieties with respect to antifungal activity and importance in counteracting mutational resistance.

The main modification in this research is introducing the amide linker core to develop all novel azole inhibitors; however, there are different modifications to be investigated. The first extra modifications to be investigated in this research were through, (1) different substitutions on the phenyl rings to explore the structure-activity relationship, (2) variation of the heterocyclic ring, including imidazole, triazole and/ or tetrazole, which is a very important moiety in the azole antifungal agents to interacts with the haem iron of CaCYP51, (3) replacement of one of the triazole rings with a phenyl substituted ring to optimise the filling of the small hydrophobic pocket in CaCYP51, and (4) extending the chain length to evaluate the optimal occupation within the CaCYP51 access channel (Figure 18).
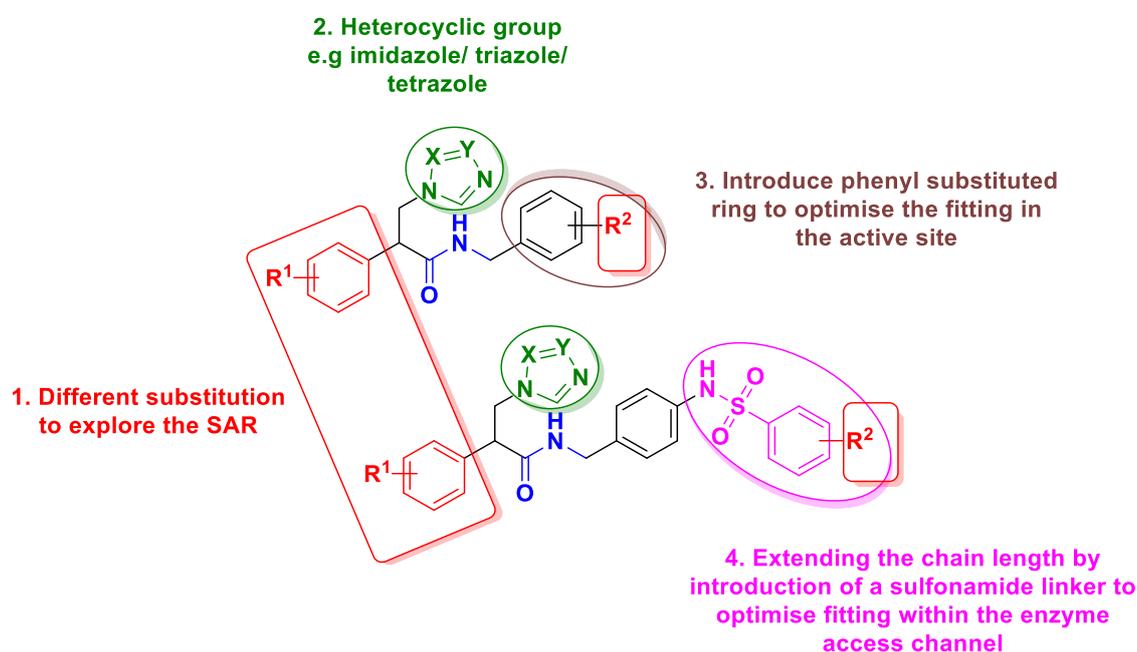
Figure 18. The first suggested modification to develop series I

The second modifications in this study to be investigated included: (1) inverting the amide linker core to investigate the fit and binding interactions within the CaCYP51 protein, (2) different substitutions on the phenyl rings to explore the structure-activity relationship, (3) variation of the chain length that links the heterocyclic ring by shortening one carbon atom to investigate the fit in the active site of CaCYP51, (4) retaining the essential moiety in the azole antifungal agents, which is the triazole heterocyclic ring, (5) extending the chain length with different linkers to evaluate the optimal occupation within the CaCYP51 access channel (Figure 19).

4. Heterocyclic group such as triazole

3. Varying in the chain length to optimise fit in the active site

Linker

R^1

R^2

2. Different substitution to explore the SAR

1. Inver the amide linker to investigate binding and fit within the active site

5. Extending the chain length with different linker to optimise the fitting within the enzyme access channel
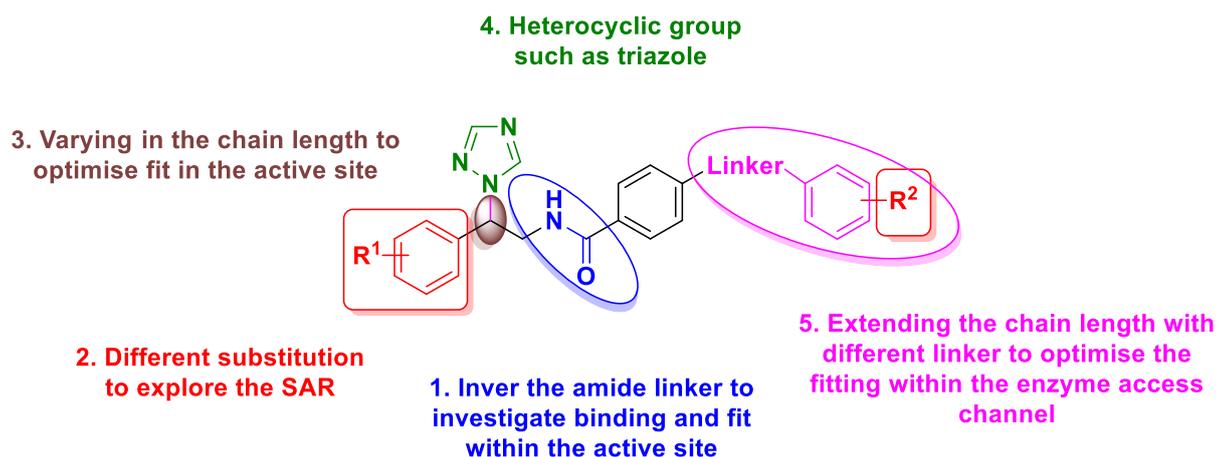
Figure 19. The second suggested modification to develop series II

The third modifications in this research will be investigated by: (1) keeping the hydroxyl group and the amide linker core to investigate the fit and binding interactions within the CaCYP51 protein, (2) different substitutions on the phenyl rings to explore the structure-activity relationship, (3) retaining the triazole heterocyclic ring, (4) replacement of one of the triazole rings with a phenyl substituted ring to optimise the filling of the small hydrophobic pocket, (5) extending the chain length with different linkers to evaluate the optimal occupation within the CaCYP51 access channel (Figure 20).

3. Heterocyclic group such as triazole

R^1 OH R^2

4. Introduce phenyl substituted ring to optimise the fitting in the active site

2. Different substitution to explore the SAR

R^1 OH   **Linker** R^2

5. Extending the chain length by introduction different linker to optimise within the enzyme access channel

1. Inver the amide linker to investigate binding and fit within the active site

Figure 20. The third suggested modification to develop series III

Therefore, the strategy applied to achieve these aims can be divided into the following steps:

1. Design of selective novel antifungal azole inhibitors for CaCYP51 considering the results of computational studies of molecular binding interactions of fluconazole and posaconazole within CaCYP51 protein (PDB: 5FSA) using Molecular Operating Environment (MOE) software[78].

2. Analysing the docking studies of the novel designed inhibitors in the CaCYP51 protein to explore computationally the effect of certain groups in the designed compounds on the binding interactions that could counteract resistance mutations by forming additional binding interactions.

3. Literature survey for the possible chemical pathways to synthesise the target compounds using Scifinder.

4. Laboratory synthesis of the designed compounds and their structure elucidation using the spectroscopic tools ^{1}H and ^{13}C NMR, HRMS or elemental microanalysis, and HPLC.

5. Further analysis of the novel inhibitors structure-activity relationships and investigating of the inhibitors through determining the minimum inhibitory concentration (MIC) against *C. albicans* SC5314 (*C. albicans* laboratory strain) and CAI4 (*C. albicans* wild type clinical isolation), CaCYP51 inhibitory activity and binding affinity (K_d). These studies will be performed by our collaborators at Swansea University.

6. Study the selectivity for CaCYP51 against hCYP51 of the most active designed compounds and also a sterol profile study, which shows the accumulation of 14α-methylated sterols, especially 14α-methyl ergosta-8,24[28]-dien-3,6-diol in both *C. albicans* strains to confirm if these compounds are akin to fluconazole in their mechanism of action. These studies will be performed by our collaborators at Swansea University.

7. Further computational studies using molecular dynamic simulations for the novel designed compounds within the wild type and a representative double mutant strain (Y132H + K143R) of CaCYP51 to investigate the relation between the binding interactions within the CaCYP51 protein and the biological results.

8. The importance of CYP51 in protozoa, including *Trypanosoma* and *Leishmania*, would suggest CYP51 as an important target for inhibitor design, however a possible

bypass mechanisms, as seen with ergosterol synthesis in fungi (Figure 12), resulting in reduced effectiveness in protozoa has been linked to recently identified orphan CYP, CYP5122A1. CYP5122A1 is found in *Trypanosoma* and *Leishmania*,[79] however, no crystal structure is available. Therefore, a homology model was generated using the SWISS-MODEL server with further optimization using molecular dynamic simulations using Maestro software.

9. Validation of the model will be performed using Ramachandran plot and ProSA analysis as well as docking studies of known inhibitors.

10. Furthermore, as azole antifungal inhibitors were studies *in vitro* or *in vivo* and showed promising results against *Leishmania* species,[43,45,47,80] some of the novel compounds designed in this PhD research also will be tested against *Leishmania donovani* to investigate the inhibitory potential. This evaluation will be performed by our collaborators at the University of Dundee.

Chapter II

Series I

2.1 Introduction

As described in Chapter I, there is an urgent need to design new azole antifungal agents to overcome azole drug resistance. Fluconazole is the first-line treatment for fungal diseases; however, the resistance of this mainstay drug arises widely, therefore short derivatives and its extended modification were designed to determined and explore binding interactions within the CaCYP51 active site (Figure 21).

Short derivatives   **Extended derivatives**
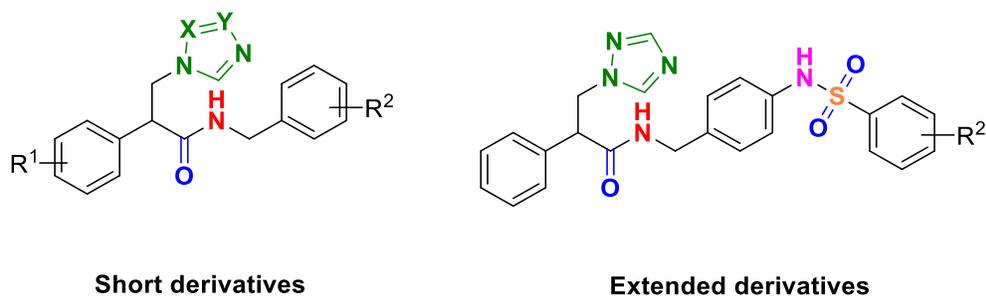
Figure 21. (*R/S*)-*N*-Benzyl-3(1*H*-azol-1-yl)-2-phenylpropanamide structures investigated in this chapter (Chapter II)

(*R/S*)-*N*-Benzyl-3(1*H*-azol-1-yl)-2-phenylpropanamide derivatives were studied to explore additional binding interactions within the hydrophobic substrate access channel of CaCYP51. The synthesis, evaluation of inhibitory activity against CaCYP51 and MIC against *C. albicans* strains and preliminary structure-activity relationships (SARs) will be investigated for (*R/S*)-*N*-benzyl-3(1*H*-azol-1-yl)-2-phenylpropanamide derivatives in this chapter.
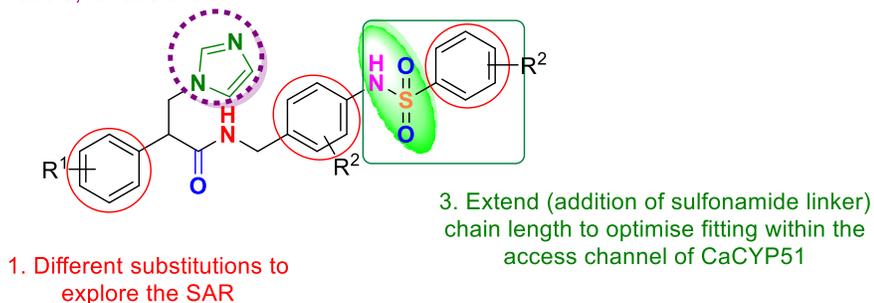
Figure 22. Sites of investigation of (*R/S*)-*N*-benzyl-3(1*H*-azol-1-yl)-2-phenylpropanamide structures

This chapter is focused on the development and modification of (*R/S*)-*N*-benzyl-3(1*H*-azol-1-yl)-2-phenylpropanamide derivatives (Figure 22), specifically through:

i.   Substitution of the phenyl rings to explore the structure-activity relationship (SAR), where the R^1/R^2-group could be an electron-withdrawing or electron-donating group in different positions.

ii. Introduction of a heterocyclic group such as imidazole, triazole and/ or tetrazole, which interacts with the haem iron of CaCYP51 as well as to evaluate the biological activity and selectivity with respect to human CYP51 (hCYP51).

iii. Extending the structure of inhibitors could lead to optimal occupation of the long channel of the access channel that may lead to more hydrophobic and/ or hydrophilic interactions with the amino acids in the active site that may enhance the activity and selectivity.

This chapter is divided into 5 parts as follows:

1. Molecular modelling
2. Results and discussion:

    a. Development of short derivatives with different aryl substitutions and azole rings

Where X:
C, N

Where Y:
C, N

Where R^1:
a= 4-H
b= 4-Cl

Where R^2:
a= 4-H   b= 4-F
c= 4-Cl   d= 2,4-diCl
e= 4-CH$_3$ f= 4-CF$_3$
g= 4-OCH$_3$ h= 3,4-diOCH$_3$
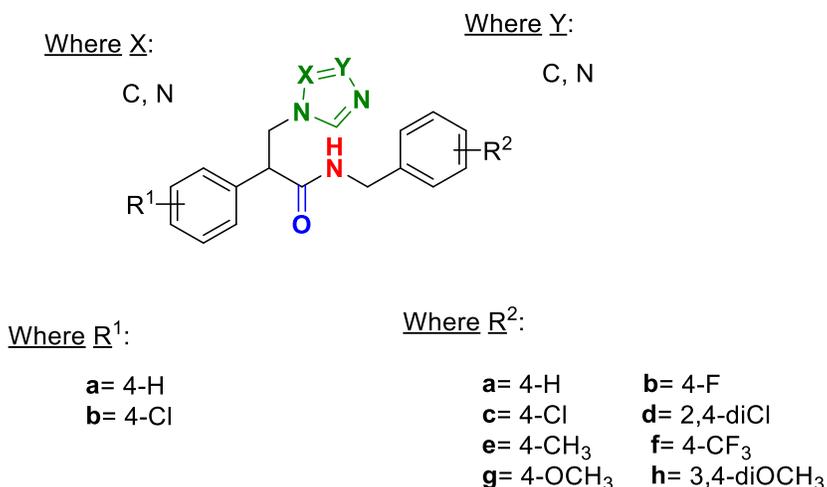
Figure   *23.*   (*R/S*)-*N*-(4-Arylpyridinyl/benzyl)-3(1*H*-azol-1-yl)-2-phenyl/chlorophenyl propanamide derivatives

b. Extended derivatives by introduction of a sulfonamide linker
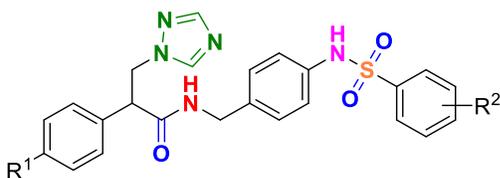
Where R^1:

    a= H

Where R^2:

    a= 4-H
    b= 4-F
    c= 4-Cl
    d= 2,4-diCl

Figure   *24.*   (*R/S*)-2-Phenyl-*N*-(4-(aryl-phenylsulfonamido)benzyl)-3-(1*H*-1,2,4-triazol-1-yl) propanamide derivatives

3. Biological evaluation
4. Molecular dynamics
5. Conclusion

2.2 Molecular modelling

The crystal structure of CaCYP51 wild type (PDB 5FSA)[35] was downloaded from the protein data bank.[76,77] To perform docking studies, inhibitors were created using ChemDraw professional (16.0) and introduced into the Molecular Operating Environment (MOE) programme.[78] After that, all designed inhibitors were protonated at physiological pH ($\approx$ 7.4) to mimic the physiological condition in *C. albicans* endoplasmic reticulum. The inhibitors were energy minimised and saved as a database file (mdb/mol2) then docking studies were performed using MOE and LeadIT[81] software programmes.

2.2.1 Docking studies with CaCYP51 (PDB 5FSA)

To design new selective CaCYP51 inhibitors, the objective was to create a small new database of compounds and to dock them in the active site of CaCYP51 to explore optimal pharmacophores to fit within the active site domains and binding interactions, compared with posaconazole, which was co-crystallised with CaCYP51 in the crystal structure 5FSA. Posaconazole has a long hydrophobic structure with bonding primarily through multiple hydrophobic interacts (29 amino acid residues in the binding pocket) and just one H-bonding interaction between Ala61 and the carbonyl oxygen of the 1,2,4-triazol-5(4*H*)-one ring. Moreover, posaconazole interacts perpendicularly with the haem iron and the N4 of the triazole ring with a distance of 2.08 Å as shown in figure 25.
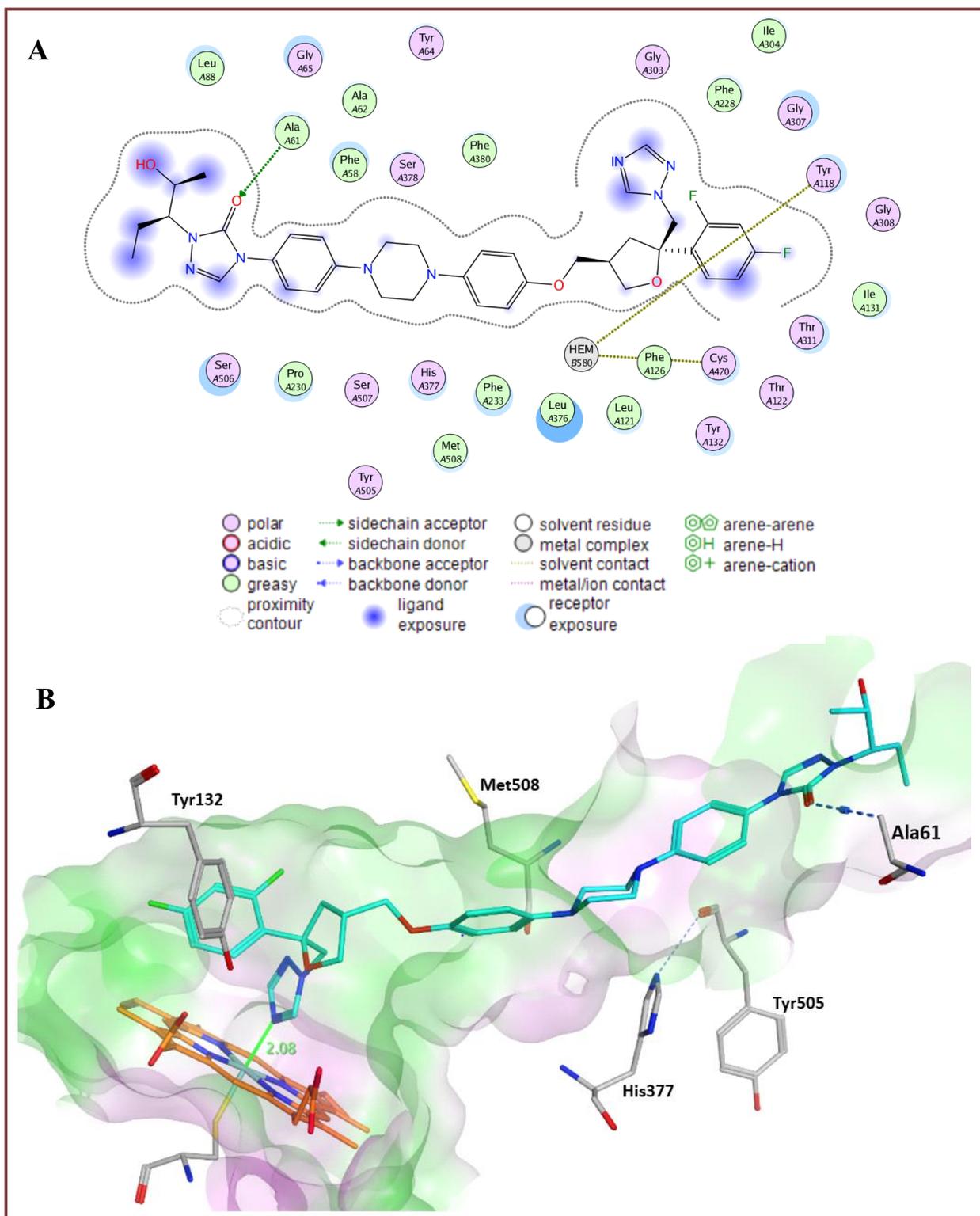
Figure 25. (A) 2D ligand interaction of posaconazole in the CaCYP51 protein. (B) 3D view of posaconazole (cyan) in the active site of CaCYP51. Lipophilic regions are shown in green, hydrophilic regions in pink. The haem group can be seen in orange

Fluconazole was docked in the CaCYP51 crystal structure and showed hydrophobic binding interactions with 12 amino acid residues and one arene-arene interaction between a triazole ring and Tyr118, which interacts with the haem (Figure 26a). Furthermore, fluconazole occupies the haem area and interacts perpendicularly with the haem iron with a distance of 2.64 Å (Figure 26B).
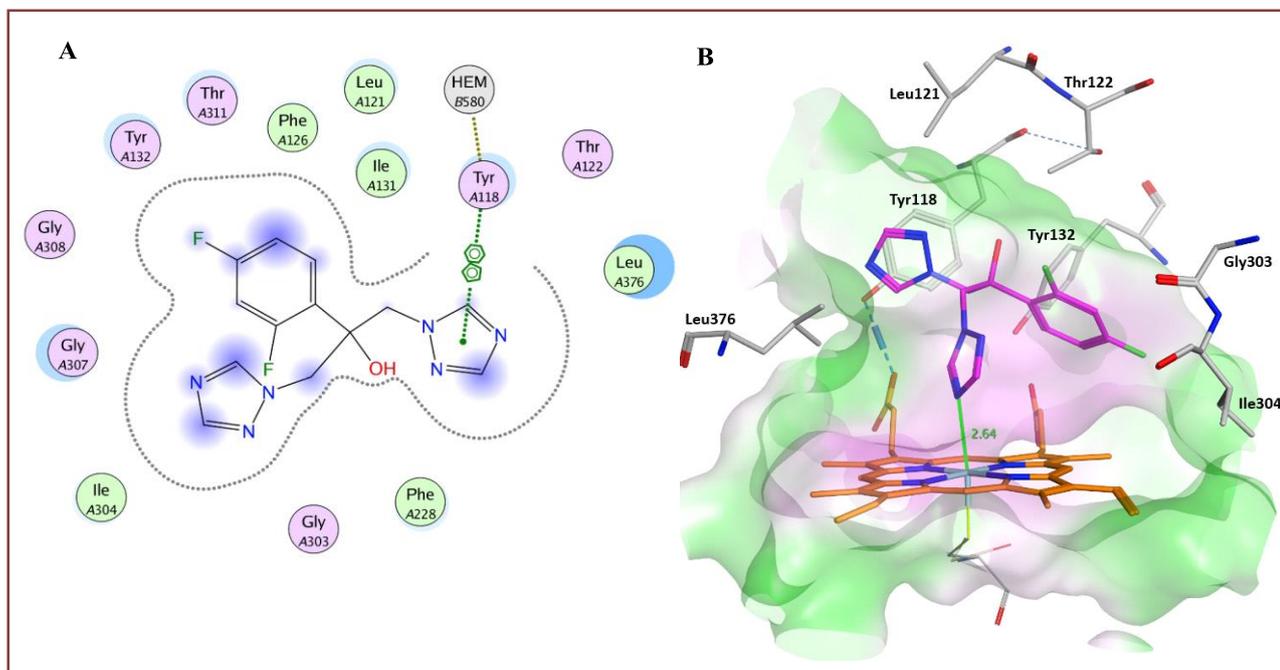
Figure 26. (A) 2D ligand interaction visualisation of fluconazole in the CaCYP51 protein. (B) A 3D view of fluconazole (magenta) in the active site of CaCYP51

The design of the novel inhibitors incorporated an amide linker to form a Y-shape. From docking studies using MOE and LeadIT programmes, the novel short azoles derivatives (**8**) and extended derivatives (**18**), interacted perpendicularly with the haem iron with a distance of < 3.0 Å.

The docking study showed azole derivatives docked within the active site of CaCYP51 in both (*R*)- and (*S*)-configurations forming both hydrophobic and hydrophilic interaction with Phe233, Tyr118, Leu121, Phe126, Gly307, Tyr132, Met508, Ser378, Ile304, Leu376, Phe228, Ile131, Thr311, Gly303, Thr122 and Phe380 amino acid residues as shown in the 2D ligand interaction and 3D visualisation e.g. Figures 27 and 28.
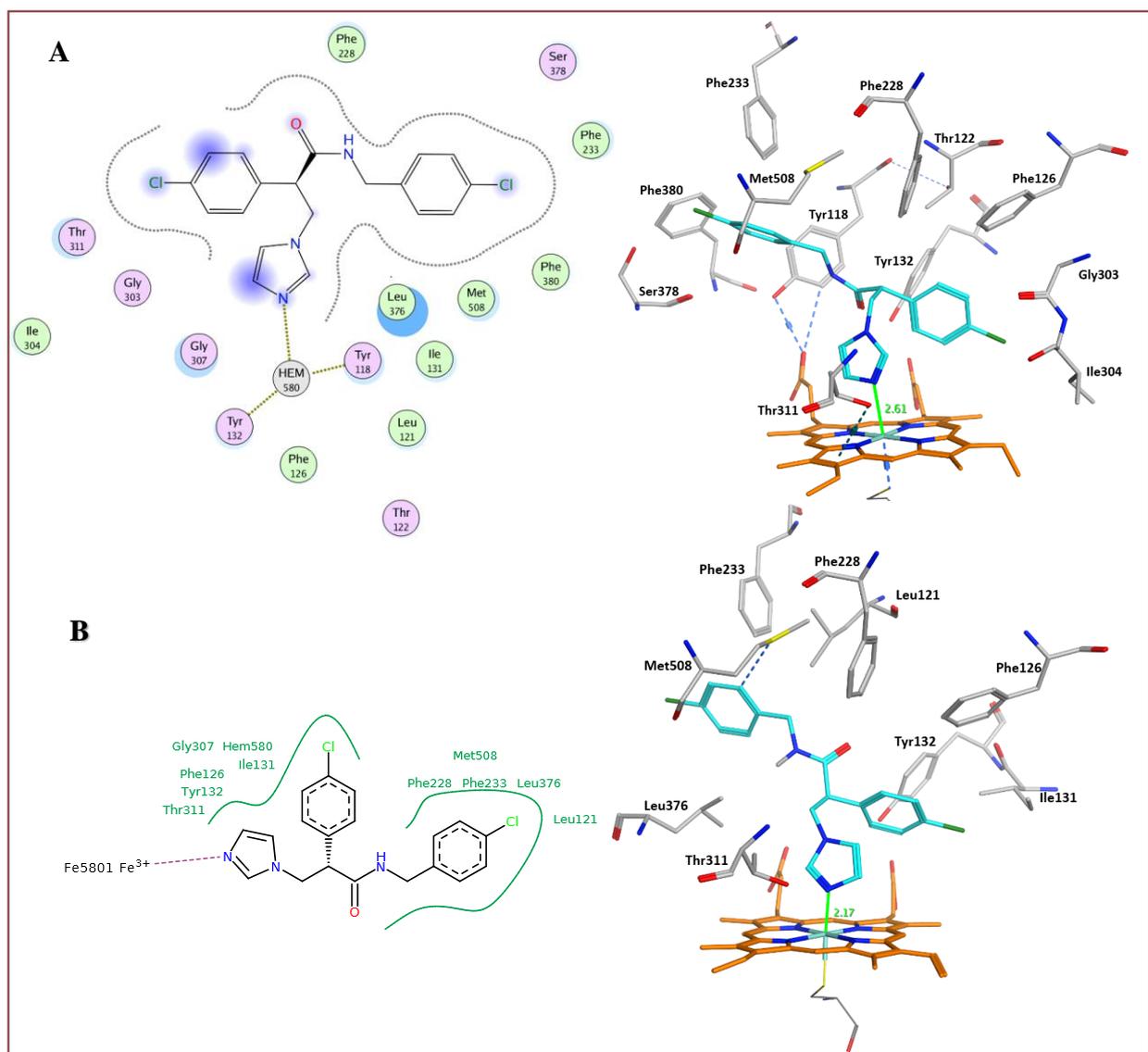
Figure 27. 2D ligplot and 3D image of (*R*)-configuration of short series exemplar in (A) MOE docking programme and (B) in LeadIT programme in the CaCYP51 active site

In the 3D image, MOE docking showed the *(R)*-configuration of the short series fit in the active site in a similar position to fluconazole, with regards to the occupancy of the pocket, and interacted through hydrophobic interaction with 16 amino acids. Moreover, the 2D ligplot showed good fitting within the pocket. Furthermore, using LeadIT software the haem iron interacted directly with N atom of the azole ring and through hydrophobic interactions with 10 amino acids.
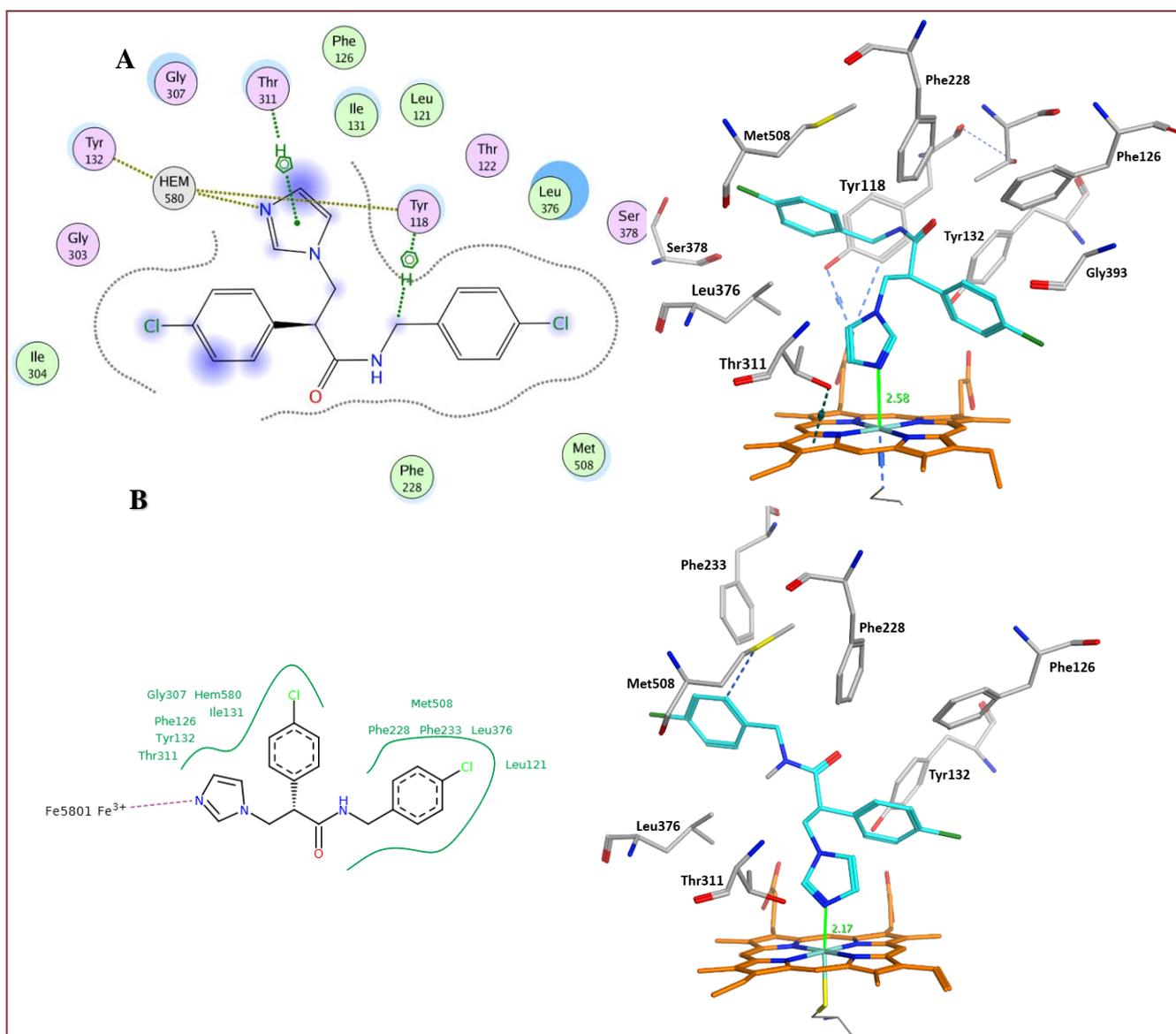
Figure 28. 2D ligplot and 3D image of (*S*)-configuration of short series exemplar in (A)
MOE docking programme and (B) LeadIT programme in the CaCYP51 active
site

The (*S*)-configuration of the short series (Figure 28) using the LeadIT software was
comparable with the (*R*)-configuration (Figure 27) with direct interaction with the haem iron.
However, the MOE programme showed H-arene interactions between the imidazole ring
and CH_2 adjacent to the amide group with Thr311 and Tyr311 respectively as shown in
figure 28A. These results indicated very slight differences were observed between the two
programmes however MOE programme was preferred owing to clearer visualisation in the
2D ligplot ligand interaction diagramme.

The extended derivatives were docked using MOE, and the results can be seen in figure 29 using an exemplar of this series. The (*R*)-configuration displayed perpendicular binding between the N-atom of the triazole ring and the haem iron with a distance of 2.49 Å and hydrophobic interactions with 22 amino acids (Table1).
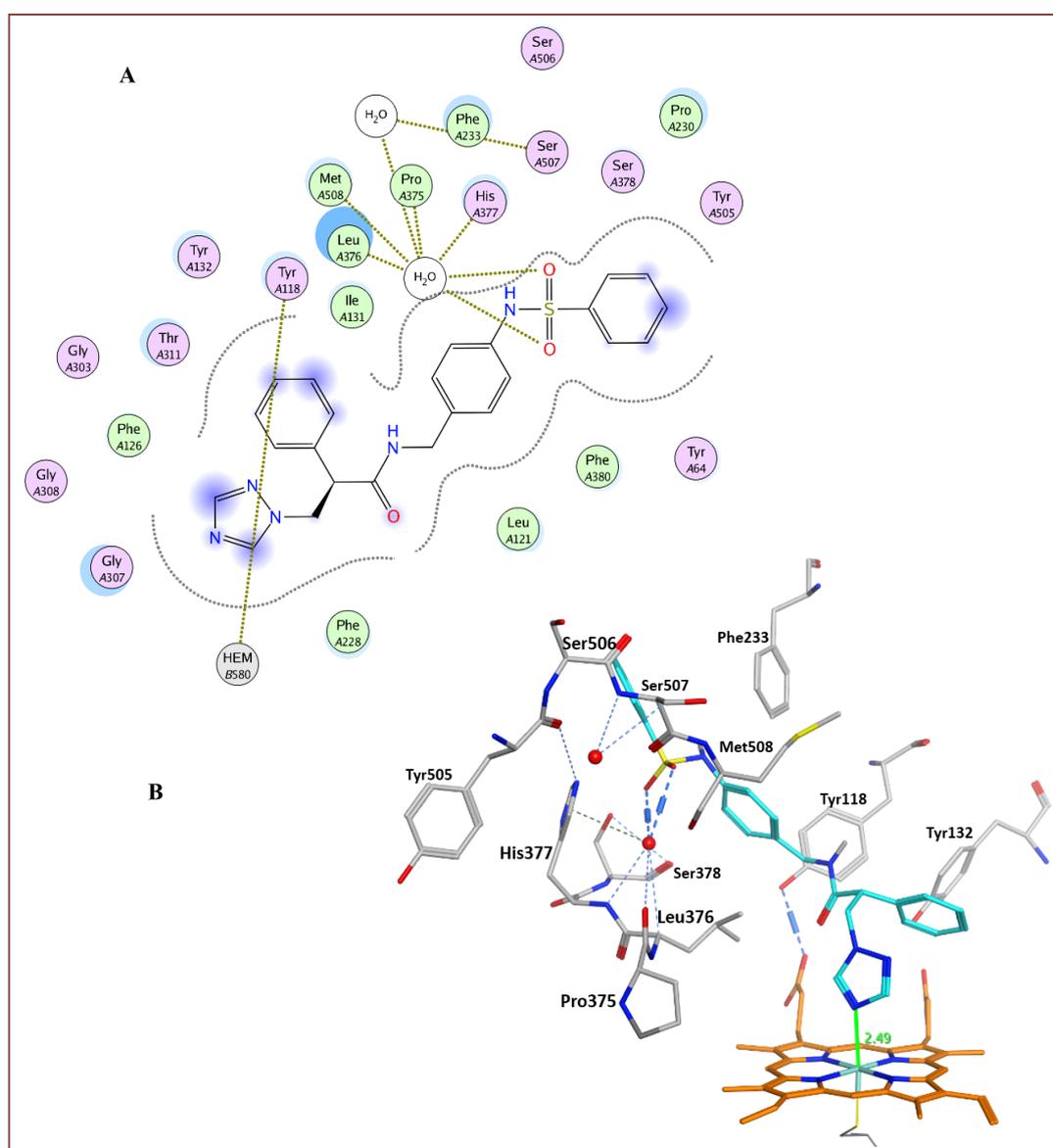
Figure 29. (A) 2D ligand interaction visualisation of the (*R*)-configuration of an exemplar of the extended series in the CaCYP51 protein. (B) A 3D image showing key binding interactions of the (*R*)-configuration of an exemplar of the extended series (cyan) within the active site of CaCYP51

Table 1. Key binding interactions between the (*R*)-configuration of extended series exemplar and the amino acids in the active site of CaCYP51

	Key binding interactions	
Distance	**Interactions through water molecules**	**Hydrophobic interactions**
2.49 Å	Leu376, Met508, Pro375, Ser507, His377	Leu121, Phe126, Phe380, Phe228, Phe233, Ile131, Pro230, Gly303, Gly307, Gly308, Tyr64, Tyr118, Tyr132, Tyr505, Thr311, Ser506, Ser378

The (*S*)-configurations of the extended series were also docked in the CaCYP51 active site and also showed water mediated binding interactions and multiple hydrophobic interactions (Figure 30).
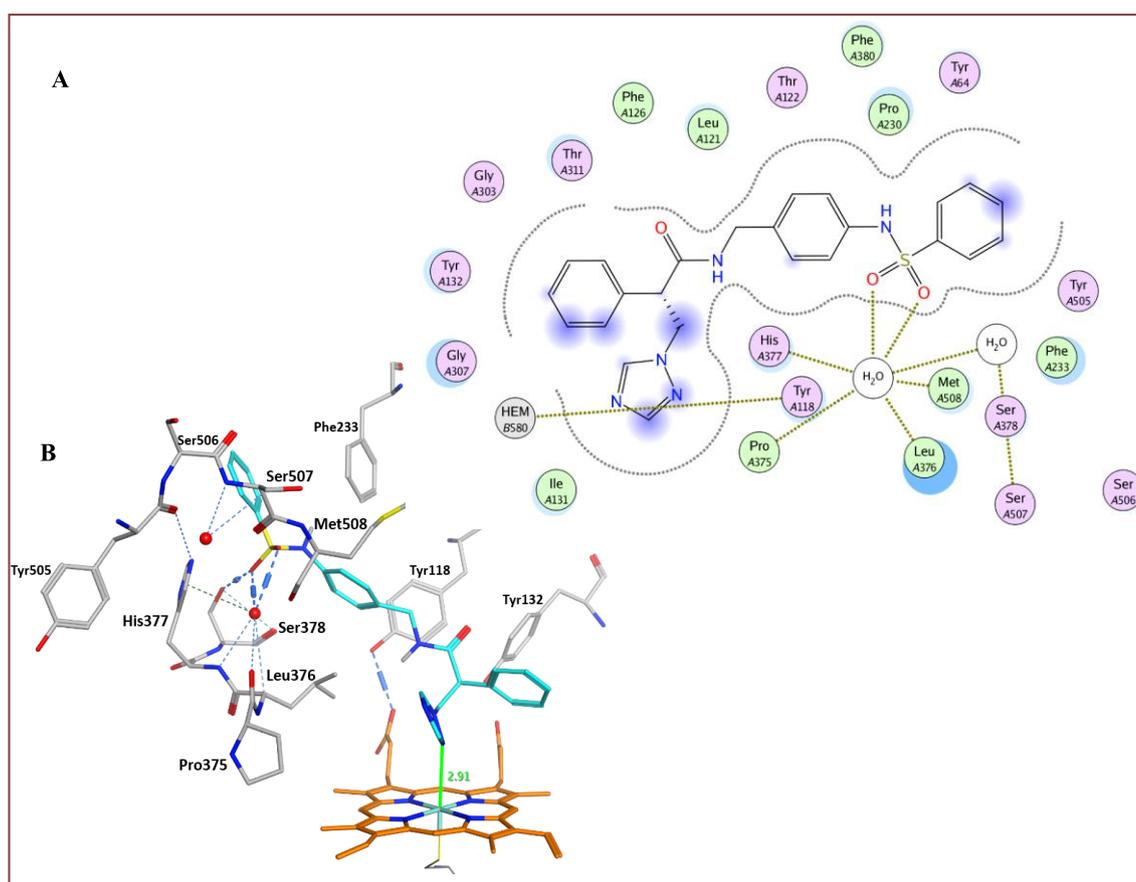
Figure 30. (A) 2D ligand interaction visualisation of the (*S*)-configuration of an exemplar of the extended series in the CaCYP51 protein. (B) A 3D view of the (*S*)-configuration of an exemplar of the extended series (cyan) in the active site of CaCYP51

2.3 Result and discussion

Following the promising results obtained from the docking studies, a synthetic pathway was developed to prepare the short derivatives incorporating different substituted aryl groups and azole rings (Figure 23).

2.3.1 Synthesis of (*R/S*)-*N*-(4-arylbenzyl)-3(1*H*-imidazol-1-yl)-2-phenylpropanamide (8)

- **General chemistry**

The synthesis of (*R/S*)-*N*-(4-arylbenzyl)-3(1*H*-imidazol-1-yl)-2-phenylpropanamide (**8**) was performed according to a sequence of six steps (Scheme 2.1):

❖ Esterification of carboxylic acid

❖ Addition of alkyl hydroxide

❖ Hydrolysis of ester to acid

❖ Amidation reaction

❖ Mesylation of the hydroxyl group

❖ Addition of an azole ring

The starting reagent 3-hydroxy-2-phenylpropanoic acid (tropic acid, **4a**) was commercially available, while the 4-chloride derivative (**4b**) was prepared using a 3-step synthesis.[82,83]
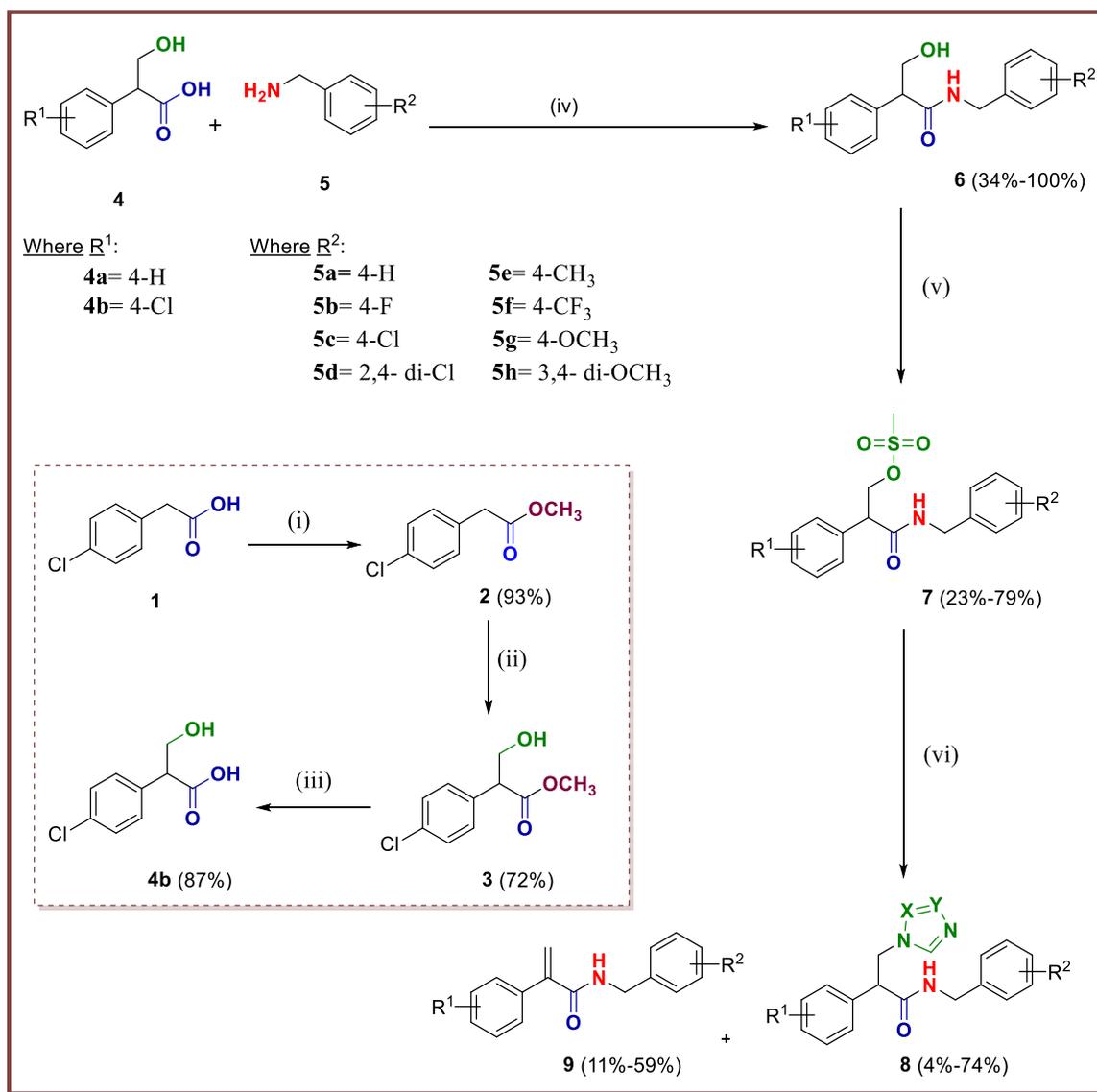
Scheme 2.1 Synthetic route for the synthesis of (*R/S*)-*N*-(4-arylbenzyl)-3(1*H*-imidazol-1-yl)-2-phenylpropanamide (**8**). *Reagents and conditions:* (i) MeOH, SOCl$_2$, 60 °C 3 h (ii) DMSO, NaOMe, paraformaldehyde, rt 4 h (iii) (a) LiOH·H$_2$O, rt 1 h (b) pH 3 with 2N HCl (iv) CPME, aliphatic amine, B(OCH$_3$)$_3$, molecular sieves, reflux 100 °C o/n (v) CH$_2$Cl$_2$, methanesulfonyl chloride, rt o/n (vi) (a) K$_2$CO$_3$, imidazole/triazole/tetrazole, CH$_3$CN, 45 °C 1 h (b) **7**, 70 °C 1-24 h

Synthesis of methyl 2-(4-chlorophenyl)acetate (2)

Methyl 2-(4-chlorophenyl)acetate (**2**) was obtained by the esterification of the carboxylic acid (**1**) using thionyl chloride (SOCl$_2$) in MeOH at 60 °C 3 h.[82]

The reaction mechanism of this step is shown in scheme 2.1.1, which involves the addition of SOCl$_2$ to convert the hydroxyl group of the carboxylic acid into a good leaving group that can be displaced by methanol to form the corresponding ester.
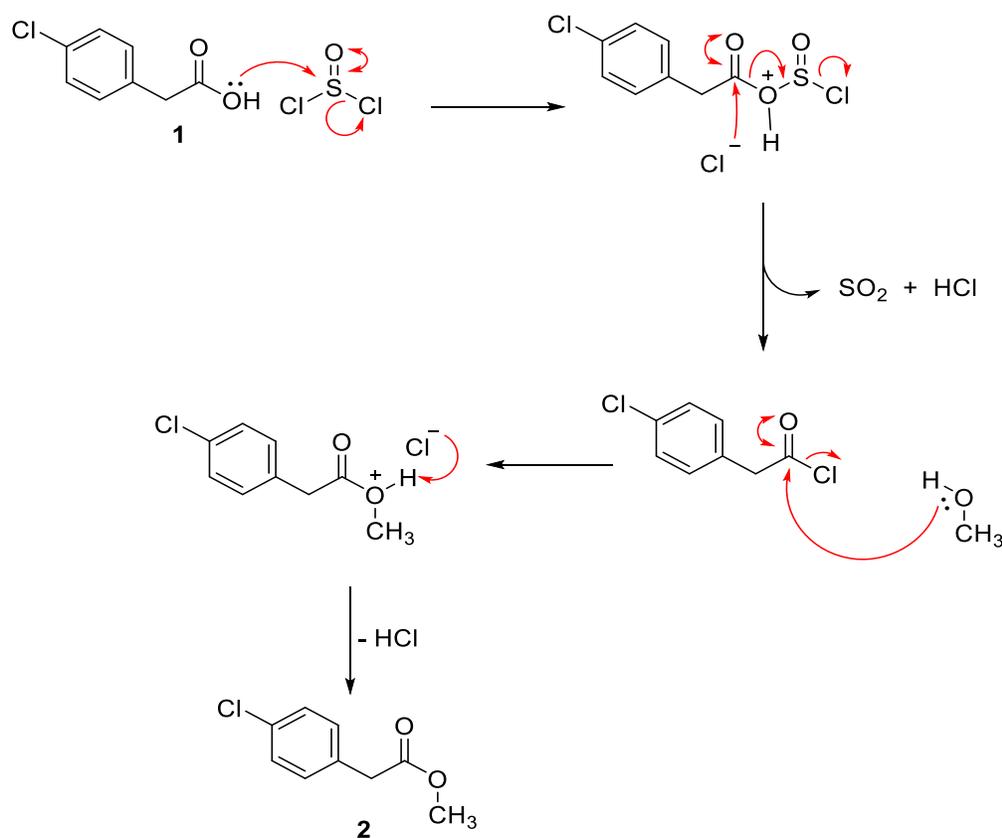
Scheme 2.1.1 Mechanism of formation of methyl 2-(4-chlorophenyl)acetate (**2**)

After aqueous work up ^{1}H NMR confirmed formation of the product with a characteristic C*H$_3$* singlet observed at δ 3.72. Methyl 2-(4-chlorophenyl) acetate (**2**) was obtained as a colourless liquid in a yield of 93 %.

Synthesis of (*R/S*)-methyl 2-(4-chlorophenyl)-3-hydroxypropanoate (3)

The synthesis of (*R/S*)-methyl 2-(4-chlorophenyl)-3-hydroxypropanoate (**3**) was carried out by the addition of paraformaldehyde in the presence of NaOMe and anhydrous DMSO as solvent at room temperature (rt) for 4 h.[83]

The mechanism of this reaction involves initial deprotonation of the acidic α-H by sodium methoxide. The resulting carbanion then attacks the electrophilic carbonyl carbon of formaldehyde, forming a new C-C bond.
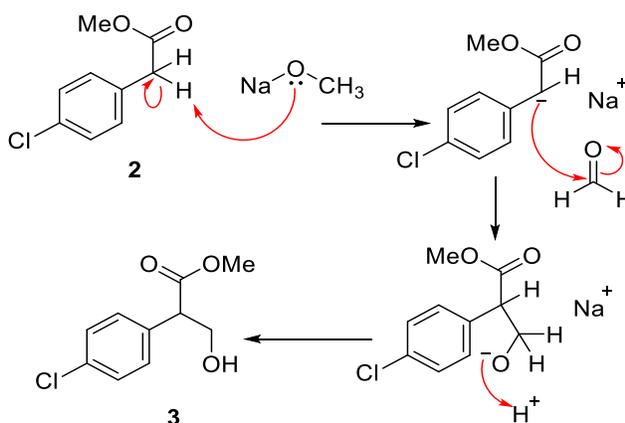
Scheme   2.1.2   Mechanism   of   formation   of   (R/S)-methyl   2-(4-chlorophenyl)-3-hydroxypropanoate (3)

After aqueous work up ^{1}H NMR confirmed formation of the product with characteristic aliphatic signals observed at δ 4.15-4.09 as a multiplet for C*H*CH$_2$OH, the CHC*H$_2$*OH was observed as a multiplet for each proton at δ 3.86-3.81 and a broad signal at δ 2.49 for O*H*. (*R/S*)-Methyl 2-(4-chlorophenyl)-3-hydroxypropanoate (**3**) was obtained as a colourless liquid after purification by gradient column chromatography in a yield of 72 %.

Synthesis of (*R/S*)-2-(4-chlorophenyl)-3-hydroxypropanoate (4b)

(*R/S*)-Methyl 2-(4-chlorophenyl)-3-hydroxypropanoate (**3**) was then converted to (*R/S*)-2-(4-chlorophenyl)-3-hydroxypropanoate (**4b**) by hydrolysis of the ester group of (*R/S*)-methyl 2-(4-chlorophenyl)-3-hydroxypropanoate (**3**) using lithium hydroxide monohydrate in tetrahydrofuran at rt for 1 h.[83] After acidification of the reaction with 2N HCl and work up ^{1}H

NMR established the formation of the product with characteristic signal of the carboxylic acid O*H* observed as a broad singlet at δ 12.42, and disappearance of the C*H₃* signal. (*R/S*)-2-(4-Chlorophenyl)-3-hydroxypropanoate (**4b**) was obtained as a white powder in a yield of 87 %.

Synthesis of (*R/S*)-*N*-(4-Arylbenzyl)-3-hydroxy-2-phenylpropanamide (6)

(*R/S*)-*N*-(4-Arylbenzyl)-3-hydroxy-2-phenylpropanamide (**6**) was prepared by stirring (*R/S*)-2-(4-chlorophenyl)-3-hydroxypropanoate/tropic acid (**4**) in dry cyclopentyl methyl ether (CPME) with molecular sieves, followed by the addition of amine (**5**) and trimethyl borate (B(OMe)₃). The resulting mixture was heated at 100 °C overnight (o/n).[84]

The reaction mechanism of this step is shown in scheme 2.1.3, which involves the addition of trimethyl borate to convert the hydroxyl group of the carboxylic acid into a good leaving group that can be displaced by the aliphatic amine to form the corresponding amide linkage.
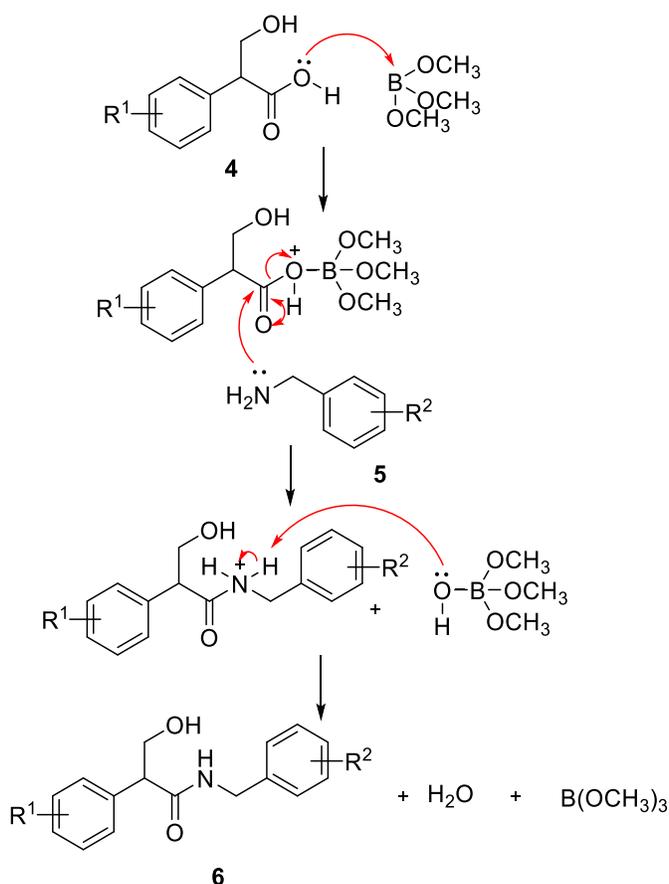
Scheme 2.1.3 Mechanism of formation of (*R/S*)-*N*-(4-arylbenzyl)-3-hydroxy-2-phenylpropanamide (**6**)

Upon completion, the reaction mixture was diluted with acetone and H_2O, and purified using a solid phase work up: stirring with Amberlite IRA743 (base resin to remove the borate), Amberlyst 15 (acid resin to take unreacted amine) and Amberlyst A26 (OH) (base resin to remove the unreacted acid from the media) resins for 2 h before drying ($MgSO_4$) and filtration. The filtrate was concentrated under pressure to give pure amine, which was characterised by the coupling pattern of the signals of NHC*HaHb* and C*H*C*HaHb* (Figure 31).
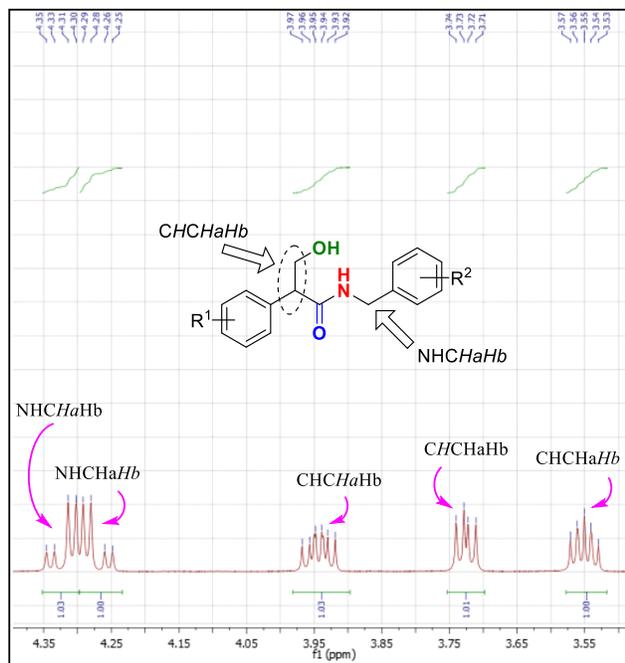
Figure 31. Characteristic ^{1}H NMR pattern of C*H*C*H2* and NHC*H2* signals of the alcohols (**6**)

Synthesis of (*R/S*)-3-[(4-arylbenzyl)amino]-3-oxo-2-phenylpropyl methanesulfonate (7)

The synthesis of (*R/S*)-3-[(4-arylbenzyl)amino]-3-oxo-2-phenylpropyl methanesulfonate (**7**) was achieved by mesylation of the alcohol (**6**) with methanesulfonyl chloride in the presence of Et_3N as base for 1 h at 0 °C then rt for 1-24 h.[85]

The product was obtained after purified by gradient column chromatography to give the product as a white solid that had characteristic shifting in the pattern of NHC*HaHb* and C*H*C*HaHb* signals (Figure 32) compared with the alcohol **6** (Figure 31). ^{13}C NMR confirmed the formation of the product by observing at δ ~71.13, ~50.89 and ~41.94 for C*H2*OMe, C*H*CH$_2$OMe and

NHCH_2 respectively, compared with alcohol (**6**) where the signals were observed at δ ~63.83, ~54.99 and ~42.46 for CH_2OH, CHCH_2OH and NHCH_2 respectively.
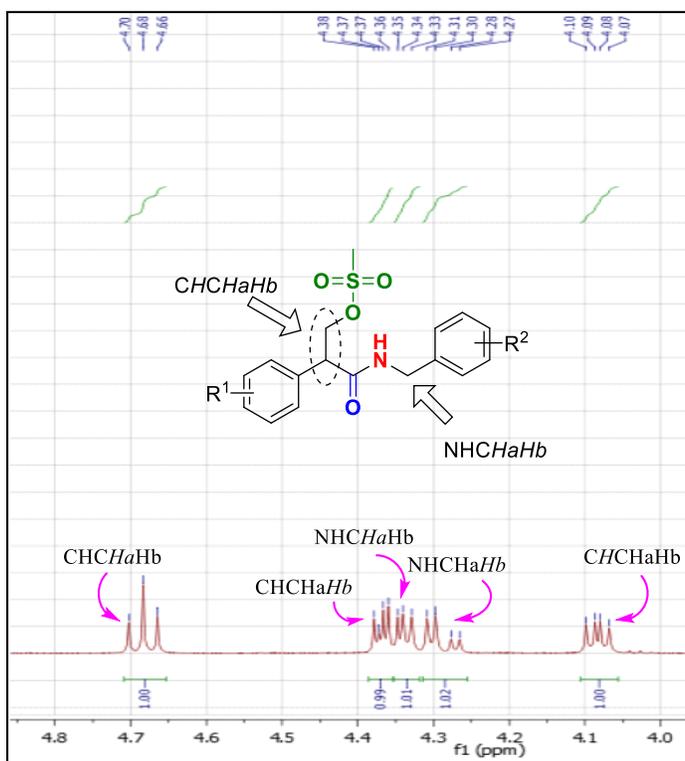
Figure 32. The ^{1}H NMR pattern of C*H*CH_2 and NHCH_2 in the mesylated compounds (**7**)

Synthesis of (*R/S*)-*N*-(4-arylbenzyl)-3(1*H*-imidazol-1-yl)-2-phenylpropanamide (8a-l)

(*R/S*)-*N*-(4-Arylbenzyl)-3(1*H*-imidazol-1-yl)-2-phenylpropanamide (**8**) was prepared by reaction of the mesylate (**7**) with the imidazolate anion (obtained by reaction of imidazole in dry acetonitrile and potassium carbonate 1 h at 45 °C), at 70 °C for 4 ¾ -24 h.[86]

After aqueous work up two new products were observed by TLC. The crude product was purified by gradient column chromatography petroleum ether–EtOAc 9:1 to petroleum ether–EtOAc 1:1 v/v to obtain the fast running spot, then the eluent was changed to CH$_2$Cl$_2$-MeOH 9:1 v/v to give the slower running spot.

The slower eluting spot was confirmed as the required product (**8**) by three broad singlets in the ^{1}H NMR characteristic of the imidazole ring. The fast running spot was confirmed by NMR to be an alkene by-product (elimination product) that could have resulted from the long duration

of the reaction. This was studied by decreasing the heating reaction time to less than 1-2 h but the alkene was still formed. Moreover, the percentage of the formation of the alkene seems to have some relevance to the substituent (R^2). For one derivative ($R^1 = H$, $R^2 = Cl$) the imidazole, triazole and tetrazole were attempted, with the triazole and tetrazole generated as described for imidazole.

Table 2 details the percentage of imidazole/ triazole/ tetrazole derivatives and the corresponding elimination products of the derivatives.
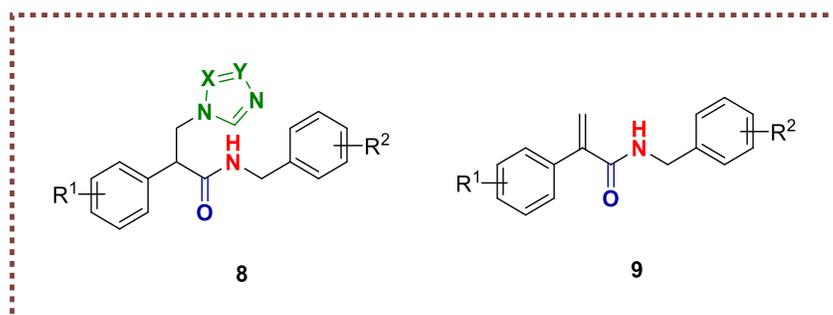
Table 2. The percentage of azole derivatives (**8a-l**) and the alkene derivatives (**9a-l**) and the ratio obtained

Compd	R^1	R^2	Azole product (%)	Compd	Alkene product (%)	Ratio 8:9
			Imidazole (X=Y=CH)			
8a	H	H	-	**9a**	62	0:1
8b	H	4-F	34	**9b**	39	1:1.14
8c	H	4-Cl	56	**9c**	-	1:0
8d	4-Cl	4-Cl	50*	**9d**	22	1:0.44
8e	H	2,4-di-Cl	74	**9e**	11	1:0.15
8f	4-Cl	2,4-di-Cl	41	**9f**	37	1:0.90
8g	H	4-CH$_3$	5	**9g**	59	1:11.48

8h	H	4-CF$_3$	4	9h	59	1:16
8i	H	4-OCH$_3$	27	9i	50	1:1.84
8j	H	3,4-di-OCH$_3$	51	9j	23	1:0.36
		Triazole (X=N,Y=CH)				
8k	H	4-Cl	77	9k	-	1:0
		Tetrazole (X=Y=N)				
8l	H	4-Cl	-	9l	23	0:1

* The compound was then recrystallised from CH$_3$CN to give 0.108g, 26%.

Electron-donating groups on the phenyl ring (R^2), such as methyl, were more likely to drive this reaction towards elimination even though the phenyl ring is far away from the site of the reaction and logically seems unlikely to affect the reaction so dramatically. Further experimentation must be done on the position of the substitution in the phenyl ring to rationalise this effect on the reaction.

Scheme 2.1.4 show the elimination mechanism of the mesyl group to form the elimination product, which is characterised by a singlet for each proton in C=C*HaHb* at δ 5.65 in the ^{1}H NMR and simplification of NHC*H$_2$* to give a doublet peak integrated for two protons.
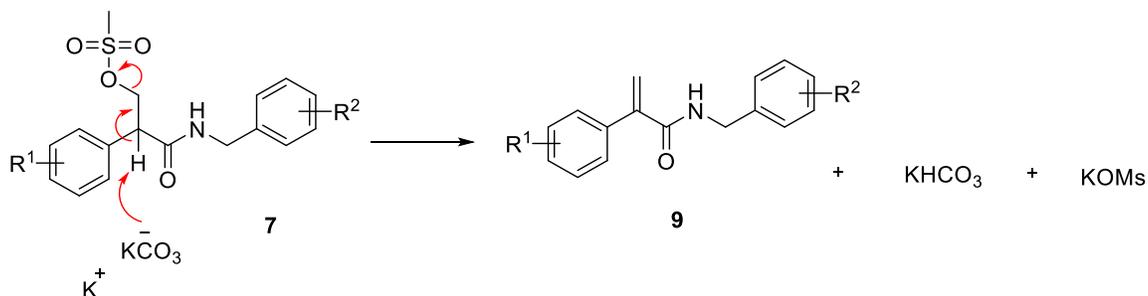
Scheme 2.1.4 Mechanism of formation of elimination products (**9**)

2.3.2 Preparation of extended derivatives by introduction of a sulfonamide linker

The extended derivatives were designed to be closer to posaconazole in length by extending the short series (**8**) with different substitutions to explore SAR. **18 (a-d)** were designed by using benzenesulfonamide derivatives to extend the length of the compound enabling it to occupy more space of the hydrophobic access channel of CaCYP51 (Figures 29 and 30).

Synthesis of (*R/S*)-2-phenyl-*N*-(4-(aryl-phenylsulfonamido)benzyl)-3-(1*H*-1,2,4-triazol-1-yl)propanamide (18a- d)

- **General chemistry**

The synthesis of (*R/S*)-2-phenyl-*N*-(4-(aryl-phenylsulfonamido)benzyl)-3-(1*H*-1,2,4-triazol-1-yl)propanamide (**18a- d**) was planned according to a sequence of seven steps (Scheme 2.2):

❖ Fmoc protection for the amino-group

❖ Amidation reaction to form the amide group

❖ Mesylation of the hydroxy group

❖ The addition of an azole ring

❖ Fmoc deprotection

❖ Generate the free amine

❖ Conversion of the amino-group to sulfonamide
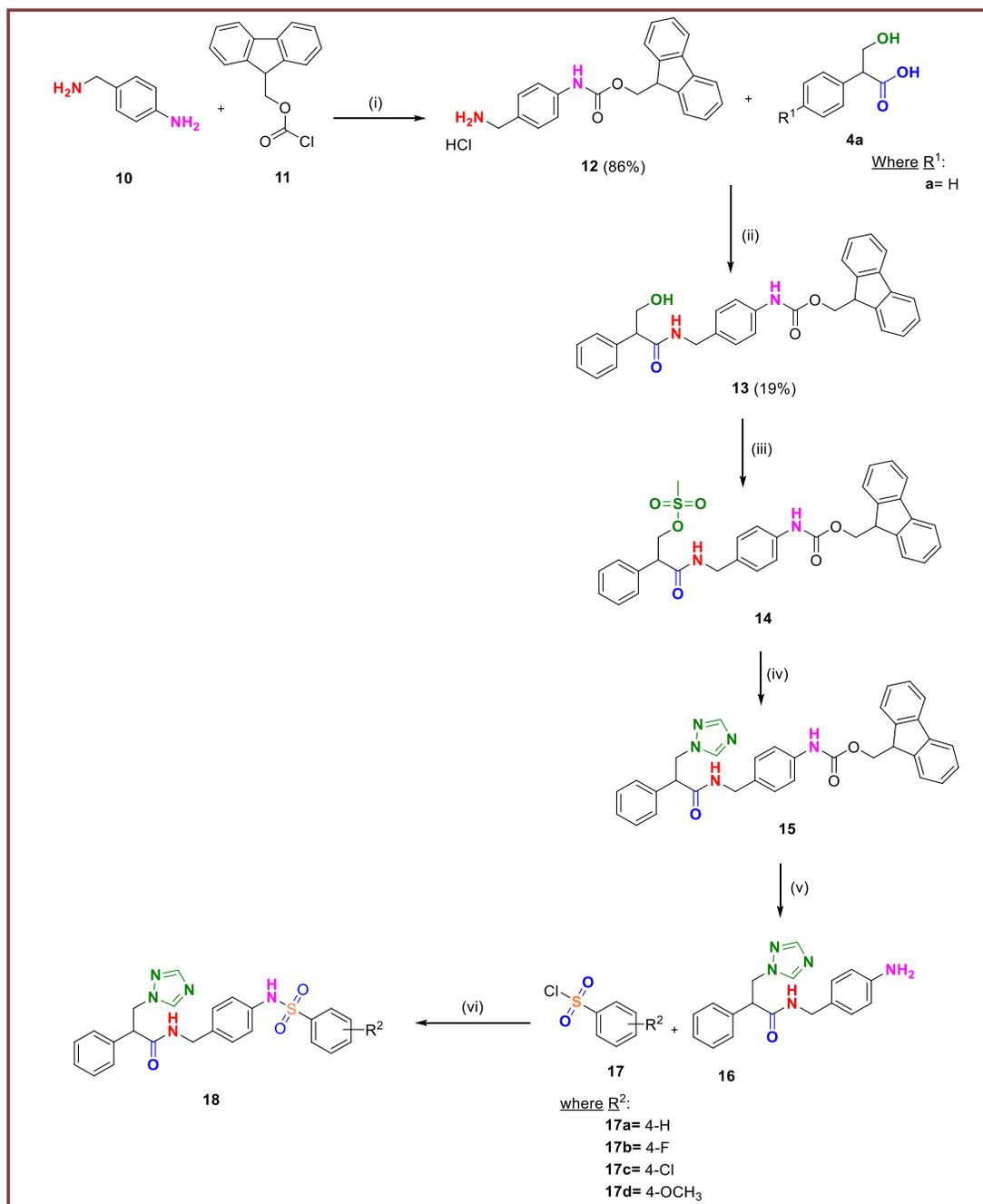
Scheme 2.2 Proposed synthetic route for (*R/S*)-2-phenyl-*N*-(4-(aryl-phenylsulfonamido)benzyl)-3-(1*H*-1,2,4-triazol-1-yl)propanamide (**18**). *Reagents and conditions:* (i) (a) 10% aq. AcOH, 1,4-dioxane, rt o/n (b) 2N aqueous HCl, pH 1, Et$_2$O (ii) (a) Tropic acid, HOBt, EtOAc, rt o/n (b) hexane, 0 °C o/n (iii) CH$_2$Cl$_2$, methanesulfonyl chloride, rt o/n (iv) (a) K$_2$CO$_3$, azole, CH$_3$CN, 45 °C 1 h (b) **14**, 70 °C, 24 h (v) piperidine, DMF, rt 2 h (iv) Et$_3$N, CH$_3$CN, benzenesulfonyl chloride derivatives, rt o/n

Method [I]

Synthesis of (9*H*-Fluoren-9-yl)methyl (4-(aminomethyl)phenyl)carbamate hydrochloride (12)

To a solution of 4-aminobenzylamine (**10**) in 10% aq. AcOH was added FmocCl (**11**) dissolved in 1,4-dioxane and the reaction stirred at rt o/n.[87]

The nonpolar impurities were extracted with Et_2O then the reaction mixture was acidified with 2N aq. HCl to pH 1. ^{1}H NMR confirmed formation of the product with characteristic aliphatic signals observed at δ 3.92 as a triplet for NH_2CH_2. ^{13}C NMR confirmed the amide group (*C*ONH), which was observed at δ ~153.88. (9*H*-Fluoren-9-yl)methyl(4-(aminomethyl)phenyl)carbamate hydrochloride (**12**) was obtained as a white solid in a yield of 86 %.

Synthesis of (*R/S*)-(9*H*-fluoren-9-yl)methyl(4-((3-hydroxy-2-phenylpropanamido)methyl) phenyl)carbamate (13)

The amide (**13**) was prepared by reaction of tropic acid (**4a**) with hydroxybenzotriazole (HOBt)/ DCC in EtOAc at 0 °C for 30 minute to which a mixture of 9*H*-fluoren-9-yl)methyl (4-(aminomethyl)phenyl)carbamate hydrochloride (**12**) in EtOAc and Et_3N (previously stirred at rt for 30 min to produce the free amine) was added and the reaction stirred at rt o/n. Hexane was then added to the mixture precipitate DCU and the reaction left after shaking in a freezer overnight.[88]

After removing DCU and aqueous work up, ^{1}H NMR showed triplet signals at δ 8.47 for N*H*CH$_2$ and the complicated pattern, previously shown in the short series, as doublet of doublet for each proton of NHC*H₂* at δ 4.23-4.16 and a triplet at δ 3.92 for NH_2CH_2. A white solid with a yield of 19 % was obtained.

The low yield obtained may be owing to the base lability of Fmoc in the conditions used to generate the free amine of **12**. A different amine protecting group, namely acid labile Boc, was used instead (scheme 2.3).
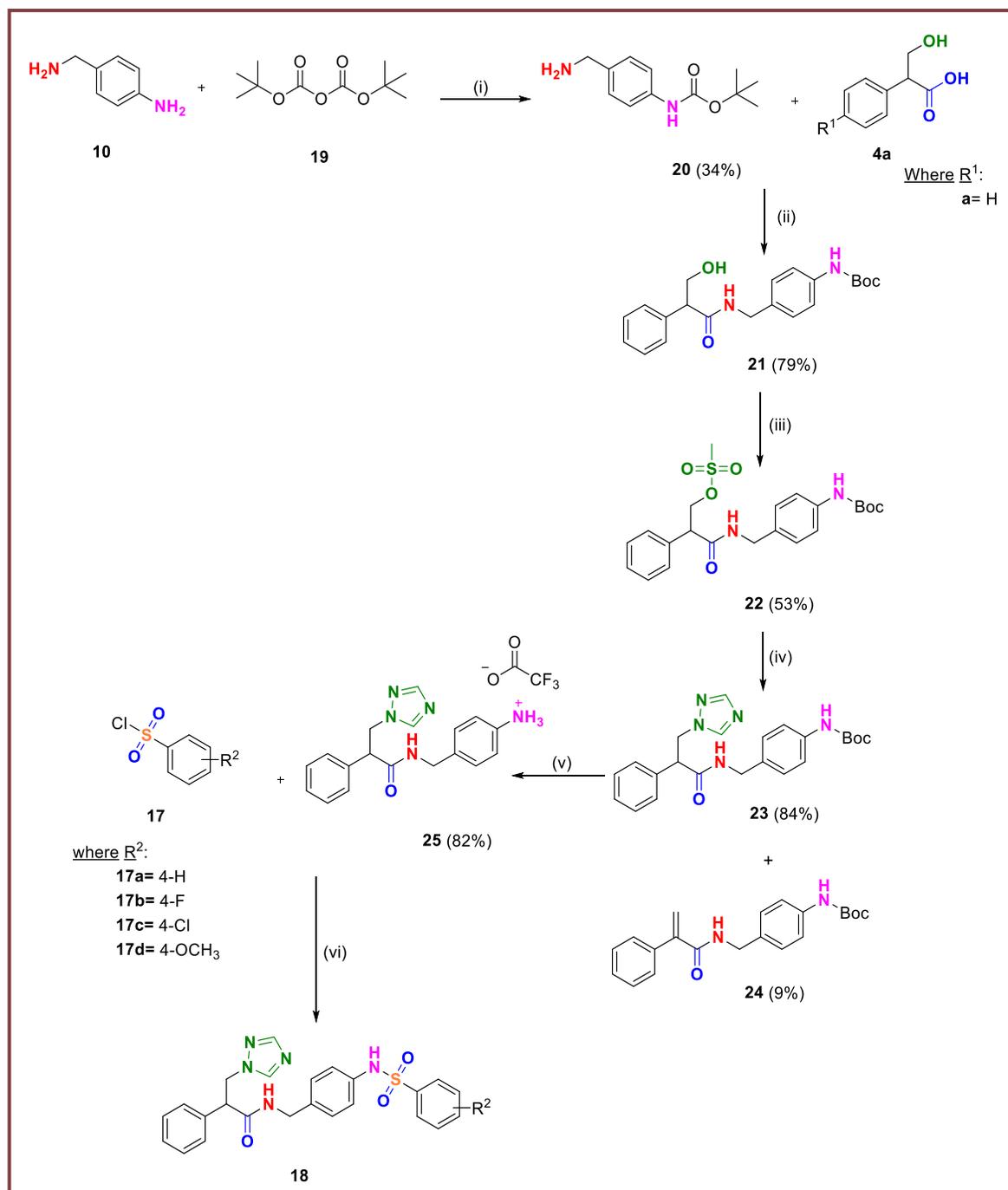
Scheme 2.3 Synthetic route for (*R/S*)-2-phenyl-*N*-(4-(phenylsulfonamido)benzyl)-3-(1*H*-1,2,4-triazol-1-yl)propanamide (**18**). *Reagents and conditions:* (i) (a) 10% aq. AcOH, 1,4-dioxane, rt o/n (b) 2N aqueous NaOH, pH 14, Et$_2$O (ii) CPME, tropic acid (**4a**), B(OCH$_3$)$_3$, molecular sieves, 100 °C o/n (iii) CH$_2$Cl$_2$, methanesulfonyl chloride, rt o/n (iv) (a) K$_2$CO$_3$, azole, CH$_3$CN, 45 °C 1 h (b) **22**, 70 °C 1 h, rt o/n (v) CH$_2$Cl$_2$, TFA, rt 1.5 h (iv) Et$_3$N, CH$_3$CN, benzenesulfonyl chloride derivatives (**17**), rt o/n

In the pathway illustrated in Scheme 2.3, the Boc protected 4-aminobenzylamine was coupled with tropic acid and then the mesylation reaction, and introduction of the azole ring completed. After removal of Boc group to give the free amine, extension of the structure by reaction of the free amine with different benzenesulfonamide derivatives would provide a more convergent and efficient preparation of a small series for biological evaluation.

Method [II]

Synthesis of *tert*-butyl(4-(aminomethyl)phenyl)carbamate (20)

tert-Butyl-(4-(aminomethyl)phenyl)carbamate (**20**) was obtained by dissolving 4-aminobenzylamine (**10**) in 10% aqueous AcOH, and addition of di-*tert*-butylcarbonate (**19**) in 1,4-dioxane followed by stirring at rt for 1 h 20 min.[87]

After work up ^{1}H NMR confirmed formation of the product with a characteristic NH_2 singlet observed at δ 3.72 and ^{13}C NMR confirmed the amide group (*C*ONH), which was observed at δ ~152.86. *tert*-butyl(4-(aminomethyl)phenyl)carbamate (**20**) was obtained as an off-white solid in a yield of 34 % (lit. yield 57 %)[87].

Synthesis of (*R/S*)-*tert*-butyl(4-((3-hydroxy-2-phenylpropanamido)methyl)phenyl) carbamate (21)

tert-Butyl(4-(aminomethyl)phenyl)carbamate (**20**) was then converted to (*R/S*)-*tert*-butyl(4-((3-hydroxy-2-phenylpropanamido)methyl)phenyl)carbamate (**21**) in the presence of tropic acid (**4a**) in CPME and molecular sieves followed by B(OMe)$_3$ and the resulting mixture was heated at 100 °C o/n.[84]

After aqueous work up ^{1}H NMR confirmed formation of the product with characteristic aliphatic signals observed for C*H*C*H$_2$*OH as well as the 9H of the Boc group at δ 1.46. (*R/S*)-*tert*-Butyl(4-((3-hydroxy-2-phenylpropanamido)methyl)phenyl)carbamate (**21**) was obtained as a yellow-orange powder after Et$_2$O wash in a yield of 79 %.

Synthesis of (*R/S*)-3-((4-((*tert*-butoxycarbonyl)amino)benzyl)amino)-3-oxo-2-phenylpropyl methanesulfonate (22)

The synthesis of (*R/S*)-3-((4-((*tert*-butoxycarbonyl)amino)benzyl)amino)-3-oxo-2-phenylpropyl methanesulfonate (**22**) was performed as previously described and obtained as a white solid in a yield 53 %.

Synthesis of (*R/S*)-*tert*-butyl(4-((2-phenyl-3-(1*H*-1,2,4-triazol-1-yl)propanamido)methyl)phenyl)carbamate (23)

(*R/S*)-*tert*-Butyl(4-((2-phenyl-3-(1*H*-1,2,4-triazol-1-yl)propanamido)methyl)phenyl)carbamate (**23**) was obtained as previously described with the alkene by-product (**25**), then the azole product (**24**) obtained after purification by gradient column chromatography. The triazole (**24**) had the two broad singlet signals characteristic of the triazole ring in the ¹H NMR.

Synthesis of (*R/S*)-4-((2-phenyl-3-(1*H*-1,2,4-triazol-1-yl)propanamide)methyl)benzenaminium trifluoroacetic acid salt (25)

(*R/S*)-*tert*-Butyl(4-((2-phenyl-3-(1*H*-1,2,4-triazol-1-yl)propanamido)methyl)phenyl)carbamate (**23**) was then converted to (*R/S*)-4-((2-phenyl-3-(1*H*-1,2,4-triazol-1-yl)propanamide)methyl)benzenaminium trifluoroacetic acid salt (**25**) in 82 % yield by using TFA in CH₂Cl₂ at rt o/n.[89] ¹H NMR established the formation of the product with the disappearance of the signal of (CH₃)₃ of the Boc moiety.

Synthesis of (*R/S*)-2-phenyl-*N*-(4-(phenylsulfonamido)benzyl)-3-(1*H*-1,2,4-triazol-1-yl)propanamide (18a)

The synthesis of (*R/S*)-2-phenyl-*N*-(4-(phenylsulfonamido)benzyl)-3-(1*H*-1,2,4-triazol-1-yl)propanamide (**18a**) was carried out by addition of Et₃N to a solution of triflate salt (**25**) in dry CH₃CN followed by the addition of benzenesulfonyl chloride (**17a**). The reaction was stirred at rt o/n.[90]

After aqueous work up, the crude product was purified by gradient column chromatography and ¹H NMR confirmed formation of the product however traces of unknown mixture were still present that could not be removed after additional washes with aqueous HCl. A second attempt to prepare **18a** using pyridine as a solvent and stronger base instead of Et₃N in the reaction at rt o/n was performed, however attempts to purify the crude product by gradient column chromatography were unsuccessful with a complex ¹H NMR spectrum observed.

This was not an optimal method in terms of purity and yield, so preparation of (*R/S*)-2-phenyl-*N*-(4-(aryl-phenylsulfonamido)benzyl)-3-(1*H*-1,2,4-triazol-1-yl)propanamide   (**18a-d**)   was attempted by protecting the other amine group of 4-aminobenzylamine (**10**) and addition of the sulfonyl linker prior to amide coupling with tropic acid (**4a**). This rearrangement in the synthetic scheme, which would hopefully overcome the low yield and the purity of the products, is shown in scheme 2.4.
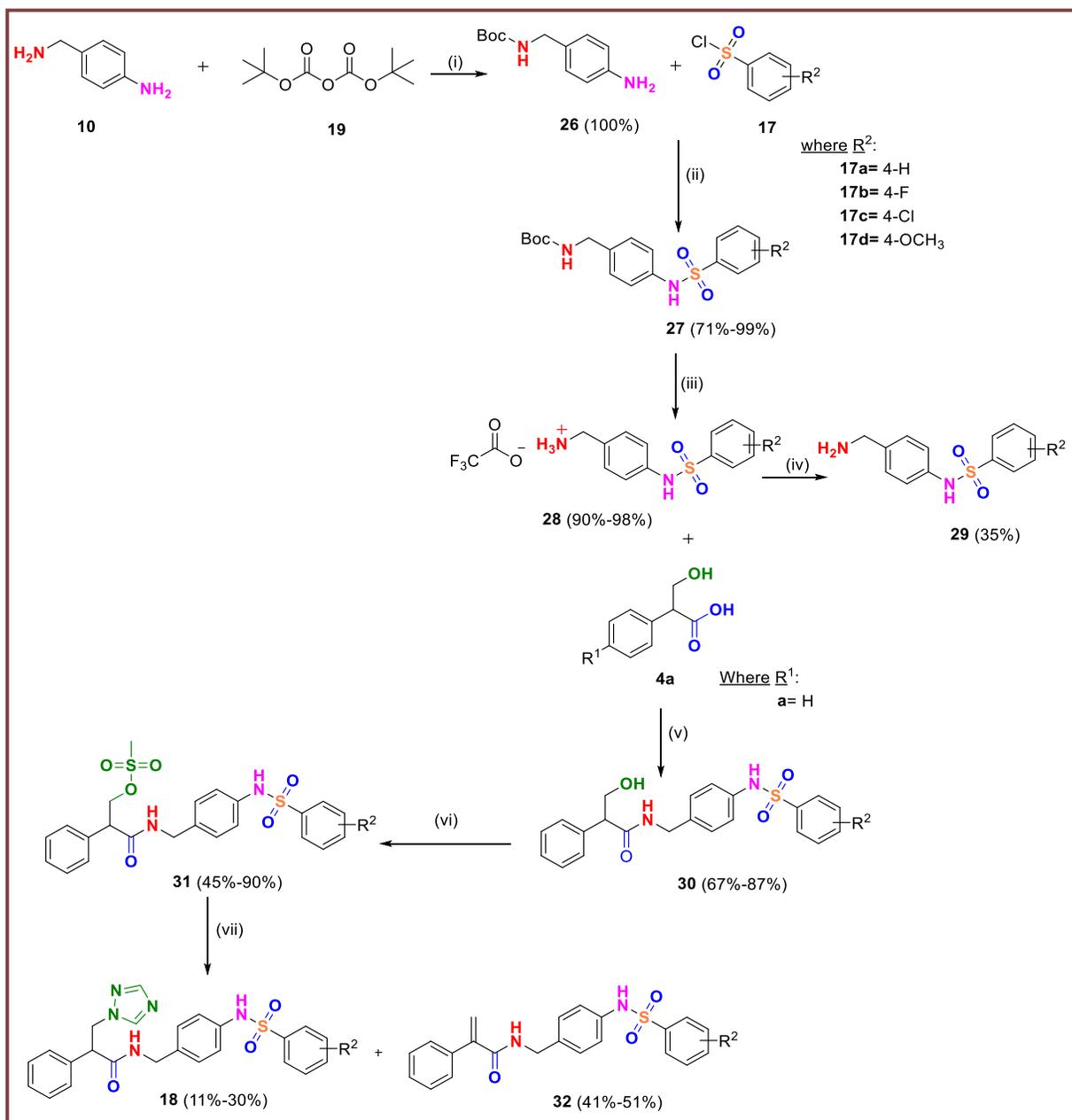
Scheme 2.4   Alternative synthetic route for (*R/S*)-2-phenyl-*N*-(4-(aryl-phenylsulfonamido)benzyl)-3-(1*H*-1,2,4-triazol-1-yl)propanamide (**18**). *Reagents and conditions:* (i) THF/ rt, 1 h 20 min (ii) pyridine, rt 2 h (iii) CH$_2$Cl$_2$, TFA, rt 1.5 h (iv) 2M aq. NaOH (v) CPME, tropic acid (**4a**), B(OCH$_3$)$_3$, molecular sieves, 100 °C o/n (vi) CH$_2$Cl$_2$, methanesulfonyl chloride, rt o/n (vii) (a) K$_2$CO$_3$, imidazole, CH$_3$CN, 45 °C 1 h (b) **31**, 70 °C 1 h, rt o/n

Method [III]

Synthesis of *tert*-butyl(4-aminobenzyl)carbamate (26)

tert-Butyl-(4-aminobenzyl)carbamate (**26**) was obtained on reaction of 4-aminobenzylamine (**10**) and di-*tert*-butylcarbonate (**19**) in THF at rt for 1 h 20 min.[90] The aliphatic amine was selectively Boc protected and the product obtained in quantitative yield. ^{1}H NMR confirmed formation of the product with a characteristic $(CH_3)_3$ singlet signal observed at δ 1.48 for the Boc group that integrated for 9 protons.

Synthesis of *tert*-butyl-(4-(aryl-phenylsulfonamido)benzyl)carbamate derivatives (27a-d)

The synthesis of *tert*-butyl-(4-(aryl-phenylsulfonamido)benzyl)carbamate derivatives (**27**) were carried out reaction of *tert*-butyl(4-aminobenzyl)carbamate (**26**) with benzenesulfonyl chloride derivatives (**17a-d**) in pyridine at rt for 2 h.[90] After work up and Et_2O trituration, ^{1}H NMR confirmed formation of the product with a characteristic N*H* singlet observed at δ 10.2. *tert*-Butyl-(4-(aryl-phenylsulfonamido)benzyl)carbamates (**27a-d**) were obtained with good yields as shown in Table 3.

Table 3. Percentage yield, melting points and physical properties of *tert*-butyl-(4-(aryl-phenylsulfonamido)benzyl)carbamates (**27a- d**)

Compd	Chemical structure	Yield (%)	Physical properties	M.p. (°C)
27a		92	White solid	160-162
27b		87	Light orange solid	174-176
27c		71	Orange solid	136-138
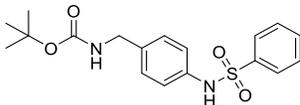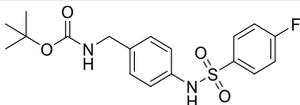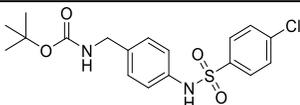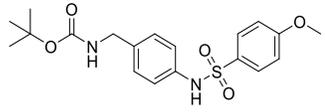
27d		99	Orange semi-solid	-

Synthesis of (4-(phenylsulfonamido)phenyl)methanaminium trifluoroacetic acid salt (28a-d)

Removal of the Boc group of *tert*-butyl-(4-(aryl-phenylsulfonamido)benzyl)carbamates (**27a-d**) with TFA in CH_2Cl_2 for 1.5 h at 0 °C, gave (4-(aryl-phenylsulfonamido)phenyl)methanaminium trifluoroacetic acid salts (**28a-d**)[90] in 90-98 % yield.

The deprotection of the Boc group uses TFA which protonates the oxygen atom of the *tert*-butyl carbamate resulting in dissociation of the *tert*-butyl cation, leaving carbamic acid. After that, decarboxylation of carbamic acid results free amine which finally protonated by TFA as shown in scheme 2.4.1.
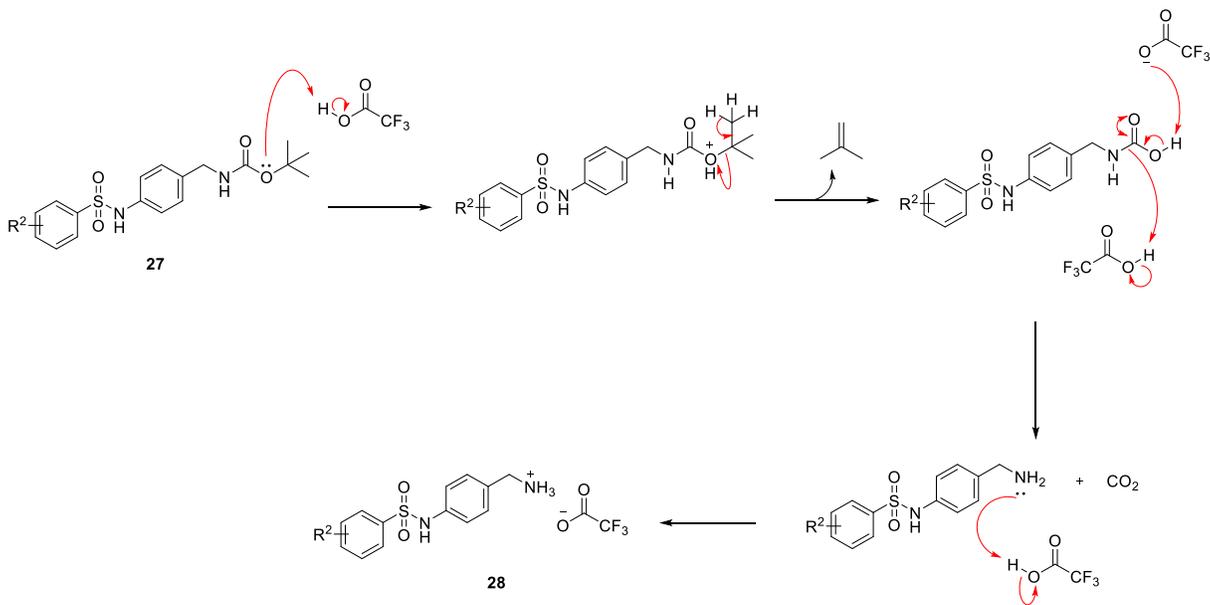
Scheme 2.4.1 Mechanism of Boc deprotection

^{1}H NMR established the formation of the product with the disappearance of the signal of $(CH_3)_3$ of the Boc moiety.

N-(4-(Aminomethyl)phenyl)benzenesulfonamide (**29a**) was obtained by dissolving (4-(phenylsulfonamido)phenyl)methanaminium trifluoroacetic acid salt (**28a**) in 2M aq. NaOH.[91] After aqueous work up, ^{1}H NMR showed a broad signal that confirmed formation of the free amine in a yield 35%.

To convert compound (**29a**) to the final compound 2-phenyl-*N*-(4-(phenylsulfonamido)benzyl)-3-(1*H*-1,2,4-triazol-1-yl)propanamide (**18a**), three more steps remained (amidation, mesylation and nucleophilic substitution to produce the azole compound), however the low yield obtained for the free amine was not optimal.

Rather than isolating the free amine, which was low yielding, the free amine could be generated *in situ* using a strong base.

Synthesis of (*R/S*)-3-hydroxy-2-phenyl-*N*-(4-(aryl-phenylsulfonamido)benzyl) propanamide derivatives (30a-d)

The synthesis of (*R/S*)-3-hydroxy-2-phenyl-*N*-(4-(phenylsulfonamido)benzyl) propanamide (**30a**) was carried out by stirring (4-(phenylsulfonamido)phenyl)methanaminium trifluoroacetic acid salt (**28a**) in CPME and Et$_3$N to produce the free amine followed by the addition of tropic acid (**4a**), B(OCH$_3$)$_3$ and molecular sieves. The resulting mixture was heated at 100 °C overnight[84] (mechanism of action in scheme 2.1.1).

After aqueous work up ^{1}H NMR confirmed formation of the product with characteristic aliphatic signals observed for C*H*C*H*$_2$OH as described previously. (*R/S*)-3-Hydroxy-2-phenyl-*N*-(4-(phenylsulfonamido)benzyl)propanamide (**30a**) was obtained as a pale yellow gum after purification by gradient column chromatography in a yield of 30 %.

Owing to the low yield of the amidation reaction a different coupling reagent (HOBt/ DCC) used previously to prepare (**13**) was tried to determine if the yield could be improved.

Tropic acid (**4a**) was reacted with hydroxybenzotriazole (HOBt) and DCC at 0 °C for 30 minute before addition of a mixture of (4-(arylphenylsulfonamido)phenyl)methanaminium trifluoroacetic acid salt (**28a-d**) in EtOAc and Et$_3$N, previously stirred at rt for 30 min to produce

the free amine. The reaction mixture was stirred at rt overnight before addition of hexane and the mixture left to stand in the freezer overnight to precipitate DCU.[88]

After removing DCU and aqueous work up, ^{1}H NMR showed the triplet signals at δ 8.43 for N*H*CH$_2$ and the doublet of doublet for each proton of NHC*H$_2$* at δ 4.20-4.10. (*R/S*)-3-Hydroxy-2-phenyl-*N*-(4-(aryl-phenylsulfonamido)benzyl)propanamides (**30a-d**) were obtained in good yields (Table 4).

Table 4. The percentage yield, melting points and the physical properties of (*R/S*)-3-hydroxy-2-phenyl-*N*-(4-(aryl-phenylsulfonamido)benzyl)propanamide derivatives (**30a-d**)

Compd	Yield (%)		M.p. (°C)	Physical properties
	Method I	**Method II**		
30a	30	68	58- 60	White solid
30b	-	67	62- 64	White solid
30c	-	84	150- 152	White solid
30d	-	87	126- 128	Off-white solid

Synthesis of (*R/S*)-3-oxo-2-phenyl-3-((4-(phenylsulfonamido)benzyl)amino)propylmethane sulfonate (31a-d)

The synthesis of (*R/S*)-3-oxo-2-phenyl-3-((4-(aryl-phenylsulfonamido)benzyl)amino)propyl methane sulfonate (**31a-d**) was carried out as previously described by reaction of (*R/S*)-3-hydroxy-2-phenyl-*N*-(4-(aryl-phenylsulfonamido)benzyl)propanamide (**30a-d**) with Et$_3$N and methanesulfonyl chloride.[85]

After work up, the crude product was purified by gradient column chromatography eluting with petroleum ether – EtOAc 4:6 v/v to give the products as white solids with characteristic ^{1}H NMR pattern of NHC*HaHb* and C*H*C*HaHb* signals and characteristic ^{13}C NMR signals (Table 5).

Table 5. The NMR pattern of NHC*HaHb* and C*HCHaHb* of (*R/S*)-3-oxo-2-phenyl-3-((4-(phenylsulfonamido)benzyl)amino)propylmethane sulfonates (**31a-d**)

Compd	¹H NMR	¹³C NMR
31a	4.74 (t, *J* = 9.6 Hz, 1H, CHC*Ha*Hb), 4.38 (ddd, *J* = 5.9, 11.9, 16.5 Hz, 2H, NHC*Ha*Hb + CHCHa*Hb*), 4.28 (dd, *J* = 5.7, 15.8 Hz, 1H, NHCHa*Hb*), 4.04 (dd, *J* = 5.9, 8.4 Hz, 1H, C*H*CHaHb).	71.09 (CHC*H₂*OMs), 50.85 (*C*HCH₂OMs), 42.08 (NH*CH₂*).
31b	4.73 (t, *J* = 9.6 Hz, 1H, CHC*Ha*Hb), 4.38 (d dd, *J* = 6.2; 5.6, 9.4 Hz, 2H, NHC*Ha*Hb + CHCHa*Hb*), 4.28 (dd, *J* = 5.7, 15.9 Hz, 1H, NHCHa*Hb*), 4.04 (dd, *J* = 5.3, 9.4 Hz, 1H, C*H*CHaHb).	71.10 (CHC*H₂*OMs), 50.86 (*C*HCH₂OMs), 42.08 (NH*CH₂*).
31c	4.74 (t, *J* = 9.1 Hz, 1H, CHC*Ha*Hb), 4.38 (m, 2H, NHC*Ha*Hb + CHCHa*Hb*), 4.29 (dd, *J* = 5.7, 15.8 Hz, 1H, NHCHa*Hb*), 4.05 (m, 1H, C*H*CHaHb).	71.10 (CHC*H₂*OMs), 50.85 (*C*HCH₂OMs), 42.08 (NH*CH₂*).
31d	4.73 (t, *J* = 9.6 Hz, 1H, CHC*Ha*Hb), 4.37 (ddd, *J* = 4.2, 9.8, 13.8 Hz, 2H, NHC*Ha*Hb + CHCHa*Hb*), 4.28 (dd, *J* = 5.7, 15.8 Hz, 1H, NHCHa*Hb*), 4.03 (d, *J* = 7.2 Hz, 1H, C*H*CHaHb).	71.10 (CHC*H₂*OMs), 50.85 (*C*HCH₂OMs), 42.01 (NH*CH₂*).

Synthesis of (*R/S*)-*N*-(4-((3-arylphenyl)sulfonamido)benzyl)-2-phenyl-3-(1*H*-1,2,4-triazol-1-yl) propanamide (18a-d)

(*R/S*)-*N*-(4-((3-arylphenyl)sulfonamido)benzyl)-2-phenyl-3-(1*H*-1,2,4-triazol-1-yl)propanamides (**18a-d**) were obtained as previously described by reaction of triazole anion with mesylated compounds (*R/S*)- (3-oxo-2-phenyl-3-((4-(aryl-phenylsulfonamido)benzyl)amino)propylmethane sulfonate (**31a-d**) at 70 °C[86] for 1 h then rt, o/n.

After aqueous work up the crude product was purified by gradient column chromatography to obtain the alkene by-product (**32**) and the slower eluting triazole product (**18**).

Table 6. The percentage of azole derivatives (**18a-d**) and the alkene derivatives (**32a-d**) and the ratio of azoles to alkenes

Compd	R^2	Azole product (%)	Compd	Alkene product (%)	Ratio 18:32
18a	4-H	19	**32a**	51	1:2.68
18b	4-F	30	**32b**	41	1:1.37
18c	4-Cl	11	**32c**	50	1:4.55
18d	4-OCH$_3$	17	**32d**	44	1:2.59

In this series the is no different between electron-donating and electron-withdrawing substitution on the phenyl ring (R^2) and percentage of azole/ elimination products, with the elimination product the major compound obtained.

Further optimisation must be done on this step; one option explores other leaving groups, for example chloride, rather than mesyl, to try and reduce the acidity of the α-proton which would favour nucleophilic substitution.

An alternative route was to synthesise a series that lacks an acidic α-proton, which would avoid alkene formation.

The route was designed by reversing the amide group and shortening by one carbon to synthesise (*R/S*)-4-aryl-*N*-(2-(1*H*-triazol-1-yl)-1-arylphenylethyl)benzamide derivatives (**37**) via three synthetic steps started by the formation of amide bond, mesylation of the hydroxyl group and addition of a triazole ring (Scheme 2.5).
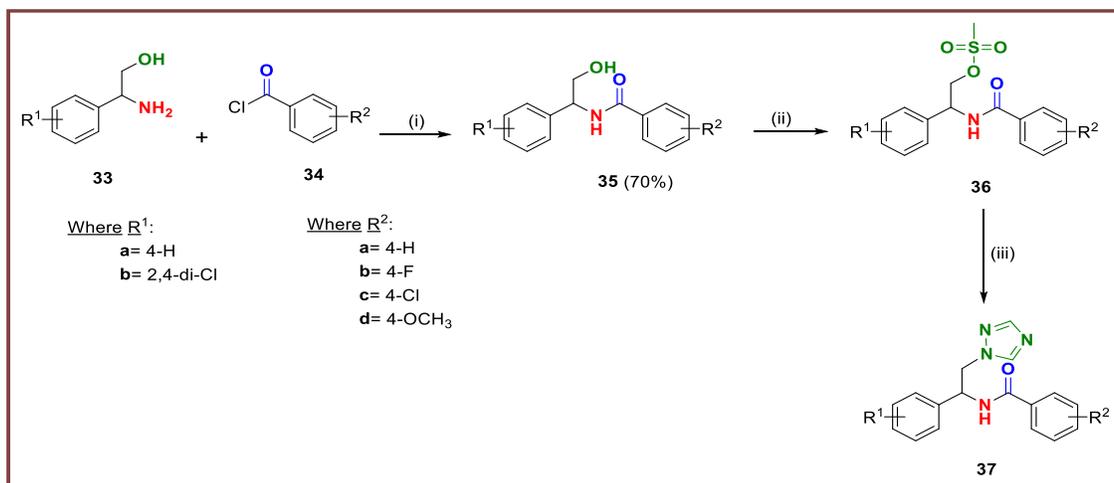
Scheme 2.5 Synthetic route for (*R/S*)-4-aryl-*N*-(2-(1*H*-triazol-1-yl)-1-aryl-phenylethyl)benzamide (**37**). *Reagents and conditions:* (i) (a) Et₃N, CH₂Cl₂, 0 °C 5 min then rt 1 h (ii) methanesulfonyl chloride, CH₂Cl₂, Et₃N, rt o/n (iii) (a) K₂CO₃, triazole, CH₃CN, 45 °C 1 h (b) **36**, 70 °C, 24 h

To investigate and optimise this synthetic pathway, (*R/S*)-*N*-(2-(1*H*-triazol-1-yl)-1-phenylethyl)benzamide (**37a**) was synthesised first.

Synthesis of (*R/S*)-*N*-(2-hydroxy-1-phenylethyl)benzamide (35)

(*R/S*)-*N*-(2-hydroxy-1-phenylethyl)benzamide (**35**) was prepared by reaction of (*R/S*)-2-amino-2-phenylethan-1-ol (**33**) with benzoyl chloride (**34a**) in the present of Et₃N at rt for 1 h.[92]

After aqueous work up ¹H NMR confirmed formation of the product and amide bond formation with characteristic aromatic signals observed at δ 7.23-7.93 and the N*H* as a doublet at δ 8.71. (*R/S*)-*N*-(2-Hydroxy-1-phenylethyl) benzamide (**35**) was obtained as a white solid in a yield of 70 %.

Synthesis of (*R/S*)-2-benzamido-2-phenylethyl methanesulfonate (36)

(*R/S*)-*N*-(2-Hydroxy-1-phenylethyl) benzamide (**35**) was then converted to (*R/S*)-2-benzamido-2-phenylethyl methanesulfonate (**36**) by reaction of (*R/S*)-*N*-(2-hydroxy-1-phenylethyl) benzamide (**35**) with methanesulfonyl chloride in CH₂Cl₂ and Et₃N or pyridine at rt o/n.

After aqueous work up and purification by gradient column chromatography ^{1}H NMR did not confirm the compound.

Alternatively the preparation of (*R/S*)-*N*-(2-chloro-1-phenylethyl)benzamide (**38**) was attempted by chlorination of the hydroxyl group of (*R/S*)-*N*-(2-hydroxy-1-phenylethyl)benzamide (**35**) using SOCl$_2$ in CH$_2$Cl$_2$ at rt for 4 h.[93] After quenching the reaction with NaHCO$_3$ and subsequent work up, ^{1}H NMR confirmed the product in quantitative yield, however it was used without further purification owing to instability.
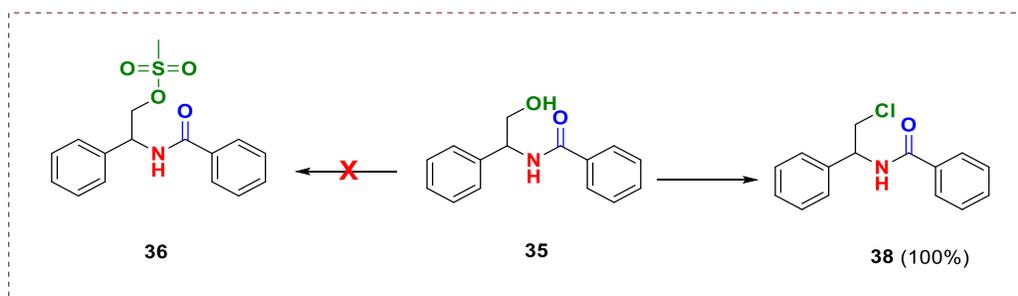
Figure 33. Conversion of the hydroxy group of (*R/S*)-*N*-(2-hydroxy-1-phenylethyl)benzamide (**35**) to a good leaving group

Synthesis of (*R/S*)-*N*-(2-(1*H*-triazol-1-yl)-1-phenylethyl)benzamide (37a)

To obtain the final product (*R/S*)-*N*-(2-(1*H*-triazol-1-yl)-1-phenylethyl)benzamide (**37a**), triazole was reacted with (*R/S*)-*N*-(2-chloro-1-phenylethyl)benzamide (**38**) in the presence of K$_2$CO$_3$ in dry CH$_3$CN at 70 °C for 24 h.[86] However, the final step produced preferentially a cyclised (*R/S*)-4,5-dihydrooxazole [2,4-diphenyl-4,5-dihydrooxazole][92] (**39**) rather than the desired azole.
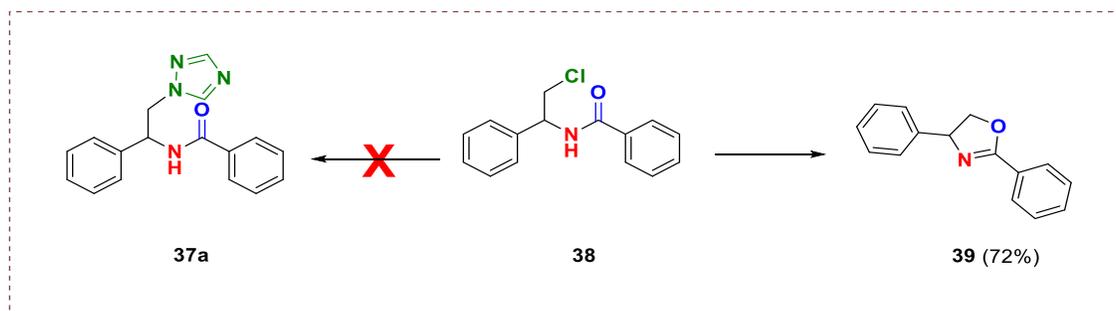
Figure 34. Formation of 2,4-diphenyl-4,5-dihydrooxazole (**39**) instead of azole product (**37a**)

On studying the ^{1}H NMR of the product of the mesylation reaction (**36**) it was determined that this was the (*R/S*)-2,4-diphenyl-4,5-dihydrooxazole (**39**) with the characteristic pattern shown in figure 35 and the proposed cyclisation mechanism in scheme 2.5.1.
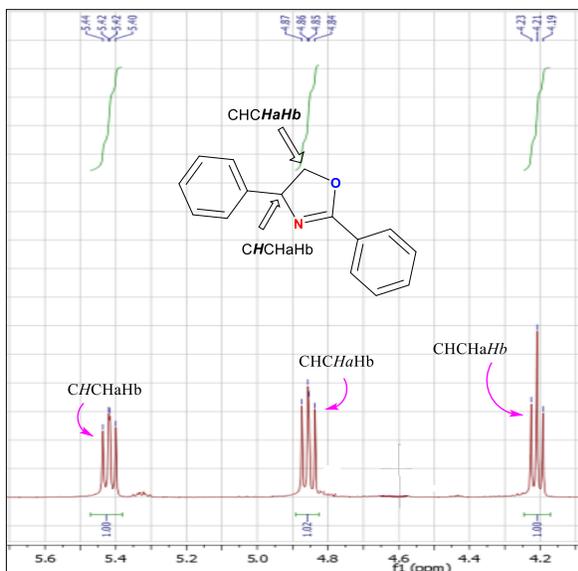
Figure 35. The ^{1}H NMR pattern of C*H*C*HaHb* in 2,4-diphenyl-4,5-dihydrooxazole (**39**)
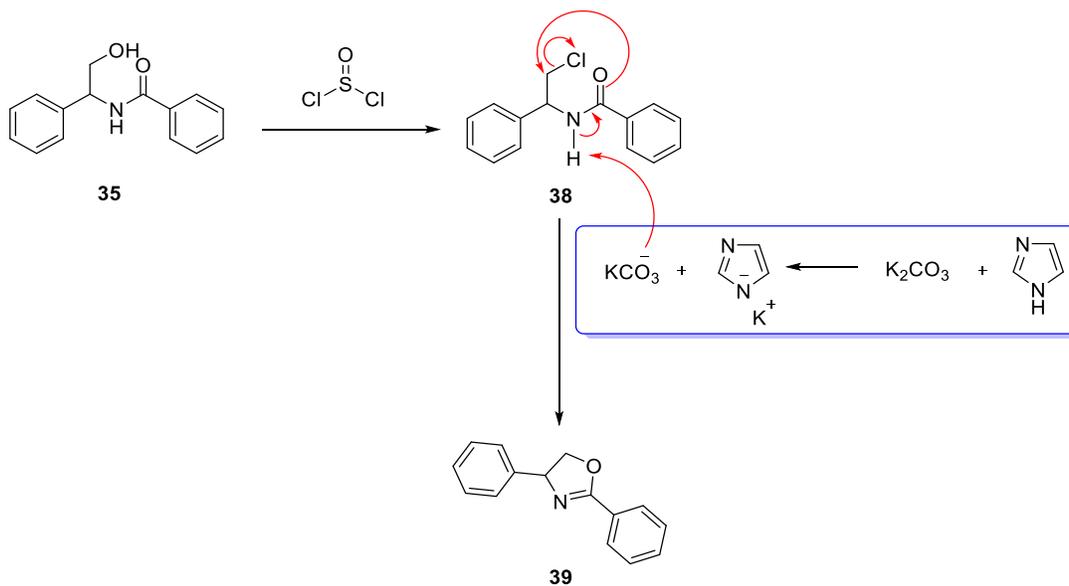
Scheme 2.5.1 Proposed reaction mechanism of cyclisation forming (*R/S*)-2,4-diphenyl-4,5-dihydrooxazole (**39**)

This step was prepared again by reacting (*R/S*)-*N*-(2-hydroxy-1-phenylethyl)benzamide (**35**) with methanesulfonyl chloride in cold dry THF and the resulting mixture stirred at rt for 3 h. Et₃N was then added dropwise and the solution was stirred at rt o/n.[94] Upon completion, the mixture was quenched by the addition of NH₄OH (25%) and after an aqueous work up ¹H NMR confirmed formation of the product with the characteristic pattern of the oxazoline ring. (*R/S*)-2,4-Diphenyl-4,5-dihydrooxazole (**39**) was obtained in quantitative yield using this method; and used in the next step without further purification.

After that, opening the oxazoline ring by reaction of (*R/S*)-2,4-diphenyl-4,5-dihydrooxazole (**39**) with excess 1,2,4-triazole at 125 °C for 48 h[94] in the presence of a small volume of isopropyl acetate was needed to form the final compound.
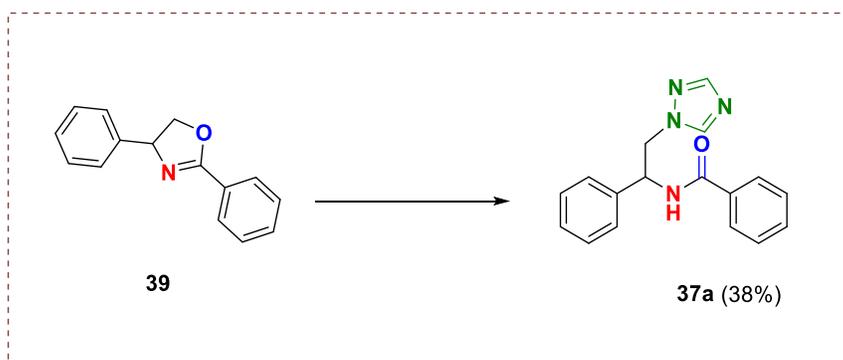
Figure 36. Formation of the azole product (**37a**)

¹H NMR confirmed the formation of the triazole by observing the two singlets characteristic of the triazole ring at δ 8.45 and 7.97. (*R/S*)-*N*-(2-(1*H*-triazol-1-yl)-1-phenylethyl)benzamide (**37a**) was obtained after purification by gradient column chromatography as a white solid in a yield of 38 %.

From the synthesis point of view, the modification by reversing the amide group and shortening the chain in the short derivatives was not optimal because the preference to form the five-member (oxazoline ring) was higher than nucleophilic addition of azole ring. However concomitant opening of the ring and introduction of the azole ring has provided a synthetic route for a different series (see Chapter III).

2.4 Biological assay

All final compounds were evaluated by reconstitution assays to evaluate inhibitory activity (IC_{50}) against CaCYP51, binding affinity (K_d) and MIC against *C. albicans* strains at the Centre for Cytochrome P450 Biodiversity, Swansea University Medical School. Assays were performed by Dr Josie Parker and Dr Andrew Warrilow.

2.4.1 Antifungal susceptibility testing (MIC)

The antifungal susceptibility testing or minimum inhibitory concentration (MIC) is defined as the lowest concentration of any antimicrobial agent (such as antifungal) that prevents the visible growth of fungi after incubation, reported as µg/mL.

The susceptibilities of the SC5314 (*Candida albicans* wild type laboratory strain) and CA14 *C. albicans* (azole sensitive) strains to all novel azole derivatives (**8**, **18**, **25** and **37a**) were determined (Table 7) together with fluconazole as a control, using the standardised CLSI M27-S4 broth dilution method.[95]

Table 7. MIC values for compounds against *C. albicans* SC5314 and CA14 at 48 hours
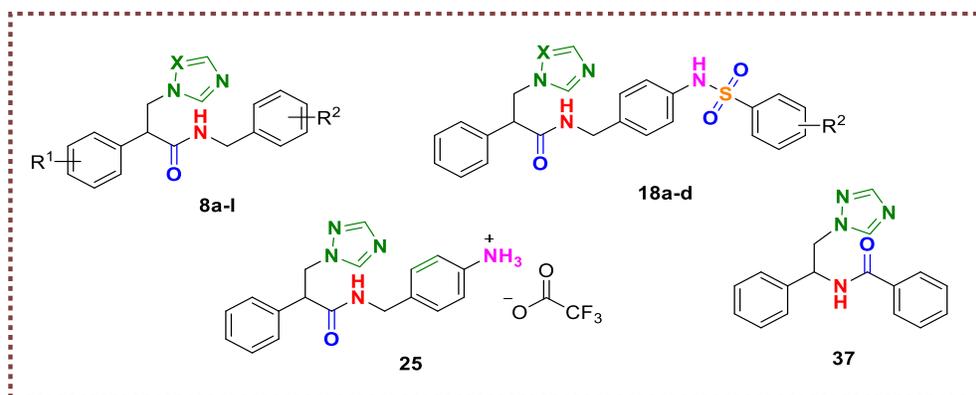
Compd	R¹	R²	X	MIC (µg/mL)		cLogP[a]
				SC5134	CA14	
8a*	4-H	4-H	CH			
8b	4-H	4-F	CH	8	4	3.14
8c	4-H	4-Cl	CH	8	4	3.54

8d	4-Cl	4-Cl	CH	0.125	0.125	4.1
8e	4-H	2,4-diCl	CH	1	1	4.1
8f	4-Cl	2,4-diCl	CH	< 0.03	< 0.03	4.66
8g	4-H	4-CH$_3$	CH	8	8	3.47
8h	4-H	4-CF$_3$	CH	4	4	3.91
8i	4-H	4-OCH$_3$	CH	8	8	2.86
8j	4-H	3,4-diOCH$_3$	CH	>16	>16	2.73
8k	4-H	4-Cl	N	8	8	3.05
8l*	4-H	4-Cl	Tetrazole			
18a	-	4-H	N	4	4	2.9
18b	-	4-F	N	4	2	3.06
18c	-	4-Cl	N	1	1	3.46
18d	-	4-OCH$_3$	N	8	4	2.77
25	-	-	-	>16	>16	1.69
37a	4-H	4-H	N	>16	>16	2.57
Fluconazole				0.125	0.125	0.86

* Synthesis unsuccessful, ^{a}cLogP was determined using Crippen's fragmentation[96]

With the exception of the dimethoxy derivative (**8j**), all the short derivatives (**8**) displayed antifungal activity against both *C. albicans* wild type strains SC5314 and CA14. However, the chloro derivatives were the most effective with **8d** (R^1= Cl, R^2= 4-Cl) comparable with the standard fluconazole (MIC 0.125 µg/mL against both strains) and **8f** (R^1 = Cl, R^2 = 2,4-diCl) more effective than fluconazole with MIC < 0.03 µg/mL against both strains. The introduction of a chloro group at R^1 was clearly beneficial (**8c** vs **8d** and **8e** vs **8f**) as was the presence of two chloro substituents at R^2 (**8c** vs **8e** and **8d** vs **8f**). Generally, the more lipophilic (cLogP) the short derivative (**8**) the better the MIC observed (Table 7). The MIC obtained was comparable whether the azole group was an imidazole (**8c**) or a triazole ring (**8k**).

For the extended derivatives (**18**) a trend was observed between MIC and cLogP with the more lipophilic derivatives more effective at inhibiting fungal growth, for example: **18c**, R^2 = 4-Cl, cLogP 3.46, MIC 1 µg/mL compared with **18a**, R^2 = H, cLogP 2.9, MIC 4 µg/mL (Table 7), while the free amine (**25**) and modified short series compound (**37a**) were ineffective against both *C. albicans* strains (MIC > 16 µg/mL).

2.4.2 Enzyme inhibition study of CaCYP51 (IC$_{50}$ determination)

IC$_{50}$, the half maximal inhibitory concentration, is a quantitative measurement by molar concentration, which shows how much concentration of an inhibitor is required to inhibit biological function or component (as enzyme) by 50%.

CYP51 reconstitution assays containing 1 µM CaCYP51 were performed as previously described.[97] For CaCYP51, the concentrations of fluconazole and novel compounds (**8**, **18** and **25**) were varied from 0 to 10 µM. Exemplar IC$_{50}$ profiles for fluconazole, **8d**, **8f** and **18c** are shown in figure 37. For a very tight binding inhibitor of CaCYP51 an IC$_{50}$ value equal to half the enzyme concentration would be expected (~0.5 µM). In the short series (**8**) the chloro derivatives **8d** (R^1 = 4-Cl, R^2 = 4-Cl) and **8f** (R^1 = 4-Cl, R^2 = 2,4-diCl) showed optimal inhibitory activity with IC$_{50}$ values of 0.39 and 0.46 µM respectively compared with fluconazole IC$_{50}$ 0.31 µM (Table 8). In addition, the 4-methoxy derivative (**8i**), showed promising inhibitory activity with an IC$_{50}$ of 0.91 µM. The extended derivatives (**18**) all showed very good inhibitory activity against CaCYP51 (IC$_{50}$ 0.20-0.79 µM), with the halide derivatives **18b** (R^2 = 4-F, IC$_{50}$ 0.20 µM) and **18c** (R^2 = 4-Cl, IC$_{50}$ 0.33 µM) having similar activity to fluconazole (Table 8). The free amine (**25**) showed weaker inhibitory activity (IC$_{50}$ 1.96 µM).

Table 8. IC$_{50}$ values for compounds against CaCYP51
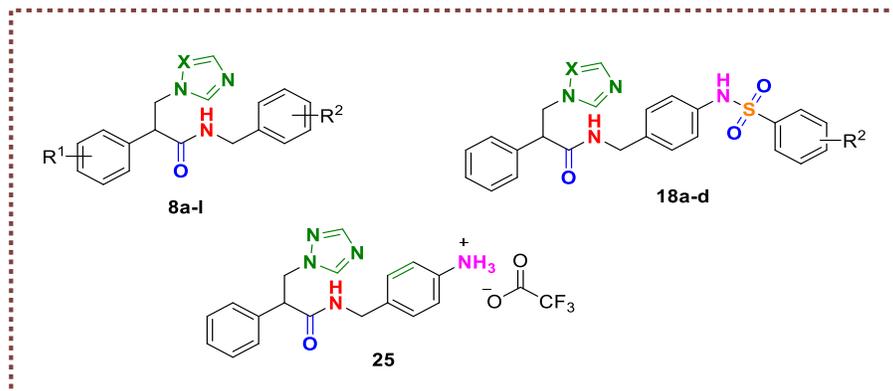
Compd	R^1	R^2	X	CaCYP51 IC$_{50}$ (μM)[a]
8b	4-H	4-F	CH	1.41
8c	4-H	4-Cl	CH	1.01
8d	4-Cl	4-Cl	CH	0.39
8e	4-H	2,4-diCl	CH	0.99
8f	4-Cl	2,4-diCl	CH	0.46
8g	4-H	4-CH$_3$	CH	2.45
8h	4-H	4-CF$_3$	CH	2.21
8i	4-H	4-OCH$_3$	CH	0.91
8j	4-H	3,4-diOCH$_3$	CH	6.15
8k	4-H	4-Cl	N	4.32
18a	-	4-H	N	0.54
18b	-	4-F	N	0.20
18c	-	4-Cl	N	0.33
18d	-	4-OCH$_3$	N	0.79
25	-	-	-	1.96
Fluconazole				0.31

[a]Curve fitted IC$_{50}$s ($v_i = z_o + \{v_o/1+([I]/IC_{50})^n\}$)

Compounds **8d** and **8f** both had MIC values comparable with or lower than fluconazole against azole-susceptible *C. albicans* strains and low IC_{50} values comparable with fluconazole (Table 8) against recombinant CaCYP51 indicating both compounds are good biochemical candidates for further study as antifungal agents. Compound **18c**, whilst having a low IC_{50} value towards CaCYP51, had a MIC value that was 8-fold higher than fluconazole, suggesting a bioavailability problem within the *C. albicans* cells.

Previously IC_{50} values of 0.38 to 0.6, 0.2, 0.39 and 0.2 µM were obtained for fluconazole, voriconazole, itraconazole and posaconazole, respectively, using 1 µM CaCYP51 in CYP51 reconstitution assays.[60,98] CYP51 reconstitution assays were also performed using 0.25 µM truncated human CYP51 (Δ60HsCYP51) in the presence of varying concentrations of compounds **8d**, **8f**, **18c**, fluconazole, voriconazole and posaconazole and the inhibition profiles obtained are shown in figures 37 and 38.
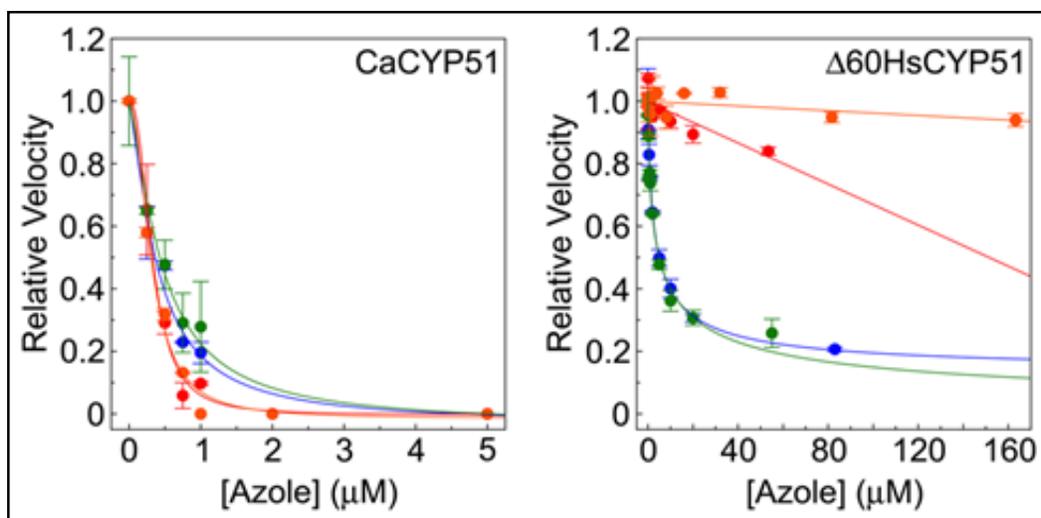
Figure 37. CYP51 azole inhibition profiles. Inhibition profiles for **8d** (●),**8f** (●), **18c** (●) and fluconazole (●) were determined using CYP51 reconstitution assays containing 1 µM CaCYP51 or 0.25 µM Δ60HsCYP51 with lanosterol as substrate. IC_{50} determinations were performed in duplicate with mean values shown along with standard deviations. Relative velocities of 1.00 correspond to actual velocities of 0.911 ±0.141 min^{-1} for CaCYP51 and 8.16 ±2.84 min^{-1} for Δ60HsCYP51
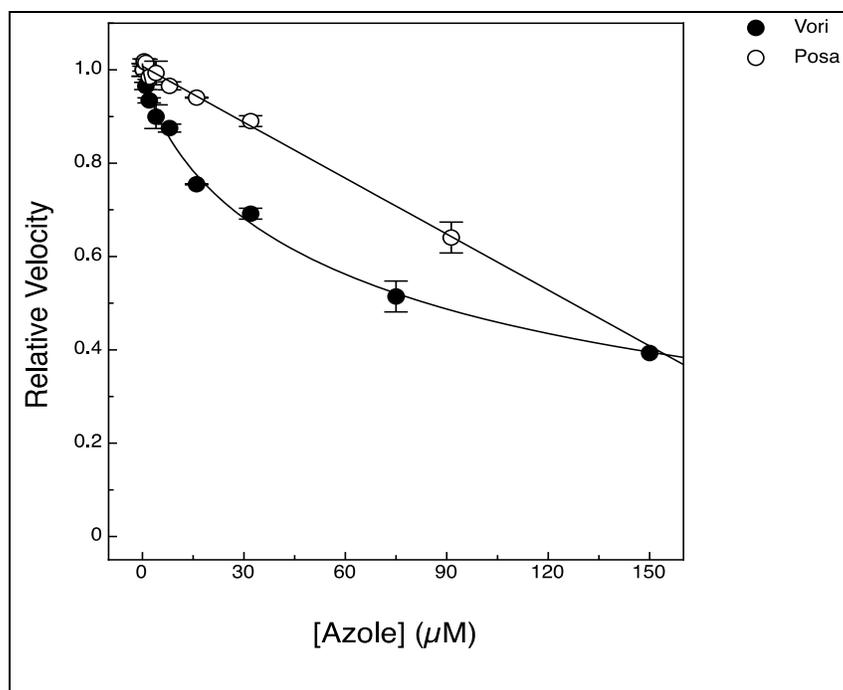
Figure 38. Δ60HsCYP51 azole inhibition profiles. Inhibition profiles for voriconazole (●) and posaconazole (○) were determined using CYP51 reconstitution assays containing 0.25 μM Δ60HsCYP51, 1 μM HsCPR and lanosterol as substrate. IC_{50} determinations were performed in duplicate with mean values shown along with standard deviations. A relative velocity of 1.00 corresponds to an actual velocity of 8.16 ±2.84 min^{-1}

2.4.3 CaCYP51 ligand binding affinity

The absolute spectra of the purified CaCYP51 and Δ60HsCYP51 (figure 39A) were typical for cytochrome P450 enzymes isolated primarily in the low spin state. Dithionite reduced carbon monoxide difference spectra (Figure 39B) produced the characteristic red- shift of the Soret peak to ~450 nm[70] indicating the proteins were isolated in their native state and confirmed by the CYP51 reconstitution assays used to determine azole IC_{50} values.
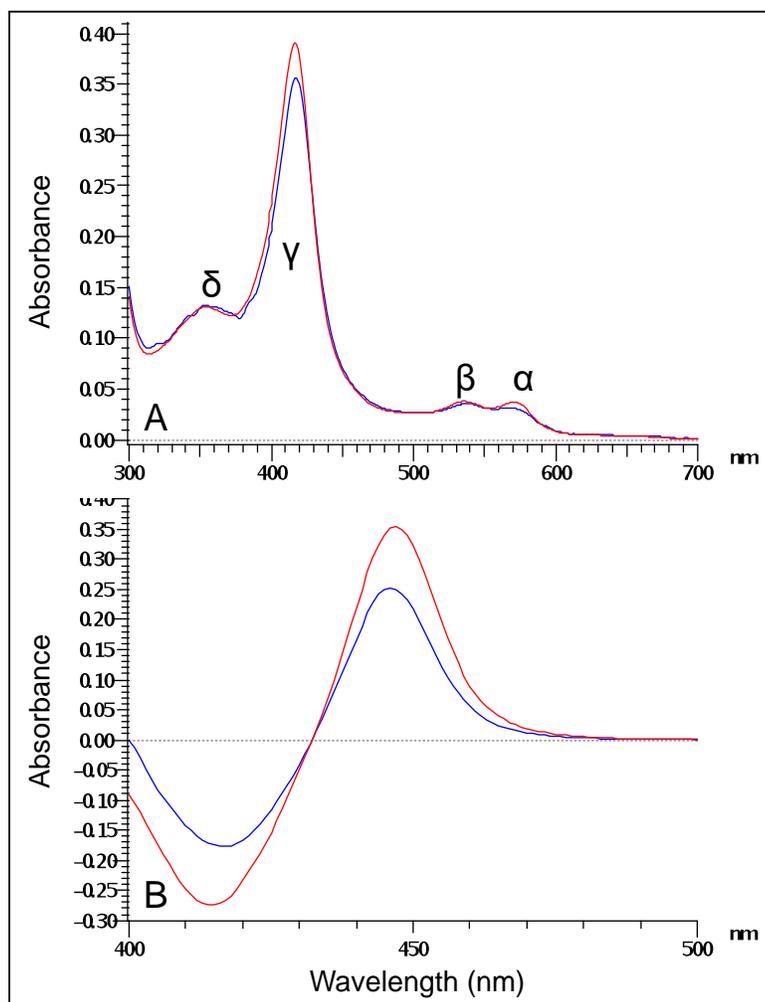
Figure 39. Spectral characterisation of CaCYP51 and Δ60HsCYP51. Absolute spectra (A) for ten-
fold dilutions of purified CaCYP51 (blue line) and Δ60HsCYP51 (red line) are shown along
with the dithionite-reduced carbon monoxide difference spectra (B)

The novel short derivatives (**8**) and extended derivatives (**18**) with MIC < 16 µg/mL and the
standard, fluconazole, were then evaluated for CaCYP51 binding affinity (K_d) by progressively
titrating against 5 µM CaCYP51 (Table 9).

Table 9. Binding affinity (K_d) values for compounds against CaCYP51
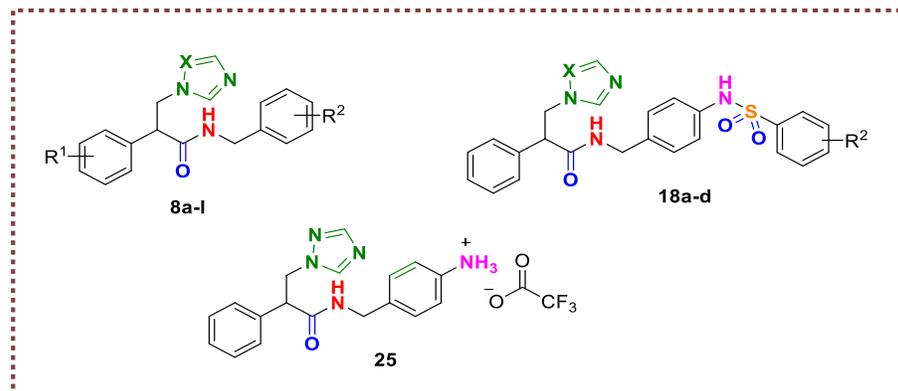
Compd	R^1	R^2	X	K_d (nM)
8b	4-H	4-F	CH	87 ± 27
8c	4-H	4-Cl	CH	60 ± 4
8d	4-Cl	4-Cl	CH	17 ± 5
8e	4-H	2,4-diCl	CH	83 ± 26
8f	4-Cl	2,4-diCl	CH	62 ± 17
8g	4-H	4-CH$_3$	CH	144 ± 47
8h	4-H	4-CF$_3$	CH	85 ± 19
8i	4-H	4-OCH$_3$	CH	55 ± 10
8j	4-H	3,4-diOCH$_3$	CH	-
8k	4-H	4-Cl	N	167 ± 17
18a	-	4-H	N	115 ± 16
18b	-	4-F	N	55 ± 27
18c	-	4-Cl	N	43 ± 18
18d	-	4-OCH$_3$	N	110 ± 22
Fluconazole				41 ± 13

In the short series tightest binding was observed for the chloro derivative **8d** (R^1 = Cl, R^2 = 4-Cl, K_d 17 ± 5 nM), which was slightly better than fluconazole (K_d = 41 ± 13 nM). Good binding affinity was also observed for other chloro derivatives **8c** (R^1 = H, R^2 = 4-Cl), **8f** (R^1 = Cl, R^2 =2,4-diCl) and the 4-methoxy derivative **8i** (R^1 = H, R^2 = 4-OCH$_3$) with K_d of 60 ± 4, 62 ± 17 and 55 ± 10 nM, respectively. In the extended series, the halide derivatives **18b** (R^2 = 4-F, K_d 55 ± 27 nM) and **18c** (R^2 = 4-Cl, K_d 43 ± 18 nM) showed good binding affinity comparable with fluconazole.

Binding saturation curves were constructed from the absorbance difference ($\Delta A_{peak\text{-}trough}$) derived from the difference spectra against the antifungal concentration for CaCYP51.[99] Type II difference binding spectra were observed for all compounds titrated against 5 µM CaCYP51 (Exemplar is shown in Figure 40) indicating the direct coordination of the imidazole or triazole nitrogen atom as the sixth axial ligand with the haem ferric ion of CaCYP51.

Titration of **8d**, **8f**, **18c**, and fluconazole with 5 µM Δ60HsCYP51 also gave type II difference binding spectra, albeit the intensity (ΔA) obtained with **18c** and fluconazole was smaller than the other two azoles (Figure 40). The rearranged Morrison equation[100] gave the best fit to the ligand saturation curves against 5 µM CaCYP51 (Figure 41) indicating the selected compounds bound tightly to the purified CaCYP51 protein in free solution. Likewise, the rearranged Morrison equation[100] gave the best fit for binding **8d** and **8f** to 5 µM Δ60HsCYP51 indicating tight binding in free solution (Figure 41). However, the Michaelis-Menten equation best fit the binding of **18c** and fluconazole to Δ60HsCYP51, indicating the binding was less tight (Figure 41). Previously Δ60HsCYP51 was shown to behave near identically to the full length HsCYP51 in terms of azole binding properties.[98]

Furthermore, the Morrison equation gave estimates of K_i^{app} from the inhibition profiles with CaCYP51 of 160, 200 and 110 nM for compounds **8d**, **8f** and **18c**, respectively, compared with 30 nM for fluconazole, confirming all four compounds bound tightly to CaCYP51.
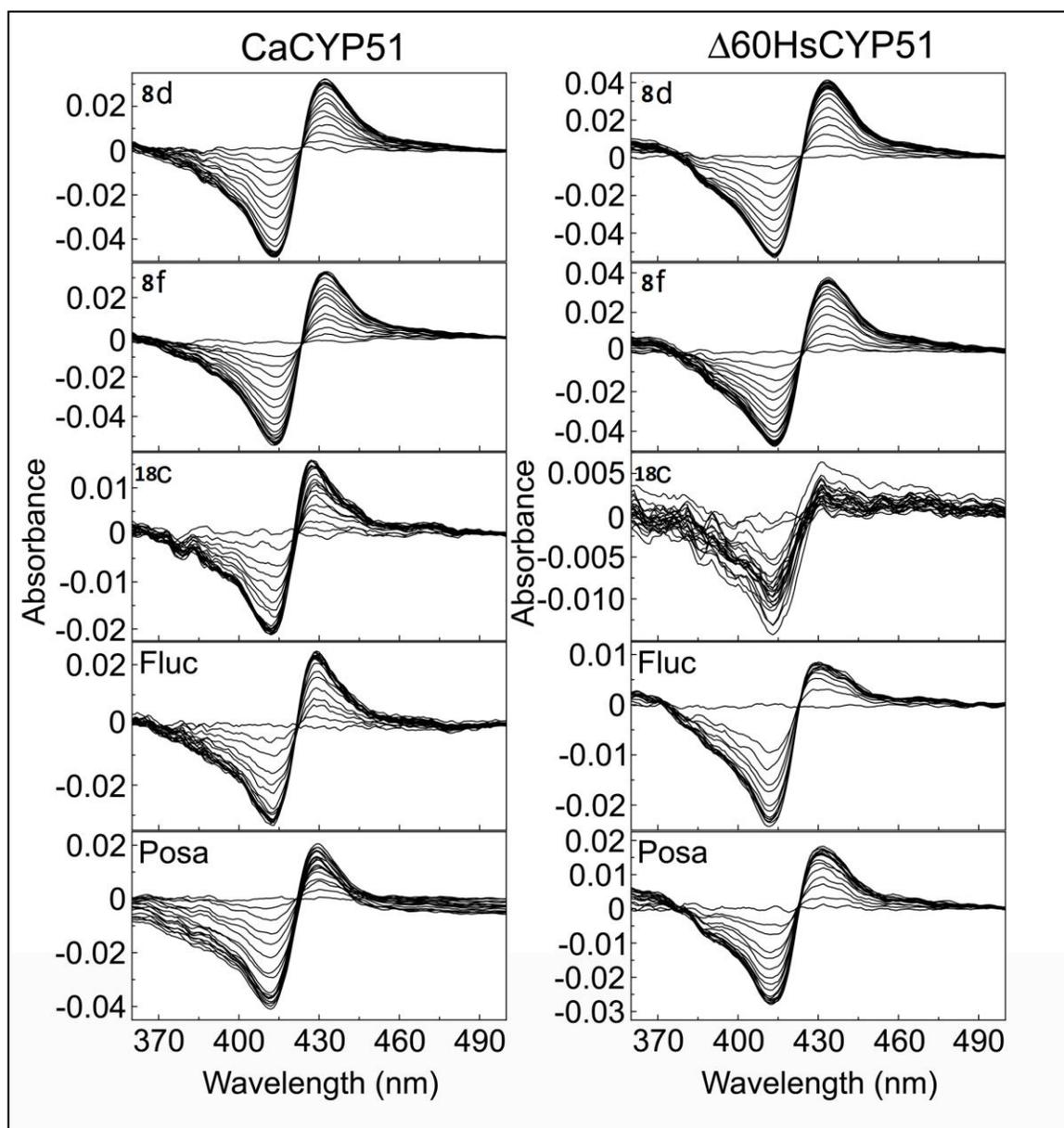
Figure 40. Azole binding difference spectra. Type II difference spectra obtained during the progressive titration of 5 μM CaCYP51 and Δ60HsCYP51 with compounds **8d**, **8f**, **18c**, fluconazole and posaconazole are shown. Each azole titration was performed in triplicate, although only one replicate is shown. The ligand saturation curves for these difference spectra are shown in figure 41
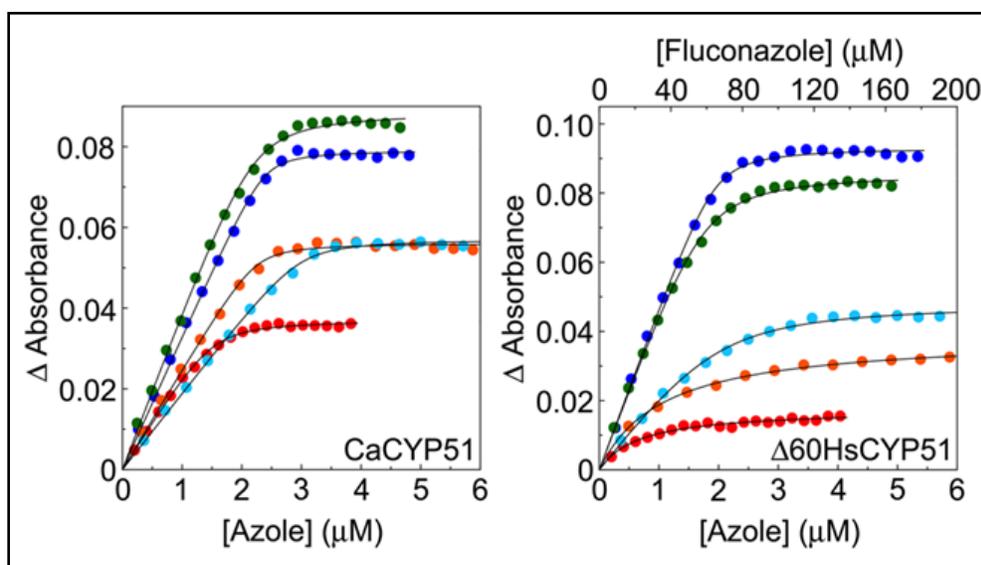
Figure 41. CYP51 azole saturation curves. Ligand binding saturation curves derived from the type II difference spectra in figure 40 are shown for compounds **8d** (●),**8f** (●), **18c** (●), fluconazole (●) and posaconazole (●) with 5 μM CaCYP51 and 5 μM Δ60HsCYP51. Each azole titration was performed in triplicate although only one replicate is shown

The selectivity for CaCYP51 over the human homologue was relatively poor for compounds **8d** and **8f** with only ~8-fold difference in IC_{50} values (Table 10), exhibiting a similar selectivity as ketoconazole.[98] This could limit the use of these two compounds as antifungal drugs. In contrast compound **18c** exhibited high selectivity at 461-fold (Table 10), which is similar to that observed with voriconazole (390-fold) and better than the previously observed 175-fold selectivity of itraconazole,[98] suggesting this compound could be useful as an antifungal drug if uptake and bioavailability could be improved in *C. albicans* by further refinement of the chemical structure. However, compound **18c** was less selective than posaconazole (615-fold) and well behind the best compound fluconazole, which exhibited over 4000-fold selectivity for CaCYP51 over the human homologue based on apparent IC_{50} values. By comparison the tetrazole VT-1161 (oteseconazole) did not inhibit Δ60HsCYP51 activity at concentrations up to 50 μM and selectivity in excess of 2000-fold was predicted.[101]

Both **8d** and **8f** bound tightly to Δ60HsCYP51 in free solution with K_d values of 45 and 74 nM, respectively, whilst binding of **18c** was less tight and more variable with a mean K_d of 923±509 nM (n=6) (Table 10). Therefore, selectivity for CaCYP51 over the human homolog based on K_d

values was poor for compounds **8d** and **8f** at 2.6- and 1.2-fold, respectively. However, selectivity of compound **18c** was higher at 21.5-fold and was higher than posaconazole (4.7-fold) and higher than previously observed with itraconazole and ketoconazole (Table 10). However, the selectivity of compound **18c** based on K_d values was still substantially lower than those observed for voriconazole (229-fold) and fluconazole (938-fold).

Table 10. Selectivity of compounds for CaCYP51 (Ca) over Δ60HsCYP51 (Hs) based on K_d and IC_{50}

Compd	K_d (nM)		Selectivity	IC_{50} (µM)		Selectivity
	Ca	Hs	Hs/Ca (fold)	Ca	Hs	Hs/Ca (fold)
8d	17 ± 5	45 ± 13	2.6	0.39	3.37	8.6
8f	62 ± 17	74 ± 13	1.2	0.46	3.73	8.1
18c	43 ± 18	923 ± 509	21.5	0.33	152	461
Fluconazole	41 ± 13	38460 ± 4840	938	0.31	~1327	4281
Posaconazole	43 ± 11	204 ± 63	4.7	0.2[b]	123[c]	615
Voriconazole	10 ± 2[a]	2290 ± 120[a]	229	0.2[b]	78[c]	390
Itraconazole	19 ± 5[a]	92 ± 7[a]	4.8	0.4[a]	70[a]	175
Ketoconazole	12 ± 3[a]	42 ± 16[a]	3.5	0.5[a]	4.5[a]	9

[a]Reference 98. [b]Reference 60. [c]Figure 38

Mean K_d values are shown along with associated standard deviations. For IC_{50} determinations CYP51 assays contained 1 µM CaCYP51 (all azoles) or 0.25 µM Δ60HsCYP51 (**8d**, **8f**, **18c** and fluconazole) or 0.4 µM Δ60HsCYP51 (posaconazole, voriconazole, itraconazole and ketoconazole).

2.4.4 Sterol profiles

C. albicans strains (CA14 and SC5314) were grown in MOPS buffered RPMI in the presence of DMSO (untreated) or DMSO and antifungal (at half the MIC) for 18 hours, at 37 °C. Sterols were then extracted and analysed by GCMS and sterol profiles (% of the total sterol extracted) were determined.

Table 11. Sterol composition (% of total sterols) of untreated and treated wild-type *C. albicans* strains

	Sterol Composition (%)									
	Untreated (DMSO only)		Fluconazole 0.06 µg/mL		8d 0.06 µg/mL		8f 0.015 µg/mL		18c 0.5 µg/mL	
	CA14	SC5314	CA14	SC5314	CA14	SC5314	CA14	SC5314	CA14	SC5314
Ergosterol	76.9±3.8	77.2±3.8	63.8±3.4	728 ±3.3	7.8±6.5	2.7±2.3	4.3±0.5	9.1±5.5	3.5±1.3	24.9±5.5
Diol[a]			0.2±0.4		8.2±6.0	17.6±7.1	7.5±4.6	11.7±1.4	9.2±1.2	7.2±5.2
Lanosterol	3.8±0.6	5.2±5.0	19.6±1.5	14.5±1.7	40.4±2.2	41.0±5.5	43.6±1.8	38.6±3.6	43.6±1.5	34.5±2.9
Eburicol		0.4±0.3	8.5±1.0	4.0±0.4	26.4±5.0	20.5±4.4	26.1±0.1	21.0±3.3	22.4±1.1	14.0±3.5
Total 14α-methylated sterols	2.8	5.6	31.4	22.2	90.0	95.8	77.2	89.3	93.3	70.6

[a]14α-methyl ergosta-8,24(28)-dien-3,6-diol

The sterol profiles showed an accumulation of 14α-methylated sterols in both *C. albicans* strains treated with fluconazole, **8d**, **8f** and **18c**. This confirms that the mechanism of action of **8d**, **8f** and **18c** as for fluconazole, is the inhibition of sterol 14α-demethylase (CYP51). The accumulation of 14α-methylated sterols in the fungal membrane inhibits the growth of the *C. albicans*. In particular, the accumulation of 14α-methyl ergosta-8,24(28)-dien-3,6-diol is believed to disrupt the fungal membrane in Candida, resulting in growth inhibition. Importantly, treatment with 0.06 µg/mL **8d** resulted in a much higher accumulation of the 'diol'sterol and concomitant depletion of ergosterol, indicating that **8d** is more effective at inhibiting CYP51 activity than fluconazole.

2.5 Molecular dynamic (MD) simulations

2.5.1 Wild type docking

For further investigation of the binding modes of the short (**8**) and extended (**18**) azole derivatives, the best ligand pose was chosen and molecular dynamics simulations were run for 100 ns using the CaCYP51 crystal structure (PDB 5FSA)[35] and representative short (**8f** and **8i**) and extended (**18c**) azole derivative complexes, using the Desmond programme of Maestro[102] are presented here. All the compounds formed a coordination interaction between the imidazole or triazole N and the haem Fe^{3+}.

Different binding profiles were observed for the short derivatives (**8**). The (*R*)-enantiomer of **8f** formed additional binding interactions within the haem binding site, specifically water mediated H-bonding interactions with His310 and Tyr132 and the amide heteroatoms, and hydrophobic interactions with Tyr118, Met508 and Phe126. The (*S*)-enantiomer of **8f** interacted primarily via hydrophobic interactions, positioned to form π-π stacking with Tyr118 and hydrophobic interactions with Phe126. The (*R*)-methoxy derivative (**8i**) formed additional water mediated H-bonding interaction through the methoxy oxygen and Ser378, π-π stacking interaction with Tyr118 and hydrophobic interactions with Ile131. Whereas, the (*S*)-enantiomer interacted primarily via hydrophobic interactions, positioned to form π-π stacking with Phe380 and hydrophobic interactions with Tyr118 and Met508 (Figure 42).
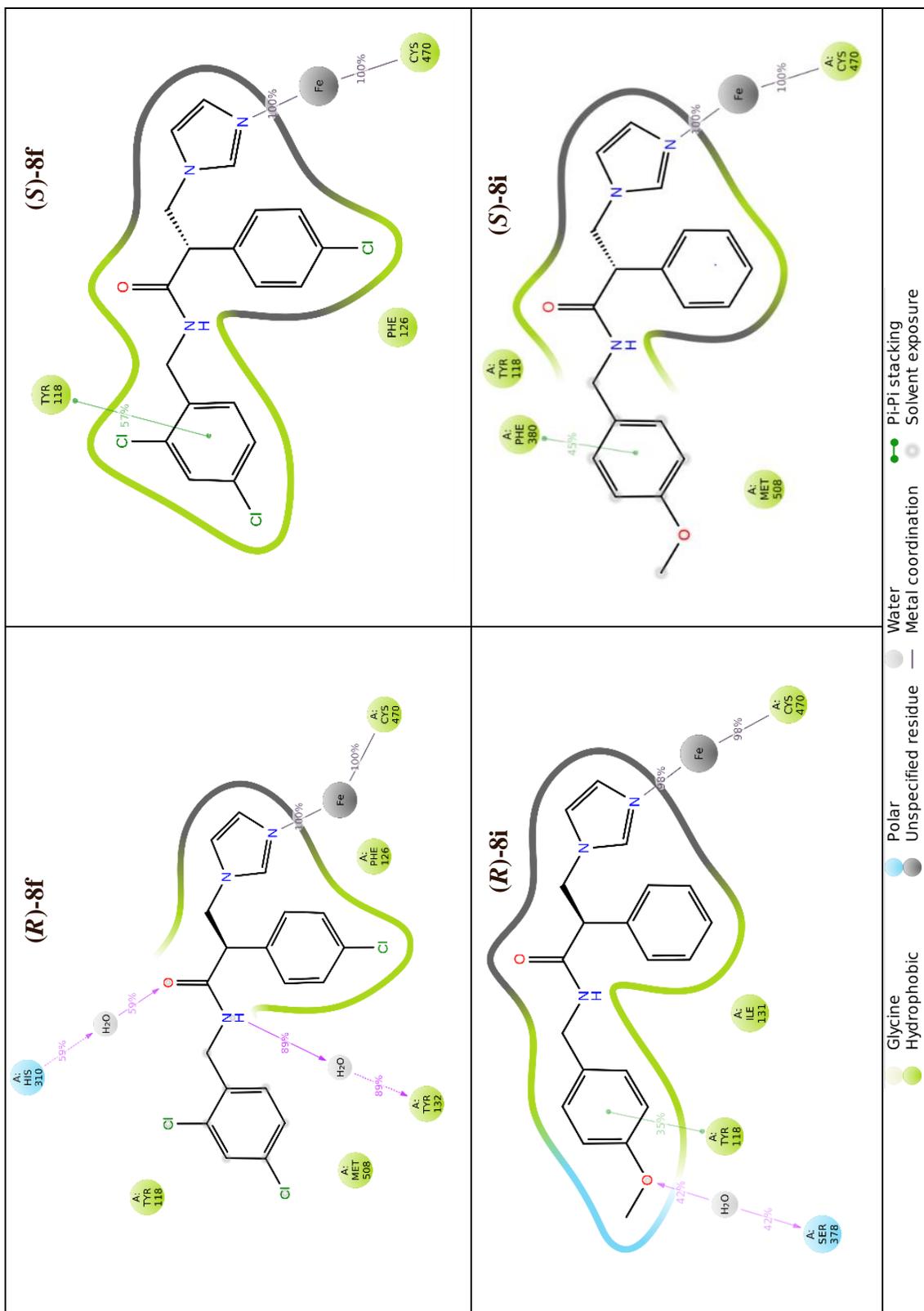
Figure 42. A schematic of detailed ligand atom interactions of representative (*R*)- and (*S*)-enantiomers of short derivatives **8** with the amino acids of CaCYP51 active site Interactions that occur more than 30.0% of the simulation time in the selected trajectory (0 through 100 ns) are shown

The (*R*)-enantiomers of the extended compounds showed preferential binding with H-bonding interactions between the sulphonamide group and Ser378 and His377, while the amide NH formed a water mediated interaction with Leu121. The three benzene rings formed π-π stacking interactions with Phe126, Tyr118 and Phe380. The (*S*)-enantiomer formed H-bonding interaction between the sulphonamide and Ser378 and the amide formed a water mediated interaction with Tyr132 (e.g. **18c**, Figure 43).
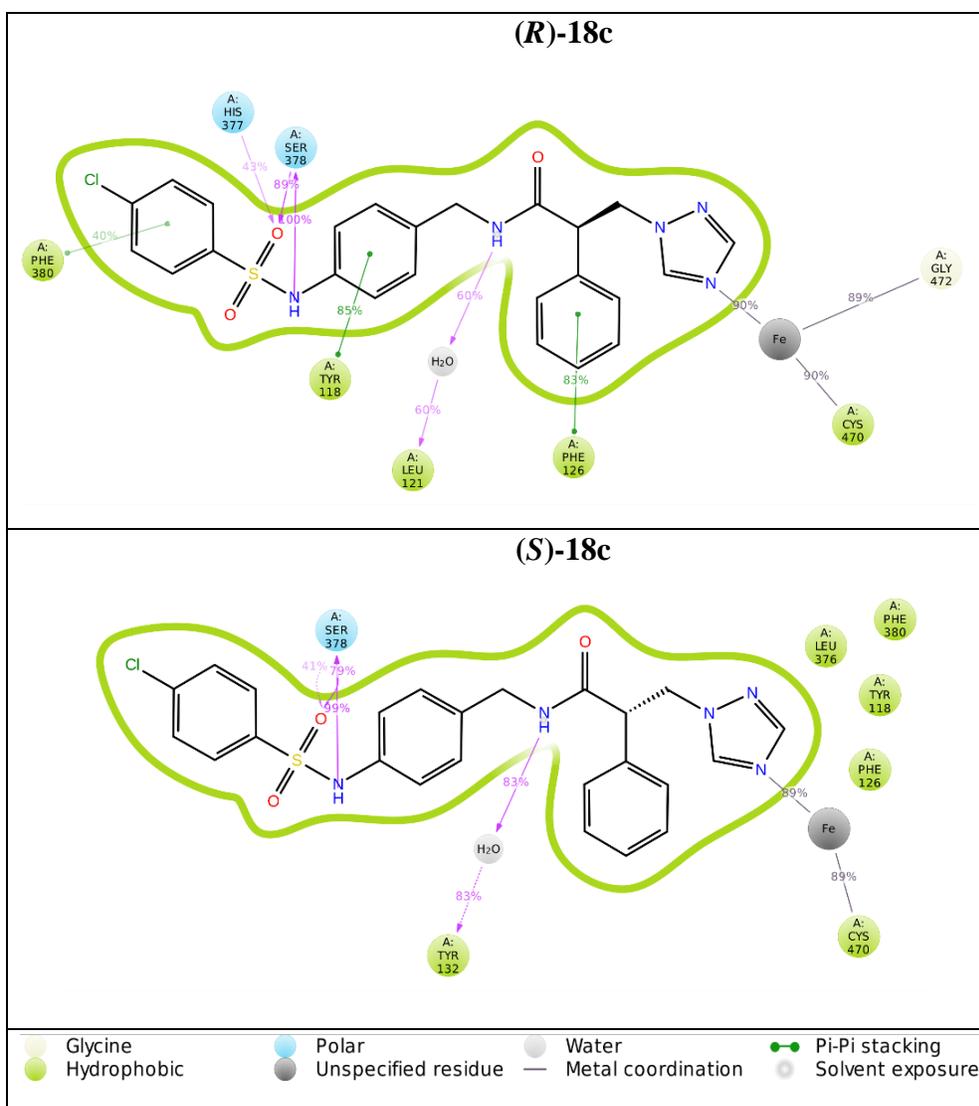
Figure 43. A schematic of detailed ligand atom interactions of representative (*R*)- and (*S*)-enantiomers of extended derivative **18c** with the protein residues of CaCYP51 active site. Interactions that occur more than 30.0% of the simulation time in the selected trajectory (0 through 100 ns) are shown

The placement of the azole derivatives in comparison with posaconazole and fluconazole in the CaCYP51 active site was visualised using MOE. Posaconazole (Figure 44, magenta) sits in a long hydrophobic channel with bonding primarily through multiple hydrophobic interactions with just one H-bonding interaction observed between Ala61 and the carbonyl oxygen of the 1,2,4-triazol-5(4*H*)-one ring. The optimal placement of fluconazole (Figure 44, cyan) was obtained after molecular dynamics simulations and, as expected, occupies a smaller area of the ligand binding channel compared with posaconazole with consequently fewer binding interactions. The short azole derivatives (**8**) mimic the positioning of fluconazole, whereas the more extended derivatives (e.g. **18c**, yellow, Figure 44) sit between posaconazole and fluconazole, however importantly they form additional H-bonding interactions with residues in the access channel compared with posaconazole, primarily through the sulphonamide group and also hydrophilic (π-π stacking) interactions with the benzene rings.
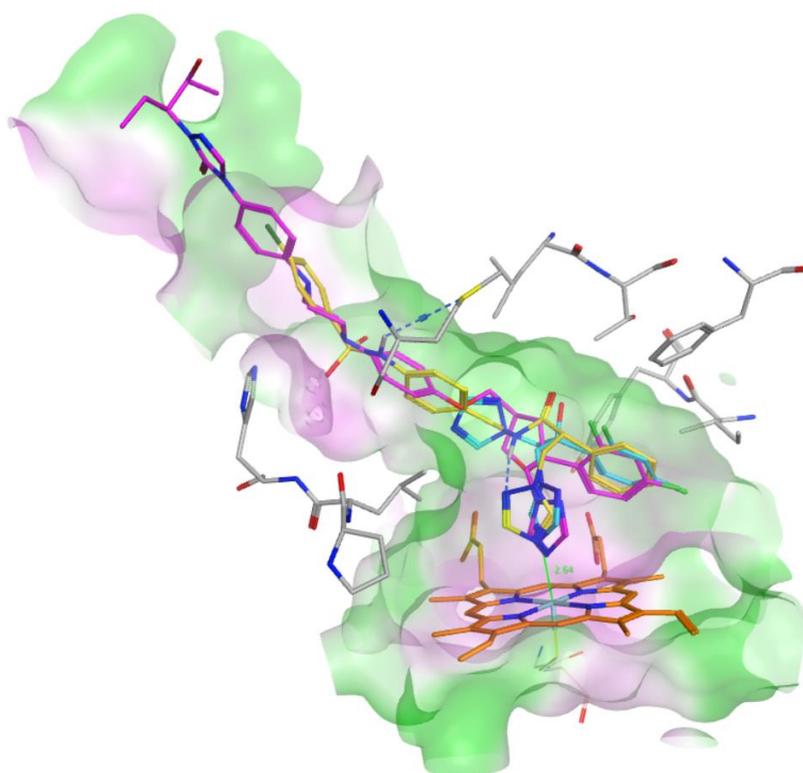
Figure 44. CaCYP51-posaconazole (magenta) complex (PDB 5FSA) with posaconazole positioned along the hydrophobic active site cavity and above the haem (orange). Fluconazole (cyan) and extended derivative **18c** (yellow) are aligned after MD simulations

2.5.2 Mutant strain docking

Several studies have shown that CaCYP51 mutation increases the resistance to fluconazole with the double mutation effect greater than the single mutant effect in CaCYP51.[60] From this point the docking of novel azole agent were studied in a double mutant strain and compared with fluconazole.

MD with a simulation time of 100 ns was performed using a representative mutant strain (Y132H+K143R) of CaCYP51 with (*R*)-configuration of short derivative (**5f**) and extended azole derivative (**18c**) compared with fluconazole.
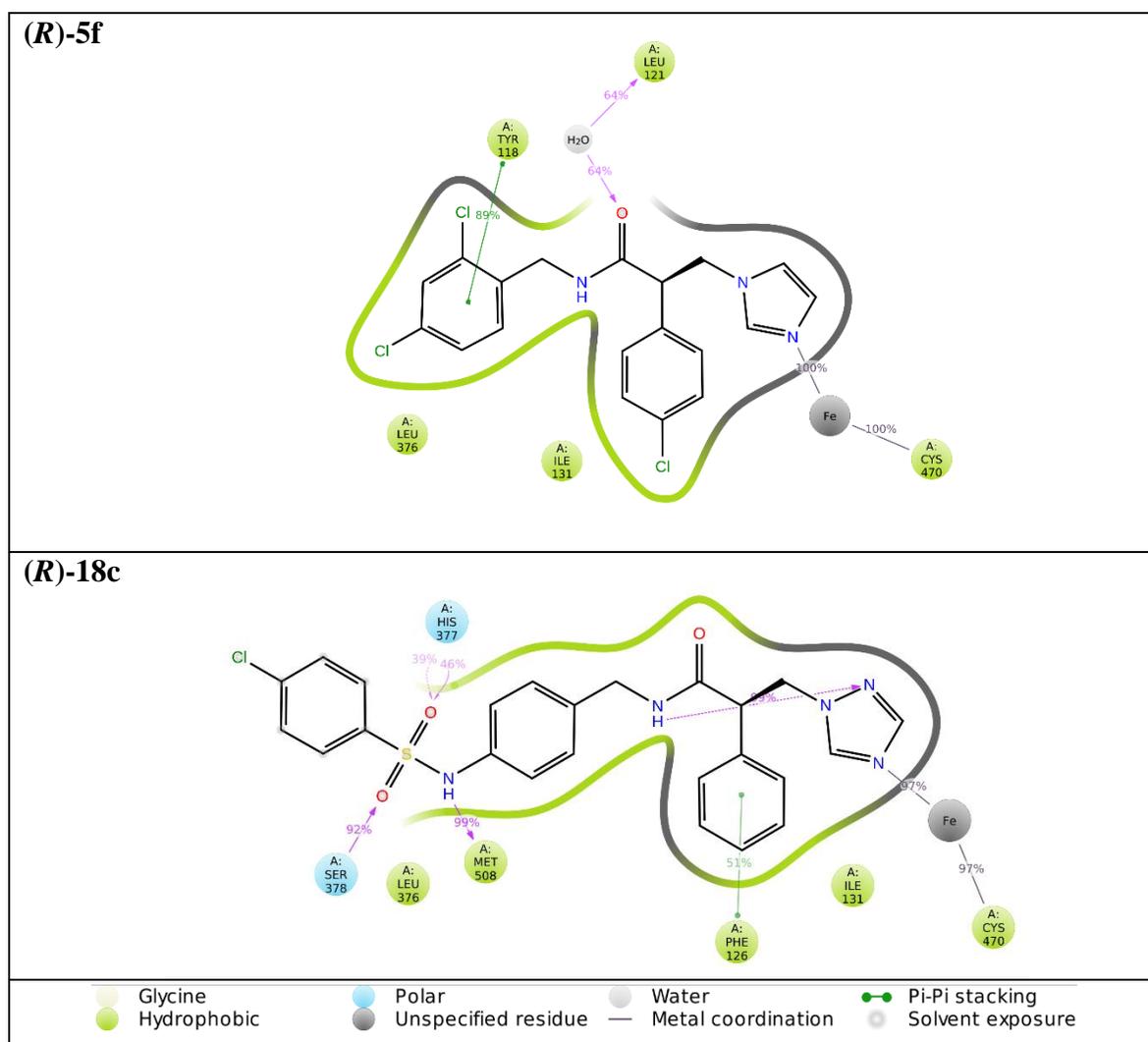
Figure 45. A schematic of detailed ligand atom interactions of representative (*R*)-enantiomer of **5f** and **18c** with the amino acids of mutant strain (Y132H+K143R) CaCYP51 active site. Interactions that occur more than 30.0% of the simulation time in the selected trajectory (0 through 100 ns) are shown

The (*R*)- enantiomer for **5f** forms water mediated H-bonding interaction with Leu121 and oxygen of the amide group and forms π-π stacking interaction with Tyr118 and aryl substituted ring, also hydrophobic interactions with Ile131 and Leu376 are observed in the Y132H+K143R mutant strain of CaCYP51. While, the (*R*)-enantiomer of the extended compound (**18c**) lost the π-π stacking interactions with Tyr118 and Phe380 and the two benzene rings, additional direct H-bonding interaction between NH of sulphonamide group and Met508, and hydrophobic interactions with Ile131 and Leu376 were formed (Figure 45) compared with the wild type CaCYP51.
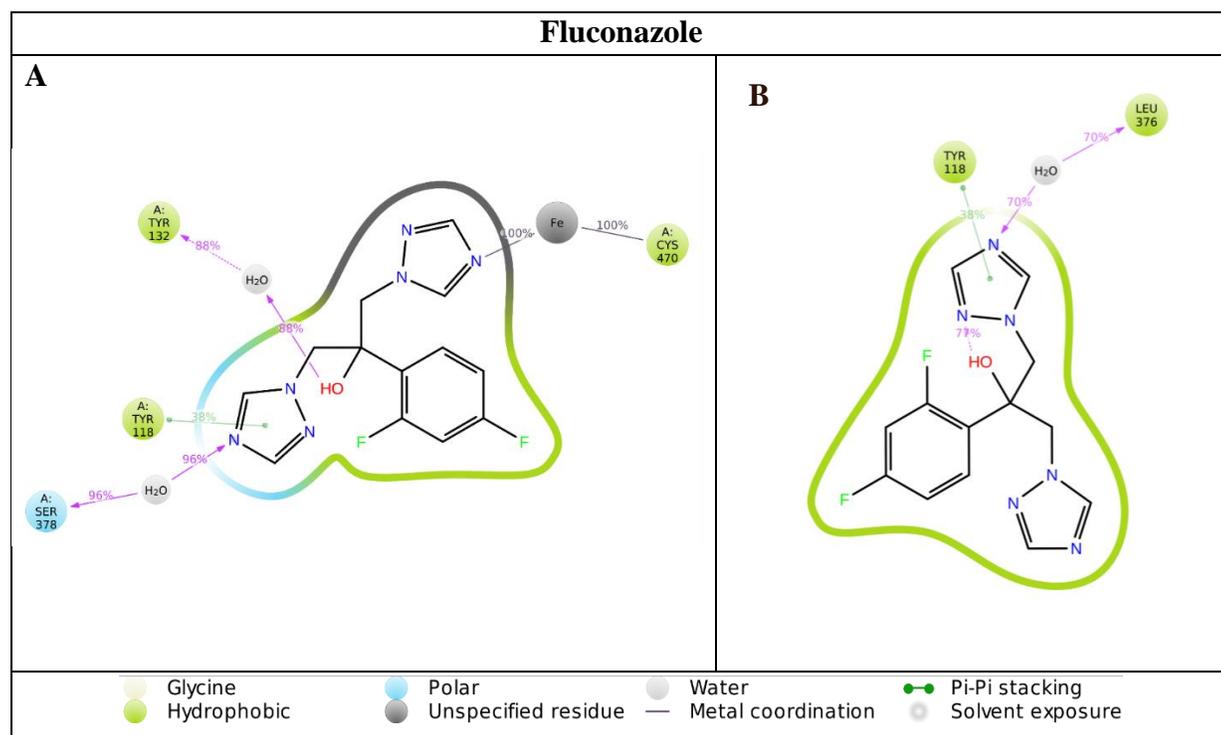
Figure 46. A schematic of detailed ligand atom interactions of fluconazole with the protein residues of wild type and mutant strain (Y132H+K143R) CaCYP51 active site. Interactions that occur more than 30.0% of the simulation time in the selected trajectory (0 through 100 ns) are shown

In the wild type CaCYP51 fluconazole binds through water mediated H-bonding interactions with Ser378 and the nitrogen of a triazole ring, Tyr132 with the hydroxy group and π-π stacking with Tyr118 (Figure 46A).

In the mutant strain Y132H+K143R fluconazole loses the key interaction with Tyr132 and is limited to indirect H-bonding interaction with Leu376 and π-π stacking with Tyr118 (Figure 46B).

For the (*R*)-**8f** and (*R*)-**18c** CaCYP51 (Y132H+K143R) complexes, the mean ΔG (bind) was calculated[103] from each frame from the point where the complex reached equilibrium to the final frame of the MD simulation with respect to RMSD. The ΔG values indicate positioning within the mutant (Y132H +K143R) CaCYP51 was optimal with respect to fit of the two ligands. The (*R*)-**18c** complex, with ΔG of -69.86 ± 5.46 kcal/mol would appear to have better binding affinity, however this ΔG calculation does not provide information with respect to haem binding and subsequently water mediated biotransformation. To determine this measurement of the distance from the azole N and the haem Fe^{3+} before and after MD simulation needs to be determined.

Complex	ΔG (kcal/mol)
Mutant strain CaCYP51-8f	-46.3480 ± 3.73
Mutant strain CaCYP51-18c	-69.8646 ± 5.46

In the wild type CaCYP51 complexes a relatively small shift is observed after MD stimulation (Table 12), however a more significant shift is observed in the case of the double mutant (Y132H+K143R) CaCYP51 complexes (Figure 47). For fluconazole a shift of 2.37 Å (pre-MD) to 4.10 Å (post-MD) reflects the loss of haem binding (Figure 46) and may explain the reduced effect of fluconazole against this mutant CaCYP51.[57,60] A less significant shift, compared with fluconazole, is observed with the mutant strain (Y132H+K143R) CaCYP51 complexes of (*R*)-**8f** and (*R*)-**18c** from 2.39 and 2.33 Å (pre-MD) to 3.08 and 3.11 Å (post-MD) respectively (Table 12). This shift still allows binding with the haem Fe^{3+}, as seen in Figure 47, and the additional bonding interactions, in particular for (*R*)-**18c**, is reflected in the ΔG (bind) calculations.

Table 12. The distance between the N-azole ring and the haem iron in the wild type of CaCYP51 active site at 0 ns and 100 ns MD stimulation

	Wild type CaCYP51 complex (Å)	
	Ligand complex at 0 ns	Ligand complex at 100 ns
8f	2.20	2.50
18c	2.67	3.38
Fluconazole	2.74	2.28

This finding needs more investigation with testing these ligands in the mutant strain to confirm it, which could help in the designing approach for selective antifungal agents.
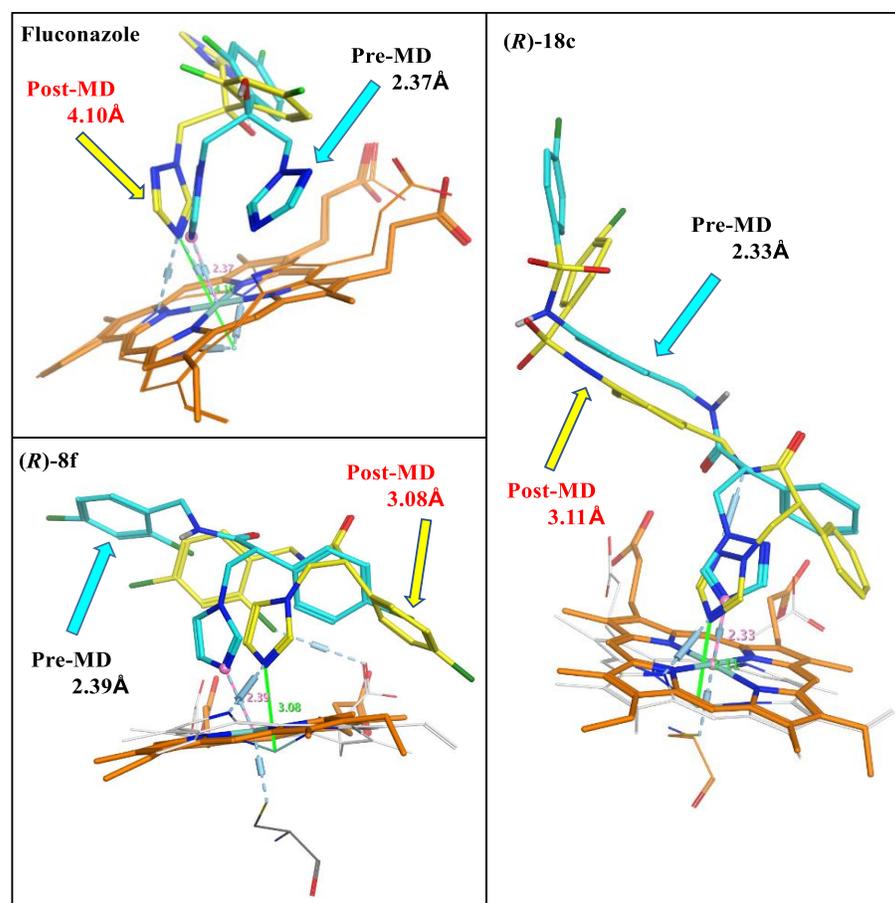
Figure 47. Complex structure of **8f** and **18c** in mutant strain (Y132H + K143R) of CaCYP51 at 0 ns (cyan) and 100 ns MD stimulation (yellow)

2.6 Conclusion

Two series of novel azole derivatives, short (**8**) and extended (**18**) series have been designed, synthesised and investigated for CYP51 inhibitory activity, binding affinity and MIC against *C. albicans* strains, with a synthetic route to a third modified short series (**37**) were determined.

Docking studies of all final novel compounds were investigated for binding interactions using the CaCYP51 crystal structure co-crystalised with posaconazole (PDB: 5FSA) generated in MOE and performs using two programmes MOE and LeadIT. No significant differences were observed between the two programmes, with respect to binding interactions and occupancy in the active site pocket of CaCYP51. MOE was preferred owing to clearer visualisation in the 2D ligplot ligand interaction diagramme. All the compounds formed a coordination interaction between the N atom of imidazole or triazole and the haem Fe^{3+} with good distance (< 3.0 Å). The short derivatives (**8**) occupied the active site pocket of CaCYP51 in a similar manner to fluconazole. The docking study of the extended derivatives (**18**) showed several interactions through water molecules as well as direct H-bonding within the access channel, which could overcome the resistance to fluconazole. Compound **37a** from the modified short series occupied the CaCYP51 active site pocket in a similar manner as the short series.

The synthesis of the short derivatives (**8**) was successfully achieved via a three steps synthetic route initiated with a trimethyl borate ($B(OCH_3)_3$) to accelerate the amidation reaction. The extended derivatives (**18**) were synthesised through a three step synthetic route after the aryl sulfonyl extension was established at an earlier stage as (4-(arylsulfonamido)phenyl) methanaminium 2,2,2-trifluoroacetate derivatives and then coupled with tropic acid. The final step needs more investigation to overcome the elimination product to improve yield. Compound **37a** was achieved via three synthetic steps initiated with the conversion the amino group to amide group, oxazoline ring formation and addition of triazole ring.

All final compounds were $\geq 95\%$ pure and were tested CaCYP51 activity to determine IC_{50}, K_d and MIC. The short derivatives were more potent against the *C. albicans* strains (e.g. **8f**, MIC <0.03 µg/mL, **18c**, MIC 1 µg/mL, fluconazole 0.125 µg/mL) but both displayed comparable enzyme binding and inhibition (**8f** K_d 62 ± 17 nM, IC_{50} 0.46 µM; **18c** K_d 43 ± 18 nM, IC_{50} 0.33 µM, fluconazole K_d 41 ± 13 nM, IC_{50} 0.31 µM). To determine whether any specific physicochemical factors may account for the difference in MIC, the physicochemical properties

of the most promising prepared compounds and reference antifungal agents were calculated (Table 13). The cLogP was determined using Crippen's fragmentation,[96] and the molecular weight (MW), number of H-bond acceptors (nON), H-bond donors (nOHNH), rotatable bonds (nrot), along with the molecular volume (MV) and topological polar surface area (TPSA) were calculated using Molinspiration software.[104] The number of violations (nviol) of Lipinskys is determined from the data presented (violations italicised in Table 13).

The two series have a significantly increased cLogP, although still within Lipinsky range, when compared with fluconazole but are similar to voriconazole and oteseconazole. The short series fits between fluconazole and voriconazole, while the extended series more closely resembles oteseconazole in all other physicochemical properties but, unlike the clinically described azoles, the extended series does not violate Lipinskys, showing more optimal drug like properties. There is a considerable range in all the physicochemical properties calculated for the clinically used potent azole antifungals, and the only clear difference observed with the two described series is for compound **18c**, which has two H-donors whereas all other compounds have one H-donor.

Table 13. Physicochemical properties of selected derivatives and clinical antifungal agents

Compd	MW	cLogP	nON/ nOHNH	nrot	MV (Å^3)	TPSA (Å^2)	nviol
8d	374.264	4.1	4/1	6	316.96	46.92	*0*
8f	408.709	4.66	4/1	9	414.51	46.92	*0*
18c	495.981	3.46	8/2	9	414.51	105.98	*0*
Fluconazole	306.271	0.87	7/1	5	248.96	81.66	*0*
Voriconazole	349.311	2.59	6/1	5	285.11	76.73	*0*
Itraconazole	*705.633*	*7.07*	*12*/1	11	607.90	104.73	*3*
Posaconazole	*700.777*	*5.74*	*12*/1	12	623.35	115.72	*3*
Oteseconazole	*527.394*	*5.2*	7/1	9	401.65	85.96	*2*

nON = H-bond acceptor; nOHNH = H-bond donor; nrot = number of rotatable bonds; MV = molecular volume; TPSA = topological polar surface area; nviol = number of Lipinsky violations

The short series had poor selectivity for CaCYP51 over the human homolog based on K_d values, while the selectivity of the extended series, e.g. compound **18c**, was higher at 21.5-fold and was higher than posaconazole (4.7-fold) and higher than previously observed with itraconazole and ketoconazole, suggesting the extended series as optimal for further development. The extended series is better able to fill the access channel and haem binding sites of CaCYP51 and forms additional binding interactions (H-bonds with His377, Ser378, π-π stacking interactions with Phe126, Tyr118 and Phe380).

In addition, molecular dynamic simulations were performed to investigate the binding and position of inhibitors; owing to the ability of both ligand and protein to move, a more accurate reflection of physiological conditions may be provided. The MD simulations for the short and extended derivatives were performed in the wild and selected double mutant (Y132H+K143R) strains of CaCYP51 compared with fluconazole. The resulting data showed good binding interaction for the short derivatives with hydrophobic interactions and some H-bonding interactions through water molecules. However, the extended derivative showed extra H-bonding interactions with some of the amino acid in the access channel of the CaCYP51 pocket. All these results reflect the biological results that the extended derivatives with extra H-bonding interaction could overcome the fluconazole resistance.

Owing to the time in enzyme preparation, extraction and the costs involved only three compounds were evaluated for IC_{50}, binding affinity and selectivity against human CYP51. The research described here will be developed further through computational studies to optimise binding interactions for CaCYP51 *vs* HsCYP51 and 'design in' selectivity of extended azole inhibitors, while maintaining optimal drug like properties and to overcome the resistance of fluconazole.

Chapter III

Series II

3.1 Introduction

In the previous chapter extended azole derivatives (**18**) showed promising CaCYP51 inhibitory activity (IC$_{50}$ 0.54-0.79 μM) as well as good selectivity compared with clinically used azole antifungals. Therefore, the designed novel inhibitors **18** were used as the lead compounds for this series.

The extended azole derivatives (**18**), which were able to access the enzyme channel with an extra binding interaction through water molecule in both configurations (Figures 29 and 30), were modified and developed in this chapter (Figure 48), specifically through:

i. Substitution of the phenyl rings to explore structure-activity relationship (SAR).
ii. Reversal of the amide link
iii. Different extension linkers to investigate the binding and the fit within the CaCYP51 access channel.
iv. Shorted the chain length to the azole ring, which should eliminate formation of the alkene by-product.

This chapter is divided into 5 parts as follows:

1. Results and discussion
2. Molecular modelling
3. Biological assay
4. Molecular dynamic
5. Conclusion

3.2 Results and discussion

Novel compounds were designed by modifying the extended derivatives (**18**) as illustrated in figure 48.
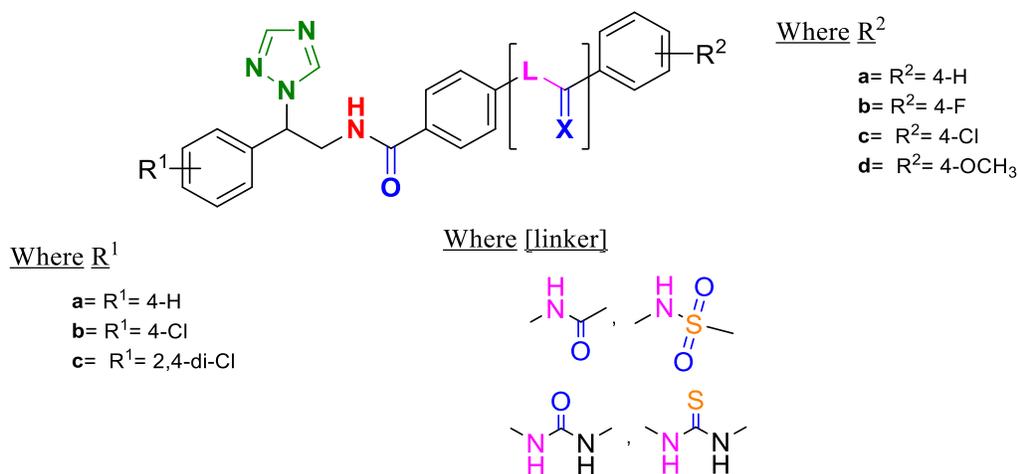
Figure 48. (*R/S*)-2-(Arylphenyl)-*N*-(4-((4-arylphenyl)amido)benzyl)-3-(1*H*-1,2,4-triazol-1-yl)propanamides derivatives

A synthetic pathway was designed for preparing the modified inhibitors.

3.2.1 Synthesis of (*R/S*)-2-(arylphenyl)-*N*-(4-((4-arylphenyl)amido)benzyl)-3-(1*H*-1,2,4-triazol-1-yl)propanamide derivatives (48, 49, 51 and 53)

• **General chemistry**

The synthesis of (*R/S*)-2-(arylphenyl)-*N*-(4-((4-arylphenyl)amido)benzyl)-3-(1*H*-1,2,4-triazol-1-yl)propanamide derivatives (**48**, **49**, **51** and **53**) was performed according to a sequence of six steps (Scheme 3.1):

❖ Boc protection of the amino group

❖ Coupling of the acid with 2-amino-1-arylphenylethan-1-ol to form the amide bond

❖ Cyclisation to form the oxazoline ring

❖ Nucleophilic ring opening with triazole

❖ Boc deprotection

❖ Extension through addition of different linkers to the amine group
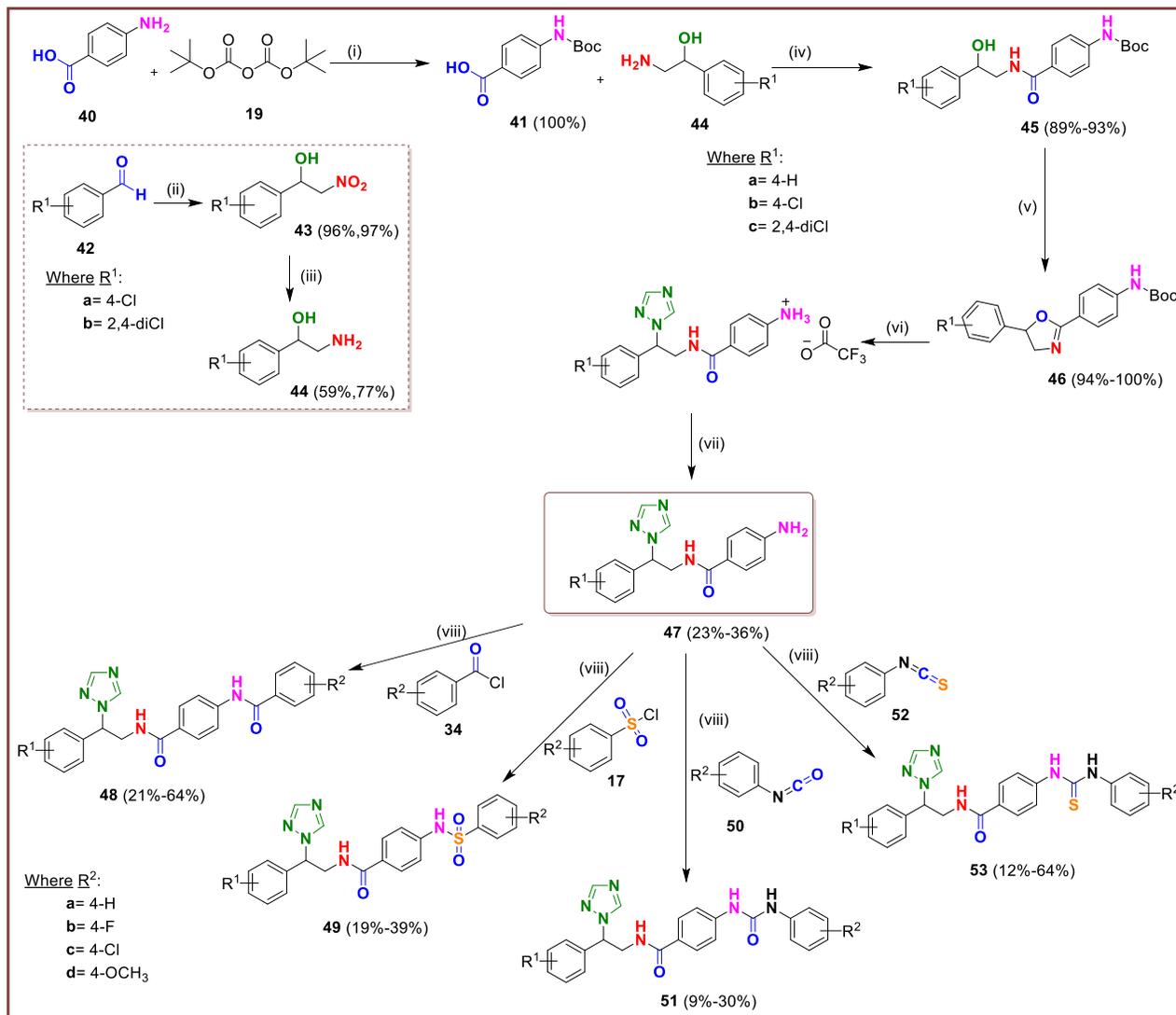
Scheme 3.1 Synthetic route for the preparation of (*R/S*)-2-(arylphenyl)-*N*-(4-((4-arylphenyl)amido)benzyl)-3-(1*H*-1,2,4-triazol-1-yl)propanamide derivatives (**48**, **49**, **51** and **53**). *Reagents and conditions:* (i) (Boc)$_2$O, H$_2$O/dioxane, Et$_3$N, rt 24 h (ii) nitromethane, AmberSep 900 (OH), rt, o/n (iii) Raney nickel (50 % slurry in H$_2$O), MeOH, formic acid under 46 psi H$_2$, 3 h (iv) CDI, DMF, rt o/n (v) MsCl, THF, rt/ 3 h then Et$_3$N, rt o/n (vi) (a) 1,2,4-triazole, 125 °C, 48 h (b) CH$_2$Cl$_2$, TFA, rt o/n (vii) 2M aq. NaOH (viii) pyridine, aryl-benzoyl chloride/aryl-benzenesulfonyl chloride/aryl-phenyl isocyanate or aryl-phenyl isothiocyanate, rt, 24 h

Synthesis of 4-((*tert*-butoxycarbonyl)amino)benzoic acid (41)[105]

4-((*tert*-Butoxycarbonyl)amino)benzoic acid **(41)** was obtained from the protection of 4-aminobenzoic acid **(40)** using (Boc)$_2$O **(19)** and Et$_3$N in water/dioxane (scheme 3.1) at rt for 24 h.

After aqueous acidification with 1N HCl and water wash ^{1}H NMR confirmed formation of the product with a characteristic N*H* singlet observed at δ 9.73 and a singlet signal for 9H at δ 1.49 for (C*H$_3$*)$_3$ of the Boc protection group. 4-((*tert*-Butoxycarbonyl)amino)benzoic acid **(41)** was obtained in quantitative yield as a white solid.

Synthesis of (*R/S*)-2-nitro-1-arylphenylethan-1-ol (43)

The synthesis of (*R/S*)-2-nitro-1-arylphenylethan-1-ol **(43)** was carried out by condensation of benzaldehyde derivatives **(46)** with nitromethane in the presence of 10 % wt/wt of AmberSep 900 (OH) at rt o/n.[94] This reaction is called the Henry reaction (nitroaldol), which is the reaction between aldehyde and nitroalkane in the present of base to form a carbon-carbon bond (β-nitro alcohol).[106]

The mechanism of this reaction involves initial deprotonation of the α-H of nitromethane by AmberSep 99 (OH). The resulting carbanion then attacks the electrophilic carbonyl carbon of formaldehyde, forming a new C-C bond.
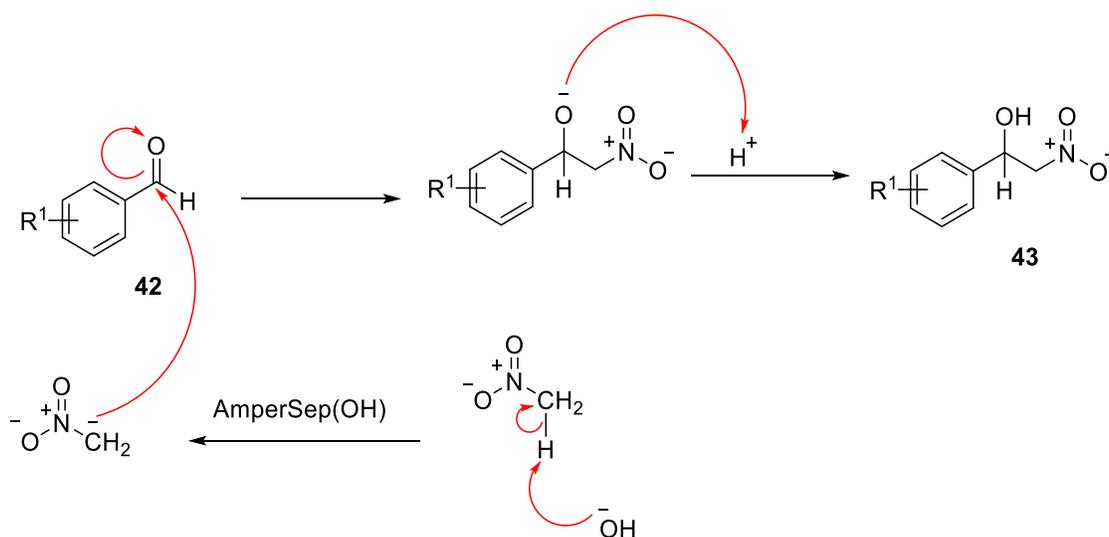
Scheme 3.1.1 Mechanism of formation of (*R/S*)-2-nitro-1-arylphenylethan-1-ol **(43)**

After aqueous work up ^{1}H NMR confirmed formation of the product with disappearance of the singlet signal of the starting material (aldehyde) and observed characteristic aliphatic signals at δ 5.28-5.56 as a pentet for C*H*CH$_a$CH$_b$, the CHC*H$_a$*C*H*$_b$ signals were observed as a doublet of doublets for each proton at δ 4.86-4.52 and a doublet signal at δ 6.18 for O*H*. Table 14 describes the physical properties, yield and melting points of (*R/S*)-2-nitro-1-arylphenylethan-1-ol derivatives (**43**).

Table 14. Yield, m.p. and physical properties of (*R/S*)-2-nitro-1-arylphenylethan-1-ol derivatives (**43**)

Compd	Yield (%)	R*f* (petroleum ether- EtOAc 3:1 v/v)	M.p.	Physical properties
43a	96	0.54	-	A pale-yellow oil
43b	97	0.63	62-64 ºC	An off-white solid

Synthesis of (*R/S*)-2-amino-1-arylphenylethan-1-ol (44)

(*R/S*)-2-Nitro-1-arylphenylethan-1-ol (**43**) was then converted to (*R/S*)-2-amino-1-phenylethan-1-ol (**44**) by catalytic hydrogenation. The nitro group of *β*-nitroalcohol derivatives (**43**) in MeOH was reduced using Raney nickel (50 % slurry in H$_2$O) and formic acid under 46 psi H$_2$ atmosphere using a Paar hydrogenator to give the corresponding amine derivatives.[94] ^{1}H NMR established the formation of the product with characteristic signals of free amine N*H$_2$* observed as a broad singlet at δ 3.31. (*R/S*)-2-Amino-1-arylphenylethan-1-ol derivatives (**44**) were obtained in good yields as shown in table 15.

Table 15. Yield, m.p. and physical properties of (*R/S*)-2-amino-1-arylphenylethan-1-ol derivatives (**44**)

Compd	Yield (%)	M.p. (°C)	Lit. M.p. (°C)	Physical properties
44a	Not synthesised as commercially available			
44b	59	72-74	(106- 110 lit)[94] (94- 95 lit)[107]	An off-white solid

44c	77	76-80	-	A pale-yellow solid

Synthesis of (*R/S*)-*tert*-butyl (4-((2-hydroxy-2-(4-arylphenyl)ethyl)carbamoyl)phenyl)carbamate derivatives (45)

(*R/S*)-*tert*-Butyl (4-((2-hydroxy-2-(4-arylphenyl)ethyl)carbamoyl)phenyl)carbamate derivatives (**45**) were obtained by coupling 4-((*tert*-butoxycarbonyl)amino)benzoic acid (**41**) with (*R/S*)-2-amino-1-arylphenylethan-1-ol (**44**) to form the amide bond using CDI as the coupling reagent in dimethylformamide at rt o/n.[94] ^{1}H NMR confirmed formation of the product with a characteristic N*H* triplet signal observed at δ 8.36 and disappearance of the broad signal of the free amine at δ 3.31. ^{13}C NMR confirmed the amide group (*C*ONH), which was observed at δ ~166.43. (*R/S*)-*tert*-Butyl (4-((2-hydroxy-2-(4-arylphenyl)ethyl)carbamoyl)phenyl)carbamate derivatives (**45**) were obtained as white solids.

Table 16. Analytical properties of (*R/S*)-*tert*-butyl (4-((2-hydroxy-2-(4-arylphenyl)ethyl)carbamoyl) phenyl)carbamate derivatives (**45**)

Compd	Yield (%)	R*f* (petroleum ether- EtOAc 1:1v/v)	M.p. (ºC)	HPLC purity
45a	93	0.48	194-196	95 %
45b	89	0.38	212-214	96 %
45c	93	0.63	198-200	96 %

As shown in Table 16, (*R/S*)-*tert*-butyl (4-((2-hydroxy-2-(4-arylphenyl)ethyl)carbamoyl)phenyl) carbamate derivatives (**45**) were obtained in excellent yield with high purity.

Synthesis of (*R/S*)-*tert*-butyl (4-(5-(arylphenyl)-4,5-dihydrooxazol-2-yl)phenyl)carbamate (46)

A solution of (*R/S*)-*tert*-butyl (4-((2-hydroxy-2-arylphenylethyl)carbamoyl)phenyl)carbamate (**45**) in dry THF was cooled to 0 °C. Then

methanesulfonyl chloride was added and the resulting mixture stirred at rt for 3 h. Et_3N was then added dropwise and the solution was stirred o/n at rt.[94]

The cyclisation to form the oxazoline ring involves initial nucleophilic attack by hydroxy with methanesulfonyl chloride with loss of HCl. Then Et_3N deprotonates the amide NH to form the enolate with subsequent displacement of the mesyl group on nucleophilic attack from the enolate anion (scheme 3.1.2).
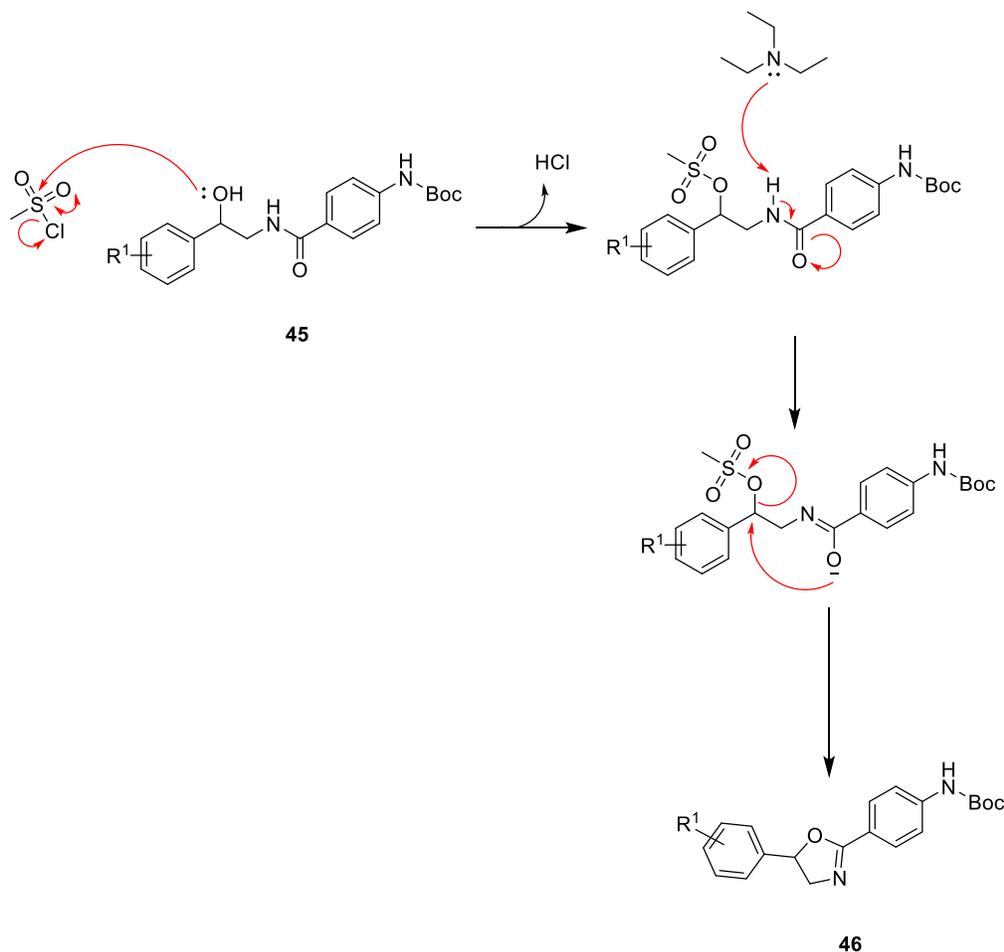
Scheme 3.1.2 Mechanism of formation of (*R/S*)-*tert*-butyl (4-(5-(arylphenyl)-4,5-dihydrooxazol-2-yl)phenyl)carbamate (**46**)

Upon completion, the mixture was quenched by the addition of NH_4OH (25%) and after an aqueous work up, ^{1}H NMR spectra confirmed formation of the product with loss of the N*H* of the amide bond at δ 3.31 as well as the O*H* doublet signal at δ 5.51 and the presence of a doublet

of doublet signals at δ ~ 5.78, 4.41 and 3.82 for each proton in the oxazoline ring. ^{13}C NMR confirmed the *C*=N (oxazole ring), which was observed at *δ* ~163.18 and the disappearance of *C*ONH at *δ* ~166.43. (*R/S*)-*tert*-Butyl (4-(5-(arylphenyl)-4,5-dihydrooxazol-2-yl)phenyl)carbamates (**46**) were obtained in very good yield, however they were found to be unstable with two compounds observed on TLC so were used in the next step without further purification.

Table 17. Yield, R*f* and physical properties of (*R/S*)-*tert*-butyl (4-(5-(arylphenyl)-4,5-dihydrooxazol-2-yl)phenyl)carbamates (**46**)

Compd	Yield (%)	R*f* (petroleum ether- EtOAc 1:1 v/v)		Physical properties
		1st spot	2nd spot	
46a	94	0.88	0.80	An off-white solid
46b	100	0.83	0.85	An orange syrup
46c	93	0.88	0.85	An orange syrup

As can be seen in Table 17, the cyclised compounds (**46**) were obtained in high yields and the R*f* of the two spots observed were very close to each other.

Synthesis of (*R/S*)-4-amino-*N*-(2-arylphenyl-2-(1*H*-1,2,4-triazol-1-yl)ethyl)benzamide derivatives (47)

The synthesis of (*R/S*)-4-amino-*N*-(2-arylphenyl-2-(1*H*-1,2,4-triazol-1-yl)ethyl)benzamide derivatives (**47**) was carried out by heating (*R/S*)-*tert*-butyl (4-(5-arylphenyl-4,5-dihydrooxazol-2-yl)phenyl)carbamates (**46**) with excess 1,2,4-triazole at 125 °C for 48 h.[94]

The mechanism of this reaction involves opening of the oxazoline ring, initiated by protonation of the nitrogen atom in the oxazoline ring with the proton of 1,2,4-triazole. Then the

deprotonated triazole attacks a carbon atom in the ring resulting in ring opening and formation of the triazole-benzamide derivatives (Scheme 3.1.3).
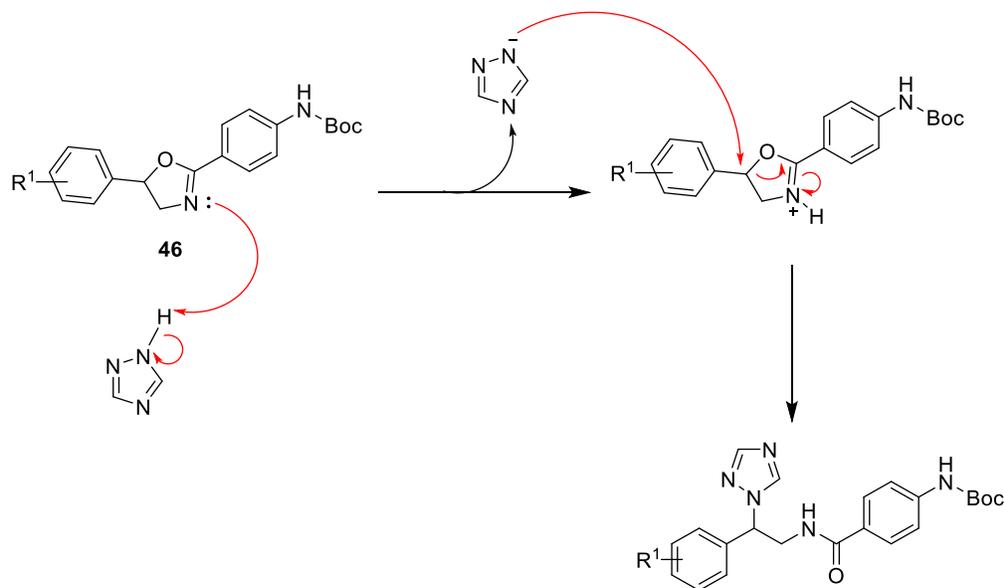
Scheme 3.1.3 Mechanism of action of oxazoline ring opening and formation of triazole-benzamide derivatives

^{1}H NMR confirmed the formation of the triazole with two singlets, characteristic of the triazole ring, observed at δ 8.72 and δ 8.01. ^{13}C NMR also confirmed the product formation by two signals observed at $δ$ ~152.08 and $δ$ ~144.52, characteristic of the *C*H of the triazole ring. Surprisingly, ^{1}H NMR also confirmed the disappearance of the singlet at δ 1.49 for 9H of (C*H$_3$*)$_3$ of the Boc protection group and the presence of a singlet integrated by two protons at δ 5.62 indicating the generation of the free amine.

The mechanism to generate the free amine could occur by protonation of the *tert*-butyl by the excess triazole, with high temperature (125 °C) and long duration (48 h) of the reaction, forming the carbamic acid. Decarboxylation with the aid of triazole in the mixture would form the free amine (Scheme 3.1.4).
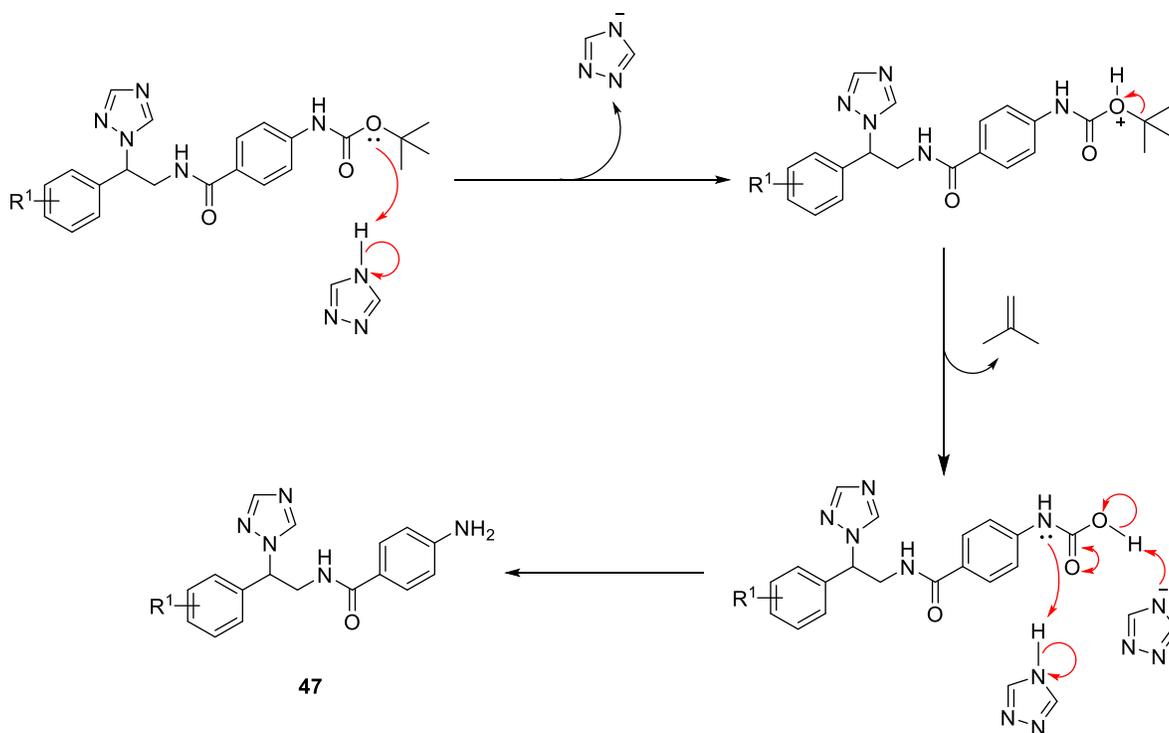
Scheme 3.1.4 Proposed mechanism of formation of (*R/S*)-4-amino-*N*-(2-arylphenyl-2-(1*H*-1,2,4-triazol-1-yl)ethyl)benzamide derivatives (**47**)

(*R/S*)-4-Amino-*N*-(2-arylphenyl-2-(1*H*-1,2,4-triazol-1-yl)ethyl)benzamide derivatives (**47**) were obtained with high purity (~96-98%) after purification by gradient column chromatography. Table 18 shows the yield, m.p., column chromatography % eluent and physical characteristics of the derivatives.

Table 18. Yield, m.p., column chromatography % eluent and physical properties of (*R/S*)-4-amino-*N*-(2-arylphenyl-2-(1*H*-1,2,4-triazol-1-yl)ethyl)benzamide derivatives (**47**)

Compd	Yield (%)	M.p. (°C)	CH₂Cl₂-MeOH (% eluent)	Physical properties
47a	23	124-126	98: 2 v/v	An off-white solid
47b	36	148-150	99: 1 to 98.5: 1.5 v/v	An off-white solid
47c	24	158-160	99: 1 v/v	A pale-yellow solid

This step proved to have a number of limitations, specifically:

Using a larger scale of starting material (1.49 g), the obtained residue was a very thick syrup that had poor solubility in ~100 mL EtOAc, resulting in a difficult extraction work up and a significant decrease in the yield e.g. for **47a** the yield decreased from 65% to 23%.

Addition of a small volume of isopropyl acetate improved the extraction work up, however the volume added must be carefully controlled as this can affect the yield.[94]

Synthesis of (*R/S*)-2-(arylphenyl)-*N*-(4-((4-arylphenyl)amido)benzyl)-3-(1*H*-1,2,4-triazol-1-yl)propanamide derivatives with different linkers (48, 49, 51 and 53)

The final compounds were obtained by stirring a solution of (*R/S*)-4-amino-*N*-(2-arylphenyl-2-(1*H*-1,2,4-triazol-1-yl)ethyl)benzamide (**47**) and aryl-benzoyl chloride (**34**)/aryl-benzenesulfonyl chloride (**17**) or aryl-phenyl isocyanate (**50**) in dry pyridine at room temperature overnight.[108] To form the thiourea compounds (**53**), (*R/S*)-4-amino-*N*-(2-arylphenyl-2-(1*H*-1,2,4-triazol-1-yl)ethyl)benzamide (**47**) was reacted with aryl-phenyl isothiocyanate (**52**) in THF and Et$_3$N and the reaction stirred at 60°C for 24 h.[109]

After aqueous work up and purification by gradient column chromatography, ^{1}H and ^{13}C NMR confirmed the formation of the product. The observed N*H* of the different linkers in ^{1}H NMR and *C*=O or *C*=S in ^{13}C NMR are presented in Table 19.

Table 19. Splitting and chemical shift of N*H*-linker and *C*=O/*C*=S of final compounds (**48**, **49**, **51** and **53**)

Compd	Linkers	^{1}H NMR N*H*	^{13}C NMR
48	**Amide**	Singlet at δ 10.28- 10.51	*C*=O at δ ~165.58
49	**Sulfonamide**	Broad singlet at δ 10.52- 10.72	-
51	**Urea**	Two singlets at δ ~8.92 and 8.73	*C*=O at δ ~152.73
53	**Thiourea**	Two singlets at δ ~9.82 and 10.02	*C*=S at δ ~179.90

All final compounds were obtained as off-white to white solids with high purity (Table 20).

Table 20. Analytical properties of novel final compounds (**48**, **49**, **51** and **53**)

Compd	R^1	R^2	Yield (%)	M.p. (°C)	HPLC purity
48a	4-H	4-H	21	248-250	99 %
48b	4-H	4-F	46	234-236	99 %
48c	4-H	4-Cl	23	236-238	97 %
48d	4-Cl	4-Cl	24	242-244	98 %
48e	2,4-diCl	4-Cl	64	194-196	98 %
48f	4-H	4-OCH$_3$	43	238-246	98 %
49a	4-H	4-H	39	200-202	99 %
49b	4-H	4-F	32	200-202	98 %
49c	4-H	4-Cl	19	186-188	99 %
49d	4-H	4-OCH$_3$	28	210-212	99 %
51a	4-H	4-H	12.4	244-246	99 %
51b	4-H	4-F	30	234-236	97 %
51c	4-H	4-Cl	26	224-226	99 %
51d	4-H	4-OCH$_3$	9	218-220	97 %
53a	4-H	4-H	18	152-154	99 %
53b	4-H	4-F	17	166-168	98 %
53c	4-H	4-Cl	59	156-158	98 %
53d	4-Cl	4-Cl	64	150-152	99 %

53e	2,4-diCl	4-Cl	18	190-192	96 %
53f	4-H	4-OCH$_3$	12	164-166	95 %

The relative low yields obtained could be owing to the free amine (**47**) being used directly without further purification, this step requires further optimisation in the future with purification of the free amine prior to reaction.

3.3 Molecular modelling

3.3.1 Wild type CaCYP51 docking studies

All the modified designed inhibitors in this chapter (Figure 48) were docked in the wild type of CaCYP51 active site to study the binding interactions between these inhibitors and the amino acids found in the CaCYP51 pocket. Figure 49 showed a superimposed between the novel extended derivatives (**18**, nude) and the modified derivatives (**48**, cyan) that both good occupy the haem pocket and having a comparable length which 'fill' the access channel of CaCYP51 active site.
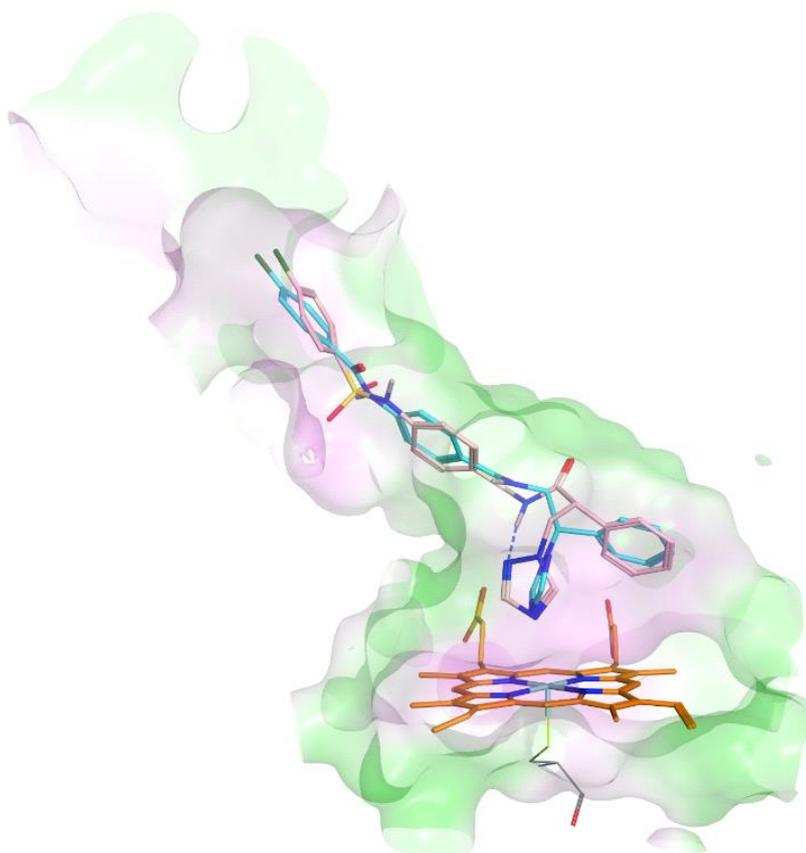
Figure 49. Extended derivative **18** (nude) and modified designed inhibitor **48** (cyan) are aligned along the hydrophobic active site of CaCYP51 enzyme cavity above the haem (orange)

All prepared azole derivatives (**48**, **49**, **51** and **53**) in both configurations were docked with the CaCYP51 protein using MOE to study the binding interactions. All the modified

compounds interacted with the haem iron of the CaCYP51 enzyme with a distance between 2.60 Å and 3.0 Å.

Four different linkers were introduced in the modified designed compounds:

A. *Amide linker derivatives:*

The amide linker compounds **48a-f** interacted by hydrophobic interactions and H-bonding interactions directly or through water molecules with different amino acid residues in the active site (Table 21).

Table 21. Key binding interactions between **48a-f** and the amino acids in the active site of CaCYP51

Compd	Distance Å	Key binding interactions	
		Direct/ or through water molecules	Hydrophobic interaction
(**R**)-**48a**	2.74 Å	Met508-OCNH (Direct interaction)	Tyr132, Gly307, Phe126, Ile131, Thr311, Phe228, Gly303, Leu121, Tyr118, Leu376, Ser507, Ser378, Phe233, Phe380, Pro230, Tyr505, His377, Tyr64
(**S**)-**48a**	2.65 Å	Met508-OCNH (Direct interaction)	Tyr132, Gly307, Phe126, Ile131, Thr311, Phe228, Gly303, Leu121, Tyr118, Leu376, Ser507, Ser378, Phe233, Phe380, Pro230, Tyr505, His377, Tyr64
(**R**)-**48b**	2.79 Å	(Leu376, Met508, Pro375, Ser507, His377)-OCNH (Through H_2O molecule)	Tyr132, Gly307, Phe126, Ile131, Thr311, Phe228, Gly303, Leu121, Tyr118, Leu88, Leu87, Ser378, Phe233, Phe380, Pro230, Tyr64
(**S**)-**48b**	2.91 Å	Met508-OCNH (Direct interaction)	Tyr132, Gly307, Phe126, Ile131, Thr311, Phe228, Gly303, Leu121, Tyr118, Leu87, Ser378, Phe233,

			Leu376, Phe380, Ser507, Pro230, His377, Tyr505, Tyr64
(*R*)-48c	2.75 Å	Met508-OCNH (Direct interaction)	Tyr132, Gly307, Phe126, Ile131, Thr311, Phe228, Gly303, Leu121, Tyr118, Leu87, Ser378, Phe233, Leu376, Phe380, Ser507, Pro230, His377, Tyr505, Tyr64
(*S*)-48c	2.76 Å	Met508-OCNH (Direct interaction)	Tyr132, Gly307, Phe126, Ile131, Thr311, Gly65, Gly303, Leu121, Tyr118, Leu87, Ser378, Phe233, Leu376, Ser506, Phe380, Ser507, Pro230, His377, Tyr505, Tyr64
(*R*)-48d	2.79 Å	(Leu376, Met508, Pro375, Ser507, His377)-OCNH (Through H$_2$O molecule)	Tyr132, Gly307, Phe126, Ile131, Thr311, Gly303, Leu121, Tyr118, Ile304, Leu87, Ser378, Phe228, Phe380, Leu88, Phe233, Pro230, Tyr505, Tyr64
(*S*)-48d	2.91 Å	Met508-OCNH (Direct interaction)	Tyr132, Gly307, Phe126, Ile131, Thr311, Gly303, Leu121, Tyr118, Ile304, Ser507, Leu87, Ser506, Leu376, Gly65, Ser378, Phe380, His377, Phe233, Pro230, Tyr505, Tyr64
(*R*)-48e	2.80 Å	Met508-OCNH, Gly303-(4-Cl) in 2,4-di-Cl phenyl ring, Tyr118- triazole ring (Direct interaction)	Tyr132, Gly307, Phe126, Ile131, Thr311, Leu121, Ile304, His377, Leu87, Thr122, Leu376, Ser378, Phe228, Phe380, Ser507, Met306, Phe233, Pro230, Tyr505, Tyr64
(*S*)-48e	2.78 Å	-	Tyr132, Gly307, Phe126, Ile131, Thr311, Gly303, Leu121, Tyr118, Ile304, Ser507, Ser506, Leu376,

			Met508, Phe228, Ser378, Phe380, His377, Phe233, Pro230, Tyr505, Tyr64
(*R*)-48f	2.91 Å	(Leu376, Met508, Pro375, Ser507, His377)-OCNH (Through H₂O molecule) and Met508-OCNH (Direct interaction)	Tyr132, Gly307, Phe126, Ile131, Thr311, Gly303, Thr122, Leu121, Ile304, Tyr118, Leu87, Ser378, Phe228, Phe380, Leu88, Phe233, Pro230, Tyr505, Tyr64
(*S*)-48f	2.93 Å	-	Tyr132, Gly307, Phe126, Ile131, Thr311, Gly303, Leu121, Ile304, Tyr118, Ser506, Leu376, Ser378, Met508, Phe380, His377, Ser507, Phe233, Pro230, Tyr505, Tyr64

The N of triazole ring interacted perpendicular with the haem iron of CaCYP51 with a distance less than 3.0 Å. An exemplar (**48c**) is shown in Figure 50, to illustrate hydrophobic interactions H-bonding interaction between Met508 and the carbonyl oxygen of the amide linker for both enantiomers.
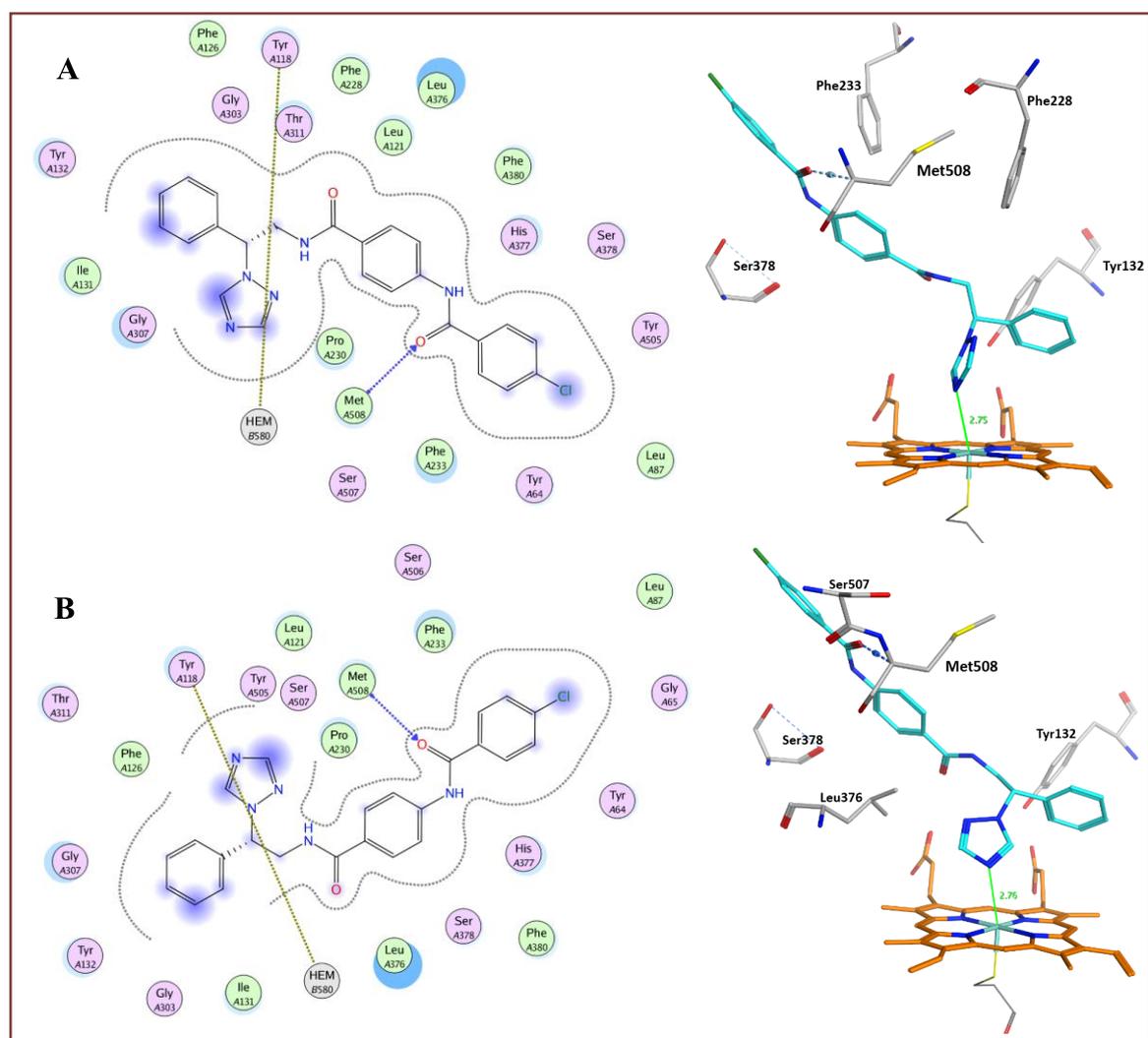
Figure 50. (A) 2D ligplot and 3D image showing key binding interactions of the (*R*)-configuration of **48c** within the CaCYP51 protein. (B) 2D ligplot and 3D image showing key binding interactions of the (*S*)-configuration of **48c** within the CaCYP51 protein

B. *Sulfonamide Linker:*

The designed inhibitors with sulfonamide linker (**49a-d**) interacted, via water molecules, with Met508, Leu376, Ser507, His377, Pro375 and the oxygen atoms of the sulfonamide linker in both configurations, as well as through hydrophobic interaction with several amino acid residues of CaCYP51 (Figure 51). In addition, a direct arene-H bond interaction was observed between Phe380 and the nitrogen atom of the sulfonamide linker in **49b** (2D ligplot, Figure 51). Furthermore, a direct H-bonding interaction between Ser378, Met508

and one of the oxygen atoms of the sulfonamide linker was seen with this derivative in the 3D image for both enantiomers (Figure 51).
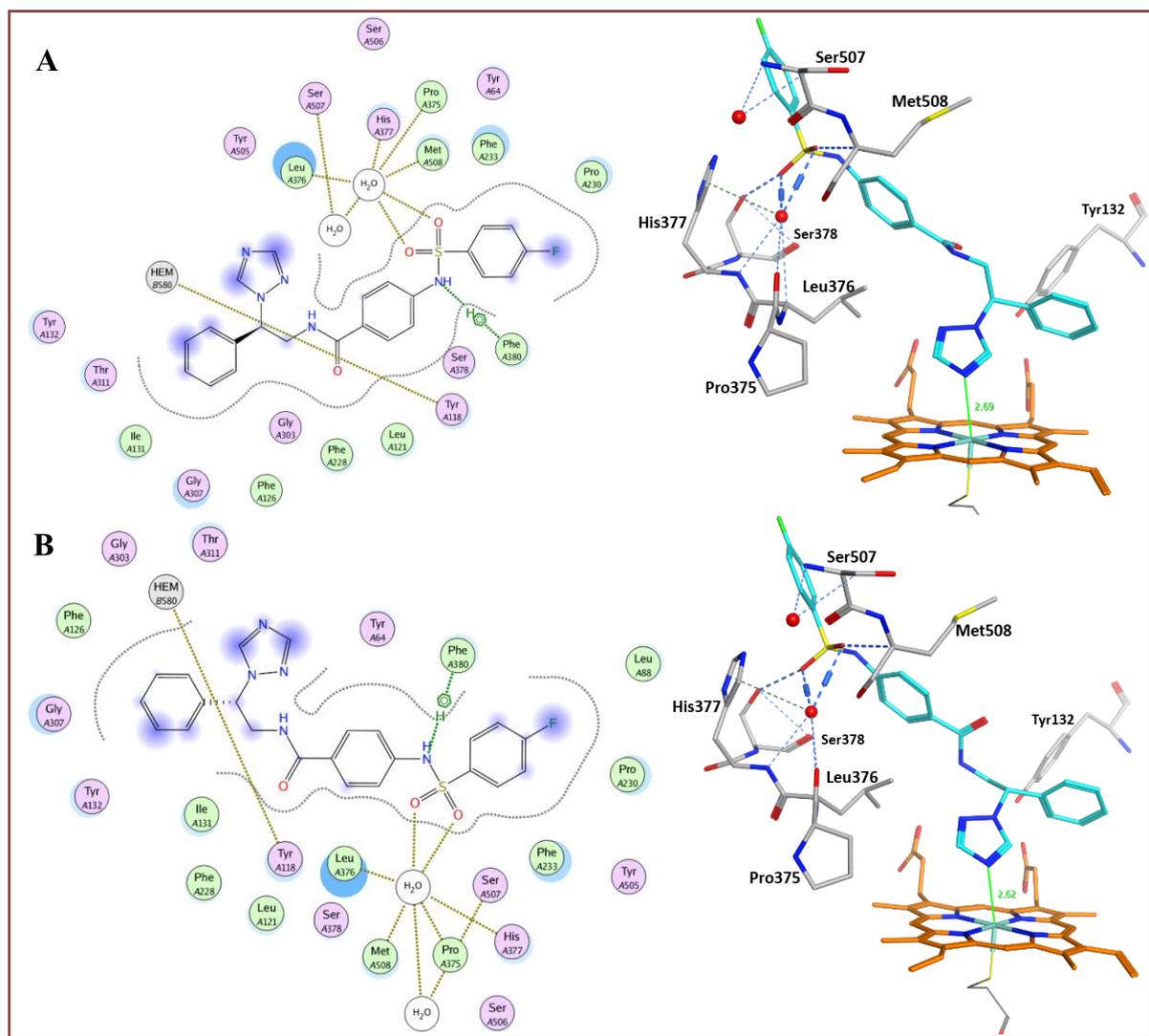
Figure 51. (A) 2D ligplot and 3D image showing key binding interactions of the (*R*)-configuration of **49b** within the CaCYP51 protein. (B) 2D ligplot and 3D image showing key binding interactions of the (*S*)-configuration of **49b** within the CaCYP51 protein

C. *Urea linker:*

The urea linked derivatives **51a-d** showed hydrophobic interactions with access channel amino acids Tyr132, Thr311, Ile131, Ile304, Gly303, Phe228, Tyr118, Tyr505, Pro230, Gly307, Ser378, Leu121, Phe126, Ser506, Phe233, Thr122, Phe380, Tyr64, Gly65, Leu87, Ala61 (see exemplar **51d**, Figure 52). In addition, water mediated hydrophobic interactions

were observed between Met508, Leu376, His377 and Pro375 with the carbonyl oxygen of the urea linker for both enantiomers. The *R*-enantiomer showed additional H-bonding interaction between Met508 and the nitrogen of the urea linker whereas the *S*-configuration showed additional H-bonding interaction between Ser378 and the nitrogen of the urea linker (3D image, Figure 52).
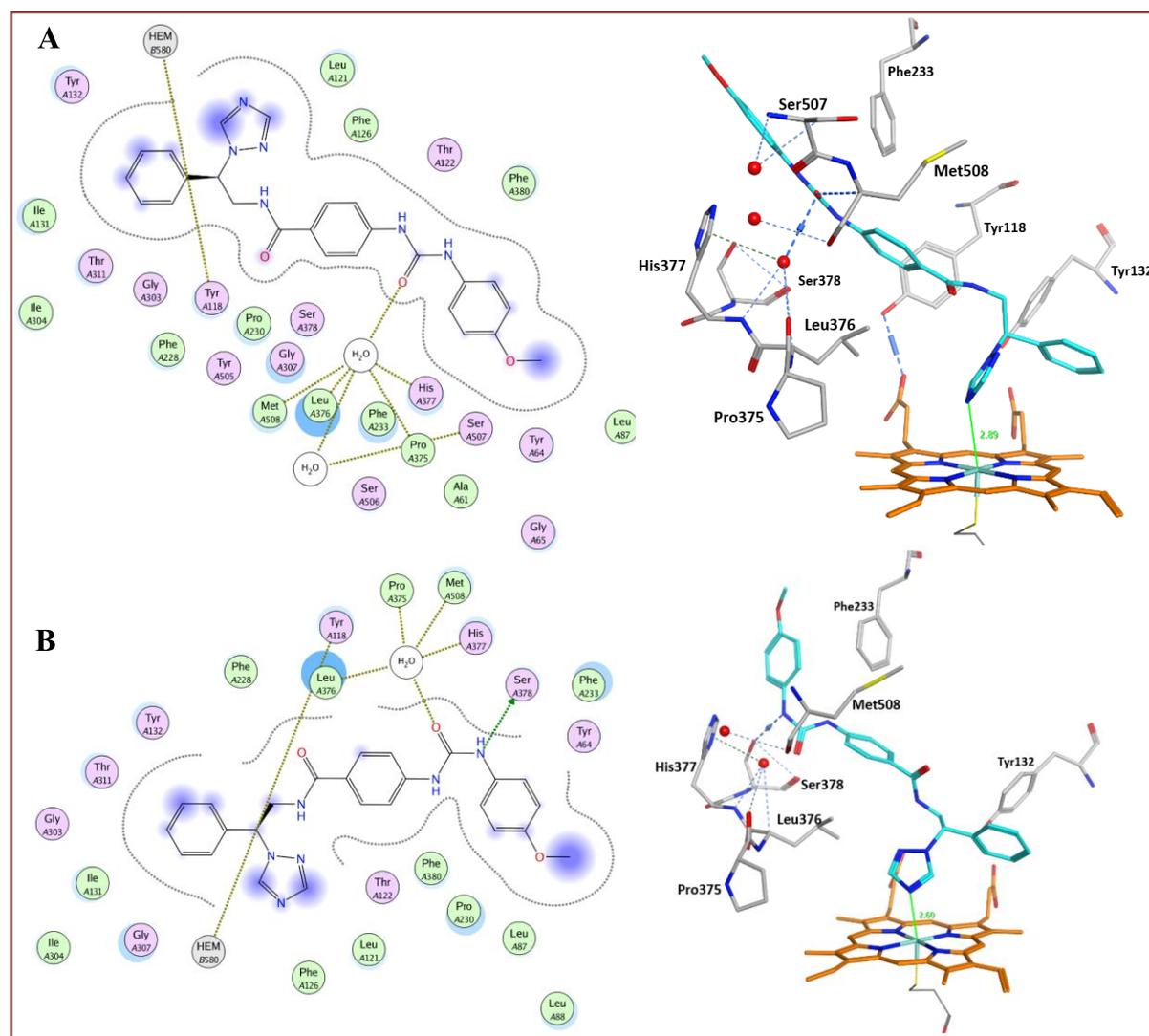
Figure 52. (A) 2D ligplot and 3D image showing key binding interactions of the (*R*)-configuration of **51d** within the CaCYP51 protein. (B) 2D ligplot and 3D image showing key binding interactions of the (*S*)-configuration of **51d** within the CaCYP51 protein

D. *Thiourea linker:*

The thiourea linked derivatives (**53a**-**f**) showed promising water mediated interactions between Met508, Leu376, His377 and Pro375 with the sulfur atom in the urea linker for both enantiomers as well as multiple hydrophobic interactions as observed for the other linkers (see exemplar **53d,** Figure 53). A direct H-bonding interaction between Ser378, Met508 and the sulfur heteroatom of the thiourea linker was also observed for the (*R*)-enantiomer whereas the (*S*)-enantiomer showed a direct H-bonding interaction between Met508 and the sulfur heteroatom of the thiourea linker (3D image, Figure 53)
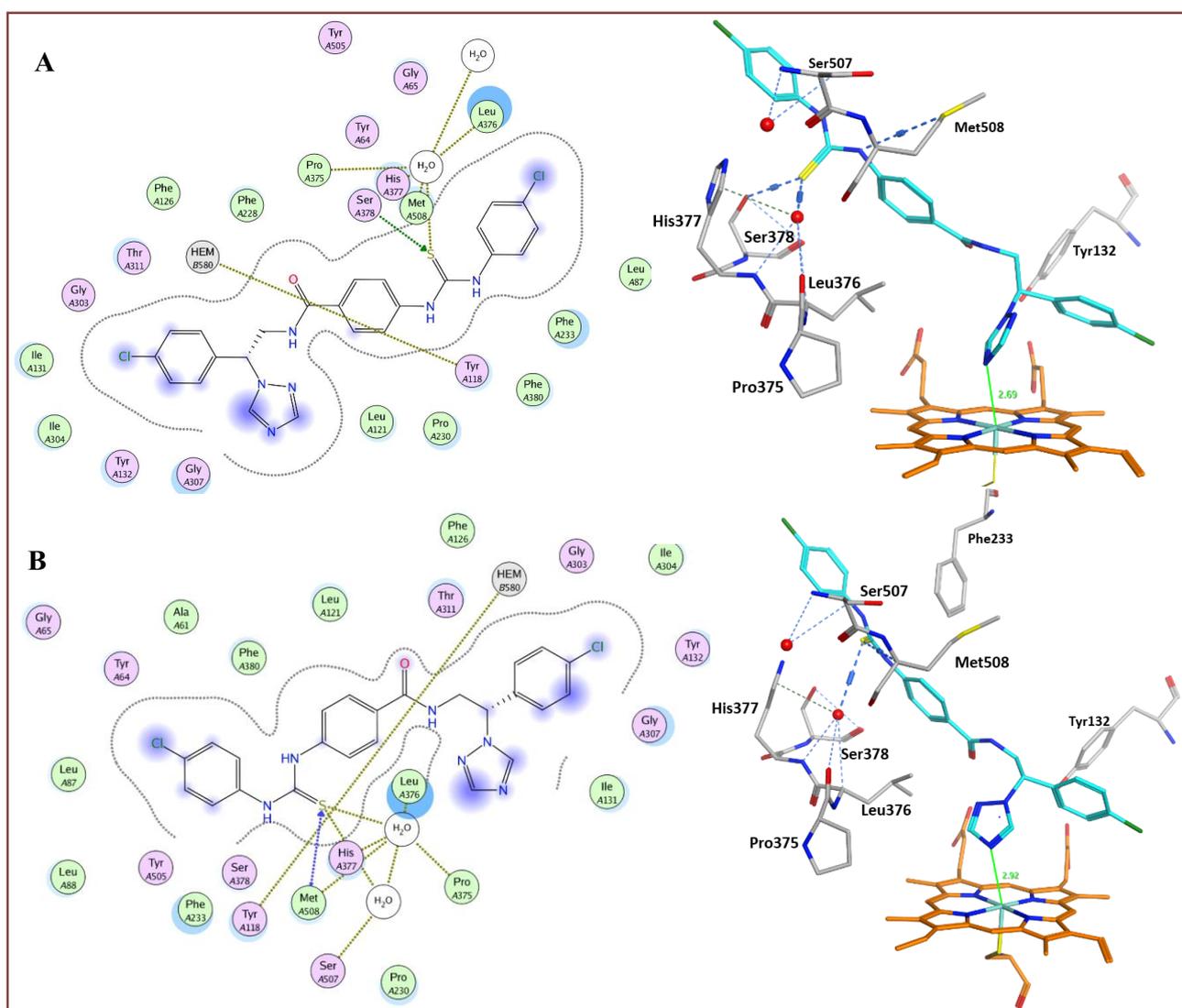
Figure 53. (A) 2D ligplot and 3D image showing key binding interactions of the (*R*)-configuration of **53d** within the CaCYP51 protein. (B) 2D ligplot and 3D image showing key binding interactions of the (*S*)-configuration of **53d** within the CaCYP51 protein

3.4 Biological assay

All final compounds were evaluated by reconstitution assays to evaluate inhibitory activity against CaCYP51, binding affinity and MIC against *C. albicans* strains at the Centre for Cytochrome P450 Biodiversity, Swansea University Medical School as previously described in chapter II. All assays were performed by Dr Josie Parker and Dr Andrew Warrilow.

3.4.1 Antifungal susceptibility testing (MIC)

The MIC test was determined for all the final derivatives in the same *C. albicans* strains (SC5314 and CA14) using the same method described in chapter II.

Table 22. MIC values for compounds against *C. albicans* SC5314 and CA14 at 48 hours
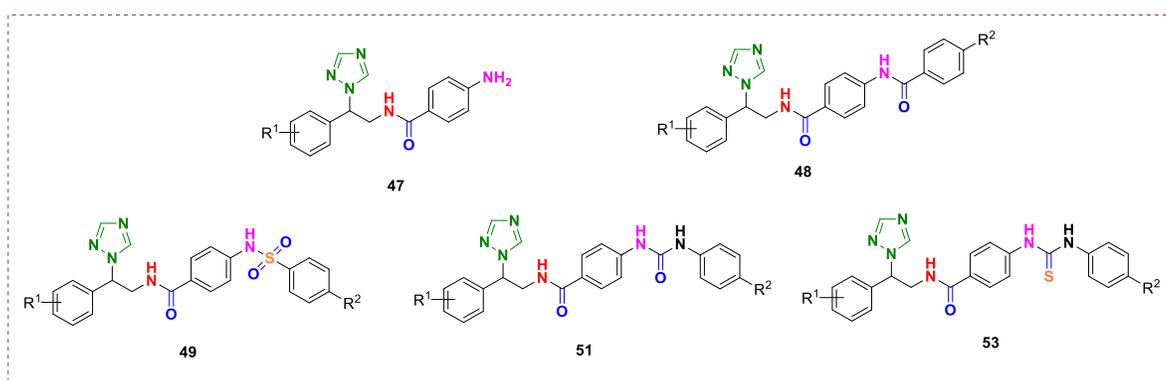
Compd	R^1	R^2	MIC (µg /mL)		cLogP^a
			SC5314	CA14	
47a	4-H	-	>16	>16	1.76
47b	4-Cl	-	>16	>16	2.32
47c	2,4-diCl	-	>16	>16	2.88
48a	4-H	H	>16	>16	3.37
48b	4-H	F	>16	>16	3.53
48c	4-H	Cl	>16	>16	3.93
48d	4-Cl	Cl	>16	>16	4.49
48e	2,4-diCl	Cl	>16	>16	5.05
48f	4-H	OCH$_3$	>16	>16	3.25

49a	4-H	H	>16	>16	2.97
49b	4-H	F	>16	>16	3.13
49c	4-H	Cl	>16	>16	3.53
49d	4-H	OCH$_3$	>16	>16	2.85
51a	4-H	H	>16	>16	3.05
51b	4-H	F	>16	>16	3.2
51c	4-H	Cl	>16	>16	3.6
51d	4-H	OCH$_3$	>16	>16	2.92
53a	4-H	H	>16	>16	4.19
53b	4-H	F	>16	>16	4.35
53c	4-H	Cl	>16	>16	4.75
53d	4-Cl	Cl	>16	>16	5.31
53e	2,4-diCl	Cl	>16	>16	5.87
53f	4-H	OCH$_3$	>16	>16	4.07
Fluconazole			0.125	0.125	0.86

^{a}cLogP was determined using Crippen's fragmentation[96]

Unfortunately, all the synthesised derivatives with different linkers were ineffective against both *C. albicans* wild type strains SC5314 and CA14 (MIC > 16 µg/mL). Although the lipophilicity (cLogP) of the compounds is good (e.g. **48c**, cLogP= 3.93; **49b**, cLogP= 3.13; **51d**, cLogP= 2.92; **53c**, cLogP= 4.75), which could help the compounds to penetrate the cell membrane of *C.albicans*. The linker groups (amide, sulfonamide, urea, thiourea) with additional H-bond donor/acceptor properties may be susceptible to efflux or the compounds may not enter the cells but might be there is a chance to bind with CaCYP51. To determine whether binding with CaCYP51 occurs, the chloro derivatives were evaluated further for IC$_{50}$ and K_d vs CaCYP51.

3.4.2 IC$_{50}$ determination and CaCYP51 ligand binding affinity

The IC$_{50}$ and binding affinity (K_d) determination were performed as described in chapter II for the chloro substituted derivatives (Table 23).

Table 23. IC$_{50}$ and K_d values for novel compounds compared with **18c** and fluconazole against CaCYP51
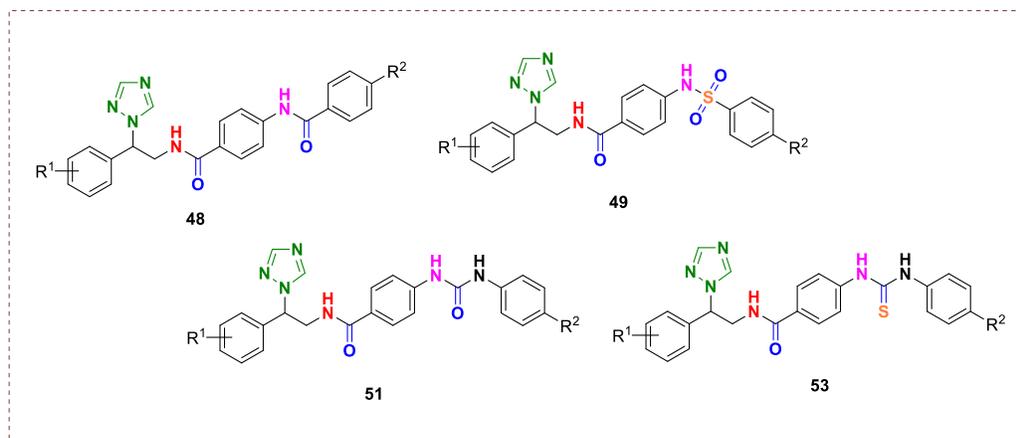
Compd	R^1	R^2	CaCYP51 IC$_{50}$ (μM)	K_d (nM)
48c	4-H	Cl	4.6	nd
48d	4-Cl	Cl	1.3	78[a]
48e	2,4-diCl	Cl	nd	1331[a]
49c	4-H	Cl	nd	nd
51c	4-H	Cl	nd	nd
53c	4-H	Cl	6.2	nd
53d	4-Cl	Cl	nd	749[a]
53e	2,4-diCl	Cl	nd	185[a]
18c			0.33	43 ± 18
Fluconazole			0.31	41 ± 13

[a] binding affinity only done in one replicate, nd= no data.

CaCYP51 IC$_{50}$ was determined for **48c**, **49c**, **51c** and **53c**, compounds **48c** (R^1 = 4-H, R^2 = Cl) and **53c** (R^1 = 4-H, R^2 = Cl) showed some inhibition with IC$_{50}$ 4.6 μM and 6.2 μM respectively compared with fluconazole (IC$_{50}$ 0.31 μM) and **18c** (IC$_{50}$ 0.33 μM). However,

compounds **49c** (R^1 = 4-H, R^2 = Cl) and **51c** (R^1 = 4-Cl, R^2 = Cl) did not show any inhibitory activity (Table 23 and Figure 54).
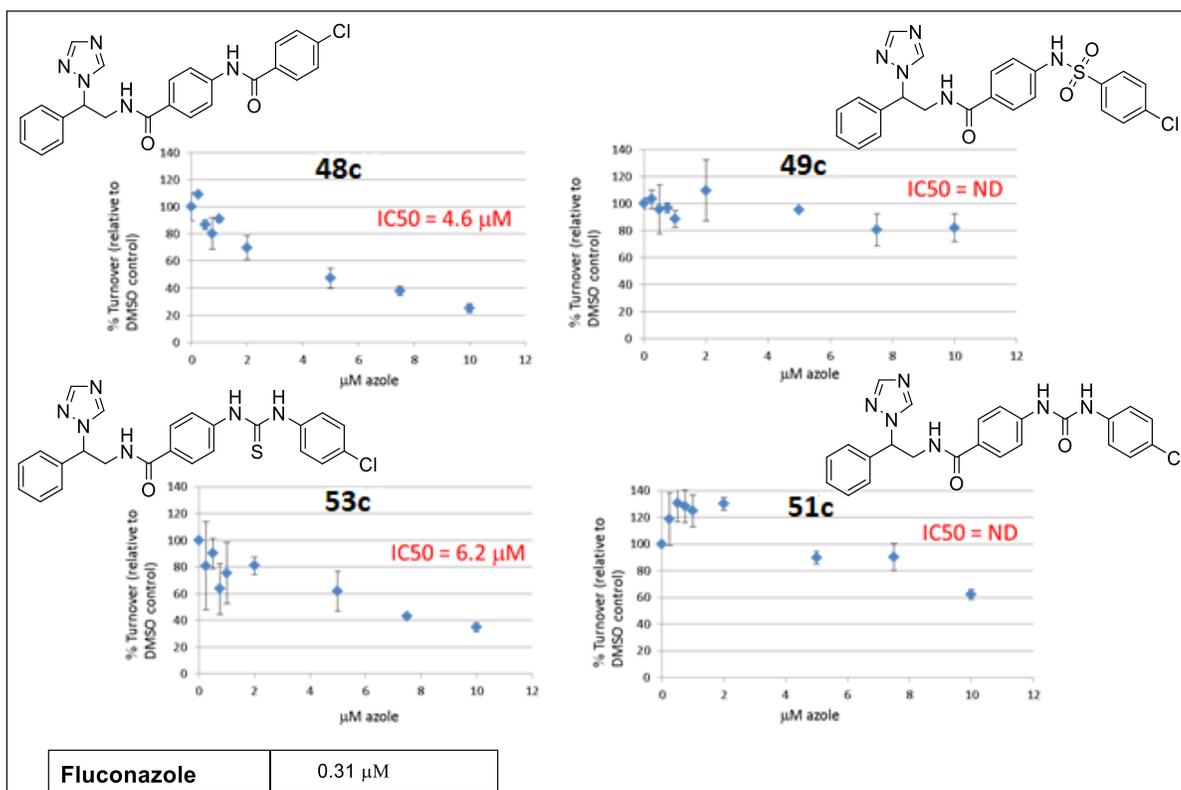
Figure 54. IC$_{50}$ (μM) for four synthesised compounds compared with fluconazole as a reference inhibitor of *C. albicans* CYP51

As some CaCYP51 inhibition was observed for the chloro derivatives **48c** with an amide linker and **53c** with a thiourea linker; the binding affinity (K_d) was obtained for **48d**, **48e**, **53d** and **53e**. Compound **48d** (R^1 = 4-Cl, R^2 = Cl) with K_d = 78 nM was better than **53d** (R^1 = 4-Cl, R^2 = Cl) with K_d = 749 nM, whereas **48e** (R^1 = 2,4-diCl, R^2 = Cl) with K_d = 1331 nM was less effective than **53e** (R^1 = 2,4-diCl, R^2 = Cl) with K_d = 185 nM (Figure 55 and 56). Binding data would indicate for **48e**, **53d**, and **53e** the azoles do not bind. Compound **48d** (R^1 = 4-Cl, R^2 = Cl) with K_d = 78 nM was evaluated further to determine IC$_{50}$ and it showed some inhibitory activity against CaCYP51 (IC$_{50}$ = 1.3 μM). Although the binding affinity of **48d** was close to fluconazole and **18c**, the IC$_{50}$ (1.3 μM) was not comparable, suggesting that **48d** may not be able to displace the natural substrate lanosterol however sterol profiles could give a better understanding. The high MIC may also be due to other factors such as efflux system.
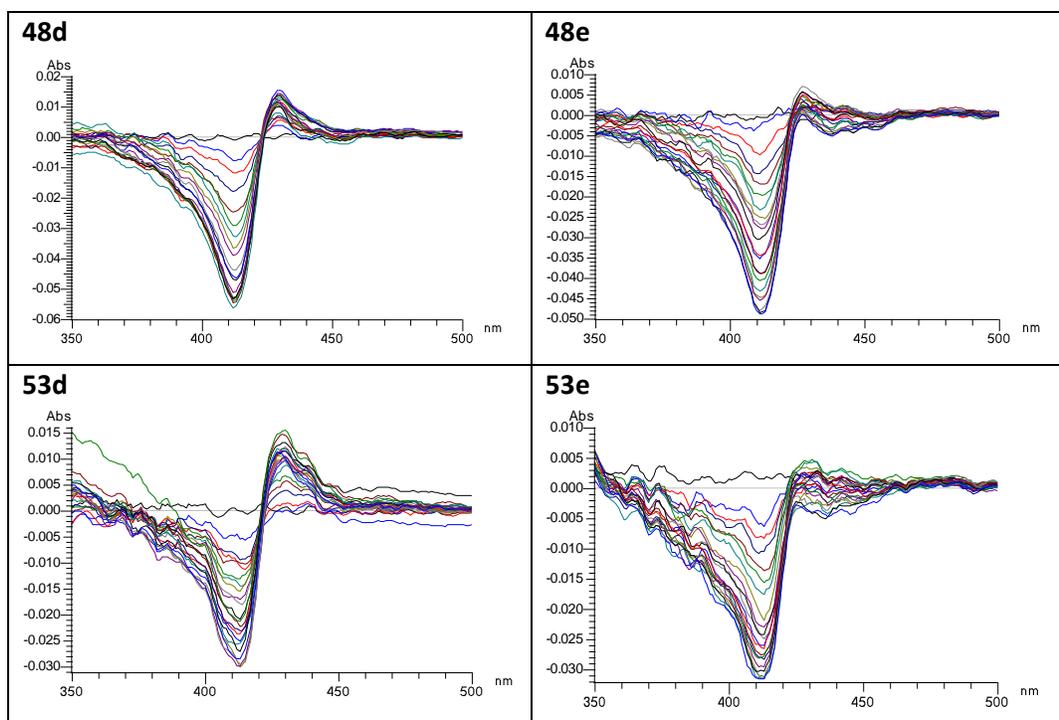
Figure 55. Azole binding difference spectra. Type II difference spectra obtained during the progressive titration of 5 μM CaCYP51 with compounds **48d**, **48e**, **53d** and **53e** are shown. Each azole titration was performed once, the ligand saturation curves for these difference spectra are shown in figure 56
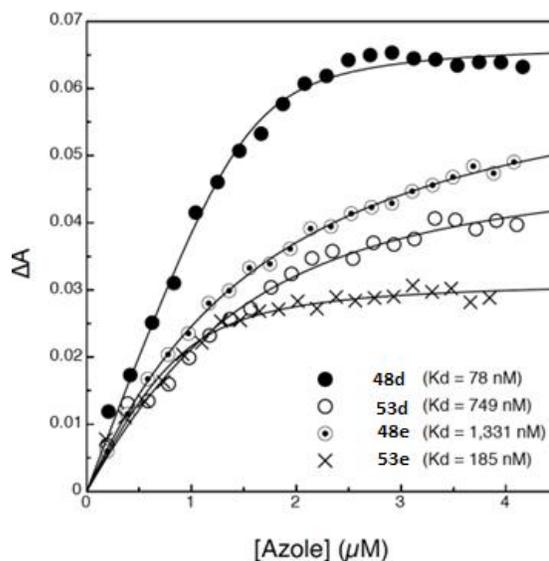
Figure 56. CYP51 azole saturation curves. Ligand binding saturation curves derived from the type II difference spectra in figure 55 are shown for compounds **48d** (●), **48e** (◉), **53d** (○) and **53e** (✕) with 5 μM CaCYP51. Each azole titration was performed once

3.5 Molecular dynamic (MD) simulations

3.5.1 Wild type docking

For further investigation of the binding modes of derivative **48d**, the best ligand pose was chosen for both configurations, and molecular dynamics simulations were run for 100 ns using the CaCYP51 crystal structure (PDB 5FSA)[35], using the Desmond programme of Maestro.[102] The novel compound in both configurations formed a coordinate bonding interaction between the triazole N and the haem Fe^{3+}. The (*R*)-enantiomer for **48d** formed water mediated H-bonding interactions between Tyr132, Ser378 and the amide NH group, also a direct H-bonding interaction with Met508 and NH atom of the amide group, and a hydrophobic interaction with Ile131. The (*S*)-enantiomer formed a water mediated H-bonding interaction between Ser378 and the amide NH group and hydrophobic interactions with Ile131, Pro230 and Met508. Furthermore, the water mediated H-bonding interaction between Tyr132, and the amide NH group shown in the (*R*)-enantiomer was not observed for the (*S*)-enantiomer (Figure 57).

Compound **48d** did show binding affinity (K_d= 78 nM) and further evaluation of sterol profiles will be performed by our collaborators at Swansea University.
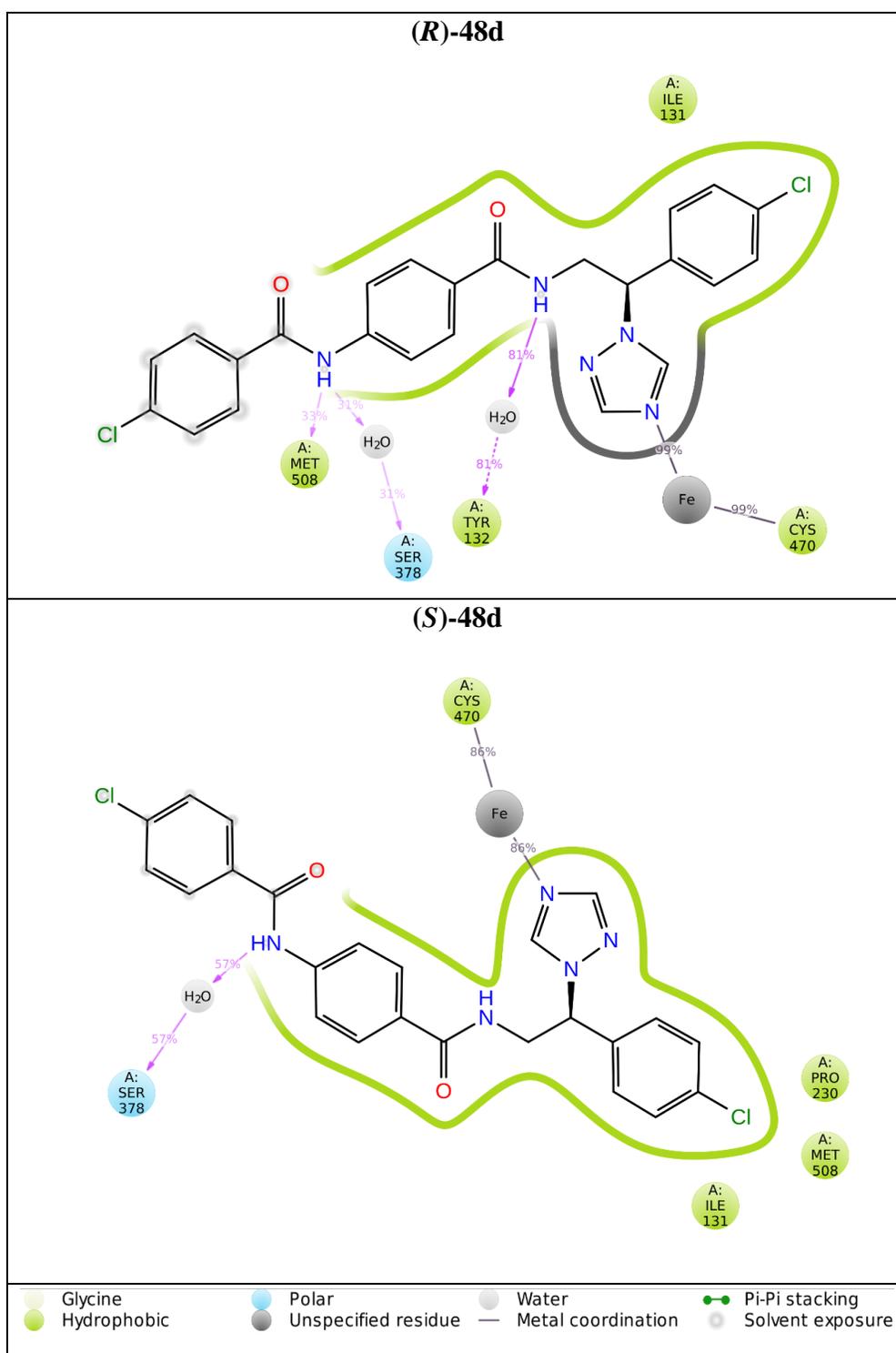
Figure 57. A schematic of detailed ligand atom interactions of representative (*R*)- and (*S*)-enantiomers of **48d** with the amino acids of CaCYP51 protein. Interactions that occur more than 30.0% of the simulation time in the selected trajectory (0 through 100 ns) are shown

3.6 Conclusion

The final modified extended derivatives with different linkers (**48**, **49**, **51** and **53**) were designed, synthesised and investigated for CaCYP51 inhibitory activity, binding affinity, and MIC against *C. albicans* strains.

Computational docking studies were performed for all final compounds investigated to determine binding interaction within the CaCYP51 protein using the CaCYP51 crystal structure co-crystalized with posaconazole (PDB 5FSA)[35]. All the compounds filled the haem and access channel sites with coordination interaction between the triazole heteroatom and the haem Fe^{3+} with good distance (< 3.0 Å) and the length of the modified compounds was comparable with the extended derivatives (**18**).

The modified extended derivatives **48**, **49**, **51** and **53** filled the access channel of CaCYP51 and interacted through water molecules with Leu376, Met508, Pro375, His377 and the amide heteroatoms as well as hydrophobic interactions within the CaCYP51 protein.

The synthesis of the final compounds with different linkers was successfully achieved with pure compounds and reasonable yield, after several trials, via five synthetic steps. All final compounds were $\geq 95\%$ pure.

All the novel compounds were ineffective against *C. albicans* strains with MIC > 16 µg/mL. An additional chloro atom showed a small improvement in the IC_{50}, for example **48c** (R^1= 4-H, R^2= Cl, $IC_{50} = 4.6$ μM) compared with **48d** (R^1= 4-Cl, R^2= Cl, $IC_{50} = 1.3$ μM), but they were much less effective than fluconazole suggesting the compounds may interact at another site within the enzyme pocket. Regarding the K_d results there was weak binding affinity to the CaCYP51 enzyme that could suggest:

- The design for these compounds is not optimal for CaCYP51 even through docking showed good results, however computational studies are limited.
- The rigidity of the designed structures lacking the CH_2 before the triazole ring removed the complication of the alkene by-product, however this also led to loss of the antifungal activity against *C. albicans*.
- The reversal of the amide group (Figure 48) of the extended derivatives (**18**) could affect the activity against CaCYP51.

All the results obtained from these studies will be considered in the design of selective CaCYP51 inhibitors.

Chapter IV

Series III

4.1 Introduction

The novel inhibitors in this chapter were designed to maximise access and fill of the hydrophobic channel of CaCYP51, through additional H-bonding interaction in CaCYP51 binding sites, to circumvent antifungal resistance shown with fluconazole.

The designed compounds were modified by introducing a linker into the 'long arm' of the "Y-shape" derivative that may lead to optimal fitting within the haem area of the active site while maximising the occupancy in the access channel (Figure 58).

Where R¹:

a= 4-Cl
b= 2,4-diCl

Where Linker:
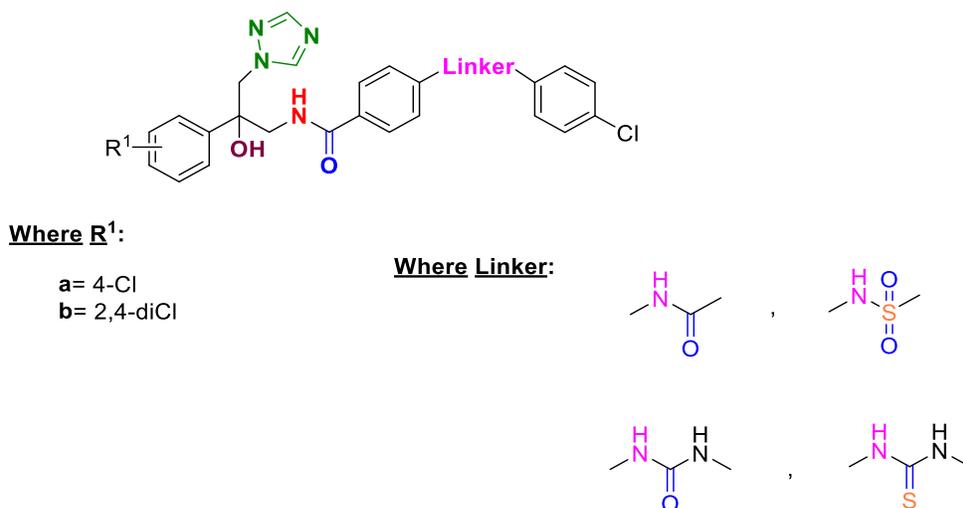
Figure 58. (*R/S*)-*N*-(2-(Arylphenyl)-2-hydroxy-3-(1*H*-1,2,4-triazol-1-yl)butanamide derivatives

This chapter is divided into 5 parts as follows:

1. Molecular modelling
2. Result and discussion
3. Biological assay
4. Molecular dynamic
5. Conclusion

4.2 Molecular modelling

4.2.1 Wild type docking

The designed compounds were docked using the MOE programme in both (*R*)- and (*S*)-configurations to study the binding interaction in the CaCYP51 protein. Docking results showed that the N atom of triazole ring interacted perpendicular with the haem iron with a distance < 3.0 Å.

Figure 59. (A) 2D ligplot and 3D image showing key binding interactions of the (*R*)-configuration of an exemplar of the new series in the CaCYP51 protein. (B) 2D ligplot and 3D image showing key binding interactions of the (*S*)-configuration of an exemplar of the new series in the CaCYP51 protein

Both (*R*)- and (*S*)-configurations showed water mediated interactions with Met508, Leu376, Ser507, His377 and Pro375 and the oxygen of the sulfonamide linker as well as hydrophobic interactions with several amino acid residues (Figure 59). In addition, a direct H-bonding interaction between Phe380 and the phenyl ring of the (*R*)-configuration was observed, while for the (*S*)-enantiomer a H-arene binding interaction between Tyr118 and the CH_2 adjacent to amide linker was formed.

4.2.2 Mutant strains docking

The novel compounds in both configurations were docked using MOE to study the binding interactions in a mutant strain of *C. albicans,* (Y132H+K143R) CaCYP51. Figure 60 shows an example of the new azole derivatives compared with the wild type docking (Figure 59).

The (*R*) and (*S*)- configurations in the mutant strain formed a water mediated H-arene binding interaction between the phenyl ring and Leu376, Met508, His377, Ser507 (Figure 60) compared with the wild type, which formed a water mediated interaction with the oxygen of the sulfonamide linker (figure 59). The (*R*) enantiomer also formed an additional H-bond between Ser378 and N atom of sulfonamide group and between Met508 and the N heteroatom of the amide linker in the mutant CaCYP51 protein.

In the (*S*)-enantiomer a direct H-arene interaction was observed between His377 and the N atom of the sulfonamide group and also a direct H-bonding interaction between Met508 and the phenyl ring (Figure 60).
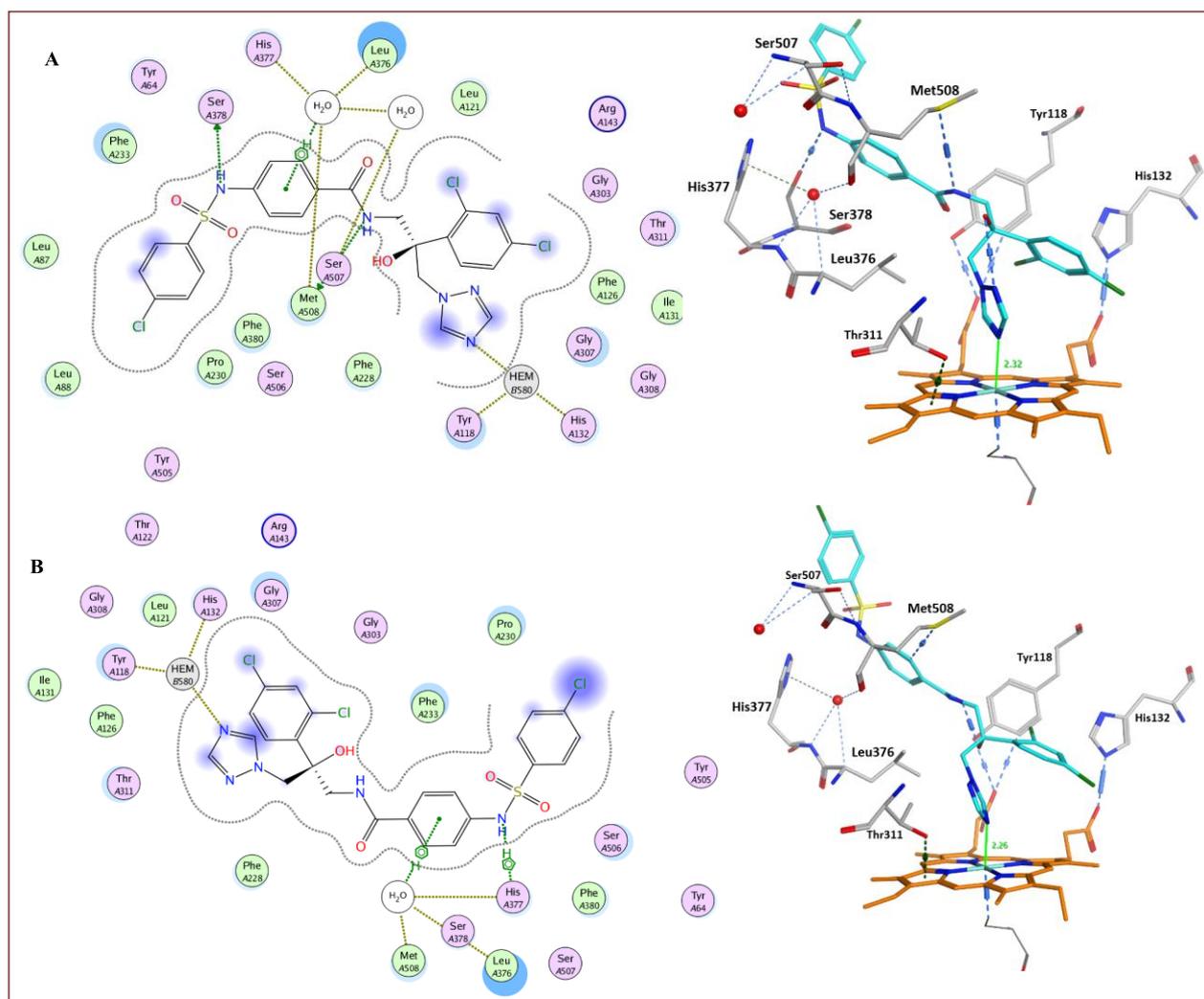
Figure 60. (A) 2D ligplot and 3D image showing key binding interactions of the (*R*)-configuration of a representative derivative of the new series in the mutant strain (Y132H+K143R) CaCYP51. (B) 2D ligplot and 3D image showing key binding interactions of the (*S*)-configuration of a representative derivative of the new series with the protein residues of mutant strain (Y132H+K143R) CaCYP51 protein

4.3 Result and discussion

Following the promising results obtained from the docking studies, synthetic pathways were designed to achieve the desired novel compounds.

4.3.1 Synthesis of *N*-(2-hydroxy-2-phenyl-3-(1*H*-1,2,4-triazol-1-yl)propyl)benzamide (57)

N-(2-Hydroxy-2-phenyl-3-(1*H*-1,2,4-triazol-1-yl)propyl)benzamide   (**57**)   was synthesised as illustrated in scheme 4.1.
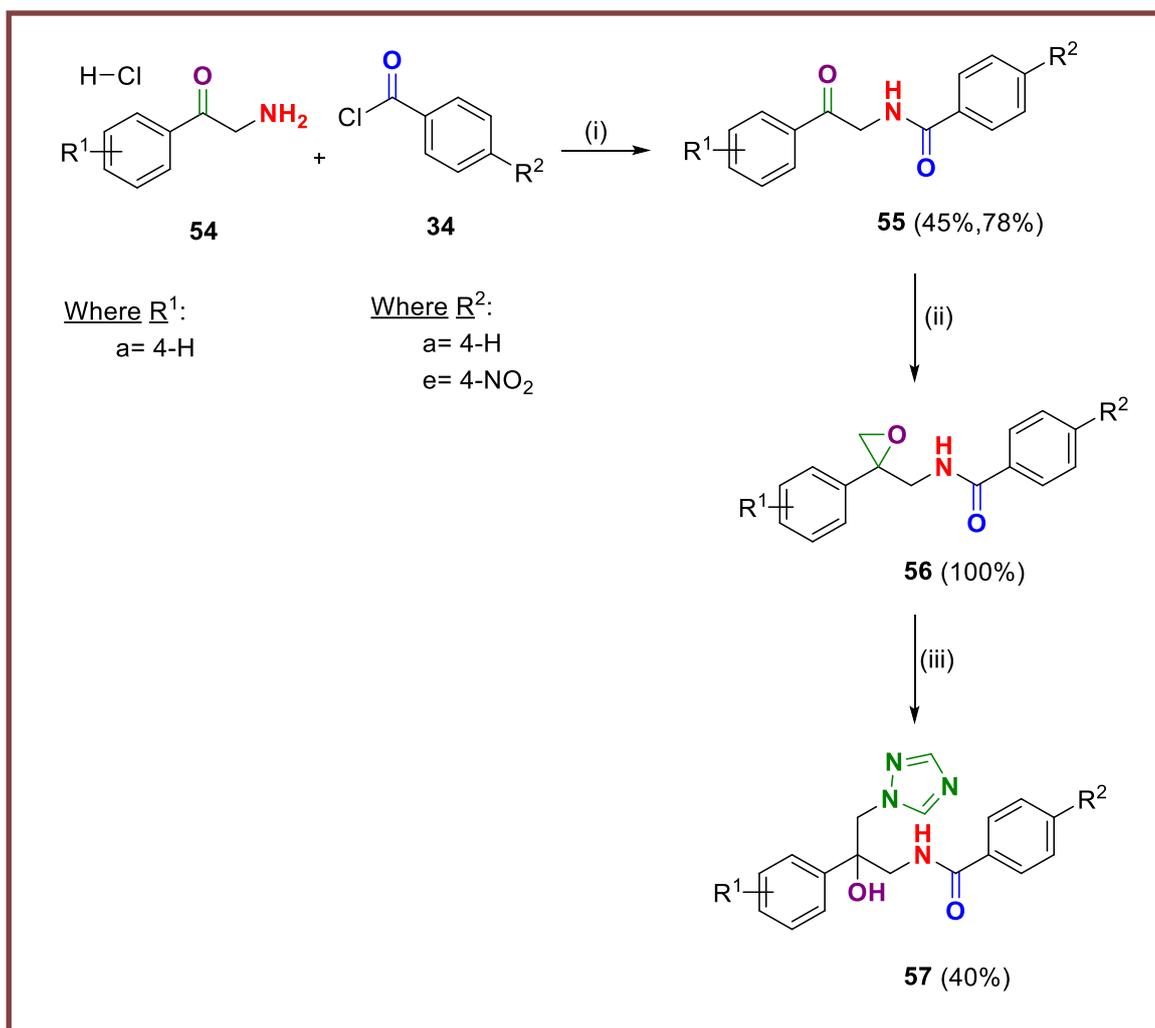
Scheme 4.1 Synthetic route for the preparation of (*R/S*)-*N*-(2-hydroxy-2-phenyl-3-(1*H*-1,2,4-triazol-1-yl)propyl)benzamide (**57**). *Reagents and conditions:* (i) CH_2Cl_2, sat. aqueous $NaHCO_3$, rt, 2 h (ii) Trimethylsulfoxonium iodide (TMSOI), 20% NaOH, toluene, 60 °C, 4 h (iii) (a) K_2CO_3, triazole, CH_3CN, 45 °C, 1 h (b) **56**, 70 °C, 24 h

Synthesis of *N*-(2-oxo-2-phenylethyl)benzamide derivatives (55)

To prepare *N*-(2-oxo-2-phenylethyl)benzamides (**55**) aminoacetophenone hydrochloride (**68**) was added to a cooled solution of benzoyl chloride (**34**) in CH_2Cl_2 and saturated aqueous $NaHCO_3$ and the mixture was stirred for 2 h at room temperature.[110]

Upon completion and aqueous work up, ^{1}H NMR confirmed the formation of product with characteristic N*H* triplet signal at δ 8.87.

Table 24. Yield, m.p. and physical properties of *N*-(2-oxo-2-phenylethyl)benzamide derivatives (**55**)

Compd	Yield (%)	M.p. (°C)	Lit. M.p. (°C)	Physical properties
55a	45	116-118	124-125.5[110]	White crystals from CH_3CN
55b	78	188-190	-	White fluffy solid

Synthesis of (*R/S*)-*N*-((2-phenyloxiran-2-yl)methyl)benzamide (56a)

N-(2-oxo-2-phenylethyl)benzamide (**55**) was then converted to (*R/S*)-*N*-((2-phenyloxiran-2-yl)methyl)benzamide (**56a**) by dissolving *N*-(2-oxo-2-phenylethyl)benzamide (**55**) in toluene and trimethylsulfoxonium iodide (TMSOI) added, followed by the addition of 20% NaOH aqueous solution. The reaction mixture was then heated at 60 °C for 4 h.[111]

The reaction is a Corey-Chaykovsky epoxidation using TMSOI (Corey-Chaykovsky reagent),[112] which on treatment with base generates an ylide. The mechanism involves the generation of ylide in the present of NaOH base, which then acts as a nucleophile towards the carbonyl compound. The resulting oxygen anion reacts as an intramolecular nucleophile toward the new electrophilic ylide carbon, which bears a sulfonium cation as a good leaving group (Scheme 4.1.1).
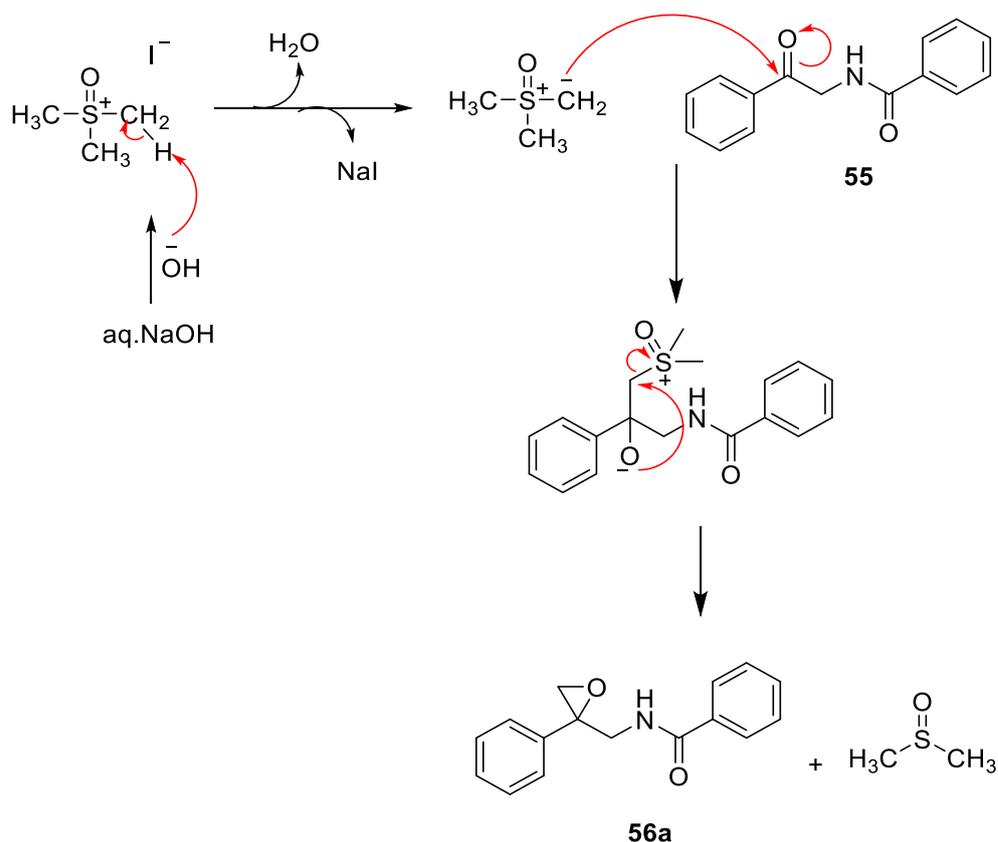
Scheme 4.1.1 Mechanism of formation of (*R/S*)-*N*-((2-phenyloxiran-2-yl)methyl)benzamide (**56a**)

After disappearance of starting material as monitored by TLC, an aqueous work up was done however ^{1}H NMR indicated a complex mixture.

A modification in this method used CH_2Cl_2 as solvent and 48% aqueous NaOH[112] and this was applied by stirring a solution of *N*-(2-oxo-2-phenylethyl)benzamide (**55a**) in CH_2Cl_2 with TMSOI and 48% NaOH aqueous solution at 48 °C for 48 h.[113] After aqueous work up, ^{1}H NMR confirmed the formation of the epoxide ring with characteristic C*H$_2$* doublet at δ 3.05 and δ 2.78 for each proton of the epoxide ring and ^{13}C NMR indicated disappearance of the quaternary carbonyl carbon of **55a** at δ 195.81 and the presence of a new signal at δ 59.23 for the quaternary carbon of the epoxide ring. (*R/S*)-*N*-((2-Phenyloxiran-2-yl)methyl)benzamide (**56a**) was obtained in quantitative yield as a pale-orange semi-solid, which was used in the next step without further purification.

Attempts to prepare the epoxide of the nitro derivative, (*R/S*)-4-nitro-*N*-((2-phenyloxiran-2-yl)methyl)benzamide (**56b**) was unsuccessful. This was studied by increasing the reaction duration, but the same result was obtained.

Synthesis of (*R/S*)-*N*-(2-hydroxy-2-phenyl-3-(1*H*-1,2,4-triazol-1-yl)propyl)benzamide (57a)

The synthesis of (*R/S*)-*N*-(2-hydroxy-2-phenyl-3-(1*H*-1,2,4-triazol-1-yl)propyl)benzamide (**57a**) was performed by the addition of a triazole ring to (*R/S*)-*N*-((2-phenyloxiran-2-yl)methyl)benzamide (**56a**) in the present of K_2CO_3 in dry CH_3CN and heated for 24 h at 70 °C.[86]

After aqueous work up, the crude product was purified by gradient column chromatography, ^{1}H NMR had the two singlets characteristic of the triazole ring at δ 8.20 and δ 7.84 and singlet at δ 6.02 for O*H*. ^{13}C NMR also confirmed the product formation by two signals observed at *δ* 150.97 and *δ* 145.39, characteristic of *C*H triazole ring. (*R/S*)-*N*-(2-Hydroxy-2-phenyl-3-(1*H*-1,2,4-triazol-1-yl)propyl)benzamide (**57a**) was obtained as an off-white solid.

The unsubstituted compound (**57a**, $R^1 = R^2 = $ 4-H) was synthesised to optimise the method since the starting material was commercially available and relatively cheap. The unsubstituted derivative (**57a**) is comparatively the same length as fluconazole with similar occupancy of the haem area of CaCYP51, which may not overcome the fluconazole resistance. Therefore, having optimised the method, this was then applied to the preparation of chloro-substituted derivatives (Scheme 4.2).
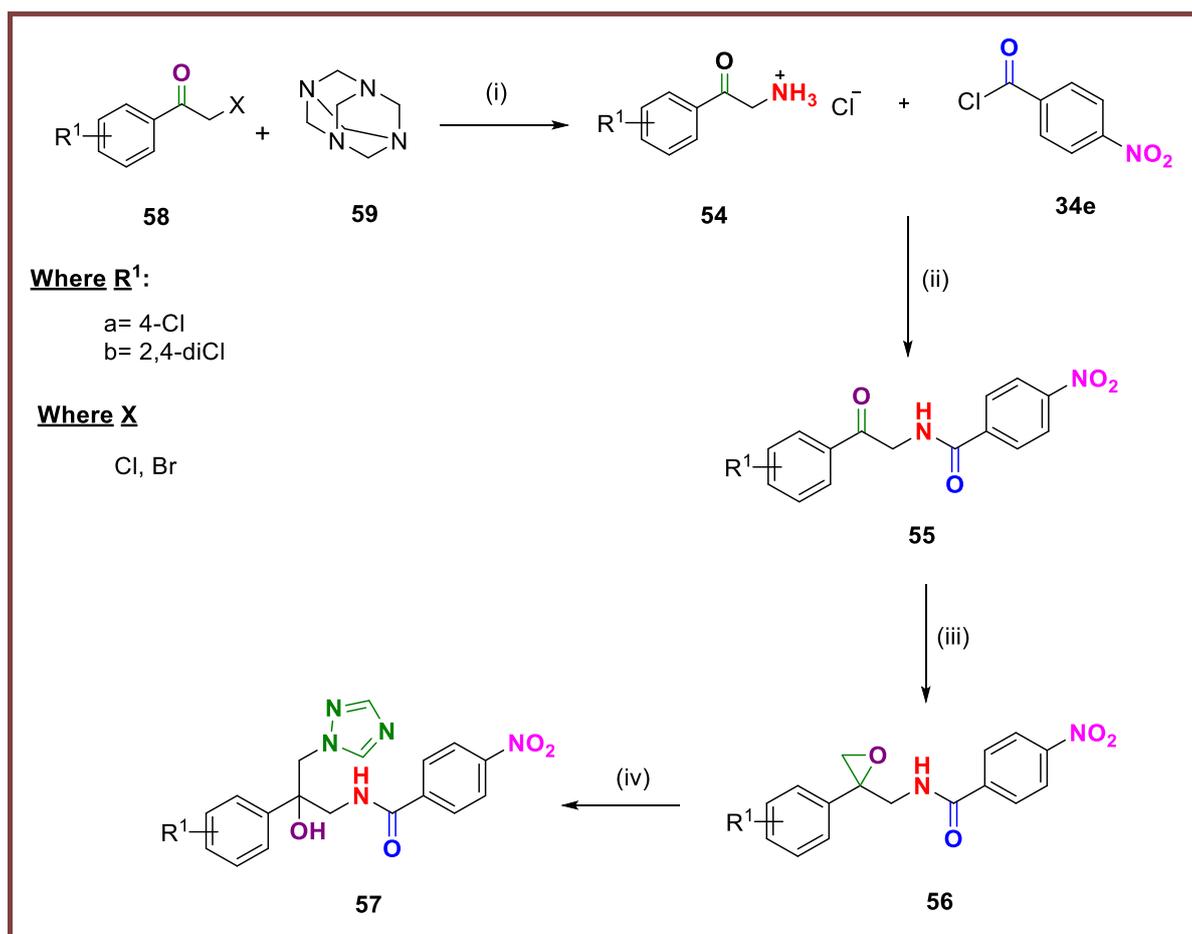
Scheme 4.2 Synthetic route for the preparation of (*R/S*)-*N*-(2-(arylphenyl)-2-hydroxy-3-(1*H*-1,2,4-triazol-1-yl)propyl)-4-nitrobenzamide (**57**). *Reagents and conditions:* (i) (a) CHCl$_3$, rt, 1 h (b) MeOH, conc HCl, 67 °C, 3 h (ii) CH$_2$Cl$_2$, sat. aqueous NaHCO$_3$, rt, 2 h (iii) TMSOI, 48% NaOH, CH$_2$Cl$_2$, 48 °C, 48 h (iv) (a) K$_2$CO$_3$, triazole, CH$_3$CN, 45 °C, 1 h (b) **56**, 70 °C, 24 h

(*R/S*)-*N*-(2-(2,4-Dichlorophenyl)-2-hydroxy-3-(1*H*-1,2,4-triazol-1-yl)propyl)-4-nitrobenzamide (**57c**) was investigated first to optimise this synthetic pathway.

Synthesis of 2-amino-1-(2,4-dichlorophenyl)ethan-1-one hydrochloride (54c)

The first attempt to prepare 2-amino-1-(2,4-dichlorophenyl)ethan-1-one hydrochloride (**54c**) used hexamethylenetetramine (**59**) as the amine source,[114] which on reaction with 2,2',4'-trichloroacetophenone (**58b**, X= Cl) gave a white solid of the assumed complex of hexamethylenetetramine-2',4'-dichloroacetophenone (Scheme 4.2.1). The reaction mechanism of this step follows the Delépine reaction, which involves reaction of

alkyl halides and hexamethylenetetramine to produce primary amines after acid hydrolysis of the quaternary ammonium salt. Treatment with methanolic HCl at 67 °C for 3 h should give the required product **54c**.[114] However, ^{1}H NMR did not confirm product and increasing the reaction time from 1 h to overnight or changing the sequence of addition were also unsuccessful. A modified method (reference 115) that involved reaction at 40 °C for 72 h then at rt for 72 h was also unsuccessful and changing 2,2',4'-trichloroacetophenone (**58b**, X= Cl) for the more reactive 2-bromo-1-(2,4-dichlorophenyl)ethan-1-one (**58b**, X= Br) did not improve the outcome.
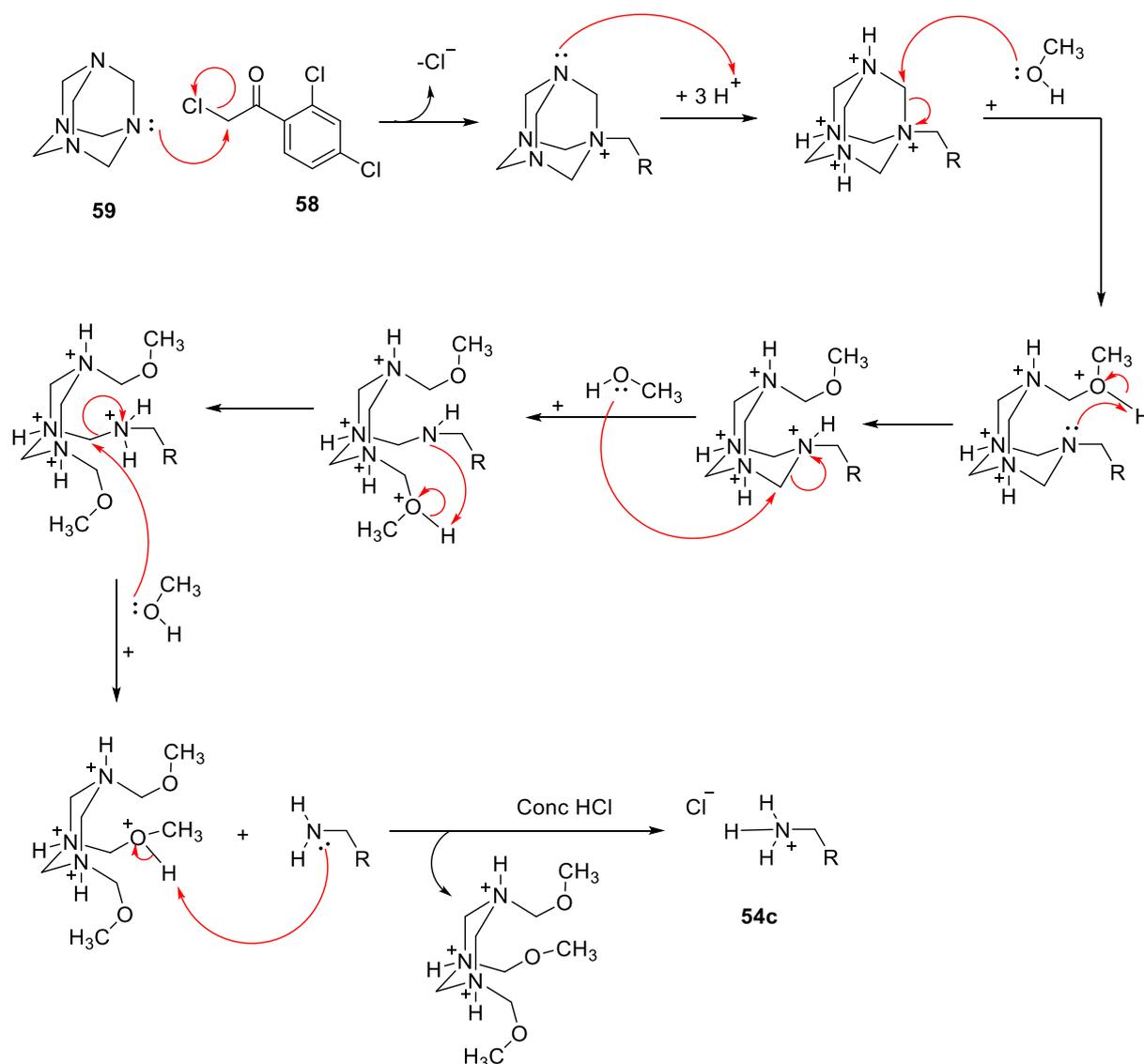
Scheme 4.2.1 Mechanism of Delépine reaction to form 2-amino-1-(2,4-dichlorophenyl)ethan-1-one hydrochloride (**54c**)

At this point another pathway was investigated to synthesise the novel compounds (Scheme 4.3).
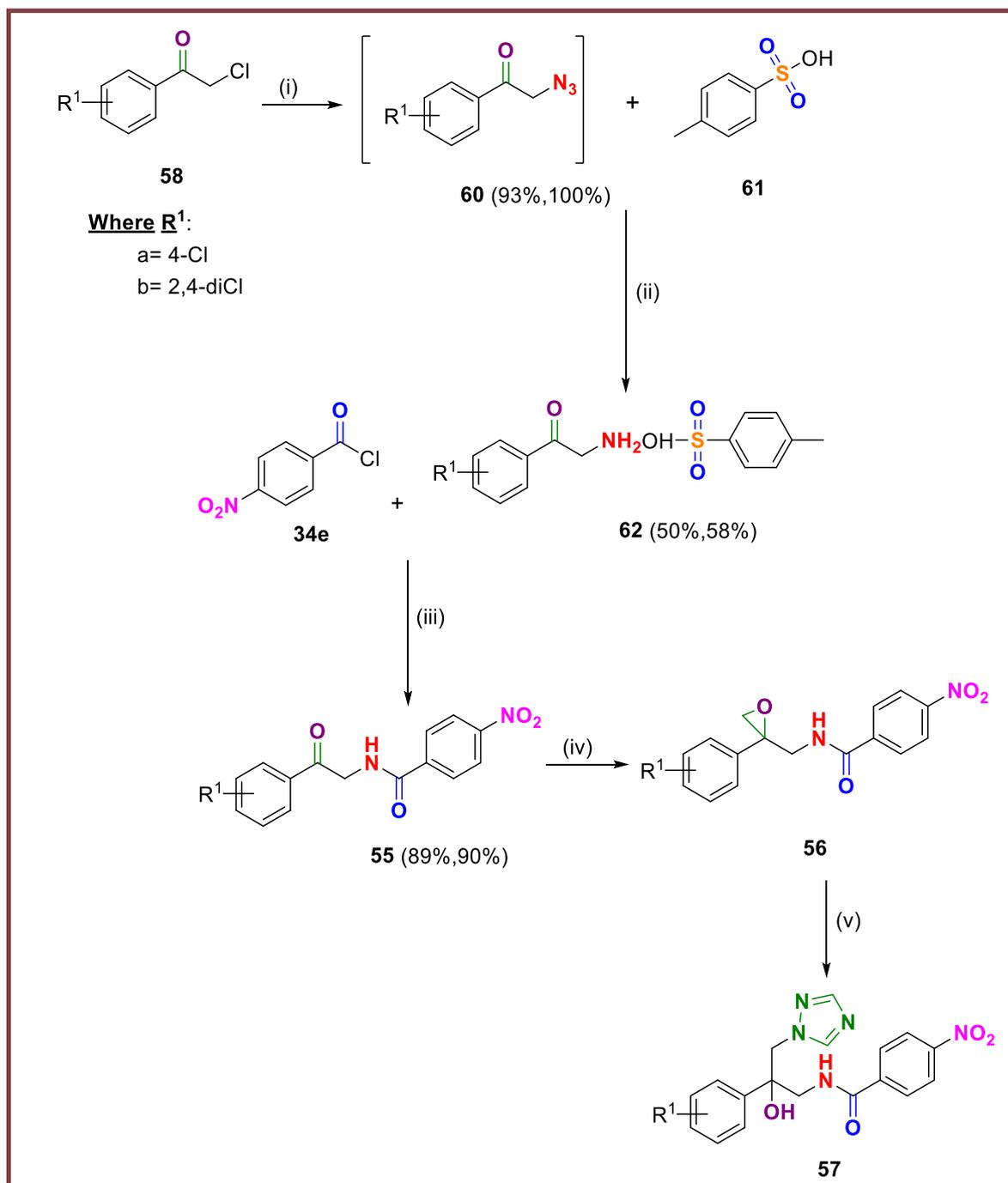
Scheme 4.3 Synthetic route for the preparation of (*R/S*)-*N*-(2-(arylphenyl)-2-hydroxy-3-(1*H*-1,2,4-triazol-1-yl)propyl)-4-nitrobenzamide (**57**). *Reagents and conditions:* (i) NaN₃, CH₃CN: H₂O (3:1 v/v), KI, 60 °C, 2 h (ii) THF, triphenylphosphine, 40 °C, o/n (iii) CH₂Cl₂, sat. aqueous NaHCO₃, rt, 2 h (iv) TMSOI, 48% NaOH, CH₂Cl₂, 48 °C, 48 h (v) (a) K₂CO₃, triazole, CH₃CN, 45 °C, 1 h (b) **56**, 70 °C, 24 h

Synthesis of 2-azido-1-(arylphenyl)ethan-1-one (60)

2-Azido-1-(arylphenyl)ethan-1-one (**60**) was prepared by the reaction of sodium azide with acetophenone derivatives (**58**) in the presence of KI in CH_3CN: H_2O (3:1 v/v) at 60 °C for 2 h.[116] After aqueous work up, ^1H NMR confirmed the formation of β-ketoazide with the characteristic shift of the CH_2 singlet observed at δ ~ 4.75 rather than δ 5.06 in acetophenone (**58**). The azides (**60**) were obtained in good yields and used in the next step without further purification.

Table 25. Yield, m.p. and physical properties of 2-azido-1-(arylphenyl)ethan-1-one derivatives (**60**)

Compd	Yield (%)	*Rf* (petroleum ether- EtOAc 4:1 v/v)	Physical properties
60a	100	0.64	Orange oil
60b	93	0.71	Orange oil

Synthesis of 2-amino-1-(arylphenyl)ethan-1-one 4-methylbenzenesulfonate (62)

The Staudinger reaction was then applied to convert 2-azido-1-(arylphenyl)ethan-1-one (**60**) to 2-amino-1-(arylphenyl)ethan-1-one 4-methylbenzenesulfonate (**62**) by reaction of β-ketoazide (**60**) with triphenylphosphine (PPh₃) and catalytic *p*-toluenesulfonic acid (*p*-TsOH) (**61**) in THF at rt until effervescence finished then heated at 40 °C o/n.[116] The Staudinger reaction is a very mild azide reduction to produce free amine. The mechanism of this step starts by nucleophilic attack of PPh₃ with the azide to generate a phosphazide. Then a nucleophilic rearrangement occurs with loss of N_2 gas (as effervescence in the reaction) to form an iminophosphorane (N=P ylide). After aqueous work up the very stable phosphine oxide by-product was produced and the amine compound as shown in scheme 4.3.1.
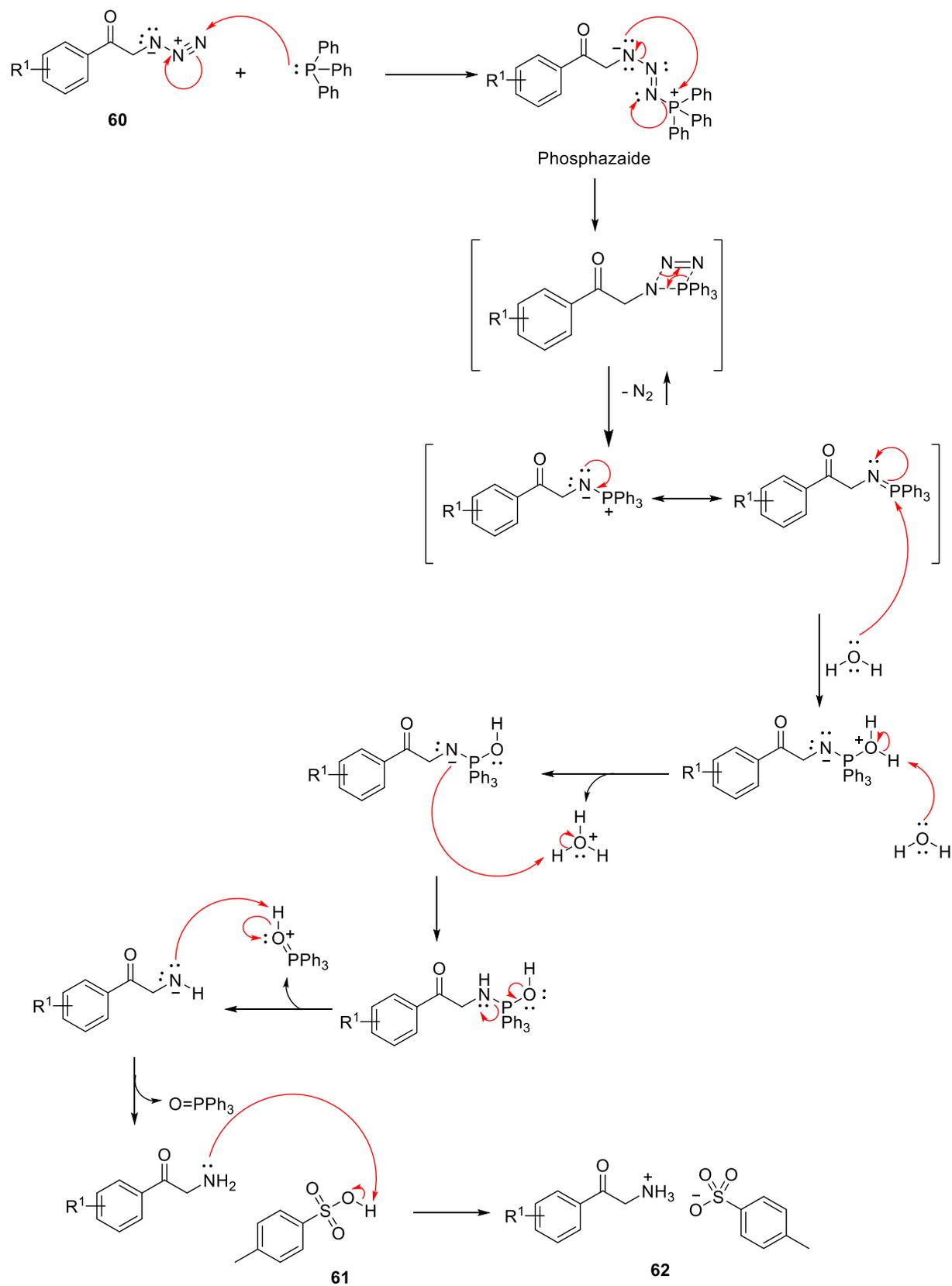
Scheme 4.3.1 Mechanism of formation of 2-amino-1-(arylphenyl)ethan-1-one 4-methylbenzenesulfonate (**62**)

^{1}H NMR confirmed the formation of β-keto-ammonium tosylate salts (**62**) with characteristic broad singlet at δ 8.28 integrated by three protons for NH_3 and a singlet at δ 2.29 integrated by three protons for CH_3 of the tosylate salt. 2-Amino-1-(arylphenyl)ethan-1-one 4-methylbenzenesulfonate (tosylate salt) (**62**) were obtained as white solids (Table 26).

Table 26. Yield, m.p. and HPLC of tosylate salts (**62**)

Compd	Yield (%)	M.p. (°C)	Lit. M.p. (°C)	HPLC
62a	58	238-240	226-227[116]	-
62b	78	188-190	-	98 %

Synthesis of *N*-(2-(arylphenyl)-2-oxoethyl)-4-nitrobenzamide (55)

To prepare *N*-(2-(arylphenyl)-2-oxoethyl)-4-nitrobenzamide (**55**) a solution of CH_2Cl_2 and saturated aqueous $NaHCO_3$ were stirred vigorously and chilled in an ice bath. After that, 4-nitrobenzoyl chloride (**34e**) was added and stirred until all the solid dissolved followed by β-keto-ammonium tosylate salts (**62**) and the mixture was stirred for 2 h at room temperature.[110]

After aqueous work up, ^{1}H NMR confirmed the formation of product with the characteristic N*H* triplet at δ ~ 9.38 and C*H₂* as a doublet at δ ~ 4.63. ^{13}C NMR confirmed the amide group (*C*ONH), which was observed at *δ* ~165.50. *N*-(2-(Arylphenyl)-2-oxoethyl)-4-nitrobenzamides (**55**) were obtained as white solids in excellent yield (Table 27).

Table 27. Yield, m.p. and HRMS of 2-azido-1-(arylphenyl)ethan-1-one derivatives (**55**)

Compd	Yield (%)	M.p. (°C)	HRMS
55c	89	168-170	Calcd for $C_{15}H_{11}ClN_2O_4$ ([M + H]⁺), 319.0485; found, 319.0482
55d	90	146-148	Calcd for $C_{15}H_{10}Cl_2N_2O_4$ ([M + H]⁺), 355.0252; found, 355.0038

Synthesis of (*R/S*)-*N*-((2-(arylphenyl)oxiran-2-yl)methyl)-4-nitrobenzamide (56)

The synthesis of the oxiranes, (*R/S*)-*N*-((2-(arylphenyl)oxiran-2-yl)methyl)-4-nitrobenzamide (**56**) from *N*-(2-(arylphenyl)-2-oxoethyl)-4-nitrobenzamide (**55**) followed the previously described method used to prepare **56a**, however ^{1}H NMR indicated a complex mixture. As this pathway (Scheme 4.3) was not optimal a third pathway was investigated (Scheme 4.4).

Scheme 4.4 Synthetic route for the preparation of (*R/S*)-2-((2-(arylphenyl)-2-hydroxy-3-(1*H*-1,2,4-triazol-1-yl)propyl)amino)-1-phenylethan-1-one (**65**). *Reagents and conditions:* (i) NaHCO$_3$, triazole, toluene, 113 °C, 4 h (ii) TMSOI, 48% NaOH, CH$_2$Cl$_2$, 48 °C, 48 h (iii) **54**, CH$_2$Cl$_2$, sat. aqueous NaHCO$_3$, rt, 2 h

1-(2,4-Dichlorophenyl)-2-(1*H*-1,2,4-triazol-1-yl)ethan-1-one (**63b**) was investigated first to optimise this synthetic pathway.

Synthesis of 1-(2,4-dichlorophenyl)-2-(1*H*-1,2,4-triazol-1-yl)ethan-1-one (63b)

The synthesis of 1-(2,4-dichlorophenyl)-2-(1*H*-1,2,4-triazol-1-yl)ethan-1-one (**63b**) was performed by the addition of triazole to 2,2',4'-trichloroacetophenone (**58b**) in the present of NaHCO$_3$ in dry toluene and reflux for 4 h at 113 °C.[111]

After aqueous work up ^{1}H NMR confirmed the formation of 1-(2,4-dichlorophenyl)-2-(1*H*-

1,2,4-triazol-1-yl)ethan-1-one (**63b**) with the characteristic triazole singlets observed at δ 8.54 and δ 8.03. 1-(2,4-Dichlorophenyl)-2-(1*H*-1,2,4-triazol-1-yl)ethan-1-one (**63b**) was obtained in a good yield (74 %) and used in the next step without further purification.

Synthesis of (*R/S*)-1-((2-(2,4-dichlorophenyl)oxiran-2-yl)methyl)-1*H*-1,2,4-triazole (64b)

1-(2,4-Dichlorophenyl)-2-(1*H*-1,2,4-triazol-1-yl)ethan-1-one (**63b**) was then converted to the oxiran-2-yl (**64b**) as previously described for **56a**, and after work up, ¹H NMR confirmed the formation of the product from the characteristic two doublets of the epoxide- C*H₂* at δ ~ 3.04 and δ ~ 2.87. (*R/S*)-1-((2-(2,4-Dichlorophenyl)oxiran-2-yl)methyl)-1*H*-1,2,4-triazole (**64b**) was obtained in excellent yield (95 %) and used directly in the next step.

Synthesis of (*R/S*)-2-((2-(2,4-dichlorophenyl)-2-hydroxy-3-(1*H*-1,2,4-triazol-1-yl)propyl)amino)-1-(4-nitrophenyl)ethan-1-one (65b)

Ring opening of (*R/S*)-1-((2-(2,4-dichlorophenyl)oxiran-2-yl)methyl)-1*H*-1,2,4-triazole (**64b**) with saturated aq. NaHCO₃, followed the method described for **55**. However, a mixture was obtained that was very difficult to purify by column chromatography. Two spots were collected, neither of which was the product.

Rather than opening the epoxide ring with saturated aq. NaHCO₃ or triazole, an alternative route (Scheme 4.5) with first introduction of triazole followed by epoxide ring opening with a more nucleophilic base (e.g. azide anion) was explored to determine if this was a more viable approach.
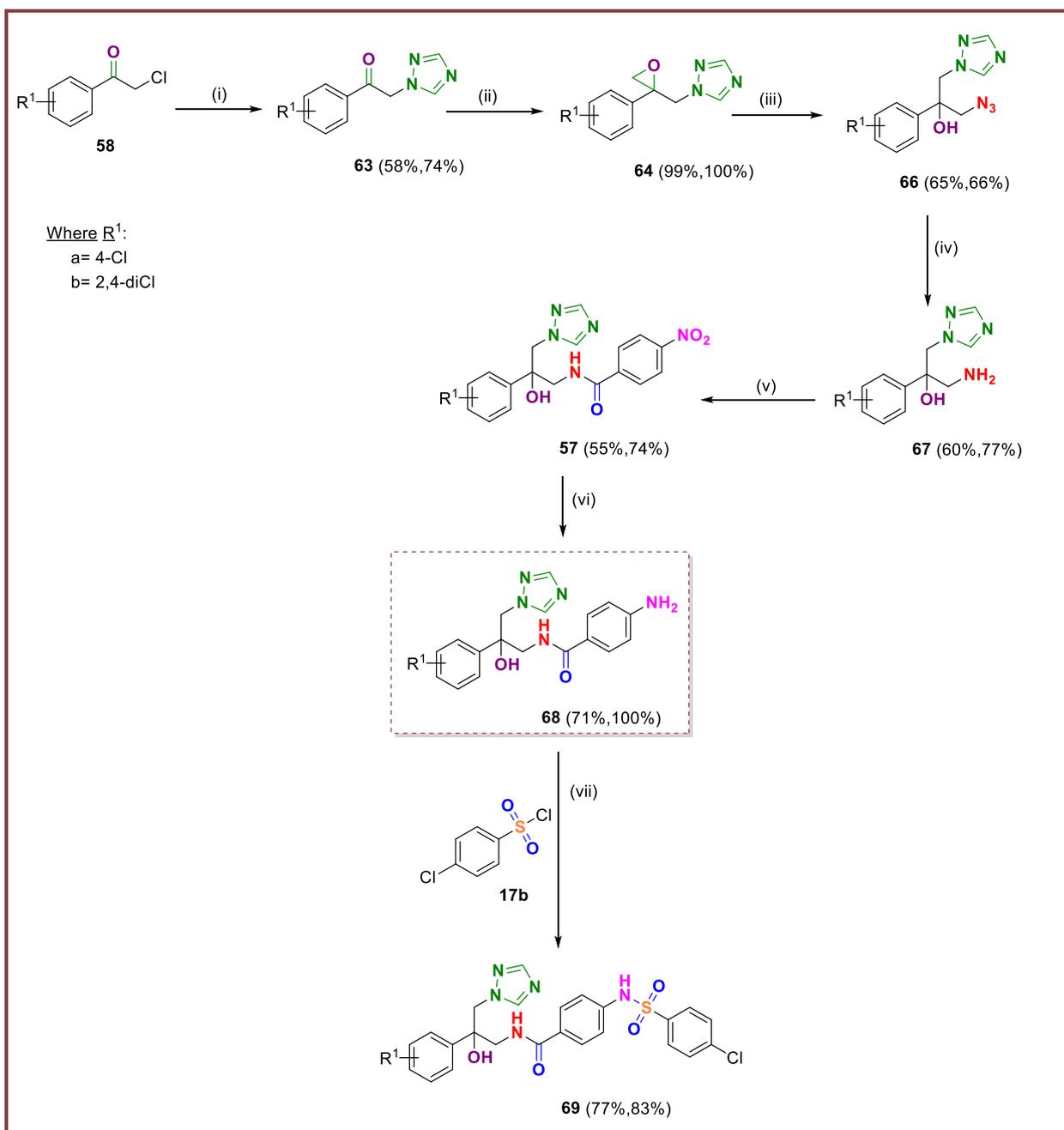
Scheme 4.5 Synthetic route for the preparation of (*R/S*)-4-chloro-*N*-(4-((aryl-phenyl)-2-hydroxy-3-(1*H*-1,2,4-triazol-1-yl)propyl)sulfonamidocarbamoyl)phenyl) benzamide derivatives (**69**). *Reagents and conditions:* (i) Triazole, NaHCO₃, toluene, 113 °C 4 h (ii) TMSOI, 20% aq. NaOH, toluene, 60 °C, 6 h then rt o/n (iii) NaN₃, NH₄Cl, DMF, 60 °C, 2 h then rt o/n (iv) (a) PPh₃, THF, rt, 1 h (b) H₂O, 60 °C, 4 h (v) 4-Nitrobenzoic acid (**34e**), CH₂Cl₂, sat. aqueous NaHCO₃, rt, 2 h (vi) Pd/C, MeOH, rt, 3 h under H₂ balloon (vii) pyridine, **17b**, rt, 24 h

Synthesis of 1-(4-arylphenyl)-2-(1*H*-1,2,4-triazol-1-yl)ethenone (63)

To prepare 1-(4-arylphenyl)-2-(1*H*-1,2,4-triazol-1-yl)ethenone (**63**) the acetophenone derivatives in dry toluene were reacted with triazole and NaHCO$_3$ and heated at 113 °C for 4 h.[111] After aqueous work up and trituration of the residue with Et$_2$O to remove remaining acetophenone derivatives,[117] ^{1}H NMR confirmed the formation of 1-(4-arylphenyl)-2-(1*H*-1,2,4-triazol-1-yl)ethenone derivatives (**63**). Table 28 shows the yield, m.p. and physical properties of 1-(arylphenyl)-2-(1*H*-1,2,4-triazol-1-yl)ethenones (**63**).

Table 28. Yield, m.p. and physical properties of 1-(arylphenyl)-2-(1*H*-1,2,4-triazol-1-yl)ethenones (**63**)

Compd	Yield (%)	M.p. (°C)	Lit. M.p. (°C)	Physical properties
63a	58	148-150	149-150[117]	White solid
63b	49	100-102	115-116[118]	Pale-yellow solid

Synthesis of (*R/S*)-1-((2-(arylphenyl)oxiran-2-yl)methyl)-1*H*-1,2,4-triazole (64)

1-(4-Arylphenyl)-2-(1*H*-1,2,4-triazol-1-yl)ethenone (**63**) was then converted to (*R/S*)-1-((2-(arylphenyl)oxiran-2-yl)methyl)-1*H*-1,2,4-triazole (**64**) by dissolving 1-(4-arylphenyl)-2-(1*H*-1,2,4-triazol-1-yl)ethenone (**63**) in toluene followed by addition of TMSOI and 20% aqueous NaOH and the reaction heated at 60 °C for 6 h[119] then rt o/n. After aqueous work up ^{1}H NMR confirmed the formation of (*R/S*)-1-((2-(arylphenyl)oxiran-2-yl)methyl)-1*H*-1,2,4-triazole (**64**) with the characteristic two doublets at δ ~ 3.05 and δ ~ 2.87 for the epoxide-C*H*$_2$. (*R/S*)-1-((2-(Arylphenyl)oxiran-2-yl)methyl)-1*H*-1,2,4-triazole derivatives (**64**) were obtained as a crude pale-yellow/orange oil (Table 29) which were used without further purification in the next step.

Table 29. Yield and R*f* of (*R/S*)-1-((2-(arylphenyl)oxiran-2-yl)methyl)-1*H*-1,2,4-triazole derivatives (**64**)

Compd	Yield (%)	R*f* (petroleum ether- EtOAc 1:2 v/v)
64a	100	0.28

64b	99	0.38

Synthesis of (*R/S*)-1-azido-2-(arylphenyl)-3-(1*H*-1,2,4-triazol-1-yl)propan-2-ol (66)

(*R/S*)-1-Azido-2-(arylphenyl)-3-(1*H*-1,2,4-triazol-1-yl)propan-2-ol (**66**) was prepared by adding NaN$_3$ and NH$_4$Cl to a solution of (*R/S*)-1-((2-(arylphenyl)oxiran-2-yl)methyl)-1*H*-1,2,4-triazole (**64**) in DMF and the reaction heated at 60 °C for 2 h then rt o/n.[120] After work up ^{1}H NMR confirmed the formation of products by a characteristic singlet at 6.02 for O*H*. ^{13}C NMR confirmed the hydroxy group (*C*-OH), which was observed at $\delta \sim 75.95$. (*R/S*)-1-Azido-2-(arylphenyl)-3-(1*H*-1,2,4-triazol-1-yl)propan-2-ol derivatives (**66**) were obtained as thick yellow syrups after purification by gradient column chromatography with good yield and purity as shown in Table 30.

Table 30. Yield, HPLC and HRMS of (*R/S*)-1-azido-2-(arylphenyl)-3-(1*H*-1,2,4-triazol-1-yl)propan-2-ol derivatives (**66**)

Compd	Yield (%)	HPLC	HRMS
66a	65	100 %	Calcd for C$_{11}$H$_{11}$ClN$_6$O ([M + H]$^+$), 279.0761; found, 279.0761
66b	66	100 %	Calcd for C$_{11}$H$_{10}$Cl$_2$N$_6$O ([M + H]$^+$), 313.0371; found, 313.0373

Synthesis of (*R/S*)-1-amino-2-(arylphenyl)-3-(1*H*-1,2,4-triazol-1-yl)propan-2-ol (67)

(*R/S*)-1-Amino-2-(arylphenyl)-3-(1*H*-1,2,4-triazol-1-yl)propan-2-ol derivatives were prepared by Staudinger reaction of (*R/S*)-1-azido-2-(arylphenyl)-3-(1*H*-1,2,4-triazol-1-yl)propan-2-ols (**66**) in THF with triphenylphosphine as previously described.[116,121] The free amine was obtained after acid-base work up to give the products as white solids and ^{1}H NMR showed the broad singlet at $\delta \sim 2.8$ and $\delta \sim 1.6$ for N*H$_2$* of **67a** and **67b** respectively.

Table 31. Yield, m.p. and HRMS of (*R/S*)-1-amino-2-(arylphenyl)-3-(1*H*-1,2,4-triazol-1-yl)propan-2-ol derivatives (**67**)

Compd	Yield (%)	M.p. (°C)	HRMS
67a	77	94-96	Calcd for $C_{11}H_{13}ClN_4O$ ([M + H]$^+$), 253.0856; found, 253.0855
67b	60	70-72	Calcd for $C_{11}H_{12}Cl_2N_4O$ ([M + H]$^+$), 287.0466; found, 287.0467

Synthesis of (*R/S*)-*N*-(2-(arylphenyl)-2-hydroxy-3-(1*H*-1,2,4-triazol-1-yl)propyl)-4-nitrobenzamide (57)

Reaction of 4-nitrobenzoyl chloride (**34e**) and (*R/S*)-1-amino-2-(arylphenyl)-3-(1*H*-1,2,4-triazol-1-yl)propan-2-ol (**67**) in CH_2Cl_2 and sat. NaHCO$_3$[110] gave (*R/S*)-*N*-(2-(arylphenyl)-2-hydroxy-3-(1*H*-1,2,4-triazol-1-yl)propyl)-4-nitrobenzamide derivatives (**57**), with characteristic N*H* triplet at δ ~ 8.63 for the amide bond observed by ^{1}H NMR. ^{13}C NMR confirmed the amide group (*C*ONH), which was observed at *δ* ~166.09. (*R/S*)-*N*-(2-(arylphenyl)-2-hydroxy-3-(1*H*-1,2,4-triazol-1-yl)propyl)-4-nitrobenzamide derivatives (**57**) were obtained with good yields after gradient column chromatography (Table 32).

Table 32. Yield, m.p. and HRMS of (*R/S*)-*N*-(2-(arylphenyl)-2-hydroxy-3-(1*H*-1,2,4-triazol-1-yl)propyl)-4-nitrobenzamide derivatives (**57**)

Compd	Yield (%)	M.p. (°C)	HRMS
57b	74	228-230	Calcd for $C_{18}H_{16}ClN_5O_4$ ([M + H]$^+$), 402.0969; found, 402.0969
57c	55	228-230	Calcd for $C_{18}H_{15}Cl_2N_5O_4$ ([M + H]$^+$), 436.0579; found, 436.0578

Synthesis of (*R/S*)-4-amino-*N*-(2-(arylphenyl)-2-hydroxy-3-(1*H*-1,2,4-triazol-1-yl)propyl)benzamide (68)

Reduction of (*R/S*)-*N*-(2-(arylphenyl)-2-hydroxy-3-(1*H*-1,2,4-triazol-1-yl)propyl)-4-nitrobenzamide (**57**) was achieved by catalytic hydrogenation using 10 % Pd/C in MeOH and H$_2$ (using hydrogen balloon) and the mixture was stirred at rt for 3 h.[122] The crude product with purified by gradient column chromatography to give (*R/S*)-4-amino-*N*-(2-(arylphenyl)-2-hydroxy-3-(1*H*-1,2,4-triazol-1-yl)propyl)benzamide derivatives (**68**) in excellent yields as off-white to pale-yellow waxes (Table 33).

Table 33. Yield, m.p. and HRMS of (*R/S*)-4-amino-*N*-(2-(arylphenyl)-2-hydroxy-3-(1*H*-1,2,4-triazol-1-yl)propyl)benzamide derivatives (**68**)

Compd	Yield (%)	R*f* (CH$_2$Cl$_2$- MeOH 9.5: 0.5 v/v)	HRMS
68a	71	0.35	Calcd for C$_{18}$H$_{18}$ClN$_5$O$_2$ ([M + Na]$^+$), 394.1047; found, 394.1047
68b	100	0.36	Calcd for C$_{18}$H$_{17}$Cl$_2$N$_5$O$_2$ ([M + Na]$^+$), 428.0657; found, 428.0660

Synthesis of (*R/S*)-*N*-(2-(arylphenyl)-2-hydroxy-3-(1*H*-1,2,4-triazol-1-yl)propyl)-4-((4-chlorophenyl)sulfonamido)benzamide (69)

(*R/S*)-4-Amino-*N*-(2-(arylphenyl)-2-hydroxy-3-(1*H*-1,2,4-triazol-1-yl)propyl)benzamide (**68**) was converted to (*R/S*)-*N*-(2-(arylphenyl)-2-hydroxy-3-(1*H*-1,2,4-triazol-1-yl)propyl)-4-((4-chlorophenyl)sulfonamido)benzamide derivatives (**69**) by reaction of (*R/S*)-4-amino-*N*-(2-(4-chlorophenyl)-2-hydroxy-3-(1*H*-1,2,4-triazol-1-yl)propyl)benzamide derivatives (**68**) with 4-chlorobenzenesulfonyl chloride (**17b**) in pyridine at rt o/n.[108] After aqueous work up the crude compound was purified by gradient column chromatography to obtain the products as white solids with excellent yields and high purity (Table 34). ^{1}H NMR confirmed the production of the product with the characteristic N*H* sulfonamide linker as a broad singlet at δ 10.7.

Table 34. Yield, m.p., R*f* and HPLC of (*R/S*)-*N*-(2-(arylphenyl)-2-hydroxy-3-(1*H*-1,2,4-triazol-1-yl)propyl)-4-((4-chlorophenyl)sulfonamido) benzamide derivatives (**69**)

Compd	Yield (%)	M.p. (°C)	R*f* (CH$_2$Cl$_2$- MeOH 9.5: 0.5 v/v)	HPLC
69a	77	236-238	0.45	100 %
69b	83	228- 230	0.46	99.69 %

Further work on this series is ongoing by another PhD student, Marwa Alsulaimany, to extend and further develop this series.

4.4 Biological assays

All final compounds were evaluated IC_{50}, binding affinity and MIC against *C. albicans* strains at the Centre for Cytochrome P450 Biodiversity, Swansea University Medical School as previously described in chapter II. All assays were performed by Dr Josie Parker and Dr Andrew Warrilow.

4.4.1 Antifungal susceptibility testing (MIC)

The MIC test was determined for all novel azole derivatives in the same *C. albicans* strains (SC5314 and CA14) using the same method described in chapter II.

Table 35. MIC values for compounds against *C. albicans* SC5314 and CA14 at 48 hours
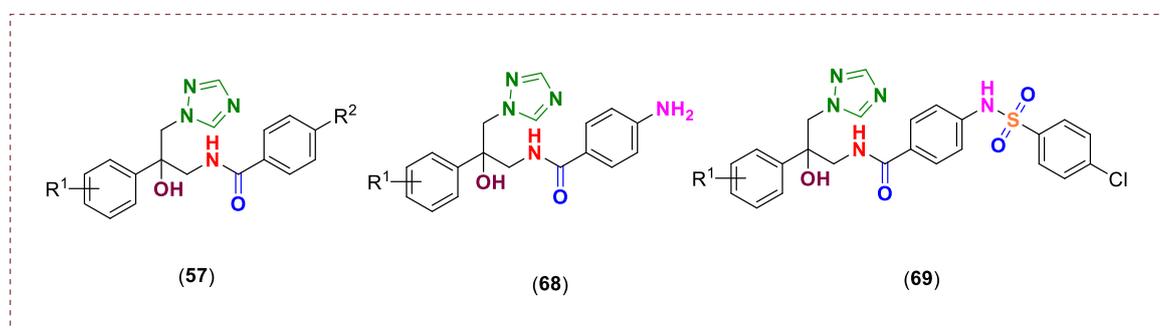
Compd	R^1	R^2	MIC (μg /mL)		cLogP[a]	miLogP[b]
			SC5314	CA14		
57a	4-H	4-H	1	1	1.93	1.30
57b	4-Cl	4-NO$_2$	0.125	0.125	-	1.94
57c	2,4-diCl	4-NO$_2$	<0.03	<0.03	-	2.54
68a	4-Cl	-	1	1	1.69	1.05
68b	2,4-diCl	-	0.25	0.25	2.24	1.66
69a	4-Cl	-	1	1	3.45	3.42
69b	2,4-diCl	-	0.25	0.25	4.01	4.03
Fluconazole			0.125	0.125	0.86	-0.12

[a]cLogP was determined using Crippens fragmentation,[96] [b]miLogP was determined using Molinspiration service[104]

All the novel derivatives (**57, 68** and **69**) displayed antifungal activity against both *C. albicans* wild type strains SC5314 and CA14. The chloro-derivatives were more effective

with **57b** (R^1= 4-Cl, R^2= 4-NO_2) comparable with the reference standard fluconazole (MIC 0.125 µg/mL) and **57c** (R^1= 2,4-diCl, R^2= 4-NO_2) more effective than fluconazole with MIC < 0.03 µg/mL against both strains. Moreover, the diCl derivatives **68b** and **69b** with MIC 0.25 µg/mL (in both strains) were more effective than **57a**, **68a** and **69a** (MIC 1 µg/mL) but less effective than fluconazole. The addition of another chloro-group at R^1 was clearly valuable (**57b** vs **57c**, **68a** vs **68b** and **69a** vs **69b**) (Table 35).

Generally the more lipophilic the novel derivatives the better the MIC observed although compounds **69a** and **69b** did not show the best results even though they have good lipophilicity (**69a**, cLogP= 3.45; **69b**, cLogP= 4.01), which could be due to other factors such as the efflux system.

4.4.2 Enzyme inhibition study of *C. albicans* CYP51

The IC_{50} test was conducted as described in chapter II (Biological section) for the novel design compounds that showed promising MIC results compared with fluconazole (Table 36).

Table 36. IC_{50} values for the novel compounds compared with fluconazole against CaCYP51
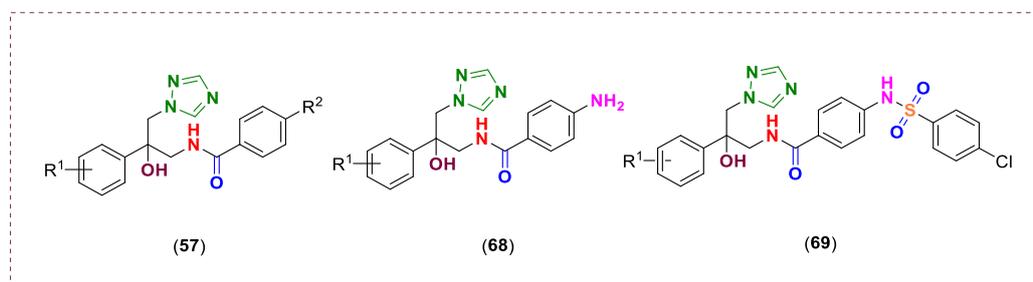
Compd	R^1	R^2	CaCYP51 IC_{50} (µM)
57a	4-H	4-H	nd
57b	4-Cl	4-NO_2	0.79
57c	2,4-diCl	4-NO_2	1.24
68a	4-Cl	-	nd
68b	2,4-diCl	-	1.6
69a	4-Cl	-	nd
69b	2,4-diCl	-	0.78
Fluconazole			0.31

nd= no data

Compounds **57b** (R^1 = 4-Cl, R^2 = 4-NO$_2$) and **69b** (R^1 = 2,4-di-Cl) showed good inhibition for CaCYP51 with IC$_{50}$ values of 0.79 μM and 0.78 μM respectively compared with fluconazole (IC$_{50}$ 0.31 μM). However, compounds **57c** (R^1 = 4-Cl, R^2 = 4-NO$_2$; IC$_{50}$ 1.24 μM) and **68b** (R^1 = 2,4-di-Cl; IC$_{50}$ 1.6 μM) showed a 4-5 fold reduced inhibition compared with fluconazole.

4.4.3 CaCYP51 ligand binding affinity

Derivatives **57**, **68** and **69** with good MIC values were evaluated for CaCYP51 binding affinity (K_d) as previously described (Table 37).

Table 37. K_d values for the novel compounds compared with fluconazole against CaCYP51
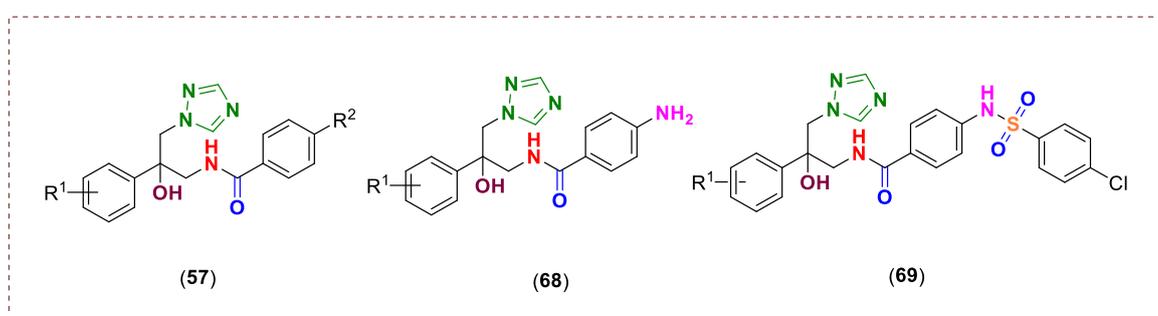
Compd	R^1	R^1	K_d (nM)
57a	4-H	4-H	nd
57b	4-Cl	4-NO$_2$	nd
57c	2,4-diCl	4-NO$_2$	108 ± 34.4
68a	4-Cl	-	nd
68b	2,4-diCl	-	159 ± 17.6
69a	4-Cl	-	nd
69b	2,4-diCl	-	94 ± 24.4
Fluconazole			41 ± 13

nd= no data

Good binding affinity was observed for the diCl derivatives **57c** (R^1 = 2,4-diCl, R^2 = 4-NO$_2$) with K_d 108 ± 34.4 and compound **68b** (R^1 = 2,4-diCl) with K_d 159 ± 17.6. While the

extended sulfonamide derivative **69b** (R^1 = 2,4-diCl) with K_d 94 ± 24.4 showed tighter binding to the haem compared with **57c** and **68b**.

The novel compounds of this series could be beneficial as shown for **69b**, which has tight binding and good IC_{50} and MIC. However, compounds **57c** and **68b** showed good MIC and IC_{50} values but the binding affinity did not reflect this finding. Sterol profile analysis could give an explanation as if these compounds (**57c** and **68b**) compete with the natural substrate lanosterol, they could bind in the access channel away from the haem, which would explain the lower binding affinity as the binding affinity assay measures how the compound binds directly with the haem Fe^{3+}.

4.5 Molecular dynamic (MD) simulations

4.5.1 Wild type docking

For further investigation of the binding modes of the novel compounds of this series, the best ligand pose was chosen and molecular dynamics simulations were run for 100 ns using the CaCYP51 crystal structure (PDB 5FSA)[35] and representative novel (**57c** and **69b**) azole derivative complexes, using the Desmond programme of Maestro[102]. All the compounds formed a coordinate binding interaction between the triazole N and the haem Fe^{3+}.

Different binding profiles were observed for the enantiomers of **57c**. (*R*)-**57c** formed additional binding interactions within the haem binding site, specifically water mediated H-bonding interactions with Gly307 and the N atom of triazole ring as well as the hydroxyl group, as well as hydrophobic interactions with Tyr118 and Met508. In addition, a direct H-bonding interaction with Ser378 and the oxygen atoms of the nitro group, and π-cationic interaction from His377 and the nitrogen of the nitro group. Whereas, (*S*)-**57c** interacted primarily via hydrophobic interactions, positioned to form π-π stacking with Tyr118, Tyr132 and the two phenyl rings, and hydrophobic interactions with Phe126, Leu376 and Met508. Further direct H-bonding interactions with Ser378 and the oxygen atoms of the nitro group, and H-bonding interaction between Tyr132 and hydroxyl group were observed (Figure 61).

The (*R*)-enantiomer of the extended sulfonamide derivative (**69b**) formed additional water mediated H-bonding interactions through the sulfonamide oxygen atom and Ser378 as well as the NH heteroatom of sulfonamide group and Ser507. Further interactions noted were a π-π stacking interaction between Phe380 and phenyl ring, and hydrophobic interaction with Phe228. (*S*)-**69b** interacted primarily via hydrophobic interactions with Tyr118, Pro230 and Leu376, and the amide NH heteroatom of sulfonamide group formed a water mediated H-bonding interaction with Tyr64. The two phenyl rings formed π-π stacking interactions with Tyr132 and Phe380 (Figure 61).
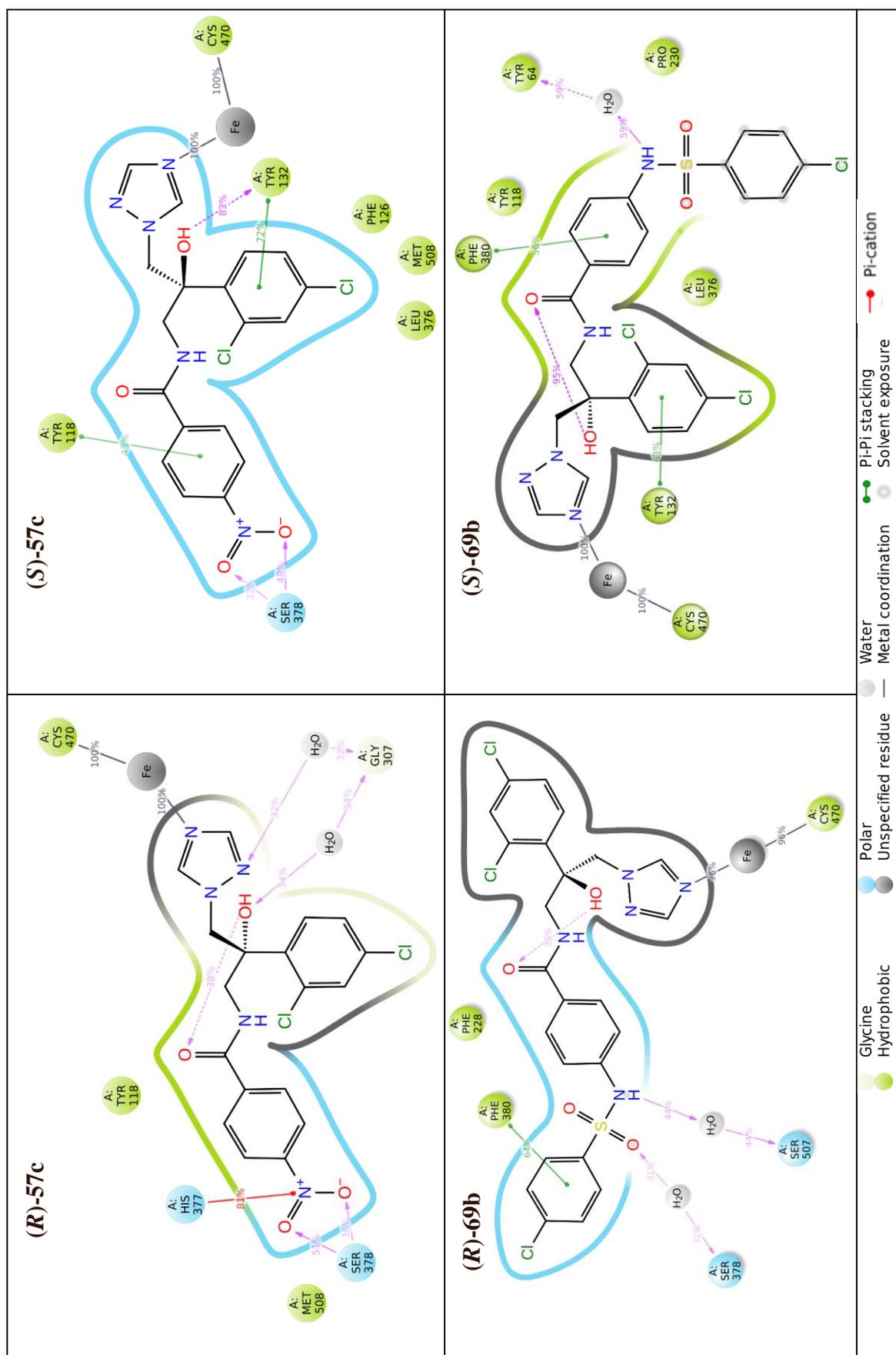
Figure 61. A schematic of detailed ligand atom interactions of representative (*R*)- and (*S*)-enantiomers of (**57c** and **69b**) with the amino acids of the wild type CaCYP51 protein. Interactions that occur more than 30.0% of the simulation time in the selected trajectory (0 through 100 ns) are shown

4.5.2 Mutant strain docking

Several studies have shown that mutations in CaCYP51 increases the resistance to fluconazole with the double mutation effect greater than the single mutant effect.[60,98] From this point, the docking of novel azole agents were studied in a double mutant strain and compared with the docking in the wild type CaCYP51 protein. MD simulations of 100 ns were performed using a representative mutant strain (Y132H+K143R) of CaCYP51 with (*R*) and (*S*)-configurations of **57c** and the extended sulfonamide derivative **69b** compared with the docking studies in the wild type which were shown in figure 61.

The (*R*)-enantiomer of **57c** lost all interactions previously observed in the wild type CaCYP51 (Figure 61) except a hydrophobic interaction with Tyr118 in the Y132H+K143R mutant strain of CaCYP51 (Figure 62). However, the (*S*)-enantiomer primarily interacted via water mediated H-bonding interactions with Met508, Ser378 and the oxygen atoms of the nitro group, and hydrophobic interactions with Ile131 and Leu376. In addition, a π-π stacking interaction between Tyr118 and a phenyl ring (Figure 62). The interaction between the hydroxyl group and Gly307 observed in wild type CaCYP51 was not observed in the Y132H+K143R double mutant.

The (*R*)-enantiomer of the extended sulfonamide derivative (**69b**) formed additional binding interactions in the active site of the Y132H+K143R mutant strain of CaCYP51, mainly water mediated H-bonding interactions with Pro375, His377 and the oxygen atom of the sulfonamide linker, and a direct H-bonding interaction between Ser378 and the NH heteroatom of sulfonamide linker as well as the oxygen atom of the sulfonamide group. Hydrophobic interactions with Tyr118, Phe380 were observed in the Y132H+K143R double mutant compared with the π-π stacking interaction shown in wild type CaCYP51. The (*S*)-enantiomer of **69b** showed a H-bonding interaction with Asn232 and the oxygen atom of the sulfonamide group, a π-π stacking interaction with Phe380 and phenyl ring, and a hydrophobic interaction with Phe126 (Figure 62) with the loss of water mediated interaction between Tyr64 and NH of sulfonamide group observed in the wild type CaCYP51 (Figure 61).
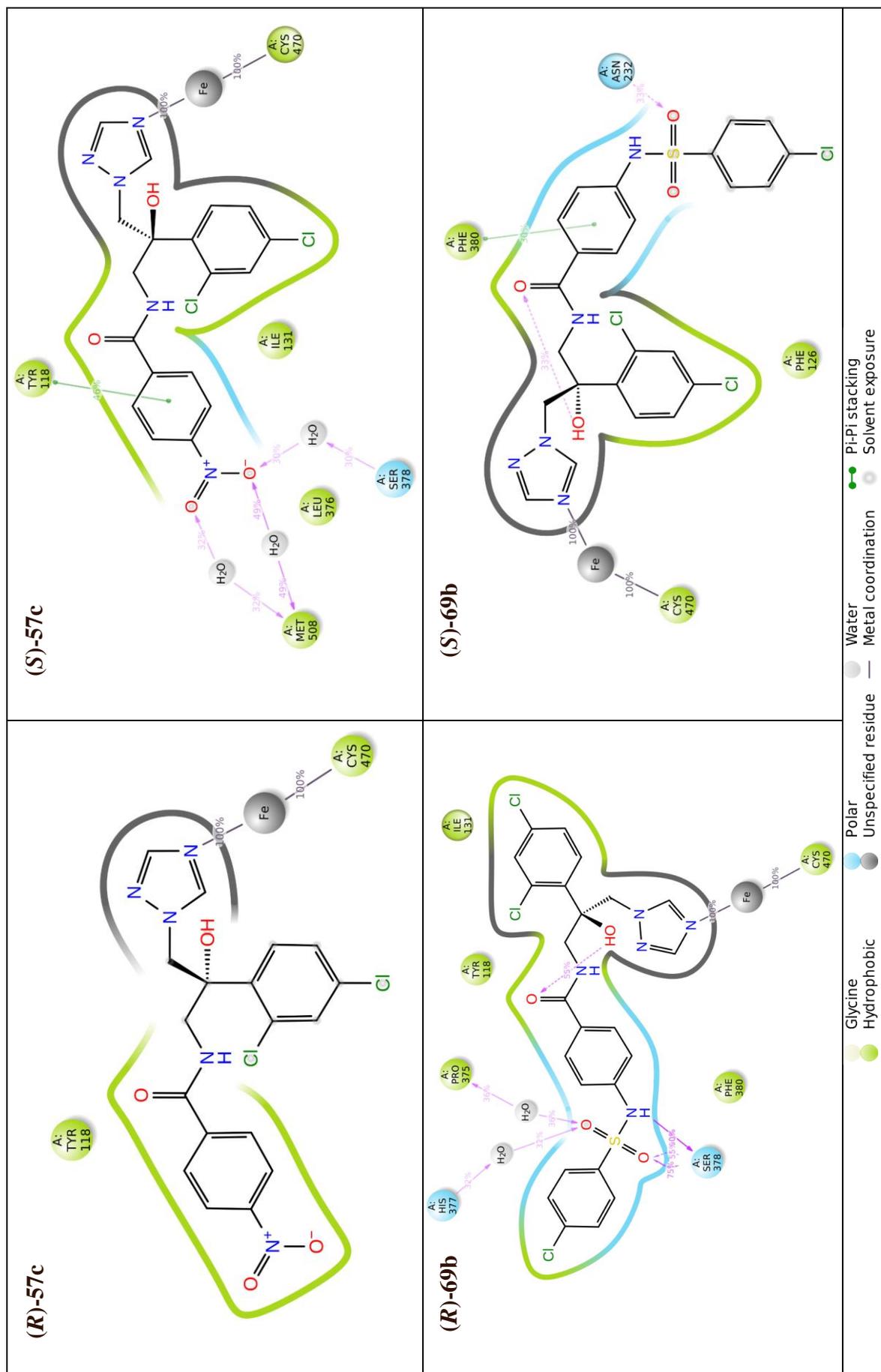
Figure 62. A schematic of detailed ligand atom interactions of representative (*R*)- and (*S*)-enantiomers of (**57c** and **69b**) with the amino acids of mutant strain (Y132H+K143R) CaCYP51 protein. Interactions that occur more than 30.0% of the simulation time in the selected trajectory (0 through 100 ns) are shown

Additionally, the measurement of the distance between the azole N and the haem Fe^{3+} before and after MD simulation was also studied in both configurations of **57c** and **69b** in wild type CaCYP51 as well as the representative mutant strain (Y132H+K143R) CaCYP51.

In the wild type CaCYP51-ligand complexes, a relatively small shift is observed after MD simulation (Figure 63) and this was also the case in the double mutant (Y132H+K143R) CaCYP51-ligand complexes (Table 38) of the novel agents.
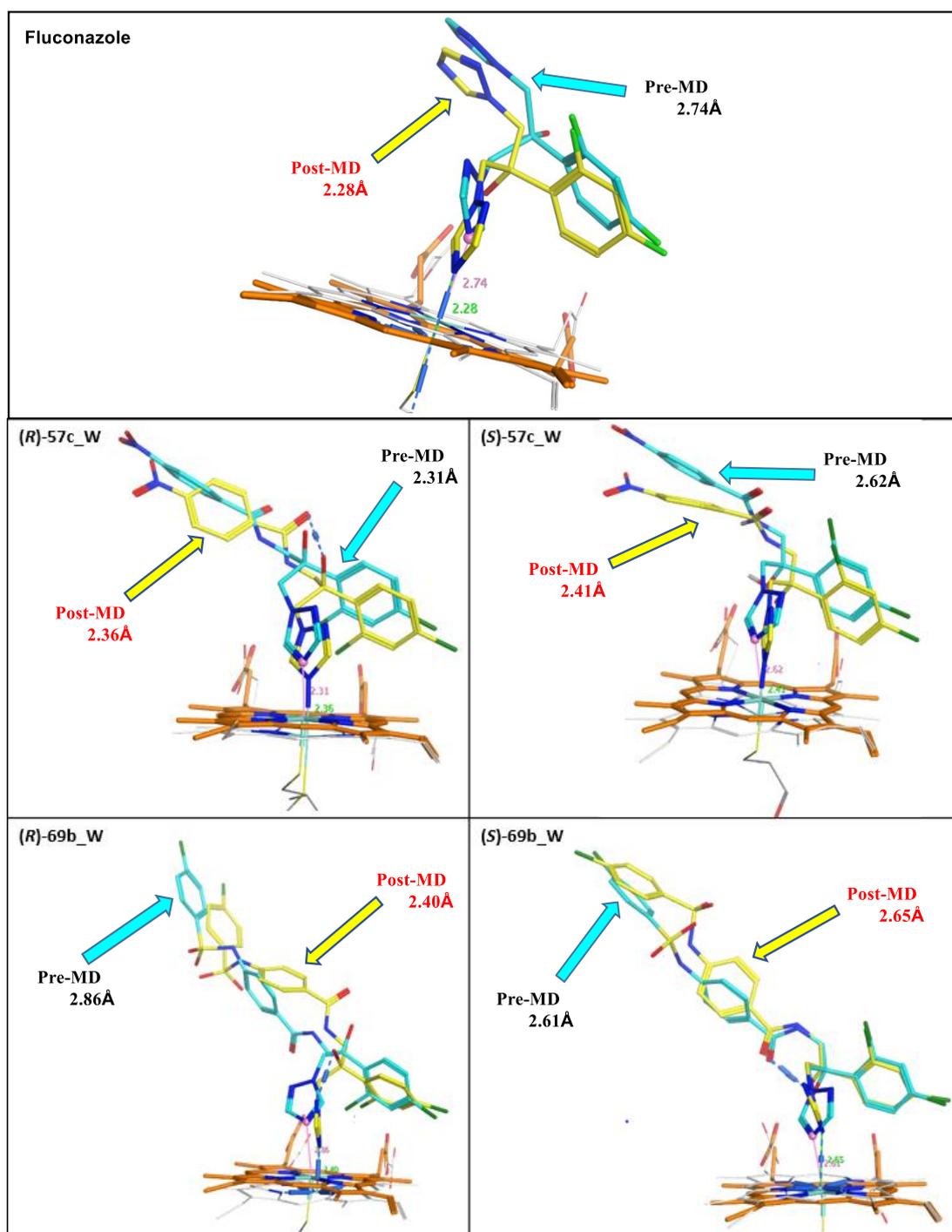
Figure 63. Wild type CaCYP51-ligand complexes of both configurations of **57c** and **69b** at 0 ns (cyan) and 100 ns MD simulation (yellow) compared with fluconazole

A less significant shift, compared with fluconazole (from 2.28 Å (pre-MD) to 2.74 Å (post-MD)), is observed with the wild type CaCYP51-ligand complexes of (*R*)-**57c** and (*S*)-**57c** from 2.31 and 2.62 Å (pre-MD) to 2.36 and 2.41 Å (post-MD) respectively, and for (*R*)-**69b** and (*S*)-**69b** a slightly increased shift in the distance was observed, from 2.86 and 2.61 Å (pre-MD) to 2.40 and 2.65 Å (post-MD) respectively (Figure 63), which might reflect the biological result obtained.

In the mutant strain (Y132H+K143R) CaCYP51-ligand complexes, a very slight shift in the distance between the N triazole ring and the haem Fe^{3+} was observed for (*R*)-**57c** and (*S*)-**57c** (2.36 and 2.25 Å (pre-MD) to 2.43 and 2.31 Å (post-MD) respectively) compared with fluconazole for which a significant shift from 2.37 Å (pre-MD) to 4.10 Å (post-MD) was noted and reflects the loss of haem binding (Table 38) and may explain the reduced effect of fluconazole against this mutant CaCYP51.[98,123] Furthermore, the distance measurements for the mutant strain (Y132H+K143R) CaCYP51-ligand complexes of (*R*)-**69b** and (*S*)-**69b** also showed a small shift from 2.32 and 2.26 Å (pre-MD) to 2.36 and 2.34 Å (post-MD) respectively (Table 38).

Table 38. The distance between the N-azole ring and the haem iron in the mutant strain (Y132H+K143R) of CaCYP51 at 0 ns and 100 ns MD simulation

	Distance (Å) between N-azole ring and haem iron in the CaCYP51 (Y132H+K143R)-ligand complexes	
	Ligand complex at 0 ns	Ligand complex at 100 ns
(*R*)-enantiomer 57c	2.36	2.43
(*S*)-enantiomer 57c	2.25	2.31
(*R*)-enantiomer 69b	2.32	2.36
(*S*)-enantiomer 69b	2.26	2.34
Fluconazole	2.37	4.10

These finding might indicate that these novel inhibitors could give promising antifungal activity and may overcome fluconazole resistance in the representative mutant strain with respect to the modelling studies, however more investigation with testing these novel inhibitors in the mutant strain is needed to confirm these observations, which could help in the design approach for selective antifungal agents.

4.6 Conclusion

All optimised novel azole compounds have been designed, synthesised and investigated for CYP51 inhibitory activity, binding affinity and MIC against *C. albicans* strains.

All novel derivatives have been docked to investigate the binding interactions using the co-crystallised CaCYP51-posaconazole crystal structure (PDB 5FSA)[35] as previously used in chapter II and chapter III. All the compounds of this series formed a coordinate bonding interaction between the haem Fe^{3+} and the N of triazole ring at a distance of < 3.0 Å. The docking studies of novel derivatives (**57**, **68** and **69**) showed several water mediated interactions between Pro375, Leu376, His377, Ser507 and Met508 and the sulfonamide group as well as a direct H-bonding interaction between the amide group and Tyr118 that may overcome the fluconazole resistance.

Subsequently, a seven step synthetic pathway was successfully achieved, after several trials to optimise this pathway, which was initiated by the addition of the triazole ring, Corey-Chaykovsky epoxidation reaction, azide formation, reducing azide to amine, coupling to form an amide group, reduction of the nitro group to free amine by catalytic hydrogenation and finally coupling to form the sulfonamide linker. All novel tested compounds were $\geq 95\%$ pure.

The novel derivatives were effective against *C. albicans* strains (e.g. **57c,** MIC < 0.03 µg/mL: **69b**, MIC 0.25 µg/mL; fluconazole MIC 0.125 µg/mL) and **57c** and **69b** exhibited some binding affinity and inhibitory activity (K_d 108 ± 34.4, IC_{50} 1.24 µM) (K_d 94 ± 24.4, IC_{50} 0.78 µM) respectively. To determine whether any specific physicochemical factors may account for the difference in MIC, the physicochemical properties of the most promising prepared compounds were calculated (Table 39) and compared with reference antifungal agents (previously detailed in Chapter II (Table 13)). The cLogP was determined using Crippen's fragmentation,[96] and the molecular weight (MW), number of H-bond acceptors (nON), H-bond donors (nOHNH) rotatable bonds (nrot), along with the molecular volume (MV) and topological polar surface area (TPSA) were calculated using Molinspiration software.[104] The number of violations (nviol) of Lipinskys is determined from the data presented (violations italicised in Table 13 (Chapter II) and Table 39).

The most promising prepared compounds have a significantly increased cLogP, although still within Lipinsky range, when compared with fluconazole but are similar to voriconazole

and oteseconazole. Compound **57c** fits closely with voriconazole, while **69b** is more similar to oteseconazole in all other physicochemical properties but, unlike the clinically described azoles, these inhibitors do not violate Lipinskys rules, showing more optimal drug like properties. There is a considerable range in all the physicochemical properties calculated for the clinically used potent azole antifungals, and the clear difference observed with the two novel inhibitors is for compound **57c**, which has two H-donors whereas **69b** has three H-donors compared with the clinically used azole antifungals, which have one H-donor (Table 13 (Chapter II) and Table 39).

Table 39. Physicochemical properties of selected derivatives

Compd	MW	cLogP	nON/ nOHNH	nrot	MV (Å^3)	TPSA (Å^2)	nviol
57c	436.25	2.54*	9/2	7	343.83	125.87	0
69b	580.88	4.01	9/3	9	449.28	126.21	*1*

nON = H-bond acceptor; nOHNH = H-bond donor; nrot = number of rotatable bonds; MV = molecular volume; TPSA = topological polar surface area; nviol = number of Lipinsky violations. *miLogP was calculated using Molinspiration software[104]

Additionally, MD simulations were performed to investigate the binding and position of inhibitors; owing to the ability of both ligand and protein to move during MD simulations a more accurate reflection of physiological conditions may be provided. The MD simulations for both configurations of **57c** and **69b**, chosen as representatives of the compounds described in this Chapter, were performed in the wild type and double mutant (Y132H+K143R) strains of CaCYP51 compared with fluconazole. The resulting data showed good binding interactions for **57c** and **69b** derivatives in both configurations with hydrophobic interactions and some H-bonding interactions through water molecules along with direct interactions with could overcome the fluconazole resistance.

Although the nitro derivatives (**57**) showed good activity against *C. albicans* strains they would be likely to undergo first pass metabolism owing to the nitro group, therefore replacement of the NO$_2$ group with alternative electron withdrawing groups or bioisosteres would be useful to prepare and evaluate. Likewise, the amine derivatives (**68**) would be subject to Phase II biotransformation so alternative H-bond donors should be considered.

Owing to the time required for enzyme preparation, extraction, and the lockdown necessitated by the COVID-19 epidemic, further biological evaluation including testing in the mutant strains with the collaborator at the Centre for Cytochrome P450 Biodiversity, Swansea University Medical School, has been delayed.

This novel series is very promising and is being continued by another PhD student, Marwa Alsulaimany, in Dr Claire's Lab with further development through computational studies to investigate the binding interactions with CaCYP51 leading to the design of selective azole inhibitors to overcome fluconazole resistance.

Chapter V

Homology model of Leishmania donovani orphan CYP5122A1

5.1 Introduction

Leishmaniasis is a diverse and complex vector-borne infection, designated by the World Health Organization (WHO) as a neglected tropical disease, which can be found in Asia, the Middle East, Africa, Southern Europe and South America.[80,124] Leishmaniasis is caused by a protozoa parasite from over 20 *Leishmania* species, which belong to the *kinetoplastids*, and is transmitted to humans by the bite of infected female phlebotomine sandflies replicating intracellularly within macrophages.[80,125,126,127] Leishmania alternates between two life stages: promastigote, inside the digestive tube of the vector where it differentiates into the infective form; amastigote, representing the clinically relevant stage of the parasite and occurring inside the mammalian host (Figure 64).[80,124-128]
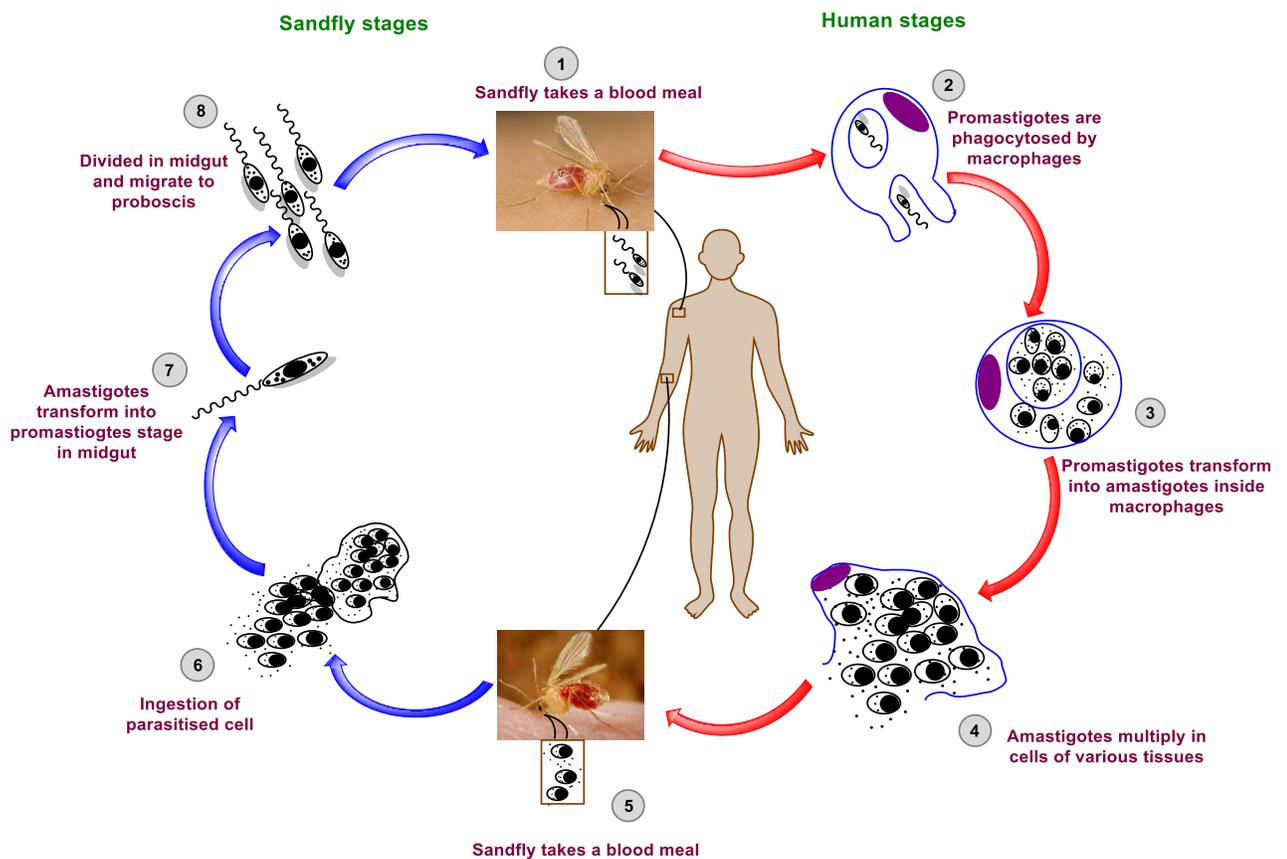
Figure 64. Leishmaniasis life cycle. (1) Leishmaniasis is transmitted by the bite of infected female phlebotomine sandflies. The sandflies inject the infective stage (i.e., promastigotes) from their proboscis during blood meals to the skin of the host. (2) Promastigotes that reach the puncture wound are phagocytosed by macrophages. (3) Promastigotes transform in these cells into the tissue stage of the parasite (i.e., amastigotes), (4) which multiply by simple

division and proceed to infect other mononuclear phagocytic cells. Sandflies become infected by ingesting infected cells with amastigotes during blood meals ((5), (6)). (7) In sandflies, amastigotes transform into promastigotes, develop in the gut, and migrate to the proboscis (8) to start the cycle again.

Leishmaniasis infection can range from asymptomatic to more severe conditions; cutaneous and mucosal leishmaniasis can cause substantial morbidity, whereas visceral leishmaniasis can be life-threatening.[124] Leishmaniasis is the ninth cause of disease burden among all infectious diseases and thus remains a severe public health problem, especially in developing countries.[127] The number of incidences of visceral leishmaniasis due to *Leishmania donovani* (*L. donovani*) and *Leishmania infantum* (*L. infantum*) is approximately 50,000-90,000 new cases with more than 95 % deaths each year globally.[129] Based on its clinical manifestations, the disease is classified into four main clinical forms: cutaneous leishmaniasis (CL); mucocutaneous leishmaniasis (ML); visceral leishmaniasis (VL, also known as kala-azar); and post-kala-azar dermal leishmaniasis (PKDL).[128]

Cutaneous leishmaniasis (CL) causes skin lesions.[128] The first sign of an infection is small erythema, which develops at the site of the sandfly bite.[43,130] The erythema enlarges into a papule, then into a nodule, and the nodule ulcerates over two weeks to six months, to become a lesion.[130] CL is the most common form of the disease with about 1.5 million new cases of cutaneous leishmaniasis occurring each year.[128,131] More than 70% of CL occurred in 10 countries: Afghanistan, Algeria, Brazil, Colombia, Costa Rica, Ethiopia, the Islamic Republic of Iran, Peru, Sudan, and the Syrian Arab Republic.[128]

Mucocutaneous leishmaniasis (ML) affects the mucous lining of the nose, mouth, and throat.[128] ML tends to occur 1 to 5 years after CL caused by these organisms has healed, but it can also be seen while skin lesions are still present.[130] ML can cause disfigurement, which leads to the stigma of those who are severely affected.[128] Ninety percent of patients with ML are seen in Bolivia, Brazil, and Peru.[128]

Visceral leishmaniasis (VL) is also known as kala-azar in the Indian subcontinent or black fever, which affects internal organs such as the liver, bone marrow and spleen.[124,128,132] VL is the most severe form of the disease and is fatal if left untreated. VL is associated with high fever, weight loss, decreased appetite and hepatosplenomegaly; other symptoms may include coughing, chronic diarrhoea and darkening of the skin. [130,132] About 90% of cases of VL are found in India,

Brazil, Sudan, Nepal, and Bangladesh, although in India, the state of Bihar alone accounts for ninety percent of cases.[133]

Post-Kala-azar Dermal Leishmaniasis (PKDL) may arise six months or more after recovery, in some cases of VL.[128,130] This manifest as a rash and occurs mainly in East Africa and the Indian subcontinent.[128]

The current treatment of leishmaniasis (pentavalent antimonial, amphotericin B, paromomycin, pentamidine and miltefosine), relies exclusively on chemotherapy, regardless of the species responsible.[134-137]

5.1.1 Leishmaniasis treatments

For more than 70 years, pentavalent antimonials have been the first choice of treatment for leishmaniasis with two commercially available: meglumine antimoniate (Glucantime®) and sodium stibogluconate (Pentostam®) (Figure 65), which are administered via slow intravenous (IV) or intramuscular (IM) injections.[126,127,132,136] The mechanism of pentavalent antimony action is not fully understood but based on extensive investigations one major hypothesis involves the biological reduction of Sb (V) to Sb (III) by the parasite or by the infected host cells to create antileishmanial activity.[126] As a result of the route of administration and the severe adverse effects such as gastrointestinal intolerance, nephrotoxicity, pancreatitis and cardiotoxicity, patients should be hospitalised and monitored, which can lead to the patient abandoning the therapy which increases drug-resistant parasites.[127,132,136]

Meglumine antimonate   **Sodium stibagluconate**
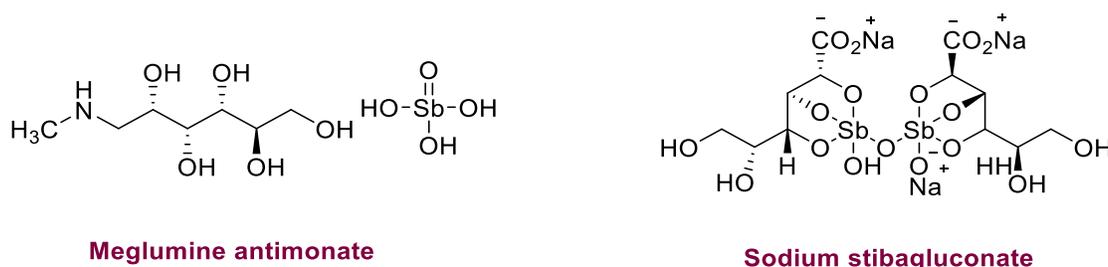
Figure 65. Pentavalent antimonials antileishmaniasis agents

In cases of drug intolerance or parasite resistance to antimonials, amphotericin B (AmBisome®) (Figure 66), a polyene antifungal agent, and its liposomal formulations are second choice drugs with high efficacy leading to 99.5% clearance of the parasite in the treated patients.[34,50,79] Even

with the high cure rate, the cost of AmBisome® treatment is a limiting factor for patients in developing countries.[50] Despite negotiations between the WHO and Gilead, the producer of AmBisome®, to reduce the price of the treatment ($18 per 50 mg ampoule), the treatment is still expensive.[50] Amphotericin B binds to ergosterol, in the fungus or the parasite rather than to human cholesterol, the major sterol present in Leishmania cell membranes, which alters the ion balance and leads to cell death.[22,50,79] However, amphotericin B causes acute adverse effects such as nausea, vomiting, fever, hypertension/hypotension; and chronic effects such as nephrotoxicity.[34,50,79] Also, amphotericin B requires long term intravenous administration, and it is inaccessible to patients in low-income countries.[79]

Amphotericin B

Figure 66. Amphotericin B antileishmaniasis agent

Another drug that has also proved its efficacy with a 94.6% cure rate towards VL caused by *L. donovani* is paromomycin, an aminoglycoside antibiotic[22,50,79] (Figure 67). In the 1960s the antileishmanial activity of paromomycin was first identified.[50] However, it must be given by IM injection over a period of three weeks, which is a significant limitation.[27,79] The mechanism of paromomycin action in Leishmania is not precisely known, but there is some evidence that it inhibits protein synthesis, alteration of membrane fluidity and lipid metabolism along with impairment of the mitochondrial membrane potential.[22,50]

Paromomycin

Figure 67. Paromomycin antileishmaniasis agent

Furthermore, pentamidine, an aromatic diamidine (Figure 68), is used as a second-line drug mainly against VL and for refractory patients following pentavalent antimonial treatment.[126,127] The cellular target of pentamidine in *Leishmania* and other *Kinetoplastids* is unknown, but studies suggest that it inhibits the active transport system and disrupts mitochondrial membrane potential.[126,132] High toxicity, combined with an increasing rate of treatment failure in patients suggesting resistance, has resulted in the complete abandonment of this drug to treat VL in India.[127]
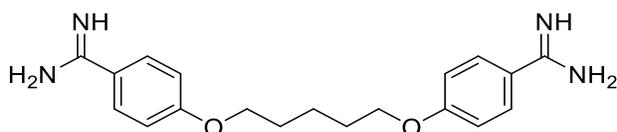
Pentamidine

Figure 68. Pentamidine antileishmaniasis agent

Miltefosine (Impavido®), an alkyl-phosphocholine drug was identified in the early 1980s as an anticancer and antileishmanial drug[126,127,132,136] (Figure 69). The mechanism of action of miltefosine is not fully understood; it is proposed to be direct action against the parasite by impairing the lipid metabolism causing an apoptosis-like death of Leishmania parasite.[127,132]

Miltefosine was approved in 2002 to be the first oral antileishmanial drug for treating VL in India.[80,126] Although its toxicity is not very high; its teratogenicity is a problem as well as long-term administration and relatively high cost.[80,127,132]
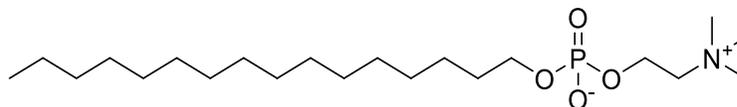
Miltefosine

Figure 69. Miltefosine antileishmaniasis agent

However, these drugs are severely limited by factors such as significant side-effects, growing incidence of parasitic resistance, toxicity or route of administration and high cost, a heavy burden for the majority of patients who live under poverty standards.[134,138] All these factors make the development of new, inexpensive oral agents with improved efficacy against existing drug-resistant strains and reduced toxicity as well as searching for new targets are an urgent need .

Currently, the new research is strongly focused on a combination treatment and/or new formulations of the existing therapies to rapidly introduce new agents for clinical use to treat the neglected leishmaniasis, such as research under DND*i*.[126] DND*i* is Drug for Neglected Diseases *initiative*, which could be one of the leading organisations driving research to deliver cures for leishmaniasis, one combination therapy being investigated is miltefosine + paromomycin for the treatment of VL in Africa, and is currently in Phase III clinical studies.[139]

Although there have been some recent advances in leishmaniasis chemotherapy, the need for a new target with different modes of action may allow a degree of selectivity and activity against existing drug resistance strains. For interest, CYP51 is found in all biological kingdoms such as fungi, animals and protozoa, that catalyses the removal of the methyl group at carbon 14 from lanosterol.[21,45,47,48] Unlike mammalian cells, but similar to fungi, the *Leishmania* parasite cell membrane produces ergosterol and ergosterol-like molecules rather than cholesterol.[43,125] Although there is significant variation at the protein sequence level, CYP51 is highly conserved across eukaryotes at the structural level. The major advantage of CYP51 as an antiprotozoal drug target relates to its high drugability for inhibitor design.[45,47] Inhibitors of this enzyme (azole

antifungals) are already used in clinical and agricultural settings.[45,46,47] These drugs inhibit CYP51, and their potency is enhanced by the accumulation of toxic methylated sterols, which are unable to replace ergosterol in the membrane owing to steric hindrance resulting in fungal/parasite growth arrest and cell death.[45,46,48,140] The treatment of Leishmania infections has been studied by azole antifungals with varying efficacy.[43] Another member of cytochrome P450 family, CYP5122A1 has been shown to be essential for survival, virulence, drug response, and ergosterol metabolism in *Leishmania*, in addition a synergism has been found between CYP5122A1 and CYP51, which could be a bypass mechanism in leishmania parasites to maintain the essential ergosterol needed for survival and may be the cause of the variable activity of azoles in protozoa.[43,79,80]

CYP5122A1 has been identified as an orphan cytochrome P450 enzyme found specifically in *Trypanosoma* (*T.*) and *Leishmania* (*L.*) species; particularly *L. donovani* that causes VL, and is mainly distributed in the endoplasmic reticulum, but also in the glycosomes and the mitochondria in small amounts.[79] Since the sequence identity between *L. donovani* and *L. major* are high (94.7 %) and in the absence of the genome sequence of CYP5122A1 *L. donovani*, the CYP sequence of *L. major* was used as a representative source to investigate this orphan enzyme.[79,141] CYP5122A1 sequence exhibited all the essential amino acids that characterise CYP which include: a transmembrane domain (38 to 60 amino acids), a proton transfer groove (348 to 353 amino acids), a motif for stabilisation of the core (418 to 421 amino acids) and a haem binding loop (516 to 525 amino acids); which will be illustrated later in this chapter.[79] Furthermore, a research study indicated that arylimidamide BD766 [*N*, *N''*-(furan-2,5-diylbis(3-isopropoxy-4,1-phenylene))dipicolinimidamide] (Figure 70), which was designed from pentamidine, had potent antileishmanial activity using *in vitro* and *in vivo* studies with a distinct mechanism of action.[80] BD766 is thought to be an inhibitor for CYP5122A1 and its antileishmanial activity is not fully understood but might be due to the interference related to ergosterol biosynthesis.[80] In addition, it was found that BD766 had a synergistic activity with posaconazole in *in vitro* studies possibly as a result of decreased expression of CY5122A1 forcing the parasite to rely more on CYP51 for sterol biosynthesis.[80]
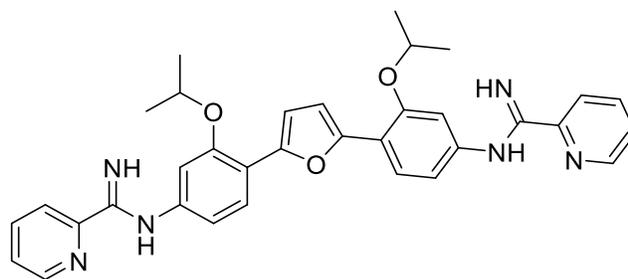
BD766

Figure 70. Structure of BD766

Ergosterol, which is the primary component of the Leishmania membrane, is functionally linked to maintenance of structural integrity.[79] Thus, interference with ergosterol biosynthesis could result in disruption of parasite function and demethylated products involved in this pathway could serve as potential drug targets. The aim in this chapter is to use molecular modelling methodologies (homology modelling, molecular dynamics, molecular docking) to identify novel potential compounds that could inhibit the target enzyme (CYP5122A1), with subsequent synthesis and biological evaluation.

5.2 Homology modelling

Research centres in the past two decades have changed the traditional method of research to generate novel bioactive molecules by using advances in molecular modelling techniques through the identification of enzymes using X-ray crystallography, after which, drugs were designed which could bind with enzymes as ligands. Furthermore, molecular modelling is a computational technique used in pharmaceutical research to design and discover potentially useful proteins, which are visualised as three-dimensional structures.[142] Molecular modelling also helps to understand and to interpret experimental observations and provide data not available from actual experiments.

Proteins are essential to life, as they play critical roles in most biological processes, X-ray crystallography is the main method for determining the structure of proteins; however, the majority of proteins are currently challenging to crystallise. The protein data bank (PDB)[76,77] is an available source of protein crystal structures, but only a small percentage of all known proteins are available as three-dimensional structures. Homology modelling is used for the determination of a protein structure based on the crystal structure of a protein (template), which has a similar amino acid sequence. Ideally, the similarity between a query sequence and the template sequence should be above 20 %.[143]

Four steps are involved in the homology process. First, one or more appropriate structural templates are identified from the PDB.[144] The second step aligns the query sequence with the template sequence. The third step develops the general skeleton from the alignment. Finally, the homology model is subject to validation .

CYP enzymes are promising protein/enzyme targets, particularly CYP5122A1 in leishmania ergosterol biosynthesis. A homology model for this enzyme was needed as no crystal structure is currently available. This can provide an excellent tool to evaluate potential inhibitory activity when docking the designed ligands .

The only previous homology model described for *L. donovani* CYP5122A1 used the crystal structure of *Bacillus megaterium* (CYP107) with PDB: 1ZOA as the template;[79] however the large number of outliers (34 amino acids residues in the outlier region) would suggest a poor-quality model. In addition, this template includes a mutation (Ala328 to Val328) within the binding site, which would also rule the template out.

5.3 Identification of a template

The Expert Protein Analysis System (ExPASy)[145] proteomics server was used to obtain the amino acid sequence of the target gene *L. donovani* CYP5122A1. Using the UniProtKB database[141] from the ExPASy server, the protein sequence for *L. donovani* CYP5122A1 was obtained.

Figure 71 below illustrates the amino acid sequence for CYP5122A1 *L. donovani* in FASTA format, which is composed of 606 amino acids and has a molecular weight of 68.67 kilodaltons. This protein has a primary (citable) accession number Q2XQE3, according to UniProtKB, which is a unique number with entry name Q2XQE3_LEIDO. All information regarding CYP5122A1 was integrated into UniProtKB on December 20, 2005.

```
>tr|Q2XQE3|Q2XQE3_LEIDO Cytochrome P450-like protein OS=Leishmania donovani
PE=2 SV=1

MVFDTDFLFVNRSQMAANALQSYIVAALHNAAAKLPSSVQPYAMVLTREDMVSTTLATAI
ATAVILYTVIAVVLPVLRMDFYLSKLPTIKHGIPFLGHALLLAGPSPWSKMSNWSLYPEK
NLPQKKKGVDGSKTSRLVTFNVAGMRVIYINEPRLLRRVLLTHQRNYRKALAAAYKHFMC
LLGTGLVTSEDEQWKKGRLLLSHALRIDILDSVPEMAMKAVDRILLKLDAVNAKNPSVDL
NEEYRHMTLQVISESALSLSAEESDRIFPALYLPIVHECNKRVWAPWRAYMPFLHGSRVR
NHCLSELNKVLRDIICRRWEQRNDSKYTAKPDILALCISQIDRIDEKMIVGLIDDVKTIL
LAGHETSAALLTFATYEVLRHPEIRQRVLEEATRLFDPARCTRTVQTRYGPRGVPSVNDV
RDLVWTPAVLRETLRRHSVVPLVMRYAAKDDVWPAEDTGLDADVRIPAGCTIAVGIEGVH
NNPDVWNKPEVFDPTRFIDAEIANDTNYLNRSTKDVKFAKKIHPYAFIPFINGPRNCLGQ
HLSMIETQVALSYMMLNYDLTIYRDPSYKGDVAAYEDAVGRHHDFIIPQVPHDGLKVWGT
PNKLFM
```

Figure 71. The query sequence of *L. donovani* CYP5122A1 in FASTA format

Initial screening for possible templates was performed using BLAST analysis[146] of the amino acid sequence of CYP5122A1 *L. donovani* by an alignment of the query protein against the all known proteins in the Uniprot database. The selection of templates depends on factors and parameters such as length alignment, E-value (a better protein sequence when E-value < 0.005), % sequence identity, and BLAST score. BLAST analysis from UniProtKB[141] found 22.8%-95.3% identity between the query CYP5122A1 and proteins from five organisms. The organisms were human, mouse, zebrafish, *Arabidopsis thaliana* and rat. The seven proteins with highest % identity with the query are shown in table 40; however, none of the proteins were available as crystal structures in the PDB.

Table 40. The sequence templates identified from the CYP5122A1 BLAST (UniProtKB) results

Protein name	Accession number (Entry)	PDB code	Blast score	Sequence identity %	Chain length	E-value
Cytochrome p450-like protein (*L. major*)	E9ACY6	NA	3007	94.7 %	606	0.0
Cytochrome p450-like protein (*L. infantum*)	A4I2K5	NA	2959	95.3 %	592	0.0
Cytochrome p450-like protein (*L. braziliensis*)	A4HFC8	NA	2759	87.7 %	592	0.0
Cytochrome P450 (*T. theileri*)	A0A1X0NLV1	NA	1669	56.9 %	581	0.0
Cytochrome P450, putative (*T. brucei*)	Q57WV1	NA	1625	59.0 %	584	0.0
Cytochrome P450, putative (*T. cruzi*)	Q4D7J7	NA	1576	57.1 %	573	0.0
Cytochrome P450, putative (*T. cruzi*)	Q4D0S6	NA	1572	57.3 %	573	0.0

NA= not available

Another alignment for CYP5122A1 was performed using NCBI-Blast[147], and the results showed 20.79%-28.85% identity between the query enzyme and available PDB protein structures from human and bacteria.

For a structure to be considered as a template, it should be wild type, rather than mutant or engineered, have reasonable sequence identity with the query enzyme (CYP5122A1), should be from the same family or close to it and also have the same function. From these respective points, a search in the protein data bank was taken, and the only crystal structure found for leishmania with the same function of the query was *L. infantum* (CYP51). The crystal structure of *L. infantum* could be the most beneficial template for the homology modelling for the query protein sequence of CYP5122A1 as it is from the same genus.

To obtain more information related to the best possible template the phylogeny server[148] was used to construct a phylogenetic tree between CYP5122A1 protein sequences and the chosen CYP templates to determine the relative distances between these enzymes and the query sequence (Figure 72).
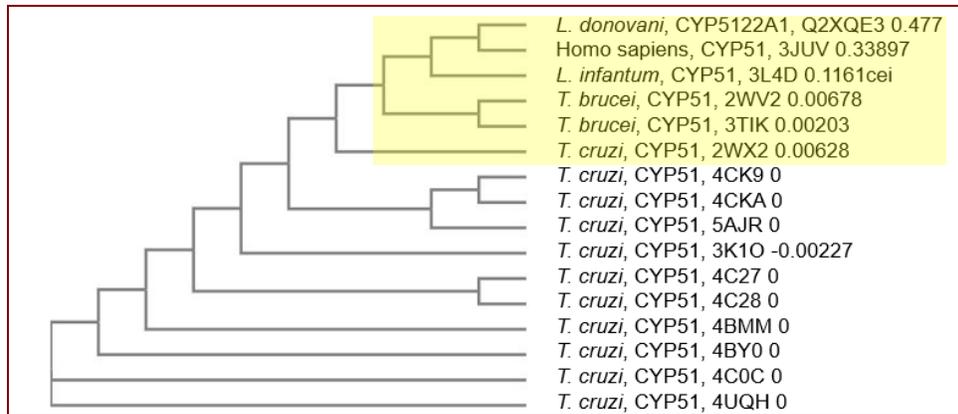
Figure 72. Phylogenetic tree generated for CYP5122A1 in relation to other CYP51 selected
         proteins from different species

After that, the Percent Identity Matrix[148] was used from the result summary tool to illustrate percent identity with the query protein; the result is shown in figure 73.

Figure 73. The percent identity matrix for CYP5122A1 in relation to other CYP51 enzyme

The phylogenetic tree indicates that CYP5122A1 is a distinct enzyme and the evolutionary distance between human CYP51 (PDB 3JUV), *L. infantum* CYP51 (PDB 3L4D), *T. brucei* CYP51 (PDB 2WV2) and *T. cruzi* CYP51 (PDB 2WX2) is short. The tree illustrates the amino acid sequence identity between these proteins: *L. infantum* CYP51 (18.06 %); *T. brucei* CYP51 (20.09 %); and *T. cruzi* CYP51 (19.00 %). The PDB 3JUV is human CYP51, and the identity was 18.40 %, which indicates the low similarity between these enzymes. Furthermore, the sequence identity of *T. brucei* CYP51 (PDB 3TIK (20.50 %)) is the highest percent similarity

for the query, however, PDB 3TIK was not chosen as one of the best templates owing to the distance indicated in the phylogenetic tree. A phylogenetic tree between CYP5122A1 protein sequence and the chosen template *L. infantum* CYP51 (PDB 3L4D) was aligned again to show the accurate distance between these enzymes as well as the Percent Identity Matrix to identify the similarity between the query enzyme CYP5122A1 and the template *L. infantum* CYP51 (PDB 3L4D).

```
                                            L. donovani, Q2XQE3_LEIDO 0.76429
                                            L. infantum, 3L4D 0.76429
```

```
#
#
#   Percent Identity  Matrix - created by Clustal2.1
#
#

  1: L. donovani, Q2XQE3_LEIDO   100.00    23.57
  2: L. infantum, 3L4D            23.57   100.00
```

From all the results, *L. infantum* CYP51 (PDB 3L4D) appeared to be the best template for the target sequence, CYP5122A1, as they are from the same family.

5.4 Multiple sequence alignment

The Clustal Omega tool[149] from the European Bioinformatics Institute, part of the European Molecular Biology Laboratory (EMBL-EBI)[148] was used to align the preferred template sequences and the query sequence of CYP5122A1 which would reveal the most conserved residues and could also be used to understand some of the expected structural and functional similarity between these enzymes (Figure 74).

In figure 74, all helices and beta strands are underlined and labelled clearly. The substrate recognition sites (SRS) regions from one to six are identified,[150] the SRS have several functions in CYPs such as oxygen binding and its activation, interaction with redox partners, structural roles including membrane association and haem binding.[69] In addition, the conserved cysteine in **FXXGXXXCXG** motif in each of these sequences is a crucial residue as it contributes to the thiol group, which is the fifth ligand that binds the iron atom in these haemoproteins. The query sequence was aligned against the best three CYP51 templates from different species (PDB: 3L4D, 2WV2 and 2WX2) using Clustal Omega. From this alignment, there are 70 amino acids conserved between the four proteins and 108 identical amino acids.
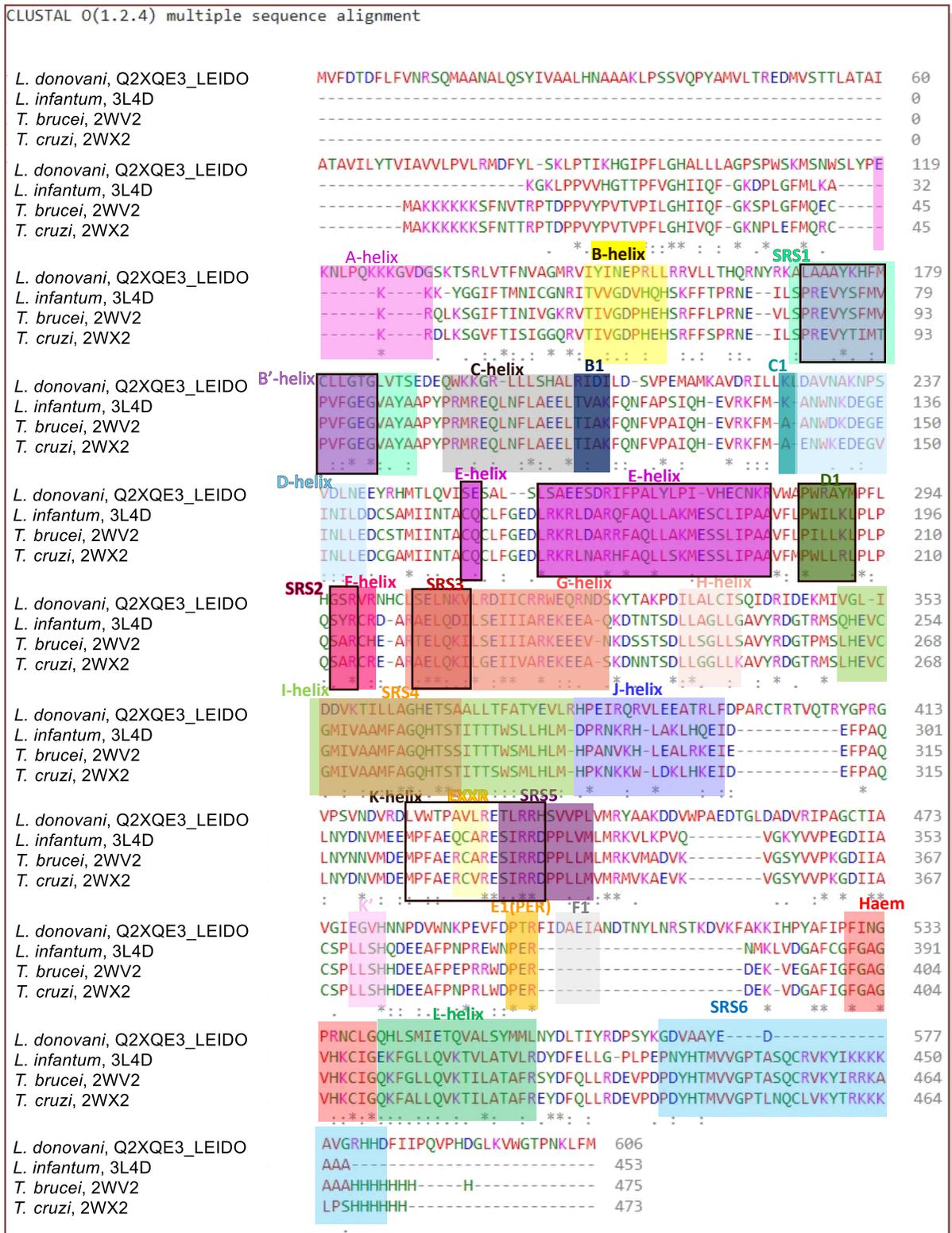
Figure 74. EMBL-EBI Clustal Omega alignment of Q2XQE3_LEIDO, 3L4D, 2WV2 and 2WX2 using ClustalW. "*" means the residues are highly conserved, ":" means the residues are identical, "." means the residue are somewhat similar

5.5 Second structure prediction

The PSIPRED[151] programme was used to predict the secondary structure of CYP5122A1 and the template (Figure 75). The prediction showed a good overlap between the template and the query secondary structure especially in positions of the A, B, B', C, D, E, F, G, I, J, K and L helices, which are interrupted by coil moieties in different sequences in the target enzyme compared with the template.

On the other hand, the query enzyme lacks the H helix; the SRS6 sequence is also missing from the query whereas in the template was predicted as β-strand. E1 and F1 helices, which are located between the K' and L-helix, are missing in the template. These findings are illustrated in more detail in table 41.
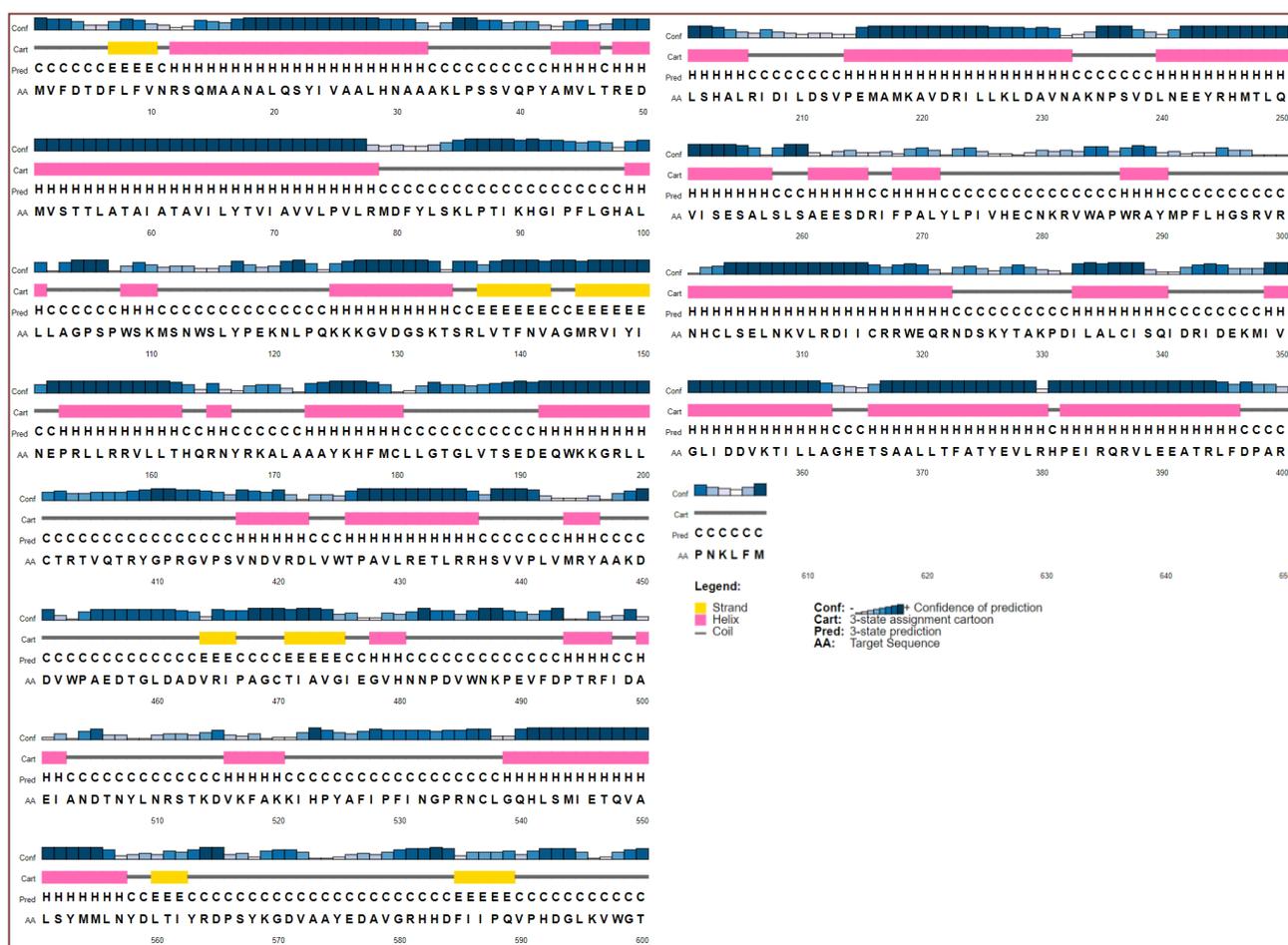
Figure 75. Secondary structure of CYP5122A1 predicted using PSIPRED software, showing helix (pink rectangle), β-strand (yellow rectangle) and coil (continuous line) with confidence level of prediction

Table 41. Comparison between the template *L. infantum* CYP51 and the query enzyme *L. donovani* CYP5122A1

The template (*L. infantum* CYP51)		The query (CYP5122A1)	
Secondary structure	*Residues*	*Secondary structure*	*Residues*
		β -Strand	Phe7-Val10
A-Helix	Ile18-Gln20	A-Helix	Arg12-Ala32
A-Helix	Pro25-Tyr36		
β -Strand	Ile39-Ile44		
β -Strand	Asn47-Val52		
B-Helix	Val55-Phe61	Helix	Ala43-Leu46
B'-Helix (SRS1)	Tyr75-Phe82	B & B'-Helix (SRS1)	Arg48-Arg78
C & C1-Helix	Met95-Lys110	C-Helix	Ala99-Leu101
		C1-Helix	Trp108-Lys110
D-Helix	Ser117- Asn131	D-Helix	Lys125-Thr134
		β -Strand	Leu137-Val142
		β -Strand	Met145-lle150
E-Helix	Asp142-Phe156	E-Helix	Pro153-Thr162
D1	Leu160-Arg163	D1	Arg165-Asn166
F-Helix (SRS2)	Arg166-Cys179	F-Helix (SRS2)	Ala173-Cys180
F-Helix (SRS2)	Ala183-Val185		
Helix	Pro188-Lys192	G-Helix	Gln192-Leu205
G-Helix (SRS3)	Ala204-Gln225	G-Helix	Pro214-Asn232
H-Helix	Asp232-Tyr242		
I-Helix (SRS4)	Gln250-Phe262	I-Helix	Leu240-Leu257
		I-Helix (SRS4)	Ala261-Asp265
I-Helix (SRS4)	Thr267-Leu279	I-Helix (SRS4)	Phe268-Leu271
J-Helix	Arg283-Ile295	J-Helix	Leu287-Tyr290
J'-Helix	Asp305-Met308	J' & K-Helix	Asn301-Arg322
K-Helix	Pro312- Arg324		
β -Strand	Arg333-Val335	Helix	Ile333-Gln340
β -Strand	Val339-Val341		
β -Strand	Tyr344-Val346		
β -Strand	Ile351-Cys354		
K'-Helix	Pro356- His360	K'-Helix	Ile349-Ala362
Helix	Glu363-Ala365	E1-Helix	Thr366- Arg380
		F1-Helix	Pro382- Phe396
L-Helix	Gly397- Asp415	L-Helix	Val417-Asp422
		Helix	Thr426-Arg436
β -Strand (SRS6)	Asp417-Leu420		
β -Strand	Arg442-Lys447		
Helix	Lys450-Ala451	Helix	Met444-Tyr446
		β -Strand	Val464- Ile466
		β -Strand	Thr471- Gly475
		Helix	Gly478- His480

	Helix	Pro494-Phe497
	Helix	Ala500-Ile502
	Helix	Val516-Lys520
	Helix	Gly539-Asn557
	β -Strand	Leu560-Ile562
	β -Strand	Phe585-Gln589

5.6 Building 3D homology model

The homology model was constructed using *L. infantum* CYP51 (PDB 3L4D) crystal structure as a template for the query enzyme. The SWISS-MODEL server[152] was used to generate a homology model for CYP5122A1, as the SWISS-MODEL server automatically fixes the loop gaps in the query sequence, this would provide a complete model.
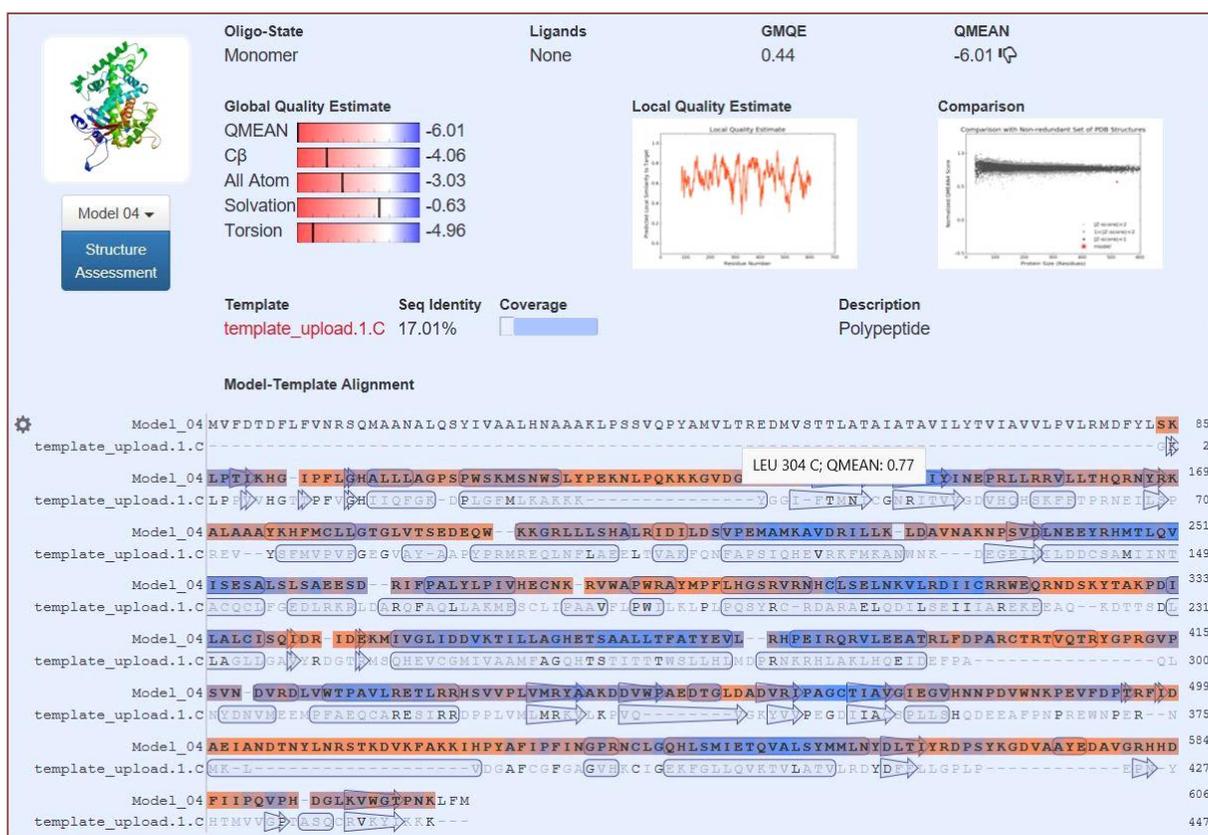
Figure 76. SWISS-MODEL for CYP5122A1

The constructed model was subjected to a number of checks to assess its quality. Stereochemical quality was evaluated by Ramachandran plots using the RAMPAGE server[153], and the overall protein structure was evaluated using ProSA.[154,155]

5.7 Homology validation

Every homology model contains errors, with the number of errors depending on various factors: first, regarding the % sequence identity between template and target, if it is greater than 90 %, the accuracy of the model can be compared with the crystal structure, except for a few individual side chains.[156] From 26 % to 90 % identity, the error will start. If the sequence identity is 25 % or less, the homology model will have very large errors. If errors in the template are located far from the active site, the error becomes less important. Validation should be taken for both the template as well as the model, and the results would propose that the model performed well in terms of the backbone stereochemistry and amino acid environment.

5.7.1 Validation by Ramachandran plots

Ramachandran plots were generated using the RAMPAGE server[153] to verify the quality of the template and the query model. A Ramachandran plot interprets phi-psi torsion angles (φ-ψ) for all residues in the structure. Importantly, glycine residues appear unique and separated from other residues in the plot region. In addition, glycine and proline residues are represented in different plots due to a difference in the phi-psi angles.

In the Ramachandran plot, a total of 95.7 % of the residues were in the favoured and allowed region, which compared with the template 3L4D (100 %), revealing that the main chain dihedral and Ψ angles in the model were reasonable. The template had no residues in the outlier region, and the CYP5122A1 model showed 22 amino acid residues in the outlier region (Table 42).

Table 42. Ramachandran plot evaluation of the template and the corresponding model

PDB	No. of residues in favoured region	No. of residues in allowed region	No. of residues in outlier region	Amino acid outlier
3L4D	437	9	0	-
CYP5122A1 model	456	40	22	Ile93, Pro94, Ser106, Leu116, Tyr117, Pro123, Val129, Pro236, Ala329,

				Thr402, Arg412, Val414, Ala500, ASP505, His523, Tyr525, Ile528, Asp565, Asp571, Val572, Arg581, His592

Visualisation of the outlier amino acid residues in the CYP5122A1 model by MOE,[78] showed them away from the haem active site (Figure 77).
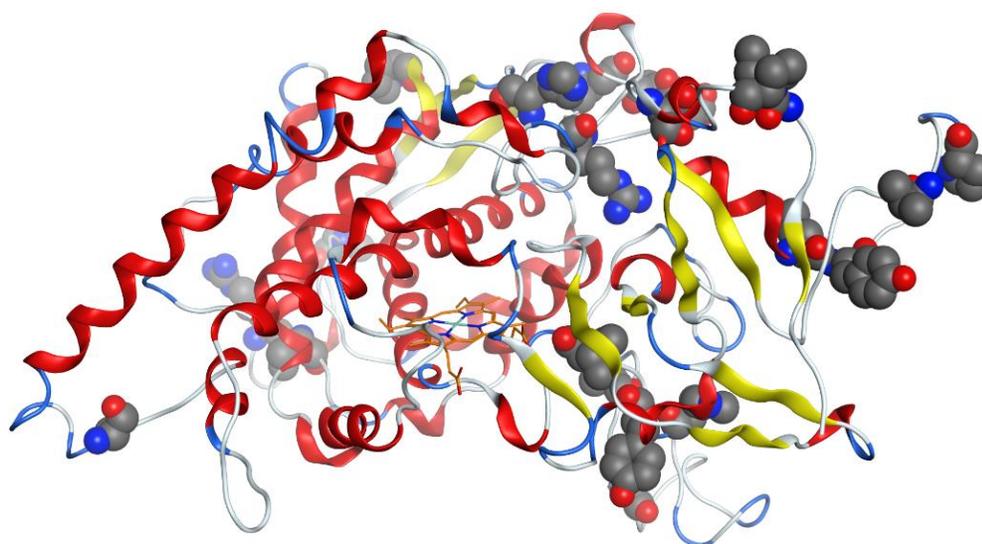
Figure 77. Outlier amino acids (space filled) identified by Ramachandran plot for the CYP5122A1 model

5.8 Molecular dynamic simulation

5.8.1 Molecular dynamic for CYP5122A1

Molecular dynamics can be used to correct protein structure issues, for example, folding, conformational flexibility, and stability. A molecular dynamics simulation of CYP5122A1 was

performed for 100 ns using Desmond[102] at 300 K temperature, which represents normal body temperature.

The Root Mean Square Deviation (RMSD) is used to measure the average change in displacement of a selection of atoms for a particular frame with respect to a reference frame. RMSD values of the backbone atoms were plotted as a time-dependent function of the molecular dynamic situation. The outcomes support the CYP5122A1 model structure, as they show time dependence of constant RMSD (Å) of the backbone atoms throughout the whole simulation process. This demonstrates the model achieved equilibrium after some initial fluctuations. The chart plainly shows that there is an adjustment in the RMSD from 1.85 Å at 0 ns until it reached a plateau from 10 ns at 4.16 Å (Figure 78).
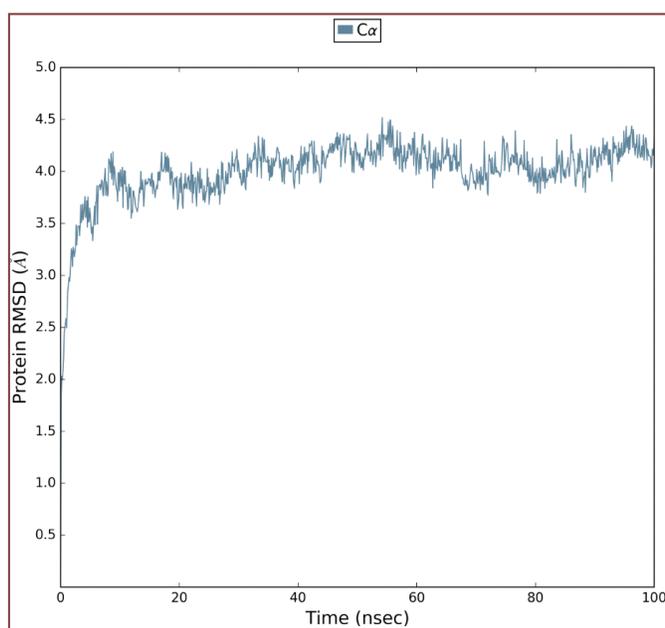
Figure 78. Time-dependent RMSD (Å) of backbone atoms of CYP5122A1 model

5.8.2 Ramachandran plots validation for CYP5122A1 model after MD simulation

A validation of CYP5122A1 model structure using Ramachandran plots was also run after MD simulation, and the structure was analysed using the RAMPAGE server.[153] The results show that 87.6 % of amino acid residues are in the most favourable regions, with 9.8 % in allowed regions, and 2.5 % were in disallowed regions (Table 43). As a result, the CYP5122A1 model had improved after MD simulations by ~ 2 %.

Table 43. Ramachandran plot evaluation of CYP5122A1 model pre and post MD simulations

CYP5122A1 model	No. of residues in favoured region	No. of residues in allowed region	No. of residues in outlier region	Amino acid outlier
Pre-MD	456	40	22	Ile93, Pro94, Ser106, Leu116, Tyr117, Pro123, Val129, Pro236, Ala329, Thr402, Arg412, Val414, Ala500, ASP505, His523, Tyr525, Ile528, Asp565, Asp571, Val572, Arg581, His592
Post-MD	454	51	13	Ser106, Ala174, His177, Ser253, Leu259, Ala 289, Pro382, Thr393, Pro441, Lys488, Asp515, Ile531, Phe585

The outlier amino acid residues in the CYP5122A1 model visualised by MOE showed the residues to be quite a distance from the haem active site (Figure 79).
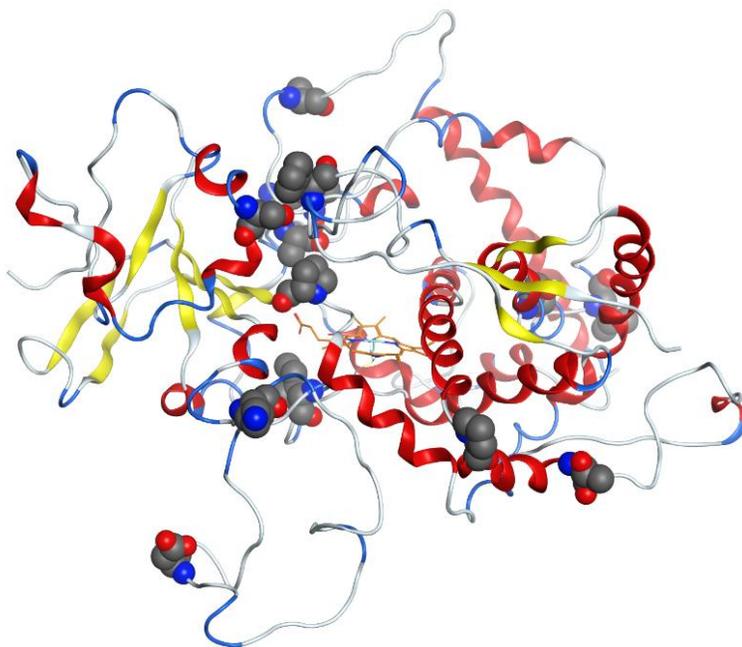
Figure 79. Outlier amino acids (space filled) identified by Ramachandran plot for the CYP5122A1 model after MD simulation at 100 ns

5.8.3 ProSA validation for CYP5122A1 model after MD simulation

Protein statistical analysis (ProSA)[155] is a programming tool that determines native fold of the protein based on statistical analysis. ProSA provides two plots; the first column (Table 44) shows the local model quality by plotting energies as a function of amino acid sequence position, generally positive values relate to erroneous parts of the input structure. The second column indicates overall model quality from which the z-score is calculated, and its value is displayed in a plot which has the z-scores of all experimentally determined protein chains in the current PDB determined by X-ray crystallography or NMR spectroscopy, a negative score shows a good model. In contrast, a positive value would show errors. The z-score of the CYP5122A1 model was -7.85 (Table 44) compared with the z-score of the template 3L4D, which was -9.87.

Table 44. ProSA output of CYP5122A1 model after MD simulations. (A) Shows the local model quality by plotting energies as a function of amino acid sequence position. (B) Shows the overall model quality by calculating z-score (dark spot)

CYP5122A1 model	Z-score	Local model quality	Overall model quality (X-ray, NMR)
Post-MD	-7.85		

To further investigate the protein, inhibitors/ligands were docked to study the binding interactions with the amino acids of CYP5122A1 protein.

5.8.4 MD simulations in *L. donovani* CYP5122A1 model

For the MD simulation studies, some ligands have been chosen and docked in the CYP5122A1 model using MOE-dock[78], and the best ligand poses chosen for further optimisation using MD simulations using Desmond[102] to improve the understanding of the binding mode achieved from molecular docking. BD766 was used for these studies as it is been believed to be an inhibitor of CYP5122A1.[80] *L. infantum* CYP51 (PDB 3L4D), the template of the CYP5122A1 model, was co-crystallised with fluconazole therefore fluconazole was selected as a ligand. Posaconazole was nominated as an example of azole drugs with an extended structure to study the fitting within the CYP5122A1 model. Furthermore, posaconazole showed good activity in *Trypanosoma* species,[43,45] and as CYP5122A1 can be found in these species as well as *Leishmania* species, it was good to investigate the binding interactions of posaconazole within *L. donovani* CYP5122A1 model. Two of the novel inhibitors (**8f** (short) and **18a** (extended), series I) from this PhD research were also studied. The dynamic stabilities of the ligand-protein complex systems were predicted using RMSD changes during the MD simulations.

All the MD simulations for *L. donovani* CYP5122A1-ligand complex systems were run for 150 ns, and the stability of the complexes was measured by their deviation from the initial structure in terms of RMSD during the MD simulations. This indicates that, after an initial increase in the magnitude of the fluctuation of the ligand atoms, the ligand reached equilibrium characterised by RMSD profile (Figure 80), showing that the complex has attained equilibration and is stable. Additionally, the ligand RMSD (right, *Y-axis* Figure 80) indicates how stable the ligand is with respect to the protein and its binding pocket. The red fluctuation line explains the RMSD of a ligand when the CYP5122A1 model-ligand complex is first aligned on the protein backbone of the reference, and then the RMSD of the ligand heavy atoms is measured. If the values observed are significantly larger than the RMSD of the protein, then it is likely that the ligand has diffused far from its initial binding site.
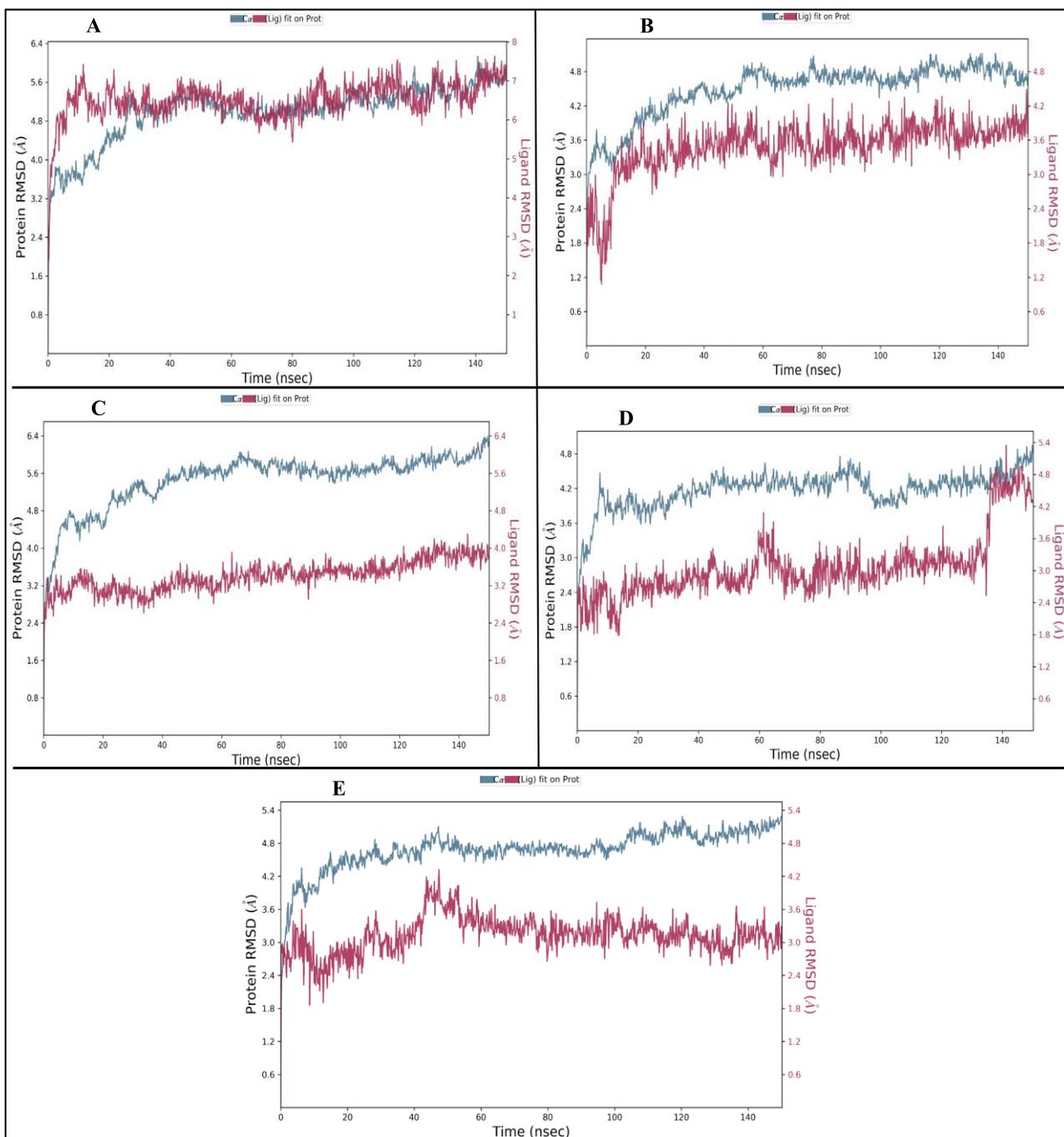
Figure 80. RMSD (in angstrom) plot with respect to time in nanoseconds during 150 ns MD simulation of (A) *L. donovani* CYP5122A1 model-BD766 complex, (B) *L. donovani* CYP5122A1 model-fluconazole complex, and (C) *L. donovani* CYP5122A1 model-posaconazole complex, (D) *L. donovani* CYP5122A1 model-(*R*)-**8f** complex, (E) *L. donovani* CYP5122A1 model-(*R*)-**18a** complex

Table 45. The RMSD of *L. donovani* CYP5122A1 complex with the selected ligand during the MD simulation

Ligand	The RMSD (Å) of protein/ligand complex at 0 ns	The RMSD (Å) of protein/ligand complex at 150 ns
BD766	2.91/4.21	5.82/7.21
Fluconazole	3.03/2.60	4.70/4.21
Posaconazole	2.62/2.47	6.28/3.77
(*R*)-8f	2.54/2.47	4.66/4.29
(*R*)-18a	2.53/2.97	5.20/3.13

As can be seen from the RMSD results (Figure 80 and Table 45), BD766, fluconazole and (*R*)-**8f** showed close values with the RMSD of the protein model, which suggest they still bind within the original binding site. However, posaconazole and (*R*)-**18a** showed slightly different variations in the RMSD, which indicate that these ligands were slightly diffuse from their original binding site.

According to the binding interactions, different binding profiles were observed for the selected ligands and the amino acids of CYP5122A1. BD766 formed a direct H-bonding interaction through the NH heteroatom and Glu365 and Asp584 as well as hydrophobic interactions with Tyr175, Val440 and Pro441. Fluconazole only showed direct H-bonding interaction with Thr366 and the N atom of one triazole ring (Figure 81). Posaconazole formed a hydrophobic interaction with Pro441 and Ile587; π-cation interaction with Lys281 and phenyl ring as well as two interactions between the oxygen atom of the 2,4-dihydro-3*H*-1,2,4-triazol-3-one ring; a direct H-bonding interaction with His583 and a water mediated H-bonding interaction with Asp584. The (*R*)-enantiomer of **8f** formed additional water mediated H-bonding interaction with Thr366 and the oxygen atom of amide group; π-π stacking interaction with Phe178 and diCl substituted phenyl ring, and hydrophobic interactions with Leu182 and Val440. The (*R*)-enantiomer of **18a** formed π-π stacking interactions with Tyr175, Phe178 and the phenyl rings; water mediated H-bonding interactions with His177 and the oxygen atom of sulphonamide linker as well as with Glu365, Asp584 and the NH of sulphonamide linker also a hydrophobic interaction with Val440 (Figure 81). However, none of the ligands interact with the haem iron.
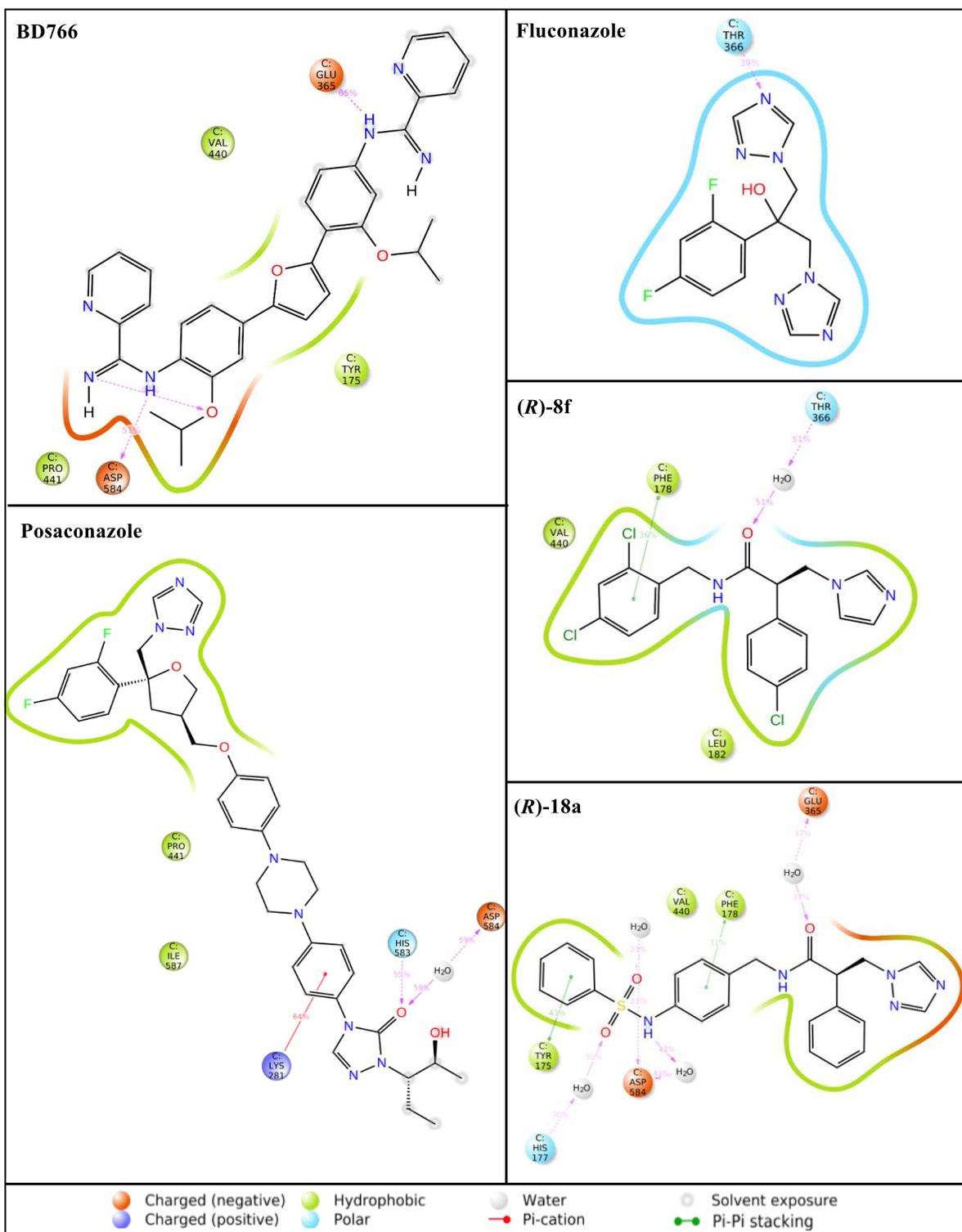
Figure 81. A schematic of detailed ligand atom interactions of BD766, fluconazole, posaconazole, (*R*)-enantiomers of **8f** and **18a** with the amino acid residues of the *L. donovani* CYP5122A1 model. Interactions that occur more than 30.0% of the simulation time in the selected trajectory (0 through 150 ns) are shown

The docking results of the selected ligands for CYP5122A1 model showed consistent amino acids Glu365, Thr366 and Val440 in the haem binding pocket, which form direct or water mediated H-bonding interactions; and in the access channel Tyr175, Phe178, Pro441 and Asp584 form H-bonding interaction or π-π stacking interactions with the inhibitors.

Superimposition of BD766, posaconazole and (*R*)-**18a** in CYP5122A1 model illustrates the occupancy of the ligands within the binding site. All the selected ligands fill the active site differently and posaconazole and (*R*)-**18a** are too far from the haem to form a binding interaction.
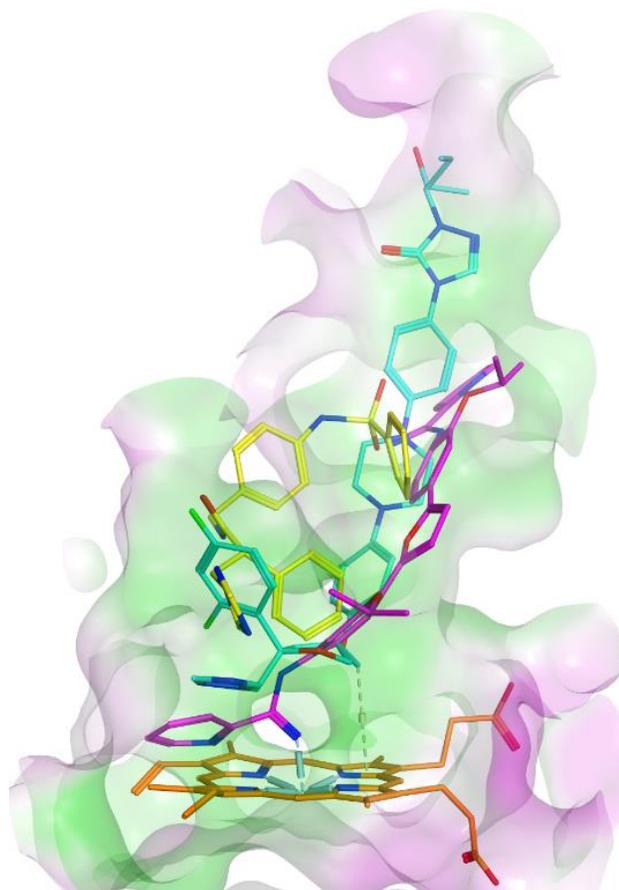
Figure 82. BD766 (magenta), posaconazole (cyan) and extended derivative (*R*)-**18a** (yellow) are aligned after MD simulations within the CYP5122A1 homology model active site cavity positioned above the haem (orange)

Owing to the low 23% homology of the CYP5122A1 homology model obtained from the available template (PDB 3L4D), the computational studies, including ligand binding, may not be an accurate representation owing to expected errors in the 3D protein structure of the model.

5.8.5 MD simulations in *L. infantum* CYP51

Since the crystal structure of *L. infantum* CYP51 (LiCYP51) was used as a template for the CYP5122A1 homology model, it was thought, it could be a good idea to investigate and compare the active site of LiCYP51 and CYP5122A1 homology model by studying the binding interactions of the selected compounds with LiCYP51, and the MD simulation studies were also run for 150 ns using Desmond[102] programme after the best ligand poses were obtained from docking studies.
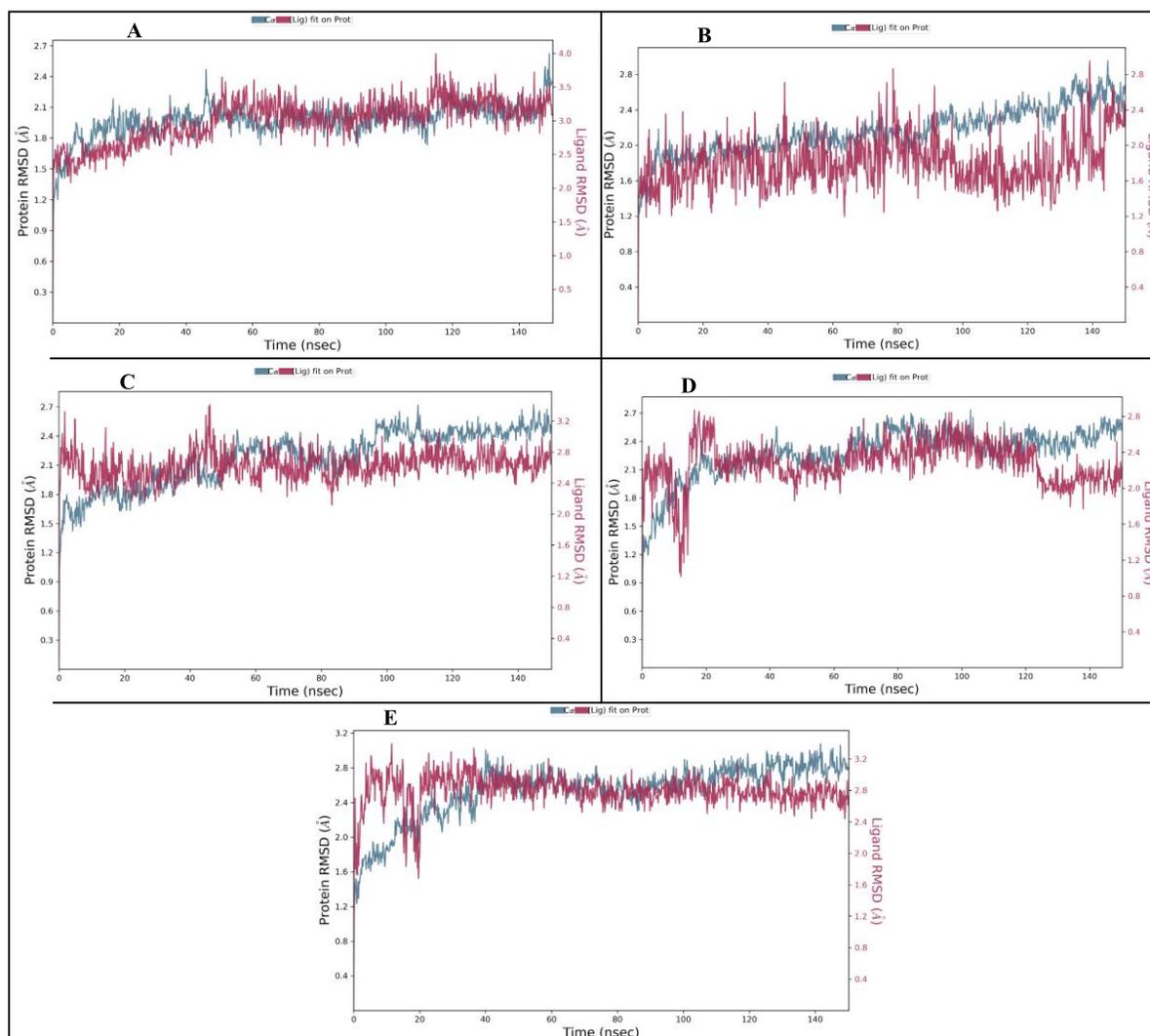
Figure 83. RMSD (in angstrom) plot with respect to time in nanoseconds during 150 ns MD simulation of LiCYP51 complex with (A) BD766, (B) fluconazole, (C) posaconazole, (D) (*R*)-**8f**, and (E) (*R*)-**18a**

Table 46. The RMSD of LiCYP51 complex with the selected ligand during the MD simulation

Ligand	The RMSD (Å) of protein/ligand complex at 0 ns	The RMSD (Å) of protein/ligand complex at 150 ns
BD766	1.22/2.29	2.31/3.23
Fluconazole	1.32/1.43	2.58/2.51
Posaconazole	1.21/2.52	2.51/2.65
(*R*)-8f	1.24/1.63	2.63/2.20
(*R*)-18a	1.46/1.80	2.81/2.73

These results (Figure 83 and Table 46) indicate that the chosen ligands bind closely to their initial (haem) binding site.

Regarding the binding interactions, the BD766 complex formed additional water mediated H-bonding interaction through the NH heteroatom and Tyr456; π-π stacking interactions between Tyr102, Phe104 and furan ring as well as with phenyl ring; a direct H-bonding interaction between Met459 and the NH heteroatom was observed as well as hydrophobic interactions with Met105 and Val356. Fluconazole showed water mediated H-bonding interaction between Met357 and the N atom of one triazole ring and hydrophobic interaction with Tyr102 in the active site of LiCYP51 (Figure 84). Posaconazole mainly forms hydrophobic interaction with Tyr102, Pro209, Ala290 and Met459. The (*R*)-enantiomer of **8f** formed H-bonding interaction with His293 and the NH atom of the amide group. In addition, the (*R*)-enantiomer of **18a** formed a direct H-bonding interactions with Val356, Met357 and the oxygen atom of sulphonamide linker as well as with Met459 and the NH atom of sulfonamide group, in addition hydrophobic interactions formed with Met105, Phe109, Phe213, Ala290 and Leu355 (Figure 84). With the exception of BD766, all the ligands interaction with the haem iron via the triazole N atom. Furthermore, docking results of the selected ligands for LiCYP51 showed amino acids Tyr102 and Ala290 in the haem binding pocket and Met105, Val356 and Met459 in the access channel of LiCYP51, which could have an important role in binding interaction to form H-bonding interaction, π-π stacking interactions as well as hydrophobic interaction with the ligands.
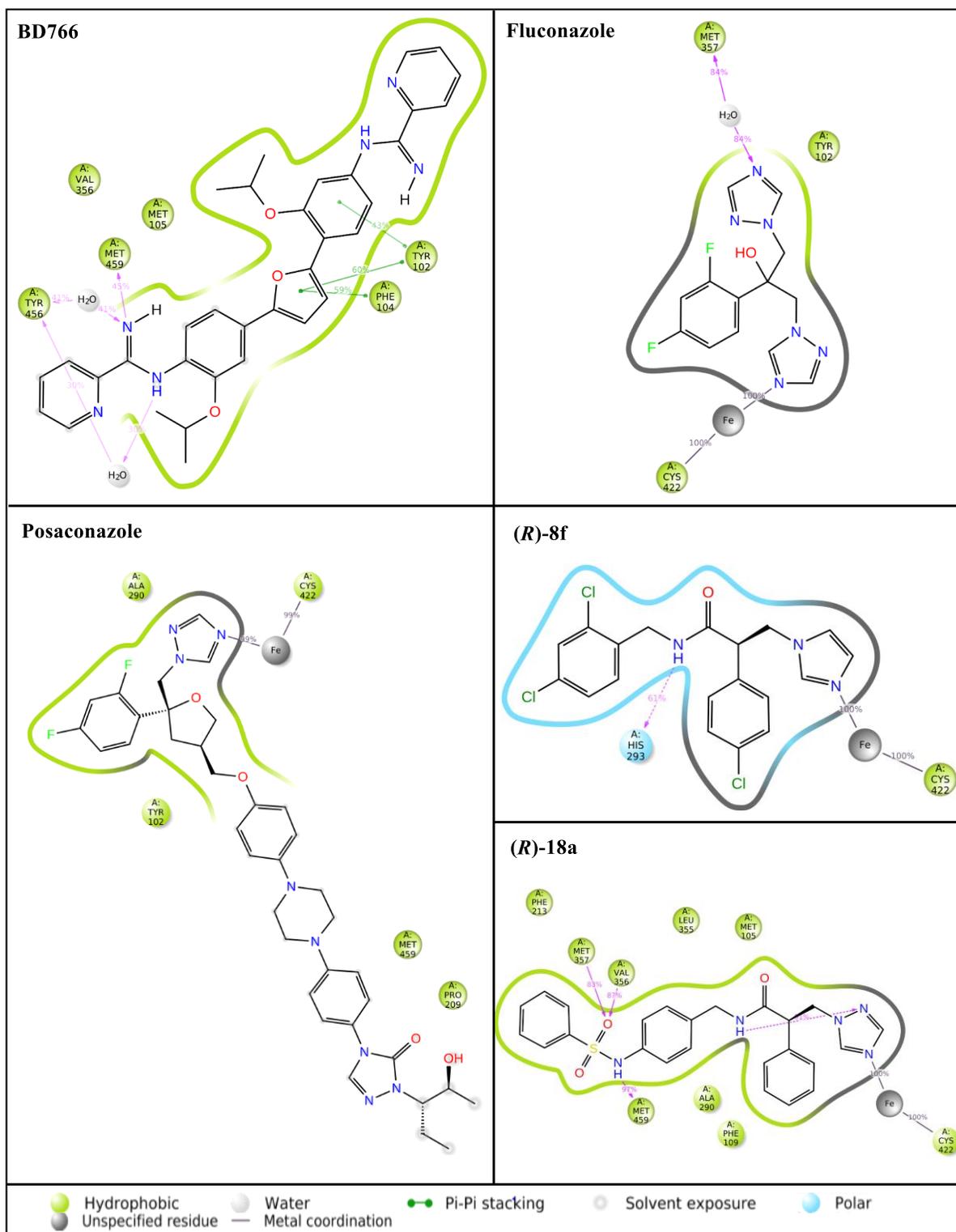
Figure 84. A schematic of detailed ligand atom interactions of BD766, fluconazole, posaconazole, (*R*)-enantiomers of **8f** and **18a** with the amino acids of the LiCYP51. Interactions that occur more than 30.0% of the simulation time in the selected trajectory (0 through 150 ns) are shown

The placement of the selected ligands in the LiCYP51 active site was visualised using MOE. BD766 (Figure 85, magenta), posaconazole (Figure 85, cyan) and (*R*)-**18a** (Figure 85, yellow) occupied the haem area and the long access channel.
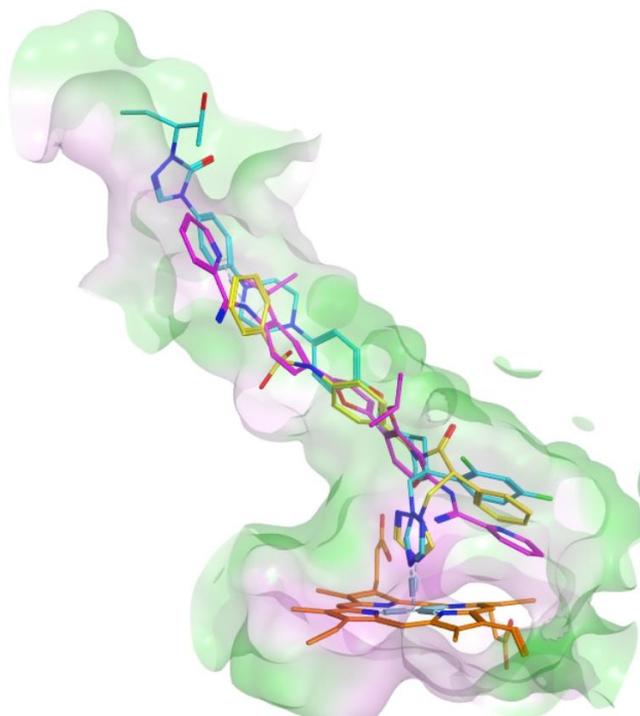
Figure 85. BD766 (magenta), posaconazole (cyan) and extended derivative (*R*)-**18a** (yellow) are positioned along the hydrophobic active site cavity and above the haem (orange) after MD simulations within the LiCYP51 crystal structure (PDB 3L4D)

5.9 Biological assay

The final compounds of series I (15 novel compounds, Chapter II) were evaluated against *L. donovani* at the Drug Discovery Unit, University of Dundee by Dr Sujatha Manthri.

5.9.1 Intra-macrophage assay (InMac) for *Leishmania*

InMac is an assay used to identify new inhibitors that are active against *L. donovani*. InMac is a high-throughput screening assay with free-living parasites using amastigotes, which have been growth outside the host cell in a growth media (more detail in the experimental section).[157]

The InMac assay was performed on all the novel derivatives of series I (**8**, **18** and **25**) and compared against two standards for comparison (Table 47).[157]

Table 47. InMac (pEC$_{50}$) values of novel derivatives (**8**, **18** and **25**) in parasite and host cell
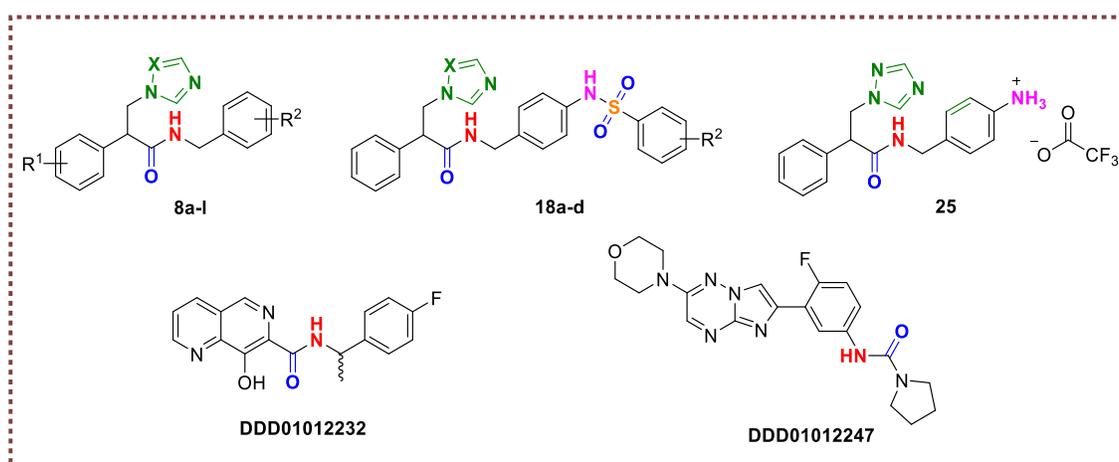
Compd	Compd ID	R^1	R^2	X	InMac pEC$_{50}$ (M)	THP-1 pEC$_{50}$
8b	DDD01867934	4-H	4-F	CH	4.3	4.3
8c	DDD01867932	4-H	4-Cl	CH	4.3	4.3
8d	DDD01867937	4-Cl	4-Cl	CH	4.3	4.3
8e	DDD01867935	4-H	2,4-diCl	CH	4.5	4.3
8f	DDD01932296	4-Cl	2,4-diCl	CH	4.8	4.3

8g	DDD01867939	4-H	4-CH$_3$	CH	4.3	4.3
8h	DDD01867940	4-H	4-CF$_3$	CH	4.3	4.3
8i	DDD01867936	4-H	4-OCH$_3$	CH	4.3	4.3
8j	DDD01867933	4-H	3,4-diOCH$_3$	CH	4.3	4.3
8k	DDD01871145	4-H	4-Cl	N	4.3	4.3
18a	DDD01871151	-	4-H	N	4.5	4.3
18b	DDD01871147	-	4-F	N	4.4	4.3
18c	DDD01932294	-	4-Cl	N	4.3	4.3
18d	DDD01932295	-	4-OCH$_3$	N	4.3	4.3
25	DDD01871146	-	-	-	4.3	4.3
Reference	DDD01012232	-	-	-	6.8	<4.3
	DDD01012247	-	-	-	6.4	<4.3

Where pEC$_{50}$ is the negative logarithm of EC$_{50}$ which measure the drug's potency in molar unit and define as the concentration of a compound where 50% of its maximal effect is observed; THP-1 is refer to human monocytic cell line (host cell) which was derived from an acute monocytic leukaemia patient.

All compounds were screened at the highest concentration of 50 µM that is a pEC$_{50}$ value of >4.3 M. For a compound to be active it should have a pEC$_{50}$ of >4.3 against the parasite (representative in the 6th column, Table 47) and it should not be toxic to the host cell so should have a pEC$_{50}$ of < 4.3 (last column in Table 47). Four compounds showed some activity with pEC$_{50}$ value of 4.5 M, 4.8 M, 4.5 M and 4.4 M for **8e**, **8f**, **18a** and **18b** respectively.

However, the results for the host cell indicate that they were toxic with pEC$_{50}$ of 4.3. The poor effectiveness could be owing to the complicated life cycle of *Leishmania* as the parasite adopts a defence mechanism when it penetrates the host cell by hiding inside a phagolysosome, (parasitophorous vacuole) in the macrophages of the host cell where the pH is acidic (5.5), to avoid the lysis from the immune system.[126,134,158,159] Inhibitors should have the ability to cross this phagolysosome (pH 5.5) before entering the amastigotes, which have a pH of 7.4, to inhibit the parasite and to be an effective inhibitor (Figure 86).[126,134,158,159]
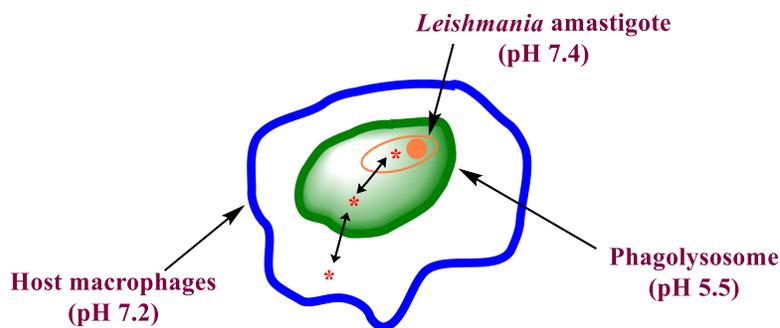
Where * = Antileishmaniasis agent,   ⟷   = Passive permiability between two compartments

Figure 86. *Leishmania* amastigotes parasite within the host macrophages and the passive permeability of antileishmaniasis agents

The results were analysed as a dose-response curve compared with the control compounds. Figure 87 shows an exemplar of the analysis data by ten-point potency curve for (*R*)-**8f** and one reference compound (DDD01012232) tested in the intracellular *Leishmania* assay.
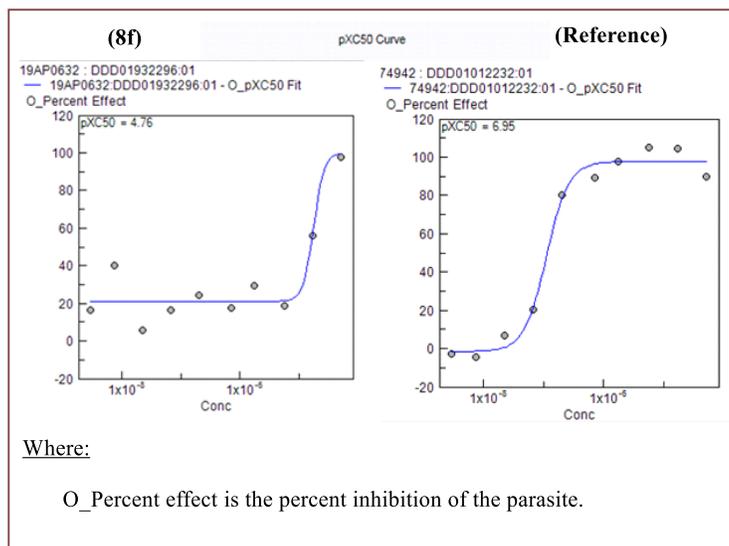
Figure 87. Dose-response curve for a representative example (*R*)-**8f** and DDD01012232 as control compound

5.10 Conclusion

A homology model of *L. donovani* CYP5122A1 has been developed using SWISS-MODEL and validated for stereochemical and amino acid environment quality using appropriate programmes, with further optimisation of the active site architecture achieved by MD simulations. Understanding protein-ligand interactions is essential for designing more selective and potent CYP5122A1 inhibitors. This chapter used a combination of homology modelling, molecular dynamic simulations, and molecular docking to understand the requirements for binding interactions of the CYP5122A1 model with selected inhibitor complexes as to date there is no crystal structure for the query protein. Examining RMSD during simulations indicated that the homology model is structurally stable. Docking results of BD766, fluconazole, posaconazole and the representative of series I (short (**8f**) and extended series (**18a**) in chapter II) in the CYP5122A1 homology model protein showed different binding interactions with amino acids Glu365, Thr366, Val440 in the haem binding pocket and Tyr175, Phe178, Pro441, Asp584 in the access channel compared with the docking studies for the same ligands in LiCYP51 crystal structure (PDB 3L4D) that showed different amino acids Tyr102, Ala290 in the haem binding pocket and in the access channel Met105, Val356, Met459 which was used as a template for the homology model of *L. donovani* CYP5122A1 in this PhD research project, which indicates that the orphan *L. donovani* CYP5122A1 has distinct active site pocket.

Fifteen novel inhibitors were evaluated by intramacrophage (InMac) assay against *Leishmania donovani*, four of which (**8e**, **8f**, **18a** and **18b**) gave some activity, however they were not as active as the control agents that displayed promising activity against *L. donovani* in *in vitro* studies. Furthermore, these inhibitors need further investigation by testing them against CYP5122A1/ CYP51 enzyme, however functional CYP5122A1 required for enzyme assays is not currently available.

The identification of the whole model with its active binding sites and key binding residues can serve as a crucial step in rational drug design for the development of new antileishmanial agents, however as noted the low similarity could reflect that the model may be far away from accurate and this is owing to the limited available templates, which have low homology to CYP5122A1. A more accurate understanding of the 3D protein structure of CYP5122A1 is dependent on either X-ray crystallography or NMR studies or identification of templates with higher homology.

Chapter VI

Conclusions

6. Conclusions

Cytochrome P450 lanosterol 14α-demethylase (CYP51) is an enzyme involved in the biosynthesis of ergosterol, which is an integral component of the fungal/protozoal cell membrane. Therefore, inhibiting ergosterol formation by inhibiting CYP51 will hinder the spread and growth of the pathogens (Figure 88).
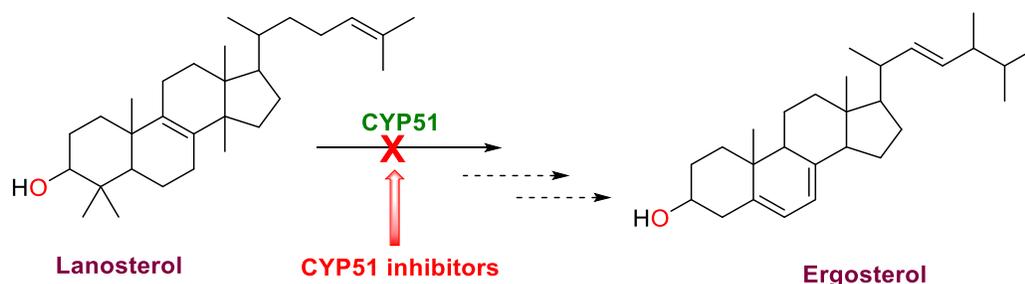
Figure 88. CYP51 inhibition site in ergosterol biosynthesis

Azoles antifungals are the mainstay treatment targeting CYP51, however prolonged treatment regimens and prophylactic use of azole drugs in the clinic as well as the extensive use in agriculture, have led to an increase in the incidence of resistance for these agents, especially the mainstay treatment fluconazole.

Thus, the aim of this research was to design and synthesise novel azole inhibitors effective against wild type and fluconazole-resistant *Candida* strains. Computational studies were very helpful in the investigation of the binding and the occupancy of the designed novel inhibitors within the crystal structure of CaCYP51 using the available protein crystal structure in the protein data bank that is co-crystallised with posaconazole (PDB 5FSA). Three novel azole series were developed by modifying fluconazole to be potent and selective for CaCYP51 and were investigated for CYP51 inhibitory activity, binding affinity, and minimum inhibitory concentration against *C. albicans* strains both biologically and computationally. According to the computational studies (molecular modeling, molecular docking studies and molecular dynamic simulations) all series interacted perpendicularly to the haem iron and the N atom of azole group with good distance (< 3.0 Å). The short derivatives in this research occupied the haem area in a similar manner to fluconazole, whereas the extended derivatives occupied the haem pocket and the long access channel of CaCYP51 with extra H-bonding interactions, either

directly or via water molecule, with the amino acids in the active site (such as Tyr118, Leu376, His377, Ser507 and Met508), which could overcome the fluconazole resistance. Furthermore, the MD simulations studies were performed in both the wild type CaCYP51 and a representative double mutant strain CaCYP51 (Y132H+K143R), which allowed the study of the binding and position of inhibitors more accurately owing to the ability of both ligand and protein to move during the MD simulations.

Development of the first series (Figure 89), short and its extended novel imidazole/triazole derivatives were synthesised successfully with high purity (> 95 %), however an unexpected alkene by-product was obtained when producing the final compounds resulting in decreased yields.
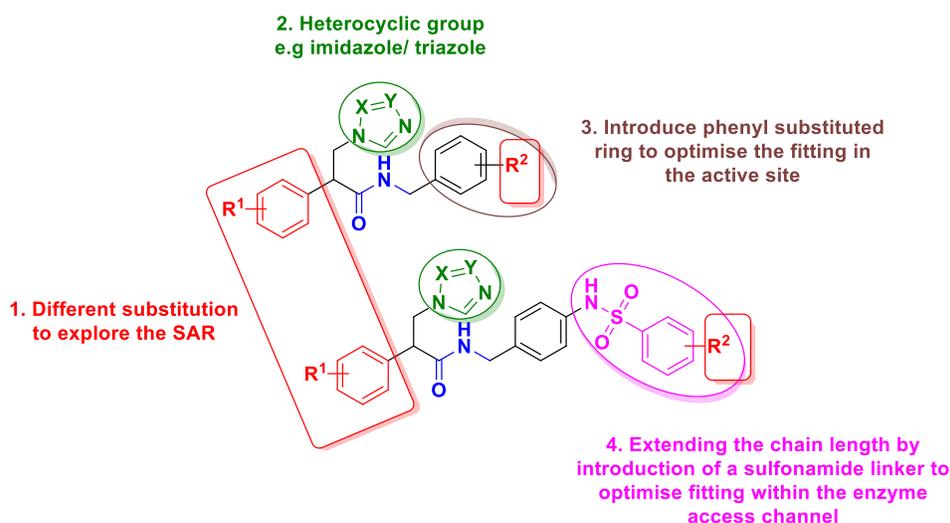
Figure 89. Series I modifications

The short derivatives were more potent against the *C. albicans* strains (e.g. MIC **8f** <0.03 µg/mL, **18c**, 1 µg/mL, fluconazole 0.125 µg/mL) but both series displayed comparable enzyme binding and inhibition (**8f** K_d 62 ± 17 nM, IC_{50} 0.46 µM; **18c** K_d 43 ± 18 nM, IC_{50} 0.33 µM, fluconazole K_d 41 ± 13 nM, IC_{50} 0.31 µM, posaconazole K_d 43 ± 11 nM, IC_{50} 0.2 µM). The short series had poor selectivity for CaCYP51 over the human homolog, while the selectivity of the extended series, e.g. compound **18c**, was higher (21.5-fold) than posaconazole (4.7-fold) based on K_d values, although posaconazole was more selective (615-fold) compared with **18c** (461-fold) based on IC_{50} values. Additionally, the distance from the azole N and the haem iron before and after MD simulation was investigated computationally and correlated with the

biological results obtained in the wild type CaCYP51 and gave comparable results. However, investigation in the mutant strains biologically is still needed to confirm the computational studies obtained, which could help in the design approach for selective antifungal agents.

The second series (Figure 90) were synthesised successfully with high purity (> 95 %) and comparatively low yields obtained. The low yields could be due to the free amine (**47**) step, which needs further optimisation in the future.
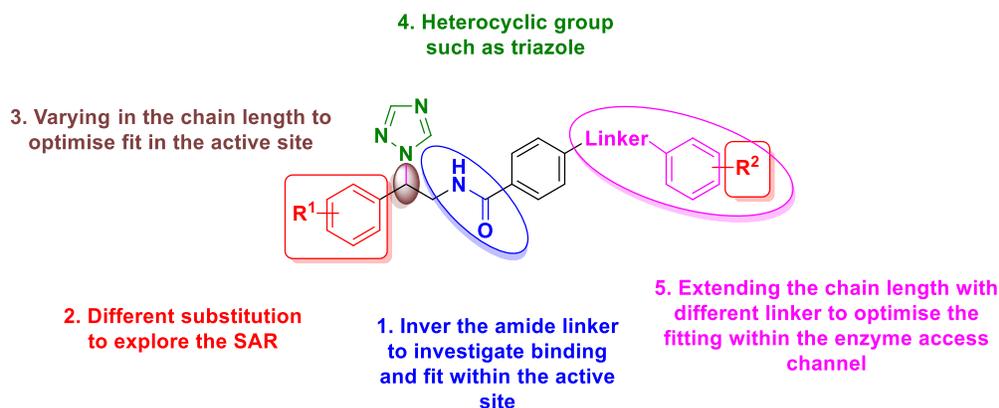
Figure 90. Series II modifications

The novel inhibitors of this series lost the activity against *C. albicans* strains due to the loss of a CH_2 before the triazole ring, which indicates the important of CH_2 for the antifungal activity when designing new antifungal azole inhibitors; however, a slight improvement in the IC_{50} was shown particularly in compound **48d** (R^1 = 4-Cl, R^2 = Cl, 1.3 µM) with K_d 78 nM compared with fluconazole (IC_{50} 0.31 µM, K_d 41 ± 13 nM) and further testing of the sterol profiles are needed, which could give a better understanding regarding these results.

A third series of novel derivatives was synthesised successfully after several trials (Figure 91) with high purity (> 95 %).
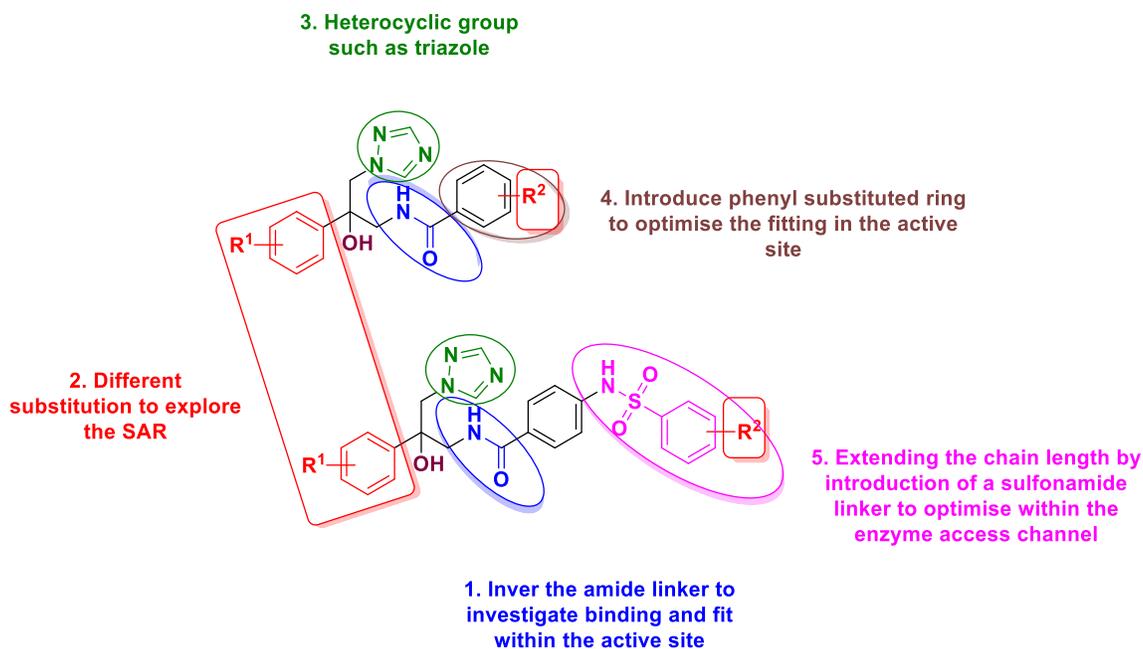
Figure 91. Series III modifications

All tested novel azole derivatives showed potent inhibitory activity against the *C. albicans* strains (MIC <0.03 to 1 µg/mL) and potent inhibitors of CaCYP51 (IC$_{50}$ 0.78 -1.61 µM) compared with the standard fluconazole. For example, compound **57c** is more effective than fluconazole with MIC < 0.03 µg/mL against both strains with IC$_{50}$ 1.24 µM and good binding affinity (K_d 108 ± 34.4), however further testing of sterol profiles is needed. In addition, comparable results were obtained in the wild type CaCYP51 when measuring the distance from the azole N and the haem iron before and after MD simulations with the biological data. This novel series is very promising and is being continued by another PhD student, Marwa Alsulaimany, in Dr Claire's Lab with further development through computational studies to investigate the binding interactions with CaCYP51 leading to the design of selective azole inhibitors to overcome fluconazole resistance.

As all the novel azole derivatives obtained in this research have been tested against CYP51 *C. albicans* strains, it was of interest to test them against different fungi to investigate broad spectrum activities. Therefore, the novel inhibitors were tested against two strains of *C. auris* (CBS10913 and CBS12372) by the team at the Centre for Cytochrome P450 Biodiversity, Swansea University Medical School; however the COVID-19 pandemic restricted completion

of this work and only preliminary data for five novel inhibitors (from the first series, Chapter II) were obtained.

The susceptibilities of the CBS10913 (*C. auris* wild type laboratory strain) and CBS12372 (azole sensitive) strains to five novel azole derivatives (**8** and **18**) were determined (Table 48), together with voriconazole as a control, using the same method described in chapter II.

Table 48. MIC values for compounds against *C. auris* CBS10913 and CBS12372 at 48 hours
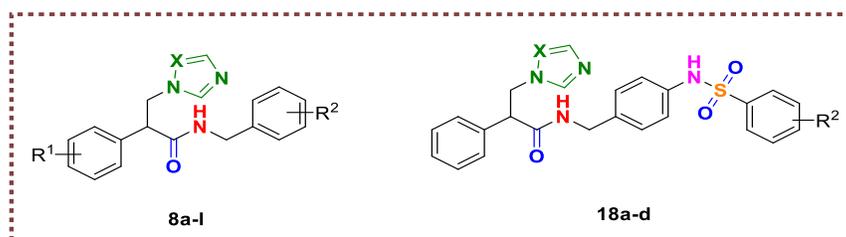
Compound	R^1	R^2	X	MIC (µg/mL)		cLogP^a
				CBS10913	**CBS12372**	
8d	4-Cl	4-Cl	CH	0.5	16	4.1
8f	4-Cl	2,4-diCl	CH	0.25	16	4.66
18a	-	4-H	N	>16	8	2.9
18b	-	4-F	N	16	>16	3.06
18c	-	4-Cl	N	4	>16	3.46
Voriconazole				<0.03	1	1.49

^{a}cLogP was determined using Crippen's fragmentation[96]

A pattern was observed between MIC and cLogP with the more lipophilic derivatives more effective at inhibiting fungal growth (Table 48). For the short derivatives (**8**) both compounds displayed antifungal activity against both *C. auris* wild type strains CBS10913 and CBS12372; **8f**, R^1 = 4-Cl, R^2 = 2,4-diCl, cLogP 4.66, MIC 0.25 µg/mL and **8d**, R^1 = 4-Cl, R^2 = 4-Cl, cLogP 4.1, MIC 0.5 µg/mL.

In addition, the extended derivatives (**18**) showed the same pattern but with less inhibitory activity than the short derivatives, however the chloro derivative displayed some activity **18c,** R^2 = 4-Cl, cLogP 3.46, MIC 4 µg/mL compared with unsubstituted derivative **18a,** R^2 = 4-H, cLogP 2.9, MIC >16 µg/mL (Table 48).

Sterol profiles were performed for the most effective compounds (**8d** and **8f**) and voriconazole (Table 49) using the same method as described in chapter II by the team at Swansea University.

The sterol profiles prove that the mechanism of action of both novel compounds, **8d** and **8f**, was inhibition of sterol 14α-demethylase (CYP51), as is the case for voriconazole (Table 49). The accumulation of 14α-methylated sterols in the fungal membrane inhibits the growth of *C. auris*, in particular, the accumulation of 14α-methyl ergosta-8,24(28)-dien-3,6-diol is believed to disrupt the fungal membrane in Candida, resulting in growth inhibition.

Table 49. Sterol composition (% of total sterols) of untreated and treated wild type *C. auris* strains

Sterol Composition (%)	Untreated (DMSO only)		Voriconazole		8d		8f	
	CBS10913	CBS12372	CBS10913 (0.03 µg/mL)	CBS12372 (1 µg/mL)	CBS10913 (0.25 µg/mL)	CBS12372 (8 µg/mL)	CBS10913 (0.125 µg/mL)	CBS12372 (8 µg/mL)
Ergosterol	77.1±1.5	82.4±0.5	20.0±0.8	58.8 ±2.3	37.8±1.3	63.6±6.8	13.4±0.8	68.5±1.4
Diol[a]			10.0±0.7	2.6±0.3	7.3±0.8	1.7±0.5	7.5±1.6	0.9±0.2
Lanosterol	0.8±0.1	0.8±0.0	35.5±1.2	24.6±1.5	28.7±0.7	22.5±4.0	42.9±2.7	18.6±0.3
Eburicol			0.9±0.0	2.0±0.2	0.6±0.1	1.1±0.3	1.0±0.3	1.2±0.3
Total 14α-methylated sterols	0.8	0.8	68.9	38.0	52.9	32.2	76.1	26.8

[a] 14α-methyl ergosta-8,24(28)-diein-3,6-diol

An extension of this research was the development of a homology model of the orphan CYP5122A1 in *L. donovani*, for which no crystal structure is currently available. This orphan CYP is of interest because it has shown to be essential for survival, virulence, drug response, and ergosterol metabolism in *Leishmania*, in addition a synergism has been found between CYP5122A1 and CYP51, which could be a bypass mechanism in leishmania parasites to maintain the essential ergosterol needed for survival and may be the cause of the variable activity of azoles in protozoa. The homology model was built using SWISS-MODEL server using the only available crystal structure template LiCYP51 (PDB 3L4D) with low similarity with the query enzyme. The CYP5122A1 homology model was subjected to validation with further optimisation of the active site architecture achieved by MD simulations. Fifteen novel designed inhibitors were tested for inhibitory activity against *L. donovani* with only four of the novel inhibitors (**8e**, **8f**, **18a** and **18b**) showing low activity, however they were toxic to the host cell. The low similarity of the available template for CYP5122A1 may well limit the accuracy of the model, which is a limitation that can only be addressed when a template with higher percent similarity is available. Another limitation is that to date no functional CYP5122A1 protein has been obtained or described in the literature to perform enzyme inhibitory assays.

Finally, owing to the time required for enzyme preparation, extraction, costs and the lockdown necessitated by the COVID-19 epidemic, further biological evaluation including testing in the mutant strains as well as testing in different fungi and some sterol profiles with the research team at the Centre for Cytochrome P450 Biodiversity, Swansea University Medical School, have been delayed. Despite this the results presented here describe some interesting finding that will be developed further through computational studies to optimise binding interactions for Candida CYP51 *vs* hCYP51 and 'design in' selectivity of azole inhibitors to overcome the resistance of fluconazole.

Chapter VII

Experimental

7. Experimental

7.1 General considerations

All reagents and solvents employed were of general purpose or analytical grade and purchased from Sigma-Aldrich Ltd, Alfa Aesar Chemicals, Fisher Scientific, Fluka and Acros Chemicals. Lanosterol and fluconazole were supplied by Sigma-Aldrich (Poole, UK). Ni^{2+}-nitrilotriacetic acid agarose (Ni^{2+}-NTA agarose) affinity chromatography matrix was obtained from Qiagen (Crawley, UK). All solvents were dried prior to use and stored over 4 Å molecular sieves, under nitrogen.

^1H and ^{13}C NMR spectra were recorded on a Bruker Avance DPX500 spectrometer operating at 500 MHz and 125 MHz respectively. Each resonance signal was reported according to the following principle:

- Chemical shifts (δ) are given in parts per million (ppm) relative to the internal standard tetramethyl silane (Me_4Si) (TMS).

- Coupling constants (*J* in hertz (Hz)).

- Multiplicities are denoted as s (singlet), bs (broad singlet), d (doublet), dd (doublet of doublet), ddd (doublet of doublet of doublet), t (triplet), q (quartet), m (multiplet) or combinations.

All NMR characterisations were made by comparison with previous NMR spectra reported in the literature or the prediction of the structure NMR from ChemDraw (Professional 16.0) software.

For gradient column chromatography, a glass column was packed in the appropriate eluent with silica gel 60 nm (230-400 mesh) (Merck) and flash column chromatography was performed with the aid of a pump. Thin layer chromatography (TLC) for analysis was carried out on pre-coated silica plates (Kiesel gel 60 F_{254}, BDH) with visualisation via UV light (254 nm /or 365 nm).

Melting points were determined using a Gallenkamp melting point apparatus and were uncorrected.

cLog P obtained from ChemDraw (Professional 16.0) using Crippen's fragmentation.[96]

Mass spectra, high resolution mass spectra (HRMS) were determined by the Engineering and Physical Sciences Research Council National Mass Spectrometry Service Centre at Swansea University (Swansea, UK) and University of Bath (UK). Elemental analysis was performed by MEDAC Ltd (Chobham, Surrey, UK).

HPLC (Method A, University of Bath) was performed on a Zorbax Eclipse Plus C18 Rapid Resolution 2.1 x 50 mm, 1.8 µm particle size using a 7.5 minute gradient method 5:95 v/v water: methanol with 0.1% formic acid as additive; (Method B1, Cardiff University) was performed on a Shimadzu LC-2030C Plus C18 Rapid Resolution 250 x 4.6 mm, 5 µm particle size using a 7 minute gradient method 5:95 v/v water: methanol; (Method B2, Cardiff University) was performed on a Shimadzu LC-2030C Plus C18 Rapid Resolution 250 x 4.6 mm, 5 µm particle size using a 10 minute gradient method 5:95 v/v water: methanol.

7.2 Computational methods

Molecular Modelling and Docking

Docking studies were performed using the MOE programme[78] and CaCYP51 (PDB 5FSA)[35] to generate PDB files of the CaCYP51 crystal structure and some representative azole derivative complexes. All minimisations were performed with MOE until a RMSD gradient of 0.01 Kcal/mol/Å with the MMFF94 forcefield and partial charges were automatically calculated. The charge of the haem iron at physiological pH was set to 3^+ (geometry d2sp3) through the atom manager in MOE. The Alpha Triangle placement was chosen to determine the poses, refinement of the results was done and rescoring of the refined results using the London ΔG scoring function was applied. The output database dock file was created with different poses for each ligand and arranged according to the final score function (S), which is the score of the last stage that was not set to zero. The docking studies were also performed using FlexX module in LeadIT version 2.3.2 by BioSolveIT.[81] The ligand database saved in mol2 format, which was prepared using MOE,[78] was used as input for the docking library and the haem iron atom of the catalytic site was set as essential pharmacophoric feature. Ligand docking was performed using the default values, configured with flexible torsion, external formal charges, Corina for generation, volume overlap factor 2.9, ligand clash factor 0.6 and water molecules were considered. Thirty output

solution were obtained from each input compound and a visual inspection in MOE was used to identify the interaction between ligand and protein.

Molecular Dynamics Simulations

Molecular dynamics simulations were run on the CaCYP51 protein, wild-type and a representative mutant strain, in complex with fluconazole and the (*R*)- and (*S*)-enantiomers of some representative. PDB files were first optimised with protein preparation wizard in Maestro (Schrödinger release 2019-1)[102], by assigning bond orders, adding hydrogen, and correcting incorrect bond types. A default quick relaxation protocol was used to minimise the MD systems with the Desmond programme.[102] In Desmond, the volume of space in which the simulation takes place, the global cell, is built up by regular 3D simulation boxes, which was utilised as part of this system for protein interactions. The orthorhombic water box allowed for a 10 Å buffer region between protein atoms and box sides. Overlapping water molecules were deleted, and the systems were neutralised with Na^+ ions and salt concentration 0.15 M. Force-field parameters for the complexes were assigned using the OPLS_ 2005 forcefield, that is, a 100ns molecular dynamic run in the NPT ensemble (T = 300 K) at a constant pressure of 1 bar. Energy and trajectory atomic coordinate data were recorded at each 1.2 ns.

Binding affinity (ΔG) calculations

Prime/MMGBAS[103], available in Schrödinger Prime suite[102], was used to calculate the binding free energy of the ligands with CaCYP51.

ΔG (bind) = E_complex (minimised) – (E_ligand (minimised) + E_receptor (minimised))

The mean ΔG (bind) was calculated from each frame from the point where the complex reached equilibrium to the final frame of the MD stimulation.

7.3 Biological studies *(Performed by Dr Josie Parker and Dr Andrew Warrilow at the Centre for Cytochrome P450 Biodiversity, Swansea University Medical School during the PhD time)*

Susceptibility testing of C. albicans strains

Minimum Inhibitory Concentration (MIC) determinations were performed according to recommendations outlined in the Clinical and Laboratory Standards Institute (CLSI) document M27-S4;[95] this includes testing in RPMI-1640 with 0.165 M MOPS as the buffer (pH 7.0), an inoculum size of 1-5 x 10^4 cells mL^{-1}, and incubation at 37 °C for 48 hours. The MICs were measured as the lowest concentrations of each antifungal agent that resulted in an 80% reduction in turbidity as compared with a drug-free, growth control well. Stock solutions of each agent were prepared in DMSO. Further dilutions were made in RPMI-1640, and the final concentration of DMSO was 1% (v/v). The final testing concentrations for all compounds ranged from 0.03-16 µg mL^{-1}.

CYP51 reconstitution assays

IC$_{50}$ used to determine the values for individual azole compounds[57,60] using lanosterol as substrate. Azoles were introduced using 2.5 µL of stock solutions in DMSO. CaCYP51 assays contained 1 µM CaCYP51 and 2 µM *H. sapiens* cytochrome P450 reductase (HsCPR - UniProtKB accession number P16435) and were incubated for 20 min at 37 °C. HsCYP51 assays contained 0.25 µM Δ60HsCYP51 and 1 µM HsCPR and were incubated for 10 min at 37 °C. Sterol metabolites were extracted with EtOAc and dried down under vacuum prior to derivatisation with trimethylchlorosilane[123] followed by analysis by gas chromatography mass spectrometry (GC/MS). Each IC$_{50}$ experiment was performed in duplicate. IC$_{50}$ is defined here as the inhibitory concentration of compound that causes a 50% reduction in observed enzyme activity under the stated assay conditions.

The dissociation constant (K_d)

Each CYP51-azole complex was determined by non-linear regression (Levenberg-Marquardt algorithm) using a rearrangement of the Morrison equation for tight ligand binding.[100] Tight binding is normally observed where the K_d for a ligand is similar or lower than the concentration of the enzyme present.[160] Where ligand binding was weaker, the Michaelis-Menten equation was used to fit the data (Figure 38). Curve fitting azole saturation curves was performed using the computer program ProFit 6.1.12 (QuantumSoft, Zurich, Switzerland) for Mac OSX. K_d values were determined for each of the three replicate titrations per azole compound and then mean K_d values and standard deviations calculated.

Sterol profile analysis of C. albicans strains

Sterol extractions were performed on cells grown in 10 mL of morpholinopropanesulfonic acid (MOPS) buffered (0.165 M) RPMI-1640, pH 7.0 containing either DMSO alone (1% v/v), or DMSO containing antifungal agent (final concentration at half the MIC). The culture medium was then inoculated with *C. albicans*, (either CA14 or SC5314), to a final density of 5×10^4 cells mL^{-1} and the cultures grown at 37 °C, 180 rpm, for 18 h. Cells were pelleted and washed with ddH_2O and non-saponifiable lipids were extracted using alcoholic KOH as reported previously.[123] Samples were dried in a vacuum centrifuge and were derivatised by the addition of 100 µL 90% BSTFA / 10% TMS (Sigma), 200 µL anhydrous pyridine (Sigma) and heating for 2 h at 80 °C. TMS-derivatised sterols were analysed and identified using GC/MS (Thermo 1300 GC coupled to a Thermo ISQ mass spectrometer, Thermo Scientific) with reference to retention times and fragmentation spectra for known standards. GC/MS data files were analysed using Xcalibur software (Thermo Scientific) to determine sterol profiles for all isolates and to integrate peak areas.

7.4 Chemistry

7.4.1 Methyl 2-(4-chlorophenyl)acetate (2)[82]

(**1**)

Chemical Formula: $C_8H_7ClO_2$
Molecular Weight: 170.59
cLog P = 2.09

(**2**)

Chemical Formula: $C_9H_9ClO_2$
Molecular Weight: 184.62
cLog P = 2.36
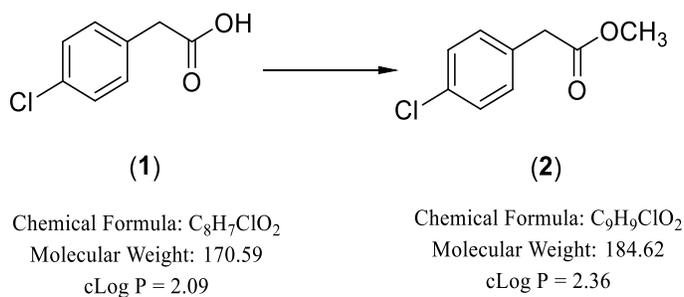
To a colourless solution of 2-(4-chlorophenyl)acetic acid (**1**) (2.5 g, 15.24 mmol) in dry MeOH (31 mL) was added $SOCl_2$ (2.2 mL, 30.48 mmol) dropwise while cooling in an ice-bath. This mixture was heated to 60 °C for 3 h before evaporation. The residue was dissolved in CH_2Cl_2 (30 mL), washed with aqueous $NaHCO_3$ (3 x 50 mL), water (3 x 50 mL) and brine (20 mL), dried ($MgSO_4$), and concentrated under vacuum to give the product that was used in the next step without further purification. Product obtained as a colourless liquid, yield: 2.60 g (93 %). TLC (petroleum ether-EtOAc 3:1 v/v), Rf = 0.64. ^{1}H NMR (CDCl$_3$): δ 7.32 (d, *J* = 8.5 Hz, 2H, Ar), 7.24 (d, *J* = 8.5 Hz, 2H, Ar), 3.72 (s, 3H, OC*H$_3$*), 3.62 (s, 2H, ArC*H$_2$*C=O).

7.4.2 (*R/S*)-Methyl 2-(4-chlorophenyl)-3-hydroxypropanoate (3)[83]

(2)	**(3)**
Chemical Formula: $C_9H_9ClO_2$	Chemical Formula: $C_{10}H_{11}ClO_3$
Molecular Weight: 184.62	Molecular Weight: 214.65
cLog P = 2.36	cLog P = 1.86
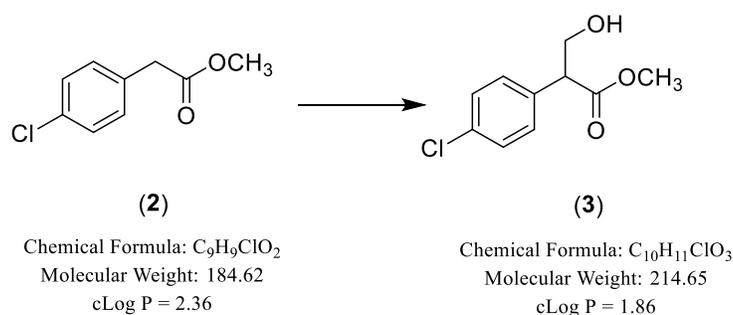
To a stirred solution of (4-chlorophenyl) acetic acid methyl ester (**2**) (2.37 g, 12.81 mmol) in dry DMSO (26 mL) was added sodium methoxide (0.03 g, 0.63 mmol) at 0 °C. Paraformaldehyde (0.40 g, 13.45 mmol) was then added and the reaction mixture was stirred at room temperature for 4 h. The reaction mixture was diluted with EtOAc (100 mL), washed with water (3 x 50 mL), brine (20 mL), dried (MgSO₄) and evaporated *in vacuo* to afford the product as a crude colourless liquid. The crude material was purified by gradient column chromatography eluting with n-hexane-EtOAc 60:40 v/v. Product obtained as a colourless liquid, yield: 1.98 g (72 %). TLC (n-hexane-EtOAc 1:1 v/v), R*f* = 0.46. ¹H NMR (CDCl₃): δ 7.33 (d, *J* = 8.5 Hz, 2H, Ar), 7.23 (d, *J* = 8.5 Hz, 2H, Ar), 4.13 (m, 1H, C*H*CHaHb), 3.84 (m, 2H, CHC*HaHb*), 2.49 (brs, 1H, O*H*).

7.4.3 (*R/S*)-2-(4-Chlorophenyl)-3-hydroxypropanoate (4b)[83]

(3)	**(4b)**
Chemical Formula: $C_{10}H_{11}ClO_3$	Chemical Formula: $C_9H_9ClO_3$
Molecular Weight: 214.65	Molecular Weight: 200.62
cLogP = 1.86	cLogP = 1.6
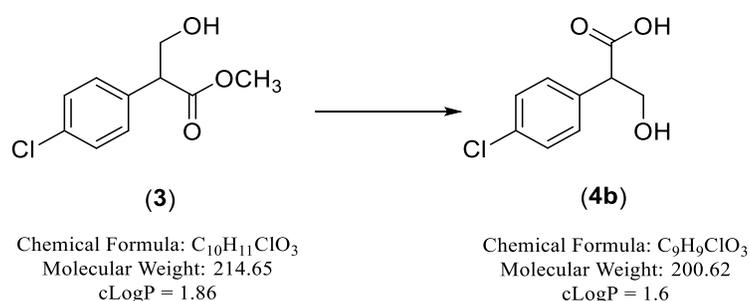
To a stirred solution of (*R/S*)-methyl 2-(4-chlorophenyl)-3-hydroxypropanoate (**3**) (0.60 g, 2.78 mmoL) in dry THF (8.4 mL) was added a solution of lithium hydroxide monohydrate (LiOH·H₂O) (0.29 g, 6.94 mmoL) in water (2.4 mL) dropwise at 0 °C and the resulting mixture stirred at room temperature for 1 h. The reaction mixture was acidified (pH 3) with 2N aqueous HCl and extracted with EtOAc (3 x 20 mL). The combined organic layers were washed with brine (3 x 50 mL), water (50 mL), dried (MgSO₄) and evaporated under vacuum. Product

obtained as a white powder, yield: 0.49 g (87 %). TLC (n-hexane-EtOAc 1:1 v/v), $Rf = 0.0$, (n-hexane-EtOAc 1:2 v/v), $Rf = 0.49$. M.p. 135-136 °C (lit. M.p. 151-154 °C)[161]. ^{1}H NMR (CDCl$_3$): δ 12.42 (brs, 1H, COO*H*), 7.39 (d, *J*= 8.5 Hz, 2H, Ar), 7.33 (d, *J*= 8.5 Hz, 2H, Ar), 4.95 (brs, 1H, CHCH$_2$O*H*), 3.89 (dd, *J*= 8.0, 10.0 Hz, 1H, CHC*H$_a$*H$_b$OH), 3.67 (dd, *J*= 6.5, 8.0 Hz, 1H, CHCH$_a$*H$_b$*OH), 3.60 (dd, *J*= 6.0, 10.5 Hz, 1H, C*H*CH$_a$H$_b$OH).

7.4.4 General method of amidation reaction (6)

Where R^1: **a**= 4-H   **Where R^2:** **a**= 4-H   **e**= 4-CH$_3$
              b= 4-Cl   **b**= 4-F   **f**= 4-CF$_3$
                                        c= 4-Cl   **g**= 4-OCH$_3$
                                        d= 2,4-di-Cl   **h**= 4-di-OCH$_3$
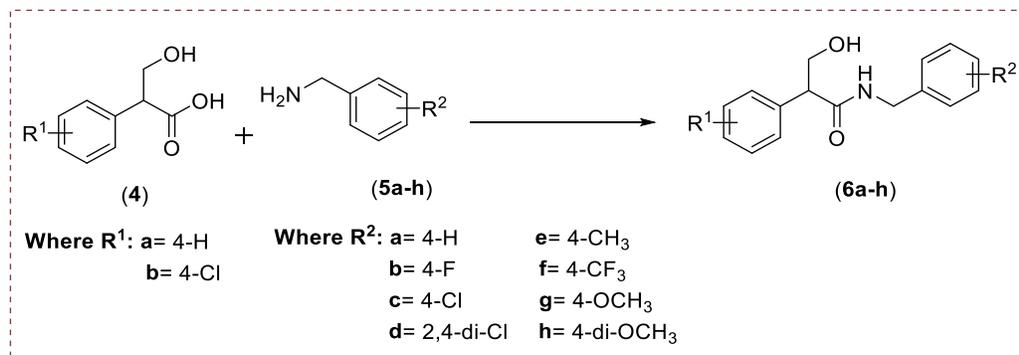
To a suspension of acid (**4**) (5 mmol) in dry CPME (15 mL) and activated 4Å molecular sieves (~ 1 mg/mmol) was added benzylamine (**5**) (5.5 mmol) followed by B(OMe)$_3$ (1.14 mL, 10 mmol). The resulting mixture was heated at 100 °C overnight. Upon completion, the reaction mixture was cooled to room temperature, diluted with acetone (10 mL) and H$_2$O (1 mL). Amberlite IRA743 (0.5 g), Amberlyst 15 (0.5 g) and Amberlyst A26 (OH) (0.5 g) resins were added, and the resulting suspension was stirred for 2 h. After disappearance of any remaining starting materials (monitored by TLC), anhydrous MgSO4 was added to the mixture. The reaction mixture was filtered, and the residue washed with acetone (2 x 10 mL), and the combined filtrates concentrated under reduced pressure to give the product, which was washed with Et$_2$O/petroleum ether to remove any remaining CPME.

(*R/S*)-*N*-Benzyl-3-hydroxy-2-phenylpropanamide (6a)

                (4a)   **(5a)**   **(6a)**

Chemical Formula: C$_9$H$_{10}$O$_3$ Chemical Formula: C$_7$H$_9$N   Chemical Formula: C$_{16}$H$_{17}$NO$_2$
Molecular Weight: 166.18   Molecular Weight: 107.16   Molecular Weight: 255.32
cLogP =1.04   cLogP= 1.08   cLogP= 2.36
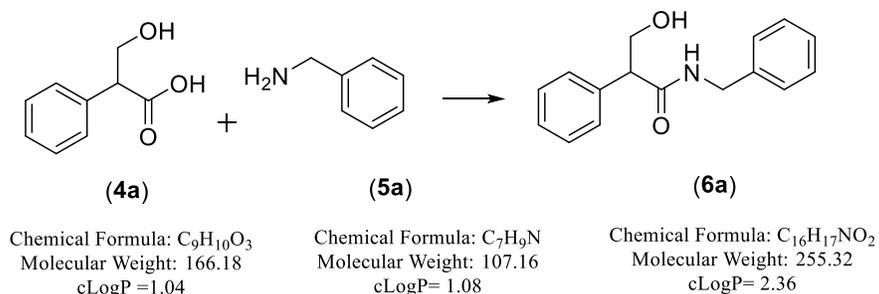
Prepared from tropic acid (**1a**, R^1=H) and benzylamine (**5a**, R^2= H) (0.6 mL, 5.5 mmoL) followed by trimethyl borate (B(OMe)$_3$) (1.14 mL, 10 mmoL). The product obtained as an off-white solid, yield 1.25 g (98%). TLC (petroleum ether-EtOAc 1:1 v/v), Rf = 0.28. M.p. 108-110 °C (lit. M.p. 117-119 °C).[84] ^{1}H NMR (DMSO-d_6): δ 8.53 (t, J = 5.9 Hz, 1H, NH), 7.26 (m, 10H, Ar), 4.86 (t, J = 5.2 Hz, 1H, O*H*), 4.31 (dd, J = 6.0, 15.3 Hz, 1H, NHC*Ha*Hb), 4.24 (dd, J = 5.8, 15.3 Hz, 1H, NHCHa*Hb*), 4.00 (ddd, J = 5.6, 9.2, 15.4 Hz, CHC*Ha*Hb), 3.68 (dd, J = 5.5, 9.0 Hz, C*H*CHaHb), 3.55 (pentet, J = 5.1 Hz, CHCHa*Hb*). ^{13}C NMR (DMSO-d_6): δ 172.18 (C, C=O), 139.92 (C, Ar), 138.90 (C, Ar), 128.65 (2 x CH, Ar), 128.63 (2 x CH, Ar), 128.41 (2 x CH, Ar), 127.50 (2 x CH, Ar), 127.20 (CH, Ar), 127.11 (CH, Ar), 63.83 (*C*H$_2$OH), 54.99 (*C*HCH$_2$OH), 42.46 (NH*C*H$_2$). HRMS (ESI), m/z. calcd for $C_{16}H_{18}NO_2$ ([M + H]$^+$), 256.1368; found, 256.1332; and calcd for $C_{16}H_{17}NO_2Na$ ([M + Na]$^+$), 278.1193; found, 278.1151. HPLC (Method A): 100%, R$_t$= 0.7 min.

(*R/S*)-*N*-(4-Fluorobenzyl)-3-hydroxy-2-phenylpropanamide (6b)

(**4a**)	(**5b**)	(**6b**)
Chemical Formula: $C_9H_{10}O_3$	Chemical Formula: C_7H_8FN	Chemical Formula: $C_{16}H_{16}FNO_2$
Molecular Weight: 166.18	Molecular Weight: 125.15	Molecular Weight: 273.31
cLogP= 1.04	cLogP= 1.24	cLogP= 2.52
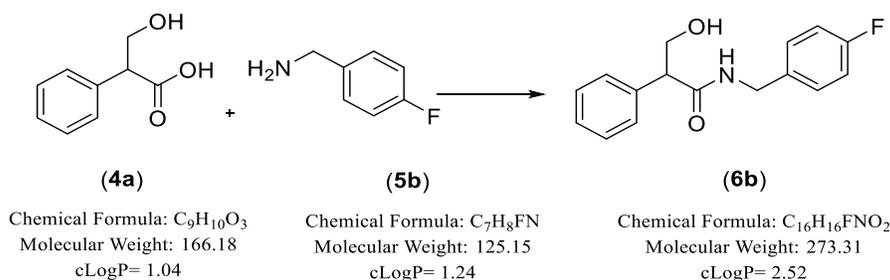
Prepared from tropic acid (**1a**, R^1=H) and 4-fluorobenzylamine (**5b**, R^2= 4-F). Product obtained as a cream coloured solid, yield 1.22 g (89 %). TLC (petroleum ether-EtOAc 1:1 v/v), Rf = 0.21. M.p. 114-116 °C. ^{1}H NMR (DMSO-d_6): δ 8.54 (t, J = 5.6 Hz, 1H, N*H*), 7.31 (m, 4H, Ar), 7.23 (m, 3H, Ar), 7.09 (t, J = 8.8 Hz, 2H, Ar), 4.87 (brs, 1H, OH), 4.31 (dd, J = 6.1, 15.3 Hz, 1H, NHC*Ha*Hb), 4.22 (dd, J = 5.7, 15.3 Hz, 1H, NHCHa*Hb*), 4.00 (t, J = 9.0 Hz, 1H, CHC*Ha*Hb), 3.67 (dd, J = 5.6, 8.8 Hz, 1H, C*H*CHaHb), 3.56 (dd, J = 5.6, 9.0 Hz, 1H, CHCHa*Hb*). ^{13}C NMR (DMSO-d_6): δ 172.24 (C, C=O), 162.52 and 160.60 (C, C-F), 138.82 (C, Ar), 136.14 (C, Ar), 129.47 (CH, Ar), 129.41 (CH, Ar), 128.67 (2 x CH, Ar), 128.40 (2 x CH, Ar), 127.23 (CH, Ar), 115.42 (CH, Ar), 115.25 (CH, Ar), 63.84 (CH*C*H$_2$OH), 55.01 (*C*HCH$_2$OH), 41.79 (NH*C*H$_2$). LRMS (ES+TOF, *m/z*): 274.13 [$C_{16}H_{16}FNO_2$ + H]$^+$, 179.02 [$C_{10}H_{13}NO_2$]$^+$. HRMS (ES+TOF) *m/z*. calcd for $C_{16}H_{17}FNO_2$ ([M + H]$^+$), 274.1243; found, 274.1250.

(*R/S*)-*N*-(4-Chlorobenzyl)-3-hydroxy-2-phenylpropanamide (6c)

(4a)

Chemical Formula: $C_9H_{10}O_3$
Molecular Weight: 166.18
cLogP =1.04

(5c)

Chemical Formula: C_7H_8ClN
Molecular Weight: 141.60
cLogP= 1.64

(6c)

Chemical Formula: $C_{16}H_{16}ClNO_2$
Molecular Weight: 289.76
cLogP= 2.92
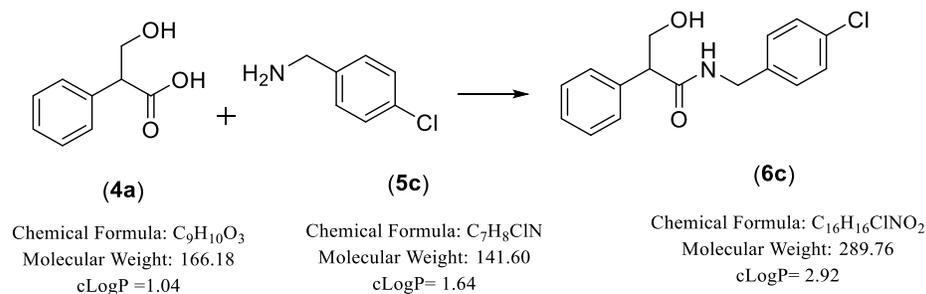
Prepared from tropic acid (**1a**, R^1=H) and 4-chlorobenzylamine (**5c**, R^2= 4-Cl). The product obtained as a cream coloured solid, yield 1.19 g (85%). TLC (petroleum ether-EtOAc 1:1 v/v), R*f* = 0.42. ^{1}H NMR (DMSO-d_6): δ 8.59 (t, *J* = 6.0 Hz, 1H, N*H*), 7.40 (s, 2H, Ar), 7.30 (m, 5H, Ar), 7.22 (m, 2H, Ar), 4.30 (dd, *J* = 6.1, 15.5 Hz, 1H, NHC*Ha*Hb), 4.21 (dd, *J* = 5.8, 15.5 Hz, 1H, NHCHa*Hb*), 3.99 (t, *J* = 9.6 Hz, 1H, O*H*), 3.86 (m, 2H, CHC*Ha*H*b*), 3.67 (dd, *J* = 5.5, 9.1 Hz, 1H, C*H*CHaHb). ^{13}C NMR (DMSO-d_6): δ 172.29 (C, C=O), 139.07 (C, Ar), 138.87 (C, C-Cl), 138.77 (C, C-Cl), 131.65 (C, Ar), 130.26 (CH, Ar), 129.36 (2 x CH, Ar), 128.65 (2 x CH, Ar), 128.56 (CH, Ar), 128.39 (CH, Ar), 127.24 (CH, Ar), 127.08 (CH, Ar), 64.32 (*CH₂*OH), 54.99 (*C*HCH₂OH), 43.63 (NH*C*H₂).

Method (2)

Tris(2,2,2-trifluoroethyl)borate (B(OCH₂CF₃)₃) (0.86 mL, 4 mmol) was added to a solution of tropic acid (**4a**) (0.33g, 2 mmol) and 4-chlorobenzylamine (**5c**) (0.24 mL, 2 mmol) in CPME (4 mL). The resulting mixture was then stirred at 100 °C overnight. Upon completion the reaction mixture was diluted with EtOAc (8 mL) and water (1 mL). Amberlyst A-26(OH) (300 mg), Amberlyst 15 (300 mg) and Amberlite IRA743 (300 mg) were added together to the mixture and it was stirred for 30 min. The mixture was then dried (MgSO₄), filtered to remove resins and MgSO₄ and washed with EtOAc (3 x 30 mL). The filtrate was concentrated *in vacuo* to yield the desired amide product.

Product obtained as an off-white solid, yield 0.35 g (60%). TLC (petroleum ether-EtOAc 1:1 v/v), R*f* = 0.42. M.p. 135-136 °C. ^{1}H NMR (CDCl₃): δ 7.35 (m, 3H, Ar), 7.28 (m, 4H, Ar), 7.11 (d, *J* = 8.5 Hz, 2H, Ar), 5.95 (s, 1H, N*H*), 4.40 (dd, *J* = 2.2, 6.0 Hz, 2H, NHC*H₂*), 4.18 (dd, *J* = 8.8, 11.1 Hz, CHC*Ha*Hb), 3.81 (dd, *J* = 4.3, 11.1 Hz, CHCHa*Hb*), 3.71 (dd, *J* = 4.5, 8.8 Hz,

C*H*CHaHb), 3.30 (s, 1H, OH). ^{1}H NMR (DMSO-d_6): δ 8.60 (t, J = 5.9 Hz, 1H, N*H*), 7.32 (m, 6H, Ar), 7.25 (d, J = 8.5 Hz, 1H, Ar), 7.21 (d, J = 8.5 Hz, 2H, Ar), 4.90 (t, J = 5.2 Hz, 1H, OH), 4.30 (dd, J = 6.1, 15.5 Hz, 1H, NHC*Ha*Hb), 4.21 (dd, J = 5.8, 15.5 Hz, 1H, NHCHa*Hb*), 4.00 (dt, J = 5.6, 9.7 Hz, CHC*Ha*Hb), 3.67 (dd, J = 5.5, 9.1 Hz, CHCHa*Hb*), 3.54 (pentet, J = 5.0 Hz, C*H*CHaHb). ^{13}C NMR (CDCl$_3$): δ 173.6 (C, C=O), 136.5 (C, Ar), 136.4 (C, Ar), 133.3 (C, C-Cl), 129.2 (3 x CH, Ar), 128.8 (2 x CH, Ar), 128.5 (3 x CH, Ar), 128.1 (CH, Ar), 64.9 (*C*H$_2$OH), 54.4 (*C*HCH$_2$OH), 42.8 (NH*C*H$_2$). Anal. Calcd for C$_{16}$H$_{16}$ClNO$_2$•0.2H$_2$O (293.3630): C, 65.51%; H, 5.63%; N, 4.77%. Found: C, 65.36%; H, 5.47%; N, 4.84%.

(*R/S*)-*N*-(4-Chlorobenzyl)-2-(4-chlorophenyl)-3-hydroxypropanamide (6d)

(4b)
Chemical Formula: C$_9$H$_9$ClO$_3$
Molecular Weight: 200.62
cLogP= 1.6

(5c)
Chemical Formula: C$_7$H$_8$ClN
Molecular Weight: 141.60
cLogP= 1.64

(6d)
Chemical Formula: C$_{16}$H$_{15}$Cl$_2$NO$_2$
Molecular Weight: 324.20
cLogP= 3.47
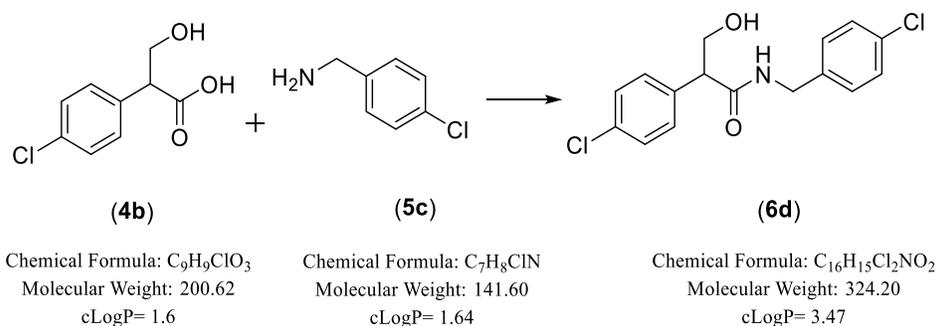
Method: see 7.4.4. The product was washed with petroleum ether to remove any remaining CPME.

Prepared from (*R/S*)-2-(4-chlorophenyl)-3-hydroxy propanoic acid[82] (**4b**, R[1]= 4-Cl) and 4-chlorobenzylamine (**5c**, R[2]= 4-Cl). Product obtained as a cream coloured solid, yield: 1.621 g (100 %). TLC (petroleum ether-EtOAc 1:1 v/v), Rf = 0.74. M.p. 126-128 °C.

Method: see 7.4.4, method (2).

Prepared from (*R/S*)-2-(4-chlorophenyl)-3-hydroxy propanoic acid (**4b**, R[1]= 4-Cl) (0.40 g, 2 mmoL) and 4-chlorobenzylamine (**5c**, R[2]= 4-Cl) (0.24 mL, 2.00 mmoL). Product obtained as a cream coloured solid, yield: 0.54 g (84 %). TLC (petroleum ether-EtOAc 1:1 v/v), Rf = 0.3. M.p. 126-128 °C. ^{1}H NMR (DMSO-d_6): δ 8.64 (t, J = 5.9 Hz, 1H, N*H*), 7.40 (m, 6H, Ar), 7.26 (d, J = 8.5 Hz, 2H, Ar), 4.95 (brs, 1H, O*H*), 4.35 (dd, J = 6.1, 15.5 Hz, 1H, NHC*Ha*Hb), 4.26 (dd, J = 5.8, 15.5 Hz, 1H, NHCHa*Hb*), 4.00 (t, J = 8.9 Hz, 1H, CHC*Ha*Hb), 3.73 (dd, J = 5.9, 8.6 Hz, 1H, C*H*CHaHb), 3.59 (dd, J = 8.3, 14.5 Hz, 1H, CHCHa*Hb*). ^{13}C NMR (DMSO-d_6): δ

171.92 (C, C=O), 158.93 (C, Ar), 137.76 (C, Ar), 131.95 (C, *C*-Cl), 131.72 (C, *C*-Cl), 130.28 (2 x CH, Ar), 129.39 (2 x CH, Ar), 128.64 (2 x CH, Ar), 128.61 (2 x CH, Ar), 63.68 (CH*C*H$_2$OH), 54.21 (*C*HCH$_2$OH), 41.87 (NH*C*H$_2$). LRMS (ES+TOF, *m/z*): 326.05 [C$_{16}$H$_{15}$^{37}Cl$_2$NO$_2$+H]$^+$, 324.06 [C$_{16}$H$_{15}$^{35}Cl$_2$NO$_2$+H]$^+$, 157.03 [C$_8$H$_8$^{35}ClO+H]$^+$. HRMS (ES+TOF), *m/z*. calcd for C$_{16}$H$_{16}$Cl$_2$NO$_2$ ([M + H]$^+$), 324.0558; found, 324.0555.

(*R/S*)-*N*-(2,4-Dichlorobenzyl)-3-hydroxy-2-phenylpropanamide (6e)

(4a)	(5d)	(6e)
Chemical Formula: C$_9$H$_{10}$O$_3$	Chemical Formula: C$_7$H$_7$Cl$_2$N	Chemical Formula: C$_{16}$H$_{15}$Cl$_2$NO$_2$
Molecular Weight: 166.18	Molecular Weight: 176.04	Molecular Weight: 324.20
cLogP= 1.04	cLogP= 2.20	cLogP= 3.47
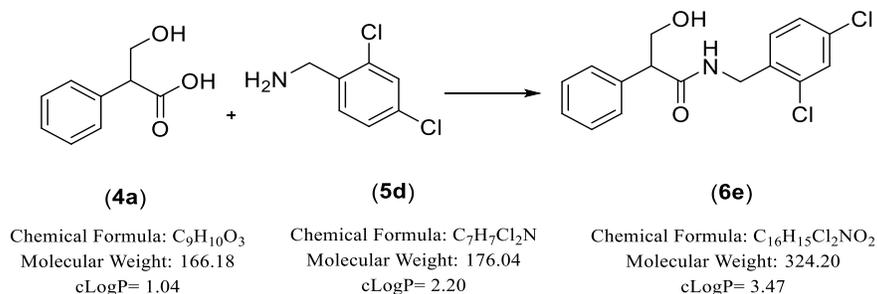
Prepared from tropic acid (**1a**, R^1= H) and 2,4-dichlorobenzylamine (**5d**, R^2= 2,4-di-Cl). Product obtained as a brown solid, yield 1.62 g (100%). TLC (petroleum ether-EtOAc 1:1 v/v), R*f* = 0.47. M.p. 78- 80 °C. ^{1}H NMR (DMSO-*d$_6$*): δ 8.61 (t, *J* = 5.8 Hz, 1H, N*H*), 7.57 (d, *J* = 2.0 Hz, 1H, Ar), 7.32 (m, 5H, Ar), 7.25 (m, 2H, Ar), 4.90 (t, *J* = 7.1 Hz, 1H, O*H*), 4.33 (dd, *J* = 5.9, 16.1 Hz, 1H, NHC*Ha*Hb), 4.27 (dd, *J* = 5.8, 16.1 Hz, 1H, NHCHa*Hb*), 3.99 (ddd, *J* = 5.6, 9.7, 15.1 Hz, 1H, CHC*Ha*Hb), 3.72 (dd, *J* = 5.5, 9.1 Hz, 1H, C*H*CHaHb), 3.56 (d dd, *J* = 1.2, 5.1, 10.0 Hz, 1H, CHCHa*Hb*). ^{13}C NMR (DMSO-*d$_6$*): δ 172.54 (C, C=O), 158.58 (C, Ar), 136.07 (C, Ar), 133.32 (C, C-Cl), 132.57 (C, C-Cl), 130.38 (CH, Ar), 128.94 (CH, Ar), 128.70 (2 x CH, Ar), 128.42 (2 x CH, Ar), 127.58 (CH, Ar), 127.31 (CH, Ar), 63.79 (CH*C*H$_2$OH), 54.95 (*C*HCH$_2$OH), 39.98 (NH*C*H$_2$). LRMS (ES+TOF, *m/z*): 326.05 [C$_{16}$H$_{15}$^{37}Cl$_2$NO$_2$ + H] $^+$, 324.06 [C$_{16}$H$_{15}$^{35}Cl$_2$NO$_2$ + H] $^+$, 159.03 [C$_7$H$_5$^{37}Cl$_2$ + H] $^+$, 157.03 [C$_7$H$_5$^{35}Cl$_2$ + H] $^+$. HRMS (ES+TOF), *m/z*. calcd for C$_{16}$H$_{16}$Cl$_2$NO$_2$ ([M + H]$^+$), 324.0558; found, 324.0562.

(*R/S*)-*N*-(2,4-Dichlorobenzyl)- 2-(4-chlorophenyl)-3-hydroxypropanamide (6f)

(4b)	(5d)	(6f)
Chemical Formula: $C_9H_9ClO_3$	Chemical Formula: $C_7H_7Cl_2N$	Chemical Formula: $C_{16}H_{14}Cl_3NO_2$
Molecular Weight: 200.62	Molecular Weight: 176.04	Molecular Weight: 358.64
cLogP= 1.6	cLogP= 2.2	cLogP= 4.03
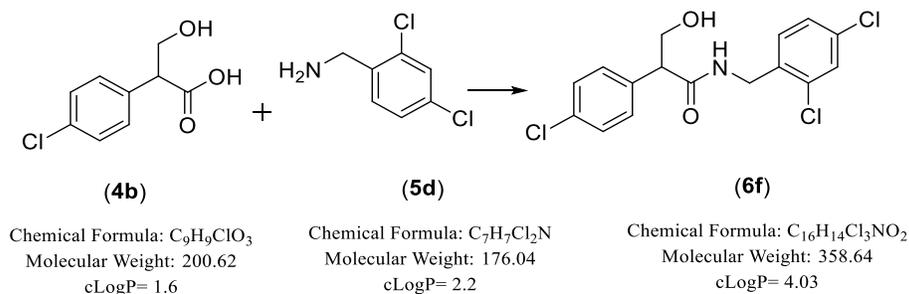
Prepared from (*R/S*)-2-(4-chlorophenyl)-3-hydroxy propanoic acid[82] (**4b**, R^1= 4-Cl) and 2,4-dichlorobenzyl amine (**5d**, R^2= 2,4-di-Cl). Product obtained as a white solid, yield: 0.71 g (40 %). TLC (petroleum ether-EtOAc 1:1 v/v), R*f* = 0.3. M.p. 106-108 °C. ^{1}H NMR (DMSO-*d*$_6$): δ 8.63 (t, *J* = 5.8 Hz, 1H, N*H*), 7.58 (d, *J* = 2.1 Hz, 1H, Ar), 7.36 (m, 5H, Ar), 7.25 (d, *J* = 8.4 Hz, 1H, Ar), 4.94 (t, *J* = 5.1 Hz, 1H, O*H*), 4.30 (m, 2H, NHC*Ha*Hb), 3.94 (ddd, *J* = 5.5, 8.9, 15.6 Hz, 1H, CHC*Ha*Hb), 3.73 (dd, *J* = 5.8, 8.8 Hz, 1H, C*H*CHaHb), 3.55 (pentet, *J* = 5.2 Hz, 1H, CHCHa*Hb*). ^{13}C NMR (DMSO-*d*$_6$): δ 172.13 (C, C=O), 137.57 (C, Ar), 135.95 (C, Ar), 133.37 (C, C-Cl), 132.63 (C, C-Cl), 131.99 (C, C-Cl), 130.45 (CH, Ar), 130.30 (2 x CH, Ar), 128.99 (CH, Ar), 128.66 (2 x CH, Ar), 127.65 (CH, Ar), 63.67 (CH*CH$_2$*OH), 54.12 (*C*HCH$_2$OH), 40.12 (NH*CH$_2$*). Anal. Calcd for $C_{16}H_{14}Cl_3NO_2$ (358.6469): C, 53.58%; H, 3.93%; N, 3.90%. Found: C, 53.72%; H, 4.06%; N, 3.85%. HRMS (ESI), *m/z*. calcd for $C_{16}H_{15}Cl_3{}^{35}NO_2$ ([M + H]$^+$), 358.0199; found, 358.0163; calcd for $C_{16}H_{14}Cl_3{}^{35}NO_2Na$ ([M + Na]$^+$), 380.0021; found, 379.9982; calcd for $C_{16}H_{15}Cl_3{}^{37}NO_2$ ([M + H]$^+$), 360.0170; found, 360.0135, and calcd for $C_{16}H_{14}Cl_3{}^{37}NO_2Na$ ([M + Na]$^+$), 381.9992; found, 381.9955.

(*R/S*)-3-Hydroxy-*N*-(4-methybenzyl)-2-phenylpropanamide (6g)

(4a)	(5e)	(6g)
Chemical Formula: $C_9H_{10}O_3$	Chemical Formula: $C_8H_{11}N$	Chemical Formula: $C_{17}H_{19}NO_2$
Molecular Weight: 166.18	Molecular Weight: 121.18	Molecular Weight: 269.34
cLogP= 1.04	cLogP= 1.57	cLogP= 2.85
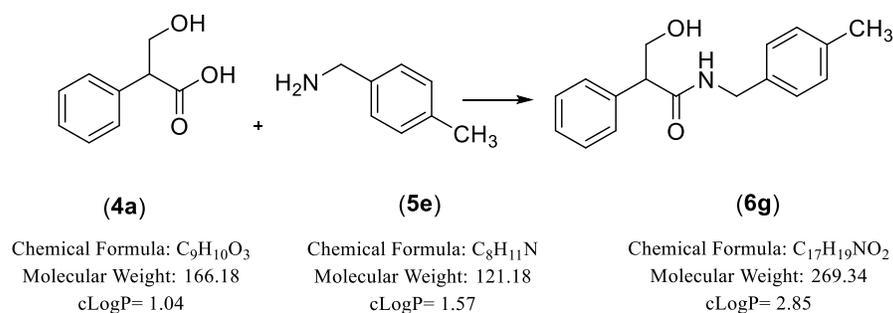
Prepared from tropic acid (**1a**, R^1= H) and 4-methybenzylamine (**5e**, R^2= 4-CH$_3$). Product obtained as a cream coloured solid, yield: 1.35 g (100%). TLC (petroleum ether-EtOAc 1:1 v/v), Rf = 0.29. M.p. 96-98 °C. ^{1}H NMR (DMSO-d_6): δ 8.47 (t, J = 5.9 Hz, 1H, NH), 7.28 (m, 5H, Ar), 7.06 (m, 3H, Ar), 6.53 (s, 1H, Ar), 4.84 (t, J = 5.2 Hz, 1H, OH), 4.25 (dd, J = 6.0, 15.1 Hz, 1H, NHCHaHb), 4.19 (dd, J = 5.9, 15.1 Hz, 1H, NHCHaHb), 3.99 (ddd, J = 5.6, 9.1, 15.5 Hz, 1H, CHCHaHb), 3.66 (dd, J = 5.5, 9.0 Hz, 1H, CHCHaHb), 3.54 (pentet, J = 5.1 Hz, 1H, CHCHaHb), 2.25 (s, 3H, CH_3). ^{13}C NMR (DMSO-d_6): δ 172.09 (C, C=O), 138.95 (C, Ar), 136.87 (C, C-CH$_3$), 136.13 (C, Ar), 129.18 (2 x CH, Ar), 128.63 (2 x CH, Ar), 128.41 (2 x CH, Ar), 127.51 (2 X CH, Ar), 127.18 (CH, Ar), 63.81 (CHCH$_2$OH), 54.97 (CHCH$_2$OH), 42.21 (NHCH$_2$), 21.09 (CH$_3$). HRMS (ESI), m/z. calcd for C$_{17}$H$_{20}$NO$_2$ ([M + H]$^+$), 270.1499; found, 270.1489, and calcd for C$_{17}$H$_{19}$NO$_2$Na ([M + Na]$^+$), 292.1322; found, 292.1308. HPLC (Method A): 92%, R$_t$ = 0.8 min.

(*R/S*)-3-Hydroxy-2-phenyl-*N*-(4-trifluoromethy)benzyl)propanamide (6h)

(**4a**)	(**5f**)	(**6h**)
Chemical Formula: C$_9$H$_{10}$O$_3$	Chemical Formula: C$_8$H$_8$F$_3$N	Chemical Formula: C$_{17}$H$_{16}$F$_3$NO$_2$
Molecular Weight: 166.18	Molecular Weight: 175.15	Molecular Weight: 323.32
cLogP= 1.04	cLogP= 2	cLogP= 3.28
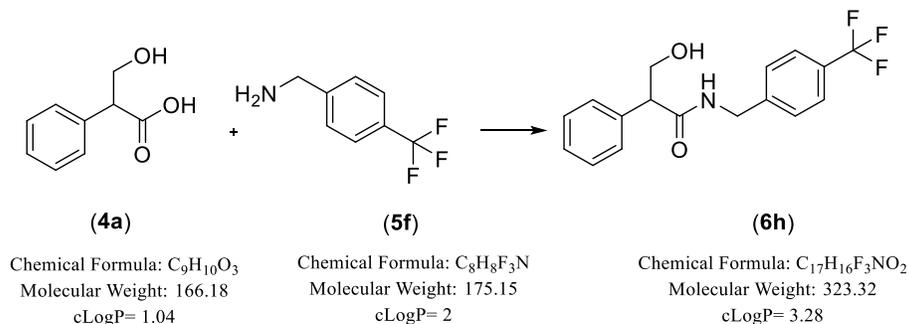
Prepared from tropic acid (**1a**, R^1= H) and 4-(trifluoromethyl)benzylamine (**5f**, R^2= 4-CF$_3$). Further purification by extraction with EtOAc (50 mL) washing with 1M HCl (2 x 25 mL), water (25 mL) and dried over (MgSO$_4$) before concentration under vacuum to give pure amine as a cream coloured solid, yield: 0.54 g (34%). TLC (petroleum ether-EtOAc 1:1 v/v), Rf = 0.2. M.p. 104-106 °C. ^{1}H NMR (DMSO-d_6): δ 8.66 (t, J = 6.0 Hz, 1H, NH),), 7.62 (d, J = 8.1 Hz, 2H, Ar), 7.40 (d, J = 8.0 Hz, 2H, Ar), 7.28 (m, 5H, Ar), 4.81 (brs, 1H, OH), 4.40 (dd, J = 6.1, 15.9 Hz, 1H, NHCHaHb), 4.31 (dd, J = 5.8, 15.8 Hz, 1H, NHCHaHb), 4.00 (t, J = 9.6 Hz, 1H, CHCHaHb), 3.69 (dd, J = 5.5, 9.1 Hz, 1H, CHCHaHb), 3.55 (dd, J = 5.5, 10.1 Hz, 1H, CHCHaHb). ^{13}C NMR (DMSO-d_6): δ 172.43 (C, C=O), 144.97 (C, Ar), 138.71 (C, Ar), 128.69 (2 x CH, Ar), 128.40 (3 x CH, Ar), 128.12 (3 x CH, Ar), 127.70 (C, Ar), 127.27 (CH, Ar), 125.50 & 125.47 (C, C-F$_3$), 63.79 (CHCH$_2$OH), 55.02 (CHCH$_2$OH), 42.13 (NHCH$_2$). ^{19}F-NMR

(DMSO-d_6): δ -60.80. Anal. Calcd for $C_{17}H_{16}F_3NO_2$•0.2H_2O (326.91714): C, 62.46%; H, 5.12%; N, 4.28%. Found: C, 62.31%; H, 4.88%; N, 3.93%. HRMS (ESI) *m/z.* calcd for $C_{17}H_{17}F_3NO_2$ ([M + H]$^+$), 324.1218; found, 324.1206, and calcd for $C_{17}H_{16}F_3NO_2Na$ ([M + Na]$^+$), 346.1037; found, 346.1025.

(*R/S*)-3-Hydroxy-*N*-(4-methoxybenzyl)-2-phenylpropanamide (6i)

(**4a**)	(**5g**)	(**6i**)
Chemical Formula: $C_9H_{10}O_3$	Chemical Formula: $C_8H_{11}NO$	Chemical Formula: $C_{17}H_{19}NO_3$
Molecular Weight: 166.18	Molecular Weight: 137.18	Molecular Weight: 285.34
cLogP= 1.04	cLogP= 0.95	cLogP= 2.23
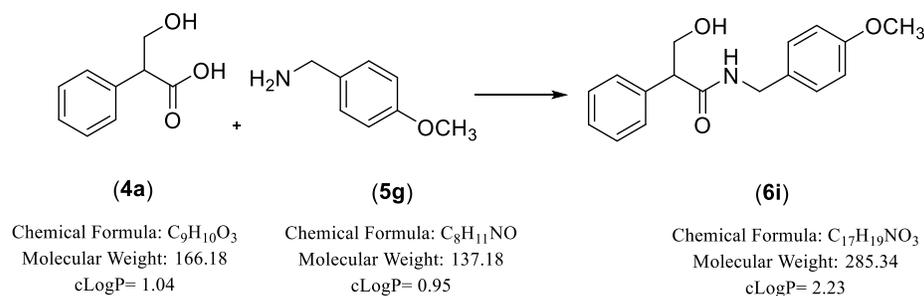
Prepared from tropic acid (**1a**, R^1=H) and 4-methoxybenzylamine (**5g**, R^2= OCH$_3$). Product obtained as a white powder, yield: 1.40 g (98 %). TLC (petroleum ether-EtOAc 1:1 v/v), Rf = 0.36. M.p. 126-128 °C. ^{1}H NMR (DMSO-d_6): δ 8.45 (t, *J* = 5.8 Hz, 1H, N*H*), 7.32 (m, 4H, Ar), 7.23 (m, 1H, Ar), 7.12 (d, *J* = 8.7 Hz, 2H, Ar), 6.83 (d, *J* = 8.7 Hz, 2H, Ar), 4.67 (dd, *J* = 8.8, 9.7 Hz, 1H, OH), 4.25 (dd, *J* = 6.0, 15.0 Hz, 1H, NHC*Ha*Hb), 4.17 (dd, *J* = 5.8, 15.0 Hz, 1H, NHCHa*Hb*), 4.00 (dd, *J* = 9.2, 9.9 Hz, 1H, CHC*Ha*Hb), 3.72 (s, 3H, C*H₃*), 3.57 (dd, *J* = 5.5, 8.9 Hz, 1H, C*H*CHaHb), 3.55 (dd, *J* = 5.5, 10.1 Hz, 1H, CHCHa*Hb*). ^{13}C NMR (DMSO-d_6): δ 172.06 (C, C=O), 158.61 (C, C-OCH$_3$), 138.97 (C, Ar), 131.83 (C, Ar), 128.86 (2 x CH, Ar), 128.63 (2 x CH, Ar), 128.42 (2 x CH, Ar), 127.17 (CH, Ar), 114.07 (2 x CH, Ar), 63.87 (CHC*H₂*OH), 55.51 (OC*H₃*), 54.97 (*C*HCH$_2$OH), 41.95 (NHC*H₂*). Anal. Calcd for $C_{17}H_{19}NO_3$ (285.3420): C, 71.56%; H, 6.71%; N, 4.91%. Found: C, 71.57%; H, 6.68%; N, 5.08%.

(*R/S*)-*N*-(3,4-Dimethoxybenzyl)-3-hydroxy-2-phenylpropanamide (6j)

(**4a**)	(**5h**)	(**6j**)
Chemical Formula: $C_9H_{10}O_3$	Chemical Formula: $C_9H_{13}NO_2$	Chemical Formula: $C_{18}H_{21}NO_4$
Molecular Weight: 166.18	Molecular Weight: 167.21	Molecular Weight: 315.37
cLogP= 1.04	cLogP= 0.83	cLogP= 2.11
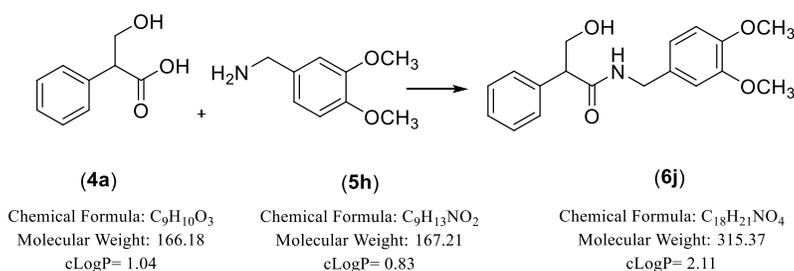
Method: see 7.4.4 method (2) but upon completion diluted with acetone instead of EtOAc.

Prepared from tropic acid (**4a**, R^1= H) and 3, 4-dimethoxybenzylamine (**5h**, R^2= 3,4-di-OCH$_3$). Product obtained as a yellow solid, yield: 1.05 g (83 %). TLC (petroleum ether-EtOAc 1:1 v/v), Rf = 0.16. M.p. 116- 118 °C. ^{1}H NMR (DMSO-d_6): δ 8.49 (t, J = 5.9 Hz, 1H, NH), 7.35 (d, J = 7.5 Hz, 2H, Ar), 7.30 (t, J = 7.5 Hz, 2H, Ar), 7.23 (t, J = 7.1 Hz, 1H, Ar), 6.83 (d, J = 8.1 Hz, 1H, Ar), 6.72 (d, J = 3.2 Hz, 1H, Ar), 6.54 (s, 1H, Ar), 4.86 (t, J = 5.1 Hz, 1H, OH), 4.23 (m, 2H, NHCHaHb), 4.02 (ddd, J = 5.6, 9.6, 15.0 Hz, 1H, CHCHaHb), 3.76 (dd, J = 5.3, 14.9 Hz, 1H, CHCHaHb), 3.70 (s, 3H, OCH_3), 3.68 (φt, J = 3.7, 5.5 Hz, 1H, CHCHaHb), 3.58 (s, 3H, OCH_3). ^{13}C NMR (DMSO-d_6): δ 172.12 (C, C=O), 149.11 (C, COCH$_3$), 148.04 (C, COCH$_3$), 138.96 (C, Ar), 132.43 (C, Ar), 128.66 (2 x CH, Ar), 128.41 (2 x CH, Ar), 127.19 (CH, Ar), 119.39 (CH, Ar), 112.11 (CH, Ar), 111.13 (CH, Ar), 63.83 (CHCH$_2$OH), 56.03 (OCH$_3$), 55.63 (OCH$_3$), 55.04 (CHCH$_2$OH), 42.02 (NHCH$_2$). LRMS (ES+TOF, m/z): 316.15 [C$_{18}$H$_{21}$NO$_4$ + H]$^+$. HRMS (ES+TOF), m/z. calcd for C$_{18}$H$_{22}$NO$_4$ ([M + H]$^+$), 316.1549; found, 316.1544.

7.4.5 <u>General method (1) of mesylation reaction (7)</u>

Where R^1: a= 4-H   **Where R^2: a**= 4-H   **e**= 4-CH$_3$
              b= 4-Cl   **b**= 4-F   **f**= 4-CF$_3$
                                       c= 4-Cl   **g**= 4-OCH$_3$
                                     d= 2,4-di-Cl   **d**= 4-di-OCH$_3$
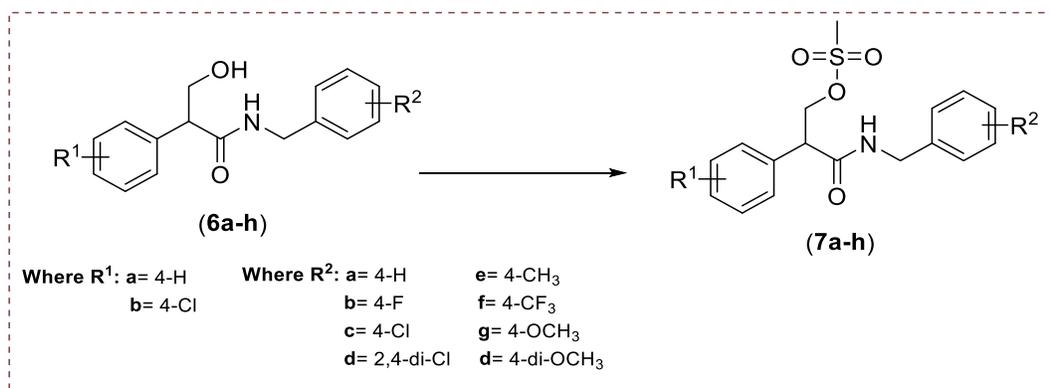
     To an ice-cooled suspension of alcohol (**6**) (1 eq) in dry CH$_2$Cl$_2$ (2 mL/mmol), was added Et$_3$N (1.5 eq) followed by methane sulfonyl chloride (2.5 eq) dropwise. The reaction was stirred at 0 °C for 1 h then at room temperature overnight. The reaction was diluted with CH$_2$Cl$_2$ (10 mL/mmol), washed with 1% aqueous/1 M HCl (10 mL/mmol), water (2 x 10 mL/mmol), dried (MgSO$_4$) and evaporated under vacuum. The product was purified by petroleum ether – EtOAc gradient column chromatography.

(*R/S*)-3-(Benzylamino)-3-oxo-2-phenylpropyl methanesulfonate (7a)

(6a)
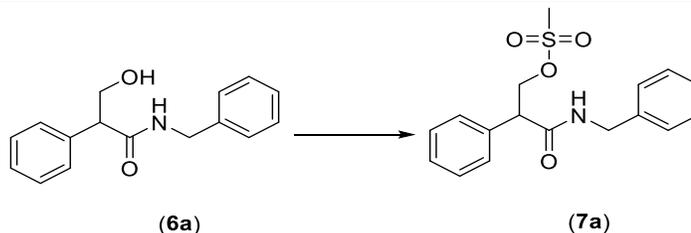
Chemical Formula: $C_{16}H_{17}NO_2$
Molecular Weight: 255.32
cLogP= 2.36

(7a)

Chemical Formula: $C_{17}H_{19}NO_4S$
Molecular Weight: 333.40
cLogP= 1.9

Prepared from (*R/S*)-*N*-benzyl-3-hydroxy-2-phenylpropanamide (**6a**) (1.21 g, 4.73 mmol) and purified by petroleum ether – EtOAc gradient column chromatography eluting with 50:50 v/v. Product obtained as a white solid, yield: 0.53 g (35 %). TLC (petroleum ether-EtOAc 1:1 v/v), Rf = 0.71. M.p. 78-80 °C. ^{1}H NMR (DMSO-d_6): δ 8.77 (t, *J* = 5.9 Hz, 1H, N*H*), 7.28 (m, 10H, Ar), 4.74 (t, *J* = 9.6 Hz, 1H, CHC*Ha*Hb), 4.34 (dd d, *J* = 5.7, 9.5; 6.0 Hz, 2H, CHCHa*Hb* + NHC*Ha*Hb), 4.26 (dd, *J* = 5.8, 15.3 Hz, 1H, NHCHa*Hb*), 4.03 (dd, *J* = 5.6, 9.4 Hz, 1H, C*H*CHaHb), 3.14 (s, 3H, C*H₃*). ^{13}C NMR(DMSO-d_6): δ 170.18 (C, C=O), 139.48 (C, Ar), 136.28 (C, Ar), 129.06 (2 x CH, Ar), 128.71 (2 x CH, Ar), 128.46 (2 x CH, Ar), 128.13 (CH, Ar), 127.50 (2 x CH, Ar), 127.27 (CH, Ar), 71.14 (*CH₂*OMs), 50.84 (*CH*CH₂OMs), 42.60 (NHC*H₂*), 37.02 (*CH₃*). Anal. Calcd for $C_{17}H_{19}NO_4S$ (333.4014): C, 61.24%; H, 5.74%; N, 4.20%. Found: C, 61.32%; H, 5.73%; N, 4.15%.

(*R/S*)-3-((4-Fluorobenzyl) amino)-3-oxo-2-phenylpropyl methanesulfonate (7b)

(6b)
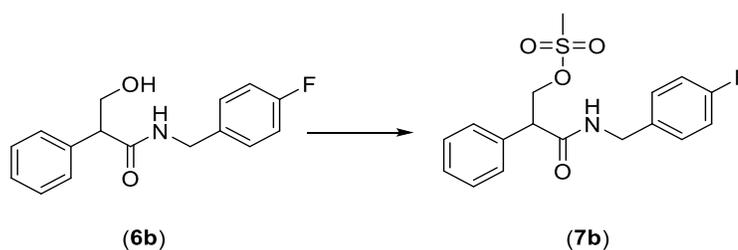
Chemical Formula: $C_{16}H_{16}FNO_2$
Molecular Weight: 273.31
cLogP= 2.52

(7b)

Chemical Formula: $C_{17}H_{18}FNO_4S$
Molecular Weight: 351.39
cLogP= 2.06

Method: see 7.4.5 method. Product was eluted with petroleum ether – EtOAc 50:50 v/v.

Prepared from (*R/S*)-*N*-(4-fluorobenzyl)-3-hydroxy-2-phenylpropanamide (**6b**) (1.17 g, 4.27 mmoL). Product obtained as an off- white solid, yield: 0.75 g (50 %). TLC (petroleum ether-

EtOAc 1:1 v/v), Rf = 0.67. M.p. 110-112 °C. ^{1}H NMR (DMSO-d_6): δ 8.78 (t, J = 5.6 Hz, 1H, N*H*), 7.38 (m, 4H, Ar), 7.32 (m, 1H, Ar), 7.22 (dd, J = 5.6, 8.5 Hz, 2H, Ar), 7.09 (t, J = 8.8 Hz, 2H, Ar), 4.74 (t, J = 9.6 Hz, 1H, CHC*H*aHb), 4.37 (dd, J = 5.6, 9.6 Hz, 1H, CHCHa*Hb*), 4.33 (dd, J = 6.0, 15.3 Hz, 1H, NHC*H*aHb), 4.24 (dd, J = 5.6, 15.2 Hz, 1H, NHCHa*Hb*), 4.03 (dd, J = 5.6, 9.6 Hz, 1H, C*H*CHaHb), 3.15 (s, 3H, C*H*$_3$). ^{13}C NMR(DMSO-d_6): δ 170.21 (C, C=O), 162.59 and 160.66 (C, *C*-F), 136.23 (C, Ar), 135.69 (C, Ar), 129.53 (CH, Ar), 129.46 (CH, Ar),129.08 (2 x CH, Ar), 128.46 (2 x CH, Ar), 128.15 (CH, Ar), 115.50 (CH, Ar), 115.33 (CH, Ar), 71.13 (*C*H$_2$OMs), 50.86 (*C*HCH$_2$OMs), 41.94 (NH*C*H$_2$), 37.05 (*C*H$_3$). LRMS (ESI, *m/z*): 352.10 [C$_{17}$H$_{18}$FNO$_4$S + H]$^+$. HRMS (ES+TOF), *m/z*. calcd for C$_{17}$H$_{19}$FNO$_4$S ([M + H]$^+$), 352.1013; found, 352.1016.

(*R/S*)-3-((4-Chlorobenzyl)amino)-3-oxo-2-phenylpropyl methanesulfonate (7c)
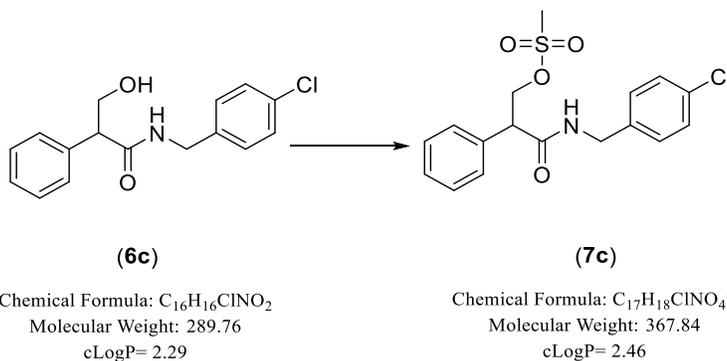
(6c)

Chemical Formula: C$_{16}$H$_{16}$ClNO$_2$
Molecular Weight: 289.76
cLogP= 2.29

(7c)

Chemical Formula: C$_{17}$H$_{18}$ClNO$_4$S
Molecular Weight: 367.84
cLogP= 2.46

Method: see 7.4.5 method. Product was eluted with petroleum ether – EtOAc 60:40 v/v.

Prepared from (*R/S*)-*N*-(4-chlorobenzyl)-3-hydroxy-2-phenylpropanamide (**6c**) (0.54 g, 1.86 mmoL). Product obtained as a white solid, yield: 0.48 g (70 %). TLC (petroleum ether-EtOAc 1:1 v/v), Rf = 0.73. M.p. 110-112 °C. ^{1}H NMR (DMSO-d_6): δ 8.84 (t, J = 5.9 Hz, 1H, N*H*), 7.37 (m, 4H, Ar), 7.33 (m, 3H, Ar), 7.19 (d, J = 8.5 Hz, 2H, Ar), 4.73 (t, J = 9.6 Hz, 1H, C*H*CHaHb), 4.37 (dd, J = 5.7, 9.5 Hz, 1H, CHC*H*aHb), 4.32 (dd, J = 6.1, 15.6 Hz, 1H, NHC*H*aHb), 4.24 (dd, J = 5.8, 15.5 Hz, 1H, NHCHa*Hb*), 4.02 (dd, J = 5.7, 9.7 Hz, 1H, CHCHa*Hb*), 3.15 (s, 3H, CH$_3$). ^{13}C NMR(DMSO-d_6): δ 170.3 (C, C=O), 138.6 (C, Ar), 136.1 (C, Ar), 131.8 (C, C-Cl), 129.9 (2 x CH, Ar), 129.4 (2 x CH, Ar), 128.8 (2 x CH, Ar), 128.5 (2 x CH, Ar), 128.2 (CH, Ar), 71.1 (*C*H$_2$OMs), 50.8 (*C*HCH$_2$OMs), 41.9 (NH*C*H$_2$), 37.0 (CH$_3$). Anal. Calcd for C$_{17}$H$_{18}$ClNO$_4$S•0.1H$_2$O (369.6486): C, 55.24%; H, 4.96%; N, 3.80%. Found: C, 54.89%; H, 5.12%; N, 3.84%.

(*R/S*)-3-((4-Chlorobenzyl)amino-2-(4-chlorophenyl)-3-oxopropyl (7d)
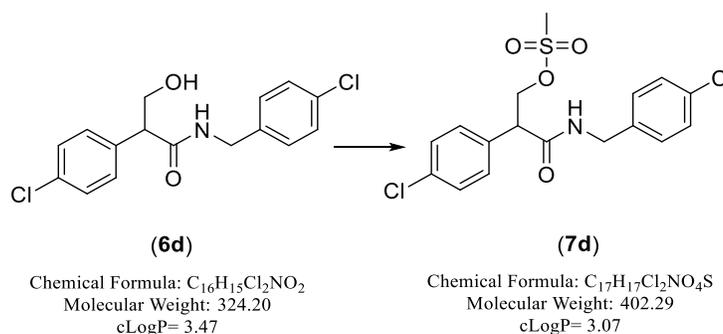
(6d)
Chemical Formula: $C_{16}H_{15}Cl_2NO_2$
Molecular Weight: 324.20
cLogP= 3.47

(7d)
Chemical Formula: $C_{17}H_{17}Cl_2NO_4S$
Molecular Weight: 402.29
cLogP= 3.07

Method: see 7.4.5 method. The crude product was purified by gradient column chromatography eluting with n-hexane-EtOAc 60: 40 v/v.

Prepared from (*R/S*)-*N*-(4-chlorobenzyl)-2-(4-chlorophenyl)-3-hydroxypropanamide (**6d**) (1.62 g, 5 mmoL). Product obtained as a brown solid, yield: 0.45 g (23 %). TLC (petroleum ether-EtOAc 2:1 v/v), R*f* = 0.27. M.p. 106-108 °C. ^{1}H NMR (DMSO-*d*$_6$): δ 8.83 (dd, *J* = 5.0, 10.0 Hz, 1H, N*H*), 7.43 (m, 4H, Ar), 7.34 (ddd, *J* = 2.5, 4.4, 9.1 Hz, 2H, Ar), 7.20 (d, *J* = 8.5 Hz, 2H, Ar), 4.70 (t, *J* = 9.5 Hz, 1H, C*H*CHaHb), 4.37 (dd, *J* = 6.0, 9.6 Hz, 1H, CHC*Ha*Hb), 4.32 (dd, *J* = 6.1, 15.4 Hz, 1H, NHC*Ha*Hb), 4.24 (dd, *J* = 5.8, 15.4 Hz, 1H, NHCHa*Hb*), 4.04 (dd, *J* = 6.0, 9.3 Hz, 1H, CHCHa*Hb*), 3.36 (s, 3H, C*H₃*). ^{13}C NMR(DMSO-*d*$_6$): δ 169.95 (C, C=O), 138.50 (C, Ar), 135.16 (C, Ar), 132.91 (C, *C*-Cl), 131.86 (C, *C*-Cl), 130.36 (2 x CH, Ar), 129.38 (2 x CH, Ar), 129.07 (2 x CH, Ar), 128.67 (2 x CH, Ar), 70.83 (CH*CH₂*OMs), 50.13 (*CH*CH₂OMs), 42.00 (NH*CH₂*), 37.04 (*CH₃*). Anal. Calcd for $C_{17}H_{17}Cl_2NO_4S$ (402.2916): C, 50.76%; H, 4.26%; N, 3.48%. Found: C, 51.09%; H, 4.27%; N, 3.74%.

(*R/S*)-3-((2,4-Dichlorobenzyl) amino)-3-oxo-2-phenylpropyl methanesulfonate (7e)

(6e)
Chemical Formula: $C_{16}H_{15}Cl_2NO_2$
Molecular Weight: 324.20
cLogP= 3.47

(7e)
Chemical Formula: $C_{17}H_{17}Cl_2NO_4S$
Molecular Weight: 402.29
cLogP= 3.02
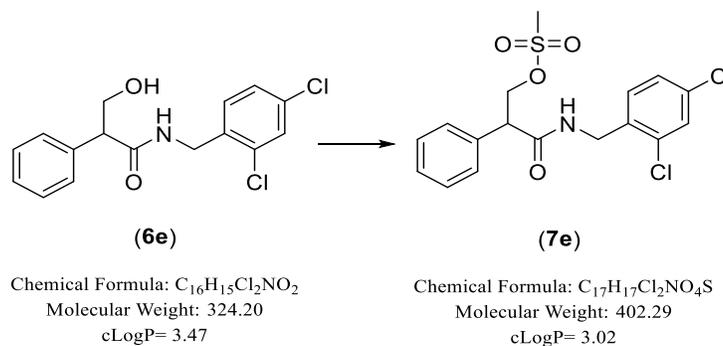
Method: see 7.4.5 method. Product was eluted with petroleum ether – EtOAc 70: 30 v/v.

Prepared from (*R/S*)-*N*-(2,4-dichlorobenzyl)-3-hydroxy-2-phenylpropanamide (**6e**) (1.62 g, 4.99 mmoL). Product obtained as a cream coloured solid, yield: 1.25 g (62 %). TLC (petroleum ether-EtOAc 1:1 v/v), R*f* = 0.75. M.p. 104-106 °C. ^{1}H NMR (DMSO-*d*$_6$): δ 8.83 (t, *J* = 5.7 Hz, 1H, N*H*), 7.59 (d, *J* = 2.1 Hz, 1H, Ar), 7.38 (m, 4H, Ar), 7.33 (m, 1H, Ar), 7.31 (dd, *J* = 2.1, 8.3 Hz, 1H, Ar), 7.20 (d, *J* = 8.4 Hz, 1H, Ar), 4.72 (t, *J* = 9.6 Hz, 1H, CHC*Ha*Hb), 4.38 (dd, *J* = 3.4, 5.6 Hz, 1H, CHCHa*Hb*), 4.35 (φt, *J* = 3.7, 5.9 Hz, 1H, NHC*Ha*Hb), 4.29 (dd, *J* = 5.7, 15.9 Hz, 1H, NHCHa*Hb*), 4.07 (dd, *J* = 5.6, 9.7 Hz, 1H, C*H*CHaHb), 3.15 (s, 3H, C*H$_3$*). ^{13}C NMR(DMSO-*d*$_6$): δ 170.47 (C, C=O), 136.01 (C, Ar), 135.65 (C, Ar), 133.51 (C, C-Cl), 132.77 (C, C-Cl), 130.45 (CH, Ar), 129.10 (3 x CH, Ar), 128.49 (2 x CH, Ar), 128.21 (CH, Ar), 127.59 (CH, Ar), 71.06 (CH*CH$_2$*OMs), 50.78 (*C*HCH$_2$OMs), 40.25 (NH*CH$_2$*), 37.05 (*C*H$_3$). Anal. Calcd for C$_{17}$H$_{17}$Cl$_2$NO$_4$S (402.2916): C, 50.76%; H, 4.26%; N, 3.48%. Found: C, 50.90%; H, 4.02%; N, 3.55%.

(*R/S*)-2-(4-Chlorophenyl)-3-((2,4-dichlorobenzyl)amino)-3-oxopropylmethane sulfonate (7f)
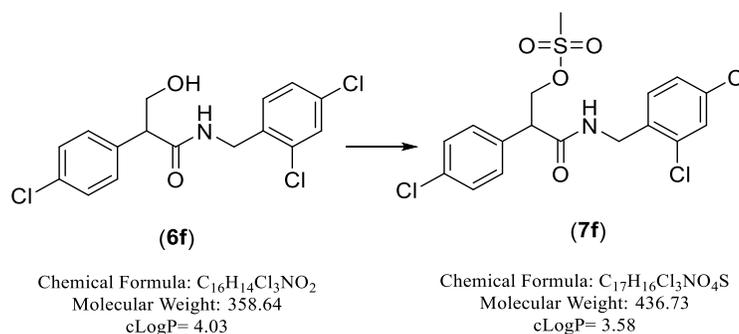
(**6f**)
Chemical Formula: C$_{16}$H$_{14}$Cl$_3$NO$_2$
Molecular Weight: 358.64
cLogP= 4.03

(**7f**)
Chemical Formula: C$_{17}$H$_{16}$Cl$_3$NO$_4$S
Molecular Weight: 436.73
cLogP= 3.58

Method: see 7.4.5 method. The crude product was purified by gradient column chromatography eluting with n-hexane-EtOAc 60: 40 v/v.

Prepared from (*R/S*)-2-(4-chlorophenyl)-*N*-(2,4-dichlorobenzyl)-3-hydroxypropanamide (**6f**) (0.6 g, 1.67 mmoL). Product obtained as a white solid, yield: 0.58 g (79 %). TLC (petroleum ether-EtOAc 2:1 v/v), R*f* = 0.83. M.p. 108-110 °C. ^{1}H NMR (DMSO-*d*$_6$): δ 8.84 (t, *J* = 5.8 Hz, 1H, N*H*), 7.60 (d, *J* = 2.1 Hz, 1H, Ar), 7.43 (dd, *J* = 8.7, 18.2 Hz, 1H, Ar), 7.33 (dd, *J* = 2.1, 8.3 Hz, 1H, Ar), 7.22 (d, *J* = 8.3 Hz, 1H, Ar), 4.68 (t, *J* = 9.5 Hz, 1H, CHC*Ha*Hb), 4.37 (dd, *J* = 3.4, 6.1 Hz, 1H, CHCHa*Hb*), 4.34 (φt, *J* = 3.5, 5.8 Hz, 1H, NHC*Ha*Hb), 4.29 (dd, *J* = 5.7, 15.8 Hz, 1H, NHCHa*Hb*), 4.08 (dd, *J* = 5.9, 9.4 Hz, 1H, C*H*CHaHb), 3.15 (s, 3H, C*H$_3$*). ^{13}C

NMR(DMSO-d_6): δ 170.10 (C, C=O), 135.53 (C, Ar), 135.00 (C, Ar), 133.55 (C, C-Cl), 132.94 (C, C-Cl), 132.84 (C, C-Cl), 130.56 (CH, Ar), 130.39 (2 x CH, Ar), 129.12 (CH, Ar), 129.07 (2 x CH, Ar), 127.65 (CH, Ar), 70.79 (CHCH_2OMs), 50.04 (*C*HCH$_2$OMs), 40.49 (NHCH_2), 37.03 (*C*H$_3$). HRMS (ESI), *m/z*. calcd for $C_{17}H_{17}Cl_3NO_4S$ ([M + H]$^+$), 434.9945; found, 437.9910. HPLC (Method A): 100%, R_t = 4.62 min.

(*R/S*)-3-((4-Methybenzyl) amino)-3-oxo-2-phenylpropyl methanesulfonate (7g)
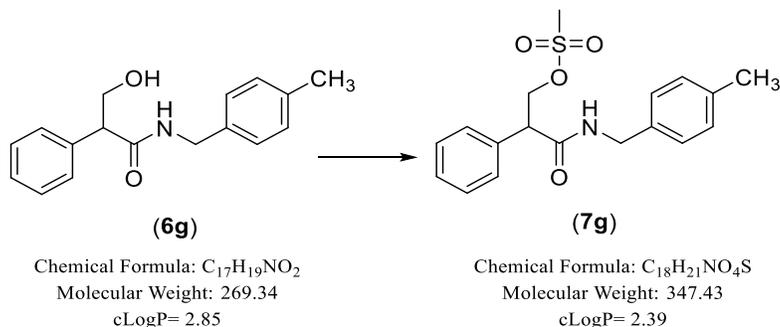
(6g)
Chemical Formula: $C_{17}H_{19}NO_2$
Molecular Weight: 269.34
cLogP= 2.85

(7g)
Chemical Formula: $C_{18}H_{21}NO_4S$
Molecular Weight: 347.43
cLogP= 2.39

Method: see 7.4.5 method. Product was eluted with petroleum ether – EtOAc 50: 50 v/v.

Prepared from (*R/S*)-3-hydroxy-*N*-(4-methylbenzyl)-2-phenylpropanamide) (**6g**) (1.30 g, 4.84 mmoL). Product obtained as an off-white solid, yield: 0.98 g (58 %). TLC (petroleum ether-EtOAc 1:1 v/v), R*f* = 0.64. M.p. 132-134 °C. ^{1}H NMR (DMSO-d_6): δ 8.80 (t, *J* = 5.7 Hz, 1H, N*H*), 7.35 (m, 5H, Ar), 7.06 (dd, *J* = 8.2, 13.7 Hz, 4H, Ar), 7.73 (t, *J* = 9.6 Hz, 1H, CHC*Ha*Hb), 4.35 (dd, *J* = 5.7, 9.5 Hz, 1H, CHCHa*Hb*), 4.27 (dd, *J* = 5.9, 15.1 Hz, 1H, NHC*Ha*Hb), 4.21 (dd, *J* = 5.8, 15.1 Hz, 1H, NHCHa*Hb*), 4.01 (dd, *J* = 5.6, 9.6 Hz, 1H, C*H*CHaHb), 3.14 (s, 3H, SO$_2$C*H$_3$*), 2.25 (s, 3H, C*H$_3$*). ^{13}C NMR (DMSO-d_6): δ 170.08 (C, C=O), 136.42 (C, Ar), 136.32 (2 x C, Ar), 129.24 (2 x CH, Ar), 129.05 (2 x CH, Ar), 128.45 (2 x CH, Ar), 128.11 (CH, Ar), 127.49 (2 x CH, Ar), 71.14 (CHCH_2OMs), 50.83 (*C*HCH$_2$OMs), 42.34 (NHCH_2), 37.02 (SO$_2$C*H$_3$*), 21.08 (OC*H$_3$*). Anal. Calcd for $C_{18}H_{21}NO_4S$ (347.4282): C, 62.23%; H, 6.09%; N, 4.03%. Found: C, 62.45%; H, 5.96%; N, 4.18%.

(*R/S*)-3-Oxo-2-phenyl-3-((4-(trifluoromethyl)benzyl)amino)propyl   methanesulfonate (7h)
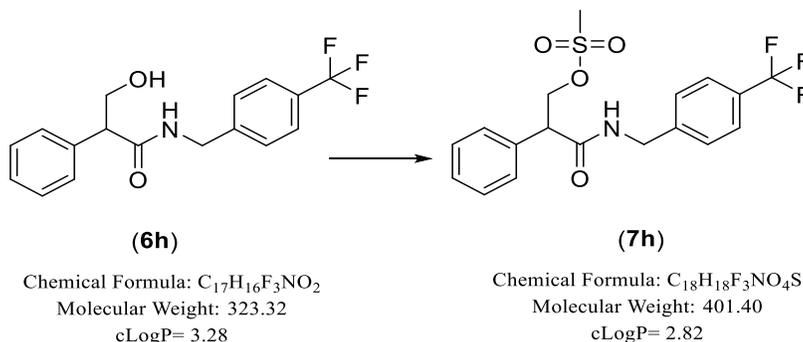
(**6h**)
Chemical Formula: $C_{17}H_{16}F_3NO_2$
Molecular Weight: 323.32
cLogP= 3.28

(**7h**)
Chemical Formula: $C_{18}H_{18}F_3NO_4S$
Molecular Weight: 401.40
cLogP= 2.82

Method: see 7.4.5 method. Product eluted with gradient petroleum ether – EtOAc 60: 40 v/v.

Prepared from (*R/S*)-3-hydroxy-2-phenyl-*N*-(4-trifluoromethy)benzyl)propanamide (**6h**) (0.43 g, 1.33 mmoL). Product obtained as a cream coloured solid, yield: 0.24 g (45 %). TLC (petroleum ether-EtOAc 1:1 v/v), R*f* = 0.60. M.p. 104-106 °C. ^{1}H NMR (DMSO-*d*$_6$): δ 8.88 (t, *J* = 6.0 Hz, 1H, N*H*), 7.62 (d, *J* = 8.2 Hz, 2H, Ar), 7.36 (m, 7H, Ar), 4.73 (t, *J* = 9.5 Hz, 1H, CHC*Ha*Hb), 4.38 (m, 3H, CHCHa*Hb* + NHC*HaHb*), 4.04 (dd, *J* = 5.7, 9.7 Hz, 1H, C*H*CHaHb), 3.15 (s, 3H, C*H₃*). ^{13}C NMR (DMSO-*d*$_6$): δ 170.45 (C, C=O), 144.51 (C, Ar), 136.20 (C, Ar), 129.11 (3 x CH, Ar), 128.46 (3 x CH, Ar), 128.20 (CH, Ar), 128.10 (2 x CH, Ar), 127.83 (C, Ar), 125.56 & 125.53 (CF₃), 71.08 (CH*CH₂*OMs), 50.87 (*C*HCH₂OMs), 42.24 (NH*CH₂*), 37.02 (*C*H₃). ^{19}F-NMR (DMSO-*d*$_6$): δ -60.83. Anal. Calcd for $C_{18}H_{18}F_3NO_4S$ (401.3997): C, 53.86%; H, 4.52%; N, 3.49%. Found: C, 53.83%; H, 4.65%; N, 3.39%. HRMS (ESI), *m/z*. calcd for $C_{18}H_{19}F_3NO_4S$ ([M + H]⁺), 402.1006; found: 402.0981, and calcd for $C_{18}H_{18}F_3NO_4SNa$ ([M + Na]⁺), 424.0828; found, 424.0801.

(*R/S*)-3-((4-Methoxybenzyl) amino)-3-oxo-2-phenylpropyl methanesulfonate (7i)
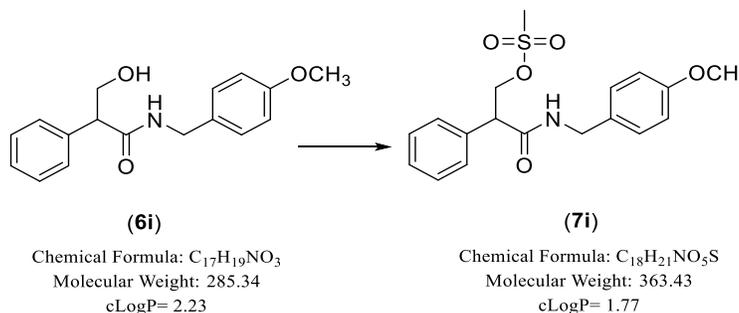
(**6i**)
Chemical Formula: $C_{17}H_{19}NO_3$
Molecular Weight: 285.34
cLogP= 2.23

(**7i**)
Chemical Formula: $C_{18}H_{21}NO_5S$
Molecular Weight: 363.43
cLogP= 1.77

Method: see 7.4.5 method. Product eluted with gradient petroleum ether –EtOAc 60: 40 v/v.

Prepared from (*R/S*)-3-hydroxy-*N*-(4-methoxybenzyl)-2-phenylpropanamide (**6i**) (1.33 g, 4.65 mmoL). Product obtained as a caramel coloured solid, yield: 0.73 g (43 %). TLC (petroleum ether-EtOAc 1:1 v/v), Rf = 0.538. M.p. 94-96 °C. ^{1}H NMR (DMSO-d_6): δ 8.68 (t, *J* = 5.7 Hz, 1H, N*H*), 7.37 (m, 4H, Ar), 7.33 (t, *J* = 6.9 Hz, 1H, Ar), 7.10 (d, *J* = 8.5 Hz, 2H, Ar), 6.83 (d, *J* = 8.5 Hz, 2H, Ar), 4.73 (t, *J* = 10.0 Hz, 1H, CHC*Ha*Hb), 4.35 (dd, *J* = 5.7, 9.5 Hz, 1H, CHCHa*Hb*), 4.26 (dd, *J* = 5.9, 14.9 Hz, 1H, NHC*Ha*Hb), 4.19 (dd, *J* = 5.7, 15.0 Hz, 1H, NHCHa*Hb*), 4.01 (dd, *J* = 5.7, 9.5 Hz, 1H, C*H*CHaHb), 3.72 (s, 3H, SO$_2$C*H$_3$*), 3.14 (s, 3H, C*H$_3$*). ^{13}C NMR (DMSO-d_6): δ 170.01 (C, C=O), 158.70 (C, *C*-OCH$_3$), 136.35 (C, Ar), 131.38 (C, Ar), 129.05 (2 x CH, Ar), 128.89 (2 x CH, Ar), 128.45 (2 x CH, Ar), 128.10 (CH, Ar), 114.13 (2 x CH, Ar), 71.17 (CH*C*H$_2$OMs), 55.52 (O*C*H$_3$), 50.82 (*C*HCH$_2$OMs), 49.07 (NH*C*H$_2$), 37.05 (SO$_2$*C*H$_3$). Anal. Calcd for C$_{18}$H$_{21}$NO$_5$S•0.1H$_2$O (365.2291): C, 59.20%; H, 5.85%; N, 3.84%. Found: C, 58.90%; H, 5.89%; N, 3.58%.

(*R/S*)-3-((3,4-Dimethoxybenzyl) amino)-3-oxo-2-phenylpropyl methanesulfonate (7j)
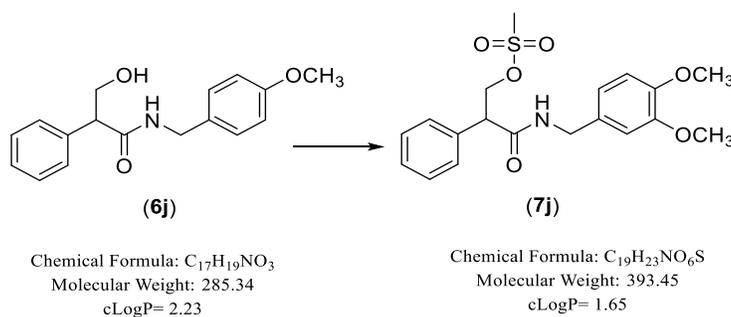
(**6j**)
Chemical Formula: C$_{17}$H$_{19}$NO$_3$
Molecular Weight: 285.34
cLogP= 2.23

(**7j**)
Chemical Formula: C$_{19}$H$_{23}$NO$_6$S
Molecular Weight: 393.45
cLogP= 1.65

Method: see 7.4.5 method. Product eluted with gradient petroleum ether – EtOAc 60: 40 v/v.

Prepared from (*R/S*)-*N*-(3,4-dimethoxybenzyl)-3-hydroxy-2-phenylpropanamide (**6j**) (0.99 g, 3.10 mmoL). Product obtained as a white solid, yield: 0.54 g (44 %). TLC (petroleum ether-EtOAc 1:1 v/v), Rf = 0.51. M.p. 114-116 °C. ^{1}H NMR (DMSO-d_6): δ 8.71 (t, *J* = 5.9 Hz, 1H, N*H*), 7.42 (d, *J* = 7.1 Hz, 2H, Ar), 7.37 (t, *J* = 7.4 Hz, 2H, Ar), 7.31 (t, *J* = 7.1 Hz, 1H, Ar), 6.83 (d, *J* = 8.0 Hz, 1H, Ar), 6.70 (d, *J* = 9.1 Hz, 2H, Ar), 4.75 (t, *J* = 9.6 Hz, 1H, CHC*Ha*Hb), 4.35 (dd, *J* = 5.6, 9.5 Hz, 1H, CHCHa*Hb*), 4.27 (dd, *J* = 6.1, 15.1 Hz, 1H, NHC*Ha*Hb), 4.15 (dd, *J* = 5.7, 15.0 Hz, 1H, NHCHa*Hb*), 4.02 (dd, *J* = 5.6, 9.6 Hz, 1H, C*H*CHaHb), 3.71 (s, 3H, OC*H$_3$*), 3.59 (s, 3H, OC*H$_3$*), 3.15 (s, 3H, SO$_2$C*H$_3$*). ^{13}C NMR (DMSO-d_6): δ 170.05 (C, C=O), 149.15

(C, *C*OCH₃), 148.19 (C, *C*OCH₃), 136.40 (C, Ar), 131.97 (C, Ar), 129.08 (2 x CH, Ar), 128.45 (2 x CH, Ar), 128.10 (CH, Ar), 119.53 (CH, Ar), 112.11 (CH, Ar), 111.11 (CH, Ar), 71.14 (CH*C*H₂OMs), 56.02 (O*C*H₃), 55.63 (O*C*H₃), 50.88 (*C*HCH₂OMs), 42.22 (NH*C*H₂), 37.02 (SO₂*C*H₃). HRMS (ESI), *m/z*. calcd for $C_{19}H_{23}NO_6SNa$ ([M + Na]⁺), 416.1144; found, 461,1138. HPLC (Method A): 92%, R_t= 4.10 min.

7.4.6 <u>General method for preparation of azoles and alkenes (8 and 9)</u>

Where R¹: a= 4-H **Where R²: a**= 4-H   **e**= 4-CH₃
        b= 4-Cl   **b**= 4-F   **f**= 4-CF₃
                          c= 4-Cl   **g**= 4-OCH₃
                          d= 2,4-di-Cl   **d**= 4-di-OCH₃
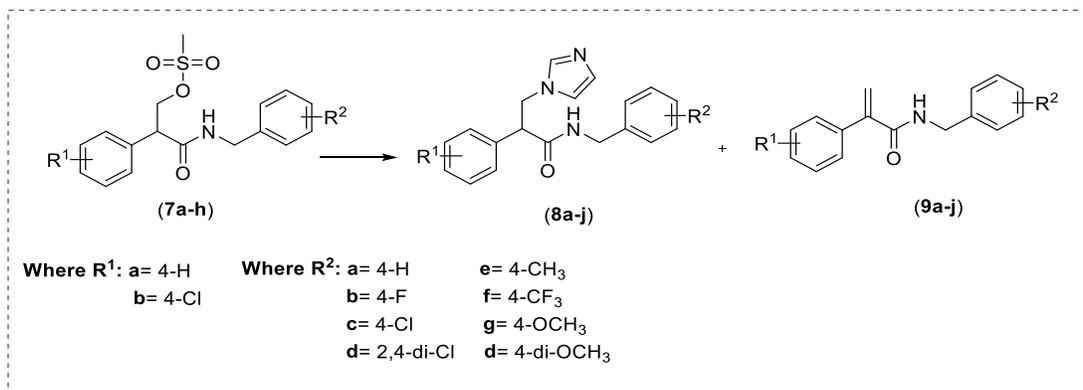
To a stirred solution of azole (imidazole or triazole or tetrazole) (4 eq) in dry CH₃CN (2 mL/mmol of azole) was added potassium carbonate (4 eq), and the mixture was heated for 1 h at 45 °C. After cooling to room temperature, mesylate (**7**) (1 eq) was added and the reaction was heated at 70 °C for 4 h then stirred at room temperature overnight. The solvent was evaporated under vacuum and the residue was extracted with EtOAc (35 mL/mmol of mesylate), washed with brine (3 x 35 mL/mmol of mesylate) and water (3 x 35 mL/mmol of mesylate). The organic layer was dried (MgSO₄) and evaporated under vacuum to give the crude product, which was purified by gradient column chromatography. Alkene (**9**) was eluted first with petroleum ether–EtOAc system, followed by the azole product (**8**) on changing the system to CH₂Cl₂-MeOH.

<u>*N*-Benzyl-2-phenylacrylamide (9a)</u>

(7a)
Chemical Formula: $C_{17}H_{19}NO_4S$
Molecular Weight: 333.40
cLogP= 1.9

(8a)
Chemical Formula: $C_{19}H_{19}N_3O$
Molecular Weight: 305.38
Log P: 2.2

(9a)
Chemical Formula: $C_{16}H_{15}NO$
Molecular Weight: 237.30
cLogP= 3.23
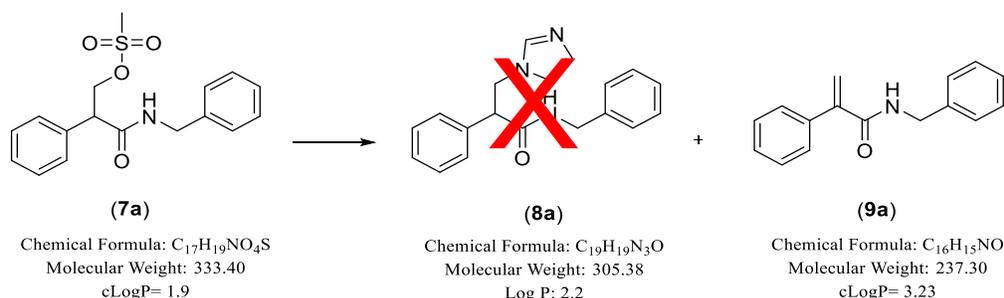
Prepared from (*R/S*)-3-(benzylamino)-3-oxo-2-phenylpropyl methanesulfonate (**7a**) (0.48 g, 1.44 mmol) and purified by gradient column chromatography eluting with petroleum ether–EtOAc 70:30 v/v. Product obtained as a white solid, yield: 0.27 g (62 %). TLC (petroleum ether-EtOAc 1:1 v/v), Rf = 0.78. M.p. 78-80 °C. ^{1}H NMR (DMSO-d_6): δ 8.74 (t, *J* = 5.9 Hz, 1H, N*H*), 7.43 (m, 2H, Ar), 7.35 (m, 7H, Ar), 7.26 (m, 1H, Ar), 5.79 (s, 1H, C=C*Ha*Hb), 5.68 (s, 1H, C=CHa*Hb*), 4.40 (d, *J* = 6.1 Hz, 2H, NHC*H₂*). ^{13}C NMR(DMSO-d_6): δ 168.70 (C, C=O), 145.65 (C, *C*=CH$_2$), 140.07 (C, Ar), 137.18 (C, Ar), 128.79 (2 x CH, Ar), 128.77 (2 x CH, Ar), 128.57 (CH, Ar), 127.61 (2 x CH, Ar), 127.52 (2 x CH, Ar), 127.21 (CH, Ar), 118.17 (C=*C*H$_2$), 42.81 (NH*C*H$_2$). HRMS (ESI), *m/z*. calcd for C$_{16}$H$_{16}$NO ([M + H]$^+$), 238.1257; found, 238.1226, and calcd for C$_{16}$H$_{15}$NONa ([M + Na]$^+$), 260.1077; found, 260.1046. HPLC (Method A): 100%, R$_t$ = 7.8 min.

(*R/S*)-*N*-(4-Fluorobenzyl)-3-(1*H*-imidazol-1-yl)-2-phenylpropanamide (8b) and *N*-(4-fluorobenzyl)-2-phenylacrylamide (9b)
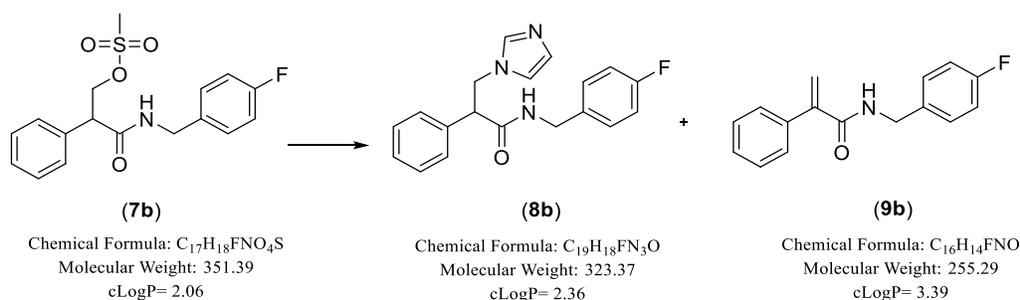
(7b)	**(8b)**	**(9b)**
Chemical Formula: C$_{17}$H$_{18}$FNO$_4$S	Chemical Formula: C$_{19}$H$_{18}$FN$_3$O	Chemical Formula: C$_{16}$H$_{14}$FNO
Molecular Weight: 351.39	Molecular Weight: 323.37	Molecular Weight: 255.29
cLogP= 2.06	cLogP= 2.36	cLogP= 3.39

Method: see 7.4.6 method but heated at 70 °C overnight. The crude product was purified by gradient column chromatography petroleum ether–EtOAc 70:30 v/v to elute (**9b**), then changed eluent to CH$_2$Cl$_2$-MeOH 90:10 v/v to elute (**8b**).

Prepared from (*R/S*)-3-((4-fluorobenzyl) amino)-3-oxo-2-phenylpropyl methanesulfonate (**7b**) (0.70 g, 1.98 mmoL). (*R/S*)-*N*-(4-Fluorobenzyl)-3-(1H-imidazol-1-yl)-2-phenylpropanamide (*8b, R^1= H, R^2= 4-F*) obtained as a cream coloured solid, yield: 0.22 g (34%). TLC (petroleum ether-EtOAc 1:1 v/v), Rf = 0.0. M.p. 100-102 °C. ^{1}H NMR (DMSO-d_6): δ 8.61 (t, *J* = 5.9 Hz, 1H, N*H*), 7.53 (brs, 1H, imid), 7.40 (d, *J* = 7.05 Hz, 2H, Ar), 7.34 (t, *J* = 7.4 Hz, 2H, Ar), 7.29 (t, *J* = 7.2 Hz, 1H, Ar), 7.11 (brs, 1H, imid), 7.03 (m, 4H, Ar), 6.88 (brs, 1H, imid), 4.63 (dd, *J* = 9.7, 13.4 Hz, 1H, CHC*Ha*Hb), 4.29 (dd, *J* = 6.4, 15.3 Hz, 1H, NHC*Ha*Hb), 4.24 (dd, *J* = 5.7,

13.4 Hz, CHCHa*Hb*), 4.10 (dd, *J* = 5.5, 15.2 Hz, NHCHa*Hb*), 4.02 (dd, *J* = 5.8, 9.6 Hz, C*H*CHaHb). ^{13}C NMR(DMSO-d_6): δ 171.06 (C, C=O), 162.52 and 160.60 (C,C-F), 137.94 (C, Ar), 135.63 (C, Ar), 130.15 (CH, imid), 130.09 (CH, imid), 129.38 (CH, Ar), 129.32 (CH, Ar), 128.93 (2 x CH, Ar), 128.27 (2 x CH, Ar), 127.86 (CH, Ar), 115.66 (CH, imid), 115.40 (CH, Ar), 115.23 (CH, Ar), 53.33 (*C*HCH$_2$imid), 48.88 (CH*CH$_2$*imid), 41.80 (NH*CH$_2$*). LRMS (ES, *m/z*): 324.1507 [C$_{19}$H$_{18}$FN$_3$O + H]$^+$. HRMS (ES+TOF), *m/z*. calcd for C$_{19}$H$_{19}$FN$_3$O ([M + H]$^+$), 324.1507; found, 324.1507. HPLC (Method B1): 98.0%, R$_t$ = 4.87 min. *N-(4-Fluorobenzyl)-2-phenylacrylamide (9b, R^1= H, R^2= 4-F)* obtained as a white fluffy solid, yield: 0.25 g (39 %). TLC (petroleum ether-EtOAc 1:1 v/v), R*f* = 0.79. M.p. 108-110 °C. ^{1}H NMR (DMSO-d_6): δ 8.74 (t, *J* = 5.4 Hz, 1H, N*H*), 7.43 (d, *J* = 7.7 Hz, 2H, Ar), 7.36 (m, 5H, Ar), 7.17 (t, *J* = 8.9 Hz, 2H, Ar), 5.79 (s, 1H, C=C*Ha*Hb), 5.69 (s, 1H, C=CHa*Hb*), 4.38 (d, *J* = 6.0 Hz, 2H, NHC*H$_2$*). ^{13}C NMR(DMSO-d_6): δ 168.68 (C, C=O), 162.60 and 160.67 (C, C-F), 145.60 (C, Ar), 137.16 (C, Ar), 136.27 (C, *C*=CH$_2$), 129.67 (CH, Ar), 129.61 (CH, Ar), 128.79 (2 x CH, Ar), 128.58 (CH, Ar), 127.53 (2 x CH, Ar), 118.29 (C=*CH$_2$*), 115.57 (CH, Ar), 115.40 (CH, Ar), 42.16 (NH*CH$_2$*). Anal. Calcd for C$_{16}$H$_{14}$FNO (255.2911): C, 75.28%; H, 5.53%; N, 5.48%. Found: C, 75.34%; H, 5.32%; N, 5.55%.

(*R/S*)-*N*-(4-Chlorobenzyl)-3(1*H*-imidazol-1-yl)-2-phenylpropanamide (8c)

(7c)
Chemical Formula: C$_{17}$H$_{18}$ClNO$_4$S
Molecular Weight: 367.84
cLogP= 2.46

(8c)
Chemical Formula: C$_{19}$H$_{18}$ClN$_3$O
Molecular Weight: 339.82
cLogp= 2.76

(9c)
Chemical Formula: C$_{16}$H$_{14}$ClNO
Molecular Weight: 271.74
cLogP= 3.79
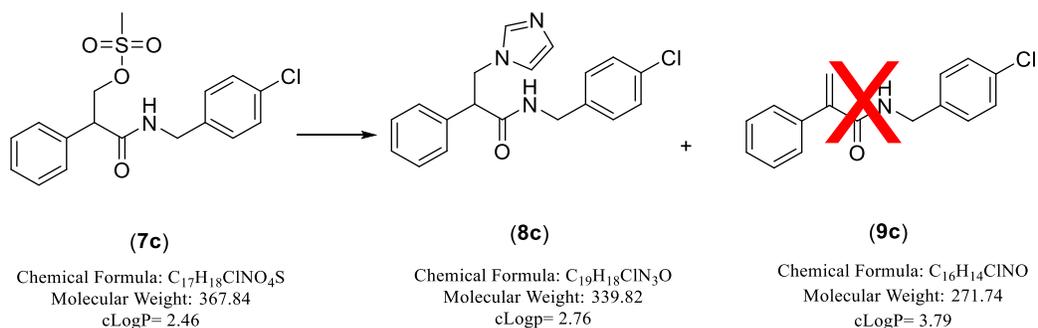
Method: see 7.4.6 method. Product purified by gradient column chromatography CH$_2$Cl$_2$-MeOH 90:10 v/v to elute (**8c**).

Prepared from (*R/S*)-3-((4-chlorobenzyl)amino)-3-oxo-2-phenylpropyl methanesulfonate (**7c**) (0.38 g, 1.0 mmoL). Product obtained as a cream coloured solid, yield: 0.20 g (56 %). TLC (petroleum ether-EtOAc 1:1 v/v), R*f* = 0.0. M.p. 136-138 °C. ^{1}H NMR (DMSO-d_6): δ 8.67 (t, *J* = 5.8 Hz, 1H, NH), 7.52 (s, 1H, imid), 7.40 (m, 2H, Ar), 7.35 (m, 2H, Ar), 7.29 (m, 3H, Ar),

7.11 (s, 1H, imid), 6.96 (d, J = 8.2 Hz, 2H, Ar), 6.88 (s, 1H, imid), 4.63 (dd, J = 9.9, 13.3 Hz, 1H, CHC*Ha*Hb), 4.30 (dd, J = 6.4, 15.5 Hz, 1H, NHC*Ha*Hb), 4.23 (dd, J = 5.6, 13.4 Hz, CHCHa*Hb*), 4.10 (dd, J = 5.4, 15.5 Hz, NHCHa*Hb*), 4.03 (dd, J = 5.7, 9.7 Hz, C*H*CHaHb). ^{13}C NMR(DMSO-d_6): δ 171.2 (C, C=O), 138.5 (C, Ar), 137.9 (C, Ar), 131.7 (C, C-Cl), 129.2 (3 x CH, Ar (2) and imid (1)), 129.0 (2 x CH, Ar), 128.6 (3 x CH, Ar (2) and imid (1)), 128.3 (2 x CH, Ar), 127.9 (CH, Ar), 120.0 (CH, imid), 53.3 (*CH*CH$_2$imid), 50.8 (CHC*H$_2$*imid), 41.8 (NHC*H$_2$*). Anal. Calcd for C$_{19}$H$_{18}$ClN$_3$O•0.1H$_2$O (341.6215): C, 66.80%; H, 5.37%; N, 12.30%. Found: C, 66.44%; H, 5.07%; N, 12.39%. HPLC (Method B2): 99.0%, R$_t$ = 4.94 min.

(*R/S*)-*N*-(4-Chlorobenzyl)-2-(4-chlorophenyl)-3(1*H*-imidazol-1-yl)propanamide (8d) and *N*-(4-chlorobenzyl)-2-(4-chlorophenyl)acrylamide (9d)
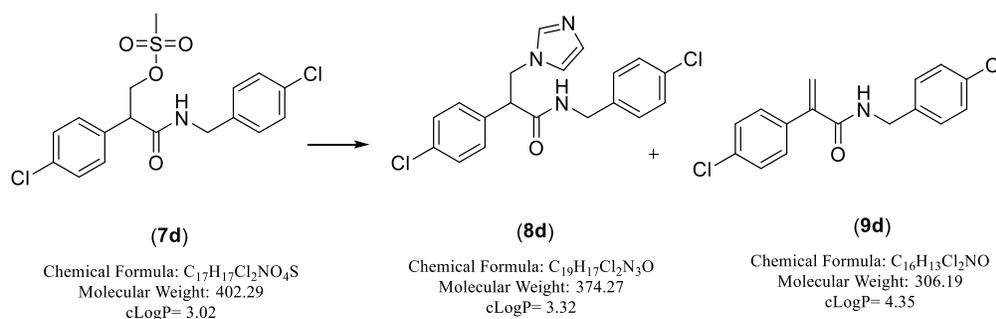
(7d)
Chemical Formula: C$_{17}$H$_{17}$Cl$_2$NO$_4$S
Molecular Weight: 402.29
cLogP= 3.02

(8d)
Chemical Formula: C$_{19}$H$_{17}$Cl$_2$N$_3$O
Molecular Weight: 374.27
cLogP= 3.32

(9d)
Chemical Formula: C$_{16}$H$_{13}$Cl$_2$NO
Molecular Weight: 306.19
cLogP= 4.35

Method: see 7.4.6 method but heated at 70 °C overnight. The crude product was purified by gradient column chromatography petroleum ether–EtOAc 70:30 v/v to elute (**9d**), then changed eluent to CH$_2$Cl$_2$-MeOH 90:10 v/v to elute (**8d**), which recrystalised the product (**8d**) from CH$_3$CN.

Prepared from (*R/S*)-3-((4-chlorobenzyl)amino)-2-(4-chlorophenyl)-3-oxopropyl methanesulfonate (**7d**) (0.44 g, 1.09 mmoL). (*R/S*)-*N*-(4-Chlorobenzyl)-2-(4-chlorophenyl)-3(1H-imidazol-1-yl)propanamide (8d, R^1= Cl, R^2= 4-Cl) obtained as a brown solid, yield: 0.11 g (26 %). TLC (petroleum ether-EtOAc 2:1 v/v), Rf = 0.0. M.p. 160-162 °C. ^{1}H NMR (DMSO-d_6): δ 8.66 (t, J = 5.9 Hz, 1H, N*H*), 7.50 (s, 1H, imid.), 7.40 (m, 4H, Ar), 7.29 (d, J = 8.5 Hz, 2H, Ar), 7.09 (s, 1H, imid.), 6.98 (d, J = 8.5 Hz, 2H, Ar), 6.86 (s, 1H, imid.), 4.59 (dd, J = 9.4, 13.5 Hz, 1H, CHC*Ha*Hb), 4.29 (dd, J = 6.4, 15.4 Hz, 1H, NHC*Ha*Hb), 4.24 (dd, J = 6.1, 13.5 Hz, 1H, CHCHa*Hb*), 4.10 (dd, J = 5.4, 15.5 Hz, 1H, NHCHa*Hb*), 4.05 (dd, J = 6.1, 9.4 Hz, 1H, C*H*CHaHb). ^{13}C NMR(DMSO-d_6): δ 170.78 (C, C=O), 138.41 (C, Ar), 138.06 (CH, imid),

136.78 (C, Ar), 132.59 (C, C-Cl), 131.75 (C, C-Cl), 130.16 (2 x CH, Ar), 129.23 (2 x CH, Ar), 128.92 (2 x CH, Ar), 128.68 (CH, imid), 128.57 (2 x CH, Ar), 119.95 (CH, imid), 52.59 (C*H*CH$_2$-imid), 48.66 (CHC*H$_2$*imid), 41.85 (NHC*H$_2$*). Anal Calcd for C$_{19}$H$_{17}$Cl$_2$N$_3$O (374.2688): C, 60.97%; H, 4.58%; N, 11.22%. Found: C, 60.99%; H, 4.50%; N, 11.20%. HPLC (Method B1): 96.3%, R$_t$ = 2.53 min. *N-(4-Chlorobenzyl)-2-(4-chlorophenyl)acrylamide (9d, R^1= Cl, R^2= 4-Cl)* obtained as an off-white solid, yield: 0.09 g (22 %). TLC (Petroleum ether-EtOAc 1:1 v/v), R*f* = 0.73. M.p. 108-110 °C. ^{1}H NMR (DMSO-*d$_6$*): δ 8.80 (t, *J* = 5.9 Hz, 1H, N*H*), 7.45 (m, 4H, Ar), 7.41 (d, *J* = 8.5 Hz, 2H, Ar), 7.33 (d, *J* = 8.5 Hz, 2H, Ar), 5.84 (s, 1H, C=C*Ha*Hb), 5.76 (s, 1H, C=CHa*Hb*), 4.37 (d, *J* = 6.1 Hz, 2H, NHC*H$_2$*). ^{13}C NMR(DMSO-*d$_6$*): δ 168.27 (C, C=O), 144.20 (C, *C*=CH$_2$), 139.02 (C, Ar), 135.98 (C, *C*-Cl), 133.27 (C, *C*-Cl), 131.80 (C, Ar), 129.55 (2 x CH, Ar), 129.46 (2 x CH, Ar), 128.80 (2 x CH, Ar), 128.74 (2 x CH, Ar), 119.40 (C=*C*H$_2$), 42.26 (NHC*H$_2$*). Anal. Calcd for C$_{16}$H$_{13}$Cl$_2$NO (306.1908): C, 62.76%; H, 4.28%; N, 4.57%. Found: C, 63.07%; H, 4.30%; N, 4.61%.

(*R/S*)-*N*-(2,4-Dichlorobenzyl)-3-(1*H*-imidazol-1-yl)-2-phenylpropanamide (8e) and *N*-(2,4-dichlorobenzyl)-2-phenylacrylamide (9e)
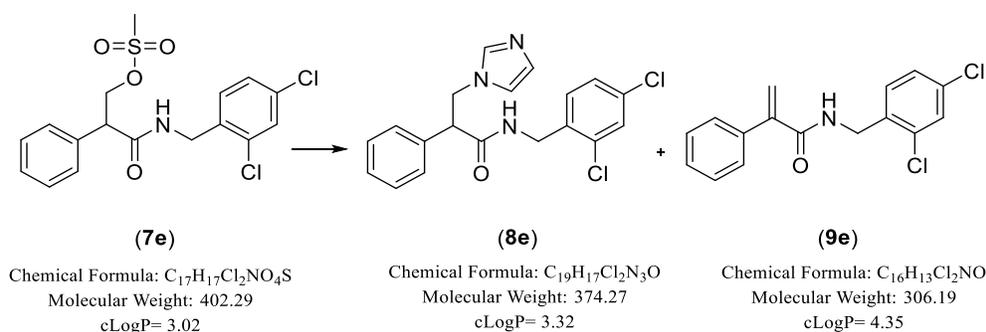
(7e)	(8e)	(9e)
Chemical Formula: C$_{17}$H$_{17}$Cl$_2$NO$_4$S	Chemical Formula: C$_{19}$H$_{17}$Cl$_2$N$_3$O	Chemical Formula: C$_{16}$H$_{13}$Cl$_2$NO
Molecular Weight: 402.29	Molecular Weight: 374.27	Molecular Weight: 306.19
cLogP= 3.02	cLogP= 3.32	cLogP= 4.35

Method: see 7.4.6 method but heated at 70 °C for overnight. The crude product was purified by gradient column chromatography petroleum ether–EtOAc 80:20 v/v to elute (**9e**), then changed eluent to CH$_2$Cl$_2$-MeOH 90:10 v/v to elute (**8e**).

Prepared from (*R/S*)-3-((2,4-dichlorobenzyl)amino)-3-oxo-2-phenylpropyl methanesulfonate (**7e**) (0.5 g, 1.24 mmoL). *(R/S)-N-(2,4-Dichlorobenzyl)-3-(1H-imidazol-1-yl)-2-phenylpropanamide (8e, R^1= H, R^2= 2, 4-di-Cl)* obtained as a cream coloured solid, yield: 0.34 g (74 %). TLC (petroleum ether-EtOAc 1:1 v/v), R*f* = 0.0. M.p. 55-57 °C. ^{1}H NMR (DMSO-*d$_6$*): δ 8.68 (t, *J* = 5.8 Hz, 1H, N*H*), 7.56 (d, *J* = 2.1 Hz, 1H, Ar), 7.54 (brs, 1H, imid), 7.41 (d,

J = 7.2 Hz, 2H, Ar), 7.36 (t, *J* = 7.4 Hz, 2H, Ar), 7.30 (t, *J* = 7.2 Hz, 1H, Ar), 7.23 (dd, *J* = 2.1, 8.4 Hz, 1H, Ar), 7.13 (brs, 1H, imid), 6.90 (brs, 1H, imid), 6.75 (d, *J* = 8.4 Hz, 1H, Ar), 4.63 (dd, *J* = 9.8, 13.4 Hz, 1H, CHC*Ha*Hb), 4.31 (dd, *J* = 6.2, 16.0 Hz, 1H, NHC*Ha*Hb), 4.23 (dd, *J* = 5.7, 13.4 Hz, 1H, CHCHa*Hb*), 4.16 (dd, *J* = 5.4, 16.0 Hz, 1H, NHCHa*Hb*), 4.10 (dd, *J* = 5.7, 9.8 Hz, 1H, C*H*CHaHb). ^{13}C NMR(DMSO-d_6): δ 171.32 (C, C=O), 137.72 (C, Ar), 135.52 (C, Ar), 133.34 (C, C-Cl), 132.63 (C, C-Cl), 130.12 (2 x CH, Ar (1) and imid (1)), 128.97 (3 x CH, Ar), 128.30 (2 x CH, Ar), 127.94 (2 x CH, Ar (1) and imid (1)), 127.51 (2 x CH, Ar (1) and imid (1)), 53.21 (*C*HCH2imid), 48.86 (CH*C*H2imid), 40.01 (NHC*H*2). Anal. Calcd for $C_{19}H_{17}Cl_2N_3O \cdot 0.2H_2O$ (377.87184): C, 60.39%; H, 4.64%; N, 11.12%. Found: C, 60.04%; H, 4.46%; N, 10.85%. HPLC (Method B1): 96.20%, R_t = 3.20 min. *N-(2,4-Dichlorobenzyl)-2-phenylacrylamide (9e, R^1= H, R^2= 2, 4-di-Cl)* obtained as a cream coloured solid, yield: 0.05 g (11 %). TLC (petroleum ether-EtOAc 1:1 v/v), R*f* = 0.85. M.p. 66-68 °C. ^{1}H NMR (DMSO-d_6): δ 8.76 (t, *J* = 5.8 Hz, 1H, N*H*), 7.63 (d, *J* = 2.1 Hz, 1H, Ar), 7.47 (m, 3H, Ar), 7.34 (m, 5H, Ar), 5.83 (s, 1H, C=C*Ha*Hb), 5.75 (s, 1H, C=CHa*Hb*), 4.44 (d, *J* = 5.9 Hz, 2H, NHC*H*2). ^{13}C NMR(DMSO-d_6): δ 168.87 (C, C=O), 145.33 (C, *C*=CH2), 137.04 (C, Ar), 136.02 (C, C-Cl), 133.41 (C, C-Cl), 132.67 (C, Ar), 130.58 (CH, Ar), 129.06 (CH, Ar), 128.82 (2 x CH, Ar), 128.63 (CH, Ar), 127.85 (CH, Ar), 127.58 (2 x CH, Ar), 118.73 (C=*C*H2), 40.01 (NHC*H*2). LRMS (ESI, *m/z*): 308.0417 $[C_{16}H_{13}{}^{37}Cl_2NO + H]^+$, 306.0447 $[C_{16}H_{13}{}^{35}Cl_2NO + H]^+$, 158.98 $[C_7H_5{}^{35}Cl_2]^+$. HRMS (ES,TOF), *m/z*. calcd for $C_{16}H_{14}{}^{35}Cl_2NO$ ($[M + H]^+$), 306.0447; found, 306.0449; and calcd for $C_{16}H_{14}{}^{37}Cl_2NO$ ($[M + H]^+$), 308.0417; found, 308.0418.

(*R/S*)-2-(4-Chlorophenyl)-*N*-(2,4-dichlorobenzyl)-3-(1*H*-imidazol-1-yl)propanamide (8f) and 2-(4-chlorophenyl)-*N*-(2,4-dichlorobenzyl)acrylamide (9f)

(7f)
Chemical Formula: $C_{17}H_{16}Cl_3NO_4S$
Molecular Weight: 436.73
cLogP= 3.58

(8f)
Chemical Formula: $C_{19}H_{16}Cl_3N_3O$
Molecular Weight: 408.71
cLogP= 3.88

(9f)
Chemical Formula: $C_{16}H_{12}Cl_3NO$
Molecular Weight: 340.63
cLogP= 4.91
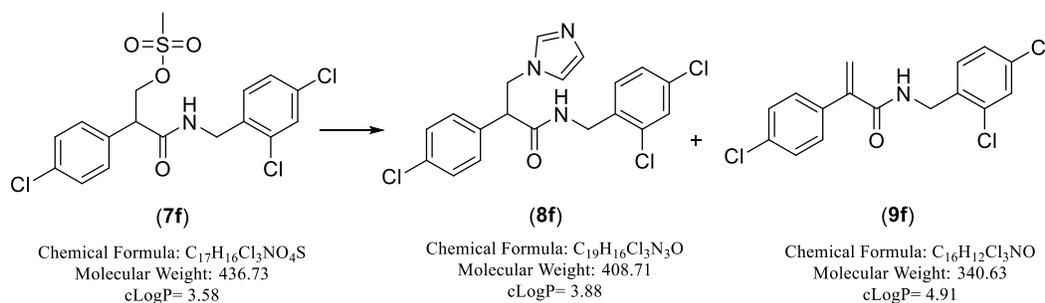
Method: see 7.4.6 method but heated at 70 °C for 30 minutes then stirred at rt for overnight. The crude product was purified by gradient column chromatography petroleum ether–EtOAc

70:30 which increased to 60:40 v/v to elute (**9f**), then changed eluent to CH_2Cl_2-MeOH 90:10 v/v to elute (**8f**).

Prepared from (*R/S*)-2-(4-chlorophenyl)-3-((2,4-dichlorobenzyl)amino)-3-oxopropyl methanesulfonate (**7f**) (0.54 g, 1.24 mmoL). *(R/S)-2-(4-Chlorophenyl)-N-(2,4-dichlorobenzyl)-3-(1H-imidazol-1-yl)propanamide (8f, R^1= Cl, R^2= 2,4-di-Cl)* obtained as a white solid, yield: 0.21 g (41%). TLC (petroleum ether-EtOAc 1:1 v/v), R*f* = 0.0. M.p. 148-150 °C. ^{1}H NMR (DMSO-*d*$_6$): δ 8.69 (t, *J* = 5.7 Hz, 1H, N*H*), 7.56 (d, *J* = 2.2 Hz, 1H, Ar), 7.50 (brs, 1H, imid), 7.41 (m, 4H, Ar), 7.26 (dd, *J* = 2.1, 8.3 Hz, 1H, Ar), 7.10 (brs, 1H, imid), 6.88 (brs, 1H, imid), 6.79 (d, *J* = 8.4 Hz, 1H, Ar), 4.58 (dd, *J* = 9.5, 13.4 Hz, 1H, CHC*Ha*Hb), 4.30 (dd, *J* = 6.1, 15.9 Hz, 1H, NHC*Ha*Hb), 4.23 (dd, *J* = 6.0, 13.5 Hz, 1H, CHCHa*Hb*), 4.16 (dd, *J* = 5.5, 15.9 Hz, 1H, NHCHa*Hb*), 4.10 (dd, *J* = 6.0, 9.5 Hz, 1H, C*H*CHaHb). ^{13}C NMR(DMSO-*d*$_6$): δ 170.96 (C, C=O), 138.02 (CH, imid), 136.64 (C, Ar), 135.41 (C, Ar), 133.40 (C, C-Cl), 132,69 (C, C-Cl), 132.63 (C, C-Cl), 130.24 (CH, Ar), 130.19 (2 x CH, Ar), 129.00 (CH, Ar), 128.94 (2 x CH, Ar), 128.74 (CH, imid), 127.57 (CH, Ar), 119.92 (CH, imid), 52.47 (*C*HCH$_2$), 48.68 (CH*C*H$_2$), 40.58 (NH*C*H$_2$). HRMS (ESI), *m/z*. calcd for $C_{19}H_{17}Cl_3N_3O$ ([M + H]$^+$), 408.0438; found, 408.0432. HPLC (Method B2): 99.6%, R$_t$ = 4.56 min. *2-(4-Chlorophenyl)-N-(2,4-dichlorobenzyl)acrylamide (9f, R^1= Cl, R^2= 2,4-di-Cl)* obtained as a white solid, yield: 0.19 g (37 %). TLC (petroleum ether-EtOAc 1:1 v/v), R*f* = 0.87. M.p. 104-106 °C. ^{1}H NMR (DMSO-*d*$_6$): δ 8.81 (t, *J* = 5.8 Hz, 1H, N*H*), 7.62 (d, *J* = 2.1 Hz, 1H, Ar), 7.46 (dd, *J* = 8.9, 16.3 Hz, 5H, Ar), 7.39 (d, *J* = 8.3 Hz, 1H, Ar), 5.88 (s, 1H, C=C*Ha*Hb), 5.80 (s, 1H, C=CHa*Hb*), 4.43 (d, *J* = 5.9 Hz, 2H, NHC*H$_2$*). ^{13}C NMR(DMSO-*d*$_6$): δ 168.43 (C, C=O), 143.97 (C, *C*=CH$_2$), 135.91 (C, Ar), 135.88 (C, *C*-Cl), 133.41 (C, *C*-Cl), 133.30 (C, *C*-Cl), 132.69 (C, Ar), 130.60 (CH, Ar), 129.49 (2 x CH, Ar), 129.07 (CH, Ar), 128.81 (2 x CH, Ar), 127.86 (CH, Ar), 119.69 (C=*C*H$_2$), 40.49 (NH*C*H$_2$). HRMS (ESI), *m/z*. calcd for $C_{16}H_{12}Cl_3NONa$ ([M + Na]$^+$), 361.9882; found, 361.9880. HPLC (Method A): 99%, R$_t$ = 4.71 min.

(*R/S*)-3-(1*H*-Imidazol-1-yl)-*N*-(4-methylbenzyl)-2-phenylpropanamide (8g) and *N*-(4-methylbenzyl)-2-phenylacrylamide (9g)

(7g)

Chemical Formula: $C_{18}H_{21}NO_4S$
Molecular Weight: 347.43
cLogP= 2.39

(8g)

Chemical Formula: $C_{20}H_{21}N_3O$
Molecular Weight: 319.41
cLogP= 2.69

(9g)

Chemical Formula: $C_{17}H_{17}NO$
Molecular Weight: 251.33
cLogP= 3.72
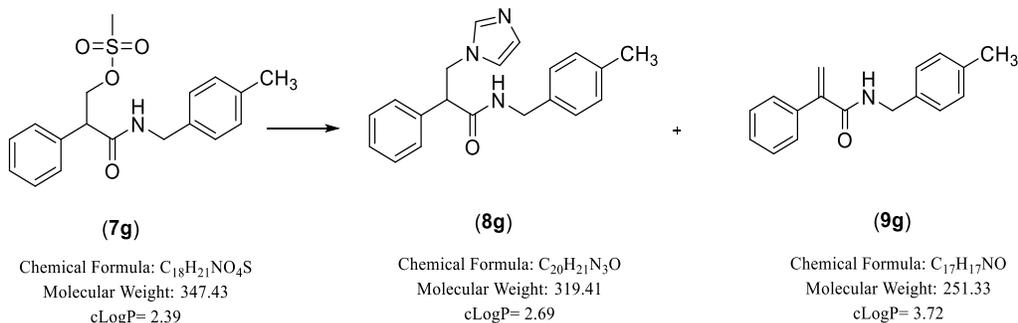
Method: see 7.4.6 method but heated at 70 °C for 2 h then stirred at room temperature overnight. The crude product was purified by gradient column chromatography petroleum ether–EtOAc 70:30 v/v to elute (**9g**), then changed eluent to CH_2Cl_2-MeOH 90:10 v/v to elute (**8g**).

Prepared from (*R/S*)-3-((4-methylbenzyl)amino)-3-oxo-2-phenylpropyl methanesulfonate (**7g**) (0.7 g, 2.0 mmoL). *(R/S)-3-(1H-Imidazol-1-yl)-N-(4-methylbenzyl)-2-phenylpropanamide (8g, R^1= H, R^2= 4-CH₃)* obtained as a cream coloured solid, yield: 0.03 g (5 %). TLC (petroleum ether-EtOAc 1:1 v/v), R*f* = 0.0. M.p. 134-136 °C. ¹H NMR (Acetone- d_6): δ 7.72 (brs, 1H, N*H*), 7.52 (brs, 1H, imid.), 7.44 (d, *J* = 7.0 Hz, 2H, Ar), 7.32 (m, 3H, Ar), 7.11 (brs, 1H, imid.), 7.04 (d, *J* = 7.9 Hz, 2H, Ar), 6.95 (d, *J* = 8.0 Hz, 2H, Ar), 6.91 (brs, 1H, imid.), 4.76 (dd, *J* = 9.3, 13.6 Hz, 1H, CHC*Ha*Hb), 4.37 (dd, *J* = 6.2, 14.8 Hz, 1H, NHC*Ha*Hb), 4.28 (dd, *J* = 5.7, 13.6 Hz, 1H, CHCHa*Hb*), 4.23 (dd, *J* = 5.6, 15.0 Hz, 1H, NHCHa*Hb*), 4.09 (dd, *J* = 5.7, 9.3 Hz, 1H, C*H*CHaHb), 2.27 (s, 3H, C*H₃*). ¹³C NMR (Acetone- d_6): δ 170.50 (C, C=O), 137.77 (C, Ar), 136.18 (C, Ar), 136.01 (C, Ar), 128.80 (2 x CH, Ar), 128.55 (3 x CH, Ar (2) and imid (1)), 128.39 (CH, imid), 127.98 (3 x CH, Ar (2) and imid (1)), 127.48 (2 x CH, Ar), 127.18 (2 x CH, Ar), 54.00 (C*H*CH₂imid), 49.20 (CHC*H₂*imid), 42.24 (NHC*H₂*) 20.10 (C*H₃*). HRMS (ESI), *m/z*. calcd for $C_{20}H_{22}N_3O$ ([M + H]⁺), 320.1786; found, 320.1757. HPLC (Method B1): 95.5%, R_t = 2.49 min. *N-(4-Methylbenzyl)-2-phenylacrylamide (9g, R^1= H, R^2= 4-CH₃)* obtained as an off-white solid, yield: 0.38 g (59 %). TLC (petroleum ether-EtOAc 1:1 v/v), R*f* = 0.78. M.p. 92-94 °C. ¹H NMR (DMSO-d_6): δ 8.69 (t, *J* = 6.0 Hz, 1H, N*H*), 7.43 (m, 2H, Ar), 7.35 (m, 3H, Ar), 7.20 (d, *J* = 8.0 Hz, 2H, Ar), 7.15 (d, *J* = 7.9 Hz, 2H, Ar), 5.78 (s, 1H, C=C*Ha*Hb), 5.66 (s, 1H, C=CHa*Hb*), 4.35 (d, *J* = 6.1 Hz, 2H, NHC*H₂*), 2.29 (s, 3H, C*H₃*). ¹³C NMR(DMSO-d_6): δ 168.63

(C, C=O), 145.68 (C, *C*=CH₂), 137.19 (C, Ar), 137.04 (C, Ar), 136.23 (C, Ar), 129.31 (2 x CH, Ar),128.78 (2 x CH, Ar), 128.55 (CH, Ar), 127.63 (2 x CH, Ar), 127.50 (2 x CH, Ar), 118.06 (C=*C*H₂), 42.54 (NH*C*H₂), 21.14 (*C*H₃). Anal. Calcd for $C_{17}H_{17}NO$ (251.3274): C, 81.24%; H, 6.82%; N, 5.57%. Found: C, 81.35%; H, 7.06%; N, 5.53%.

(*R/S*)-3-(1*H*-Imidazol-1-yl)-2-phenyl-*N*-(4-(trifluoromethyl)benzyl)propanamide   (8h) and 2-phenyl-*N*-(4-(trifluoromethyl)benzyl)acrylamide (9h)

(7h)

Chemical Formula: $C_{18}H_{18}F_3NO_4S$
Molecular Weight: 401.40
cLogP= 2.82

(8h)

Chemical Formula: $C_{20}H_{18}F_3N_3O$
Molecular Weight: 373.38
cLogP= 3.12

(9h)

Chemical Formula: $C_{17}H_{14}F_3NO$
Molecular Weight: 305.30
cLogP= 4.15
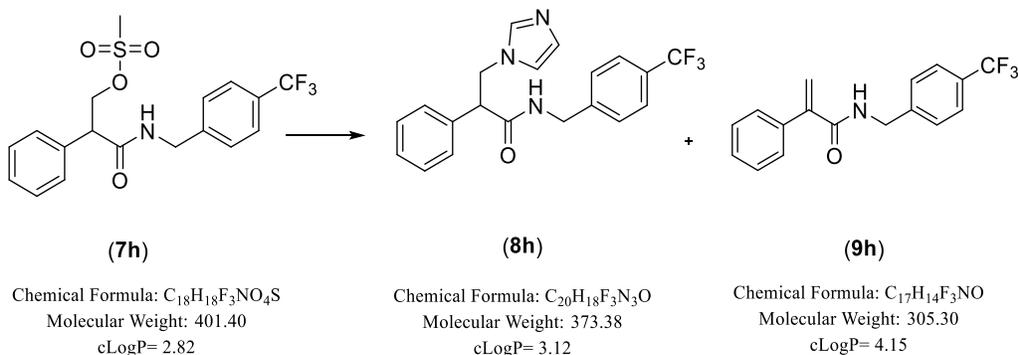
Method: see 7.4.6 method but heated at 70 °C for 1 h then stirred at room temperature overnight. The crude product was purified by gradient column chromatography petroleum ether – EtOAc 70:30 v/v to elute (**9h**), then changed eluent to CH_2Cl_2-MeOH 90:10 v/v to elute (**8h**).

Prepared   from   (*R/S*)-3-oxo-2-phenyl-3-((4-(trifluoromethyl)benzyl)amino)propyl methanesulfonate (**7h**) (0.58 g, 1.44 mmoL). (*R/S*)-3-(1H-Imidazol-1-yl)-2-phenyl-N-(4-(trifluoromethyl)benzyl)propanamide (*8h, R^1= H, R^2= 4-CF₃*) obtained as a semi-solid brown coloured, yield: 0.02 g (4 %). TLC (petroleum ether-EtOAc 1:1 v/v), R*f* = 0.0. ^{1}H NMR (Acetone- d_6): δ 7.87 (brs, 1H, N*H*), 7.50 (m, 4H, Ar (3) and imid. (1)), 7.33 (m, 2H, Ar (1) and imid. (1)), 7.21 (m, 4H, Ar (3) and imid. (1)), 7.11 (m, 2H, Ar), 4.67 (dd, *J* = 9.8, 12.8 Hz, 1H, CHC*Ha*Hb), 4.38 (dd, *J* = 6.2, 15.6 Hz, 1H, NHC*Ha*Hb), 4.22 (d, *J* = 5.3 Hz, 1H, CHCHa*Hb*), 4.20 (t, *J* = 5.2 Hz, 1H, NHCHa*Hb*), 4.05 (dd, *J* = 5.3, 8.9 Hz, 1H, C*H*CHaHb). ^{13}C NMR(Acetone-d_6): δ 170.85 (C, C=O), 143.94 (C, Ar), 137.47 (C, Ar), 128.64 (3 x CH, Ar), 128.31 (CH, imid), 128.28 (C, Ar), 128.25 (CH, imid), 127.99 (3 x CH, Ar), 127.63 (CH, Ar), 127.60 (2 X CH, Ar), 127.49 (CH, imid), 125.07 & 125.04 (CF₃), 53.82 (*C*HCH₂imid), 49.89 (CH*C*H₂imid), 42.03 (NH*C*H₂). ^{19}F-NMR (DMSO-d_6): δ -62.87. HRMS (ESI), *m/z*. calcd for $C_{20}H_{19}F_3N_3O$ ([M + H]⁺), 374.1506; found, 374.1475. HPLC (Method B1): 97.7%, R_t = 3.47

min. *2-Phenyl-N-(4-(trifluoromethyl)benzyl)acrylamide (9h, R^1= H, R^2= 4-CF$_3$)* obtained as an off-white solid, yield: 0.32 g (59 %). TLC (petroleum ether-EtOAc 1:1 v/v), R*f* = 0.74. M.p. 88-90 °C. ^{1}H NMR (DMSO-*d$_6$*): δ 8.83 (t, *J* = 6.0 Hz, 1H, N*H*), 7.72 (d, *J* = 8.1 Hz, 2H, Ar), 7.54 (d, *J* = 8.0 Hz, 2H, Ar), 7.43 (d, *J* = 6.8 Hz, 2H, Ar), 7.36 (m, 3H, Ar), 5.81 (s, 1H, C=C*Ha*Hb), 5.73 (s, 1H, C=CHa*Hb*), 4.48 (d, *J* = 6.1 Hz, 2H, NHC*H$_2$*). ^{13}C NMR(DMSO-*d$_6$*): δ 168.81 (C, C=O), 145.46 (C, =*C*=), 144.97 (C, Ar), 137.10 (C, Ar), 128.81 (2 x CH, Ar), 128.61 (CH, Ar),128.30 (3 x CH, Ar), 127.80 (C, Ar), 127.57 (3 x CH, Ar), 125.69 & 125.66 (CF$_3$), 118.60 (C=*C*H$_2$), 42.55 (NH*C*H$_2$). ^{19}F-NMR (DMSO-*d$_6$*): δ -60.78. Anal. Calcd for C$_{17}$H$_{14}$F$_3$NO•0.1H$_2$O (307.10042): C, 66.49%; H, 4.66%; N, 4.56%. Found: C, 66.43%; H, 4.75%; N, 4.48%.

(*R/S*)-3-(1*H*-Imidazol-1-yl)-*N*-(4-methoxybenzyl)-2-phenylpropanamide (8i) and *N*-(4-methoxybenzyl)-2-phenylacrylamide (9i)
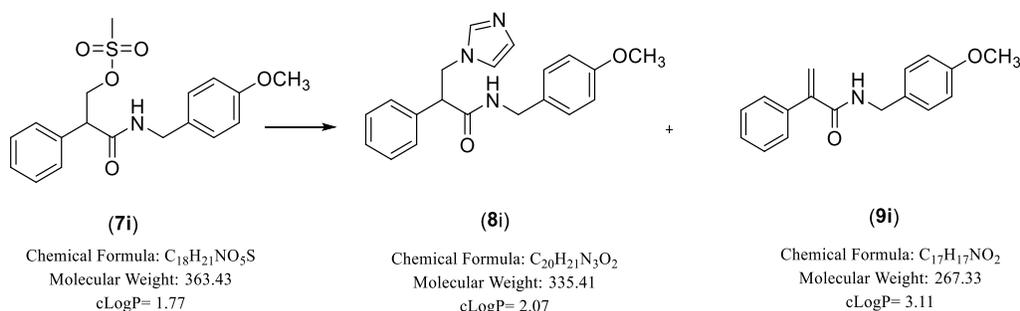
(7i)	(8i)	(9i)
Chemical Formula: C$_{18}$H$_{21}$NO$_5$S	Chemical Formula: C$_{20}$H$_{21}$N$_3$O$_2$	Chemical Formula: C$_{17}$H$_{17}$NO$_2$
Molecular Weight: 363.43	Molecular Weight: 335.41	Molecular Weight: 267.33
cLogP= 1.77	cLogP= 2.07	cLogP= 3.11

Method: see 7.4.6 method but heated at 70 °C for overnight. The crude product was purified by gradient column chromatography petroleum ether – EtOAc 70:30 v/v to elute (**9i**), then changed eluent to CH$_2$Cl$_2$-MeOH 90:10 v/v to elute (**8i**).

Prepared from (*R/S*)-3-((4-methoxybenzyl)amino)-3-oxo-2-phenylpropyl methanesulfonate (**7i**) (0.67 g, 1.85 mmoL). *(R/S)-3-(1H-Imidazol-1-yl)-N-(4-methoxybenzyl)-2-phenylpropanamide (8i, R^1= H, R^2= 4-OCH$_3$)* obtained as a brown coloured solid, yield: 0.17 g (27 %). TLC (petroleum ether-EtOAc 1:1 v/v), R*f* = 0.0. M.p. 102-104 °C. ^{1}H NMR (DMSO- *d$_6$*): δ 8.52 (t, *J* = 5.8 Hz, 1H, N*H*), 7.53 (brs, 1H, imid), 7.39 (d, *J* = 7.2 Hz, 2H, Ar), 7.34 (t, *J* = 7.4 Hz, 2H, Ar), 7.28 (t, *J* = 7.2 Hz, 1H, Ar), 7.09 (brs, 1H, imid), 6.93 (d, *J* = 8.6 Hz, 2H, Ar), 6.87 (brs, 1H, imid), 6.79 (d, *J* = 8.6 Hz, 1H, Ar), 4.62 (dd, *J* = 9.6, 13.4 Hz, 1H, CHC*Ha*Hb), 4.24 (φt, *J* = 5.6, 4.3 Hz, 1H, NHC*Ha*Hb), 4.22 (t, *J* = 5.8 Hz, 1H, CHCHa*Hb*), 4.06 (dd, *J* = 5.4, 14.9 Hz,

1H, NHCHa*Hb*), 4.00 (dd, J = 5.8, 9.5 Hz, 1H, C*H*CHaHb), 3.71 (s, 3H, C*H₃*). ^{13}C NMR (DMSO- d_6): δ 170.89 (C, C=O), 158.64 (C, *C*-OCH₃), 138.05 (C, Ar), 131.30 (C, Ar), 128.90 (2 x CH, Ar (1) and imid (1)), 128.77 (2 x CH, Ar (1) and imid (1)), 128.28 (2 x CH, Ar (1) and imid (1)), 127.81 (CH, Ar), 114.05 (2 x CH, Ar), 55.52 (OCH₃), 53.31 (*C*HCH₂imid), 48.91 (CHC*H₂*imid), 41.99 (NHC*H₂*). LRMS (ES+ TOF, *m/z*): 336.17 [C₂₀H₂₁N₃O₂+H]$^+$. HRMS (ES+ TOF), *m/z*. calcd for C₂₀H₂₂N₃O₂ ([M + H]$^+$), 336.1712; found, 336.1715. HPLC (Method B1): 95.9%, R$_t$ = 5.07 min. *N-(4-Methoxybenzyl)-2-phenylacrylamide (9i, R¹= H, R²= 4-OCH₃)* obtained as an off-white solid, yield: 0.31 g (50 %). TLC (petroleum ether-EtOAc 1:1 v/v), R*f* = 0.64. M.p. 100-102 °C. ^{1}H NMR (DMSO-d_6): δ 8.66 (t, J = 5.9 Hz, 1H, N*H*), 7.43 (d, J = 4.7 Hz, 2H, Ar), 7.36 (m, 3H, Ar), 7.25 (d, J = 8.7 Hz, 2H, Ar), 6.91 (d, J = 8.7 Hz, 2H, Ar), 5.77 (s, 1H, C=C*Ha*Hb), 5.65 (s, 1H, C=CHa*Hb*), 4.33 (d, J = 6.1 Hz, 2H, NHC*H₂*), 3.75 (s, 3H, C*H₃*). ^{13}C NMR(DMSO-d_6): δ 168.58 (C, C=O), 158.66 (C, *C*-OCH₃), 145.72 (C, *C*=CH₂), 137.22 (C, Ar), 132.02 (C, Ar), 129.00 (2 x CH, Ar),128.78 (2 x CH, Ar), 128.54 (CH, Ar), 127.50 (2 x CH, Ar), 118.04 (C=*C*H₂), 114.18 (2 x CH, Ar), 55.53 (*C*H₃), 42.27 (NHC*H₂*). Anal. Calcd for C₁₇H₁₇NO₂ (267.3268): C, 76.38%; H, 6.41%; N, 5.24%. Found: C, 76.35%; H, 6.30%; N, 5.13%.

(R/S)-N-(3,4-Dimethoxybenzyl)-3-(1*H*-imidazol-1-yl)-2-phenylpropanamide (8j) and N-(3,4-dimethoxybenzyl)-2-phenylacrylamide (9j)
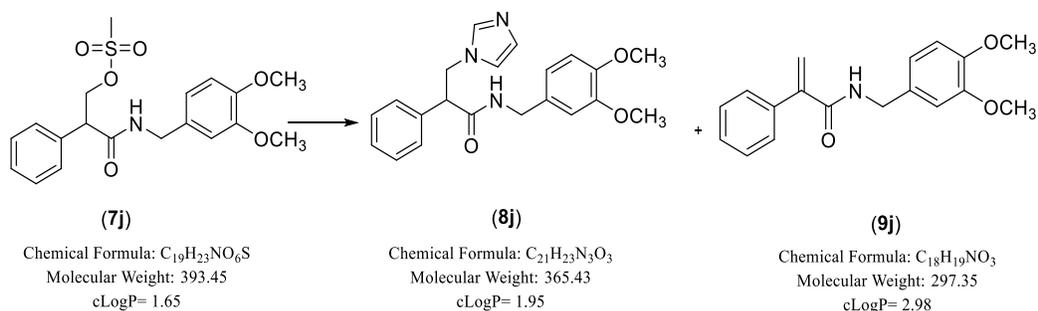
(7j)	**(8j)**	**(9j)**
Chemical Formula: C₁₉H₂₃NO₆S	Chemical Formula: C₂₁H₂₃N₃O₃	Chemical Formula: C₁₈H₁₉NO₃
Molecular Weight: 393.45	Molecular Weight: 365.43	Molecular Weight: 297.35
cLogP= 1.65	cLogP= 1.95	cLogP= 2.98

Method: see 7.4.6 method but heated at 70 °C for overnight. The crude product was purified by gradient column chromatography petroleum ether – EtOAc 60:40 v/v to elute (**9j**), then changed eluent to CH₂Cl₂-MeOH 90:10 v/v to elute (**8j**).

Prepared from (R/S)-3-((3,4-dimethoxybenzyl)amino)-3-oxo-2-phenylpropyl methanesulfonate (**7j**) (0.52 g, 1.30 mmoL). *(R/S)-N-(3,4-Dimethoxybenzyl)-3-(1H-imidazol-1-yl)-2-*

phenylpropanamide (8j, R^1= H, R^2= 3,4-di-OCH$_3$) obtained as a pale-yellow oil, yield: 0.25 g (51 %). TLC (petroleum ether-EtOAc 1:1 v/v), Rf = 0.0. ^{1}H NMR (DMSO- d_6): δ 8.55 (t, J = 5.8 Hz, 1H, NH), 7.53 (brs, 1H, imid), 7.41 (d, J = 7.2 Hz, 2H, Ar), 7.34 (t, J = 7.4 Hz, 2H, Ar), 7.28 (t, J = 7.3 Hz, 1H, Ar), 7.09 (brs, 1H, imid), 6.85 (brs, 1H, imid), 6.80 (d, J = 8.2 Hz, 1H, Ar), 6.60 (d, J = 1.8 Hz, 1H, Ar), 6.56 (dd, J = 1.8, 8.2 Hz, 1H, Ar), 4.64 (dd, J = 9.6, 13.5 Hz, 1H, CHCHaHb), 4.23 (dd, J = 7.5, 13.5 Hz, 1H, CHCHaHb), 4.16 (d, J = 5.8 Hz, 2H, NHCHaHb), 4.01 (dd, J = 5.7, 9.5 Hz, 1H, CHCHaHb), 3.70 (s, 3H, CH_3), 3.58 (s, 3H, CH_3). ^{13}C NMR(DMSO-d_6): δ 170.93 (C, C=O), 149.10 (C, COCH$_3$), 148.17 (C, COCH$_3$), 138.16 (C, Ar), 131.88 (C, Ar), 128.93 (3 x CH, Ar (2) and imid (1)), 128.52 (CH, imid), 128.27 (3 x CH, Ar (2) and imid (1)), 127.81 (CH, Ar), 119.55 (CH, Ar), 112.05 (CH, Ar), 111.14 (CH, Ar), 56.02 (OCH$_3$), 55.67 (OCH$_3$), 53.35 (CHCH$_2$imid), 48.80 (CHCH_2imid), 42.21 (NHCH_2). LRMS (ES+ TOF, m/z): 366.18 [C$_{21}$H$_{23}$N$_3$O$_3$ + H]$^+$. HRMS (ES+ TOF), m/z. calcd for C$_{21}$H$_{24}$N$_3$O$_3$ ([M + H]$^+$), 366.1818; found, 366.1826. HRMS (ESI), m/z. calcd for C$_{21}$H$_{24}$N$_3$O$_3$ ([M + H]$^+$), 366.1835; found, 366.1812. HPLC (Method B2): 99.9%, R$_t$ = 4.81 min. *N-(3,4-Dimethoxybenzyl)-2-phenylacrylamide (9j, R^1= H, R^2= 3,4-di-OCH$_3$)* obtained as a white solid, yield: 0.09 g (23 %). TLC (petroleum ether-EtOAc 1:1 v/v), Rf = 0.92. M.p. 102-104 °C. ^{1}H NMR (DMSO-d_6): δ 8.66 (t, J = 6.0 Hz, 1H, NH), 7.44 (m, 2H, Ar), 7.36 (m, 3H, Ar), 6.92 (m, 2H, Ar), 6.84 (dd, J = 1.9, 8.2 Hz, 1H, Ar), 5.78 (s, 1H, C=CHaHb), 5.65 (s, 1H, C=CHaHb), 4.33 (d, J = 6.1 Hz, 2H, NHCH_2), 3.75 (s, 3H, CH_3), 3.74 (s, 3H, CH_3). ^{13}C NMR(DMSO-d_6): δ 168.68 (C, C=O), 149.13 (C, C-OCH$_3$), 148.21 (C, C-OCH$_3$), 145.75 (C, C=CH$_2$), 137.19 (C, Ar), 132.52 (C, Ar), 128.79 (2 x CH, Ar), 128.57 (CH, Ar), 127.45 (2 x CH, Ar), 119.74 (CH, Ar), 117.87 (C=CH$_2$), 112.24 (CH, Ar), 111.69 (CH, Ar), 56.05 (CH$_3$), 55.86 (CH$_3$), 42.54 (NHCH_2). Anal. Calcd for C$_{18}$H$_{19}$NO$_3$ (299.3530): C, 72.71%; H, 6.44%; N, 4.71%. Found: C, 72.59%; H, 6.46%; N, 4.82%.

(R/S)-N-(4-Chlorobenzyl)-2-phenyl-3-(1H-1,2,4-triazol-1-yl)propanamide (8k)
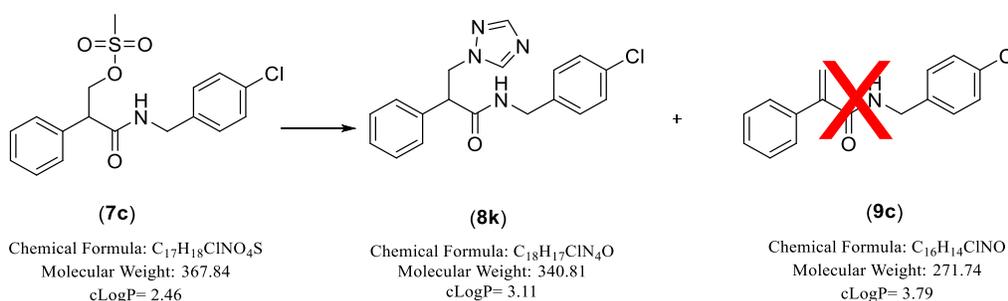
(7c)	(8k)	(9c)
Chemical Formula: C$_{17}$H$_{18}$ClNO$_4$S	Chemical Formula: C$_{18}$H$_{17}$ClN$_4$O	Chemical Formula: C$_{16}$H$_{14}$ClNO
Molecular Weight: 367.84	Molecular Weight: 340.81	Molecular Weight: 271.74
cLogP= 2.46	cLogP= 3.11	cLogP= 3.79

Method: see 7.4.6 method. The crude product was purified by gradient column chromatography petroleum ether – EtOAc 10:90 v/v to elute (**8k**).

Prepared from (*R/S*)-3-((4-chlorobenzyl)amino)-3-oxo-2-phenylpropyl methanesulfonate (**7c**) (0.59 g, 1.61 mmol). Product obtained as a white solid, yield: 0.22 g (40 %). TLC (petroleum ether-EtOAc 1:1 v/v), R*f* = 0.0. M.p. 113-115 °C. ^{1}H NMR (DMSO-d_6): δ 8.72 (t, *J* = 6.0 Hz, 1H, N*H*), 8.32 (s, 1H, triaz), 7.99 (s, 1H, triaz), 7.20 (m, 5H, Ar), 7.28 (d, *J* = 8.4 Hz, 2H, Ar), 6.97 (d, *J* = 8.5 Hz, 2H, Ar), 4.83 (dd, *J* = 9.2, 13.8 Hz, 1H, CHC*Ha*Hb), 4.44 (dd, *J* = 6.5, 13.5 Hz, 1H, CHCHa*Hb*), 4.27 (m, 2H, C*H*CHaHb + NHC*Ha*Hb), 4.08 (dd, *J* = 5.5, 15.6 Hz, NHCHa*Hb*). ^{13}C NMR(DMSO-d_6): δ 170.74 (C, C=O), 151.99 (CH, triaz), 145.08 (CH, triaz), 138.58 (C, Ar), 137.94 (C, C-Cl), 137.47 (C, C-Cl), 131.68 (C, Ar), 129.9.36 (CH, Ar), 129.07 (2 x CH, Ar), 129.02 (2 x CH, Ar), 128.78 (CH, Ar), 128.54 (2 x CH, Ar), 128.23 (CH, Ar), 51.56 (*CH*CH$_2$triaz), 51.10 (CH*CH$_2$*triaz), 41.72 (NH*CH$_2$*). HRMS (ES), *m/z*. calcd for $C_{18}H_{18}^{35}ClN_4O$ ([M + H]$^+$), 341.1188; found, 341.1164; calcd for $C_{18}H_{17}^{35}ClN_4ONa$ ([M + Na]$^+$), 363.1009; found, 363.0983; calcd for $C_{18}H_{18}^{37}ClN_4O$ ([M + H]$^+$), 343.1160, found, 343.1140; and calcd for $C_{18}H_{17}^{37}ClN_4ONa$ ([M + Na]$^+$), 365.0981; found, 365.0960. Anal. Calcd for $C_{18}H_{17}ClN_4O$ (340.8115): C, 63.44%; H, 5.03%; N, 16.43%. Found: C, 63.22%; H, 5.01%; N, 16.33%. HPLC (Method B2): 99.7%, R_t = 4.91 min.

N-(4-Chlorobenzyl)-2-phenylacrylamide (9c)
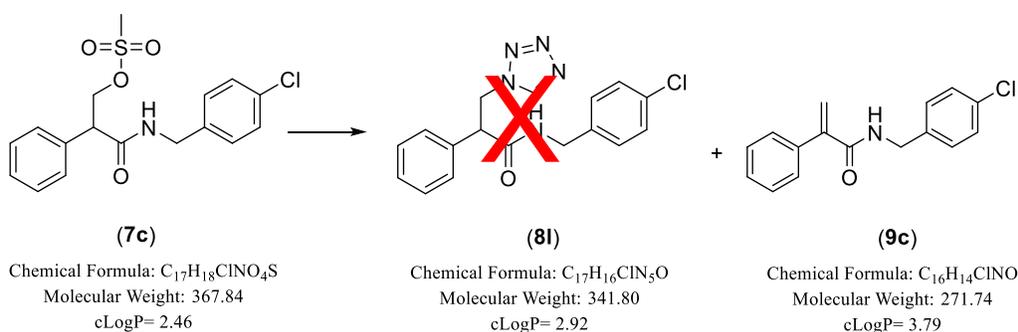
(**7c**)	(**8l**)	(**9c**)
Chemical Formula: $C_{17}H_{18}ClNO_4S$	Chemical Formula: $C_{17}H_{16}ClN_5O$	Chemical Formula: $C_{16}H_{14}ClNO$
Molecular Weight: 367.84	Molecular Weight: 341.80	Molecular Weight: 271.74
cLogP= 2.46	cLogP= 2.92	cLogP= 3.79

Method: see 7.4.6 method but heated at 70 °C for overnight. The crude product was purified by gradient column chromatography petroleum ether – EtOAc 70:30 v/v to elute (**9c**).

Prepared from (*R/S*)-3-((4-chlorobenzyl)amino)-3-oxo-2-phenylpropyl methanesulfonate (**7c**) (0.38 g, 1.03 mmol). Product obtained as a white solid, yield: 0.09 g (23 %). TLC (petroleum ether-EtOAc 1:1 v/v), R*f* = 0.75. M.p. 118-120 °C. ^{1}H NMR (DMSO-d_6): δ 8.76 (t, *J* = 5.9 Hz,

1H, N*H*), 7.38 (m, 9H, Ar), 5.79 (s, 1H, C=C*Ha*Hb), 5.69 (s, 1H, C=CHa*Hb*), 4.37 (d, $J = 6.1$ Hz, 2H, NHC*H₂*). ^{13}C NMR(DMSO-d_6): δ 168.72 (C, C=O), 145.53 (C, *C*=CH₂), 139.13 (C, Ar), 137.12 (C, Ar), 131.77 (C, C-Cl), 129.54 (2 x CH, Ar), 128.80 (2 x CH, Ar), 128.73 (2 x CH, Ar), 128.59 (CH, Ar), 127.54 (2 x CH, Ar), 118.40 (C=*C*H₂), 42.22 (NH*C*H₂). Anal. Calcd for $C_{16}H_{14}ClNO$ (271.7457): C, 70.72%; H, 5.19%; N, 5.15%. Found: C, 70.44%; H, 5.16%; N, 5.04%.

7.4.7 (9*H*-Fluoren-9-yl)methyl(4-(aminomethyl)phenyl) carbamate hydrochloride (12)

(10)	**(11)**	**(12)**
Chemical Formula: $C_7H_{10}N_2$	Chemical Formula: $C_{15}H_{11}ClO_2$	Chemical Formula: $C_{22}H_{21}ClN_2O_2$
Molecular Weight: 122.17	Molecular Weight: 258.70	Molecular Weight: 380.87
cLogP= 0.28	cLogP= 4.09	
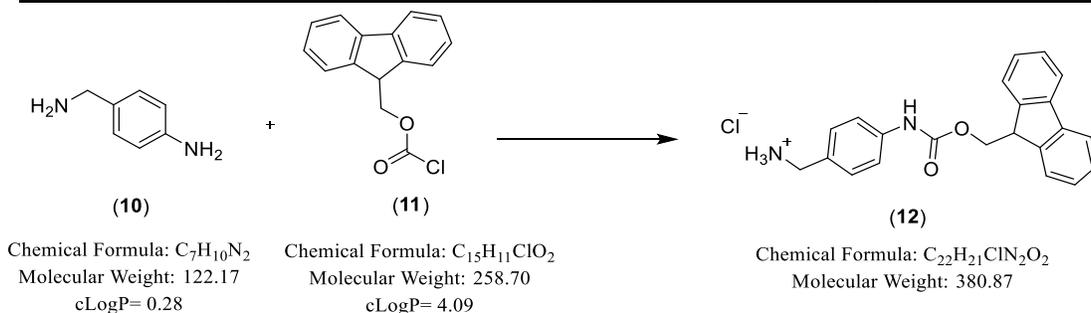
To a solution of 4-aminobenzylamine (**10**) (0.59 mL, 5.176 mmol) in 10% aq. AcOH (20 mL) was added a solution of FmocCl (**11**) (1.5380 g, 5.383 mmol) in 1,4-dioxane (20 mL). After overnight stirring at rt., Et₂O (2 × 30 mL) was added to the reaction mixture to extract the nonpolar impurities.[87] The reaction mixture was then acidified with 2N HCl to pH 1. The precipitate was collected by filtration, washed with Et₂O (15 mL) and dried in a vacuum oven at 40 °C o/n. Product obtained as a white solid, yield: 1.69 g (86 %). TLC (CH₂Cl₂-MeOH 9:1 v/v), R*f* = 0.41. M.p. 254-257 °C. ^{1}H NMR (DMSO-d_6): δ 9.82 (brs, 1H, N*H*), 8.34 (brs, 2H, N*H₂*), 7.91 (d, $J = 7.6$ Hz, 2H, Ar), 7.76 (d, $J = 7.4$ Hz, 2H, Ar), 7.41 (m, 8H, Ar), 4.50 (d, $J = 6.4$ Hz, 2H, OC*H₂*CH), 4.31 (t, $J = 6.5$ Hz, 1H, OCH₂C*H*), 3.92 (t, $J = 5.4$ Hz, 2H, NH₂C*H₂*). ^{13}C NMR (DMSO-d_6): δ 153.88 (C, C=O), 144.21 (2 x C, Ar), 141.28 (2 x C, Ar), 139.71 (C, Ar), 130.09 (2 x CH, Ar), 128.32 (C, Ar), 128.18 (2 x CH, Ar), 127.60 (2 x CH, Ar), 125.59 (2 x CH, Ar), 120.67 (2 x CH, Ar), 118.64 (2 x CH, Ar), 66.10 (O*C*H₂CH), 47.07 (OCH₂*C*H), 42.25 (NH₂*C*H₂). HPLC (Method A): 81%, R_t = 08 min.

7.4.8 General procedure to synthesise the coupling compound with tropic acid (13)

To an ice-cooled solution of tropic acid (**4a**) (1 eq) and HOBt (0.20 g, 1.33 mmol) in EtOAc (10 mL/mmol) was added DCC (1.1 eq) and the reaction stirred at 0 °C for 30 min. In a separate flask, a mixture of (9*H*-fluoren-9-yl)methyl(4-(aminomethyl)phenyl) carbamate

hydrochloride (**12**) (1 eq) in EtOAc (5 mL/mmol) and Et₃N (3 eq) was stirred at rt for 30 min to produce the free amine, The free amine mixture was then added to the cooled activated tropic acid-DCC mixture and the reaction stirred at rt o/n. Hexane (15 mL/mmol) was added to the reaction and the flask left in the freezer overnight to precipitate DCU, which was removed by filtration and washed with EtOAc. The combined filtrates were washed with 4% aqueous HCl (2 x 30 mL), saturated aqueous NaHCO₃ (3 x 25 mL) and brine (3 x 30 mL). The organic layer was dried (MgSO₄) and evaporated under reduced pressure.

(*R/S*)-(9*H*-fluoren-9-yl)methyl(4-((3-hydroxy-2-phenylpropanamido)methyl)phenyl) carbamate (13)

(**12**)	(**4a**)	(**13**)
Chemical Formula: $C_{22}H_{21}ClN_2O_2$	Chemical Formula: $C_9H_{10}O_3$	Chemical Formula: $C_{31}H_{28}N_2O_4$
Molecular Weight: 380.87	Molecular Weight: 166.18	Molecular Weight: 492.58
	cLogP= 1.04	cLogP= 5.09

Prepared from tropic acid (**4a**) (0.44 g, 2.63 mmoL) and (9*H*-Fluoren-9-yl)methyl (4-(aminomethyl)phenyl)carbamate hydrochloride (**12**) (1.00 g, 2.63 mmoL).[84]

Product obtained as a white solid, yield: 0.25 g (19 %). TLC (CH₂Cl₂-MeOH 9.5:0.5 v/v), R*f* = 0.68. M.p. 150-152 °C. ¹H NMR (DMSO-*d₆*): δ 9.64 (brs, 1H, N*H*), 8.47 (t, *J* = 5.9 Hz, 1H, N*H*CH₂), 7.91 (d, *J* = 7.5 Hz, 2H, Ar), 7.75 (d, *J* = 7.4 Hz, 2H, Ar), 7.43 (t, *J* = 7.4 Hz, 2H, Ar), 7.29 (m, 10H, Ar), 7.07 (d, *J* = 8.0 Hz, 1H, Ar), 4.86 (t, *J* = 5.2 Hz, 1H, OH), 4.47 (d, *J* = 6.2 Hz, 2H, CHC*H₂*OC=O), 4.30 (t, *J* = 6.6 Hz, 1H, C*H*CH₂OC=O), 4.23 (dd, *J* = 5.9, 15.1 Hz, 1H, NHC*Ha*Hb), 4.16 (dd, *J* = 5.8, 15.2 Hz, 1H, NHCHa*Hb*), 3.99 (pentet, *J* = 4.8 Hz, 1H, CHC*Ha*Hb), 3.66 (dd, *J* = 5.5, 9.0 Hz, 1H, C*H*CHaHb), 3.54 (pentet, *J* = 5.1 Hz, 1H, CHCHa*Hb*). ¹³C NMR (DMSO-*d₆*): δ 172.12 (C, C=O), 153.90 (C, C=O), 144.26 (C, Ar), 141.28 (C, Ar), 138.97 (C, Ar), 138.07 (C, Ar), 133.96 (C, Ar), 129.39 (CH, Ar), 128.61 (2 x CH, Ar), 128.42 (2 x CH, Ar), 128.15 (2 x CH, Ar), 127.96 (2 x CH, Ar), 127.57 (2 x CH, Ar), 127.16 (CH, Ar), 126.76 (C, Ar), 125.57 (2 x CH, Ar), 120.61 (2 x CH, Ar), 118.70 (CH, Ar), 110.09 (C, Ar), 66.04 (CHC*H₂*OC=O), 63.84 (CHC*H₂*OH), 55.01 (*C*HCH₂OH), 47.14

($CHCH_2OC{=}O$), 42.07 ($NHCH_2$). HRMS (ESI), *m/z*. calcd for $C_{31}H_{28}N_2O_4Na$ [M + Na]$^+$, 515.1947; found, 515.1938.

7.4.9 *tert*-Butyl (4-(aminomethyl)phenyl)carbamate (20)[87]

(10)	(19)	(20)
Chemical Formula: $C_7H_{10}N_2$	Chemical Formula: $C_{10}H_{18}O_5$	Chemical Formula: $C_{12}H_{18}N_2O_2$
Molecular Weight: 122.17	Molecular Weight: 218.25	Molecular Weight: 222.29
cLogP= 0.28	cLogP= 2.59	cLogP= 1.45
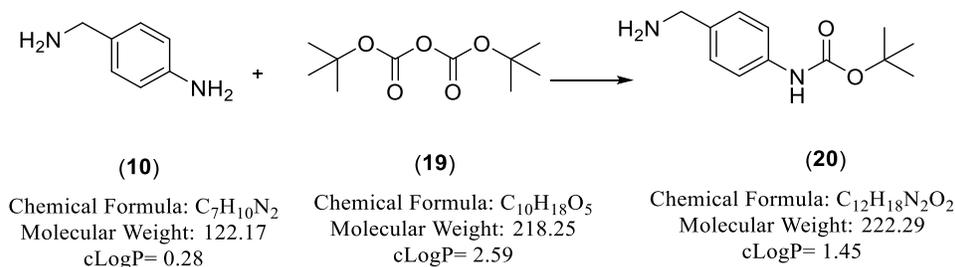
To a solution of 4-aminobenzylamine (**10**) (1.86 mL, 16.37 mmoL) in 10% aqueous acetic acid (30 mL) was added a solution of di-*tert*-butyl carbonate (($Boc)_2O$) (**19**) (3.89 g, 17.84 mmoL) in 1,4-dioxane (30 mL). After overnight stirring at room temperature, water (100 mL) was added and the mixture was washed with Et_2O (3 x 50 mL).

The aqueous phase was basified with 2N aqueous NaOH to pH 14 and extracted with Et_2O (3 x 75 mL). The combined extracts were washed with H_2O (2 x 40 mL), dried ($MgSO_4$) and concentrated under reduced pressure. Product obtained as an off-white solid, yield: 1.21 g (34 %). TLC (CH_2Cl_2-MeOH 7:3 v/v), Rf = 0.9. M.p. 72-74 °C (lit. M.p. 86-90 °C)[84]. ^{1}H NMR ($CDCl_3$): δ 7.34 (d, *J* = 8.3 Hz, 2H, Ar), 7.24 (d, *J* = 8.6 Hz, 2H, Ar), 6.64 (brs, 1H, N*H*), 3.83 (brs, 2H, NH_2CH_2), 3.72 (brs, 2H, NH_2CH_2), 1.53 (s, 9H, C(C*H_3*)_3). ^{13}C NMR ($CDCl_3$): δ 152.86 (C, C=O), 138.00 (C, Ar), 137.11 (C, Ar), 127.72 (3 x CH, Ar), 118.76 (CH, Ar), 67.09 (C, *C*(CH_3)_3), 45.99 (NH*CH_2*), 28.36 (C(*CH_3*)_3).

(*R/S*)-*tert*-Butyl (4-((3-hydroxy-2-phenylpropanamido)methyl)phenyl) carbamate (21)

(20)	(4a)	(21)
Chemical Formula: $C_{12}H_{18}N_2O_2$	Chemical Formula: $C_9H_{10}O_3$	Chemical Formula: $C_{21}H_{26}N_2O_4$
Molecular Weight: 222.29	Molecular Weight: 166.18	Molecular Weight: 370.45
cLogP= 1.45	cLogP= 1.04	cLogP= 2.73
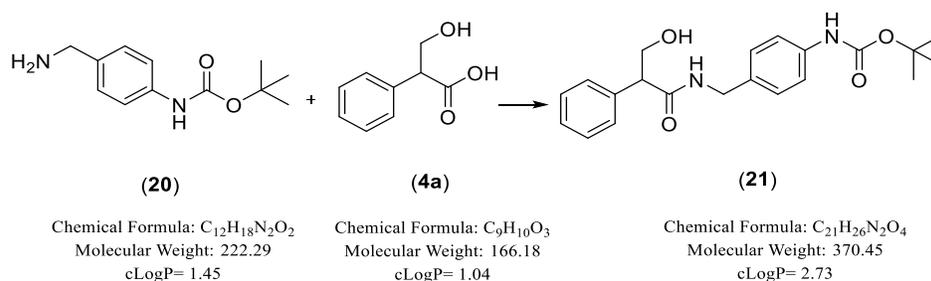
Method: see 7.4.4.

Prepared from tropic acid (**4a**, R^1= 4-H, 0.59 g, 3.54 mmoL) and *tert*-butyl (4-(aminomethyl)phenyl)carbamate[87] (**20**) (0.86 g, 3.89 mmoL). Product obtained as a yellow solid, yield: 1.03 g (79%). TLC (petroleum ether-EtOAc 1:1 v/v), Rf = 0.2. M.p. 118-120 °C. ^{1}H NMR (DMSO-d_6): δ 9.25 (brs, 1H, NH), 8.45 (t, *J* = 5.9 Hz, 1H, N*H*), 7.27 (m, 6H, Ar), 7.23 (m, 1H, Ar), 7.05 (d, *J* = 8.6 Hz, 2H, Ar), 4.83 (t, *J* = 5.2 Hz, 1H, O*H*), 4.22 (dd, *J* = 6.0, 15.2 Hz, 1H, NHC*Ha*Hb), 4.15 (dd, *J* = 5.8, 15.1 Hz, 1H, NHCHa*Hb*), 3.99 (ddd, *J* = 5.6, 9.9, 29.5 Hz, 1H, CHC*Ha*Hb), 3.65 (dd, *J* = 5.5, 9.0 Hz, 1H, C*H*CHaHb), 3.53 (pentet, *J* = 5.1 Hz, 1H, CHCHa*Hb*), 1.46 (s, 9H, C(C*H₃*)₃). ^{13}C NMR (DMSO-d_6): δ 172.06 (C, C=O), 153.22 (C, C=O), 138.95 (C, Ar), 138.59 (C, Ar), 133.39 (C, Ar), 129.91 (CH, Ar), 128.63 (2 x CH, Ar), 128.40 (2 x CH, Ar), 127.85 (2 x CH, Ar), 127.17 (CH, Ar), 118.37 (CH, Ar), 79.37 (*C*(CH₃)₃), 63.81 (*C*H₂OH), 54.96 (*C*HCH₂OH), 42.01 (NH*C*H₂), 28.60 (C(*C*H₃)₃). HRMS (ESI), *m/z*. calcd for C₂₁H₂₇N₂O₄ ([M + H]⁺), 371.1990; found, 371.1965; and calcd for C₂₁H₂₆N₂O₄Na ([M + Na]⁺), 393.1812; found, 393.1785. HPLC (Method A): 83%, R$_t$ = 7.3 min.

(*R/S*)-3-((4-((*tert*-Butoxycarbonyl)amino)benzyl)amino)-3-oxo-2-phenylpropyl methanesulfonate (22)
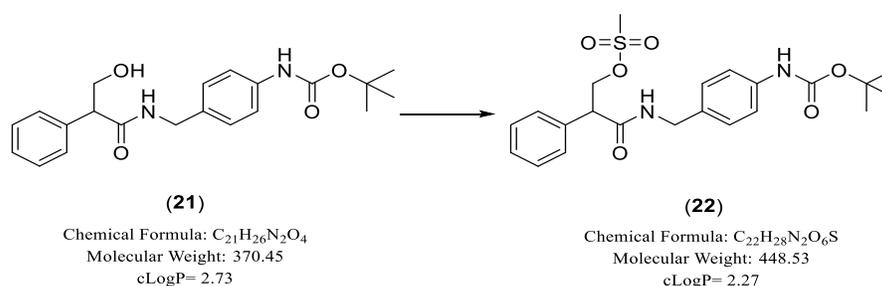
(**21**)
Chemical Formula: C₂₁H₂₆N₂O₄
Molecular Weight: 370.45
cLogP= 2.73

(**22**)
Chemical Formula: C₂₂H₂₈N₂O₆S
Molecular Weight: 448.53
cLogP= 2.27

Method: see 7.4.5. The crude product was purified by gradient column chromatography eluting with petroleum ether – EtOAc 50:50 v/v.

Prepared from (*R/S*)-*tert*-butyl (4-((3-hydroxy-2-phenylpropanamido)methyl)phenyl)carbamate (**21**) (1.00 g, 2.72 mmoL). Product obtained as a white fluffy solid, yield: 0.64 g (53%). TLC (petroleum ether-EtOAc 1:1 v/v), Rf = 0.63. M.p. 118-120 °C. ^{1}H NMR (DMSO-d_6): δ 9.26 (brs, 1H, N*H*), 8.69 (t, *J* = 5.9 Hz, 1H, N*H*), 7.35 (m, 7H, Ar), 7.03 (d, *J* = 8.6 Hz, 2H, Ar), 4.72 (t, *J* = 9.6 Hz, 1H, CHC*Ha*Hb), 4.35 (dd, *J* = 5.7, 9.5 Hz, 1H, CHCHa*Hb*), 4.24 (dd, *J* = 5.9, 15.1 Hz, 1H, NHC*Ha*Hb), 4.17 (dd, *J* = 5.8, 15.1 Hz, 1H, NHCHa*Hb*), 4.00 (dd, *J* = 5.1, 9.0 Hz, 1H, C*H*CHaHb), 3.14 (s, 3H, SO₂C*H₃*), 1.46 (s, 9H,

C(C*H₃*)₃). ¹³C NMR (DMSO-*d₆*): δ 170.04 (C, C=O), 153.21 (C, C=O), 138.73 (C, Ar), 136.32 (C, Ar), 132.92 (C, Ar), 129.04 (2 x CH, Ar), 128.58 (CH, Ar), 128.45 (2 x CH, Ar), 128.10 (CH, Ar), 127.85 (2 x CH, Ar), 118.42 (CH, Ar), 79.40 (*C*(CH₃)₃), 71.15 (CH*CH₂*OMs), 50.82 (*C*HCH₂OMs), 42.15 (NH*CH₂*), 37.02 (*C*H₃), 28.60 (C(*C*H₃)₃). HRMS (ESI), *m/z*. calcd for C₂₂H₂₉N₂O₆S ([M + H]⁺), 449.1806; found, 449.1741; and calcd for C₂₂H₂₈N₂O₆SNa ([M + Na]⁺), 471.1638; found, 471.1560. HPLC (Method A): 94%, R_t = 8.6 min.

(*R/S*)-*tert*-Butyl(4-((2-phenyl-3-(1*H*-1,2,4-triazol-1-yl)propanamido)methyl)phenyl) carbamate (23) and *tert*-butyl (4-((2-phenylacrylamido)methyl)phenyl)carbamate (24)

(22)
Chemical Formula: C₂₂H₂₈N₂O₆S
Molecular Weight: 448.53
cLogP= 2.27

(23)
Chemical Formula: C₂₃H₂₇N₅O₃
Molecular Weight: 421.50
cLogP= 2.92

(24)
Chemical Formula: C₂₁H₂₄N₂O₃
Molecular Weight: 352.43
cLogP= 3.6
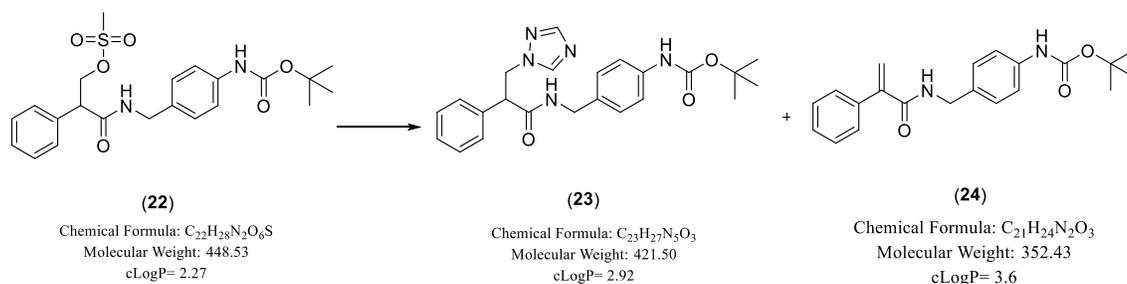
Method: see 7.4.6. Heated at 70 °C for 2.5 h then rt, o/n. The crude product was purified by gradient column chromatography petroleum ether–EtOAc 60:40 v/v to elute (**24**), then changed eluent to CH₂Cl₂-MeOH 9:1 v/v to elute (**23**).

Prepared from (*R/S*)-3-((4-((*tert*-butoxycarbonyl)amino)benzyl)amino)-3-oxo-2-phenylpropyl methane sulfonate (**22**) (0.62 g, 1.39 mmoL). (*R/S*)-*tert*-Butyl (4-((2-phenyl-3-(1H-1,2,4-triazol-1-yl)propanamido)methyl) phenyl) carbamate (*23*) obtained as a pale-yellow oil, yield: 0.49 g (84 %). TLC (petroleum ether-EtOAc 1:1 v/v), R*f* = 0.0. ¹H NMR (CDCl₃): δ 7.80 (s, 1H, triazole), 7.76 (s, 1H, triazole), 7.18 (m, 7H, Ar), 6.81 (d, *J* = 8.5 Hz, 2H, Ar), 6.61 (s, 1H, N*H*), 6.10 (t, *J* = 5.6 Hz, 1H, N*H*CHaHb), 4.83 (dd, *J* = 8.7, 13.6 Hz, 1H, CHC*Ha*Hb), 4.23 (ddd, *J* = 6.1, 14.7, 21.0 Hz, 2H, CHCHa*Hb* and NHC*Ha*Hb), 4.11 (dd, *J* = 5.5, 9.2, 14.8 Hz, 1H, NHCHa*Hb*), 3.97 (dd, *J* = 6.2, 8.7 Hz, 1H, C*H*CHaHb), 1.39 (s, 9H, C(C*H₃*)₃). ¹³C NMR (CDCl₃): δ 170.26 (C, C=O), 152.79 (C, C=O), 151.99 (CH, triaz), 144.21 (CH, triaz), 137.77 (C, Ar), 135.96 (C, Ar), 132.12 (C, Ar), 129.25 (2 x CH, Ar), 128.35 (CH, Ar), 128.14 (3 x CH, Ar), 127.81 (2 x CH, Ar), 118.75 (CH, Ar), 80.60 (*C*(CH₃)₃), 54.71 (*C*HCH₂), 52.05 (CH*CH₂*), 42.15 (NH*CH₂*), 28.33 (C(*C*H₃)₃). HRMS (ESI), *m/z*. calcd for C₂₃H₂₈N₅O₃ ([M + H]⁺)**,** 422.2218; found, 422.2187. HPLC (Method B2): 99.7%, R_t = 4.82 min. *tert*-Butyl (4-((2-

*phenylacrylamido)methyl)phenyl) carbamate (**24**)* obtained as a white solid, yield: 0.06 g (9 %).

TLC (Petroleum ether-EtOAc 1:1 v/v), Rf = 0.70. M.p. 136-138 °C. ^{1}H NMR (CDCl$_3$): δ 7.38

(m, 5H, Ar), 7.33 (d, J = 8.5 Hz, 2H, Ar), 7.21 (d, J = 8.5 Hz, 2H, Ar), 6.53 (s, 1H, NH), 6.21

(d, J = 1.3 Hz, 1H, C=CHaHb), 5.97 (brs, 1H, NH), 5.65 (d, J = 1.3 Hz, 1H, C=CHaHb), 4.49

(d, J = 5.6 Hz, 2H, NHCH_2), 1.53 (s, 9H, C(CH_3)$_3$). ^{13}C NMR (CDCl$_3$): δ 167.07 (C, C=O),

152.73 (C, C=O), 144.61 (C, C=CHaHb), 137.77 (C, Ar), 136.97 (C, Ar), 132.60 (C, Ar), 128.77

(2 x CH, Ar), 128.57 (CH, Ar), 128.50 (3 x CH, Ar), 128.82 (2 x CH, Ar), 122.64 (C=CH$_2$),

118.78 (CH, Ar), 80.64 (C(CH$_3$)$_3$), 43.46 (NHCH$_2$), 28.34 (C(CH$_3$)$_3$). HRMS (ESI), *m/z.* calcd

for C$_{21}$H$_{25}$N$_2$O$_3$ ([M + H]$^+$), 353.1876; found, 353.1860; and calcd for C$_{21}$H$_{24}$N$_2$O$_3$Na ([M +

Na]$^+$), 375.1702; found, 375.1679. HPLC (Method A): 100%, R$_t$ = 8.7 min.

7.4.10 <u>(*R/S*)-4-((2-Phenyl-3-(1*H*-1,2,4-triazol-1-yl)propanamide)methyl)benzenaminium trifluoroacetic acid salt (25)</u>

(**23**)
Chemical Formula: C$_{23}$H$_{27}$N$_5$O$_3$
Molecular Weight: 421.50
cLogP= 2.92

(**25**)
Chemical Formula: C$_{20}$H$_{20}$F$_3$N$_5$O$_3$
Molecular Weight: 435.41
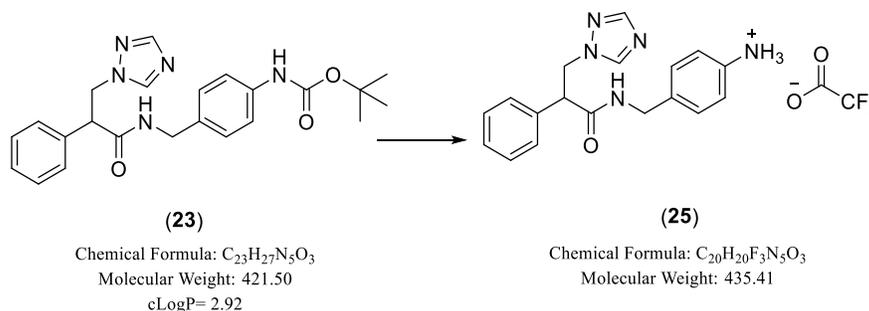
(*R/S*)-*tert*-Butyl (4-((2-phenyl-3-(1*H*-1,2,4-triazol-1-yl)propanamido)methyl)phenyl)

carbamate (**23**) (0.48 g, 1.14 mmol) was stirred overnight with a solution of trifluoroacetic

acid/CH$_2$Cl$_2$ (20 mL, 3:1 v/v). The solvent was then evaporated with further co-evaporation with

EtOH (3 x 20 mL). To the resulting residue was added Et$_2$O (75 mL) and after stirring for 2 h

the residue was collected by vacuum filtration and dried *in vacuo*. Product obtained as an orange

semi-solid, yield: 0.41 g (82 %). TLC (CH$_2$Cl$_2$-MeOH 9:1 v/v), Rf = 0.28. ^{1}H NMR (DMSO-

d$_6$): δ 8.71 (t, J = 5.8 Hz, 1H, NH), 8.34 (s, 1H, triazole), 7.97 (s, 1H, triazole), 7.38 (d, J = 7.0

Hz, 2H, Ar), 7.33 (t, J = 7.4 Hz, 2H, Ar), 7.28 (d, J = 7.2 Hz, 1H, Ar), 7.05 (d, J = 8.0 Hz, 2H,

Ar), 6.97 (d, J = 8.2 Hz, 2H, Ar), 4.83 (dd, J = 9.2, 13.5 Hz, 1H, CHCHaHb), 4.44 (dd, J = 6.4,

13.4 Hz, 1H, CHCHaHb), 4.26 (dd, J = 6.4, 9.3 Hz, 2H, CHCHaHb + NHCHaHb), 4.08 (dd, J

= 5.5, 15.4 Hz, 1H, NHCHaHb). ^{13}C NMR (DMSO-*d*$_6$): δ 170.70 (C, C=O), 158.77 (C, C=O),

158.50 (C, Ar), 158.22 (C, Ar), 151.92 (2 x CH, triaz), 137.49 (C, Ar), 134.17 (C, CF$_3$), 129.00

(2 x CH, Ar), 128.40 (3 x CH, Ar), 128.24 (2 x CH, Ar), 127.95 (CH, Ar), 121.47 (CH, Ar), 51.55 (CH*CH₂*OH), 51.14 (*C*HCH₂OH), 41.91 (NH*CH₂*). HRMS (ESI), *m/z*. calcd for $C_{18}H_{20}N_5O$ ([M + H]⁺), 322.1702; found, 322.1662; and calcd for $C_{18}H_{19}N_5ONa$ ([M + Na]⁺), 344.1525; found, 344.1482.

7.4.11 *tert*-Butyl (4-aminobenzyl)carbamate (26)[90]

(10)	(19)	(26)
Chemical Formula: $C_7H_{10}N_2$	Chemical Formula: $C_{10}H_{18}O_5$	Chemical Formula: $C_{12}H_{18}N_2O_2$
Molecular Weight: 122.17	Molecular Weight: 218.25	Molecular Weight: 222.29
cLogP= 0.28	cLogP= 2.59	cLogP= 1.67
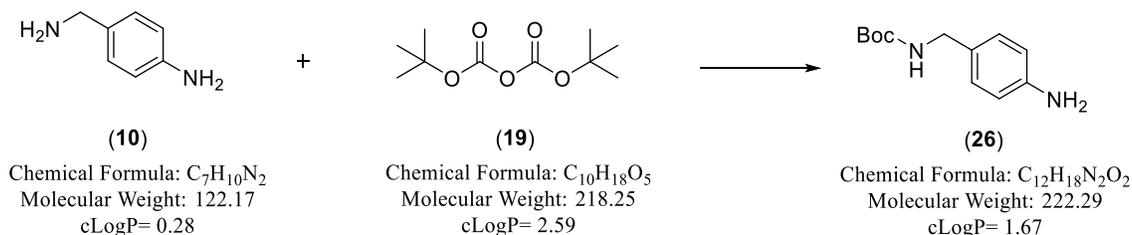
To a pale-yellow solution of 4-aminobenzylamine (**10**) (3.0 g, 24.56 mmol) in dry THF (45 mL) was added a solution of (Boc)₂O (**19**) (5.6 g, 25.78 mmol) in dry THF (30 mL) dropwise over 20 min. A white precipitate formed immediately on addition of (Boc)₂O which became a clear solution on completion of addition. The reaction was stirred at room temperature for 1 h 20 min then the solvent removed under vacuum.

Product obtained as a yellow solid, yield: 5.5 g (100 %). TLC (petroleum ether-EtOAc 1:1 v/v), R*f* = 0.68. M.p. 75-76 °C (lit. M.p. 74-75 °C)[90]. ¹H NMR (CDCl₃): δ 7.09 (d, *J* = 5.0 Hz, 2H, Ar), 6.66 (d, *J* = 5.0 Hz, 2H, Ar), 4.78 (brs, 1H, N*H*Boc), 4.21 (d, *J* = 5.0 Hz, 2H, NHC*H₂*), 3.67 (br. s, 2H, N*H₂*), 1.48 (s, 9H, C(C*H₃*)₃).

7.4.12 *tert*-Butyl (4-(arylphenylsulfonamido)benzyl)carbamate (27)

Where R²:

17a=R²= 4-H
17b=R²= 4-F
17c=R²= 4-Cl
17d=R²= 4-OCH₃
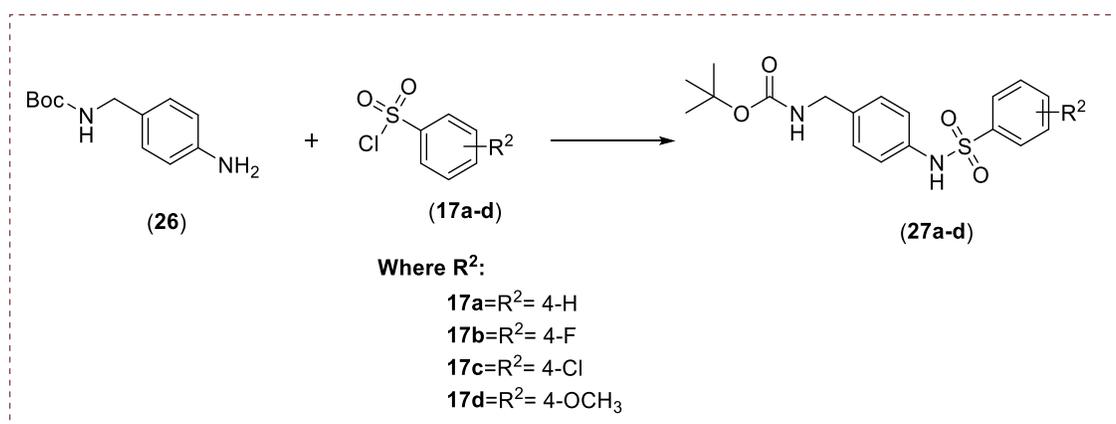
To an ice-cooled yellow solution of *tert*-butyl (4-aminobenzyl)carbamate (**26**)[90] (1 mmoL)

in dry pyridine (10 mL/mmoL) was added benzenesulfonyl chloride (**17**) (1.2 mmoL) in portions and the reaction mixture was stirred at rt for 2 h, then pyridine removed under vacuum. The resulting syrup was diluted in CH_2Cl_2 (100 mL), washed with 0.5 M aqueous HCl (50 mL), H_2O (50 mL), dried ($MgSO_4$) then concentrated under vacuum.

tert-Butyl (4-(phenylsulfonamido)benzyl)carbamate (27a)[90]

(**26**)	(**17a**)	(**27a**)
Chemical Formula: $C_{12}H_{18}N_2O_2$	Chemical Formula: $C_6H_5ClO_2S$	Chemical Formula: $C_{18}H_{22}N_2O_4S$
Molecular Weight: 222.29	Molecular Weight: 176.61	Molecular Weight: 362.44
cLogP= 1.67	cLogP= 1.77	cLogP= 2.88
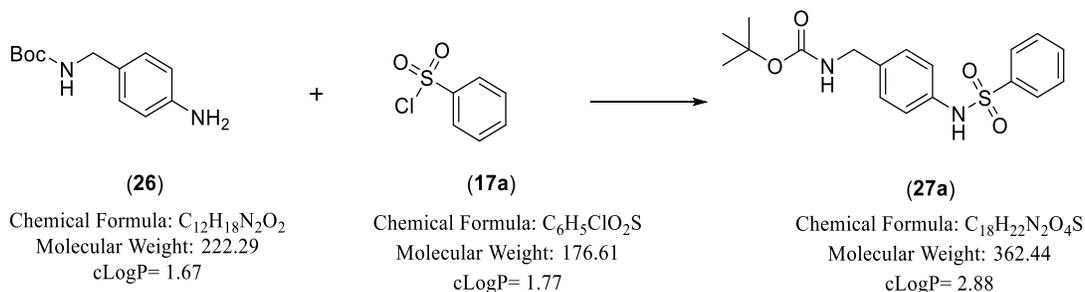
Method: see 7.4.12. The crude product was purified by gradient column chromatography eluting with petroleum ether – EtOAc 50:50 v/v.

Prepared from benzenesulfonyl chloride (**17a**, R^2= 4-H) (0.69 mL, 5.4 mmoL). Product obtained as a white solid, yield: 1.51 g (92%). TLC (petroleum ether-EtOAc 3:2 v/v), R*f* = 0.53. M.p. 160-162 °C. ^{1}H NMR (DMSO-d_6): δ 10.21 (s, 1H, N*H*SO$_2$Ar), 7.70 (d, *J* = 7.4 Hz, 2H, Ar), 7.60 (t, *J* = 7.3 Hz, 1H, Ar), 7.54 (m, 2H, Ar), 7.27 (t, *J* = 6.3 Hz, 1H, N*H*CH$_2$), 7.08 (d, *J* = 8.5 Hz, 2H, Ar), 7.02 (d, *J* = 8.5 Hz, 2H, Ar), 4.01 (d, *J* = 6.1 Hz, 2H, NHC*H$_2$*), 1.37 (s, 9H, C(C*H$_3$)$_3$*).

tert-Butyl (4-((4-fluorophenyl)sulfonamido)benzyl)carbamate (27b)

(**26**)	(**17b**)	(**27b**)
Chemical Formula: $C_{12}H_{18}N_2O_2$	Chemical Formula: $C_6H_4ClFO_2S$	Chemical Formula: $C_{18}H_{21}FN_2O_4S$
Molecular Weight: 222.29	Molecular Weight: 194.60	Molecular Weight: 380.43
cLogP= 1.67	cLogP= 1.92	cLogP= 3.04
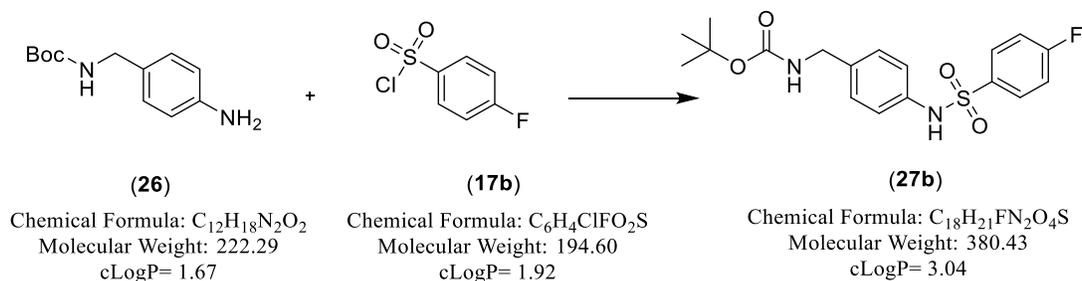
Method: see 7.4.12. The product was washed with Et$_2$O (3 x 50 mL).

Prepared from 4-fluorobenzenesulfonyl chloride (**17b**, R^2= 4-F) (1.05g, 5.4 mmoL). Product obtained as a light orange solid, yield: 1.49 g (87%). TLC (petroleum ether-EtOAc 1:1 v/v), R*f*

= 0.8. M.p. 174-176 °C. ^{1}H NMR (DMSO-d_6): δ 10.23 (brs, 1H, N*H*SO₂Ar), 7.80 (dd, J = 5.0, 10.0 Hz, 2H, Ar), 7.38 (t, J = 10.0 Hz, 2H, Ar), 7.28 (dd, J = 10.0, 5.0 Hz, 1H, N*H*CH₂), 7.10 (d, J = 5.0 Hz, 2H, Ar), 7.03 (d, J = 5.0 Hz, 2H, Ar), 4.02 (d, J = 5.0 Hz, 2H, NHC*H₂*), 1.38 (s, 9H, C(C*H₃*)₃). ^{13}C NMR (DMSO-d_6): δ 165.73 (C, *C*-F), 163.73 (C, *C*=O), 156.22 (C, Ar), 136.73 (C, Ar), 136.40 (C, Ar), 130.22 (CH, Ar), 130.14 (CH, Ar), 128.23 (2 x CH, Ar), 120.93 (2 x CH, Ar), 116.99 (CH, Ar), 116.81 (CH, Ar), 78.25 (C, *C*(CH₃)₃), 43.24 (NH*C*H₂), 28.68 (*C*(CH₃)₃). Anal. Calcd for C₁₈H₂₁FN₂O₄S•0.1H₂O (382.23482): C, 56.56%; H, 5.59%; N, 7.33%. Found: C, 56.18%; H, 5.77%; N, 7.07%.

tert-Butyl (4-((4-chlorophenyl)sulfonamido)benzyl)carbamate (27c)

(26)	**(17c)**	**(27c)**
Chemical Formula: C₁₂H₁₈N₂O₂	Chemical Formula: C₆H₄Cl₂O₂S	Chemical Formula: C₁₈H₂₁ClN₂O₄S
Molecular Weight: 222.29	Molecular Weight: 211.06	Molecular Weight: 396.89
cLogP= 1.67	cLog P= 2.32	cLog P= 3.44
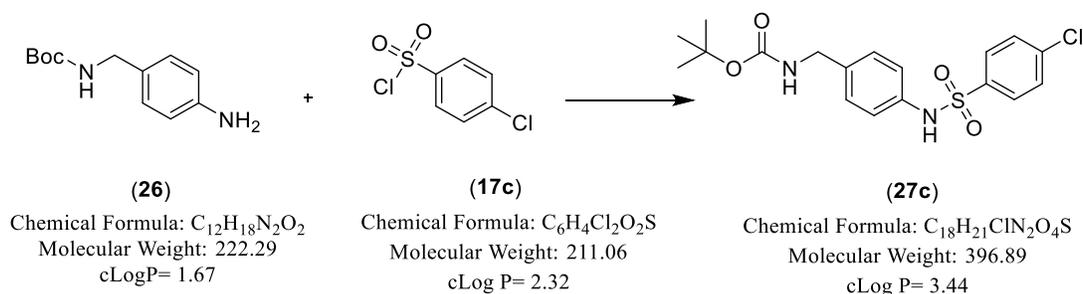
Method: see 7.4.12. The product was washed with Et₂O (3 x 50 mL).

Prepared from 4-chlorobenzenesulfonyl chloride (**17c,** R²= 4-Cl) (1.14, 5.4 mmoL). Product obtained as an orange coloured solid, yield: 1.27 g (71%). TLC (petroleum ether-EtOAc 3:2 v/v), Rf = 0.69. M.p. 136-138 °C. ^{1}H NMR (DMSO-d_6): δ 10.29 (brs, 1H, N*H*SO₂), 7.73 (d, J = 8.7 Hz, 2H, Ar), 7.62 (d, J = 8.6 Hz, 2H, Ar), 7.28 (t, J = 6.1 Hz, 1H, N*H*CH₂), 7.10 (d, J = 8.7 Hz, 2H, Ar), 7.02 (d, J = 8.5 Hz, 2H, Ar), 4.01 (d, J = 6.1 Hz, NHC*H₂*), 1.37 (s, 9H, C(C*H₃*)₃). ^{13}C NMR (DMSO-d_6): δ 156.21 (C, C=O), 138.81 (C, Ar), 138.19 (C, C-Cl), 136.83 (C, Ar), 136.25 (C, Ar), 129.88 (2 x CH, Ar), 129.07 (2 x CH, Ar), 128.26 (2 x CH, Ar), 121.03 (2 x CH, Ar), 78.26 (*C*(CH₃)₃), 43.24 (NH*C*H₂), 28.69 (C(C*H₃*)₃). Anal. Calcd for C₁₈H₂₁ClN₂O₄S (396.8879): C, 54.47%; H, 5.33%; N, 7.05%. Found: C, 54.74%; H, 5.37%; N, 7.10%. HRMS (ESI), m/z. calcd for C₁₈H₂₁ClN₂O₄SNa ([M + Na]⁺), 419.0803; found, 419.0809.

tert-**Butyl (4-((4-methoxyphenyl)sulfonamido)benzyl)carbamate (27d)**

(26)
Chemical Formula: $C_{12}H_{18}N_2O_2$
Molecular Weight: 222.29
cLogP= 1.67

(17d)
Chemical Formula: $C_7H_7ClO_3S$
Molecular Weight: 206.64
cLog P= 1.64

(27d)
Chemical Formula: $C_{19}H_{24}N_2O_5S$
Molecular Weight: 392.47
cLog P= 2.75
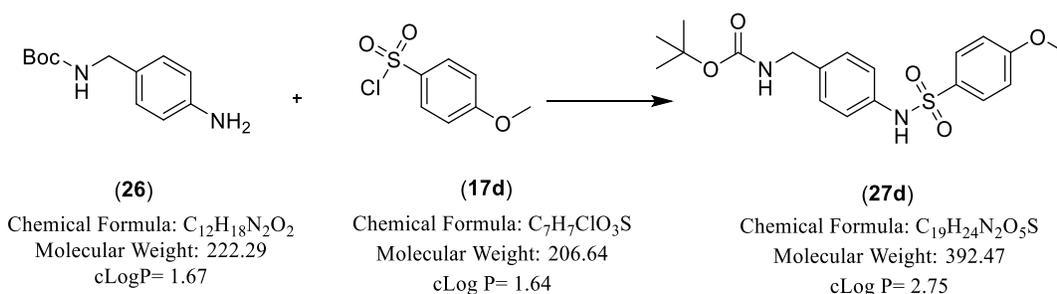
Method: see 7.4.12

Prepared from 4-methoxybenzenesulfonyl chloride (**17d**, R^2= 4-OCH_3) (1.12, 5.4 mmoL). Product obtained as a semi-solid orange coloured, yield: 1.75 g (99%). TLC (petroleum ether-EtOAc 3:2 v/v), Rf = 0.41. ^{1}H NMR (DMSO-d_6): δ 10.07 (brs, 1H, NHSO$_2$), 7.68 (d, J = 8.9 Hz, 2H, Ar), 7.27 (t, J = 6.0 Hz, 1H, NH), 7.04 (m, 6H, Ar), 4.00 (d, J = 6.1 Hz, 2H, NHCH_2), 3.79 (s, 3H, OCH_3), 1.37 (s, 9H, C(CH_3)$_3$). ^{13}C NMR (DMSO-d_6): δ 162.82 (C, C-OCH$_3$), 156.20 (C, C=O), 136.85 (C, Ar), 136.21 (C, Ar), 131.64 (C, Ar), 129.32 (2 x CH, Ar), 128.68 (2 x CH, Ar), 120.44 (2 x CH, Ar), 114.81 (2 x CH, Ar), 78.23 (C(CH$_3$)$_3$), 56.06 (OCH$_3$), 43.24 (NHCH$_2$), 28.69 (C(CH$_3$)$_3$). HRMS (ESI), m/z. calcd for $C_{19}H_{24}N_2O_5SNa$ ([M + Na]$^+$), 415.1298; found, 415.1311. HPLC (Method A): 98%, R$_t$ = 8.7 min.

(4-(Phenylsulfonamido)phenyl)methanaminium trifluoroacetic acid salt[90] (28a)

(27a)
Chemical Formula: $C_{18}H_{22}N_2O_4S$
Molecular Weight: 362.44
cLogP= 2.88

(28a)
Chemical Formula: $C_{15}H_{15}F_3N_2O_4S$
Molecular Weight: 376.35
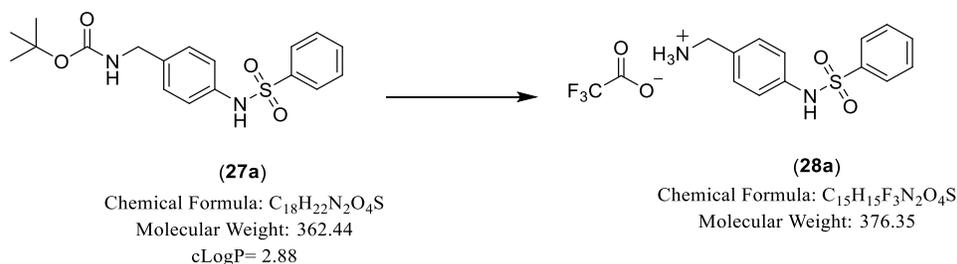
Method: see 7.4.10

Prepared from *tert*-butyl(4-(phenylsulfonamido)benzyl)carbamate (**27a**, R^2= 4-H, 1.45 g, 4.00 mmol). Product obtained as a very pale-yellow solid, yield: 1.44 g (95%). TLC (petroleum ether-EtOAc 1:1 v/v), Rf = 0.08. M.p. 212-214 °C. ^{1}H NMR (DMSO-d_6): δ 10.52 (brs, 1H, NHSO$_2$Ar), 8.20 (brs, 3H, NH_3), 7.80 (d, J = 7.3 Hz, 2H, Ar), 7.62 (t, J = 7.2 Hz, 1H, Ar), 7.56

(d, J = 7.5 Hz, 2H, Ar), 7.31 (d, J = 8.5 Hz, 2H, Ar), 7.13 (d, J = 8.5 Hz, 2H, Ar), 3.91 (s, 2H, NH$_3$CH_2). ^{13}C NMR (DMSO-d_6): δ 139.86 (C, C=O), 138.37 (C, Ar), 133.48 (CH, Ar), 130.41 (2 x CH, Ar), 129.92 (C, Ar), 129.92 (2 x CH, Ar), 127.15 (2 x CH, Ar), 120.04 (2 x CH, Ar), 42.14 (NHCH$_2$).

(4-((4-Fluorophenyl)sulfonamido)phenyl)methanaminium trifluoroacetic acid salt (28b)

(27b)
Chemical Formula: C$_{18}$H$_{21}$FN$_2$O$_4$S
Molecular Weight: 380.43
cLogP= 3.04

(28b)
Chemical Formula: C$_{15}$H$_{14}$F$_4$N$_2$O$_4$S
Molecular Weight: 394.34
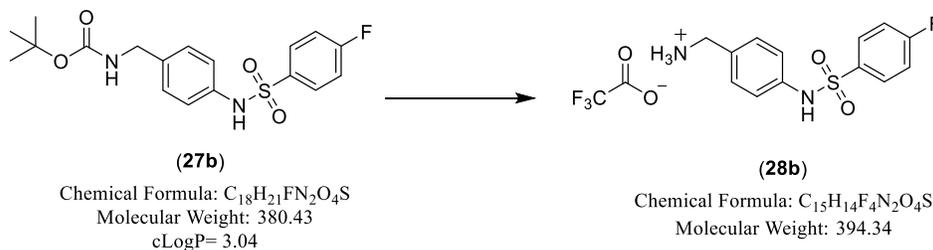
Method: see 7.4.10. The product was washed with Et$_2$O (3 x 50 mL).

Prepared from *tert*-butyl(4-((4-fluorophenyl)sulfonamido)benzyl)carbamate (**27b**, R^2= 4-F, 1.38 g, 4.00 mmol). Product obtained as an orange solid, yield: 1.39 g (97%). TLC (petroleum ether-EtOAc 1:1 v/v), Rf = 0.08. M.p. 224-226 °C. ^{1}H NMR (DMSO-d_6): δ 10.52 (brs, 1H, NHSO$_2$Ar), 8.18 (brs, 3H, NH_3), 7.86 (m, 2H, Ar), 7.41 (t, J = 8.8 Hz, 2H, Ar), 7.33 (d, J = 8.6 Hz, 2H, Ar), 7.13 (d, J = 8.6 Hz, 2H, Ar), 3.93 (s, 2H, NH$_3$CH_2). ^{13}C NMR (DMSO-d_6): δ 165.80 (C, C=O), 163.80 (C, C-F), 138.19 (C, Ar), 136.27 (C, Ar), 130.43 (2 x CH, Ar), 130.28 (CH, Ar), 130.14 (CH, Ar), 130.14 (C, Ar), 120.33 (2 x CH, Ar), 117.08 (CH, Ar), 116.90 (CH, Ar), 42.16 (NHCH$_2$). HPLC (Method A): 93%, R$_t$ = 0.5 min.

(4-((4-Chlorophenyl)sulfonamido)phenyl)methanaminium trifluoroacetic acid salt (28c)

(27c)
Chemical Formula: C$_{18}$H$_{21}$ClN$_2$O$_4$S
Molecular Weight: 396.89
cLog P= 3.44

(28c)
Chemical Formula: C$_{15}$H$_{14}$ClF$_3$N$_2$O$_4$S
Molecular Weight: 410.79
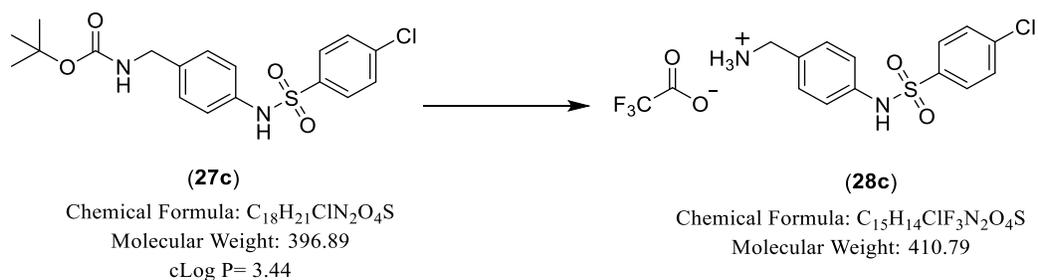
Method: see 7.4.10

Prepared from *tert*-butyl (4-((4-chlorophenyl)sulfonamido)benzyl)carbamate (**27c**, R^2= 4-Cl, 1.22 g, 3.09 mmol). Product obtained as a light orange solid, yield: 1.25 g (98 %). TLC (petroleum ether-EtOAc 1:1 v/v), Rf = 0.0. M.p. 240-242 °C. ^{1}H NMR (DMSO-d_6): δ 10.51 (s, 1H, N*H*SO$_2$), 8.10 (brs, 3H, $^+$N*H$_3$*CH$_2$), 7.78 (d, *J* = 8.8 Hz, 2H, Ar), 7.65 (d, *J* = 8.8 Hz, 2H, Ar), 7.32 (d, *J* = 8.6 Hz, 2H, Ar), 7.12 (d, *J* = 8.6 Hz, 2H, Ar), 3.92 (brs, 2H, $^+$NH$_3$C*H$_2$*). ^{19}F-NMR (DMSO-d_6): δ -73.52. ^{13}C NMR (DMSO-d_6): δ 176.62 (C, *C*=O), 158.52 & 158.27 (C, *C*F$_3$), 138.69 (C, Ar), 138.35 (C, Ar), 138.05 (C, Ar), 130.47 (2 x CH, Ar), 130.22 (C, Ar), 129.97 (2 x CH, Ar), 129.12 (2 x CH, Ar), 120.41 (2 x CH, Ar), 42.17 ($^+$NH$_3$*C*H$_2$). Anal. Calcd for (C$_{15}$H$_{14}$ClF$_3$N$_2$O$_4$S) (410.7948): C, 43.86%; H, 3.43%; N, 6.82%. Found: C, 44.06%; H, 3.59%; N, 6.81%. HPLC (Method A): 98%, R$_t$ = 0.5 min.

(4-((4-Methoxyphenyl)sulfonamido)phenyl)methanaminium trifluoroacetic acid salt (28d)

(27d)
Chemical Formula: C$_{19}$H$_{24}$N$_2$O$_5$S
Molecular Weight: 392.47
cLog P= 2.75

(28d)
Chemical Formula: C$_{16}$H$_{17}$F$_3$N$_2$O$_5$S
Molecular Weight: 406.38
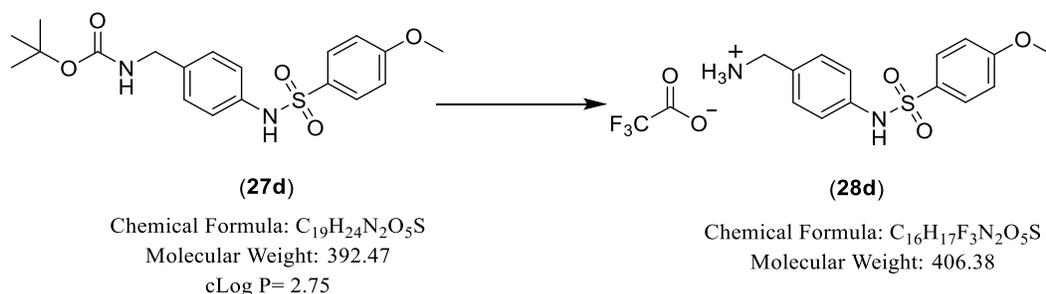
Method: see 7.4.10

Prepared from *tert*-butyl (4-((4-methoxyphenyl)sulfonamido)benzyl)carbamate (**27d**, R^2= 4-OCH$_3$, 1.71 g, 4.35 mmol). Product obtained as an orange solid, yield: 1.59 g (90 %). TLC (petroleum ether-EtOAc 1:1 v/v), Rf = 0.0. M.p. 214-216 °C. ^{1}H NMR (DMSO-d_6): δ 10.34 (s, 1H, N*H*SO$_2$), 8.11 (brs, 3H, $^+$N*H$_3$*CH$_2$), 7.72 (d, *J* = 9.0 Hz, 2H, Ar), 7.30 (d, *J* = 8.7 Hz, 2H, Ar), 7.12 (d, *J* = 8.6 Hz, 2H, Ar), 7.06 (d, *J* = 9.0 Hz, 2H, Ar), 3.91 (brs, 2H, $^+$NH$_3$C*H$_2$*), 3.80 (s, 3H, OC*H$_3$*). ^{19}F-NMR (DMSO-d_6): δ -73.53. ^{13}C NMR (DMSO-d_6): δ 176.61 (C, *C*-OCH$_3$), 162.93 (C, C=O), 158.56 & 158.32 (C, *C*F$_3$), 138.64 (C, Ar), 131.51 (C, Ar), 130.36 (2 x CH, Ar), 129.61 (C, Ar), 129.39 (2 x CH, Ar), 119.84 (2 x CH, Ar), 114.89 (2 x CH, Ar), 56.13 (OC*H$_3$*), 42.19 ($^+$NH$_3$*C*H$_2$). HPLC (Method A): 99%, R$_t$ = 0.5 min.

7.4.13 *N*-(4-(Aminomethyl)phenyl)benzenesulfonamide (29a)

(28a)
Chemical Formula: $C_{14}H_{15}F_3N_2O_4S$
Molecular Weight: 376.35

(29a)
Chemical Formula: $C_{13}H_{14}N_2O_2S$
Molecular Weight: 262.33
cLogP= 1.49
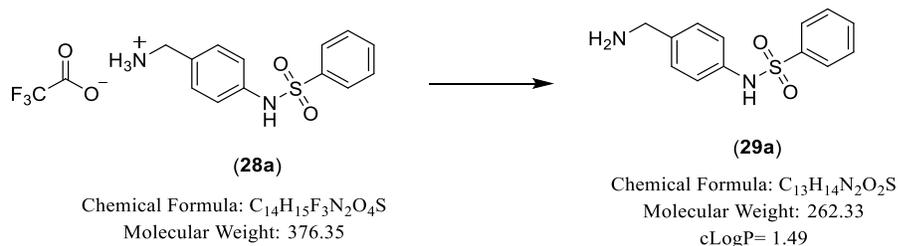
(4-(Phenylsulfonamido)phenyl)methanaminium trifluoroacetic acid salt (**29a**) (0.5 g, 1.33 mmoL) was dissolved in 2M aqueous NaOH (5 mL).[91] The solution was extracted with EtOAc (50 mL), washed with H_2O (3 x 50 mL) and dried ($MgSO_4$) then concentrated under vacuum to yield the free amine.

Product obtained as an off-white solid, yield: 0.12 g (35%). TLC (CH_2Cl_2: MeOH 9:1 v/v), R*f* = 0.15. M.p. 134-136 °C. ^{1}H NMR (DMSO-d_6): δ 7.75 (d, J = 8.3 Hz, 2H, Ar), 7.52 (m, 3H, Ar), 7.14 (d, J = 8.2 Hz, 1H, Ar), 6.99 (d, J = 8.3 Hz, 2H, Ar), 4.69 (brs, 3H, N*H*SO$_2$Ar + N*H$_2$*), 3.65 (s, 2H, NH$_2$C*H$_2$*). ^{13}C NMR (DMSO-d_6): δ 141.44 (C, Ar), 138.92 (C, Ar), 136.75 (C, Ar), 132.66 (CH, Ar), 129.44 (2 x CH, Ar), 128.49 (2 x CH, Ar), 127.04 (2 x CH, Ar), 120.66 (2 x CH, Ar), 44.83 (NH$_2$*C*H$_2$). Anal. Calcd for $C_{13}H_{14}N_2O_2S$•$0.2H_2O$ (265.92884): C, 58.72%; H, 5.46%; N, 10.53%. Found: C, 58.84%; H, 5.26%; N, 10.17%.

(*R/S*)-3-Hydroxy-2-phenyl-*N*-(4-(phenylsulfonamido)benzyl)propanamide (30a)

(28a)
Chemical Formula: $C_{15}H_{15}F_3N_2O_4S$
Molecular Weight: 376.35

(4a)
Chemical Formula: $C_9H_{10}O_3$
Molecular Weight: 166.18
cLogP= 1.04

(30a)
Chemical Formula: $C_{22}H_{22}N_2O_4S$
Molecular Weight: 410.49
cLogP= 2.76
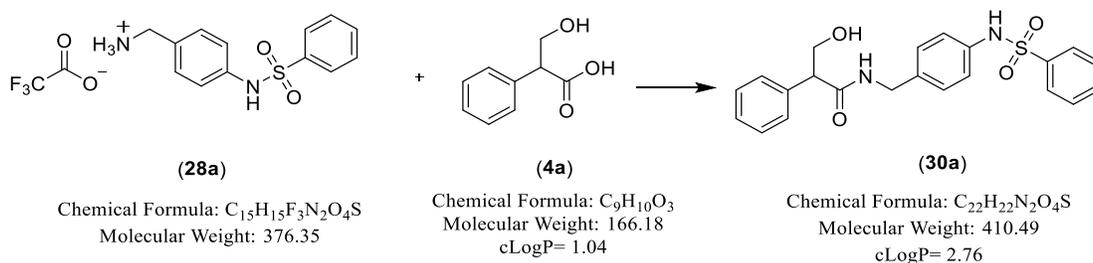
Method (1): see 7.4.4. The crude product was purified by gradient column chromatography eluting with petroleum ether – EtOAc 20:80 v/v.

Prepared from (4-(phenylsulfonamido)phenyl)methanaminium trifluoroacetic acid salt (**28a**) (0.25 g, 0.66 mmoL). Product obtained as a pale-yellow gum, yield: 0.08 g (30%). TLC (petroleum ether-EtOAc 1/1 v/v), R*f* = 0.08. ^{1}H NMR (DMSO-d_6): δ 10.21 (brs, 1H, N*H*SO$_2$Ar),

8.43 (t, J = 5.8 Hz, 1H, NH), 7.75 (d, J = 7.5 Hz, 2H, Ar), 7.60 (t, J = 7.3 Hz, 1H, Ar), 7.54 (t, J = 7.6 Hz, 2H, Ar), 7.29 (dd, J = 7.8, 14.6 Hz, 4H, Ar), 7.23 (t, J = 6.6 Hz, 1H, Ar), 7.03 (d, J = 8.5 Hz, 2H, Ar), 6.98 (d, J = 8.5 Hz, 2H, Ar), 4.84 (t, J = 5.1 Hz, 1H, OH), 4.22 (dd, J = 6.1, 15.4 Hz, 1H, NHCHaHb), 4.11 (dd, J = 5.7, 15.4 Hz, 1H, NHCHaHb), 3.98 (ddd, J = 5.7, 9.6, 15.0 Hz, 1H, CHCHaHb), 3.64 (dd, J = 5.5, 9.0 Hz, 1H, CHCHaHb), 3.53 (pentet, J = 5.0 Hz, 1H, CHCHaHb). ^{13}C NMR (DMSO-d_6): δ 172.16 (C, C=O), 140.00 (C, Ar), 138.83 (C, Ar), 136.63 (C, Ar), 135.73 (C, Ar), 133.30 (CH, Ar), 129.70 (2 x CH, Ar), 128.63 (2 x CH, Ar), 128.38 (2 x CH, Ar), 128.25 (2 x CH, Ar), 127.19 (CH, Ar), 127.10 (2 x CH, Ar), 120.58 (2 x CH, Ar), 63.79 (CHCH_2OH), 54.96 (CHCH$_2$OH), 41.86 (NHCH_2). HRMS (ESI), *m/z.* calcd for $C_{22}H_{23}N_2O_4S$ ([M + H]$^+$), 411.1400; found, 411.1373; and calcd for $C_{22}H_{22}N_2O_4SNa$ ([M + Na]$^+$), 433.1220; found, 433.1192. HPLC (Method A): 93%, R_t = 0.7 min.

Method (2): see 7.4.8

Prepared from tropic acid (**4a**, R^1= 4-H) (0.22 g, 1.33 mmol) and (4-(phenylsulfonamido)phenyl)methanaminium trifluoroacetic acid salt (**28a**, R^2= 4-H) (0.5 g, 1.33 mmoL). Product obtained as a white solid, yield: 0.37 g (68%). TLC (CH$_2$Cl$_2$-MeOH 9.5:0.5 v/v), Rf = 0.67. M.p. 58-60 °C. ^{1}H NMR (DMSO-d_6): δ 10.21 (brs, 1H, NHSO$_2$), 8.43 (t, J = 5.9 Hz, 1H, NH), 7.74 (d, J = 7.1 Hz, 2H, Ar), 7.60 (t, J = 7.4 Hz, 1H, Ar), 7.54 (t, J = 7.5 Hz, 2H, Ar), 7.26 (m, 5H, Ar), 7.02 (d, J = 8.7 Hz, 2H, Ar), 6.97 (d, J = 8.7 Hz, 2H, Ar), 4.83 (t, J = 5.2 Hz, 1H, OH), 4.20 (dd, J = 6.1, 15.4 Hz, 1H, NHCHaHb), 4.10 (dd, J = 5.7, 15.4 Hz, 1H, NHCHaHb), 3.97 (ddd, J = 5.6, 9.3, 15.5 Hz, 1H, CHCHaHb), 3.62 (dd, J = 5.4, 9.0 Hz, 1H, CHCHaHb), 3.51 (pentet, J = 5.1 Hz, 1H, CHCHaHb). ^{13}C NMR (DMSO-d_6): δ 172.14 (C, C=O), 139.96 (C, Ar), 138.82 (C, Ar), 136.61 (C, Ar), 135.72 (C, Ar), 133.31 (CH, Ar), 129.70 (2 x CH, Ar), 128.63 (2 x CH, Ar), 128.37 (2 x CH, Ar), 128.25 (2 x CH, Ar), 127.19 (CH, Ar), 127.09 (2 x CH, Ar), 120.55 (2 x CH, Ar), 63.77 (CHCH_2OH), 54.94 (CHCH$_2$OMs), 41.84 (NHCH_2). Anal. Calcd for $C_{22}H_{22}N_2O_4S$ (410.4868): C, 64.37%; H, 5.40%; N, 6.82%. Found: C, 64.40%; H, 5.72%; N, 7.22%. HRMS (ESI), m/z. calcd for $C_{22}H_{23}N_2O_4S$ ([M + H]$^+$), 411.1373; found, 411.1423; calcd for $C_{22}H_{22}N_2O_4SNa$ ([M + Na]$^+$), 433.1192; found, 433.1204.

(*R/S*)-*N*-(4-((4-Fluorophenyl)sulfonamido)benzyl)-3-hydroxy-2-phenylpropanamide (30b)

(28b)
Chemical Formula: $C_{15}H_{15}F_3N_2O_4S$
Molecular Weight: 376.35

(4a)
Chemical Formula: $C_9H_{10}O_3$
Molecular Weight: 166.18
cLogP= 1.04

(30b)
Chemical Formula: $C_{22}H_{21}FN_2O_4S$
Molecular Weight: 428.48
cLog P= 2.92
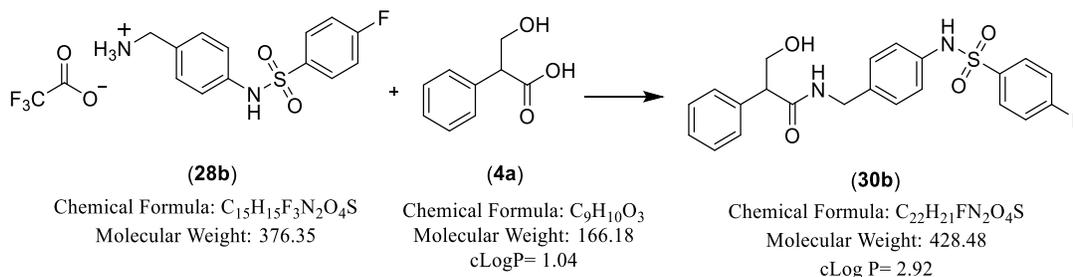
Method: see 7.4.8

Prepared from tropic acid (**4a**, R^1= 4-H) (0.21 g, 1.27 mmol) and (4-((4-fluorophenyl)sulfonamido)phenyl)methanaminium trifluoroacetic acid salt (**28b**, R^2= 4-F) (0.5 g, 1.27 mmoL).

Product obtained as a white solid, yield: 0.36 g (67%). TLC (CH_2Cl_2-MeOH 9.5:0.5 v/v), R*f* = 0.64. M.p. 62-64 °C. ^{1}H NMR (DMSO-d_4): δ 10.23 (s, 1H, N*H*SO$_2$), 8.44 (t, *J* = 5.9 Hz, 1H, N*H*), 7.78 (dd, *J* = 5.2, 9.0 Hz, 2H, Ar), 7.38 (t, *J* = 8.9 Hz, 2H, Ar), 7.28 (m, 4H, Ar), 7.22 (m, 1H, Ar), 7.03 (d, *J* = 8.6 Hz, 2H, Ar), 6.97 (d, *J* = 8.6 Hz, 2H, Ar), 4.84 (t, *J* = 5.2 Hz, 1H, O*H*), 4.21 (dd, *J* = 6.1, 15.4 Hz, 1H, NHC*Ha*Hb), 4.11 (dd, *J* = 5.7, 15.4 Hz, 1H, NHCHa*Hb*), 3.97 (ddd, *J* = 5.6, 9.9, 15.9 Hz, CHC*Ha*Hb), 3.62 (dd, *J* = 5.5, 9.1 Hz, C*H*CHaHb), 3.52 (pentet, *J* = 5.1 Hz, 1H, CHCHa*Hb*). ^{13}C NMR (DMSO-d_6): δ 172.17 (C, C=O), 156.71 (C, Ar), 163.71 (C, Ar), 138.80 (C, Ar), 136.45 (C, Ar), 135.94 (C, Ar), 130.19 (CH, Ar), 130.12 (CH, Ar), 128.63 (2 x CH, Ar), 128.37 (2 x CH, Ar), 128.29 (2 x CH, Ar), 127.19 (CH, Ar), 120.80 (2 x CH, Ar), 117.00 (CH, Ar), 116.82 (CH, Ar), 63.76 (CH*C*H$_2$OH), 54.95 (*C*HCH$_2$OH), 41.83 (NH*C*H$_2$). HRMS (ESI), *m/z*. calcd for $C_{22}H_{22}FN_2O_4S$ ([M + H]$^+$), 429.1279; found, 429.1305; calcd for $C_{22}H_{21}FN_2O_4SNa$ ([M + Na]$^+$), 451.1098; found, 451.1113. HPLC (Method A): 89%, R_t = 7.4 min.

(*R/S*)-*N*-(4-((4-Chlorophenyl)sulfonamido)benzyl)-3-hydroxy-2-phenylpropanamide (30c)

(**28c**)
Chemical Formula: $C_{15}H_{14}ClF_3N_2O_4S$
Molecular Weight: 410.79

(**4a**)
Chemical Formula: $C_9H_{10}O_3$
Molecular Weight: 166.18
cLogP= 1.04

(**30c**)
Chemical Formula: $C_{22}H_{21}ClN_2O_4S$
Molecular Weight: 444.93
cLog P: 3.32
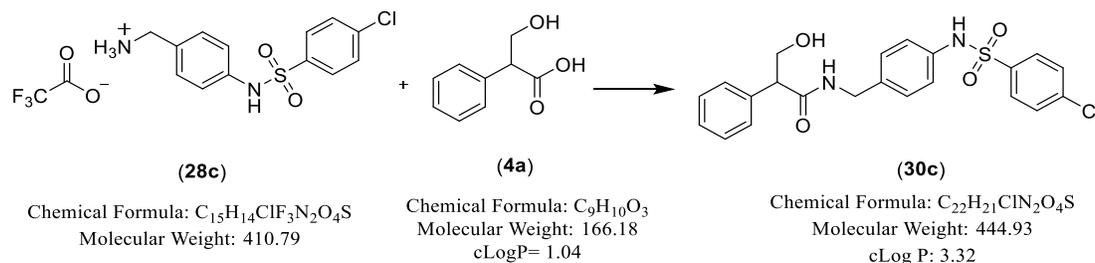
Method: see 7.4.8

Prepared from tropic acid (**4a**, R^1= 4-H) (0.20 g, 1.22 mmoL) and (4-((4-chlorophenyl)sulfonamido)phenyl)methanaminium trifluoroacetic acid salt (**28c**, R^2= 4-Cl) (0.5 g, 1.22 mmoL).

Product obtained as a white solid, yield: 0.45 g (84 %). TLC (CH_2Cl_2-MeOH 9.5:0.5 v/v), R*f* = 0.42. M.p. 150-152 °C. ^1H NMR (DMSO-d_6): δ 10.28 (brs, 1H, N*H*SO$_2$), 8.44 (t, *J* = 5.9 Hz, 1H, N*H*), 7.72 (d, *J* = 8.8 Hz, 2H, Ar), 7.62 (d, *J* = 8.8 Hz, 2H, Ar), 7.26 (m, 5H, Ar), 7.04 (d, *J* = 8.6 Hz, 2H, Ar), 6.96 (d, *J* = 8.6 Hz, 2H, Ar), 4.84 (t, *J* = 5.2 Hz, 1H, O*H*), 4.21 (dd, *J* = 6.1, 15.4 Hz, 1H, NHC*Ha*Hb), 4.11 (dd, *J* = 5.7, 15.4 Hz, 1H, NHCHa*Hb*), 4.00 (ddd, *J* = 5.6, 9.9, 14.9 Hz, 1H, CHC*Ha*Hb), 3.63 (dd, *J* = 5.4, 9.1 Hz, 1H, C*H*CHaHb), 3.52 (pentet, *J* = 5.1 Hz, 1H, CHCHa*Hb*). ^{13}C NMR (DMSO-d_6): δ 172.16 (C, C=O), 138.81 (C, Ar), 138.78 (C, *C*-Cl), 138.20 (C, Ar), 136.27 (C, Ar), 136.09 (C, Ar), 129.89 (2 x CH, Ar), 129.06 (2 x CH, Ar), 128.63 (2 x CH, Ar), 128.38 (2 x CH, Ar), 128.34 (2 x CH, Ar), 127.19 (CH, Ar), 120.89 (2 x CH, Ar), 63.77 (CH*C*H$_2$OH), 54.95 (*C*HCH$_2$OH), 41.84 (NH*C*H$_2$). HRMS (ESI), *m/z*. calcd for $C_{22}H_{21}ClN_2O_4SNa$ ([M + Na]$^+$), 467.0809; found, 467.0799. HPLC (Method A): 100%, R_t = 4.23 min.

(*R/S*)-*N*-(4-((4-Methoxyphenyl)sulfonamido)benzyl)-3-hydroxy-2-phenylpropanamide (30d)

(28d)
Chemical Formula: $C_{16}H_{17}F_3N_2O_5S$
Molecular Weight: 406.38

(4a)
Chemical Formula: $C_9H_{10}O_3$
Molecular Weight: 166.18
cLogP= 1.04

(30d)
Chemical Formula: $C_{23}H_{24}N_2O_5S$
Molecular Weight: 440.51
cLog P: 2.64
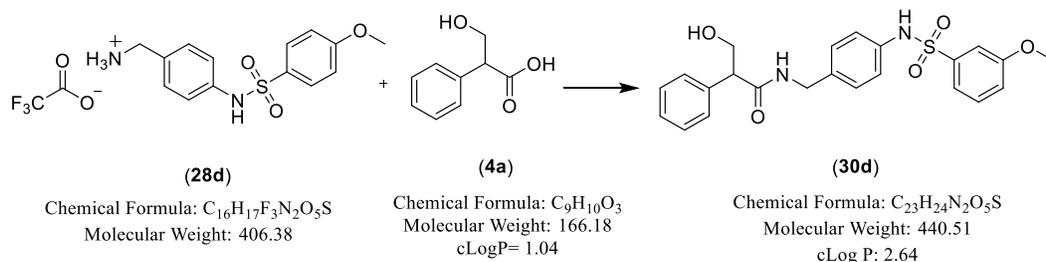
Method: see 7.4.8

Prepared from tropic acid (**4a**, R^1= 4-H) (0.20 g, 1.23 mmoL) and (4-((4-methoxyphenyl)sulfonamido)phenyl)methanaminium trifluoroacetic acid salt (**28d**, R^2= 4-OCH$_3$) (0.5 g, 1.23 mmoL).

Product obtained as an off-white solid, yield: 0.47 g (87 %). TLC (CH$_2$Cl$_2$-MeOH 9.5:0.5 v/v), Rf = 0.5. M.p. 126-128 °C. ^{1}H NMR (DMSO-d_6): δ 10.06 (brs, 1H, N*H*SO$_2$), 8.43 (t, *J* = 5.9 Hz, 1H, N*H*), 7.67 (d, *J* = 9.0 Hz, 2H, Ar), 7.26 (m, 5H, Ar), 7.05 (d, *J* = 9.0 Hz, 2H, Ar), 7.02 (d, *J* = 8.7 Hz, 2H, Ar), 6.96 (d, *J* = 8.7 Hz, 2H, Ar), 4.84 (t, *J* = 5.2 Hz, 1H, O*H*), 4.20 (dd, *J* = 6.1, 15.4 Hz, 1H, NHC*Ha*Hb), 4.10 (dd, *J* = 5.7, 15.4 Hz, 1H, NHCHa*Hb*), 3.97 (ddd, *J* = 5.7, 9.9, 14.9 Hz, 1H, CHC*Ha*Hb), 3.79 (s, 3H, OC*H$_3$*), 3.62 (dd, *J* = 5.4, 9.1 Hz, 1H, C*H*CHaHb), 3.52 (pentet, *J* = 5.1 Hz, 1H, CHCHa*Hb*). ^{13}C NMR (DMSO-d_6): δ 172.15 (C, C=O), 162.82 (C, *C*-OCH$_3$), 138.82 (C, Ar), 136.87 (C, Ar), 135.45 (C, Ar), 131.60 (C, Ar), 129.31 (2 x CH, Ar), 128.63 (2 x CH, Ar), 128.37 (2 x CH, Ar), 128.20 (2 x CH, Ar), 127.19 (CH, Ar), 120.31 (2 x CH, Ar), 114.82 (2 x CH, Ar), 63.77 (CH*C*H$_2$OH), 56.08 (O*C*H$_3$), 54.94 (*C*HCH$_2$OH), 41.85 (NH*C*H$_2$). HRMS (ESI), *m/z*. calcd for $C_{23}H_{24}N_2O_5SNa$ ([M + Na]$^+$), 463.1304; found, 463.1295. HPLC (Method A): 99%, R$_t$ = 4.06 min.

(*R/S*)-3-Oxo-2-phenyl-3-((4-(phenylsulfonamido)benzyl)amino)propyl methanesulfonate (31a)
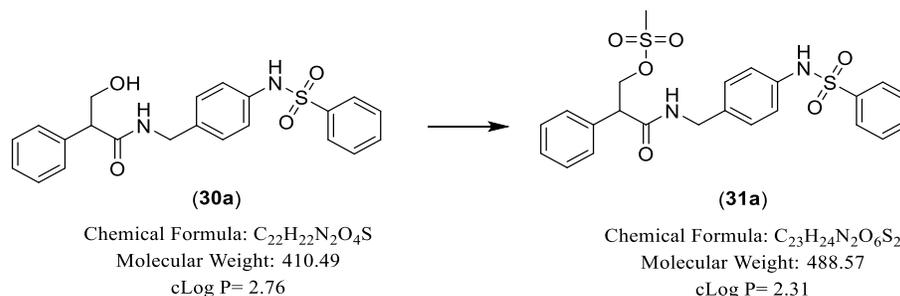
(**30a**)
Chemical Formula: $C_{22}H_{22}N_2O_4S$
Molecular Weight: 410.49
cLog P= 2.76

(**31a**)
Chemical Formula: $C_{23}H_{24}N_2O_6S_2$
Molecular Weight: 488.57
cLog P= 2.31

Method: see 7.4.5. The crude product was purified by gradient column chromatography eluting with petroleum ether – EtOAc 40:60 v/v.

Prepared from (*R/S*)-3-hydroxy-2-phenyl-*N*-(4-(phenylsulfonamido)benzyl)propanamide (**30a**, R^2= 4-H) (0.33 g, 0.81 mmoL). Product obtained as a white solid, yield: 0.35 g (90 %). TLC (petroleum ether-EtOAc 1:1 v/v), Rf = 0.37. M.p. 80-82 °C. ^{1}H NMR (DMSO-d_6): δ 10.22 (brs, 1H, N*H*SO$_2$), 8.85 (t, *J* = 6.0 Hz, 1H, N*H*), 7.81 (d, *J* = 7.7 Hz, 3H, Ar), 7.67 (t, *J* = 6.8 Hz, 2H, Ar), 7.38 (m, 5H, Ar), 7.21 (d, *J* = 8.5 Hz, 2H, Ar), 7.11 (d, *J* = 8.5 Hz, 2H, Ar), 4.74 (t, *J* = 9.6 Hz, 1H, CHC*Ha*Hb), 4.38 (ddd, *J* = 5.9, 11.9, 16.5 Hz, 2H, NHC*Ha*Hb + CHCHa*Hb*), 4.28 (dd, *J* = 5.7, 15.8 Hz, 1H, NHCHa*Hb*), 4.04 (dd, *J* = 5.9, 8.4 Hz, 1H, C*H*CHaHb), 3.14 (s, 3H, SO$_2$C*H$_3$*). ^{13}C NMR (DMSO-d_6): δ 170.41 (C, C=O), 138.86 (C, Ar), 136.15 (C, Ar), 135.05 (CH, Ar), 132.67 (C, Ar), 131.39 (2 x CH, Ar), 129.97 (2 x CH, Ar), 129.10 (2 x CH, Ar), 128.47 (2 x CH, Ar), 128.45 (2 x CH, Ar), 128.29 (2 x CH, Ar), 128.19 (CH, Ar), 71.09 (CH*C*H$_2$OMs), 50.85 (*C*HCH$_2$OMs), 42.08 (NH*C*H$_2$), 37.04 (*C*H$_3$). HRMS (ESI), *m/z.* calcd for $C_{23}H_{25}N_2O_6S_2$ ([M + H]$^+$), 489.1196; found, 489.1149; and calcd for $C_{23}H_{24}N_2O_6S_2Na$ ([M + Na]$^+$), 511.0966; found, 511.0968. HPLC (Method A): 75%, R$_t$ = 4.40 min.

(*R/S*)-3-Oxo-2-phenyl-3-((4-(4-fluorophenylsulfonamido)benzyl)amino)propyl methanesulfonate (31b)

(30b)
Chemical Formula: $C_{22}H_{21}FN_2O_4S$
Molecular Weight: 428.48
cLog P= 2.92

(31b)
Chemical Formula: $C_{23}H_{23}FN_2O_6S_2$
Molecular Weight: 506.56
cLog P= 2.47
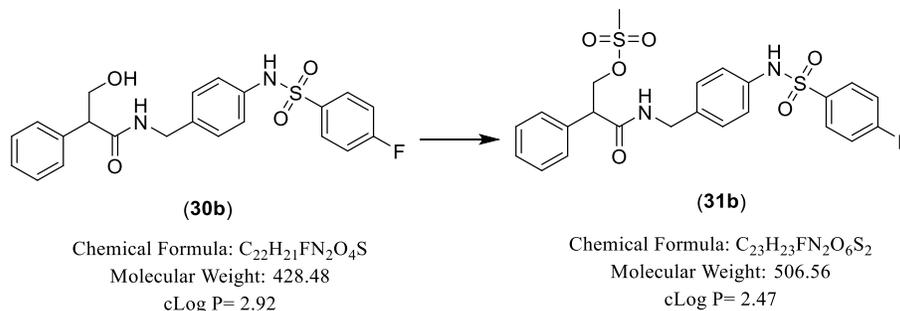
Method: see 7.4.5. The crude product was purified by gradient column chromatography eluting with petroleum ether – EtOAc 40:60 v/v.

Prepared from (*R/S*)-*N*-(4-((4-fluorophenyl)sulfonamido)benzyl)-3-hydroxy-2-phenylpropanamide (**30b**, R^2= 4-F) (0.34 g, 0.79 mmoL). Product obtained as a white solid, yield: 0.35 g (87 %). TLC (petroleum ether-EtOAc 1:1 v/v), R*f* = 0.5. M.p. 130-132 °C. ^{1}H NMR (DMSO-d_6): δ 10.24 (brs, 1H, N*H*SO$_2$), 8.85 (t, *J* = 6.0 Hz, 1H, N*H*), 7.88 (dd, *J* = 5.0, 9.0 Hz, 2H, Ar), 7.52 (t, *J* = 8.8 Hz, 2H, Ar), 7.36 (m, 5H, Ar), 7.22 (d, *J* = 8.4 Hz, 2H, Ar), 7.12 (d, *J* = 8.6 Hz, 2H, Ar), 4.73 (t, *J* = 9.6 Hz, 1H, CHC*Ha*Hb), 4.38 (d dd, *J* = 6.2; 5.6, 9.4 Hz, 2H, NHC*Ha*Hb + CHCHa*Hb*), 4.28 (dd, *J* = 5.7, 15.9 Hz, 1H, NHCHa*Hb*), 4.04 (dd, *J* = 5.3, 9.4 Hz, 1H, C*H*CHaHb), 3.14 (s, 3H, SO$_2$C*H$_3$*). ^{13}C NMR (DMSO-d_6): δ 170.42 (C, C=O), 166.77 (C, Ar), 142.05 (C, Ar), 136.14 (C, Ar), 135.10 (C, Ar), 132.55 (C, Ar), 131.86 (CH, Ar), 131.78 (CH, Ar), 131.39 (2 x CH, Ar), 129.11 (2 x CH, Ar), 128.47 (2 x CH, Ar), 128.35 (2 x CH, Ar), 128.19 (CH, Ar), 117.41 (CH, Ar), 117.23 (CH, Ar), 71.10 (CH*C*H$_2$OMs), 50.86 (*C*HCH$_2$OMs), 42.08 (NH*C*H$_2$), 37.03 (*C*H$_3$). HRMS (ESI), *m/z*. calcd for $C_{23}H_{23}FN_2O_6S_2Na$ ([M + Na]$^+$), 529.0874; found, 529.0883. HPLC (Method A): 79%, R_t = 4.47 min.

(*R/S*)-3-((4-((4-Chlorophenyl)sulfonamido)benzyl)amino)-3-oxo-2-phenylpropyl methanesulfonate (31c)
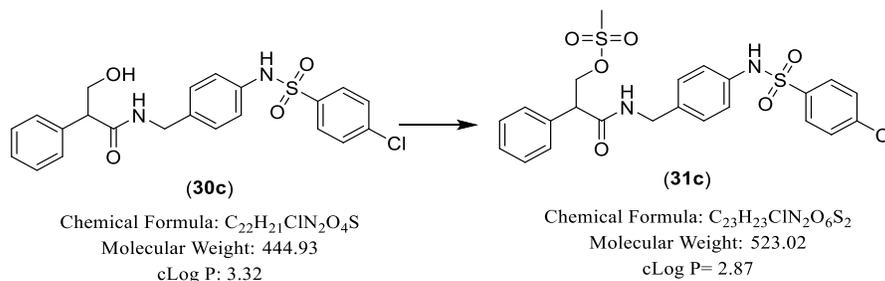
(30c)
Chemical Formula: $C_{22}H_{21}ClN_2O_4S$
Molecular Weight: 444.93
cLog P: 3.32

(31c)
Chemical Formula: $C_{23}H_{23}ClN_2O_6S_2$
Molecular Weight: 523.02
cLog P= 2.87

Method: see 7.4.5. The crude product was purified by gradient column chromatography eluting with petroleum ether – EtOAc 40:60 v/v.

Prepared from (*R/S*)-*N*-(4-((4-chlorophenyl)sulfonamido)benzyl)-3-hydroxy-2-phenylpropanamide (**30c**, R^2= 4-Cl) (0.42 g, 0.94 mmoL).

Product obtained as a white solid, yield: 0.22 g (45 %). TLC (petroleum ether-EtOAc 1:1 v/v), R*f* = 0.46. M.p. 158-160 °C. ^{1}H NMR (DMSO-d_6): δ 10.29 (brs, 1H, N*H*SO$_2$), 8.85 (t, *J* = 6.0 Hz, 1H, N*H*), 7.82 (d, *J* = 8.9 Hz, 2H, Ar), 7.76 (d, *J* = 8.9 Hz, 2H, Ar), 7.37 (m, 5H, Ar), 7.23 (d, *J* = 8.4 Hz, 2H, Ar), 7.14 (d, *J* = 8.6 Hz, 2H, Ar), 4.74 (t, *J* = 9.1 Hz, 1H, CHC*Ha*Hb), 4.38 (m, 2H, NHC*Ha*Hb + CHCHa*Hb*), 4.29 (dd, *J* = 5.7, 15.8 Hz, 1H, NHCHa*Hb*), 4.05 (m, 1H, C*H*CHaHb), 3.14 (s, 3H, SO$_2$C*H$_3$*). ^{13}C NMR (DMSO-d_6): δ 170.42 (C, C=O), 142.11 (C, Ar), 140.09 (C, C-Cl), 137.65 (C, Ar), 136.15 (C, Ar), 132.48 (C, Ar), 131.40 (2 x CH, Ar), 130.39 (2 x CH, Ar), 130.20 (2 x CH, Ar), 129.90 (CH, Ar), 129.10 (2 x CH, Ar), 128.47 (2 x CH, Ar), 128.18 (CH, Ar), 120.88 (CH, Ar), 71.10 (CH*C*H$_2$OMs), 50.85 (*C*HCH$_2$OMs), 42.08 (NH*C*H$_2$), 37.03 (*C*H$_3$). HRMS (ESI), *m/z*. calcd for $C_{23}H_{23}ClN_2O_6S_2Na$ ([M + Na]$^+$), 545.0584; found, 545.0574. HPLC (Method A): 100%, R$_t$ = 4.27 min.

(*R/S*)-3-((4-((4-Methoxyphenyl)sulfonamido)benzyl)amino)-3-oxo-2-phenylpropyl methanesulfonate (31d)

(30d)
Chemical Formula: $C_{23}H_{24}N_2O_5S$
Molecular Weight: 440.51
cLog P: 2.64

(31d)
Chemical Formula: $C_{24}H_{26}N_2O_7S_2$
Molecular Weight: 518.60
cLog P: 2.18
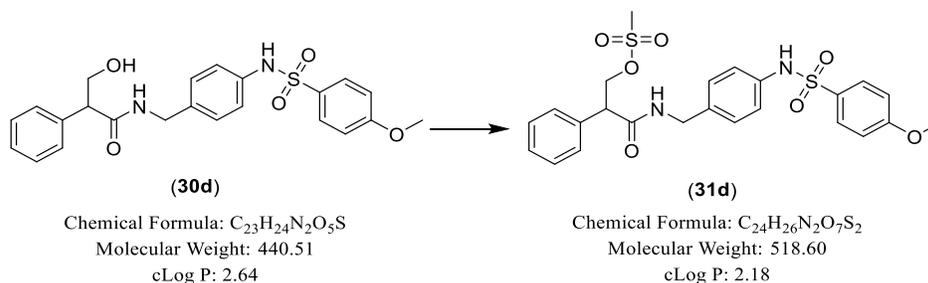
Method: see 7.4.5. The crude product was purified by gradient column chromatography eluting with petroleum ether – EtOAc 40:60 v/v.

Prepared from (*R/S*)-3-hydroxy-*N*-(4-((4-methoxyphenyl)sulfonamido)benzyl)-2-phenylpropanamide (**30d**, R^2= 4-OCH$_3$) (0.55 g, 1.26 mmoL).

Product obtained as a white solid, yield: 0.44 g (68 %). TLC (petroleum ether-EtOAc 1:1 v/v), Rf = 0.41. M.p. 110-114 °C. ^{1}H NMR (DMSO-d_6): δ 10.07 (brs, 1H, N*H*SO$_2$), 8.84 (t, *J* = 5.95 Hz, 1H, N*H*), 7.73 (d, *J* = 9.1 Hz, 2H, Ar), 7.66 (t, *J* = 9.0 Hz, 1H, Ar), 7.38 (m, 5H, Ar), 7.17 (d, *J* = 9.1 Hz, 2H, Ar), 7.04 (d, *J* = 9.0 Hz, 2H, Ar), 6.98 (d, *J* = 5.9 Hz, 2H, Ar), 4.73 (t, *J* = 9.6 Hz, 1H, CHC*Ha*Hb), 4.37 (ddd, *J* = 4.2, 9.8, 13.8 Hz, 2H, NHC*Ha*Hb + CHCHa*Hb*), 4.28 (dd, *J* = 5.7, 15.8 Hz, 1H, NHCHa*Hb*), 4.03 (d, *J* = 7.2 Hz, 1H, C*H*CHaHb), 3.89 (s, 3H, OC*H₃*), 3.14 (s, 3H, SO$_2$C*H₃*). ^{13}C NMR (DMSO-d_6): δ 170.41 (C, C=O), 164.21 (C, *C*-OCH$_3$), 141.81 (C, Ar), 136.15 (C, Ar), 132.86 (C, Ar), 131.37 (2 x CH, Ar), 130.97 (2 x CH, Ar), 130.06 (C, Ar), 129.32 (CH, Ar), 129.10 (2 x CH, Ar), 128.47 (2 x CH, Ar), 128.23 (2 x CH, Ar), 120.30 (CH, Ar), 114.82 (CH, Ar), 71.10 (CH*CH₂*OMs), 56.40 (O*CH₃*), 50.85 (*C*HCH$_2$OMs), 42.01 (NH*CH₂*), 37.03 (*C*H₃). HRMS (ESI), *m/z*. calcd for C$_{24}$H$_{26}$N$_2$O$_7$S$_2$Na ([M + Na]$^+$), 541.1079; found, 541.1068. HPLC (Method A): 100%, R$_t$ = 4.24 min.

(*R/S*)-2-Phenyl-*N*-(4-(phenylsulfonamido)benzyl)-3-(1*H*-1,2,4-triazol-1-yl) propanamide (18a) and 2-phenyl-*N*-(4-(phenylsulfonamido)benzyl)acrylamide (32a)
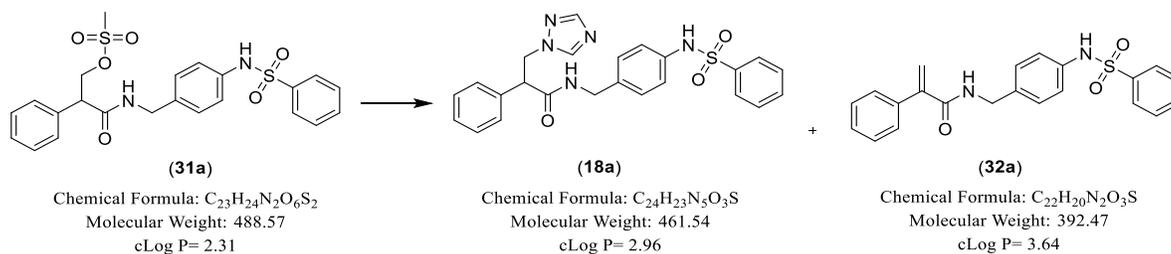
(31a)
Chemical Formula: C$_{23}$H$_{24}$N$_2$O$_6$S$_2$
Molecular Weight: 488.57
cLog P= 2.31

(18a)
Chemical Formula: C$_{24}$H$_{23}$N$_5$O$_3$S
Molecular Weight: 461.54
cLog P= 2.96

(32a)
Chemical Formula: C$_{22}$H$_{20}$N$_2$O$_3$S
Molecular Weight: 392.47
cLog P= 3.64

Method: see 7.4.6. Heated at 70 °C for 1h then rt, o/n. The crude product was purified by gradient column chromatography petroleum ether–EtOAc 40:60 v/v to elute (**32a**), then changed eluent to CH$_2$Cl$_2$-MeOH 90:10 v/v to elute (**18a**).

Prepared from (*R/S*)-3-oxo-2-phenyl-3-((4-(phenylsulfonamido)benzyl)amino)propyl methanesulfonate (**31a**) (0.32 g, 0.65 mmoL). *(R/S)-2-Phenyl-N-(4-*

*(phenylsulfonamido)benzyl)-3-(1H-1,2,4-triazol-1-yl) propanamide (**18a**, $R^2 = 4$-H)* obtained as a white solid, yield: 0.06 g (19 %). TLC (petroleum ether-EtOAc 1:1 v/v), Rf = 0.0. M.p. 96-98 °C. ^{1}H NMR (DMSO-d_6): δ 10.20 (brs, 1H, NHSO$_2$), 8.58 (t, J = 5.9 Hz, 1H, NH), 8.30 (s, 1H, triazole), 7.92 (s, 1H, triazole), 7.73 (d, J = 7.1 Hz, 2H, Ar), 7.61 (t, J = 7.4 Hz, 1H, Ar), 7.54 (t, J = 7.5 Hz, 2H, Ar), 7.31 (m, 5H, Ar), 6.93 (d, J = 8.6 Hz, 2H, Ar), 6.79 (d, J = 8.6 Hz, 2H, Ar), 4.80 (dd, J = 9.1, 13.5 Hz, 1H, CHCHaHb), 4.42 (dd, J = 6.6, 13.5 Hz, 1H, CHCHaHb), 4.18 (ddd, J = 6.5, 15.4, 20.9 Hz, 2H, CHCHaHb + NHCHaHb), 3.97 (dd, J = 5.8, 15.4 Hz, 1H, NHCHaHb). ^{13}C NMR (DMSO-d_6): δ 170.59 (C, C=O), 151.89 (CH, triazole), 145.63 (CH, triazole), 139.93 (C, Ar), 137.50 (C, Ar), 136.68 (C, Ar), 135.23 (C, Ar), 133.33 (CH, Ar), 129.70 (2 x CH, Ar), 128.96 (2 x CH, Ar), 128.21 (2 x CH, Ar), 128.05 (2 x CH, Ar), 127.91 (CH, Ar), 127.09 (2 x CH, Ar), 120.51 (2 x CH, Ar), 51.52 (CHCH$_2$), 51.08 (CHCH$_2$), 41.78 (NHCH$_2$). HRMS (ESI), m/z. calcd for C$_{24}$H$_{24}$N$_5$O$_3$S ([M + H]$^+$), 462.1594; found, 462.1613; calcd for C$_{24}$H$_{23}$N$_5$O$_3$SNa ([M + Na]$^+$), 484.1414; found, 484.1428. HPLC (Method B2): 99.9%, R$_t$ = 4.68 min. *2-Phenyl-N-(4-(phenylsulfonamido)benzyl)acrylamide (**32a**)* obtained as a white wax solid, yield: 0.15 g (51 %). TLC (petroleum ether-EtOAc 1:1 v/v), Rf = 0.46. ^{1}H NMR (DMSO-d_6): δ 10.25 (brs, 1H, NHSO$_2$), 8.63 (t, J = 6.0 Hz, 1H, NH), 7.77 (d, J = 7.1 Hz, 2H, Ar), 7.60 (t, J = 7.1 Hz, 1H, Ar), 7.54 (t, J = 7.45 Hz, 2H, Ar), 7.36 (m, 5H, Ar), 7.16 (d, J = 8.6 Hz, 2H, Ar), 7.06 (d, J = 8.6 Hz, 2H, Ar), 5.76 (s, 1H, C=CHaHb), 5.64 (s, 1H, C=CHaHb), 4.27 (d, J = 6.1 Hz, 2H, NHCH_2). ^{13}C NMR (DMSO-d_6): δ 168.65 (C, C=O), 145.56 (C, C=CH$_2$), 140.00 (C, Ar), 137.13 (C, Ar), 136.71 (C, Ar), 135.84 (C, Ar), 133.33 (CH, Ar), 129.71 (2 x CH, Ar), 128.77 (2 x CH, Ar), 128.55 (CH, Ar), 128.42 (2 x CH, Ar), 127.49 (2 x CH, Ar), 127.11 (2 x CH, Ar), 120.69 (2 x CH, Ar), 118.18 (C=CH$_2$), 42.21 (NHCH$_2$). HRMS (ESI), m/z. calcd for C$_{22}$H$_{21}$N$_2$O$_3$S ([M + H]$^+$), 393.1267; found, 393.1255; and calcd for C$_{22}$H$_{20}$N$_2$O$_3$SNa ([M + Na]$^+$), 415.1087; found, 415.1082. HPLC (Method A): 91%, R$_t$ = 8.4 min.

(*R/S*)-*N*-(4-((4-Fluorophenyl)sulfonamido)benzyl)-2-phenyl-3-(1*H*-1,2,4-triazol-1-yl) propanamide (18b) and *N*-(4-((4-fluorophenyl)sulfonamido)benzyl)-2-phenylacrylamide (32b)
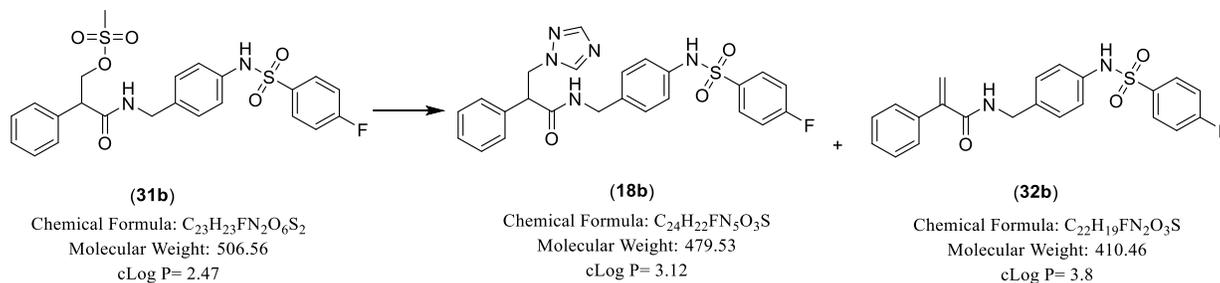
(31b)
Chemical Formula: $C_{23}H_{23}FN_2O_6S_2$
Molecular Weight: 506.56
cLog P= 2.47

(18b)
Chemical Formula: $C_{24}H_{22}FN_5O_3S$
Molecular Weight: 479.53
cLog P= 3.12

(32b)
Chemical Formula: $C_{22}H_{19}FN_2O_3S$
Molecular Weight: 410.46
cLog P= 3.8

Method: see 7.4.6. Heated at 70 °C for 1h then rt, o/n. The crude product was purified by gradient column chromatography petroleum ether–EtOAc 50:50 v/v to elute (**32b**), then changed eluent to CH_2Cl_2-MeOH 90:10 v/v to elute (**18b**).

Prepared from (*R/S*)-3-oxo-2-phenyl-3((4-(4-fluorophenylsulfonamido)benzyl)amino)propyl methanesulfonate (**31b**, R^2=4-F) (0.31 g, 0.62 mmoL). (*R/S*)-*N*-(4-((4-Fluorophenyl)sulfonamido)benzyl)-2-phenyl-3-(1H-1,2,4-triazol-1-yl) propanamide (**18b**, R^2= 4-F) obtained as a white solid, yield: 0.09 g (30 %). TLC (petroleum ether-EtOAc 1:1 v/v), R*f* = 0.0. M.p. 78-80 °C. ^{1}H NMR (DMSO-d_6): δ 10.21 (brs, 1H, N*H*SO$_2$), 8.59 (t, *J* = 5.9 Hz, 1H, N*H*), 8.31 (s, 1H, triazole), 7.93 (s, 1H, triazole), 7.79 (dd, *J* = 5.2, 8.9 Hz, 2H, Ar), 7.34 (m, 7H, Ar), 6.93 (d, *J* = 8.5 Hz, 2H, Ar), 6.81 (d, *J* = 8.5 Hz, 2H, Ar), 4.81 (dd, *J* = 9.1, 13.5 Hz, 1H, CHC*Ha*Hb), 4.43 (dd, *J* = 6.6, 13.5 Hz, 1H, CHCHa*Hb*), 4.19 (m, 2H, C*H*CHaHb + NHC*Ha*Hb), 3.99 (dd, *J* = 5.4, 15.4 Hz, 1H, NHCHa*Hb*). ^{13}C NMR (DMSO-d_6): δ 170.60 (C, C=O), 165.73 (C, Ar), 163.73 (C, Ar), 151.90 (CH, triazole), 143.33 (CH, triazole), 137.51 (C, Ar), 136.49 (C, Ar), 135.48 (C, Ar), 130.21 (CH, Ar), 130.13 (CH, Ar), 128.96 (2 x CH, Ar), 128.22 (2 x CH, Ar), 128.08 (2 x CH, Ar), 127.90 (CH, Ar), 120.76 (2 x CH, Ar), 117.00 (CH, Ar), 116.82 (CH, Ar), 51.53 (*C*HCH$_2$), 51.09 (*C*HCH$_2$), 41.78 (NH*C*H$_2$). Anal. Calcd for $C_{24}H_{22}FN_5O_3S$•0.1H$_2$O (481.32942): C, 59.89%; H, 4.65%; N, 14.55%. Found: C, 59.52%; H, 4.49%; N, 14.26%. HPLC (Method B2): 99.9%, R$_t$ = 4.69 min. *N*-(4-((4-Fluorophenyl)sulfonamido)benzyl)-2-phenylacrylamide (*32b*) obtained as a white solid, yield: 0.12 g (41 %). TLC (petroleum ether-EtOAc 1:1 v/v), R*f* = 0.5. M.p. 136-138 °C. ^{1}H NMR (DMSO-d_6): δ 10.27 (brs, 1H, N*H*SO$_2$), 8.64 (t, *J* = 6.1 Hz, 1H, N*H*), 7.81 (dd, *J* = 5.2, 9.0 Hz,

2H, Ar), 7.36 (m, 7H, Ar), 7.17 (d, J = 8.6 Hz, 2H, Ar), 7.06 (d, J = 8.6 Hz, 2H, Ar), 5.76 (s, 1H, C=C*Ha*Hb), 5.64 (s, 1H, C=CHa*Hb*), 4.28 (d, J = 6.1 Hz, 2H, NHC*H$_2$*). ^{13}C NMR (DMSO-*d$_6$*): δ 168.65 (C, C=O), 165.73 (C, Ar), 163.73 (C, Ar), 145.56 (C, *C*=CH$_2$), 137.13 (C, Ar), 136.50 (C, Ar), 136.09 (C, Ar), 130.22 (CH, Ar), 130.15 (CH, Ar), 128.76 (2 x CH, Ar), 128.54 (CH, Ar), 128.47 (2 x CH, Ar), 127.49 (2 x CH, Ar), 120.93 (2 x CH, Ar), 118.20 (C=*C*H$_2$), 117.02 (CH, Ar), 116.84 (CH, Ar), 42.20 (NHC*H$_2$*). HRMS (ESI), m/z. calcd for C$_{22}$H$_{20}$FN$_2$O$_3$S ([M + H]$^+$), 411.1173; found, 411.1173; and calcd for C$_{22}$H$_{19}$FN$_2$O$_3$SNa ([M + Na]$^+$), 433.0993; found, 433.0994. HPLC (Method A): 98%, R$_t$ = 8.6 min.

(R/S)-N-(4-((3-Chlorophenyl)sulfonamido)benzyl)-2-phenyl-3-(1H-1,2,4-triazol-1-yl) propanamide (18c) and N-(4-((3-chlorophenyl)sulfonamido)benzyl)-2-phenylacrylamide (32c)
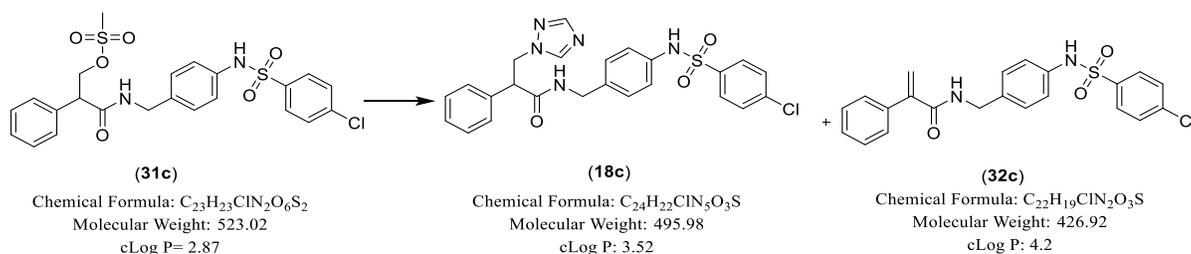
(31c)
Chemical Formula: C$_{23}$H$_{23}$ClN$_2$O$_6$S$_2$
Molecular Weight: 523.02
cLog P= 2.87

(18c)
Chemical Formula: C$_{24}$H$_{22}$ClN$_5$O$_3$S
Molecular Weight: 495.98
cLog P: 3.52

(32c)
Chemical Formula: C$_{22}$H$_{19}$ClN$_2$O$_3$S
Molecular Weight: 426.92
cLog P: 4.2

Method: see 7.4.6. Heated at 70 °C for 1h then rt, o/n. The crude product was purified by gradient column chromatography petroleum ether–EtOAc 50:50 v/v to elute (**32c**), then changed eluent to CH$_2$Cl$_2$-MeOH 90:10 v/v to elute (**18c**).

Prepared from (*R/S*)-3-((4-((4-chlorophenyl)sulfonamido)benzyl)amino)-3-oxo-2-phenylpropyl methanesulfonate (**31c**, R^2= 4-Cl) (0.20 g, 0.41 mmoL). (*R/S*)-N-(4-((3-Chlorophenyl)sulfonamido)benzyl)-2-phenyl-3-(1H-1,2,4-triazol-1-yl) propanamide (**18c**, R^2= 4-Cl) obtained as an off-white solid, yield: 0.02 g (11 %). TLC (petroleum ether-EtOAc 1:1 v/v), R*f* = 0.0. M.p. 122-124 °C. ^{1}H NMR (DMSO-*d$_6$*): δ 10.27 (brs, 1H, N*H*SO$_2$), 8.59 (t, J = 5.9 Hz, 1H, N*H*), 8.31 (s, 1H, triazole), 7.92 (s, 1H, triazole), 7.72 (d, J = 8.8 Hz, 2H, Ar), 7.63 (d, J = 8.8 Hz, 2H, Ar), 7.30 (m, 5H, Ar), 6.92 (d, J = 8.6 Hz, 2H, Ar), 6.81 (d, J = 8.6 Hz, 2H, Ar), 4.81 (dd, J = 9.1, 13.5 Hz, 1H, CHC*Ha*Hb), 4.43 (dd, J = 6.6, 13.5 Hz, 1H, CHCHa*Hb*), 4.19 (m, 2H, C*H*CHaHb + NHC*Ha*Hb), 3.99 (dd, J = 5.4, 15.4 Hz, 1H, NHCHa*Hb*). ^{13}C NMR (DMSO-*d$_6$*): δ 170.60 (C, C=O), 151.89 (CH, triazole), 143.81 (CH, triazole), 138.76 (C, Ar),

138.21 (C, C-Cl), 137.51 (C, Ar), 136.33 (C, Ar), 135.61 (C, Ar), 129.89 (2 x CH, Ar), 129.07 (2 x CH, Ar), 128.96 (2 x CH, Ar), 128.22 (2 x CH, Ar), 128.12 (2 x CH, Ar), 127.90 (CH, Ar), 120.85 (2 x CH, Ar), 51.52 (*CH*CH$_2$), 51.09 (CH*CH$_2$*), 41.78 (NH*CH$_2$*). HRMS (ESI), m/z. calcd for C$_{24}$H$_{23}$ClN$_5$O$_3$S ([M + H]$^+$), 455.1119; found, 455.1143. HPLC (Method B2): 99.9%, R$_t$ = 4.75 min. *N-(4-((4-Chlorophenyl)sulfonamido)benzyl)-2-phenylacrylamide (32c)* obtained as a white solid, yield: 0.10 g (50 %). TLC (petroleum ether-EtOAc 1:1 v/v), R*f* = 0.73. M.p. 164-166 °C. ^{1}H NMR (DMSO-*d$_6$*): δ 10.33 (brs, 1H, N*H*SO$_2$), 8.64 (t, *J* = 6.1 Hz, 1H, N*H*), 7.75 (d, *J* = 8.8 Hz, 2H, Ar), 7.63 (d, *J* = 8.8 Hz, 2H, Ar), 7.36 (m, 5H, Ar), 7.18 (d, *J* = 8.5 Hz, 2H, Ar), 7.05 (d, *J* = 8.5 Hz, 2H, Ar), 5.76 (s, 1H, C=C*Ha*Hb), 5.64 (s, 1H, C=CHa*Hb*), 4.28 (d, *J* = 6.1 Hz, 2H, NHC*H$_2$*). ^{13}C NMR (DMSO-*d$_6$*): δ 168.67 (C, C=O), 145.55 (C, *C*=CH$_2$), 138.81 (C, Ar), 138.22 (C, C-Cl), 137.12 (C, Ar), 136.20 (C, Ar), 129.90 (2 x CH, Ar), 129.08 (2 x CH, Ar), 128.77 (2 x CH, Ar), 128.55 (CH, Ar), 128.51 (2 x CH, Ar), 127.49 (2 x CH, Ar), 121.02 (2 x CH, Ar), 118.20 (C=*C*H$_2$), 42.21 (NH*CH$_2$*). HRMS (ESI), m/z. calcd for C$_{22}$H$_{20}$ClN$_2$O$_3$S ([M + H]$^+$), 427.0884; found, 427.0872. HPLC (Method A): 100%, R$_t$ = 4.37 min.

<u>(R/S)-2-Phenyl-*N*-(4-(4-methoxyphenylsulfonamido)benzyl)-3-(*1H*-1,2,4-triazol-1-yl) propanamide (18d) and 2-phenyl-*N*-(4-((4-methoxyphenylsulfonamido)benzyl) acrylamide (32d)</u>
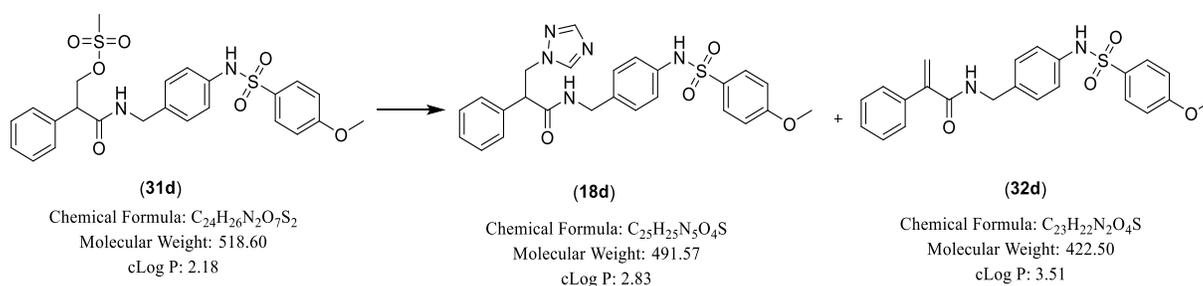
(31d)
Chemical Formula: C$_{24}$H$_{26}$N$_2$O$_7$S$_2$
Molecular Weight: 518.60
cLog P: 2.18

(18d)
Chemical Formula: C$_{25}$H$_{25}$N$_5$O$_4$S
Molecular Weight: 491.57
cLog P: 2.83

(32d)
Chemical Formula: C$_{23}$H$_{22}$N$_2$O$_4$S
Molecular Weight: 422.50
cLog P: 3.51

Method: see 7.4.6. Heated at 70 °C for 1h then rt, o/n. The crude product was purified by gradient column chromatography petroleum ether–EtOAc 40:60 v/v to elute (**32d**), then changed eluent to CH$_2$Cl$_2$-MeOH 90:10 v/v to elute (**18d**).

Prepared from (*R/S*)-3-((4-((4-methoxyphenyl)sulfonamido)benzyl)amino)-3-oxo-2-phenylpropyl methanesulfonate (**31d**, R^2= 4-OCH$_3$) (0.40 g, 0.77 mmoL). *(R/S)-2-Phenyl-N-(4-(4-methoxyphenylsulfonamido)benzyl)-3-(1H-1,2,4-triazol-1-yl)propanamide (18d, R^2= 4-*

OCH$_3$) obtained as a white solid, yield: 0.07 g (17 %). TLC (petroleum ether-EtOAc 1:1 v/v), R*f* = 0.0. M.p. 160-162 °C. ^{1}H NMR (DMSO-*d$_6$*): δ 10.05 (brs, 1H, N*H*SO$_2$), 8.58 (t, *J* = 5.9 Hz, 1H, N*H*), 8.31 (s, 1H, triazole), 7.92 (s, 1H, triazole), 7.67 (d, *J* = 9.0 Hz, 2H, Ar), 7.31 (m, 5H, Ar), 7.05 (d, *J* = 9.0 Hz, 2H, Ar), 6.93 (d, *J* = 8.5 Hz, 2H, Ar), 6.79 (d, *J* = 8.5 Hz, 2H, Ar), 4.81 (dd, *J* = 9.0, 13.4 Hz, 1H, CHC*Ha*Hb), 4.43 (dd, *J* = 6.6, 13.5 Hz, 1H, CHCHa*Hb*), 4.19 (m, 2H, C*H*CHaHb + NHC*Ha*Hb), 3.98 (dd, *J* = 5.4, 15.4 Hz, 1H, NHCHa*Hb*), 3.80 (s, 3H, OC*H$_3$*). ^{13}C NMR (DMSO-*d$_6$*): δ 170.59 (C, C=O), 162.85 (C, *C*-OCH$_3$), 151.84 (CH, triazole), 145.04 (CH, triazole), 137.57 (CH, Ar), 136.97 (C, Ar), 135.00 (C, Ar), 131.74 (C, Ar), 129.31 (2 x CH, Ar), 128.93 (2 x CH, Ar), 128.22 (2 x CH, Ar), 128.02 (2 x CH, Ar), 128.87 (CH, Ar), 120.36 (2 x CH, Ar), 114.81 (2 x CH, Ar), 56.09 (OC*H$_3$*), 51.58 (CHC*H$_2$*), 51.18 (*C*HCH$_2$), 41.87 (NHC*H$_2$*). HRMS (ESI), *m/z*. calcd for C$_{25}$H$_{26}$N$_5$O$_4$S ([M + H]$^+$), 492.1706; found, 492.1695. HPLC (Method B2): 99.99 %, R$_t$ = 4.68 min. *N-(4-((4-Methoxyphenyl)sulfonamido)benzyl)-2-phenylacrylamide (32d)* obtained as a white solid, yield: 0.17 g (44 %). TLC (petroleum ether-EtOAc 1:1 v/v), R*f* = 0.33. M.p. 98-100 °C. ^{1}H NMR (DMSO-*d$_6$*): δ 10.11 (brs, 1H, N*H*SO$_2$), 8.63 (t, *J* = 6.1 Hz, 1H, N*H*), 7.69 (d, *J* = 9.0 Hz, 2H, Ar), 7.38 (m, 5H, Ar), 8.65 (d, *J* = 8.7 Hz, 2H, Ar), 7.05 (d, *J* = 8.8 Hz, 4H, Ar), 5.76 (s, 1H, C=C*Ha*Hb), 5.64 (s, 1H, C=CHa*Hb*), 4.27 (d, *J* = 6.1 Hz, 2H, NHC*H$_2$*), 3.79 (s, 3H, OC*H$_3$*). ^{13}C NMR (DMSO-*d$_6$*): δ 168.65 (C, C=O), 162.84 (C, *C*-OCH$_3$), 145.56 (C, *C*=CH$_2$), 136.97 (C, Ar), 135.57 (C, Ar), 131.64 (C, Ar), 129.34 (2 x CH, Ar), 128.76 (2 x CH, Ar), 128.54 (CH, Ar), 128.38 (2 x CH, Ar), 127.49 (2 x CH, Ar), 120.43 (2 x CH, Ar), 118.16 (C=*C*H$_2$), 114.82 (2 x CH, Ar), 56.07 (OC*H$_3$*), 42.21 (NHC*H$_2$*). HRMS (ESI), *m/z*. calcd for C$_{23}$H$_{23}$N$_2$O$_4$S ([M + H]$^+$), 423.1379; found, 423.1368. HPLC (Method A): 100%, R$_t$ = 4.21 min.

7.4.14 *(R/S)-N-(2-Hydroxy-1-phenylethyl) benzamide (35)*[92]

(33)	(34a)	(35)
Chemical Formula: C$_8$H$_{11}$NO	Chemical Formula: C$_7$H$_5$ClO	Chemical Formula: C$_{15}$H$_{15}$NO$_2$
Molecular Weight: 137.18	Molecular Weight: 140.57	Molecular Weight: 241.29
cLog P = 0.54	cLog P= 2.17	cLog P= 2.37
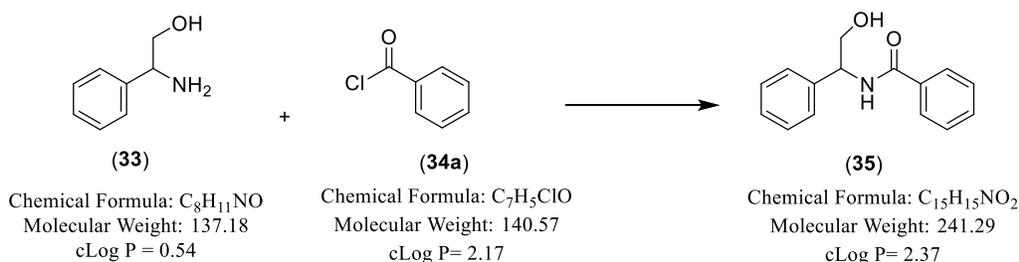
To an ice cooled solution of (*R/S*)-2-amino-2-phenylethan-1-ol (**33**) (1.00 g, 7.29 mmol) and Et$_3$N (1.5 mL, 10.95 mmol) in dry CH$_2$Cl$_2$ (14.5 mL), was added benzoyl chloride (**34a**,

R^1= 4-H) (0.84 mL, 7.29 mmol) in dry CH_2Cl_2 (14.5 mL) dropwise then the reaction was stirred at rt for 1 h. CH_2Cl_2 (20 mL) and water (20 mL) were added, and the layers were separated. The organic phase was dried ($MgSO_4$) and concentrated under vacuum. The resulting residue was triturated with Et_2O to afford the product as a white powder, yield: 1.24 g (70%). TLC (petroleum ether-EtOAc 1:1 v/v), R*f* = 0.33. M.p. 166-168 °C (lit. M.p. 158-159 °C)[92]. ^{1}H-NMR (DMSO-d$_6$): δ 8.71 (d, *J*= 8.0 Hz, 1H, N*H*), 7.93 (d, *J*= 7.5 Hz, 2H, Ar), 7.40 (m, 8H, Ar), 5.10 (dd, *J*= 7.0, 6.5 Hz, 1H, C*H*CH$_2$), 4.95 (t, *J*= 5.5 Hz, 1H, O*H*), 3.71 (m, 2H, CHC*H*$_2$).

7.4.15 (*R/S*)-2,4-Diphenyl-4,5-dihydrooxazole (39)[92]

(35)
Chemical Formula: $C_{15}H_{15}NO_2$
Molecular Weight: 241.29
cLog P= 2.37

(39)
Chemical Formula: $C_{15}H_{13}NO$
Molecular Weight: 223.28
cLogP= 3.78
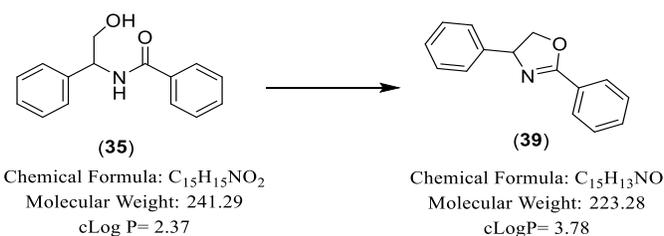
Method (1): see 7.4.5. The crude product was purified by gradient column chromatography eluted with petroleum ether – EtOAc 80:20 v/v.

Prepared from (*R/S*)-*N*-(2-hydroxy-1-phenylethyl) benzamide (**35**) (0.3 g, 1.24 mmol). Product obtained as a colourless viscous oil, yield: 0.11 g (28%). TLC (petroleum ether-EtOAc 1:1 v/v), R*f* = 0.85. ^{1}H NMR (CDCl$_3$): δ 8.09 (d, *J* = 7.1 Hz, 2H, Ar), 7.54 (t, *J* = 7.4 Hz, 1H, Ar), 7.47 (t, *J* = 7.3 Hz, 2H, Ar), 7.35 (m, 5H, Ar), 5.42 (dd, *J* = 8.2, 10.1 Hz, 1H, NC*H*CHaHb), 4.83 (dd, *J* = 8.4, 10.1 Hz, 1H, NCHC*Ha*Hb), 4.31 (t, *J* = 8.3 Hz, 1H, NCHCHa*Hb*). ^{13}C NMR (CDCl$_3$): δ 164.77 (C, *C*=N-), 142.41 (C, Ar), 131.58 (CH, Ar), 128.79 (2 x CH, Ar), 128.51 (2 x CH, Ar), 128.41 (2 x CH, Ar), 127.66 (CH, Ar), 127.59 (C, Ar), 126.79 (2 x CH, Ar), 74.92 (NCH*C*H$_2$), 70.15 (N*C*HCH$_2$).

Method (2)

To a stirred solution of (*R/S*)-*N*-(2-hydroxy-1-phenylethyl) benzamide (**35**) (0.30 g, 1.24 mmol), in dry CH_2Cl_2 (18 mL), was added $SOCl_2$ (0.9 mL, 12.43 mmol) dropwise at 0 °C. The reaction was stirred at room temperature for 4 h, then concentrated under reduced pressure.[93] The residue was quenched with saturated aqueous $NaHCO_3$ solution (5 mL) and extracted with CH_2Cl_2 (50 mL). The organic layer was separated, washed with brine (3 x 50 mL) and water (2

x 50 mL), dried ($MgSO_4$) and evaporated under vacuum. The product was obtained as an off-white semi-solid, yield: 0.23 g (72%). TLC (petroleum ether-EtOAc 3:1 v/v), Rf = 0.62.

Method (3)

A solution of (*R/S*)-*N*-(2-hydroxy-1-phenylethyl) benzamide (**35**) (1.00 g, 4.14 mmol) in dry THF (18.00 mL) was cooled to 0 °C. Then methanesulfonyl chloride (0.64 mL, 8.29) was added and the resulting mixture stirred at rt for 3 h. Et_3N (1.27 mL, 9.12 mmol) was added dropwise, and the solution was stirred overnight at rt. The mixture was quenched by the addition of NH_4OH (25%) and the reaction stirred at rt for 30 min. Then THF was removed under reduced pressure and the residue was extracted between EtOAc (100 mL) and water (2 x 100 mL). The combined organic layer dried ($MgSO_4$) and concentrated under vacuum.[94] The product obtained as a crude off-white semi-solid, yield: 0.93 g (quantitative). TLC (petroleum ether-EtOAc 1:1 v/v), Rf = 0.9 (1st spot), 0.85 (2nd spot), which was used directly in the next step without further purification.

7.4.16 (*R/S*)-*N*-(2-(1*H*-triazol-1-yl)-1-phenylethyl)benzamide (37a)

(**39**)
Chemical Formula: $C_{15}H_{13}NO$
Molecular Weight: 223.28
cLogP= 3.78

(**37a**)
Chemical Formula: $C_{17}H_{16}N_4O$
Molecular Weight: 292.34
cLogP= 2.57
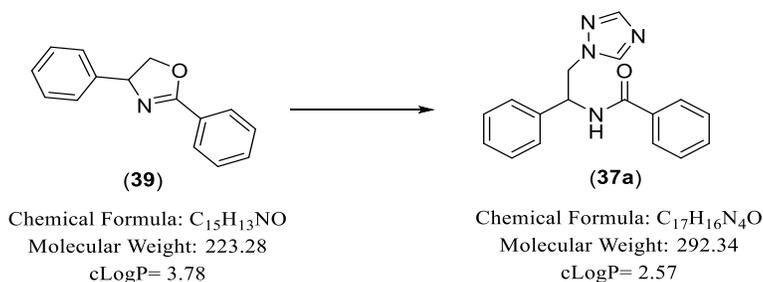
A mixture of (*R/S*)-2,4-diphenyl-4,5-dihydrooxazole (**39**) (0.90 g, 4.04 mmol) and 1,2,4-triazole (11.16 g, 161.56 mmol) was refluxed at 125 °C for 48 h. Upon completion, the mixture was extracted between EtOAc (100 mL) and brine (2 x 100 mL). The organic layer was dried ($MgSO_4$), concentrated under vacuum[94] and purified by gradient column chromatography CH_2Cl_2– MeOH (97:3 v/v) and product obtained as a white solid, yield: 0.45 g (38%). TLC (CH_2Cl_2-MeOH 9.5:0.5 v/v), Rf = 0.64. M.p. 206-208 °C ^{1}H NMR (DMSO-d_6): δ 9.01 (d, *J* = 8.7 Hz, 1H, N*H*), 8.45 (s, 1H, triazole), 7.97 (s, 1H, triazole), 7.78 (d, *J* = 7.0 Hz, 2H, Ar), 7.54 (t, *J* = 7.3 Hz, 1H, Ar), 7.47 (m, 4H, Ar), 7.37 (t, *J* = 7.5 Hz, 2H, Ar), 7.30 (t, *J* = 7.3 Hz, 1H, Ar), 5.55 (ddd, *J* = 5.6, 9.2, 14.6 Hz, 1H, C*H*CHaHb), 4.66 (dd, *J* = 9.7, 13.8 Hz, 1H,

CHC*Ha*Hb), 4.57 (dd, J = 5.6, 13.8 Hz, 1H, CHCHa*Hb*). ^{13}C NMR(DMSO-d_6): δ 166.45 (C, C=O), 151.93 (CH, triazole), 145.01 (CH, triazole), 140.33 (C, Ar), 134.59 (C, Ar), 131.88 (CH, Ar), 129.00 (2 x CH, Ar), 128.79 (2 x CH, Ar), 128.06 (CH, Ar), 127.71 (2 x CH, Ar), 127.30 (2 x CH, Ar), 53.61 (*C*HCH$_2$), 53.10 (CH*C*H$_2$). HRMS (ESI), *m/z.* calcd for $C_{17}H_{16}N_4O$ ([M + H]$^+$), 293.1402; found, 293.1395. HPLC (Method A): 98.92%, R_t = 4.00 min.

7.4.17 4-((*tert*-Butoxycarbonyl)amino)benzoic acid (41)[105]

(40)	**(19)**	**(41)**
Chemical Formula: $C_7H_7NO_2$	Chemical Formula: $C_{10}H_{18}O_5$	Chemical Formula: $C_{12}H_{15}NO_4$
Molecular Weight: 137.14	Molecular Weight: 218.25	Molecular Weight: 237.26
cLogP= 0.79	cLogP=2.59	cLogP=1.96
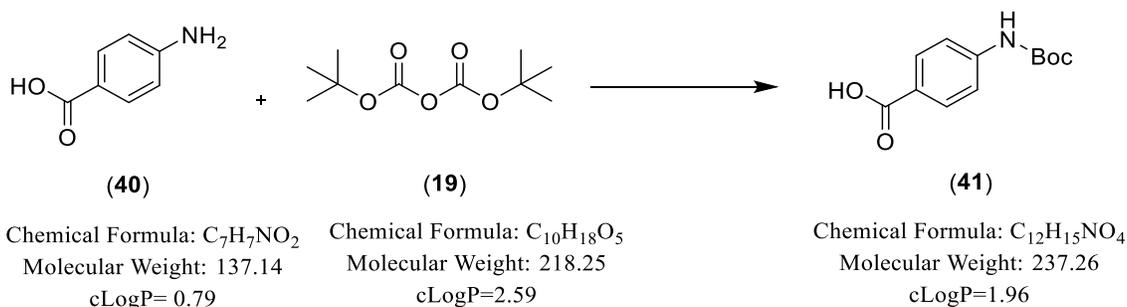
To a solution of 4-aminobenzoic acid (**40**) (5.00g, 36.46 mmoL) in water/dioxane (1:2 v/v, 50 mL) were added Et$_3$N (7.6 mL, 54.69 mmol) and (Boc)$_2$O (**19**) (11.94 g, 54.69 mmol). The resulting solution was stirred at rt for 24 h. The solvent was evaporated, and the residue was acidified with a 1N aqueous HCl solution to pH ~ 4. The obtained precipitate was washed with H$_2$O to give the product as a white solid, yield: 8.7 g (100 %). TLC (petroleum ether-EtOAc 1:1 v/v), Rf = 0.76. M.p. 192-194 °C (181 °C lit)[105]. ^{1}H NMR (DMSO-d_6): δ 12.60 (brs, 1H, COO*H*), 9.73 (s, 1H, NH), 7.84 (d, J = 8.75 Hz, 2H), 7.56 (d, J = 8.75 Hz, 2H), 1.49 (s, 9H, C(C*H$_3$*)$_3$).

7.4.18 General method for preparation of (*R/S*)-β-nitroalcohols (43)
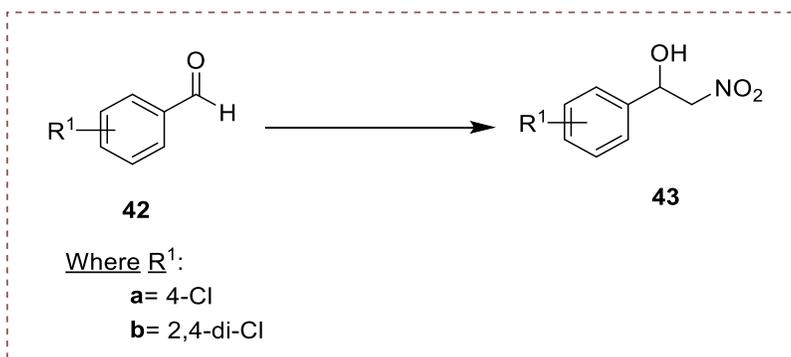
To a solution of benzaldehyde (**42**) (1.0 meq) in nitromethane (0.46 mL, 8.6 meq) was added AmberSep 900 (OH) (10 wt %). The solution was stirred overnight then the AmberSep 900 was removed by filtration. The crude product was extracted with EtOAc (100 mL), washed with brine (2 x 100 mL), dried (MgSO$_4$) and reduced *in vacuo*.[94]

(*R/S*)-1-(4-Chlorophenyl)-2-nitroethan-1-ol (43a)[94]

(**42a**)	(**43a**)
Chemical Formula: C$_7$H$_5$ClO	Chemical Formula: C$_8$H$_8$ClNO$_3$
Molecular Weight: 140.57	Molecular Weight: 201.61
cLog P= 2.34	cLog P= 1.2
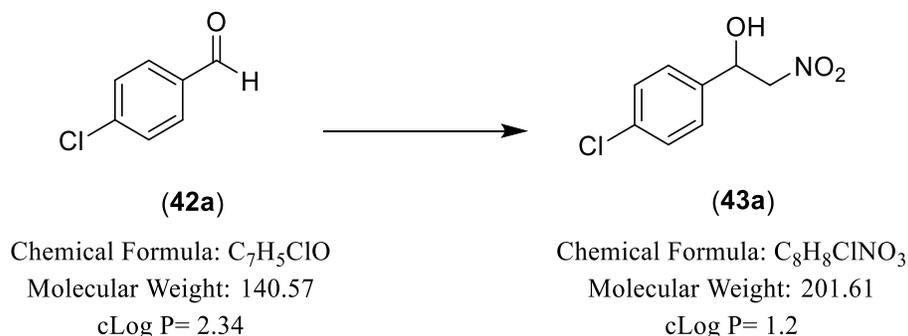
Prepared from 4-chlorobenzaldehyde (**42a**, R^1= 4-Cl) (1.00 g, 7.13 mmol) and nitromethane (3.32 mL, 61.32 mmol). Product obtained as a pale-yellow oil, yield 1.34 g (96 %). TLC (petroleum ether-EtOAc 3:1 v/v), R*f* = 0.54. ^{1}H NMR (DMSO-*d$_6$*): δ 7.47 (d, *J* = 8.5 Hz, 2H, Ar), 7.44 (d, *J* = 8.7 Hz, 2H, Ar), 6.18 (d, *J* = 5.1 Hz, 1H, O*H*), 5.28 (pentet, *J* = 4.5 Hz, 1H, C*H*CH$_a$CH$_b$), 4.86 (dd, *J* = 3.5, 12.6 Hz, 1H, CHC*H$_a$*CH$_b$), 4.57 (dd, *J* = 9.7, 12.6 Hz, 1H, CHCH$_a$C*H$_b$*).

(*R/S*)-1-(2,4-Dichlorophenyl)-2-nitroethan-1-ol (43b)

(**42b**)	(**43b**)
Chemical Formula: C$_7$H$_4$Cl$_2$O	Chemical Formula: C$_8$H$_7$Cl$_2$NO$_3$
Molecular Weight: 175.01	Molecular Weight: 236.05
cLog P= 2.9	cLog P= 1.82
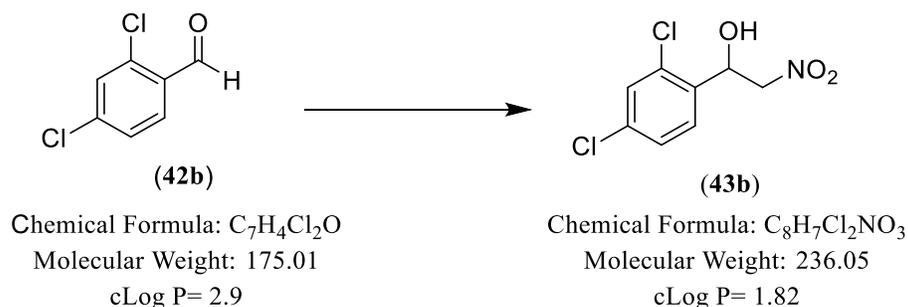
Prepared from 2,4-dichlorobenzaldehyde (**42b**, R^1= 2,4-diCl) (2.5 g, 14.28 mmol) and nitromethane (10 mL, 122.85 mmol).[162] Product obtained as an off-white solid, yield 3.27 g (97 %). TLC (petroleum ether-EtOAc 3:1 v/v), R*f* = 0.63. M.p. 62-64 °C. ^{1}H NMR (DMSO-*d$_6$*): δ

7.66 (d, J = 8.6 Hz, 2H, Ar), 7.51 (dd, J = 2.1, 8.4 Hz, 1H, Ar), 6.40 (dd, J = 1.0, 5.0 Hz, 1H, OH), 5.56 (pentet, J = 4.4 Hz, 1H, CHCH$_a$CH$_b$), 4.83 (dd, J = 2.9, 12.8 Hz, 1H, CHCH_aCH$_b$), 4.52 (dd, J = 9.6, 12.8 Hz, 1H, CHCH$_a$CH_b).

7.4.19 General procedure of reduction using Paar hydrogenator (44)
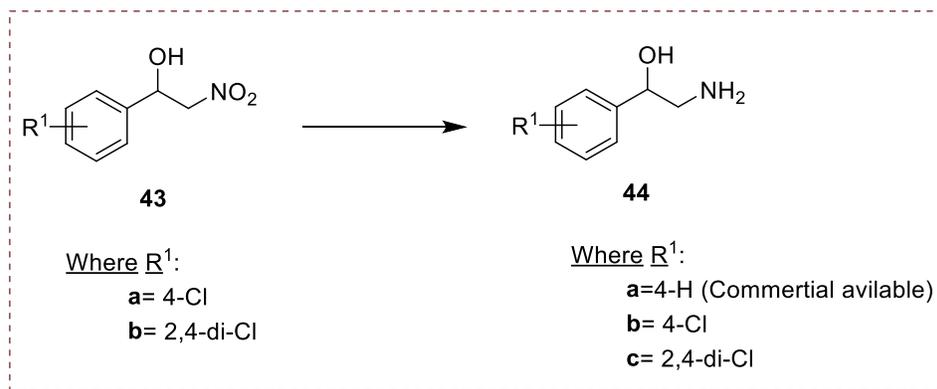
Raney nickel (50 % slurry in H$_2$O, 3 mL) was added to a solution of (*R/S*)-1-(4-arylphenyl)-2-nitroethan-1-ol (**43**) (1.0 meq) in methanol (12 mL/mmoL) and aqueous formic acid (2.5 mL/mmoL). The reaction flask was then degassed and purged with hydrogen. The reaction was carried out under 46 psi H$_2$ atmosphere using a Paar hydrogenator.[94] The reaction flask was shaken vigorously for 3h until all starting material had been consumed. After removal of hydrogen the reaction mixture was filtered, and the solvent removed *in vacuo*. The aqueous residue was made alkaline (pH ~ 10) with NH$_4$OH (25 %), extracted with EtOAc (100 mL) and washed with brine (2 × 100 mL), dried (MgSO$_4$), filtered and reduced under vacuum.

(*R/S*)-2-Amino-1-(4-chlorophenyl)ethan-1-ol (44b)

(43a)

Chemical Formula: C$_8$H$_8$ClNO$_3$
Molecular Weight: 201.61
cLog P= 1.2

(44b)

Chemical Formula: C$_8$H$_{10}$ClNO
Molecular Weight: 171.62
cLog P= 1.1
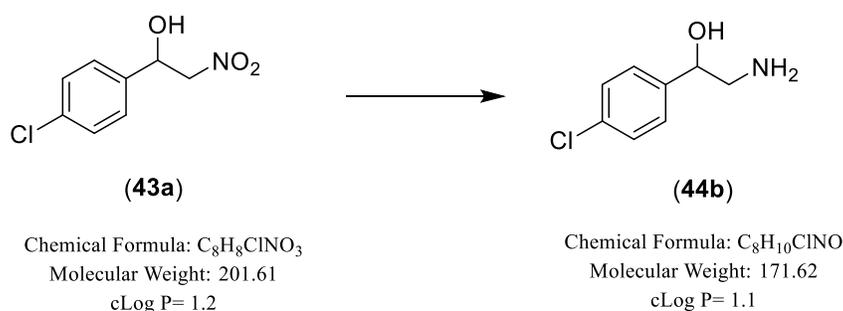
Prepared from (*R/S*)-1-(4-chlorophenyl)-2-nitroethan-1-ol (**43a**, R^1= 4-Cl) (3.4 g, 16.86 mmol). Product obtained as an off-white solid, yield: 1.69 g (59 %). TLC (CH_2Cl_2-CH_3OH 9:1 v/v), R*f* = 0.15. M.p. 72-74 °C (106-110 °C lit)[94], (94-95 °C lit)[107]. ^{1}H NMR (DMSO-d_6): δ 7.37 (d, *J* = 8.7 Hz, 2H, Ar), 7.34 (d, *J* = 8.7 Hz, 2H, Ar), 5.35 (brs, 1H, O*H*), 4.44 (dd, *J* = 4.3, 7.5 Hz, 1H, C*H*CH$_a$CH$_b$), 3.31 (brs, 2H, N*H$_2$*), 2.65 (dd, *J* = 4.3, 12.9 Hz, 1H, CHC*H$_a$*CH$_b$), 2.56 (dd, *J* = 7.9, 12.6 Hz, 1H, CHCH$_a$C*H$_b$*). ^{13}C NMR (DMSO-d_6): δ 143.94 (C, Ar), 131.58 (C, C-Cl), 128.31 (2 x CH, Ar), 128.28 (2 x CH, Ar), 74.28 (*C*HCH$_2$NH$_2$), 50.55 (CH*C*H$_2$NH$_2$). ^{1}H NMR (CDCl$_3$): δ 7.34 (d, *J* = 8.8 Hz, 2H, Ar), 7.31 (d, *J* = 8.6 Hz, 2H, Ar), 4.62 (dd, *J* = 3.9, 7.8 Hz, 1H, C*H*CH$_a$CH$_b$), 3.02 (dd, *J* = 3.7, 12.8 Hz, 1H, CHC*H$_a$*CH$_b$), 2.77 (dd, *J* = 7.9, 12.7 Hz, 1H, CHCH$_a$C*H$_b$*), 1.87 (brs, 3H, O*H* + N*H$_2$*). ^{13}C NMR (CDCl$_3$): δ 141.00 (C, Ar), 133.19 (C, *C*-Cl), 128.55 (2 x CH, Ar), 127.25 (2 x CH, Ar), 73.46 (*C*HCH$_2$NH$_2$), 49.15 (CH*C*H$_2$NH$_2$).

(*R/S*)-2-Amino-1-(2,4-dichlorophenyl)ethan-1-ol (44c)
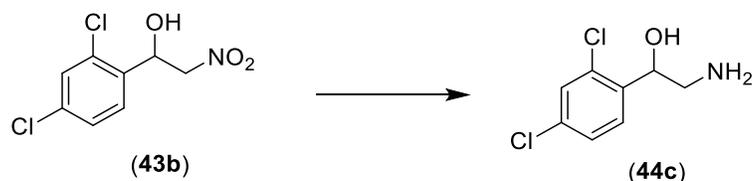
(**43b**)
Chemical Formula: $C_8H_7Cl_2NO_3$
Molecular Weight: 236.05
cLog P= 1.82

(**44c**)
Chemical Formula: $C_8H_9Cl_2NO$
Molecular Weight: 206.07
Log P= 1.66

Prepared from (*R/S*)-1-(2,4-dichlorophenyl)-2-nitroethan-1-ol (**44b**, R^1= 2,4-diCl) (3.28 g, 13.89 mmol).[163] Product obtained as a pale-yellow solid, yield: 2.19 g (77 %). TLC (CH_2Cl_2-CH_3OH 9:1 v/v), R*f* = 0.25. M.p. 76-80 °C. ^{1}H NMR (DMSO-d_6): δ 7.55 (d, *J* = 8.4 Hz, 1H, Ar), 7.53 (d, *J* = 2.1 Hz, 1H, Ar), 7.43 (dd, *J* = 2.1, 8.2 Hz, 1H, Ar), 5.56 (brs, 1H, O*H*), 4.77 (dd, *J* = 3.4, 7.6 Hz, 1H, C*H*CH$_a$CH$_b$), 2.74 (dd, *J* = 3.4, 13.1 Hz, 1H, CHC*H$_a$*CH$_b$), 2.48 (dd, *J* = 7.2, 12.6 Hz, 1H, CHCH$_a$C*H$_b$*), 1.58 (brs, 2H, N*H$_2$*).

7.4.20 General method of CDI coupling reaction (45)

Where R[1]:
a= 4-H
b= 4-Cl
c= 2,4-di-Cl
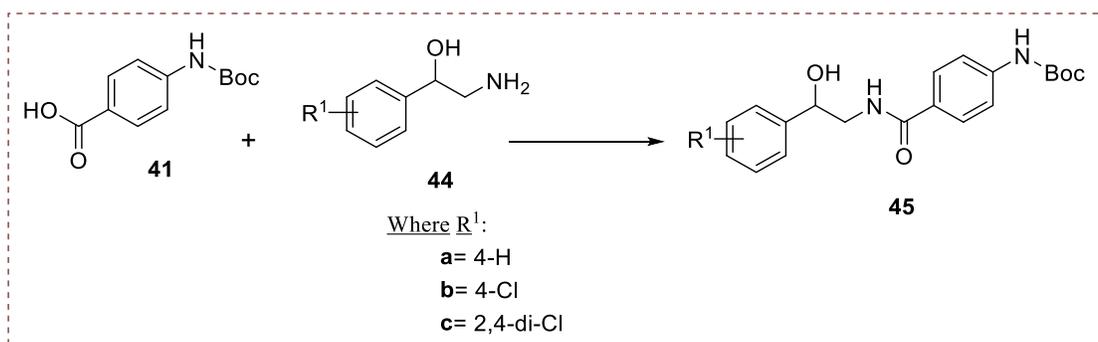
A solution of 4-((*tert*-butoxycarbonyl)amino)benzoic acid (**41**) (1.00 meq) in dry DMF (8 mL/mmoL) was combined with CDI (1.1 meq). The reaction was stirred for 1 h at rt under nitrogen. The mixture was cooled to 0 °C then added to a solution of (*R/S*)-2-amino-1-arylphenylethan-1-ol (**44**) (1.00 meq) in dry DMF (5 mL/mmoL). The resulting mixture was stirred at room temperature overnight and on completion, ice was added into the flask. The resulting white precipitate was collected by filtration, washed with ice-cold water and dried.[94]

(*R/S*)-*tert*-Butyl (4-((2-hydroxy-2-phenylethyl)carbamoyl)phenyl)carbamate (45a)

(**41**)
Chemical Formula: $C_{12}H_{15}NO_4$
Molecular Weight: 237.26
cLogP=1.96

(**44a**)
Chemical Formula: $C_8H_{11}NO$
Molecular Weight: 137.18
cLogP= 0.54

(**45a**)
Chemical Formula: $C_{20}H_{24}N_2O_4$
Molecular Weight: 356.42
cLogP= 2.74
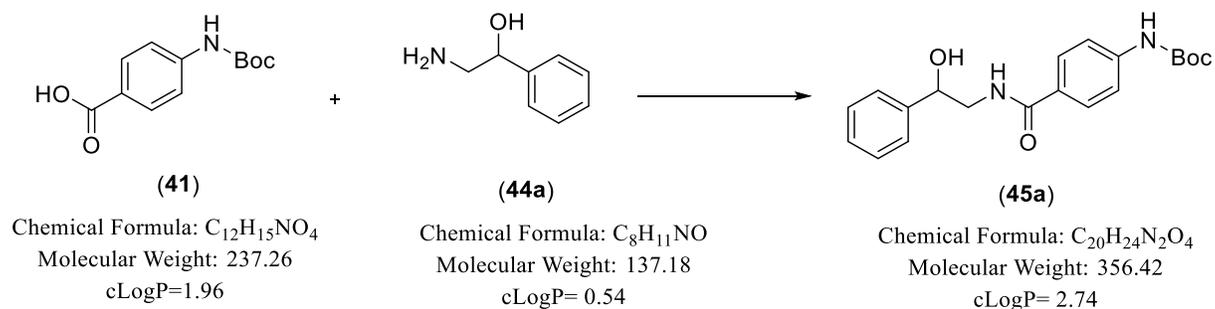
Prepared from (*R/S*)-2-amino-1-phenylethan-1-ol (**44a**, R[1]= 4-H) (1.12 g, 8.2 mmol). Product obtained as a white solid, yield: 2.71 g (93 %). TLC (petroleum ether-EtOAc 1:1 v/v), R*f* = 0.48. M.p. 194-196 °C. ^{1}H NMR (DMSO-*d₆*): δ 9.54 (s, 1H, CON*H*), 8.28 (t, *J* = 5.6 Hz, 1H, N*H*CH₂), 7.76 (d, *J* = 8.8 Hz, 2H, Ar), 7.51 (d, *J* = 8.8 Hz, 2H, Ar), 7.35 (pentet, *J* = 7.6 Hz, 4H, Ar), 7.25 (t, *J* = 7.1 Hz, 1H, Ar), 5.33 (d, *J* = 4.2 Hz, 1H, O*H*), 4.78 (pentet, *J* = 4.2 Hz, 1H, CH₂C*H*OH), 3.49 (pentet, *J* = 6.0 Hz, 1H, NHC*Ha*Hb), 3.32 (dd, *J* = 5.3, 7.9 Hz, 1H, NHCHa*Hb*), 1.49 (s, 9H, C(C*H₃*)*₃*). ^{13}C NMR (DMSO-*d₆*): δ 166.43 (C, *C*ONH), 153.09 (C, *C*O₂), 144.31 (C, Ar), 142.65 (C, Ar), 128.47 (4 x CH, Ar), 128.38 (C, Ar), 127.43 (CH, Ar), 126.43 (2 x CH, Ar),

117.61 (2 x CH, Ar), 79.93 (C, $C(CH_3)_3$), 71.81 ($NHCH_2CH$), 48.15 ($NHCH_2CH$), 28.57 ($C(CH_3)_3$). HRMS (ESI), m/z. calcd for $C_{20}H_{24}N_2O_4$ ($[M + Na]^+$), 379.1634; found, 379.1629. HPLC (Method A): 95.20 %, R_t= 4.33 min.

(R/S)-*tert*-Butyl (4-((2-(4-chlorophenyl)-2-hydroxyethyl)carbamoyl)phenyl)carbamate (45b)

(41)	(44b)	(45b)
Chemical Formula: $C_{12}H_{15}NO_4$	Chemical Formula: $C_8H_{10}ClNO$	Chemical Formula: $C_{20}H_{23}ClN_2O_4$
Molecular Weight: 237.26	Molecular Weight: 171.62	Molecular Weight: 390.86
cLog P= 1.96	cLog P= 1.1	cLog P= 3.3
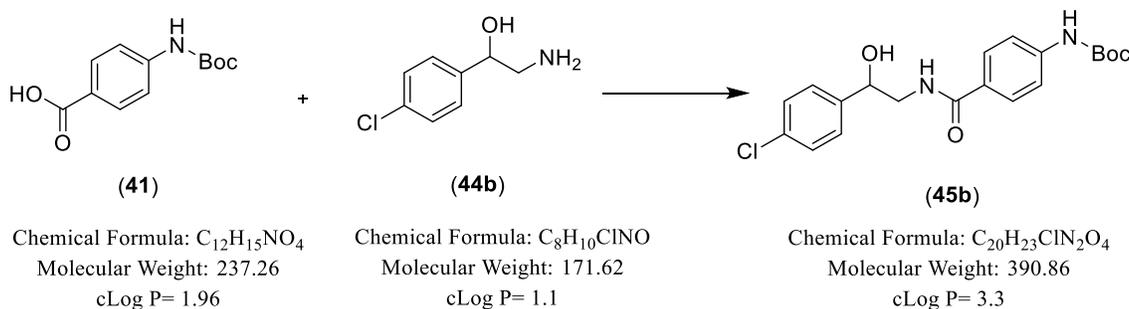
Prepared from (R/S)-2-amino-1-(4-chlorophenyl)ethan-1-ol (**44b**, R^1= 4-Cl) (1.12 g, 6.55 mmoL). Product obtained as a white solid, yield: 2.28 g (89 %). TLC (petroleum ether-EtOAc 1:1 v/v), Rf = 0.38. M.p. 212-214 °C. ^{1}H NMR (DMSO-d_6): δ 9.60 (s, 1H, CONH), 8.35 (t, J = 5.7 Hz, 1H, NHCH$_2$), 7.74 (d, J = 8.8 Hz, 2H, Ar), 7.51 (d, J = 8.8 Hz, 2H, Ar), 7.38 (m, 4H, Ar), 5.62 (d, J = 4.5 Hz, 1H, OH), 4.76 (ddd, J = 4.8, 7.5, 9.4 Hz, 1H, CH$_2$CHOH), 3.44 (ddd, J = 5.9, 11.5, 13.1 Hz, 1H, NHCHaHb), 3.30 (dd, J = 5.4, 7.7 Hz, 1H, NHCHaHb), 1.49 (s, 9H, C(CH_3)$_3$). ^{13}C NMR (DMSO-d_6): δ 166.44 (C, CONH), 153.07 (C, CO$_2$), 143.31 (C, Ar), 142.68 (C, Ar), 131.90 (C, C-Cl), 128.50 (2 x CH, Ar), 128.43 (2 x CH, Ar), 128.35 (2 x CH, Ar), 128.22 (C, Ar), 117.54 (2 x CH, Ar), 79.93 (C, C(CH$_3$)$_3$), 71.07 ($NHCH_2CH$), 47.88 ($NHCH_2CH$), 28.54 ($C(CH_3)_3$). HRMS (ESI), m/z. calcd for $C_{20}H_{23}ClN_2O_4$ ($[M + H]^+$), 391.1424; found, 391.1425. HPLC (Method B2): 96.22%, R_t= 5.03 min.

(*R/S*)-*tert*-Butyl   (4-((2-(2,4-dichlorophenyl)-2-hydroxyethyl)carbamoyl)phenyl) carbamate (45c)

(41)	(44c)	(45c)
Chemical Formula: $C_{12}H_{15}NO_4$	Chemical Formula: $C_8H_9Cl_2NO$	Chemical Formula: $C_{20}H_{22}Cl_2N_2O_4$
Molecular Weight: 237.26	Molecular Weight: 206.07	Molecular Weight: 425.31
cLog P= 1.96	cLog P: 1.66	cLog P= 3.86
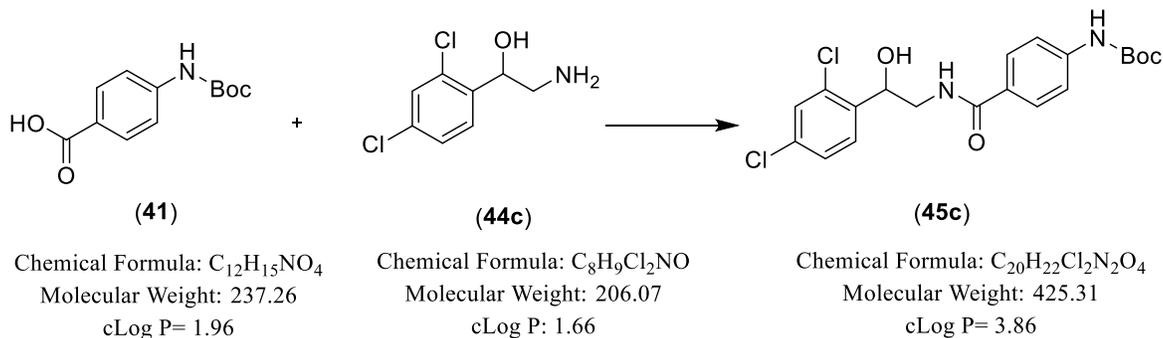
Prepared from (*R/S*)-2-amino-1-(2,4-dichlorophenyl)ethan-1-ol (**44c**, R^1= 2,4-diCl) (1.1 g, 5.31 mmoL). Product obtained as a white solid, yield: 2.11 g (93 %). TLC (petroleum ether-EtOAc 1:1 v/v), R*f* = 0.63. M.p. 198-200 °C. ^{1}H NMR (DMSO-d_6): δ 9.60 (s, 1H, CON*H*), 8.36 (t, *J* = 5.8 Hz, 1H, N*H*CH$_2$), 7.74 (d, *J* = 8.8 Hz, 2H, Ar), 7.61 (d, *J* = 8.4 Hz, 1H, Ar), 7.54 (d, *J* = 2.1 Hz, 1H, Ar), 7.50 (d, *J* = 8.7 Hz, 2H, Ar), 7.45 (dd, *J* = 2.1, 8.4 Hz, 1H, Ar), 5.79 (d, *J* = 4.6 Hz, 1H, O*H*), 5.11 (dd, *J* = 4.7, 11.7 Hz, 1H, CH$_2$C*H*OH), 3.47 (ddd, *J* = 5.4, 10.6, 13.2 Hz, 1H, NHC*Ha*Hb), 3.39 (dd, *J* = 6.7, 13.8 Hz, 1H, NHCHa*Hb*), 1.49 (s, 9H, C(C*H$_3$*)$_3$). ^{13}C NMR (DMSO-d_6): δ 166.57 (C, *C*ONH), 153.08 (C, *C*O$_2$), 142.65 (C, Ar), 140.72 (C, Ar), 132.69 (C, *C*-Cl), 132.63 (C, *C*-Cl), 130.04 (CH, Ar), 128.71 (CH, Ar), 128.54 (2 x CH, Ar), 128.22 (C, Ar), 127.85 (CH, Ar), 117.51 (2 x CH, Ar), 79.93 (C, *C*(CH$_3$)$_3$), 68.11 (NHCH$_2$*C*H), 46.15 (NH*C*H$_2$CH), 28.54 (C(*C*H$_3$)$_3$). HRMS (ESI), m/z. calcd for $C_{20}H_{22}Cl_2N_2O_4$ ([M + Na]$^+$), 447.0855; found, 447.0855. HPLC (Method B2): 95.83%, R$_t$= 6.01 min.

(*R/S*)-*tert*-Butyl (4-(5-phenyl-4,5-dihydrooxazol-2-yl)phenyl)carbamate (46a)

(45a)	(46a)
Chemical Formula: $C_{20}H_{24}N_2O_4$	Chemical Formula: $C_{20}H_{22}N_2O_3$
Molecular Weight: 356.42	Molecular Weight: 338.41
cLogP= 2.74	cLogP= 4.15
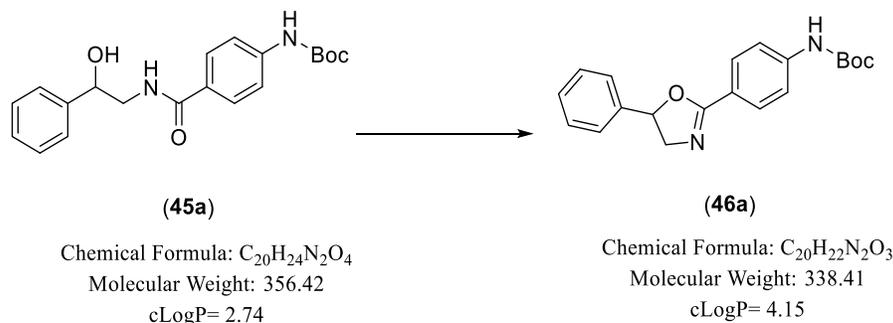
Method: see 7.4.15 method (3)

Prepared from (*R/S*)-*tert*-butyl (4-((2-hydroxy-2-phenylethyl)carbamoyl)phenyl)carbamate (**45a**, R^1= 4-H) (1.67 g, 4.69 mmoL). Product obtained as an off-white solid (*crude*), yield: 1.5 g (94 %). TLC (petroleum ether-EtOAc 1:1 v/v), Rf = 0.88 (1st spot), 0.80 (2nd spot). ^{1}H NMR (DMSO-d_6): δ 9.72 (s, 1H, CON*H*), 7.84 (d, *J* = 8.9 Hz, 2H, Ar), 7.59 (d, *J* = 7.6 Hz, 2H, Ar), 7.38 (m, 5H, Ar), 5.78 (dd, *J* = 7.9, 10.2 Hz, 1H, OC*H*CHaHb), 4.41 (dd, *J* = 10.1, 14.6 Hz, 1H, OCHC*Ha*Hb), 3.82 (dd, *J* = 7.6, 14.6 Hz, 1H, OCHCHa*Hb*), 1.49 (s, 9H, C(C*H₃*)₃). ^{13}C NMR (DMSO-d_6): δ 163.18 (C, *C*=N), 153.02 (C, *C*O₂), 143.37 (C, Ar), 141.45 (C, Ar), 129.36 (2 x CH, Ar), 129.23 (2 x CH, Ar), 128.68 (CH, Ar), 127.75 (C, Ar), 126.24 (2 x CH, Ar), 118.02 (2 x CH, Ar), 80.80 (O*C*HCH₂), 80.10 (C, *C*(CH₃)₃), 60.22 (OCH*C*H₂), 28.52 (C(*C*H₃)₃).

(*R/S*)-*tert*-Butyl (4-(5-(4-chlorophenyl)-4,5-dihydrooxazol-2-yl)phenyl) carbamate (46b)

(**45b**)

Chemical Formula: C₂₀H₂₃ClN₂O₄
Molecular Weight: 390.86
cLog P= 3.3

(**46b**)

Chemical Formula: C₂₀H₂₁ClN₂O₃
Molecular Weight: 372.85
cLog P= 4.71
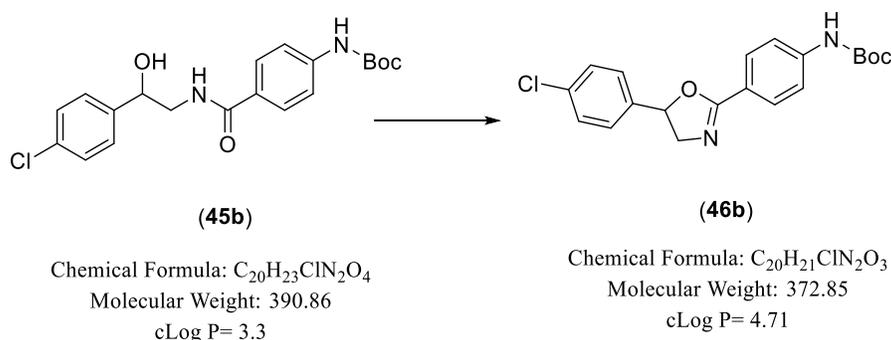
Method: see 7.4.15 method (3)

Prepared from (*R/S*)-*tert*-butyl (4-((2-(4-chlorophenyl)-2-hydroxyethyl)carbamoyl)phenyl)carbamate (**45b**, R^1= 4-Cl) (1.00 g, 2.56 mmol). Product obtained as an orange syrup (*crude*), yield: 0.95 g (100 %). TLC (petroleum ether-EtOAc 1:1 v/v), Rf = 0.83 (1st spot), 0.85 (2nd spot). ^{1}H NMR (DMSO-d_6): δ 9.72 (s, 1H, CON*H*), 7.84 (d, *J* = 8.9 Hz, 2H, Ar), 7.58 (d, *J* = 8.8 Hz, 2H, Ar), 7.47 (d, *J* = 8.6 Hz, 2H, Ar), 7.39 (d, *J* = 8.5 Hz, 2H, Ar), 5.79 (dd, *J* = 7.5, 10.0 Hz, 1H, OC*H*CHaHb), 4.41 (dd, *J* = 10.1, 14.7 Hz, 1H, OCHC*Ha*Hb), 3.79 (dd, *J* = 7.4, 14.7 Hz, 1H, OCHCHa*Hb*), 1.49 (s, 9H, C(C*H₃*)₃). ^{13}C NMR (DMSO-d_6): δ 163.03 (C, *C*=N), 153.02 (C, *C*O₂), 143.38 (C, Ar), 140.54 (C, Ar), 133.20 (C, *C*-Cl), 129.35 (2 x CH, Ar), 129.23 (2 x CH, Ar), 128.12 (2 x CH, Ar), 127.67 (C, Ar), 118.02 (2 x CH, Ar), 80.10 (O*C*HCH₂), 79.93 (C, *C*(CH₃)₃), 60.22 (OCH*C*H₂), 28.52 (C(*C*H₃)₃).

(*R/S*)-*tert*-butyl (4-(5-(2,4-dichlorophenyl)-4,5-dihydrooxazol-2-yl)phenyl)carbamate (46c)

(45c)

Chemical Formula: $C_{20}H_{22}Cl_2N_2O_4$
Molecular Weight: 425.31
cLog P: 3.86

(46c)

Chemical Formula: $C_{20}H_{20}Cl_2N_2O_3$
Molecular Weight: 407.29
cLog P: 5.26
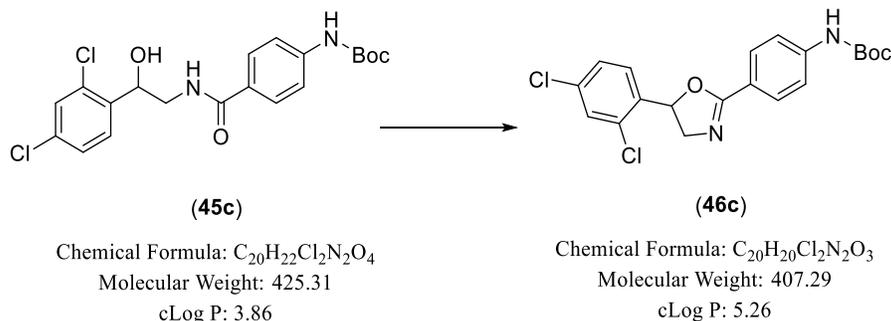
Method: see 7.4.15 method (3)

Prepared from (*R/S*)-*tert*-butyl (4-((2-(2,4-dichlorophenyl)-2-hydroxyethyl)carbamoyl)phenyl) carbamate (**45c**, R^1= 2,4-diCl) (1.00 g, 2.35 mmol). Product obtained as an orange syrup (*crude*), yield: 0.96 g (100 %). TLC (petroleum ether-EtOAc 1:1 v/v), Rf = 0.88 (1st spot), 0.85 (2nd spot). ^{1}H NMR (DMSO-d_6): δ 9.76 (s, 1H, CON*H*), 7.89 (d, *J* = 8.8 Hz, 2H, Ar), 7.72 (d, *J* = 2.2 Hz, 1H, Ar), 7.61 (d, *J* = 8.8 Hz, 2H, Ar), 7.53 (dd, *J* = 2.2, 8.5 Hz, 1H, Ar), 7.43 (d, *J* = 8.5 Hz, 1H, Ar), 6.00 (dd, *J* = 7.3, 10.2 Hz, 1H, OC*H*CHaHb), 4.53 (dd, *J* = 10.3, 14.6 Hz, 1H, OCHC*Ha*Hb), 3.78 (dd, *J* = 7.2, 14.6 Hz, 1H, OCHCHa*Hb*), 1.50 (s, 9H, C(C*H₃*)₃). ^{13}C NMR (DMSO-d_6): δ 166.64 (C, *C*=N), 153.02 (C, *C*O₂), 142.99 (C, Ar), 134.92 (C, Ar), 134.52 (C, *C*-Cl), 133.84 (C, *C*-Cl), 131.04 (CH, Ar), 129.72 (2 x CH, Ar), 129.48 (2 x CH, Ar), 128.60 (CH, Ar), 128.32 (2 x CH, Ar), 127.59 (C, Ar), 80.15 (C, *C*(CH₃)₃), 77.72 (O*C*HCH₂), 60.22 (OCH*C*H₂), 28.52 (C(C*H₃*)₃).

(*R/S*)-4-Amino-*N*-(2-phenyl-2-(1*H*-1,2,4-triazol-1-yl)ethyl)benzamide (47a)

(46a)

Chemical Formula: $C_{20}H_{22}N_2O_3$
Molecular Weight: 338.41
cLogP= 4.15

(47a)

Chemical Formula: $C_{17}H_{17}N_5O$
Molecular Weight: 307.36
cLogP= 1.76
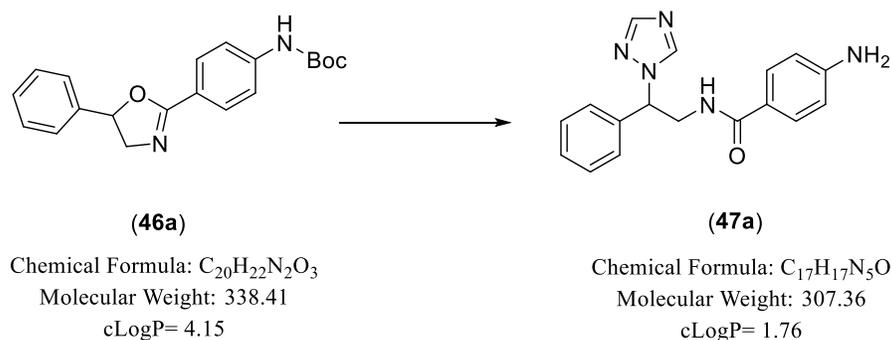
Method: see 7.4.16

Prepared from (*R/S*)-*tert*-butyl (4-(5-phenyl-4,5-dihydrooxazol-2-yl)phenyl)carbamate (**46a**, R^1= 4-H) (1.49 g, 4.40 mmol). Product obtained as an off-white solid which was purified by gradient column chromatography CH_2Cl_2-MeOH (98: 2 v/v), yield: 0.31 g (23 %). TLC (CH_2Cl_2-MeOH 9.5:0.5 v/v), R*f* = 0.45. M.p. 124-126 °C. ^{1}H NMR (DMSO-d_6): δ 8.72 (s, 1H, triazole), 8.21 (t, *J* = 5.5 Hz, 1H, N*H*CH$_2$), 8.01 (s, 1H, triazole), 7.47 (d, *J* = 8.7 Hz, 2H, Ar), 7.36 (m, 5H, Ar), 6.50 (d, *J* = 8.7 Hz, 2H, Ar), 5.88 (dd, *J* = 5.4, 9.2 Hz, 1H, NHCHaHbC*H*), 5.62 (s, 2H, N*H*$_2$), 4.02 (m, 1H, NHC*Ha*HbCH), 3.93 (ddd, *J* = 5.4, 10.8, 13.7 Hz, 1H, NHCHa*Hb*CH). ^{13}C NMR (DMSO-d_6): δ 167.23 (C, *C*ONH), 152.29 (C, *C*-NH$_2$), 152.08 (CH, triazole), 144.52 (CH, triazole), 138.64 (C, Ar), 129.22 (2 x CH, Ar), 129.10 (2 x CH, Ar), 128.65 (CH, Ar), 127.61 (2 x CH, Ar), 120.99 (C, Ar), 112.92 (2 x CH, Ar), 62.46 (NHCH$_2$*C*H), 43.86 (NH*C*H$_2$CH). HRMS (ESI), m/z. calcd for $C_{17}H_{17}N_5O$ ([M + H]$^+$), 308.1511; found, 308.1512. HPLC (Method A): 97.82%, R_t= 3.73 min.

(*R/S*)-4-Amino-*N*-(2-(4-chlorophenyl)-2-(1*H*-1,2,4-triazol-1-yl)ethyl)benzamide (47b)

(**46b**)
Chemical Formula: $C_{20}H_{21}ClN_2O_3$
Molecular Weight: 372.85
cLog P= 4.71

(**47b**)
Chemical Formula: $C_{17}H_{16}ClN_5O$
Molecular Weight: 341.80
cLog P= 2.32
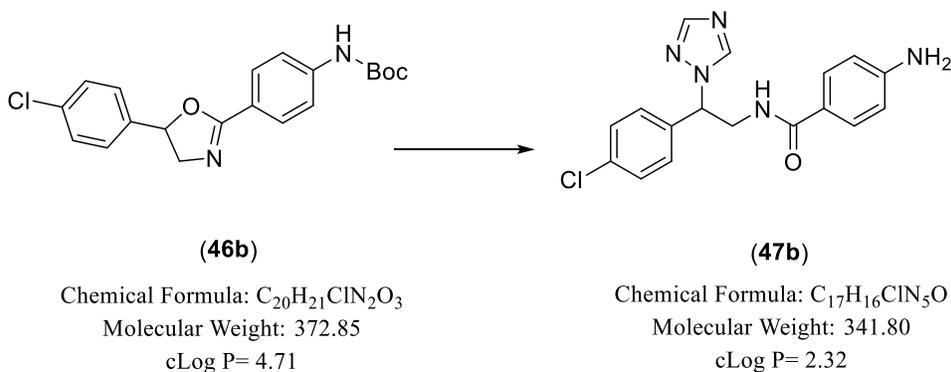
Method: see 7.4.16

Prepared from (*R/S*)-*tert*-butyl (4-(5-(4-chlorophenyl)-4,5-dihydrooxazol-2-yl)phenyl)carbamate (**46b**, R^1= 4-Cl) (0.95 g, 2.55 mmol). Product obtained as an off-white solid which was purified by gradient column chromatography CH_2Cl_2-MeOH (99: 1 to 98.5: 1.5 v/v), yield: 0.31 g (36 %). TLC (CH_2Cl_2-MeOH 9.5:0.5 v/v), R*f* = 0.45. M.p. 148-150 °C. ^{1}H NMR (DMSO-d_6): δ 8.72 (s, 1H, triazole), 8.22 (t, *J* = 5.5 Hz, 1H, N*H*CH$_2$), 8.03 (s, 1H, triazole), 7.47 (d, *J* = 8.7 Hz, 2H, Ar), 7.44 (m, 4H, Ar), 6.50 (d, *J* = 8.8 Hz, 2H, Ar), 5.90 (dd,

J = 6.0, 8.6 Hz, 1H, NHCHaHbC*H*), 5.63 (s, 2H, N*H*$_2$), 3.95 (m, 2H, NHC*Ha*HbCH). ^{13}C NMR (DMSO-*d*$_6$): δ 167.23 (C, *C*ONH), 152.33 (C, *C*-NH$_2$), 152.24 (CH, triazole), 144.63 (CH, triazole), 137.54 (C, Ar), 133.33 (C, *C*-Cl), 129.66 (2 x CH, Ar), 129.22 (2 x CH, Ar), 129.08 (2 x CH, Ar), 120.91 (C, Ar), 112.92 (2 x CH, Ar), 61.60 (NHCH$_2$*C*H), 43.73 (NH*C*H$_2$CH). HRMS (ESI), m/z. calcd for C$_{17}$H$_{16}$ClN$_5$O ([M + H]$^+$), 342.1121; found, 342.1130. HPLC (Method B2): 98.46%, R$_t$= 3.83 min.

(*R/S*)-4-Amino-*N*-(2-(2,4-dichlorophenyl)-2-(1*H*-1,2,4-triazol-1-yl)ethyl)benzamide (47c)

(46c)
Chemical Formula: C$_{20}$H$_{20}$Cl$_2$N$_2$O$_3$
Molecular Weight: 407.29
cLog P: 5.26

(47c)
Chemical Formula: C$_{17}$H$_{15}$Cl$_2$N$_5$O
Molecular Weight: 376.24
cLog P: 2.88
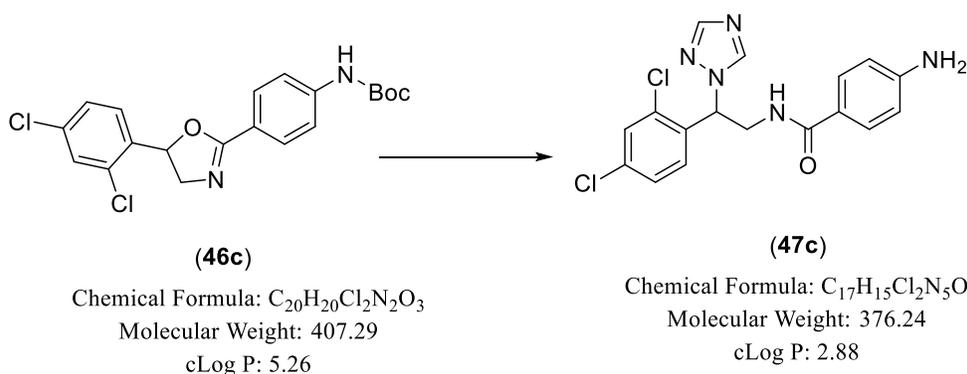
Method: see 7.4.16

Prepared from (*R/S*)-*tert*-butyl (4-(5-(2,4-dichlorophenyl)-4,5-dihydrooxazol-2-yl)phenyl)carbamate (**46c**, R^1= 2,4-diCl) (0.95 g, 2.36 mmol). Product obtained as a pale-yellow solid which was purified by gradient column chromatography CH$_2$Cl$_2$-MeOH (99: 1 v/v), yield: 0.22 g (24 %). TLC (CH$_2$Cl$_2$-MeOH 9.5:0.5 v/v), R*f* = 0.46. M.p. 158-160 °C. ^{1}H NMR (DMSO-*d*$_6$): δ 8.74 (s, 1H, triazole), 8.24 (t, *J* = 5.5 Hz, 1H, N*H*CH$_2$), 8.01 (s, 1H, triazole), 7.67 (d, *J* = 2.2 Hz, 1H, Ar), 7.62 (d, *J* = 8.5 Hz, 1H, Ar), 7.50 (dd, *J* = 2.2, 8.5 Hz, 1H, Ar), 7.47 (d, *J* = 8.7 Hz, 2H, Ar), 6.51 (d, *J* = 8.7 Hz, 2H, Ar), 6.24 (dd, *J* = 5.7, 8.8 Hz, 1H, NHCHaHbC*H*), 5.64 (s, 2H, N*H*$_2$), 4.07 (m, 1H, NHC*Ha*HbCH), 3.90 (ddd, *J* = 5.3, 10.8, 13.6 Hz, 1H, NHCHa*Hb*CH). ^{13}C NMR (DMSO-*d*$_6$): δ 167.21 (C, *C*ONH), 152.35 (C, *C*-NH$_2$), 152.29 (CH, triazole), 144.94 (CH, triazole), 134.46 (C, Ar), 134.35 (C, *C*-Cl), 134.33 (C, *C*-Cl), 130.83 (CH, Ar), 129.57 (CH, Ar), 129.24 (2 x CH, Ar), 128.34 (CH, Ar), 120.86 (C, Ar), 112.92 (2 x CH, Ar), 58.24 (NHCH$_2$*C*H), 42.72 (NH*C*H$_2$CH). HRMS (ESI), m/z. calcd for C$_{17}$H$_{15}$Cl$_2$N$_5$O ([M + H]$^+$), 376.0732; found, 376.0731. HPLC (Method B2): 96.12%, R$_t$= 4.06 min.

7.4.21 General method to form different linker (48, 49 and 51)

To an ice-cooled solution of (*R/S*)-4-amino-*N*-(2-arylphenyl-2-(1*H*-1,2,4-triazol-1-yl)ethyl)benzamide (**47**) (1.0 meq) in dry pyridine (3 mL/mmoL) was added aryl-benzoyl chloride (**34**)/aryl-benzenesulfonyl chloride (**17**) or aryl-phenyl isocyanate (**50**) (1.5 meq) in portions and the reaction mixture was stirred at rt overnight. Upon completion, the pyridine was removed under vacuum and the resulting syrup was diluted with CH_2Cl_2 (50 mL), washed with 1M aqueous HCl (50 mL) and H_2O (50 mL). The orange layer was dried ($MgSO_4$) then concentrated under reduce pressure.[108] The product was purified by CH_2Cl_2-MeOH gradient column chromatography.

(*R/S*)-4-Benzamido-*N*-(2-phenyl-2-(1*H*-1,2,4-triazol-1-yl)ethyl)benzamide (48a)

(**47a**)	(**34a**)	(**48a**)
Chemical Formula: $C_{17}H_{17}N_5O$	Chemical Formula: C_7H_5ClO	Chemical Formula: $C_{24}H_{21}N_5O_2$
Molecular Weight: 307.36	Molecular Weight: 140.57	Molecular Weight: 411.47
cLogP= 1.76	cLogP= 2.17	cLogP =3.37
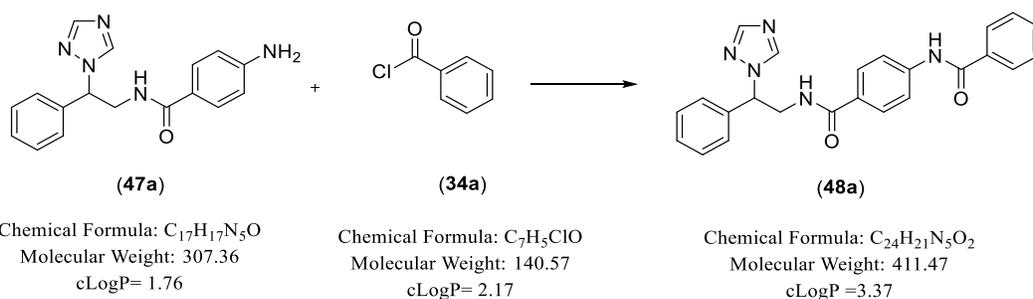
Prepared from benzoyl chloride (**34a**, R^2= 4-H) (0.08 mL, 0.70 mmoL). Product obtained as a white solid which was purified by gradient column chromatography CH_2Cl_2-MeOH (97: 3 v/v), yield: 0.06 g (21 %). TLC (CH_2Cl_2-MeOH 9.5:0.5 v/v), R*f* = 0.62. M.p. 248-250 °C. ^{1}H NMR (DMSO-d_6): δ 10.44 (s, 1H, CON*H*), 8.75 (s, 1H, triazole), 8.63 (t, *J* = 5.5 Hz, 1H, N*H*CH₂), 8.05 (m, 2H, Ar), 8.04 (s, 1H, triazole), 7.96 (d, *J* = 7.0 Hz, 2H, Ar), 7.85 (d, *J* = 8.9 Hz, 2H, Ar), 7.76 (d, *J* = 8.8 Hz, 2H, Ar), 7.62 (t, *J* = 7.4 Hz, 1H, Ar), 7.55 (t, *J* = 7.4 Hz, 2H, Ar), 7.38 (m, 5H, Ar), 5.92 (dd, *J* = 5.6, 9.1 Hz, 1H, NHCHaHbC*H*), 4.09 (m, 1H, NHC*Ha*HbCH), 4.00 (ddd, *J* = 5.4, 10.9, 13.6 Hz, 1H, NHCHa*Hb*CH). ^{13}C NMR (DMSO-d_6): δ 166.75 (C, *C*ONH), 166.29 (C, *C*ONH), 152.15 (CH, triazole), 144.61 (CH, triazole), 142.45 (C, Ar), 138.46 (C, Ar), 135.12 (C, Ar), 132.27 (CH, Ar), 129.26 (C, Ar), 129.14 (2 x CH, Ar), 128.91 (2 x CH, Ar), 128.75 (CH, Ar), 128.38 (2 x CH, Ar), 128.20 (2 x CH, Ar), 127.67 (2 x CH, Ar), 119.87 (2 x CH, Ar), 62.24 (NHCH₂*C*H), 43.95 (NH*C*H₂CH). HRMS (ESI), m/z. calcd for $C_{24}H_{21}N_5O_2$ ([M + H]⁺), 412.1773; found, 412.1766. HPLC (Method B2): 99.18%, R_t= 3.84 min.

(*R/S*)-4-Fluoro-*N*-(4-((2-phenyl-2-(1*H*-1,2,4-triazol-1-yl)ethyl)carbamoyl)phenyl) benzamide (48b)

(47a)	(34b)	(48b)
Chemical Formula: $C_{17}H_{17}N_5O$	Chemical Formula: C_7H_4ClFO	Chemical Formula: $C_{24}H_{20}FN_5O_2$
Molecular Weight: 307.36	Molecular Weight: 158.56	Molecular Weight: 429.46
cLogP= 1.76	cLogP= 2.32	cLogP =3.53
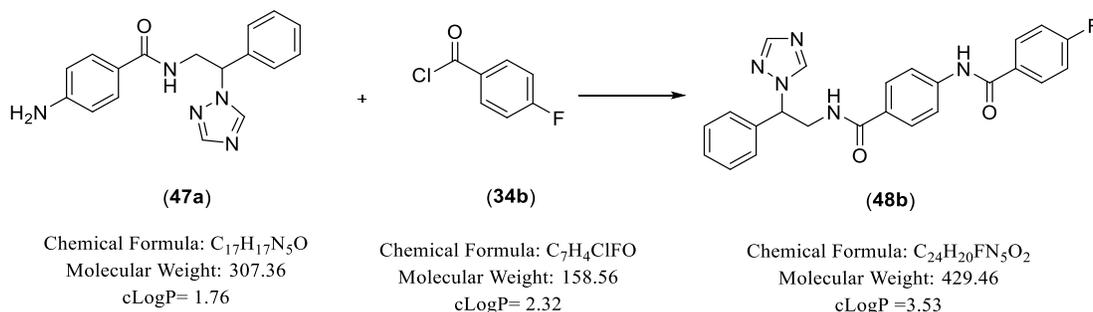
Prepared from 4-fluorobenzoyl chloride (**34b**, R^2= 4-F) (0.10 mL, 0.78 mmoL). Product obtained as a white solid which was purified by gradient column chromatography CH_2Cl_2-MeOH (96.5: 3.5 v/v), yield: 0.15 g (46 %). TLC (CH_2Cl_2-MeOH 9.5:0.5 v/v), R*f* = 0.34. M.p. 234-236 °C. ^{1}H NMR (DMSO-d_6): δ 10.46 (s, 1H, CON*H*), 8.75 (s, 1H, triazole), 8.63 (t, *J* = 5.5 Hz, 1H, N*H*CH$_2$), 8.05 (m, 2H, Ar), 8.04 (s, 1H, triazole), 7.83 (d, *J* = 8.9 Hz, 2H, Ar), 7.76 (d, *J* = 8.9 Hz, 2H, Ar), 7.44 (d, *J* = 7.1 Hz, 2H, Ar), 7.37 (m, 5H, Ar), 5.92 (dd, *J* = 5.5, 9.2 Hz, 1H, NHCHaHbC*H*), 4.09 (m, 1H, NHC*Ha*HbCH), 4.00 (ddd, *J* = 5.4, 10.8, 13.6 Hz, 1H, NHCHa*Hb*CH). ^{13}C NMR (DMSO-d_6): δ 166.72 & 165.65 (C, *C*-F), 165.15 (C, *C*ONH), 163.67 (C, *C*ONH), 152.15 (CH, triazole), 144.62 (CH, triazole), 142.35 (C, Ar), 138.48 (C, Ar), 131.54 (C, Ar), 131.02 (CH, Ar), 130.95 (CH, Ar), 129.34 (C, Ar), 129.14 (2 x CH, Ar), 128.74 (CH, Ar), 128.39 (2 x CH, Ar), 127.66 (2 x CH, Ar), 119.90 (2 x CH, Ar), 115.96 (CH, Ar), 115.78 (CH, Ar), 62.24 (NHCH$_2$*C*H), 43.96 (NH*C*H$_2$CH). HRMS (ESI), m/z. calcd for $C_{24}H_{20}FN_5O_2$ ([M + H]$^+$), 430.1679; found, 430.1678. HPLC (Method B2): 99.03%, R_t= 4.18 min.

(*R/S*)-4-Chloro-*N*-(4-((2-phenyl-2-(1*H*-1,2,4-triazol-1-yl)ethyl)carbamoyl)phenyl) benzamide (48c)

(47a)	(34c)	(48c)
Chemical Formula: $C_{17}H_{17}N_5O$	Chemical Formula: $C_7H_4Cl_2O$	Chemical Formula: $C_{24}H_{20}ClN_5O_2$
Molecular Weight: 307.36	Molecular Weight: 175.01	Molecular Weight: 445.91
cLogP= 1.76	cLogP= 2.72	cLogP =3.93
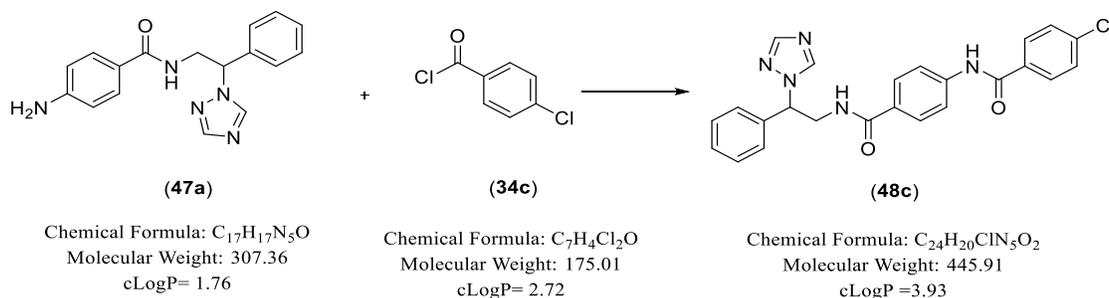
Prepared from 4-chlorobenzoyl chloride (**34c**, R^2= 4-Cl) (0.19 mL, 1.46 mmoL). Product obtained as a white solid which was purified by gradient column chromatography CH$_2$Cl$_2$-MeOH (96.5: 3.5 v/v), yield: 0.10 g (23 %). TLC (CH$_2$Cl$_2$-MeOH 9.5:0.5 v/v), Rf = 0.55. M.p. 236-238 °C. ^{1}H NMR (DMSO-d_6): δ 10.50 (s, 1H, CON*H*), 8.74 (s, 1H, triazole), 8.63 (t, J = 5.5 Hz, 1H, N*H*CH$_2$), 8.04 (s, 1H, triazole), 7.99 (d, J = 8.7 Hz, 2H, Ar), 7.84 (d, J = 8.9 Hz, 2H, Ar), 7.76 (d, J = 8.9 Hz, 2H, Ar), 7.62 (d, J = 8.7 Hz, 2H, Ar), 7.44 (d, J = 7.2 Hz, 2H, Ar), 7.39 (t, J = 7.4 Hz, 2H, Ar), 7.34 (t, J = 7.13 Hz, 1H, Ar), 5.92 (dd, J = 5.5, 9.2 Hz, 1H, NHCHaHbC*H*), 4.09 (m, 1H, NHC*Ha*HbCH), 4.00 (ddd, J = 5.4, 10.8, 13.6 Hz, 1H, NHCHa*Hb*CH). ^{13}C NMR (DMSO-d_6): δ 166.72 (C, *C*ONH), 165.16 (C, *C*ONH), 152.15 (CH, triazole), 144.62 (CH, triazole), 142.24 (C, Ar), 138.47 (C, Ar), 137.11 (C, *C*-Cl), 133.80 (C, Ar), 130.19 (2 x CH, Ar), 129.44 (C, Ar), 129.14 (2 x CH, Ar), 128.99 (2 x CH, Ar), 128.74 (CH, Ar), 128.41 (2 x CH, Ar), 127.66 (2 x CH, Ar), 119.95 (2 x CH, Ar), 62.24 (NHCH$_2$*C*H), 43.96 (NH*C*H$_2$CH). HRMS (ESI), m/z. calcd for C$_{24}$H$_{20}$ClN$_5$O$_2$ ([M + Na]$^+$), 468.1204; found, 468.1201. HPLC (Method B2): 97.47%, R$_t$= 4.69 min.

(*R/S*)-4-Chloro-*N*-(4-((2-(4-chlorophenyl)-2-(1*H*-1,2,4-triazol-1-yl)ethyl)carbamoyl) phenyl)benzamide (48d)

(47b)

Chemical Formula: C$_{17}$H$_{16}$ClN$_5$O
Molecular Weight: 341.80
cLog P: 2.32

(34c)

Chemical Formula: C$_7$H$_4$Cl$_2$O
Molecular Weight: 175.01
cLogP= 2.72

(48d)

Chemical Formula: C$_{24}$H$_{19}$Cl$_2$N$_5$O$_2$
Molecular Weight: 480.35
cLog P: 4.49
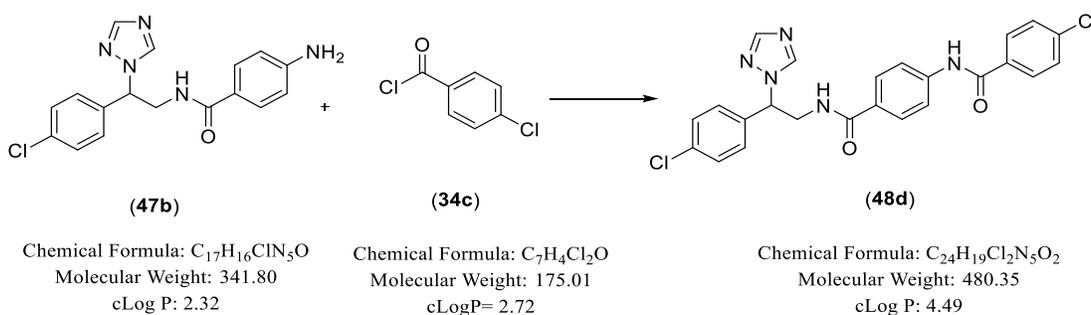
Prepared from 4-chlorobenzoyl chloride (**34c**, R^2= 4-Cl) (0.14 mL, 1.1 mmoL). Product obtained as a white solid which was purified by gradient column chromatography CH$_2$Cl$_2$-MeOH (97: 3 v/v), yield: 0.08 g (24 %). TLC (CH$_2$Cl$_2$-MeOH 9.5:0.5 v/v), Rf = 0.49. M.p. 242-244 °C. ^{1}H NMR (DMSO-d_6): δ 10.51 (s, 1H, CON*H*), 8.74 (s, 1H, triazole), 8.64 (t, J = 5.6 Hz, 1H, N*H*CH$_2$), 8.06 (s, 1H, triazole), 7.99 (d, J = 8.7 Hz, 2H, Ar), 7.84 (d, J = 8.9 Hz, 2H, Ar), 7.76 (d, J = 8.8 Hz, 2H, Ar), 7.63 (d, J = 8.7 Hz, 2H, Ar), 7.47 (brs, 4H, Ar), 5.94 (dd, J = 6.0, 8.7 Hz, 1H, NHCHaHbC*H*), 4.03 (m, 2H, NHC*HaHb*CH). ^{13}C NMR (DMSO-d_6): δ 166.72 (C, *C*ONH), 165.16 (C, *C*ONH), 152.31 (CH, triazole), 144.72 (CH, triazole), 142.27 (C, Ar),

137.37 (C, Ar), 137.12 (C, C-Cl), 133.80 (C, Ar), 133.43 (C, C-Cl), 130.19 (2 x CH, Ar), 129.70 (2 x CH, Ar), 129.37 (C, Ar), 129.13 (2 x CH, Ar), 128.99 (2 x CH, Ar), 128.41 (2 x CH, Ar), 119.95 (2 x CH, Ar), 61.40 (NHCH$_2$$C$H), 43.83 (NH$CH_2$CH). HRMS (ESI), m/z. calcd for $C_{24}H_{19}Cl_2N_5O_2$ ([M + H]$^+$), 480.0994; found, 480.0993. HPLC (Method A): 98.58%, R$_t$= 4.48 min.

(*R/S*)-4-Chloro-*N*-(4-((2-(2,4-dichlorophenyl)-2-(1*H*-1,2,4-triazol-1-yl)ethyl) carbamoyl)phenyl)benzamide (48e)

(47c)
Chemical Formula: $C_{17}H_{15}Cl_2N_5O$
Molecular Weight: 376.24
cLog P: 2.88

(34c)
Chemical Formula: $C_7H_4Cl_2O$
Molecular Weight: 175.01
cLogP= 2.72

(48e)
Chemical Formula: $C_{24}H_{18}Cl_3N_5O_2$
Molecular Weight: 514.79
cLog P: 5.05

Prepared from 4-chlorobenzoyl chloride (**34c**, R^2= 4-Cl) (0.11 mL, 0.87 mmoL). Product obtained as an off-white solid which was purified by gradient column chromatography CH$_2$Cl$_2$-MeOH (97: 3 v/v), yield: 0.20 g (64 %). TLC (CH$_2$Cl$_2$-MeOH 9.5:0.5 v/v), Rf = 0.51. M.p. 194-196 °C. ^{1}H NMR (DMSO-d_6): δ 10.51 (s, 1H, CONH), 8.78 (s, 1H, triazole), 8.65 (t, J = 5.6 Hz, 1H, NHCH$_2$), 8.04 (s, 1H, triazole), 7.99 (d, J = 8.7 Hz, 2H, Ar), 7.84 (d, J = 8.9 Hz, 2H, Ar), 7.76 (d, J = 8.9 Hz, 2H, Ar), 7.69 (d, J = 2.2 Hz, 1H, Ar), 7.67 (d, J = 8.6 Hz, 1H, Ar), 7.63 (d, J = 8.7 Hz, 2H, Ar), 7.52 (dd, J = 2.2, 8.5 Hz, 1H, Ar), 6.28 (dd, J = 5.8, 8.8 Hz, 1H, NHCHaHbCH), 4.15 (m, 1H, NHCHaHbCH), 3.96 (ddd, J = 5.2, 10.8, 13.6 Hz, 1H, NHCHaHbCH). ^{13}C NMR (DMSO-d_6): δ 166.73 (C, CONH), 165.16 (C, CONH), 152.35 (CH, triazole), 145.05 (CH, triazole), 142.29 (C, Ar), 137.12 (C, Ar), 134.42 (C, C-Cl), 134.34 (2 x C, C-Cl), 133.79 (C, Ar), 130.84 (CH, Ar), 130.19 (2 x CH, Ar), 129.60 (CH, Ar), 129.33 (C, Ar), 128.99 (2 x CH, Ar), 128.43 (2 x CH, Ar), 128.39 (CH, Ar), 119.95 (2 x CH, Ar), 58.03 (NHCH$_2$$C$H), 42.90 (NH$CH_2$CH). HRMS (ESI), m/z. calcd for $C_{24}H_{18}Cl_3N_5O_2$ ([M + H]$^+$), 514.0604; found, 514.0595. HPLC (Method B2): 98.32%, R$_t$= 6.39 min.
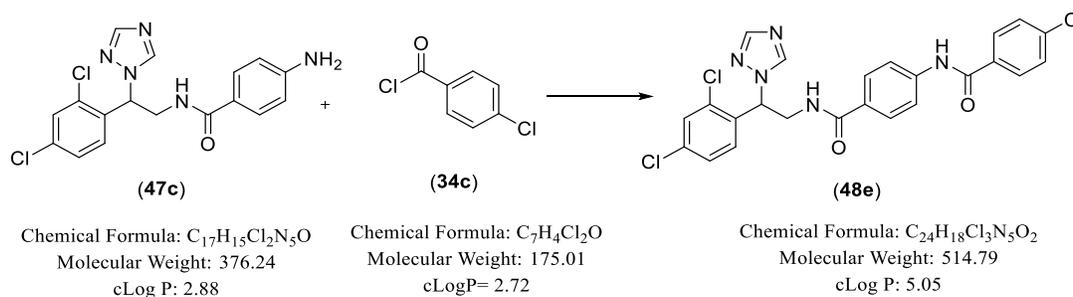
(*R/S*)-4-Methoxy-*N*-(4-((2-phenyl-2-(1*H*-1,2,4-triazol-1-yl)ethyl)carbamoyl)phenyl) benzamide (48f)

(47a)
Chemical Formula: $C_{17}H_{17}N_5O$
Molecular Weight: 307.36
cLogP= 1.76

(34d)
Chemical Formula: $C_8H_7ClO_2$
Molecular Weight: 170.59
cLogP= 2.04

(48f)
Chemical Formula: $C_{25}H_{23}N_5O_3$
Molecular Weight: 441.49
cLogP= 3.25
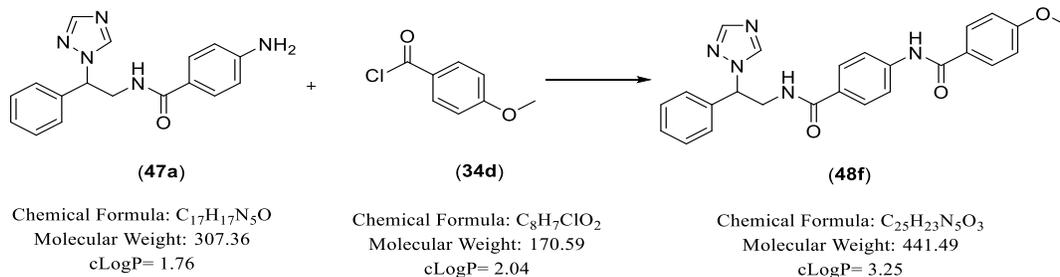
Prepared from 4-methoxybenzoyl chloride (**34d**, R^2= 4-Cl) (0.15 mL, 1.1 mmoL). Product obtained as a white solid which was purified by gradient column chromatography CH_2Cl_2-MeOH (96.5: 3.5 v/v), yield: 0.21 g (43 %). TLC (CH_2Cl_2-MeOH 9.5:0.5 v/v), R*f* = 0.27. M.p. 238-246 °C. ^{1}H NMR (DMSO-d_6): δ 10.28 (s, 1H, CON*H*), 8.74 (s, 1H, triazole), 8.61 (t, *J* = 5.5 Hz, 1H, N*H*CH$_2$), 8.04 (s, 1H, triazole), 7.97 (d, *J* = 8.9 Hz, 2H, Ar), 7.83 (d, *J* = 8.8 Hz, 2H, Ar), 7.74 (d, *J* = 8.8 Hz, 2H, Ar),7.44 (d, *J* = 7.2 Hz, 2H, Ar), 7.40 (t, *J* = 7.4 Hz, 2H, Ar), 7.34 (t, *J* = 7.2 Hz, 1H, Ar), 7.08 (d, *J* = 8.9 Hz, 2H, Ar), 5.92 (dd, *J* = 5.4, 9.1 Hz, 1H, NHCHaHbC*H*), 4.09 (m, 1H, NHC*Ha*HbCH), 3.40 (ddd, *J* = 5.4, 10.9, 13.7 Hz, 1H, NHCHa*Hb*CH), 3.85 (s, 3H, OC*H₃*). ^{13}C NMR (DMSO-d_6): δ 166.76 (C, *C*ONH), 165.58 (C, *C*ONH), 162.55 (C, *C*-OCH₃), 152.14 (CH, triazole), 143.90 (CH, triazole), 142.66 (C, Ar), 138.48 (C, Ar), 130.19 (2 x CH, Ar), 129.14 (2 x CH, Ar), 128.99 (C, Ar), 128.73 (CH, Ar), 128.34 (2 x CH, Ar), 127.66 (2 x CH, Ar), 127.08 (C, Ar), 119.78 (2 x CH, Ar), 114.13 (2 x CH, Ar), 62.25 (NHCH$_2$*C*H), 55.93 (O*C*H₃), 43.95 (NH*C*H₂CH). HRMS (ESI), m/z. calcd for $C_{25}H_{23}N_5O_3$ ([M + H]$^+$), 442.1879; found, 442.1880. HPLC (Method B2): 97.62%, R_t= 4.85 min.

(*R/S*)-*N*-(2-Phenyl-2-(1*H*-1,2,4-triazol-1-yl)ethyl)-4-(phenylsulfonamido)benzamide (49a)

(47a)	(17a)	(49a)
Chemical Formula: $C_{17}H_{17}N_5O$	Chemical Formula: $C_6H_5ClO_2S$	Chemical Formula: $C_{23}H_{21}N_5O_3S$
Molecular Weight: 307.36	Molecular Weight: 176.61	Molecular Weight: 447.51
cLogP= 1.76	cLogP=1.77	cLogP= 2.97
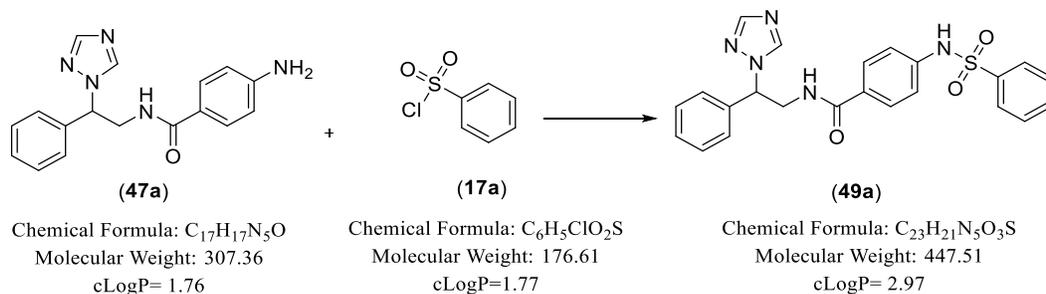
Prepared from benzenesulfonyl chloride (**17a**, R^2= 4-H) (0.10 mL, 0.78 mmoL). Product obtained as a white solid which was purified by gradient column chromatography CH_2Cl_2-MeOH (96.5: 3.5 v/v), yield: 0.11 g (39 %). TLC (CH_2Cl_2-MeOH 9.5:0.5 v/v), Rf = 0.71. M.p. 200-202 °C. ^{1}H NMR (DMSO-d_6): δ 10.67 (brs, 1H, SO_2N*H*), 8.70 (s, IH, triazole), 8.55 (t, *J* = 5.55 Hz, 1H, N*H*CH$_2$), 8.01 (s, 1H, triazole), 7.79 (d, *J* = 6.90 Hz, 2H, Ar), 7.57 (m, 5H, Ar), 7.36 (m, 5H, Ar), 7.12 (d, *J* = 8.75 Hz, 2H, Ar), 5.85 (dd, *J* = 5.4, 9.15 Hz, 1H, NHCHaHbC*H*), 4.03 (m, 1H, NHC*Ha*HbCH), 3.94 (ddd, *J* = 5.40, 10.80, 13.65 Hz, 1H, NHCHa*Hb*CH). ^{13}C NMR (DMSO-d_6): δ 166.59 (C, *C*ONH), 152.13 (CH, triazole), 144.59 (CH, triazole), 141.10 (C, Ar), 139.81 (C, Ar), 138.41 (C, Ar), 133.59 (CH, Ar), 129.85 (2 x CH, Ar), 129.53 (C, Ar), 129.12 (2 x CH, Ar), 128.93 (2 x CH, Ar), 128.73 (CH, Ar), 127.62 (2 x CH, Ar), 127.1087 (2 x CH, Ar), 118.79 (2 x CH, Ar), 62.20 (NHCH$_2$*C*H), 43.91 (NH*C*H$_2$CH). HRMS (ESI), m/z. calcd for $C_{23}H_{21}N_5O_3S$ ([M + Na]$^+$), 470.1263; found, 470.1247. HPLC (Method A): 99.19%, R_t= 4.11 min.

(*R/S*)-4-((4-Fluorophenyl)sulfonamido)-*N*-(2-phenyl-2-(1*H*-1,2,4-triazol-1-yl)ethyl) benzamide (49b)

(47a)	(17b)	(49)
Chemical Formula: $C_{17}H_{17}N_5O$	Chemical Formula: $C_6H_4ClFO_2S$	Chemical Formula: $C_{23}H_{20}FN_5O_3S$
Molecular Weight: 307.36	Molecular Weight: 194.60	Molecular Weight: 465.50
cLogP= 1.76	cLogP= 1.92	cLogP =3.13
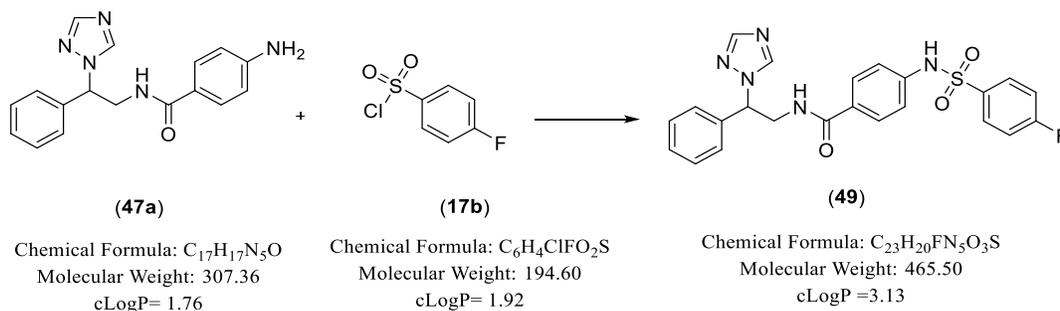
Prepared from 4-fluorobenzenesulfonyl chloride (**17b**, R^2= 4-F) (0.15 g, 0.78 mmoL). Product obtained as a white solid which was purified by gradient column chromatography CH$_2$Cl$_2$-MeOH (97: 3 v/v), yield: 0.12 g (32 %). TLC (CH$_2$Cl$_2$-MeOH 9.5:0.5 v/v), Rf = 0.38. M.p. 200-202 °C. ^{1}H NMR (DMSO-d_6): δ 10.70 (brs, 1H, SO$_2$NH), 8.74 (s, 1H, triazole), 8.56 (t, J = 5.5 Hz, 1H, NHCH$_2$), 8.01 (s, 1H, triazole), 7.85 (dd, J = 5.1, 8.9 Hz, 2H, Ar), 7.60 (d, J = 8.7 Hz, 2H, Ar), 7.36 (m, 7H, Ar), 7.12 (d, J = 8.7 Hz, 2H, Ar), 5.85 (dd, J = 5.4, 9.2 Hz, 1H, NHCHaHbCH), 4.04 (m, 1H, NHCHaHbCH), 3.93 (m, 1H, NHCHaHbCH). ^{13}C NMR (DMSO-d_6): δ 166.59 (C, CONH), 165.85 & 163.84 (C,C-F), 152.12 (CH, triazole), 144.58 (CH, triazole), 141.07 (C, Ar), 138.39 (C, Ar), 136.24 (C, Ar), 130.25 (CH, Ar), 130.17 (CH, Ar), 129.60 (C, Ar), 129.12 (2 x CH, Ar), 128.96 (2 x CH, Ar), 128.74 (CH, Ar), 127.62 (2 x CH, Ar), 119.01 (2 x CH, Ar), 117.16 (CH, Ar), 116.98 (CH, Ar), 62.19 (NHCH$_2$$C$H), 43.90 (NH$CH_2$CH). HRMS (ESI), m/z. calcd for C$_{23}$H$_{20}$FN$_5$O$_3$S ([M + Na]$^+$), 488.1169; found, 488.1161. HPLC (Method B2): 98.17%, R$_t$= 3.84 min.

(*R/S*)-4-((4-Chlorophenyl)sulfonamido)-*N*-(2-phenyl-2-(1*H*-1,2,4-triazol-1-yl)ethyl) benzamide (49c)

(**47a**)

Chemical Formula: C$_{17}$H$_{17}$N$_5$O
Molecular Weight: 307.36
cLogP= 1.76

(**17c**)

Chemical Formula: C$_6$H$_4$Cl$_2$O$_2$S
Molecular Weight: 211.06
cLogP= 2.32

(**49c**)

Chemical Formula: C$_{23}$H$_{20}$ClN$_5$O$_3$S
Molecular Weight: 481.96
cLogP =3.53

Prepared from 4-chlorobenzenesulfonyl chloride (**17c**, R^2= 4-Cl) (0.205 g, 0.97 mmoL). Product obtained as a white solid which was purified by gradient column chromatography CH$_2$Cl$_2$-MeOH (96.5: 3.5 v/v), yield: 0.09 g (19 %). TLC (CH$_2$Cl$_2$-MeOH 9.5:0.5 v/v), Rf = 0.49. M.p. 186-188 °C. ^{1}H NMR (DMSO-d_6): δ 10.72 (brs, 1H, SO$_2$NH), 8.71 (s, 1H, triazole), 8.57 (t, J = 5.5 Hz, 1H, NHCH$_2$), 8.02 (s, 1H, triazole), 7.79 (d, J = 8.8 Hz, 2H, Ar), 7.63 (dd, J = 8.8, 12.0 Hz, 4H, Ar), 7.39 (pentet, J = 7.0 Hz, 4H, Ar), 7.32 (t, J = 7.0 Hz, 1H, Ar), 7.13 (d, J = 8.8 Hz, 2H, Ar), 5.86 (dd, J = 5.3, 9.2 Hz, 1H, NHCHaHbCH), 4.04 (m, 1H, NHCHaHbCH), 3.95 (ddd, J = 5.4, 10.8, 13.7 Hz, 1H, NHCHaHbCH). ^{13}C NMR (DMSO-d_6): δ 166.56 (C, CONH), 152.13 (CH, triazole), 144.60 (CH, triazole), 140.76 (C, Ar), 138.62 (C, Ar), 138.50 (C, Ar), 138.41

(C, *C*-Cl), 130.04 (2 x CH, Ar), 129.85 (C, Ar), 129.12 (2 x CH, Ar), 129.07 (2 x CH, Ar), 129.00 (2 x CH, Ar), 128.73 (CH, Ar), 127.62 (2 x CH, Ar), 119.12 (2 x CH, Ar), 62.19 (NHCH$_2$*C*H), 43.92 (NH*C*H$_2$CH). HRMS (ESI), m/z. calcd for C$_{23}$H$_{20}$ClN$_5$O$_3$S ([M + H]$^+$), 482.1053; found, 432.1055. HPLC (Method B2): 99.31%, R$_t$= 4.12 min.

(*R/S*)-4-((4-Methoxyphenyl)sulfonamido)-*N*-(2-phenyl-2-(1*H*-1,2,4-triazol-1-yl)ethyl) benzamide (49d)

(47a)	(17d)	(49d)
Chemical Formula: C$_{17}$H$_{17}$N$_5$O	Chemical Formula: C$_7$H$_7$ClO$_3$S	Chemical Formula: C$_{24}$H$_{23}$N$_5$O$_4$S
Molecular Weight: 307.36	Molecular Weight: 206.64	Molecular Weight: 477.54
cLogP= 1.76	cLogP= 1.64	cLogP =2.85

Prepared from 4-methoxybenzenesulfonyl chloride (**17d**, R^2= 4-OCH$_3$) (0.36 g, 1.73 mmoL). Product obtained as a white solid which was purified by gradient column chromatography CH$_2$Cl$_2$-MeOH (97: 3 v/v), yield: 0.23 g (28 %). TLC (CH$_2$Cl$_2$-MeOH 9.5:0.5 v/v), R*f* = 0.43. M.p. 210-212 °C. ^{1}H NMR (DMSO-*d$_6$*): δ 10.52 (s, 1H, SO$_2$N*H*), 8.70 (s, 1H, triazole), 8.55 (t, *J* = 5.53 Hz, 1H, N*H*CH$_2$), 8.01 (s, 1H, triazole), 7.73 (d, *J* = 8.95 Hz, 2H, Ar), 7.60 (d, *J* = 8.8 Hz, 2H, Ar), 7.38 (pentet, *J* = 7.1 Hz, 4H, Ar), 7.32 (t, *J* = 7.0 Hz, 1H, Ar), 7.12 (d, *J* = 8.8 Hz, 2H, Ar), 7.1 (d, *J* = 9.0 Hz, 2H, Ar), 5.85 (dd, *J* = 5.4, 9.1 Hz, 1H, NHCHaHbC*H*), 4.03 (m, 1H, NHC*Ha*HbCH), 3.94 (ddd, *J* = 5.4, 10.8, 13.6 Hz, 1H, NHCHa*Hb*CH), 3.79 (s, 3H, OC*H$_3$*). ^{13}C NMR (DMSO-*d$_6$*): δ 166.61 (C, *C*ONH), 163.05 (C,*C*-OCH$_3$), 152.13 (CH, triazole), 144.59 (CH, triazole), 141.29 (C, Ar), 138.41 (C, Ar), 131.34 (C, Ar), 129.38 (2 x CH, Ar), 129.31 (C, Ar), 129.12 (2 x CH, Ar), 128.90 (2 x CH, Ar), 128.73 (CH, Ar), 127.62 (2 x CH, Ar), 118.55 (2 x CH, Ar), 114.97 (2 x CH, Ar), 62.21 (NHCH$_2$*C*H), 56.11 (O*C*H$_3$), 43.91 (NH*C*H$_2$CH). HRMS (ESI), m/z. calcd for C$_{24}$H$_{23}$N$_5$O$_4$S ([M + H]$^+$), 478.1549; found, 478.1554. HPLC (Method B2): 99.34%, R$_t$= 3.81 min.

(*R/S*)-*N*-(2-Phenyl-2-(1*H*-1,2,4-triazol-1-yl)ethyl)-4-(3-phenylureido)benzamide (51a)

(47a)
Chemical Formula: $C_{17}H_{17}N_5O$
Molecular Weight: 307.36
cLogP= 1.76

(50a)
Chemical Formula: C_7H_5NO
Molecular Weight: 119.12

(51a)
Chemical Formula: $C_{24}H_{22}N_6O_2$
Molecular Weight: 426.48
cLogP= 3.05

Prepared from phenyl isocyanate (**50a**, R^2= 4-H) (0.18 mL, 1.65 mmoL). Product obtained as a white solid which was purified by gradient column chromatography CH_2Cl_2-MeOH (96.5: 3.5 v/v), yield: 0.09 g (12.4 %). TLC (CH_2Cl_2-MeOH 9.5:0.5 v/v), R*f* = 0.51. M.p. 244-246 °C. ^{1}H NMR (DMSO-*d$_6$*): δ 8.92 (s, 1H, *H*NC=ONH), 8.74 (s, 1H, triazole), 8.73 (s, 1H, HNC=ON*H*), 8.54 (t, *J* = 5.5 Hz, 1H, N*H*CH$_2$), 8.03 (s, 1H, triazole), 7.69 (d, *J* = 8.8 Hz, 2H, Ar), 7.49 (d, *J* = 8.8 Hz, 2H, Ar), 7.39 (m, 7H, Ar), 7.29 (t, *J* = 7.9 Hz, 2H, Ar), 6.98 (t, *J* = 7.4 Hz, 1H, Ar), 5.91 (dd, *J* = 5.5, 9.1 Hz, 1H, NHCHaHbC*H*), 4.08 (m, 1H, NHC*Ha*HbCH), 3.98 (ddd, *J* = 5.4, 10.8, 13.6 Hz, 1H, NHCHa*Hb*CH). ^{13}C NMR (DMSO-*d$_6$*): δ 166.79 (C, *C*O), 152.73 (C, *C*O), 152.13 (CH, triazole), 144.61 (CH, triazole), 143.13 (C, Ar), 139.86 (C, Ar), 138.50 (C, Ar), 129.28 (2 x CH, Ar), 129.13 (2 x CH, Ar), 128.72 (CH, Ar), 128.67 (2 x CH, Ar), 127.65 (2 x CH, Ar), 127.42 (C, Ar), 122.56 (CH, Ar), 118.81 (2 x CH, Ar), 117.56 (2 x CH, Ar), 62.25 (NHCH$_2$*C*H), 43.93 (NH*C*H$_2$CH). HRMS (ESI), m/z. calcd for $C_{24}H_{22}N_6O_2$ ([M + Na]$^+$), 449.1702; found, 449.1694. HPLC (Method B2): 99.09%, R_t= 6.39 min.

(*R/S*)-4-(3-(4-Fluorophenyl)ureido)-*N*-(2-phenyl-2-(1*H*-1,2,4-triazol-1-yl)ethyl) benzamide (51b)

(47a)
Chemical Formula: $C_{17}H_{17}N_5O$
Molecular Weight: 307.36
cLogP= 1.76

(50b)
Chemical Formula: C_7H_4FNO
Molecular Weight: 137.11

(51b)
Chemical Formula: $C_{24}H_{21}FN_6O_2$
Molecular Weight: 444.47
cLogP= 3.2

Prepared from 4-fluorophenyl isocyanate (**50b**, R^2= 4-F) (0.16 mL, 1.44 mmoL). Product

obtained as a white solid which was purified by gradient column chromatography CH_2Cl_2-MeOH (96.5: 3.5 v/v), yield: 0.13 g (30 %). TLC (CH_2Cl_2-MeOH 9.5:0.5 v/v), Rf = 0.36. M.p. 234-236 °C. ^{1}H NMR (DMSO-d_6): δ 8.94 (s, 1H, *H*NC=ONH), 8.79 (s, 1H, HNC=ON*H*), 8.73 (s, 1H, triazole), 8.55 (t, *J* = 5.5 Hz, 1H, N*H*CH$_2$), 8.03 (s, 1H, triazole), 7.69 (d, *J* = 8.8 Hz, 2H, Ar), 7.46 (m, 6H, Ar), 7.39 (t, *J* = 7.4 Hz, 2H, Ar), 7.34 (t, *J* = 7.1 Hz, 1H, Ar), 7.13 (t, *J* = 8.9 Hz, 2H, Ar), 5.91 (dd, *J* = 5.5, 9.2 Hz, 1H, NHCHaHbC*H*), 4.07 (m, 1H, NHC*Ha*HbCH), 3.98 (ddd, *J* = 5.4, 10.8, 13.6 Hz, 1H, NHCHa*Hb*CH). ^{13}C NMR (DMSO-d_6): δ 166.79 (C, *C*O), 158.89 & 157.00 (C, *C*-F), 152.85 (C, *C*O), 152.14 (CH, triazole), 144.60 (CH, triazole), 143.11 (C, Ar), 138.95 (C, Ar), 136.20 (C, Ar), 129.13 (2 x CH, Ar), 128.72 (CH, Ar), 128.66 (2 x CH, Ar), 127.65 (2 x CH, Ar), 127.45 (C, Ar), 120.66 (CH, Ar), 120.60 (CH, Ar), 117.61 (2 x CH, Ar), 115.87 (CH, Ar), 115.69 (CH, Ar), 62.25 (NHCH$_2$*C*H), 43.94 (NH*C*H$_2$CH). HRMS (ESI), m/z. calcd for $C_{24}H_{21}FN_6O_2$ ([M + H]$^+$), 445.1788; found, 445.1787. HPLC (Method B2): 96.73%, R$_t$= 4.18 min.

(*R/S*)-4-(3-(4-Chlorophenyl)ureido)-*N*-(2-phenyl-2-(1*H*-1,2,4-triazol-1-yl)ethyl) benzamide (51c)

(47a)
Chemical Formula: $C_{17}H_{17}N_5O$
Molecular Weight: 307.36
cLogP= 1.76

(50c)
Chemical Formula: C_7H_4ClNO
Molecular Weight: 153.57

(51c)
Chemical Formula: $C_{24}H_{21}ClN_6O_2$
Molecular Weight: 460.92
cLogP= 3.6

Prepared from 4-chlorophenyl isocyanate (**50c**, R^2= 4-Cl) (0.11 mL, 0.885 mmoL). Product obtained as a white solid which was purified by gradient column chromatography CH_2Cl_2-MeOH (96.5: 3.5 v/v), yield: 0.11 g (26 %). TLC (CH_2Cl_2-MeOH 9.5:0.5 v/v), Rf = 0.38. M.p. 224-226 °C. ^{1}H NMR (DMSO-d_6): δ 8.98 (s, 1H, *H*NC=ONH), 8.94 (s, 1H, HNC=ON*H*), 8.73 (s, 1H, triazole), 8.55 (t, *J* = 5.5 Hz, 1H, N*H*CH$_2$), 8.03 (s, 1H, triazole), 7.69 (d, *J* = 8.8 Hz, 2H, Ar), 7.50 (d, *J* = 9.0 Hz, 4H, Ar), 7.41 (pentet, *J* = 7.8 Hz, 4H, Ar), 7.34 (d, *J* = 8.9 Hz, 3H, Ar), 5.91 (dd, *J* = 5.4, 9.1 Hz, 1H, NHCHaHbC*H*), 4.07 (m, 1H, NHC*Ha*HbCH), 3.98 (ddd, *J* = 5.4, 10.9, 13.6 Hz, 1H, NHCHa*Hb*CH). ^{13}C NMR (DMSO-d_6): δ 166.77 (C, *C*O), 152.66 (C, *C*O), 152.13 (CH, triazole), 144.61 (CH, triazole), 142.95 (C, Ar), 138.90 (C, Ar), 138.48 (C, Ar),

129.13 (4 x CH, Ar), 128.72 (CH, Ar), 128.67 (2 x CH, Ar), 127.65 (2 x CH, Ar), 127.59 (C, *C*-Cl), 126.08 (C, Ar), 120.35 (2 x CH, Ar), 117.70 (2 x CH, Ar), 62.25 (NHCH$_2$*C*H), 43.93 (NH*C*H$_2$CH). HRMS (ESI), m/z. calcd for C$_{24}$H$_{21}$ClN$_6$O$_2$ ([M + Na]$^+$), 483.1313; found, 483.1305. HPLC (Method B2): 99.99%, R$_t$= 4.69 min.

(*R/S*)-4-(3-(4-Methoxyphenyl)ureido)-*N*-(2-phenyl-2-(1*H*-1,2,4-triazol-1-yl)ethyl) benzamide (51d)

(47a)	(50d)	(51d)
Chemical Formula: C$_{17}$H$_{17}$N$_5$O	Chemical Formula: C$_8$H$_7$NO$_2$	Chemical Formula: C$_{25}$H$_{24}$N$_6$O$_3$
Molecular Weight: 307.36	Molecular Weight: 149.15	Molecular Weight: 456.51
cLogP= 1.76		cLogP= 2.92

Prepared from 4-methoxyphenyl isocyanate (**50d**, R^2= 4-OCH$_3$) (0.21 mL, 1.65 mmoL). Product obtained as a white solid which was purified by gradient column chromatography CH$_2$Cl$_2$-MeOH (96.5: 3.5 v/v), yield: 0.07 g (9 %). TLC (CH$_2$Cl$_2$-MeOH 9.5:0.5 v/v), R*f* = 0.38. M.p. 218-220 °C. ^{1}H NMR (DMSO-*d$_6$*): δ 8.86 (s, 1H, *H*NC=ONH), 8.73 (s, 1H, triazole), 8.57 (s, 1H, HNC=ON*H*), 8.53 (t, *J* = 5.5 Hz, 1H, N*H*CH$_2$), 8.03 (s, 1H, triazole), 7.68 (d, *J* = 8.8 Hz, 2H, Ar), 7.47 (d, *J* = 8.8 Hz, 2H, Ar), 7.38 (m, 7H, Ar), 6.87 (d, *J* = 9.1 Hz, 2H, Ar), 5.90 (dd, *J* = 5.5, 9.2 Hz, 1H, NHCHaHbC*H*), 4.06 (m, 1H, NHC*Ha*HbCH), 3.98 (ddd, *J* = 5.4, 10.9, 13.6 Hz, 1H, NHCHa*Hb*CH), 3.72 (s, 3H, OC*H$_3$*). ^{13}C NMR (DMSO-*d$_6$*): δ 166.80 (C, *C*O), 155.11 (C, *C*-OCH$_3$), 152.92 (C, *C*O), 152.13 (CH, triazole), 144.61 (CH, triazole), 143.34 (C, Ar), 138.51 (C, Ar), 132.86 (C, Ar), 129.13 (2 x CH, Ar), 128.72 (CH, Ar), 128.65 (2 x CH, Ar), 127.65 (2 x CH, Ar), 127.20 (C, Ar), 120.66 (2 x CH, Ar), 117.44 (2 x CH, Ar), 114.47 (2 x CH, Ar), 62.26 (NHCH$_2$*C*H), 55.65 (O*C*H$_3$), 43.93 (NH*C*H$_2$CH). HRMS (ESI), m/z. calcd for C$_{25}$H$_{24}$N$_6$O$_3$ ([M + H]$^+$), 457.1988; found, 457.1987. HPLC (Method B2): 97.02%, R$_t$= 4.02 min.

7.4.22 General method to form thiourea linker compounds (53)

(*R/S*)-4-Amino-*N*-(2-phenyl-2-(1*H*-1,2,4-triazol-1-yl)ethyl)benzamide (**47**) (1.0 meq) was dissolved in dry THF (10 mL/mmoL), and triethylamine (2 mmol) was added. To this mixture, aryl-phenyl isothiocyanate (**52**) (1.5 meq) was added dropwise and the reaction was stirred at 60°C for 24 h.[109] The solvent was evaporated under reduced pressure, and the residue was diluted in CH_2Cl_2 (50 mL), washed with 1M aqueous HCl (50 mL) and H_2O (50 mL), then dried ($MgSO_4$) and concentrated under reduce pressure. The product was purified by CH_2Cl_2-MeOH gradient column chromatography.

(*R/S*)-*N*-(2-Phenyl-2-(1*H*-1,2,4-triazol-1-yl)ethyl)-4-(3-phenylthioureido)benzamide (53a)

(**47a**)
Chemical Formula: $C_{17}H_{17}N_5O$
Molecular Weight: 307.36
cLogP= 1.76

(**52a**)
Chemical Formula: C_7H_5NS
Molecular Weight: 135.18
cLogP= 2.2

(**53a**)
Chemical Formula: $C_{24}H_{22}N_6OS$
Molecular Weight: 442.54
cLogP= 4.19

Prepared from phenyl isothiocyanate (**52a**, R^2= 4-H) (0.11 mL, 0.92 mmol). Product obtained as an off-white solid which was purified by gradient column chromatography CH_2Cl_2-MeOH (96.5: 3.5 v/v), yield: 0.07 g (18 %). TLC (CH_2Cl_2-MeOH 9.5:0.5 v/v), R*f* = 0.59. M.p. 152-154 °C. ^{1}H NMR (DMSO-d_6): δ 9.99 (brs, 1H, *H*NC=SNH), 9.95 (brs, 1H, HNC=SN*H*), 8.74 (s, IH, triazole), 8.63 (t, *J* = 5.48 Hz, 1H, N*H*CH₂), 8.04 (s, 1H, triazole), 7.70 (d, *J* = 8.75 Hz, 2H, Ar), 7.58 (d, *J* = 8.70 Hz, 2H, Ar), 7.48 (d, *J* = 7.45 Hz, 2H, Ar), 7.45 (d, *J* = 7.20 Hz, 2H, Ar), 7.39 (t, *J* = 7.35 Hz, 2H, Ar), 7.34 (t, *J* = 7.9 Hz, 3H, Ar), 7.14 (t, *J* = 7.38 Hz, 1H, Ar), 5.92 (dd, *J* = 5.55, 9.1 Hz, 1H, NHCHaHbC*H*), 4.08 (m, 1H, NHC*Ha*HbCH), 4.00 (ddd, *J* = 5.40, 10.90, 13.55 Hz, 1H, NHCHa*Hb*CH). ^{13}C NMR (DMSO-d_6): δ 179.90 (C, *C*=S), 166.74 (C, *C*ONH), 152.15 (CH, triazole), 144.62 (CH, triazole), 142.88 (C, Ar), 139.73 (C, Ar), 138.43 (C, Ar), 129.68 (C, Ar), 129.14 (2 x CH, Ar), 128.98 (2 x CH, Ar), 128.74 (CH, Ar), 128.06 (2 x CH, Ar), 127.67 (2 x CH, Ar), 125.10 (CH, Ar), 124.154 (2 x CH, Ar), 122.64 (2 x CH, Ar), 62.16 (NHCH₂*C*H), 43.95 (NH*C*H₂CH). HRMS (ESI), m/z. calcd for $C_{24}H_{22}N_6OS$ ([M + Na]$^+$),

465.1474; found, 465.1463. HPLC (Method A): 99.13%, R_t= 3.83 min.

(*R/S*)-4-(3-(4-Fluorophenyl)thioureido)-*N*-(2-phenyl-2-(1*H*-1,2,4-triazol-1-yl)ethyl) benzamide (53b)

(**47a**)
Chemical Formula: $C_{17}H_{17}N_5O$
Molecular Weight: 307.36
cLogP= 1.76

(**52b**)
Chemical Formula: C_7H_4FNS
Molecular Weight: 153.17
cLogP= 2.36

(**53b**)
Chemical Formula: $C_{24}H_{21}FN_6OS$
Molecular Weight: 460.53
cLogP=4.35

Prepared from 4-fluorophenyl isothiocyanate (**52b**, R^2= 4-F) (0.36 gm, 2.32 mmoL). Product obtained as a white solid which was purified by gradient column chromatography CH_2Cl_2-MeOH (97: 3 v/v), yield: 0.12 g (17 %). TLC (CH_2Cl_2-MeOH 9.5:0.5 v/v), R*f* = 0.33. M.p. 166-168 °C. ^{1}H NMR (DMSO-d_6): δ 9.99 (brs, 1H, *H*NC=SNH), 9.91 (brs, 1H, HNC=SN*H*), 8.73 (s, 1H, triazole), 8.63 (t, *J* = 5.5 Hz, 1H, N*H*CH₂), 8.03 (s, 1H, triazole), 7.70 (d, *J* = 8.7 Hz, 2H, Ar), 7.56 (d, *J* = 8.7 Hz, 2H, Ar), 7.46 (m, 4H, Ar), 7.39 (t, *J* = 7.3 Hz, 2H, Ar), 7.34 (t, *J* = 7.1 Hz, 1H, Ar), 7.18 (t, *J* = 8.9 Hz, 2H, Ar), 5.92 (dd, *J* = 5.6, 9.2 Hz, 1H, NHCHaHbC*H*), 4.08 (m, 1H, NHC*Ha*HbCH), 3.99 (ddd, *J* = 5.4, 10.9, 13.6 Hz, 1H, NHCHa*Hb*CH). ^{13}C NMR (DMSO-d_6): δ 180.29 (C, *C*=S), 166.72 (C, *C*ONH), 160.67 & 158.75 (C, *C*-F), 152.15 (CH, triazole), 144.62 (CH, triazole), 142.79 (C, Ar), 138.43 (C, Ar), 136.05 (C, Ar), 129.75 (C, Ar), 129.14 (2 x CH, Ar), 128.74 (CH, Ar), 128.08 (2 x CH, Ar), 127.67 (2 x CH, Ar), 126.74 (CH, Ar), 126.67 (CH, Ar), 122.72 (2 x CH, Ar), 115.67 (CH, Ar), 115.49 (CH, Ar), 62.15 (NHCH₂*C*H), 43.95 (NH*C*H₂CH). HRMS (ESI), m/z. calcd for $C_{24}H_{21}FN_6OS$ ([M + Na]$^+$), 483.1380; found, 483.1366. HPLC (Method B2): 98.20%, R_t= 3.96 min.

(*R/S*)-4-(3-(4-Chlorophenyl)thioureido)-*N*-(2-phenyl-2-(1*H*-1,2,4-triazol-1-yl)ethyl) benzamide (53c)

(47a)
Chemical Formula: $C_{17}H_{17}N_5O$
Molecular Weight: 307.36
cLogP= 1.76

(52c)
Chemical Formula: C_7H_4ClNS
Molecular Weight: 169.63
cLogP= 2.76

(53c)
Chemical Formula: $C_{24}H_{21}ClN_6OS$
Molecular Weight: 476.98
cLogP=4.75

Prepared from 4-chlorophenyl isothiocyanate (**52c**, R^2= 4-Cl) (0.23 gm, 1.35 mmoL). Product obtained as a white solid which was purified by gradient column chromatography CH_2Cl_2-MeOH (97: 3 v/v), yield: 0.25 g (59 %). TLC (CH_2Cl_2-MeOH 9.5:0.5 v/v), R*f* = 0.48. M.p. 156-158 °C. ^{1}H NMR (DMSO-*d*$_6$): δ 10.05 (brs, 1H, *H*NC=SNH), 10.01 (brs, 1H, HNC=SN*H*), 8.73 (s, 1H, triazole), 8.63 (t, *J* = 5.5 Hz, 1H, N*H*CH$_2$), 8.03 (s, 1H, triazole), 7.70 (d, *J* = 8.8 Hz, 2H, Ar), 7.55 (d, *J* = 8.8 Hz, 2H, Ar), 7.51 (d, *J* = 8.9 Hz, 2H, Ar), 7.43 (d, *J* = 7.2 Hz, 2H, Ar), 7.39 (m, 4H, Ar), 7.33 (t, *J* = 7.1 Hz, 1H, Ar), 5.91 (dd, *J* = 5.5, 9.1 Hz, 1H, NHCHaHbC*H*), 4.08 (m, 1H, NHC*Ha*HbCH), 3.99 (ddd, *J* = 5.4, 10.9, 13.6 Hz, 1H, NHCHa*Hb*CH). ^{13}C NMR (DMSO-*d*$_6$): δ 176.97 (C, *C*=S), 166.71 (C, *C*ONH), 152.15 (CH, triazole), 144.62 (CH, triazole), 142.71 (C, Ar), 138.79 (C, Ar), 138.42 (C, Ar), 129.85 (C, C-Cl), 129.14 (2 x CH, Ar), 128.92 (C, Ar), 128.82 (2 x CH, Ar), 128.75 (CH, Ar), 128.10 (2 x CH, Ar), 127.67 (2 x CH, Ar), 125.78 (2 x CH, Ar), 122.75 (2 x CH, Ar), 62.15 (NHCH$_2$*C*H), 43.95 (NH*C*H$_2$CH). HRMS (ESI), m/z. calcd for $C_{24}H_{21}ClN_6OS$ ([M + H]$^+$), 477.1264; found, 477.1255. HPLC (Method B2): 98.27%, R$_t$= 4.45 min.

(*R/S*)-*N*-(2-(4-Chlorophenyl)-2-(1*H*-1,2,4-triazol-1-yl)ethyl)-4-(3-(4-chlorophenyl)thioureido)benzamide (53d)

(47b)
Chemical Formula: $C_{17}H_{16}ClN_5O$
Molecular Weight: 341.80
cLog P: 2.32

(52c)
Chemical Formula: C_7H_4ClNS
Molecular Weight: 169.63
cLogP= 2.76

(53d)
Chemical Formula: $C_{24}H_{20}Cl_2N_6OS$
Molecular Weight: 511.43
cLog P: 5.31

Prepared from 4-chlorophenyl isothiocyanate (**52c**, R^2= 4-Cl) (0.19 gm, 1.10 mmoL). Product obtained as a white solid which was purified by gradient column chromatography CH$_2$Cl$_2$-MeOH (97: 3 v/v), yield: 0.24 g (64 %). TLC (CH$_2$Cl$_2$-MeOH 9.5:0.5 v/v), R*f* = 0.48. M.p. 150-152 °C. ^{1}H NMR (DMSO-d_6): δ 10.06 (brs, 1H, *H*NC=SNH), 10.01 (brs, 1H, HNC=SN*H*), 8.73 (s, 1H, triazole), 8.63 (t, *J* = 5.6 Hz, 1H, N*H*CH$_2$), 8.05 (s, 1H, triazole), 7.70 (d, *J* = 8.8 Hz, 2H, Ar), 7.56 (d, *J* = 8.8 Hz, 2H, Ar), 7.52 (d, *J* = 8.9 Hz, 2H, Ar), 7.47 (s, 4H, Ar), 7.39 (d, *J* = 8.9 Hz, 2H, Ar), 5.94 (dd, *J* = 6.0, 8.6 Hz, 1H, NHCHaHbC*H*), 4.05 (ddd, *J* = 4.4, 8.7, 13.8 Hz, 1H, NHC*Ha*HbCH), 3.99 (ddd, *J* = 5.7, 11.6, 13.5 Hz, 1H, NHCHa*Hb*CH). ^{13}C NMR (DMSO-d_6): δ 179.99 (C, *C*=S), 166.72 (C, *C*ONH), 152.30 (CH, triazole), 144.72 (CH, triazole), 142.72 (C, Ar), 138.76 (C, Ar), 137.32 (C, Ar), 133.43 (C, *C*-Cl), 129.79 (C, *C*-Cl), 129.71 (2 x CH, Ar), 129.13 (2 x CH, Ar), 128.93 (C, Ar), 128.83 (2 x CH, Ar), 128.10 (2 x CH, Ar), 125.78 (2 x CH, Ar), 122.76 (2 x CH, Ar), 61.32 (NHCH$_2$*C*H), 43.82 (NH*C*H$_2$CH). HRMS (ESI), m/z. calcd for C$_{24}$H$_{20}$Cl$_2$N$_6$OS ([M + H]$^+$), 511.0874; found, 511.0868. HPLC (Method B2): 99.42%, R$_t$= 5.22 min.

(*R/S*)-4-(3-(4-Chlorophenyl)thioureido)-*N*-(2-(2,4-dichlorophenyl)-2-(1*H*-1,2,4-triazol-1-yl)ethyl)benzamide (53e)

(47c)
Chemical Formula: C$_{17}$H$_{15}$Cl$_2$N$_5$O
Molecular Weight: 376.24
cLog P: 2.88

(52c)
Chemical Formula: C$_7$H$_4$ClNS
Molecular Weight: 169.63
cLogP= 2.76

(53e)
Chemical Formula: C$_{24}$H$_{19}$Cl$_3$N$_6$OS
Molecular Weight: 545.87
cLog P: 5.87

Prepared from 4-chlorophenyl isothiocyanate (**52c**, R^2= 4-Cl) (0.12 gm, 0.70 mmoL). Product obtained as an off-white solid which was purified by gradient column chromatography CH$_2$Cl$_2$-MeOH (97: 3 v/v), yield: 0.05 g (18 %). TLC (CH$_2$Cl$_2$-MeOH 9.5:0.5 v/v), R*f* = 0.5. M.p. 190-192 °C. ^{1}H NMR (DMSO-d_6): δ 10.07 (brs, 1H, *H*NC=SNH), 10.02 (brs, 1H, HNC=SN*H*), 8.77 (s, 1H, triazole), 8.65 (t, *J* = 5.6 Hz, 1H, N*H*CH$_2$), 8.03 (s, 1H, triazole), 7.71 (brs, 1H, Ar), 7.70 (dd, *J* = 2.1, 3.4 Hz, 2H, Ar), 7.66 (d, *J* = 8.6 Hz, 1H, Ar), 7.57 (d, *J* = 8.8 Hz, 2H, Ar), 7.52 (m, 3H, Ar), 7.39 (d, *J* = 8.9 Hz, 2H, Ar), 6.28 (dd, *J* = 5.8, 8.8 Hz, 1H, NHCHaHbC*H*), 4.14 (m, 1H, NHC*Ha*HbCH), 3.96 (ddd, *J* = 5.3, 10.8, 13.6 Hz, 1H, NHCHa*Hb*CH). ^{13}C NMR (DMSO-

d_6): δ 179.98 (C, C=S), 166.74 (C, CONH), 152.35 (CH, triazole), 145.05 (CH, triazole), 142.76 (C, Ar), 138.78 (C, Ar), 134.43 (C, Ar), 134.34 (C, C-Cl), 134.33 (C, C-Cl), 130.84 (CH, Ar), 129.74 (C, C-Cl), 129.60 (CH, Ar), 128.92 (C, Ar), 128.83 (2 x CH, Ar), 128.39 (CH, Ar), 128.13 (2 x CH, Ar), 125.77 (2 x CH, Ar), 122.75 (2 x CH, Ar), 57.96 (NHCH$_2$$C$H), 42.90 (NH$CH_2$CH). HRMS (ESI), m/z. calcd for $C_{24}H_{19}Cl_3N_6OS$ ([M + H]$^+$), 547.0485; found, 547.0452. HPLC (Method B2): 96.44%, R_t= 5.94 min.
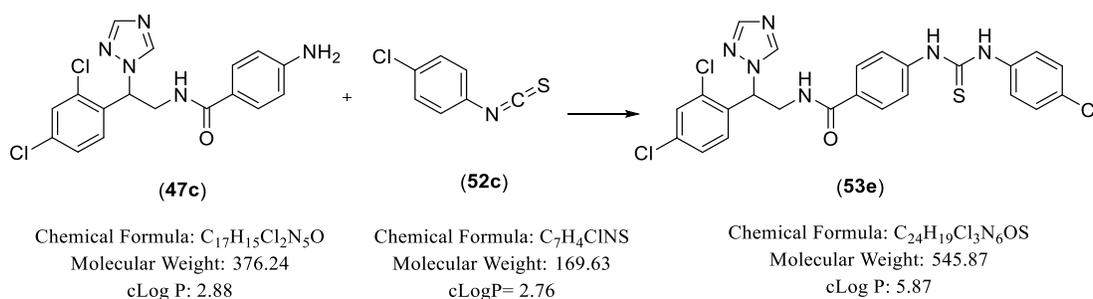
(*R/S*)-4-(3-(4-Methoxyphenyl)thioureido)-*N*-(2-phenyl-2-(1*H*-1,2,4-triazol-1-yl)ethyl) benzamide (53f)

(47a)	(52d)	(53f)
Chemical Formula: $C_{17}H_{17}N_5O$	Chemical Formula: C_8H_7NOS	Chemical Formula: $C_{25}H_{24}N_6O_2S$
Molecular Weight: 307.36	Molecular Weight: 165.21	Molecular Weight: 472.57
cLogP= 1.76	cLogP= 2.07	cLogP=4.07
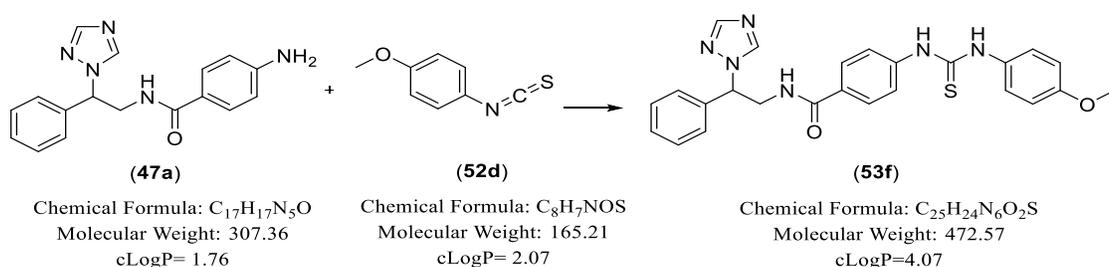
Prepared from 4-methoxyphenyl isothiocyanate (**52d**, R^2= 4-Cl) (0.2 mL, 1.46 mmoL). Product obtained as a white solid which was purified by gradient column chromatography CH$_2$Cl$_2$-MeOH (96.5: 3.5 v/v), yield: 0.07 g (12 %). TLC (CH$_2$Cl$_2$-MeOH 9.5:0.5 v/v), Rf = 0.5. M.p. 164-166 °C. ^{1}H NMR (DMSO-d_6): δ 9.82 (s, 1H, HNC=SNH), 9.77 (s, 1H, HNC=SNH), 8.73 (s, 1H, triazole), 8.61 (t, J = 5.5 Hz, 1H, NHCH$_2$), 8.03 (s, 1H, triazole), 7.69 (d, J = 8.8 Hz, 2H, Ar), 7.56 (d, J = 8.7 Hz, 2H, Ar), 7.43 (d, J = 7.2 Hz, 2H, Ar), 7.39 (t, J = 7.4 Hz, 2H, Ar), 7.33 (t, J = 7.4 Hz, 3H, Ar), 6.91 (d, J = 9.0 Hz, 2H, Ar), 5.91 (dd, J = 5.6, 9.1 Hz, 1H, NHCHaHbCH), 4.08 (m, 1H, NHCHaHbCH), 3.99 (ddd, J = 5.4, 10.9, 13.6 Hz, 1H, NHCHaHbCH), 3.75 (s, 3H, OCH_3). ^{13}C NMR (DMSO-d_6): δ 180.13 (C, C=S), 166.75 (C, CONH), 157.14 (C, C-OCH$_3$), 152.15 (CH, triazole), 144.61 (CH, triazole), 143.01 (C, Ar), 138.43 (C, Ar), 132.42 (C, Ar), 129.53 (C, Ar), 129.14 (2 x CH, Ar), 128.74 (CH, Ar), 128.01 (2 x CH, Ar), 127.67 (2 x CH, Ar), 126.45 (2 x CH, Ar), 122.60 (2 x CH, Ar), 114.20 (2 x CH, Ar), 62.16 (NHCH$_2$$C$H), 55.71 (O$CH_3$), 43.95 (NH$CH_2$CH). HRMS (ESI), m/z. calcd for $C_{24}H_{24}N_6O_2S$ ([M + Na]$^+$), 495.1579; found, 495.1571. HPLC (Method B2): 95.29%, R_t= 3.85 min.

7.4.23 General procedure to form amide linker derivatives (55)

Where R^1:
  a= 4-H
  b= 2,4-diCl

Where R^2:
  a= 4-H
  e= 4-NO$_2$
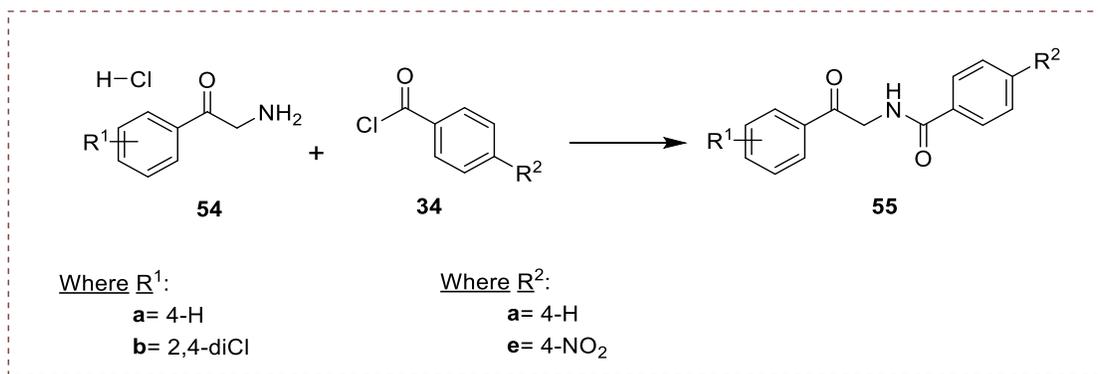
A solution of CH_2Cl_2 (7.5 mL) and saturated aqueous $NaHCO_3$ (15 mL) were stirred vigorously and chilled in an ice bath. Benzoyl chloride derivative (**34**) (4.37 mmoL) was added, stirred until all the solid dissolved, followed by acetophenone derivative (**54**) (2.91 mmoL). Stirring was continued while warming to room temperature over a period of 2 h. The reaction mixture was evaporated, and the obtained residue was diluted with EtOAc (15 mL), extracted with H_2O (5 mL), dried ($MgSO_4$) and the solvent evaporated under vacuum and purified by recrystallisation when needed.

N-(2-Oxo-2-phenylethyl)benzamide (55a)[110]

(**54a**)

Chemical Formula: $C_8H_{10}ClNO$
Molecular Weight: 171.62

(**34a**)

Chemical Formula: C_7H_5ClO
Molecular Weight: 140.57
cLog P: 2.17

(**55a**)

Chemical Formula: $C_{15}H_{13}NO_2$
Molecular Weight: 239.27
cLog P: 2.09
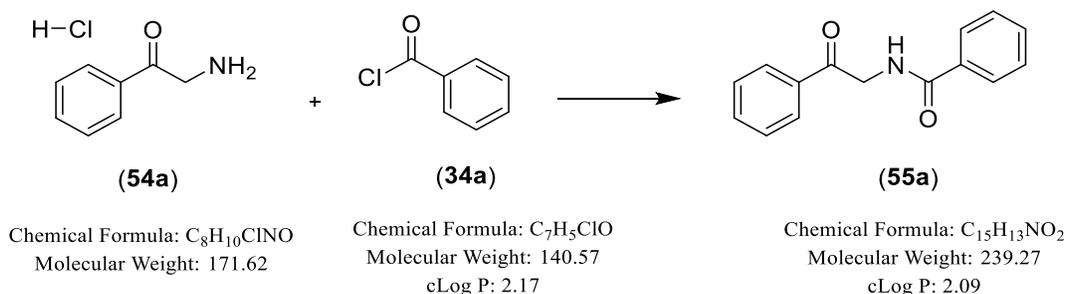
Prepared from benzoyl chloride (**34a**, R^2= 4-H) (0.51 mL, 4.37 mmoL) and aminoacetophenone hydrochloride (**54a**, R^1= 4-H) (0.5 g, 2.91 mmoL). Product obtained as white crystals after recrystallisation from CH_3CN, yield: 0.31 g (45 %). TLC (petroleum ether-EtOAc 3:1 v/v), R*f* = 0.28. M.p. 116-118 °C (124-125.5 °C lit)[110]. ^{1}H NMR (DMSO-*d*$_6$): δ 8.87 (t, *J* = 5.6 Hz, 1H, N*H*), 8.05 (d, *J* = 7.1 Hz, 2H, Ar), 7.91 (d, *J* = 7.0 Hz, 2H, Ar), 7.69 (t, *J* = 7.4 Hz, 1H, Ar), 7.57 (m, 3H, Ar), 7.51 (t, *J* = 7.4 Hz, 2H, Ar), 4.79 (d, *J* = 5.7 Hz, 2H, C*H*$_2$-NH).

4-Nitro-*N*-(2-oxo-2-phenylethyl)benzamide (55b)

(54a)

Chemical Formula: $C_8H_{10}ClNO$
Molecular Weight: 171.62

(34e)

Chemical Formula: $C_7H_4ClNO_3$
Molecular Weight: 185.56
cLog P: 1.49

(55b)

Chemical Formula: $C_{15}H_{12}N_2O_4$
Molecular Weight: 284.27
cLog P: 1.24
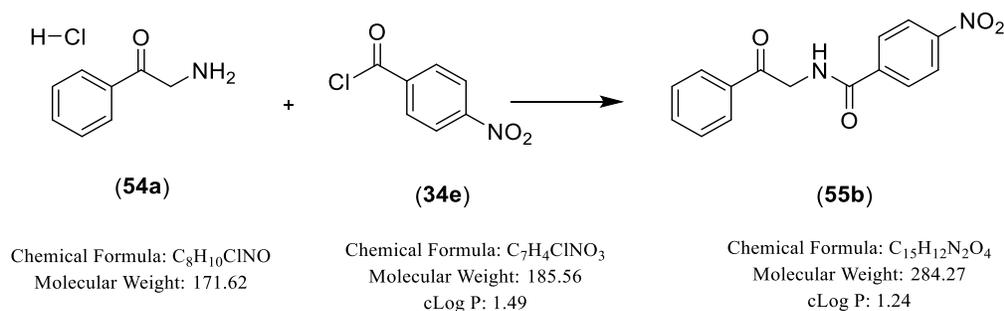
Prepared from 4-nitrobenzoyl chloride (**34e**, R^2= 4-NO_2) (0.81 g, 4.37 mmoL) and aminoacetophenone hydrochloride (**54a**, R^1= 4-H) (0.5 g, 2.91 mmoL). Product obtained as a white solid, yield: 0.64 g (78 %). TLC (petroleum ether-EtOAc 3:1 v/v), R*f* = 0.2. M.p. 188-190 °C. ^{1}H NMR (DMSO-*d*$_6$): δ 9.23 (t, *J* = 5.6 Hz, 1H, N*H*), 8.36 (d, *J* = 9.0 Hz, 2H, Ar), 8.14 (d, *J* = 8.9 Hz, 2H, Ar), 8.06 (d, *J* = 7.2 Hz, 2H, Ar), 7.70 (t, *J* = 7.4 Hz, 1H, Ar), 7.58 (t, *J* = 7.7 Hz, 2H, Ar), 4.85 (d, *J* = 5.7 Hz, 2H, C*H*$_2$NH). ^{13}C NMR (DMSO-*d*$_6$): δ 195.34 (C, C=O), 165.48 (C, C=O), 149.64 (C, Ar), 140.00 (C, Ar), 135.44 (C, Ar), 134.15 (CH, Ar), 129.35 (2 x CH, Ar), 129.48 (2 x CH, Ar), 128.37 (2 x CH, Ar), 124.14 (2 x CH, Ar), 47.06 (*C*H$_2$NH). HRMS (ESI), *m/z*. calcd for $C_{15}H_{12}N_2O_4$ ([M + H]$^+$), 285.0875; found, 285.0875. HPLC (Method B2): 97.62%, R_t = 4.85 min.

7.4.24 (*R/S*)-*N*-((2-Phenyloxiran-2-yl)methyl)benzamide (56a)

(55a)

Chemical Formula: $C_{15}H_{13}NO_2$
Molecular Weight: 239.27
cLog P: 2.09

(56a)

Chemical Formula: $C_{16}H_{15}NO_2$
Molecular Weight: 253.30
cLog P: 2.37
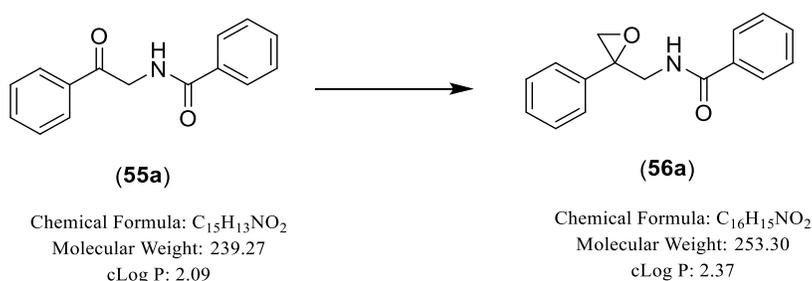
TMSOI (0.44 g, 2.02 mmoL) and 48% NaOH aqueous solution (12.5 mL) was added to a solution of *N*-(2-oxo-2-phenylethyl)benzamide (**55a**, R^1=R^2= H) (0.34 g, 1.41 mmoL) in CH_2Cl_2 (5 mL), then the reaction mixture was heated at 48 °C for 48h. The reaction was diluted with H_2O (20 mL) and extracted with CH_2Cl_2 (40 mL). The organic layer was washed with H_2O (2 x 20 mL), dried (MgSO$_4$) and evaporated under pressure.[113] The product was obtained as a

crude orange oil which was used in the next step without further purification, yield: 0.36 gm (100 %). TLC (petroleum ether-EtOAc 3:1 v/v), Rf = 0.3. ^{1}H NMR (DMSO-d_6): δ 8.63 (t, J = 5.9 Hz, 1H, NH), 7.82 (d, J = 7.1 Hz, 2H, Ar), 7.45 (m, 4H, Ar), 7.37 (t, J = 7.4 Hz, 3H, Ar), 7.31 (t, J = 7.3 Hz, 1H, Ar), 3.93 (dd, J = 5.9, 14.4 Hz, 1H, NHCHaHb), 3.87 (dd, J = 6.2, 14.4 Hz, 1H, NHCHaHb), 3.05 (d, J = 5.2 Hz, 1H, COCHaHb), 2.78 (d, J = 5.1Hz, 1H, COCHaHb). ^{13}C NMR (DMSO-d_6): δ 167.09 (C, C=O), 139.00 (C, Ar), 134.65 (C, Ar), 128.75 (2 x CH, Ar), 128.72 (2 x CH, Ar), 128.23 (CH, Ar), 127.75 (2 x CH, Ar), 127.04 (CH, Ar), 126.56 (2 x CH, Ar), 59.23 (C, COCH$_2$), 53.15 (COCH_2), 42.82 (CH_2NH).

7.4.25 (*R/S*)-*N*-(2-Hydroxy-2-phenyl-3-(1*H*-1,2,4-triazol-1-yl)propyl)benzamide (57a)
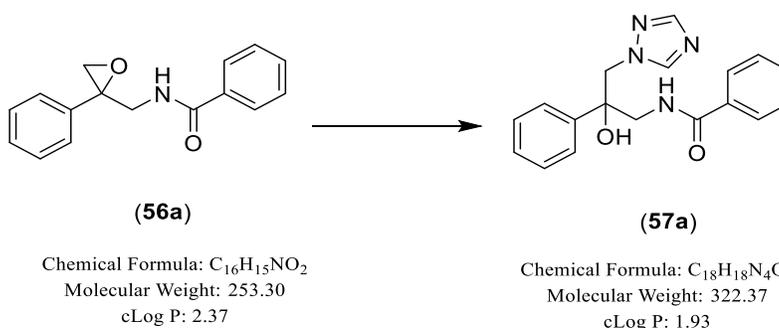
(56a)

Chemical Formula: C$_{16}$H$_{15}$NO$_2$
Molecular Weight: 253.30
cLog P: 2.37

(57a)

Chemical Formula: C$_{18}$H$_{18}$N$_4$O$_2$
Molecular Weight: 322.37
cLog P: 1.93

Method: see 7.4.6 method. The crude product was purified by gradient column chromatography eluting with CH$_2$Cl$_2$-MeOH 97.5:2.5 v/v.

Prepared from (*R/S*)-*N*-((2-phenyloxiran-2-yl)methyl)benzamide (**56a**, R^1=R^2= H) (0.32g, 1.28 mmoL) and the product obtained as an off-white solid, yield: 0.17 gm (40 %). TLC (CH$_2$Cl$_2$-MeOH 9.5:0.5 v/v), Rf = 0.54. M.p. 140-142 °C. ^{1}H NMR (DMSO-d_6): δ 8.27 (t, J = 5.8 Hz, 1H, NH), 8.20 (s, 1H, triazole), 7.84 (s, 1H, triazole), 7.72 (d, J = 7.1 Hz, 2H, Ar), 7.51 (t, J = 7.4 Hz, 1H, Ar), 7.43 (t, J = 7.8 Hz, 4H, Ar), 7.28 (t, J = 7.6 Hz, 2H, Ar), 7.21 (t, J = 7.3 Hz, 1H, Ar), 6.02 (s, 1H, OH), 4.58 (d, J = 2.0, 2H, CHaHb-triazole), 3.88 (dd, J = 6.7, 14.0 Hz, 1H, NHCHaHb), 3.63 (dd, J = 5.2, 14.0 Hz, 1H, NHCHaHb). ^{13}C NMR (DMSO-d_6): δ 167.86 (C, C=O), 150.97 (CH, triazole), 145.39 (CH, triazole), 142.43 (C, Ar), 134.55 (C, Ar), 131.81 (CH, Ar), 128.73 (2 x CH, Ar), 128.24 (2 x CH, Ar), 127.69 (2 x CH, Ar), 127.50 (CH, Ar), 126.25 (2 x CH, Ar), 76.45 (C-OH), 57.38 (CH_2-triazole), 48.34 (CH_2NH). HRMS (ESI), m/z. calcd for C$_{18}$H$_{18}$N$_4$O$_2$ ([M + H]$^+$), 323.1508; found, 323.1509. HPLC (Method B2): 99.95%, R$_t$

= 4.96 min.

7.4.26 General procedure to prepare β-ketoazide (60)
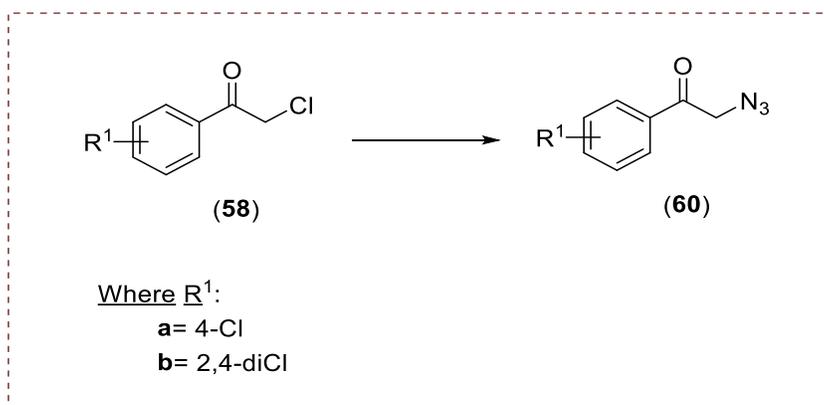
To a solution of acetophenone derivatives (**58**) (4.48 mmoL) in CH_3CN: H_2O (3:1 v/v, 6mL) was added NaN_3 (4.92 mmoL) and KI (0.22 mmoL). The reaction mixture was heated at 60 °C for 2 h. The biphasic solution was separated, and the aqueous layer was extracted with EtOAc (3 x 5 mL). The organic layers were combined, washed with brine (5 mL), dried (Mg_2SO_4) and concentrated to provide the corresponding crude β-ketoazide, which was used without further purification in the next step.[116]

2-Azido-1-(4-chlorophenyl)ethan-1-one (60a)

Chemical Formula: $C_8H_6Cl_2O$
Molecular Weight: 189.04
cLog P: 2.43
miLogP: 2.74

Chemical Formula: $C_8H_6ClN_3O$
Molecular Weight: 195.61
miLogP: 2.84
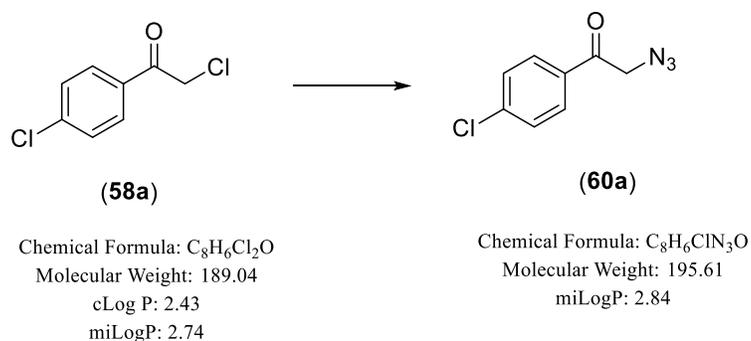
Prepared from 2,4'-dichloroacetophenone (**58a**, R^1= 4-Cl) (3.00 g, 15.87 mmoL) and the product obtained as a crude orange oil, yield: 3.10 gm (100 %). TLC (petroleum ether-EtOAc 4:1 v/v), Rf = 0.64. ^1H NMR (DMSO-d_6): δ 7.96 (d, J = 8.7 Hz, 2H, Ar), 7.64 (d, J = 8.8 Hz, 2H, Ar), 4.89 (s, 2H, CH_2N$_3$). ^{13}C NMR (DMSO-d_6): δ 194.10 (C, C=O), 139.28 (C, *C*-Cl), 133.54 (C, Ar), 130.31 (2 x CH, Ar), 129.49 (2 x CH, Ar), 55.26 (*C*H$_2$N$_3$).

2-Azido-1-(2,4-dichlorophenyl)ethan-1-one (60b)

(58b)

Chemical Formula: $C_8H_5Cl_3O$
Molecular Weight: 223.48
cLog P: 2.99
miLog P: 3.35

(60b)

Chemical Formula: $C_8H_5Cl_2N_3O$
Molecular Weight: 230.05
miLog P: 3.45
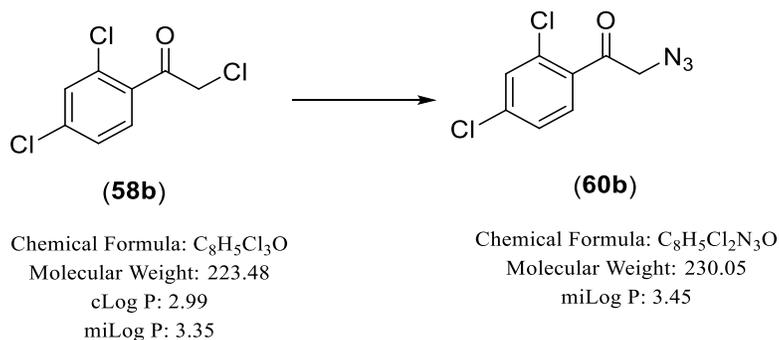
Prepared from 2,2',4'-trichloroacetophenone (**58b,** R= 2,4-di-Cl) (1.00 g, 4.48 mmoL) and the product obtained as a crude orange oil, yield: 0.95 gm (93 %). TLC (petroleum ether-EtOAc 4:1 v/v), Rf = 0.71. ^{1}H NMR (DMSO-d_6): δ 7.84 (d, J = 8.4 Hz, 1H, Ar), 7.80 (d, J = 2.0 Hz, 1H, Ar), 7.61 (dd, J = 2.1, 8.4 Hz, 1H, Ar), 4.75 (s, 2H, CH_2N$_3$). ^{13}C NMR (DMSO-d_6): δ 195.94 (C, C=O), 137.60 (C, Ar), 134.44 (C, C-Cl), 132.23 (C, C-Cl), 131.68 (CH, Ar), 130.83 (CH, Ar), 128.14 (CH, Ar), 57.40 (*C*H$_2$N$_3$).

7.4.27 General procedure to form β-keto-ammonium tosylate salts derivatives (62)
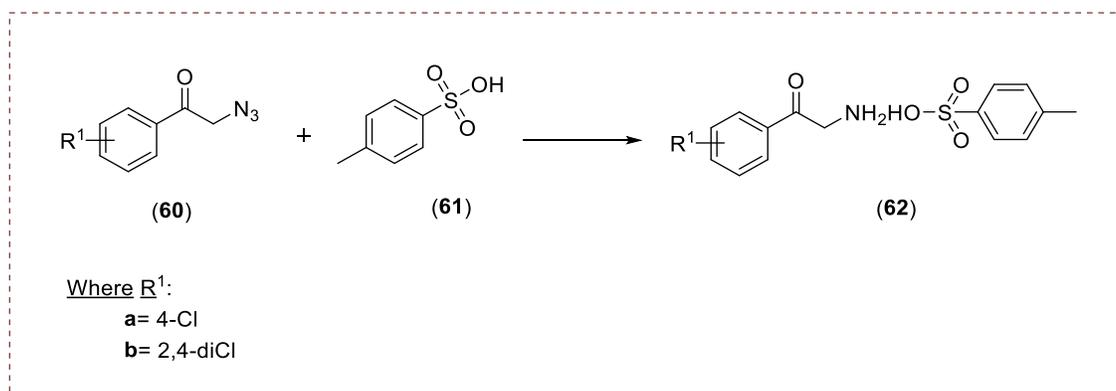
To a solution of the β-ketoazide (**60**) (4.04 mmoL) in THF (6 mL) was added *p*-TsOH (**61**) (16.152 mmoL) followed by PPh$_3$ (8.08 mmoL) in portions. The reaction stirred at room temperature until cessation of effervescence then the mixture was heated at 40 °C overnight. Upon completion, the reaction was cooled to room temperature and filtered to obtained white solid which washed with cold THF and used without further purification in the next step.[116]

2-Amino-1-(4-chlorophenyl)ethan-1-one 4-methylbenzenesulfonate (62a)

(**60a**)

Chemical Formula: $C_8H_6ClN_3O$
Molecular Weight: 195.61
miLogP: 2.84

(**61**)

Chemical Formula: $C_7H_8O_3S$
Molecular Weight: 172.20
cLog P: 1.68

(**62a**)

Chemical Formula: $C_{15}H_{16}ClNO_4S$
Molecular Weight: 341.81
miLogP: -0.18
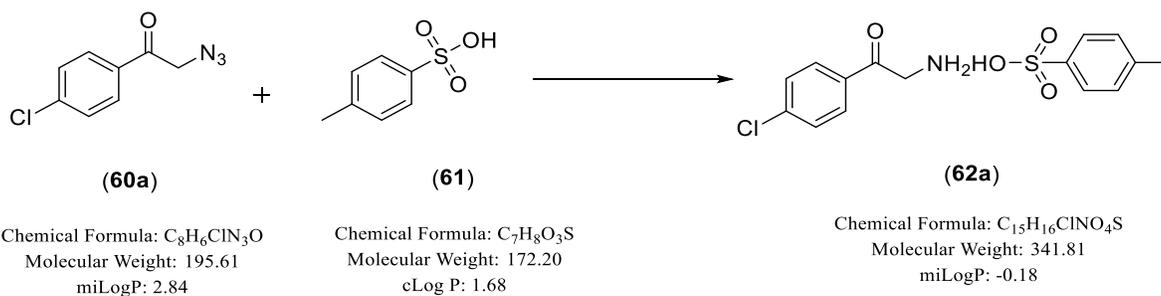
Prepared from β-ketoazide (**60a,** R^1= 4-Cl) (3.00 g, 15.34 mmoL). Product obtained as a white solid, yield: 3.05 g (58 %). TLC (CH_2Cl_2-MeOH 9.5:0.5 v/v), Rf = 0.23. M.p. 238-240 °C, (226-227 °C lit)[116]. ^{1}H NMR (DMSO-d_6): δ 8.22 (brs, 3H, NH_2 + OH), 8.04 (d, J = 8.8 Hz, 2H, Ar), 7.69 (d, J = 8.7 Hz, 2H, Ar), 7.48 (d, J = 8.0 Hz, 2H, Ar), 7.11 (d, J = 7.8 Hz, 2H, Ar), 4.61 (brs, 2H, CH_2NH$_2$), 2.29 (s, 3H, CH_3).

2-Amino-1-(2,4-dichlorophenyl)ethan-1-one 4-methylbenzenesulfonate (62b)

(**60b**)

Chemical Formula: $C_8H_5Cl_2N_3O$
Molecular Weight: 230.05
miLog P: 3.45

(**61**)

Chemical Formula: $C_7H_8O_3S$
Molecular Weight: 172.20
cLog P: 1.68

(**62b**)

Chemical Formula: $C_{15}H_{15}Cl_2NO_4S$
Molecular Weight: 376.25
miLog P: 1.55
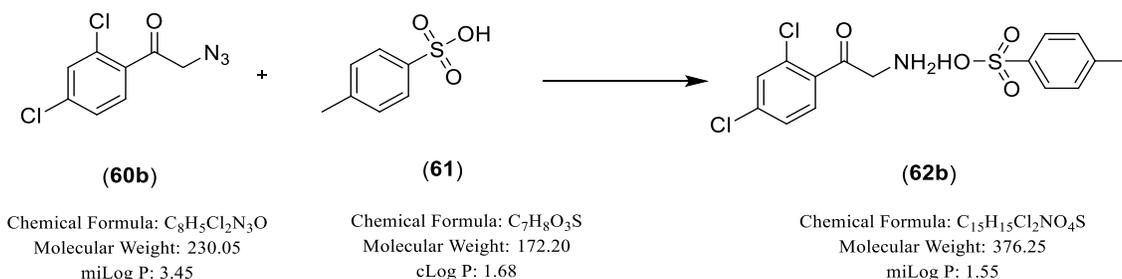
Prepared from β-ketoazide (**60a,** R^1= 2,4-di-Cl) (0.93g, 4.04 mmoL). Product obtained as a white solid, yield: 0.76 g (50 %). TLC (CH_2Cl_2-MeOH 9.5:0.5 v/v), Rf = 0.48. M.p. 188-190 °C. ^{1}H NMR (DMSO-d_6): δ 8.27 (brs, 3H, NH_2+OH), 7.98 (d, J = 8.5 Hz, 1H, Ar), 7.85 (d, J = 2.1 Hz, 1H, Ar), 7.66 (dd, J = 2.1, 8.5 Hz, 1H, Ar), 7.48 (d, J = 8.1 Hz, 2H, Ar), 7.11 (d, J = 7.8 Hz, 2H, Ar), 4.53 (s, 2H, CH_2NH$_2$), 2.29 (s, 3H, CH_3). ^{13}C NMR (DMSO-d_6): δ 193.44 (C, C=O), 146.16 (C, Ar), 138.57 (C, Ar), 138.08 (C, Ar), 133.00 (C, C-Cl), 132.81 (C, C-Cl), 132.61 (CH, Ar), 131.34 (CH, Ar), 128.52 (2 x CH, Ar), 128.29 (CH, Ar), 125.96 (2 x CH, Ar), 47.48 (CH_2NH$_2$), 21.24 (CH_3). HRMS (ESI), m/z. calcd for $C_8H_7Cl_2NO$ ([M + H]$^+$), 203.9983; found, 203.9983. HPLC (Method A): 98.13%, R$_t$ = 3.68 min.

N-(2-(4-Chlorophenyl)-2-oxoethyl)-4-nitrobenzamide (55c)

(62a)

Chemical Formula: $C_{15}H_{16}ClNO_4S$
Molecular Weight: 341.81
miLogP: -0.18

(34e)

Chemical Formula: $C_7H_4ClNO_3$
Molecular Weight: 185.56
cLog P: 1.49
miLog P: 2.35

(55c)

Chemical Formula: $C_{15}H_{11}ClN_2O_4$
Molecular Weight: 318.71
cLog P: 1.86
miLogP: 2.92

Method: see 7.4.23 method.

Prepared from 4-nitrobenzoyl chloride (**34e**, R^2= 4-NO_2) (0.81 g, 4.39 mmoL) and 2-amino-1-(4-chlorophenyl)ethan-1-one 4-methylbenzenesulfonate (**62a,** R^1= 4-Cl) (1.00 g, 2.93 mmoL). Product obtained as a white solid, yield: 0.83 g (89 %). TLC (petroleum ether-EtOAc 3:1 v/v), Rf = 0.23. M.p. 168-170 °C. ^{1}H NMR (DMSO-d_6): δ 9.24 (t, *J* = 5.6 Hz, 1H, N*H*), 8.36 (d, *J* = 8.9 Hz, 2H, Ar), 8.14 (d, *J* = 9.0 Hz, 2H, Ar), 8.07 (d, *J* = 8.7 Hz, 2H, Ar), 7.65 (d, *J* = 8.7 Hz, 2H, Ar), 4.83 (d, *J* = 5.7 Hz, 2H, C*H*$_2$NH). ^{13}C NMR (DMSO-d_6): δ 194.52 (C, C=O), 165.50 (C, C=O), 149.65 (C, Ar), 139.91 (C, Ar), 139.04 (C, *C*-Cl), 134.11 (C, Ar), 130.34 (2 x CH, Ar), 129.47 (2 x CH, Ar), 129.28 (2 x CH, Ar), 124.14 (2 x CH, Ar), 47.08 (*C*H$_2$NH). HRMS (ESI), *m/z*. calcd for $C_{15}H_{11}ClN_2O_4$ ([M + H]$^+$), 319.0485; found, 319.0482. HPLC (Method B2): 99.97%, R_t = 4.70 min.

N-(2-(2,4-Dichlorophenyl)-2-oxoethyl)-4-nitrobenzamide (55d)

(62b)

Chemical Formula: $C_{15}H_{15}Cl_2NO_4S$
Molecular Weight: 376.25
miLog P: 1.55

(34e)

Chemical Formula: $C_7H_4ClNO_3$
Molecular Weight: 185.56
cLog P: 1.49
miLog P: 2.35

(55d)

Chemical Formula: $C_{15}H_{10}Cl_2N_2O_4$
Molecular Weight: 353.16
cLog P: 2.48
miLog P: 3.52

Method: see 7.4.23 method.

Prepared from 4-nitrobenzoyl chloride (**34e**, R^2= 4-NO_2) (0.55 g, 2.97 mmoL) and 2-amino-1-(2,4-dichlorophenyl)ethan-1-one 4-methylbenzenesulfonate (**62b,** R^1= 2,4-di-Cl) (0.75 g, 1.98 mmoL). Product obtained as a white solid, yield: 0.63 g (90 %). TLC (petroleum ether-EtOAc 4:1 v/v), Rf = 0.49. M.p. 146-148 °C. ^{1}H NMR (DMSO-d_6): δ 9.38 (t, J = 5.5 Hz, 1H, N*H*), 8.35 (d, J = 8.9 Hz, 2H, Ar), 8.10 (d, J = 9.0 Hz, 2H, Ar), 7.83 (d, J = 8.4 Hz, 1H, Ar), 7.78 (d, J = 2.0 Hz, 1H, Ar), 7.60 (dd, J = 2.1, 8.4 Hz, 1H, Ar), 4.63 (d, J = 5.6 Hz, 2H, C*H*$_2$NH). ^{13}C NMR (DMSO-d_6): δ 197.35 (C, C=O), 165.55 (C, C=O), 146.70 (C, Ar), 139.61 (C, Ar), 137.11 (C, Ar), 135.61 (C, *C*-Cl), 131.94 (C, *C*-Cl), 131.49 (CH, Ar), 130.62 (CH, Ar), 129.26 (2 x CH, Ar), 128.08 (CH, Ar), 124.16 (2 x CH, Ar), 49.62 (*C*H$_2$NH$_2$). HRMS (ESI), *m/z.* calcd for $C_{15}H_{10}Cl_2N_2O_4$ ([M + H]$^+$), 353.0096; found, 353.0038. HPLC (Method A): 100%, R_t = 4.63 min.

7.4.28 General procedure to prepare triazole derivatives (63)
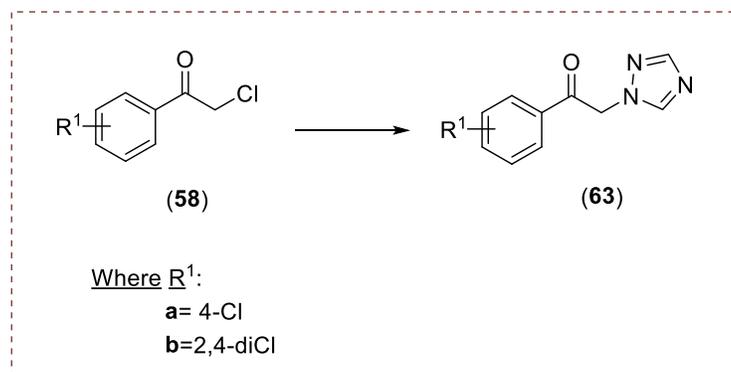
A mixture of acetophenone derivatives (**58**) (1.0 meq), 1,2,4-triazole (1.2 meq), sodium bicarbonate (1.2 meq) in toluene (1 ml/mmoL) was refluxed (113 °C) for 4 h.[116] After the reaction was complete, the mixture was poured into crushed ice and extracted with EtOAc (2 x 50 mL). The combined organic layers were washed with H_2O (2 × 20 mL), brine (20 mL), dried (Mg_2SO_4) and concentrated under reduced pressure. The residue was dissolved in EtOAc (50 mL) and H_2O (25 mL) and stirred for 15 min then the EtOAc was evaporated and the residue collected by filtration followed by recrystallisation from EtOH.[117]

1-(4-Chlorophenyl)-2-(1*H*-1,2,4-triazol-1-yl)ethan-1-one (63a)

(**58a**)

Chemical Formula: $C_8H_6Cl_2O$
Molecular Weight: 189.04
cLog P: 2.43
miLogP= 2.74

(**63a**)

Chemical Formula: $C_{10}H_8ClN_3O$
Molecular Weight: 221.64
cLog P: 1.4
miLogP= 1.28
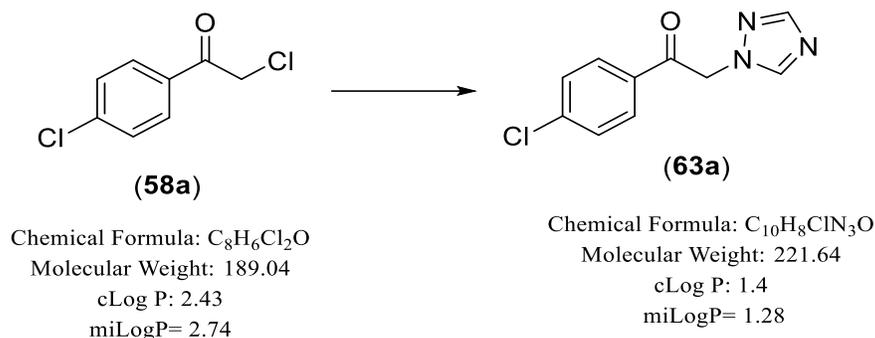
Method (1): see 7.4.28 method

Prepared from 2',4'-dichloroacetophenone (**58a,** R^1= 4-Cl) (2.00 g, 10.58 mmoL). Product obtained as a white solid, yield: 1.34 g (58 %). TLC (petroleum ether-EtOAc 1:2 v/v), R*f* = 0.36. M.p. 148-150 °C (149-150 °C lit)[117]. ^{1}H NMR (DMSO-*d*₆): δ 8.51 (s, 1H, triazole), 8.07 (d, *J* = 8.8 Hz, 2H, Ar), 8.03 (s, 1H, triazole), 7.69 (d, *J* = 8.7 Hz, 2H, Ar), 6.00 (s, 2H, C*H*₂-triazole). ^{13}C NMR (DMSO-*d*₆): δ 192.22 (C, C=O), 151.79 (CH, triazole), 146.07 (CH, triazole), 139.55 (C, *C*-Cl), 133.37 (C, Ar), 130.52 (2 x CH, Ar), 129.59 (2 x CH, Ar), 55.68 (*C*H₂-triazole).

Method (2)

To a cooled solution of 2,4'-dichloroacetophenone (**58a,** R^1= 4-Cl) (3.0 g, 15.87 mmol) in acetone (75 mL) was added 1,2,4-triazole (2.2 g, 31.74 mmol) and K_2CO_3 (2.62 g, 19.04 mmol). The reaction was stirred vigorously at 0 °C for 30 min then at room temperature overnight. The reaction mixture was filtered to remove inorganics (KCl) and the filtrate concentrated under reduced pressure. The residue obtained was extracted between EtOAc (100 mL) and washed with H_2O (3 x 50 mL), the combined aqueous extracts were back extracted with EtOAc (50 mL), then the combined organic layers dried ($MgSO_4$) and concentrated under reduced pressure.[117] The deep yellow residue was triturated with Et_2O to remove remaining acetophenone, then the yellow solid recrystallised from EtOH. The product obtained as a white crystalline solid, yield: 1.79 g (51%). TLC (petroleum ether-EtOAc 1:2 v/v), R*f* = 0.35.

1-(2,4-Dichlorophenyl)-2-(1*H*-1,2,4-triazol-1-yl)ethan-1-one (63b)

(58b)

Chemical Formula: $C_8H_5Cl_3O$
Molecular Weight: 223.48
cLog P: 2.99
miLogP= 3.35

(63b)

Chemical Formula: $C_{10}H_7Cl_2N_3O$
Molecular Weight: 256.09
cLog P= 1.96
miLogP= 1.89
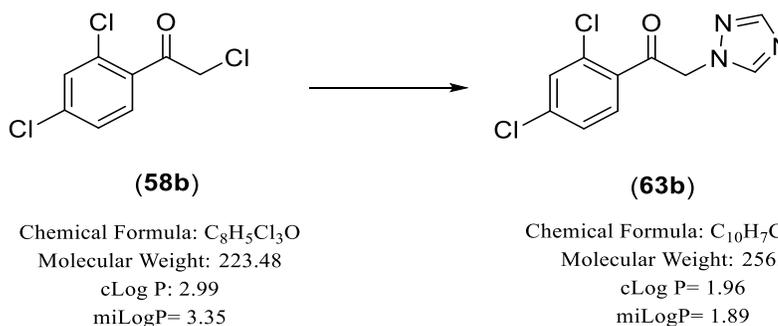
Method (1): see 7.4.28 method (2)

Prepared from 2,2',4'-trichloroacetophenone (**58b**, R^1= 2,4-di-Cl) (8.00 g, 35.81 mmoL). Product obtained as a pale-yellow solid, yield: 4.49 g (49 %). TLC (petroleum ether-EtOAc 1:2 v/v), R*f* = 0.21. M.p. 100-102 °C (115-116 °C lit)[118]. ^{1}H NMR (DMSO-d_6): δ 8.54 (s, 1H, triazole), 8.03 (s, 1H, triazole), 7.96 (d, *J* = 8.4 Hz, 1H, Ar), 7.82 (d, *J* = 2.0 Hz, 1H, Ar), 7.65 (dd, *J* = 2.1, 8.4 Hz, 1H, Ar), 5.85 (s, 2H, C*H₂*-triazole). ^{13}C NMR (DMSO-d_6): δ 193.90 (C, C=O), 152.00 (CH, triazole), 146.04 (CH, triazole), 137.85 (C, Ar), 134.04 (C, *C*-Cl), 132.51 (C, *C*-Cl), 131.86 (CH, Ar), 131.00 (CH, Ar), 128.16 (CH, Ar), 57.59 (*C*H₂-triazole).

Method (2)

A mixture of 2,2',4'-trichloroacetophenone (**58b**, R^1= 2,4-di-Cl) (1.00 g, 4.48 mmoL), 1,2,4-triazole (0.37 g, 5.37 mmoL), sodium bicarbonate (0.45 g, 5.37 mmoL) in toluene (6.0 ml) was refluxed (113 °C) for 4 h. After the reaction was complete, the mixture was poured into crushed ice and extracted with EtOAc (2 x 50 mL). The combined organic layers were washed with H_2O (2 × 20 mL), brine (20 mL), dried (Mg_2SO_4) and concentrated under reduced pressure.[111] The product obtained as an orange oil without further purification with a yield: 0.85 g (74%). TLC (CH_2Cl_2-MeOH 9.5:0.5 v/v), R*f* = 0.5.

7.4.29 **General procedure for formation of the epoxide (64)**

Where R¹:
a= 4-Cl
b= 2,4-diCl
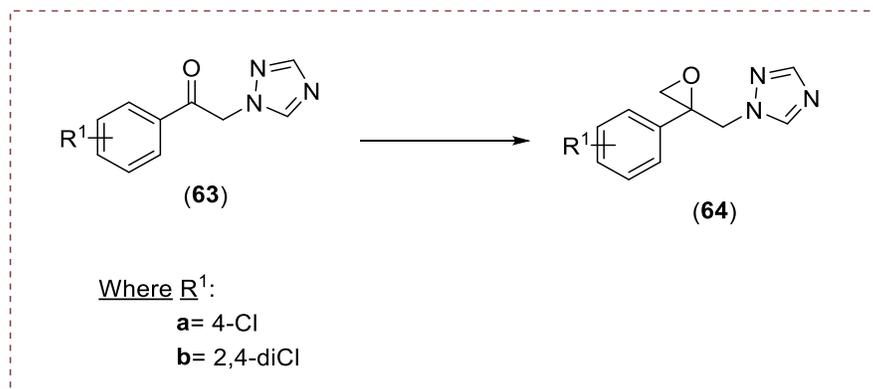
To a solution of 1-(arylphenyl)-2-(1*H*-1,2,4-triazol-1-yl)ethanone (**63**) (5 mmoL) in toluene (11 mL/mmoL) was added trimethylsulfoxonium iodide (TMSOI) (10 mmoL) followed by 20% aqueous NaOH (18.9 mmoL) and the reaction heated at 60 °C for 6 h[119] then rt o/n. Upon completion, the reaction was diluted with H_2O (30 mL) and EtOAc (30 mL). The aqueous layer was extracted with EtOAc (3 x 20 mL), then the combined organic extracts washed with H_2O (2 x 30 mL), brine (20 mL), dried ($MgSO_4$) and concentrated to give the epoxide which was used in the next step without further purification.

(*R/S*)-1-((2-(4-Chlorophenyl)oxiran-2-yl)methyl)-1*H*-1,2,4-triazole (64a)

(63a)

Chemical Formula: $C_{10}H_8ClN_3O$
Molecular Weight: 221.64
cLog P: 1.4
miLogP= 1.28

(64a)

Chemical Formula: $C_{11}H_{10}ClN_3O$
Molecular Weight: 235.67
cLog P: 1.67
miLogP= 1.64

Prepared from 1-(4-chlorophenyl)-2-(1*H*-1,2,4-triazol-1-yl)ethanone (**63a**, R¹= 4-Cl) (1.25 g, 5.66 mmoL). Product obtained as a light-yellow oil, which became dark orange on standing, yield: 1.33 g (100 %). TLC (petroleum ether – EtOAc 1:2 v/v), R*f* = 0.28. ¹H NMR (DMSO-*d6*): δ 8.39 (s, 1H, triazole), 7.91 (s, 1H, triazole), 7.40 (s, 4H, Ar), 5.06 (d, *J* = 15.0 Hz, 1H, C*Ha*Hb-triazole), 4.64 (d, *J* = 15.0 Hz, 1H, CHa*Hb*-triazole), 3.04 (d, *J* = 4.9 Hz, 1H, OC*Ha*Hb),

2.87 (d, *J* = 4.9 Hz, 1H, OCHa*Hb*). ^{13}C NMR (DMSO-d$_6$): δ 151.79 (CH, triazole), 145.40 (CH, triazole), 136.28 (C, Ar), 131.19 (C, Ar), 128.78 (2 x CH, Ar), 128.56 (2 x CH, Ar), 58.72 (*C*-epoxide), 53.99 (*C*H$_2$-triazole), 52.82 (*C*H$_2$-O).

(*R/S*)-1-((2-(2,4-Dichlorophenyl)oxiran-2-yl)methyl)-1*H*-1,2,4-triazole (64b)
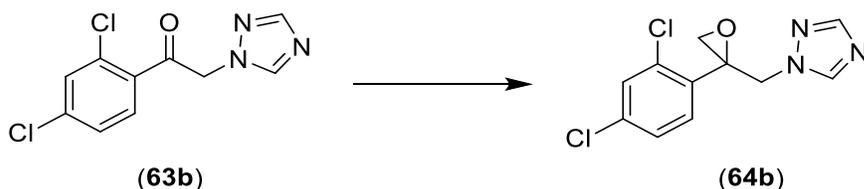
(**63b**)

Chemical Formula: $C_{10}H_7Cl_2N_3O$
Molecular Weight: 256.09
cLog P: 1.96
miLogP= 1.89

(**64b**)

Chemical Formula: $C_{11}H_9Cl_2N_3O$
Molecular Weight: 270.11
cLog P: 2.23
miLogP= 2.24

Prepared from (2,4-dichlorophenyl)-2-(1*H*-1,2,4-triazol-1-yl)ethan-1-one (**63b**, R^1= 2,4-diCl) (1.88 g, 7.32 mmoL). Product obtained as a pale yellow to orange oil, yield: 1.96 g (99 %). TLC (petroleum ether – EtOAc 1:2 v/v), R*f* = 0.38. ^{1}H NMR (DMSO-d$_6$): δ 8.40 (s, 1H, triazole), 7.91 (s, 1H, triazole), 7.67 (d, *J* = 2.1 Hz, 1H, Ar), 7.36 (dd, *J* = 2.1, 8.3 Hz, 1H, Ar), 7.12 (d, *J* = 8.4 Hz, 1H, Ar), 4.87 (d, *J* = 15.0 Hz, 1H, C*Ha*Hb-triazole), 4.55 (d, *J* = 14.9 Hz, 1H, CH*aHb*-triazole), 3.13 (d, *J* = 4.8 Hz, 1H, COC*Ha*Hb), 2.94 (d, *J* = 4.75 Hz, 1H, COCHa*Hb*). ^{13}C NMR (DMSO-d$_6$): δ 151.92 (CH, triazole), 145.50 (CH, triazole), 134.44 (C, Ar), 134.23 (C, *C*-Cl), 133.58 (C, *C*-Cl), 131.41 (CH, Ar), 129.15 (CH, Ar), 127.80 (CH, Ar), 58.95 (*C*-epoxide), 52.91 (*C*H$_2$-triazole), 52.24 (*C*H$_2$-O).

7.4.30 General method for preparation of azide derivatives (66)

(**64**)

(**66**)

Where R^1:
  a= 4-Cl
  b= 2,4-diCl
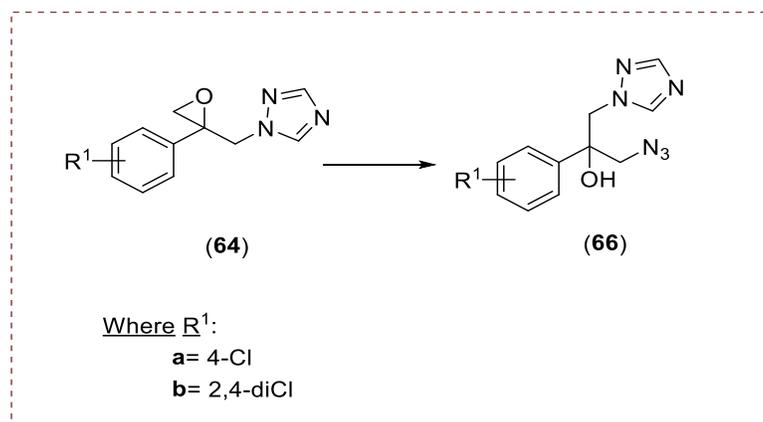
To a solution of epoxide derivative (**64**) (1.0 meq) in dry DMF (2.7 mL/mmoL) was added NaN_3 (1.95 meq) and NH_4Cl (1.2 meq) and the reaction heated at 60 °C for 2 h then rt o/n.[120] After cooling to room temperature sat. aq. $NaHCO_3$ (50 mL/meq) was added, and the reaction extracted with EtOAc (50 mL). The aqueous layer was back extracted with EtOAc (25 mL), then the combined organic layers washed with H_2O (25 mL), brine (25 mL), dried ($MgSO_4$) and concentrated under reduced pressure. The crude product was purified by gradient column chromatography.

(*R/S*)-1-Azido-2-(4-chlorophenyl)-3-(1*H*-1,2,4-triazol-1-yl)propan-2-ol (66a)

(64a)

Chemical Formula: $C_{11}H_{10}ClN_3O$
Molecular Weight: 235.67
cLog P: 1.67
miLogP= 1.64

(66a)

Chemical Formula: $C_{11}H_{11}ClN_6O$
Molecular Weight: 278.70
miLogP= 1.86
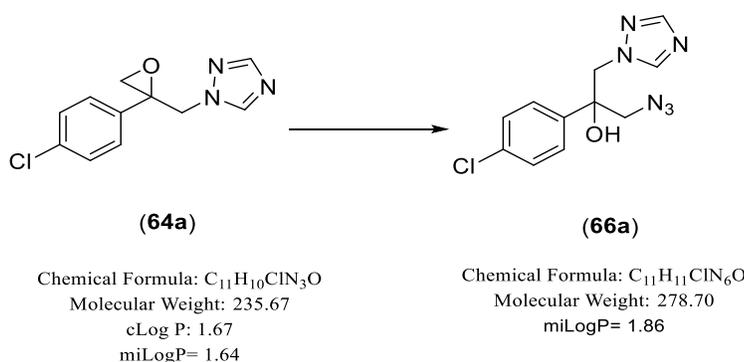
Prepared from (*R/S*)-1-((2-(4-chlorophenyl)oxiran-2-yl)methyl)-1*H*-1,2,4-triazole (**64a**, R^1= 4-Cl) (1.33 g, 5.64 mmoL). Product obtained as a thick yellow syrup after purification by gradient column chromatography (petroleum ether – EtOAc to 40:60 v/v), yield: 1.02 g (65 %). TLC (petroleum ether – EtOAc 1:2 v/v), R*f* = 0.45. ^{1}H NMR (DMSO-d_6): δ 8.22 (s, 1H, triazole), 7.85 (s, 1H, triazole), 7.43 (d, *J* = 8.8 Hz, 2H, Ar), 7.37 (d, *J* = 8.8 Hz, 2H, Ar), 6.14 (s, 1H, O*H*), 4.54 (dd, *J* = 14.3, 22.0 Hz, 2H, C*H*$_2$-triazole), 3.65 (dd, *J* = 12.9, 22.6 Hz, 2H, C*H*$_2$-N$_3$). ^{13}C NMR (DMSO-d_6): δ 151.27 (CH, triazole), 145.59 (CH, triazole), 141.06 (C, Ar), 132.54 (C, *C*-Cl), 128.32 (2 x CH, Ar), 128.24 (2 x CH, Ar), 75.95 (C, *C*-OH), 57.88 (*C*H$_2$- triazole), 56.35 (*C*H$_2$-N$_3$). HRMS (ESI), *m/z*. calcd for $C_{11}H_{11}ClN_6O$ ([M + H]$^+$), 279.0761; found, 279.0761. HPLC (Method B2): 98.99%, R_t = 4.94 min.

(*R/S*)-1-Azido-2-(2,4-dichlorophenyl)-3-(1*H*-1,2,4-triazol-1-yl)propan-2-ol (66b)

(64b)
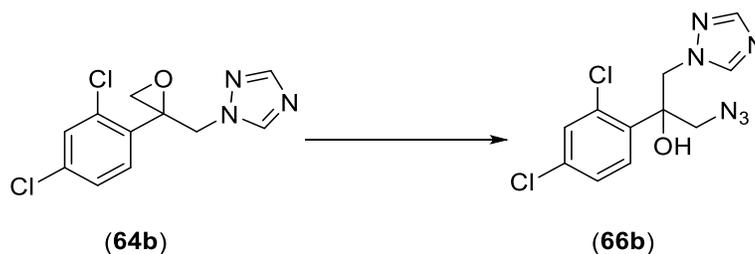
Chemical Formula: $C_{11}H_9Cl_2N_3O$
Molecular Weight: 270.11
cLog P: 2.23
miLogP= 2.24

(66b)

Chemical Formula: $C_{11}H_{10}Cl_2N_6O$
Molecular Weight: 313.14
miLogP= 2.47

Prepared from (*R/S*)-1-((2-(2,4-dichlorophenyl)oxiran-2-yl)methyl)-1*H*-1,2,4-triazole (**64b**, R^1= 2,4-diCl) (1.94 g, 7.17 mmoL). Product obtained as a thick yellow syrup after purification by gradient column chromatography (petroleum ether – EtOAc to 40:60 v/v), yield: 1.48 g (66 %). TLC (Petroleum ether – EtOAc 1:2 v/v), R*f* = 0.31. ^{1}H NMR (DMSO-d_6): δ 8.32 (s, 1H, triazole), 7.79 (s, 1H, triazole), 7.59 (t, *J* = 2.4 Hz, 2H, Ar), 7.39 (dd, *J* = 2.2, 8.7 Hz, 1H, Ar), 6.47 (s, 1H, O*H*), 4.85 (d, *J* = 14.5 Hz, 1H, C*Ha*Hb-triazole), 4.69 (d, *J* = 14.5 Hz, 1H, CHa*Hb*-triazole), 4.10 (d, *J* = 13.2 Hz, 1H, C*Ha*Hb-N₃), 3.74 (d, *J* = 13.2 Hz, 1H, CHa*Hb*-N₃). ^{13}C NMR (DMSO-d_6): δ 151.27 (CH, triazole), 145.66 (CH, triazole), 137.34 (C, Ar), 133.72 (C, *C*-Cl), 131.73 (CH, Ar), 131.54 (C, *C*-Cl), 130.46 (CH, Ar), 127.61 (CH, Ar), 76.78 (C, *C*-OH), 55.75 (*C*H₂- triazole), 53.98 (*C*H₂-N₃). HRMS (ESI), *m/z.* calcd for $C_{11}H_{10}Cl_2N_6O$ ([M + H]$^+$), 313.0371; found, 313.0373. HPLC (Method B2): 99.27%, R_t = 5.03 min.

7.4.31 **General method for preparation of amines (67)**

(66)   **(67)**

Where $\underline{R^1}$:
    a= 4-Cl
    b= 2,4-diCl
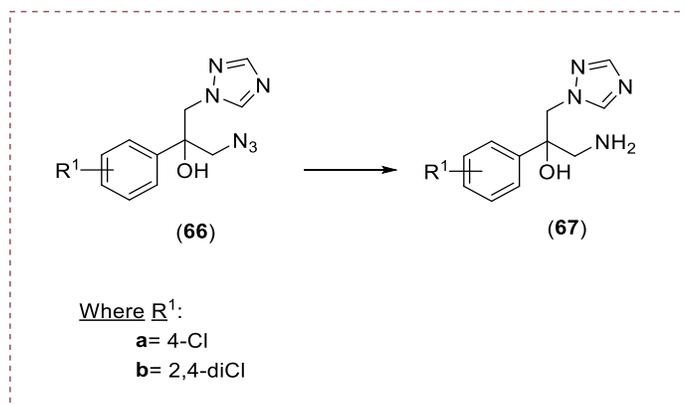
To a solution of azide derivative (**66**) (1.0 meq) in dry THF (5 mL) was added triphenylphosphine (1.15 meq) and the reaction stirred at room temperature for 1 h. H_2O (11.0 meq) was added, and the reaction heated at 60 °C for 4 h. The reaction was concentrated under reduced pressure and to the resulting residue 2M aqueous HCl (20 mL) was added, and the reaction stirred at room temperature for 20 min before extracting with CH_2Cl_2 (4 x 20 mL) to remove excess Ph_3P and triphenylphosphine oxide by-product. To the aqueous layer was added 1 M aqueous NaOH until basic pH; the free amine was then extracted with EtOAc (2 x 50 mL). The organic layers were combined, dried ($MgSO_4$) and concentrated under reduced pressure.[121]

(*R/S*)-1-Amino-2-(4-chlorophenyl)-3-(1*H*-1,2,4-triazol-1-yl)propan-2-ol (67a)

(**66a**)

Chemical Formula: $C_{11}H_{11}ClN_6O$
Molecular Weight: 278.70
miLogP= 1.86

(**67a**)

Chemical Formula: $C_{11}H_{13}ClN_4O$
Molecular Weight: 252.70
cLog P: 0.66
miLogP= -0.04
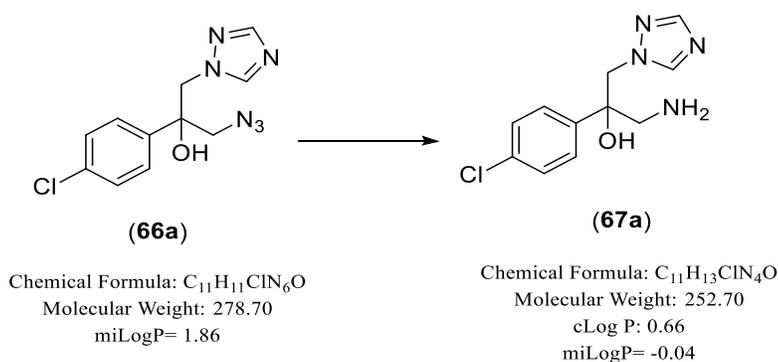
Prepared from (*R/S*)-1-azido-2-(4-chlorophenyl)-3-(1*H*-1,2,4-triazol-1-yl)propan-2-ol (**66a**, R^1= 4-Cl) (0.514 g, 1.84 mmoL). Product obtained as a white solid on standing overnight., yield: 0.36 g (77%). TLC (CH_2Cl_2-MeOH 9:1 v/v), R*f* = 0.4. M.p. 94-96 °C. ^{1}H NMR (DMSO-*d6*): δ 8.20 (s, 1H, triaz), 7.82 (s, 1H, triaz), 7.40 (d, *J* = 8.8 Hz, 2H, Ar), 7.33 (d, *J* = 8.8 Hz, 2H, Ar), 5.54 (brs, 2H, N*H2* partially exchanged), 4.50 (dd, *J* = 14.3, 19.3 Hz, 2H, C*H2*-triazole), 2.81 (s, 2H, C*H2*-NH2). (O*H* exchanged so not observed). ^{13}C NMR (DMSO-*d6*): δ 150.93 (CH, triazole), 145.30 (CH, triazole), 142.71 (C, Ar), 131.91 (C, *C*-Cl), 128.28 (2 x CH, Ar), 128.16 (2 x CH, Ar), 75.92 (C, *C*-OH), 56.51 (C*H2*-triazole), 50.00 (C*H2*-NH2). HRMS (ESI), *m/z*. calcd for $C_{11}H_{13}ClN_4O$ ([M + H]$^+$), 253.0856; found, 253.0855. HPLC (Method B2): 97.62%, R_t = 4.85 min.

(*R/S*)-1-Amino-2-(2,4-dichlorophenyl)-3-(1*H*-1,2,4-triazol-1-yl)propan-2-ol (67b)
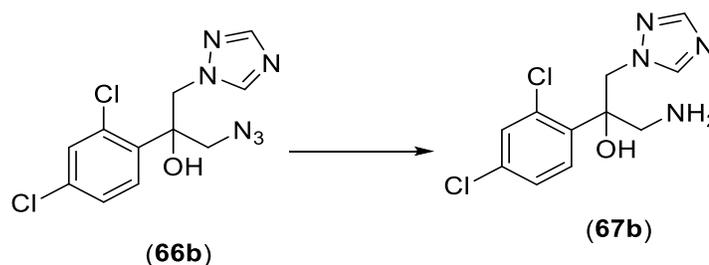
(**66b**)

Chemical Formula: $C_{11}H_{10}Cl_2N_6O$
Molecular Weight: 313.14
miLogP= 2.47

(**67b**)

Chemical Formula: $C_{11}H_{12}Cl_2N_4O$
Molecular Weight: 287.14
cLog P: 1.22
miLogP= 0.57

Prepared from (*R/S*)-1-azido-2-(2,4-dichlorophenyl)-3-(1*H*-1,2,4-triazol-1-yl)propan-2-ol (**66b**, R^1 = 2,4-diCl) (1.45 g, 4.62 mmoL). Product obtained as a white solid, yield: 0.80 g (60 %). TLC (CH₂Cl₂-MeOH 9:1 v/v), R*f* = 0.48. M.p. 70-72 °C. ¹H NMR (DMSO-*d₆*): δ 8.29 (s, 1H, triazole), 7.72 (s, 1H, triazole), 7.53 (t, *J* = 2.1 Hz, 1H, Ar), 7.52 (s, 1H, Ar), 7.30 (dd, *J* = 2.2, 8.6 Hz, 1H, Ar), 5.80 (brs, 1H, O*H*), 4.87 (d, *J* = 14.3 Hz, 1H, C*Ha*Hb-triazole), 4.50 (d, *J* = 14.4 Hz, 1H, CHa*Hb*-triazole), 3.21 (d, *J* = 13.5 Hz, 1H, C*Ha*Hb-NH₂), 3.07 (d, *J* = 13.5 Hz, 1H, CHa*Hb*-NH₂), 1.55 (brs, 2H, N*H₂*). ¹³C NMR (DMSO-d₆): δ 150.88 (CH, triazole), 145.37 (CH, triazole), 139.27 (C, Ar), 132.97 (C, *C*-Cl), 131.76 (CH, Ar), 131.58 (C, *C*-Cl), 130.36 (CH, Ar), 127.28 (CH, Ar), 76.47 (C, *C*-OH), 54.36 (*C*H₂-triazole), 47.04 (*C*H₂-NH₂).). HRMS (ESI), *m/z*. calcd for $C_{11}H_{12}Cl_2N_4O$ ([M + H]⁺), 287.0466; found, 287.0467. HPLC (Method B2): 99.33%, Rₜ = 4.78 min.

(*R/S*)-*N*-(2-(4-Chlorophenyl)-2-hydroxy-3-(1*H*-1,2,4-triazol-1-yl)propyl)-4-nitrobenzamide (57b)
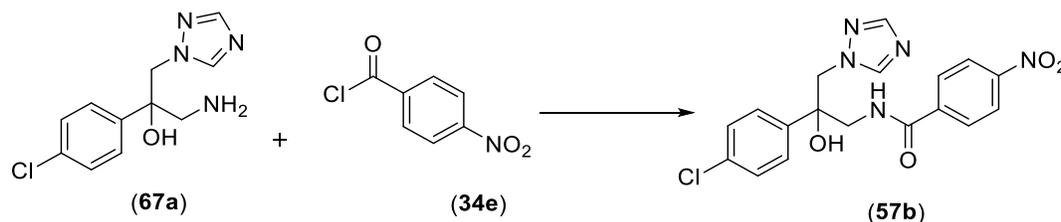
(**67a**)

Chemical Formula: $C_{11}H_{13}ClN_4O$
Molecular Weight: 252.70
cLog P: 0.66
miLogP= -0.04

(**34e**)

Chemical Formula: $C_7H_4ClNO_3$
Molecular Weight: 185.56
cLog P: 1.49
miLog P: 2.35

(**57b**)

Chemical Formula: $C_{18}H_{16}ClN_5O_4$
Molecular Weight: 401.81
miLogP= 1.94

Method: see 7.4.23 method, the reaction mixture was evaporated, and the obtained residue diluted with EtOAc (15 mL), extracted with H_2O (5 mL), dried ($MgSO_4$) and the solvent evaporated under vacuum.

Prepared from (*R/S*)-1-amino-2-(4-chlorophenyl)-3-(1*H*-1,2,4-triazol-1-yl)propan-2-ol (**67a**, R^1= 4-Cl) (0.2 g, 0.79 mmoL). Product obtained as a white solid, which was purified by gradient column chromatography CH_2Cl_2-MeOH (97: 3 v/v), yield: 0.24 g (74 %). TLC (CH_2Cl_2-MeOH 9.5:0.5 v/v), Rf = 0.44. M.p. 228-230 °C. ^{1}H NMR (DMSO-d_6): δ 8.63 (t, *J* = 5.9 Hz, 1H, N*H*), 8.29 (d, *J* = 8.9 Hz, 2H, Ar), 8.26 (s, 1H, triazole), 7.96 (d, *J* = 8.9 Hz, 2H, Ar), 7.84 (s, 1H, triazole), 7.45 (d, *J* = 8.6 Hz, 2H, Ar), 7.32 (d, *J* = 8.7 Hz, 2H, Ar), 6.00 (s, 1H, O*H*), 4.63 (dd, *J* = 14.4, 20.8 Hz, 2H, C*H*$_2$-triazole), 3.91 (dd, *J* = 6.8, 13.9 Hz, 1H, C*Ha*HbNH), 3.64 (dd, *J* = 5.3, 13.9 Hz, 1H, CHa*Hb*NH). ^{13}C NMR (DMSO-d_6): δ 166.09 (C, C=O), 151.05 (CH, triazole), 149.50 (C, Ar), 145.47 (CH, triazole), 141.28 (C, Ar), 140.34 (C, Ar), 132.22 (C, *C*-Cl), 129.28 (2 x CH, Ar), 128.37 (2 x CH, Ar), 128.11 (2 x CH, Ar), 123.93 (2 x CH, Ar), 76.12 (C, *C*-OH), 56.92 (*C*H$_2$-triazole), 49.15 (*C*H$_2$-NH$_2$). HRMS (ESI), *m/z*. calcd for $C_{18}H_{16}ClN_5O_4$ ([M + H]$^+$), 402.0969; found, 402.0969. HPLC (Method B2): 99.895%, R_t = 4.84 min.

(*R/S*)-*N*-(2-(2,4-dichlorophenyl)-2-hydroxy-3-(1*H*-1,2,4-triazol-1-yl)propyl)-4-nitrobenzamide (57c)
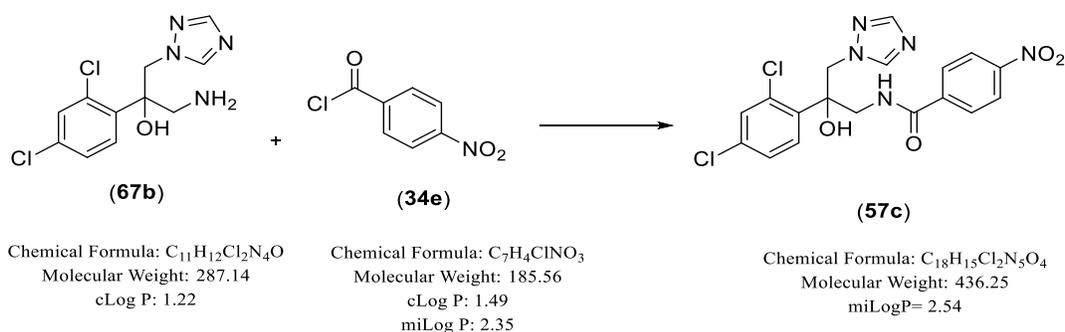
(**67b**)	(**34e**)	(**57c**)
Chemical Formula: $C_{11}H_{12}Cl_2N_4O$	Chemical Formula: $C_7H_4ClNO_3$	Chemical Formula: $C_{18}H_{15}Cl_2N_5O_4$
Molecular Weight: 287.14	Molecular Weight: 185.56	Molecular Weight: 436.25
cLog P: 1.22	cLog P: 1.49	miLogP= 2.54
	miLog P: 2.35	

Method: see 7.4.23 method, the reaction mixture was evaporated, and the obtained residue diluted with EtOAc (15 mL), extracted with H_2O (5 mL), dried ($MgSO_4$) and the solvent evaporated under vacuum.

Prepared from (*R/S*)-1-amino-2-(2,4-dichlorophenyl)-3-(1*H*-1,2,4-triazol-1-yl)propan-2-ol (**67b**, R^1= 2,4-diCl) (0.5 g, 1.74 mmoL). Product obtained as a white solid which was purified

by gradient column chromatography CH_2Cl_2-MeOH (97.5: 2.5 to 97: 3 v/v), yield: 0.42 g (55 %). TLC (CH_2Cl_2-MeOH 9.5:0.5 v/v), Rf = 0.5. M.p. 228-230 °C. ^{1}H NMR (DMSO-d_6): δ 8.79 (t, J = 6.1 Hz, 1H, NH), 8.34 (s, 1H, triazole), 8.30 (d, J = 9.0 Hz, 2H, Ar), 7.99 (d, J = 8.7 Hz, 2H, Ar), 7.75 (s, 1H, triazole), 7.58 (s, 1H, Ar), 7.56 (d, J = 2.2 Hz, 1H, Ar), 7.29 (dd, J = 2.2, 8.6 Hz, 1H, Ar), 6.26 (brs, 1H, OH), 5.10 (d, J = 14.5 Hz, 1H, CHaHb-triazole), 4.71 (d, J = 14.5 Hz, 1H, CHaHb-triazole), 4.07 (dd, J = 5.8, 14.0 Hz, 1H, CHaHbNH), 4.00 (dd, J = 6.4, 14.0 Hz, 1H, CHaHbNH). ^{13}C NMR (DMSO-d_6): δ 166.49 (C, C=O), 151.06 (CH, triazole), 149.55 (C, Ar), 145.46 (CH, triazole), 140.16 (C, Ar), 137.97 (C, Ar), 133.33 (C, C-Cl), 132.11 (C, C-Cl), 131.49 (CH, Ar), 130.46 (CH, Ar), 129.36 (2 x CH, Ar), 127.27 (CH, Ar), 123.93 (2 x CH, Ar), 76.74 (C, C-OH), 54.03 (CH_2-triazole), 45.81 (CH_2-NH$_2$). HRMS (ESI), *m/z.* calcd for $C_{18}H_{15}Cl_2N_5O_4$ ([M + H]$^+$), 436.0579; found, 436.0578. HPLC (Method B2): 99.99%, R$_t$ = 4.68 min.

7.4.32 General method for reduction of nitro derivatives to free amine derivatives (68)
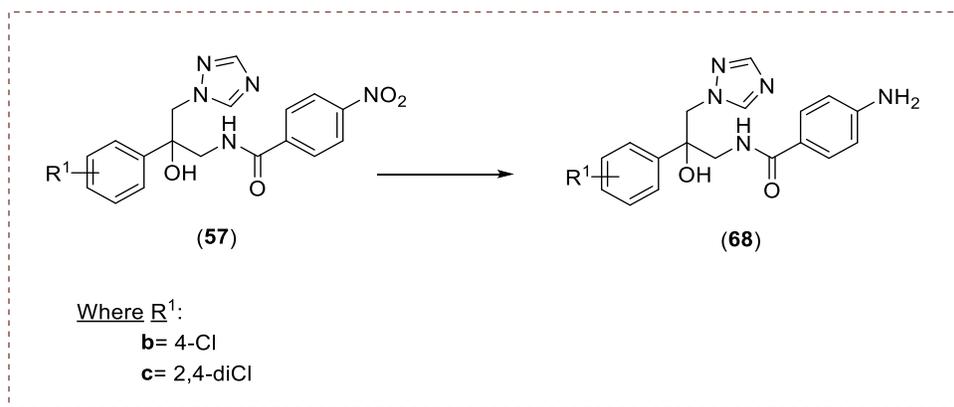
To a solution of *N*-(2-(arylphenyl)-2-hydroxy-3-(1*H*-1,2,4-triazol-1-yl)propyl)-4-nitrobenzamide derivative (**57**) (1.0 meq) in dry MeOH (15 mL) was added 10% Pd/C. Then, the reaction atmosphere was degassed, filled with hydrogen (using hydrogen balloon) and the mixture stirred at rt for 3 h.[122] The suspension was filtered through a pad of celite and the solvent removed under reduce pressure. The crude product was purified by gradient column chromatography CH_2Cl_2-MeOH (97: 3 v/v).

(*R/S*)-4-Amino-*N*-(2-(4-chlorophenyl)-2-hydroxy-3-(1*H*-1,2,4-triazol-1-yl)propyl) benzamide (68a)

(57b)

Chemical Formula: $C_{18}H_{16}ClN_5O_4$
Molecular Weight: 401.81
miLogP= 1.94

(68a)

Chemical Formula: $C_{18}H_{18}ClN_5O_2$
Molecular Weight: 371.83
Log P: 1.69
miLogP= 1.05
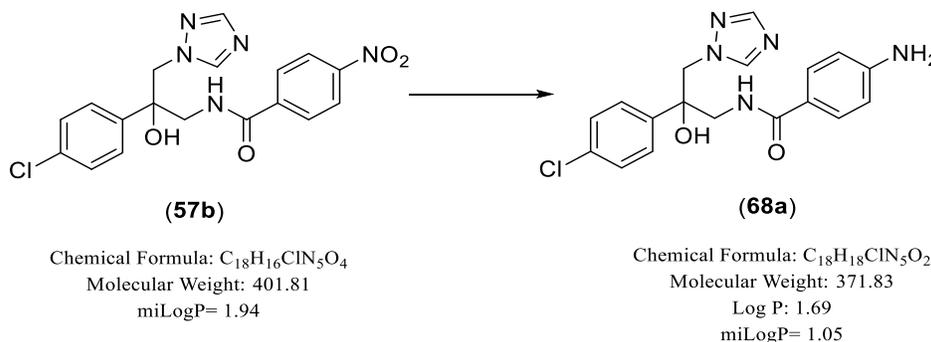
Prepared from (*R/S*)-*N*-(2-(4-chlorophenyl)-2-hydroxy-3-(1*H*-1,2,4-triazol-1-yl)propyl)-4-nitrobenzamide (**57b**, R^1= 4-Cl) (0.2 g, 0.5 mmoL). Product obtained as an off-white wax, yield: 0.13 g (71 %). TLC (CH_2Cl_2-MeOH 9.5:0.5 v/v), R*f* = 0.35. ^{1}H NMR (DMSO-*d*$_6$): δ 8.25 (s, 1H, triazole), 8.00 (t, *J* = 5.9 Hz, 1H, N*H*), 7.82 (s, 1H, triazole), 7.48 (d, *J* = 8.7 Hz, 2H, Ar), 7.42 (d, *J* = 8.8 Hz, 2H, Ar), 7.31 (d, *J* = 8.8 Hz, 2H, Ar), 6.51 (d, *J* = 8.8 Hz, 2H, Ar), 6.40 (s, 1H, O*H*), 4.53 (dd, *J* = 14.3, 20.3 Hz, 2H, C*H*$_2$-triazole), 3.79 (dd, *J* = 6.6, 14.1 Hz, 1H, C*Ha*HbNH), 3.60 (dd, *J* = 5.1, 14.1 Hz, 1H, CHa*Hb*NH). ^{13}C NMR (DMSO-*d*$_6$): δ 168.38 (C, C=O), 152.50 (C, Ar), 150.97 (CH, triazole), 145.45 (CH, triazole), 141.73 (C, Ar), 132.07 (C, *C*-Cl), 129.41 (2 x CH, Ar), 128.42 (2 x CH, Ar), 128.09 (2 x CH, Ar), 120.45 (C, Ar), 112.92 (2 x CH, Ar), 76.54 (C, *C*-OH), 57.33 (*C*H$_2$-triazole), 48.39 (*C*H$_2$-NH). HRMS (ESI), *m/z*. calcd for $C_{18}H_{18}ClN_5O_2$ ([M + Na]$^+$), 394.1047; found, 394.1047. HPLC (Method B2): 99.81%, R_t = 4.695 min.

(*R/S*)-4-Amino-*N*-(2-(2,4-dichlorophenyl)-2-hydroxy-3-(1*H*-1,2,4-triazol-1-yl)propyl) benzamide (68b)

(57c)

Chemical Formula: $C_{18}H_{15}Cl_2N_5O_4$
Molecular Weight: 436.25
miLogP= 2.54

(68b)

Chemical Formula: $C_{18}H_{17}Cl_2N_5O_2$
Molecular Weight: 406.27
cLog P: 2.24
miLogP= 1.66
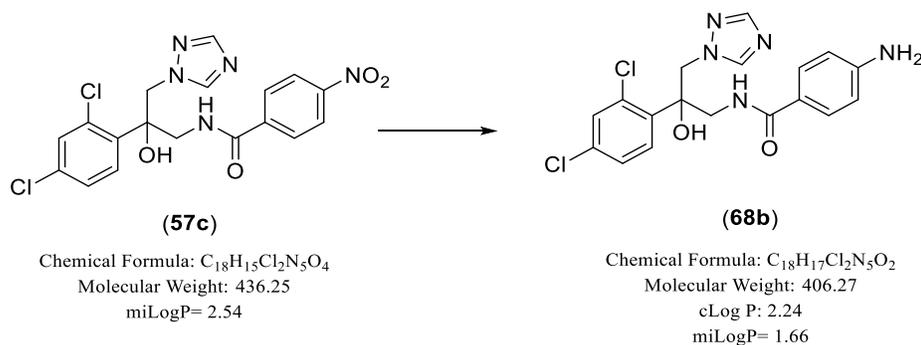
Prepared from (*R/S*)-*N*-(2-(2,4-dichlorophenyl)-2-hydroxy-3-(1*H*-1,2,4-triazol-1-yl)propyl)-4-nitrobenzamide (**57c**, R^1= 2,4-diCl) (0.38 g, 0.86 mmoL). Product obtained as a pale-yellow wax, yield: 0.35 g (100 %). TLC (CH$_2$Cl$_2$-MeOH 9.5:0.5 v/v), R*f* = 0.36. ^{1}H NMR (DMSO-*d*$_6$): δ 8.34 (s, 1H, triazole), 8.21 (t, *J* = 5.9 Hz, 1H, N*H*), 7.73 (s, 1H, triazole), 7.58 (d, *J* = 8.7 Hz, 1H, Ar), 7.55 (d, *J* = 2.2 Hz, 1H, Ar), 7.51 (d, *J* = 8.7 Hz, 2H, Ar), 7.28 (dd, *J* = 2.3, 8.7 Hz, 1H, Ar), 6.87 (s, 1H, O*H*), 6.51 (d, *J* = 8.7 Hz, 2H, Ar), 5.71 (brs, 2H, N*H*$_2$), 5.00 (d, *J* = 14.3 Hz, 1H, C*Ha*Hb-triazole), 4.65 (d, *J* = 14.3 Hz, 1H, CHa*Hb*-triazole), 3.94 (d, *J* = 5.3 Hz, 2H, C*H*$_2$-NH). ^{13}C NMR (DMSO-*d*$_6$): δ 169.23 (C, C=O), 152.67 (C, Ar), 150.96 (CH, triazole), 145.61 (CH, triazole), 138.48 (C, Ar), 133.22 (C, *C*-Cl), 131.96 (C, *C*-Cl), 131.67 (CH, Ar), 130.37 (CH, Ar), 129.59 (2 x CH, Ar), 127.29 (CH, Ar), 120.01 (C, Ar), 112.90 (2 x CH, Ar), 77.21 (C, *C*-OH), 54.33 (*C*H$_2$-triazole), 46.39 (*C*H$_2$-NH). HRMS (ESI), *m/z*. calcd for C$_{18}$H$_{17}$Cl$_2$N$_5$O$_2$ ([M + Na]$^+$), 428.0657; found, 428.0660. HPLC (Method B2): 99.98%, R$_t$ = 4.68 min.

(*R/S*)-*N*-(2-(4-Chlorophenyl)-2-hydroxy-3-(1*H*-1,2,4-triazol-1-yl)propyl)-4-((4-chlorophenyl)sulfonamido)benzamide (69a)

(**68a**)
Chemical Formula: C$_{18}$H$_{18}$ClN$_5$O$_2$
Molecular Weight: 371.83
cLog P: 1.69
miLogP= 1.05

(**17b**)
Chemical Formula: C$_6$H$_4$Cl$_2$O$_2$S
Molecular Weight: 211.06
cLog P: 2.32

(**69a**)
Chemical Formula: C$_{24}$H$_{21}$Cl$_2$N$_5$O$_4$S
Molecular Weight: 546.42
cLog P: 3.45
miLogP= 3.42
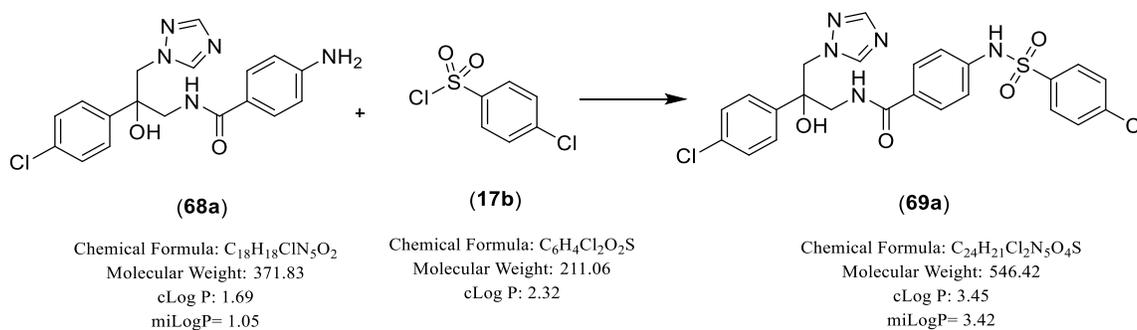
Method: see 7.4.21 method.

Prepared from (*R/S*)-4-amino-*N*-(2-(4-chlorophenyl)-2-hydroxy-3-(1*H*-1,2,4-triazol-1-yl)propyl)benzamide (**68a**, R^1= 4-Cl) (0.30 g, 0.82 mmoL) and 4-chlorobenzenesulfonyl chloride (**17b**, R^2= 4-Cl) (0.26 g, 1.23 mmoL). Product obtained as a white solid, which was purified by column chromatography CH$_2$Cl$_2$-MeOH (96.5: 3.5 v/v), yield: 0.35 g (77 %). TLC (CH$_2$Cl$_2$-MeOH 9.5:0.5 v/v), R*f* = 0.45. M.p. 236-238 °C. ^{1}H NMR (DMSO-*d*$_6$): δ 10.73 (brs, 1H, N*H*SO$_2$), 8.23 (s, 1H, triazole), 8.21 (t, *J* = 6.0 Hz, 1H, N*H*), 7.81 (s, 1H, triazole), 7.79 (d, *J* = 8.8 Hz, 2H, Ar), 7.63 (m, 4H, Ar), 7.41 (d, *J* = 8.7 Hz, 2H, Ar), 7.28 (m, 2H, Ar), 716 (m,

2H, Ar), 6.04 (s, 1H, O*H*), 4.56 (dd, *J* = 14.4, 25.0 Hz, 2H, C*H₂*- triazole), 3.79 (dd, *J* = 6.6, 14.0 Hz, 1H, NHC*Ha*Hb), 3.59 (dd, *J* = 5.3, 14.0 Hz, 1H, NHCHa*Hb*). ^{13}C NMR (DMSO-*d₆*): δ 167.19 (C, C=O), 151.00 (CH, triazole), 145.44 (CH, triazole), 141.45 (C, Ar), 140.85 (C, Ar), 138.65 (C, Ar), 138.48 (C, *C*-Cl), 132.15 (C, *C*-Cl), 130.03 (2 x CH, Ar), 129.76 (C, Ar), 129.15 (2 x CH, Ar), 129.04 (2 x CH, Ar), 128.35 (2 x CH, Ar), 128.06 (2 x CH, Ar), 119.09 (2 x CH, Ar), 76.25 (C, *C*-OH), 57.04 (*C*H₂- triazole), 48.18 (*C*H₂-NH). HRMS (ESI), *m/z*. calcd for $C_{24}H_{21}Cl_2N_5O_4S$ ([M + H]$^+$), 546.0769; found, 546.0769. HPLC (Method B2): 100%, R$_t$ = 4.77 min.

(*R/S*)-4-((4-chlorophenyl)sulfonamido)-*N*-(2-(2,4-dichlorophenyl)-2-hydroxy-3-(1*H*-1,2,4-triazol-1-yl)propyl)benzamide (69b)

(68b)
Chemical Formula: $C_{18}H_{17}Cl_2N_5O_2$
Molecular Weight: 406.27
cLog P: 2.24
miLogP= 1.66

(17b)
Chemical Formula: $C_6H_4Cl_2O_2S$
Molecular Weight: 211.06
cLog P: 2.32
miLogP= 2.50

(69b)
Chemical Formula: $C_{24}H_{20}Cl_3N_5O_4S$
Molecular Weight: 580.87
cLog P: 4.01
miLogP= 4.03
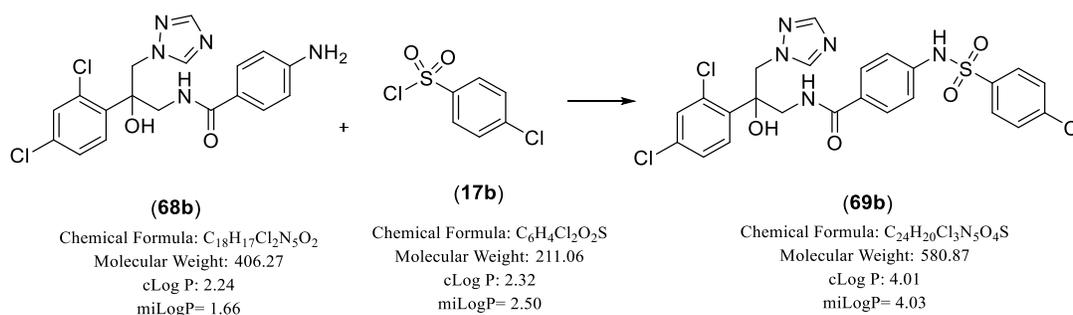
Method: see 7.4.21 method.

Prepared from (*R/S*)-4-amino-*N*-(2-(2,4-dichlorophenyl)-2-hydroxy-3-(1*H*-1,2,4-triazol-1-yl)propyl)benzamide (**68b**, R^1= 2,4-diCl) (0.17 g, 0.42 mmoL) and 4-chlorobenzenesulfonyl chloride (**17b**, R^2= 4-Cl) (0.13 g, 0.63 mmoL). Product obtained as a white solid, which was purified by column chromatography CH_2Cl_2-MeOH (96.5: 3.5 v/v), yield: 0.2 g (83 %). TLC (CH_2Cl_2-MeOH 9.5:0.5 v/v), R*f* = 0.46. M.p. 228-230 °C. ^{1}H NMR (DMSO-*d₆*): δ 10.76 (brs, 1H, N*H*SO₂), 8.40 (t, *J* = 6.0 Hz, 1H, N*H*), 8.32 (s, 1H, triazole), 7.79 (d, *J* = 8.8 Hz, 2H, Ar),), 7.72 (s, 1H, triazole), 7.60 (dd, *J* = 4.8, 8.9 Hz, 4H, Ar), 7.54 (dd, *J* = 3.2, 5.5 Hz, 2H, Ar), 7.27 (dd, *J* = 2.2, 8.7 Hz, 1H, Ar), 713 (d, *J* = 8.8 Hz, 2H, Ar), 6.36 (s, 1H, O*H*), 5.04 (d, *J* = 14.4 Hz, 1H, C*Ha*Hb-triazole), 4.63 (d, *J* = 14.4 Hz, 1H, CHa*Hb*-triazole), 4.01 (dd, *J* = 5.7, 14.1 Hz, 1H, C*Ha*HbNH), 3.89 (dd, *J* = 6.3, 14.0 Hz, 1H, CHa*Hb*NH). ^{13}C NMR (DMSO-*d₆*): δ 167.78 (C, C=O), 151.00 (CH, triazole), 145.56 (CH, triazole), 141.01 (C, Ar), 138.65 (C, Ar), 138.48 (C, Ar), 138.15 (C, *C*-Cl), 133.26 (C, *C*-Cl), 132.01 (C, *C*-Cl), 131.50 (CH, Ar), 130.41

(CH, Ar), 130.03 (2 x CH, Ar), 129.44 (C, Ar), 129.26 (2 x CH, Ar), 129.08 (2 x CH, Ar), 127.27 (CH, Ar), 119.02 (2 x CH, Ar), 76.91 (C, *C*-OH), 45.09 (*CH₂*- triazole), 45.96 (*CH₂*-NH). HRMS (ESI), *m/z*. calcd for $C_{24}H_{21}Cl_2N_5O_4S$ ([M + H]⁺), 580.038; found, 580.0304. HPLC (Method B2): 99.69%, $R_t = 4.76$ min.

7.5 Homology model

7.5.1 Construction of *L. donovani* CYP5122A1 model

Homology search

The protein sequence for CYP5122A1 of *L. donovani* was obtained from the ExPASy proteomics server at the Swiss Bioinformatics Institute.[145,164] The enzyme sequence of the target gene has the UniProt Identifier Q2XQE3 (Q2XQE3_LEIDO) and is composed of 606 residues. A homology search was performed using the SIB BLAST service[146,165] accessible from the ExPASy server, which was used to align the query sequence (CYP5122A1) against the sequences in the protein data bank[76,77] and thus the close homologous proteins were identified. The alignment parameters and the thresholds, which were used for screening expected homologues, were used with their default values and BLOSUM62 comparison matrix. The phylogeny server[148] was used to build a phylogenetic tree for these homologous proteins, the query sequence and other CYP enzymes selected from different organisms.

Multiple sequence and structure alignment

The sequence of the query enzyme was aligned with the protein sequences of the most homologous bacterial CYPs especially CYP51 templates: *L. infantum* (PDB 3L4D); *T. brucei* (PDB 2WV2); and *T. cruzi* (PDB 2WX2), using Clustal Omega.[149] The second structure of the query enzyme and the closest template (PDB 3L4D) were determined using PSIPRED.[151]

3D model building

The molecular experiments were performed using SWISS-MODEL[152], a fully automated protein structure homology-modelling server. To build a homology model using this server, the query sequence file in FASTA format was uploaded, and a search for templates run. After that, the best template (PDB 3L4D) was selected, which is from the same gene.

7.5.2 Model validation

Stereochemical quality of the polypeptide backbone and side chains was evaluated using Ramachandran plots obtained from the RAMPAGE server.[153] The ProSA server[155] was used to check defaults in the three-dimensional protein structure based on statistical analysis. Validation data from the template (PDB 3L4D) was used as the baseline to evaluate the model.

7.5.3 Molecular dynamic (MD) simulation

MD simulation of CYP5122A1 homology model was run over 150 ns using Desmond.[102] The preparation of protein was conducted as described in this chapter section 7.2.

7.5.4 Docking study

Performed as described previously in this chapter section 7.2 with one modification: the active site was defined with the dummy atoms guide, they were then selected and extended to near (4.5 Å) residues in order to include in the docking site the haem iron region and the access channel to the catalytic site with no water molecules considered.

7.5.5 Biological assay (Intra-macrophage assay) *(Performed by Dr Sujatha at the Drug Discovery Unit, University of Dundee during the PhD time)*

In a 384 well-plate the THP-1 (human monocytic leukaemia) macrophages were differentiated with 10 nM PMA (phorbol 12-myristate 13-acetate) concentration for 3 days, followed by plates washed to remove the PMA. THP-1 was infected overnight with an enhanced green fluorescent protein (eGFP) expressing amastigotes with the ratio (amastigotes to THP-1, 5:1) to facilitate the image analysis. After the infection, compounds were added to the plate after removing the extracellular amastigotes by washing the plate, followed by 72 h incubation. Finally, the plate was washed, fixed and stained to analyse the image and tabulate the data. Further details can be found in De Rycker, M. *et al.*[157]

Chapter VIII

References

8. References

1. CDC - Centre for Disease Control and Prevention. Available from: https://www.cdc.gov/fungal/diseases/candidiasis/index.html (Accessed June 1, **2020**).

2. Bongomin, F.; Gago, S.; Oladele, R.; Denning, D. Global and multi-national prevalence of fungal diseases estimate precision. *J. Fungi* **2017**, *3*, 57.

3. Sardi, J.C.O.; Scorzoni, L.; Bernardi, T.; Fusco-Almeida, A.M.; Mendes-Giannini, M.J.S. Candida Species: current epidemiology, pathogenicity, biofilm formation, natural antifungal products and new therapeutic options. *J. Med. Microbiol.* **2013**, *62*, 10-24.

4. Sanglard, D. Emerging threats in antifungal-resistant fungal pathogens. *Front. Med.* **2016**, *3*, 11.

5. Eddouzi, J.; Parker, J.E.; Vale-Silva, L.A.; Coste, A.; Ischer, F.; Kelly, S.; Manai, M.; Sanglard, D. Molecular mechanisms of drug resistance in clinical *Candida* species isolated from Tunisian hospitals. *Antimicrob. Agents Chemother.* **2013**, *57*, 3182-3193.

6. Whaley, S.G.; Berkow, E.L.; Rybak, J.M.; Nishimoto, A.T.; Barker, K.S.; Rogers, P.D. Azole antifungal resistance in *Candida albicans* and emerging non-albicans *Candida* species. *Front. Microbiol.* **2017**, *7*, 2173.

7. Cleveland, A.A.; Harrison, L.H.; Farley, M.M.; Hollick, R.; Stein, B.; Chiller, T.M.; Lockhart, S.R.; Park B.J. Declining incidence of Candidemia and the shifting epidemiology of *Candida* resistance in two US metropolitan areas, 2008-2013: results from population-based surveillance. *PLoS One* **2015**, *10*, e0120452.

8. Klingspor, L.; Tortorano, A.M.; Peman, J.; Willinger, B.; Hamal, P.; Sendid, B.; Velegraki, A.; Kbbler, C.; Meis, J.F.; Sabino, R.; Ruhnke, M.; Arikan-Akdagli, S.; Salonen, J.; Dóczi, I. Invasive *Candida* infections in surgical patients in intensive care units: aprospective, multicentre survey initiated by the European Confederation of Medical Mycology (ECMM) (2006-2008). *Clin. Microbiol. Infect.* **2015**, *21*, 87.e1-87.e10.

9. Sharifzadeh, A.; Khosravi, A.R.; Shokri, H.; Jamnani, F.A.; Hajiabdolbaghi, M.; Tamami, I.A. Oral microflora and their relation to risk factors in HIV+ patients with oropharyngeal candidiasis. *J. Mycol. Med.* **2013**, *23*, 105-112.

10. Spivak, E.S; Hanson, K.E. *Candida auris*: an emerging fungal pathogen. *J. Clin. Microbiol.* **2018**, *56*, e01588-17.

11. Centre for Disease Control and Prevention. Tracking Candida auris. Available from: https://www.cdc.gov/fungal/candidaauris/tracking-c-auris.html (Accessed June 1, **2020**).

12. Zhang, J.; Li, L.; Lv, Q.; Yan, L.; Wang, Y.; Jian, Y. The fungal CYP51s: their functions, structures, related drug resistance, and inhibitors. *Front. Microbiol*. **2019**, *10*, 691.

13. McKinnon, R.A. Cytochrome P450 multiplicity and function. *Aust. J. of Hospital Pharm.* **2000**, *30*, 54-56.

14. Brown, G.D.; Denning, D.W.; Gow, N.A.R.; Levitz, S.M.; Netea, M.G.; White, T.C. Hidden killers: human fungal infections. *Sci. Transl. Med*. **2012**, *4*, 165rv13.

15. Vázquez-González D., Perusquía-Ortiz A.M.; Hundeiker M.; Bonifaz, A. Opportunistic yeast infections: candidiasis, cryptococcosis, trichosporonosis and geotrichosis. *JDDG* **2013**, *11*, 381-93.

16. Mayer, F.L.; Wilson, D.; Hube, B. *Candida albicans* pathogenicity mechanisms. *Virulence* **2013**, *4*, 119-128.

17. Yapar, N. Epidemiology and risk factors for invasive candidiasis. *Ther. Clin. Risk Manag.* **2014**, *10*, 95-105.

18. Laboratory surveillance of candidaemia in England, Wales and Northern Ireland: 2017. Health Protection Report **2018,** 12. Available from: https://assets.publishing.service.gov.uk/government/uploads/system/uploads/attachment_data/file/742602/hpr3418_cnddm17.pdf (Accessed Feb 26, **2020**).

19. Sobel, J.D. Vulvovaginal candidosis. *Lancet* **2007**, *369*, 1961-1971.

20. Gow, N.A.R.; Latge, J.-P., Munro, C.A. 2017.The fungal cell wall: structure, biosynthesis, and function. *Microbiol. Spectrum*. **2017**, *5*, 0035-2016.

21. Riley, J.; Brand, S.; Voice, M.; Caballero, I.; Calvo, D.; Read, K.D. Development of a fluorescence-based trypanosoma cruzi CYP51 inhibition assay for effective compound triaging in drug discovery programmes for Chagas disease. *PLoS Negl. Trop. Dis.* **2015**, *9*, e0004014.

22. Kathiravan, M.L.; Salake, A.B.; Chothe, A.S.; Dudhe, P.B.; Watode, R.P.; Mukta, M.S.; Gadhwe, S. The biology and chemistry of antifungal agents: a review. *Bioorg. Med. Chem.* **2012**, *20*, 5678-5698.

23. Campoy, S.; Adrio, J.L. Antifungals. *Biochem. Pharmacol.* **2017**, *133*, 86-96.

24. Denning, D.W.; Hope, W.W. Therapy for fungal diseases: opportunities and priorities. *Trends Microbiol.* **2010**, *18*, 195-204.

25. Odds, F.C.; Brown, A.J.P.; Gow, N.A.R. Antifungal agents: mechanisms of action. *Trends Microbiol.* **2003**, *11*, 272-279.

26. Ghannoum, M.A.; Rice, L.B. Antifungal agents: mode of action, mechanisms of resistance, and correlation of these mechanisms with bacterial resistance. *Clin. Microbiol. Rev.* **1999**, *4*, 501-517.

27. Hu, Z.; He, B.; Ma, L.; Sun, Y.; Niu, Y.; Zeng, B. Recent advances in ergosterol biosynthesis and regulation mechanisms in *Saccharomyces cerevisiae. Indian J. Microbiol.* **2017**, *57*, 270-277.

28. Dupont, S.; Lemetais, G.; Ferreira, T.; Cayot, P.; Gervais, P.; Beney, L. Ergosterol biosynthesis: a fungal pathway for life on land? *Evolution* **2012**, *66*, 2961-2968.

29. Zhang, Y-Q; Gamarra, S.; Garcia-Effron, G.; Park, S.; Perlin, D.S.; Rao, R. Requirement for ergosterol in V-ATPase function underlies antifungal activity of azole drugs. *PLoS Pathog.* **2010**, *6*, e1000939.

30. Lv, Q-Z; Yan, L.; Jiang, Y-Y. The synthesis, regulation, and functions of sterols in *Candida albicans*: well-known but still lots to learn. *Virulence* **2016**, *7*, 649-659.

31. Choi, J.Y.; Podust, L.M.; Roush, W.R. Drug strategies targeting CYP51 in neglected tropical diseases. *Chem. Rev.* **2014**, *114*, 11242-11271.

32. Sanglard, D.; Ischer, F.; Parkinson, T.; Falconer, D.; Bille, J. *Candida albicans* mutations in the ergosterol biosynthetic pathway and resistance to several antifungal agents. *Antimicrob. Agents Chemother.* **2003**, *47*, 2404-2412.

33. Onyewu, C.; Blankenship, J.R.; Poeta, M.D.; Heitman, J. Ergosterol biosynthesis inhibitors become fungicidal when combined with calcineurin inhibitors against *Candida albicans*, *Candida glabrata*, and *Candida krusei. Antimicrob. Agents Chemother.* **2003**, *47*, 956-964.

34. Pianalto, K.M.; Alspaugh, J.A. New horizons in antifungal therapy. *J. Fungi* **2016**, *2*, 1-24.

35. Hargrove, T.Y.; Friggeri, L.; Wawrzak, Z.; Qi, A.; Hoekstra, W.J.; Schotzinger, R.J.; York, J.D.; Guengerich, F.P.; Lepesheva, G.I. Structural analyses of *Candida albicans* sterol 14α-demethylase complexed with azole drugs address the molecular basis of azole-mediated inhibition of fungal sterol biosynthesis. *J. Biol. Chem.* **2017**, *292*, 6728-6743.

36. Martel, C.M.; Parker, J.E.; Bader, O.; Weig, M.; Gross, U.; Warrilow, A.G.S.; Rolley, N.; Kelly, D.E.; Kelly, S.L. Identification and characterization of four azole-resistant erg3 mutants of *Candida albicans*. *Antimicrob. Agents Chemother*. **2010**, *54*, 4527-4533.

37. Shukla, P.K.; Singh, P.; Yadav, R.K.; Pandey, S.; Bhunia, S.S. Past, present and future of antifungal drug development. *Top. Med. Chem.* **2016**, *29*, 125-167.

38. Kullberg, B.J.; Arendrup, M.C. Invasive candidiasis. *N. Engl. J. Med*. **2015**, *873*, 1445-1456.

39. Pappas, P.G.; Kauffman, C.A.; Andes, D.R.; Clancy, C.J.; Marr, K.A.; Ostrosky-Zeichner, L.; Reboli, A.C.; Schuster, M.G.; Vazquez, J.A.; Walsh, T.J.; Zaoutis, T.E.; Sobel, J.D. Clinical practice guidelines for the management of candidiasis: 2016 update by the Infectious Disease Society of America. *Clin. Infec. Dis*. **2016**, *62*, e1-e50.

40. Li, Y.; Theuretzbacher, U.; Clancy, C.J.; Nguyen, M.H.; Derendorf, H. Pharmacokinetic/pharmacodynamic profile of posaconazole. *Clin. Pharmacokinet.* **2010**, *49*, 379-396.

41. Yates, C.M.; Garvey, E.P.; Shaver, S.R.; Schotzinger, R.J.; Hoekstra, W.J. Design and optimization of highly-selective, broad spectrum fungal CYP51 inhibitors. *Bioorg. Med. Chem. Lett*. **2017**, *27*, 3243-3248.

42. Garvey, E.P.; Hoekstra, W.J.; Schotzinger, R.J.; Sobel, J.D.; Lilly, E.A.; Fidel, J.P.L. Efficacy of the clinical agent VT-1161 against fluconazole-sensitive and –resistant *Candida albicans* in a murine model of vaginal candidiasis. *Antimicrob. Agents Chemother*. **2015**, *59*, 5567-5573.

43. McCall, L.-I.; El Aroussi, A., Choi, J.Y.; Vieira, D.F.; De Muylder, G.; Johnston, J.B.; Chen, S.; Kellar, D.; Siqueira-Neto, J.L.; Roush, W.R.; Podust, L.M.; McKerrow, J.H. Targeting ergosterol biosynthesis in *Leishmania donovani*: essentiality of sterol 14alpha-demethylase. *PLOS Negl. Trop. Dis.* **2015**, *9*, e0003588.

44. Hargrove, T.Y.; Wawrzak, Z.; Alexander, P.W.; Chaplin, J.H.; Keenan, M.; Charman, S.A.; Perez, C.J.; Waterman, M.R.; Chatelain, E.; Lepesheva, G.I. Complexes of *Trypanosoma cruzi* sterol 14α-demethylase (CYP51) with two pyridine-based drug candidates for Chagas disease. *J. Biol. Chem.* **2013**, *288*, 31602-31615.

45. Lepesheva, G.I.; Waterman, M.R. Sterol 14alpha-demethylase (CYP51) as a therapeutic target for human trypanosomiasis and leishmaniasis. *Curr. Top. Med. Chem.* **2011**, *11*, 2060-2071.

46. Soeiro, M.N.C.; de Souza, E.M.; de Silva, C.F.; Batista, D.G.J.; Batista, M.M.; Pavão, B.P.; Araújo, J.S.; Aiub, C.A.F.; da Silva, P.B.; Lionel, J.; Britto, C.; Kim, K.; Sulikowski, G.; Hargrove, T.Y.; Waterman, M.R.; Lepesheva, G.I. *In vitro* and *in vivo* studies of the antiparasitic activity of sterol 14α-demethylase (CYP51) inhibitor VNI against drug-resistant strains of *trypanosoma cruzi*. *Antimicrob. Agents Ch.* **2013**, *57*, 4151-4163.

47. Lepesheva, G.I.; Villalta, F.; Waterman, M.R. Targeting *trypanosoma cruzi* sterol 14α-demethylase (CYP51). *Adv. Parasitol.* **2011**, *75*, 65-87.

48. Yua, X.; Cojocarub, V.; Mustafaa, G.; Salo-Ahenc, O.M.H.; Lepeshevad, G.I.; Wadea, R.C. Dynamics of CYP51: implications for function and inhibitor design. *J. Mol. Recognit.* **2015**, *28*, 59-73.

49. Hargrove, T.Y.; Friggeri, L.; Wawrzak, Z.; Sivakumaran, S.; Yazlovitskaya, E.M.; Hiebert, S.W.; Guengerich, F.P.; Waterman, M.R.; Lepesheva, G.I. Human sterol 14α-demethylase as a target for anticancer chemotherapy: towards structure-aided drug design. *J. Lipid Res.* **2016**, *57*, 1552-1563.

50. Choi, J.Y.; Roush, W.R. Structure based design of CYP51 inhibitors. *Curr. Top. Med. Chem.* **2017**, *17*, 30-39.

51. Parker, J.E.; Warrilow, A.G.S.; Price, C.L.; Mullins, J.G.L.; Kelly, D.E.; Kelly, S.L. Resistance to antifungals that target CYP51. *J. Chem. Biol.* **2014**, *7*, 143-161.

52. Lepesheva, G.I.; Hargrove, T.Y.; Kleshchenko, W.; Nes, D.; Villalta, F.; Waterman, M.R. CYP51: a major drug target in the cytochrome P450 superfamily. *Lipids* **2008**, *43*, 1117-1125.

53. Pfaller, M.A.; Diekema, D.J. Epidemiology of invasive candidiasis: a persistent public health problem. *Clin. Microbiol. Rev*. **2007**, *20*, 133-163.

54. Richardson, M.D. Changing patterns and trends in systemic fungal infections. *J. Antimicrob. Chemother*. **2005**, *56* (Suppl 1), i5-i11.

55. Sims, C.R.; Ostrosky-Zeichner, L.; Rex, J.H. Invasive candidiasis in immunocompromised hospitalized patients. *Arch. Med. Res*. **2005**, *36*, 660-671.

56. Guengerich, F.P.; Waterman, M.R.; Egli, M. Recent structure insights into cytochrome P450 function. *Trends Pharmacol. Sci.* **2016**, *37*, 625-640.

57. Flowers, S.A.; Colón, B.; Whaley, S.G.; Schuler, M.A.; Rogers, D.P. Contribution of clinically derived mutations in ERG11 to azole resistance in *Candida albicans*. *Antimicrob. Agents Chemother.* **2015**, *59*, 450-460.

58. Omura, T.; Sato, R. A new cytochrome in liver microsomes. *J. Biol. Chem.* **1962**, *237*, PC1375-PC1376.

59. Cowen, L.E.; Sanglard, D.; Susan J. Howard, S.J.; Rogers, P.D.; Perlin, D.S. Mechanisms of antifungal drug resistance. *CSH Perspect Med.* **2014**, *5*, a019752.

60. Warrilow, A.G.; Nishimoto, A.T.; Parker, J.E.; Price, C.L.; Flowers, S.A.; Kelly, D.E.; Rogers, P.D.; Kelly, S.L. The evolution of azole resistance in *Candida albicans* sterol 14α-demethylase (CYP51) through incremental amino acid substitutions. *Antimicrob. Agents Chemother.* **2019**, *63*, e02586-18.

61. Xiang, M-J.; Liu, J-Y.; Ni, P-H.; Wang, S.; Shi, C.; Wei, B.; Ni, Y-X.; Ge, H-L. Erg11 mutations associated with azole resistance in clinical isolates of *Candida albicans*. *FEMS Yeast Res*. **2013**, *13*, 386-393.

62. Lepesheva, G.I.; Waterman, M.R.; CYP51 – the omnipotent P450. *Mol. Cell. Endocrinol*. **2004**, *215*, 165-170.

63. Sanglard, D.; Ischer, F.; Koymans, L.; Bille, J. Amino acid substitutions in the cytochrome P450 lanosterol 14-demethylase (CYP51A1) from azole-resistant *Candida albicans* clinical isolates contribute to resistance to azole antifungal agents. *Antimicrob. Agent Chemother.* **1998**, *42*, 241-253.

64. Ravikumar, S.; Win, M.S.; Chai, L.Y. Optimizing outcomes in immunocompromised hosts: understanding the role of immunotherapy in invasive fungal diseases. *Front. Microbiol.* **2015**, *6*,1322.

65. Sanguinetti, M.; Posteraro, B.; Beigelman-Aubry, C.; Lamoth, F.; Dunet, V.; Slavin, M.; Richardson, M.D. Diagnosis and treatment of invasive fungal infections: looking ahead. *J Antimicrob Chemother* **2019**, *74*, ii27-ii37.

66. Furge, L.L.; Guengerich, F.P. Cytochrome P450 enzymes in drug metabolism and chemical toxicology: an introduction. *Biochem. Mol. Biol. Educ.* **2006**, *34*, 66-74.

67. Gilardi, G.; Nardo, G.D. Heme iron centers in cytochrome P450: structure and catalytic activity. *Rend. Fis. Acc. Lincei.* **2017**, *28* (Suppl 1), S159-S167.

68. Cook, D.J.; Finnigan, J.D.; Cook, K.; Black, G.W.; Charnock, S.J. Cytochromes P450: history, classes, catalytic mechanism, and industrial application; Taylor & Francis: UK, **2016**; pp105-126.

69. Lewis, D.F.V. Guide to Cytochromes P450, 2nd ed.; Taylor & Francis, **2001**, pp 50-59.

70. Omura, T.; Sato, R. The carbon monoxide-binding pigment of liver microsomes. *J. Biol. Chem.* **1964**, *239*, 2379-2385.

71. Werck-Reichhart, D.; Feyereisen, R. Protein family review cytochromes P450: a success story. *Genome Biol.* **2000**, *1*, 1-9.

72. Meunier, B.; De Visser, S.P.; Shaik, S. Mechanism of oxidation reactions catalyzed by cytochrome P450 enzymes. *Chem. Rev.* **2004**, *104*, 3947-3980.

73. Guengerich, F.P. Invited review: common and uncommon cytochrome P450 reactions related to metabolism and chemical toxicity. *Chem. Res. Toxicol.* **2001**, *14*, 611-650.

74. Lewis, D.F.V; Hlavica, P. Interactions between redox partners in various cytochrome P450 systems: functional and structural aspects. *Biochim. Biophys. Acta* **2000**, *1460*, 353-374.

75. Huang, X.; Groves, J.T. Oxygen activation and radical transformations in heme proteins and metalloporphyrins. *Chem. Rev.* **2018**, *118*, 2491-2553.

76. Berman, H.M; Westbrook, J.; Feng, Z.; Gilliland, G.; Bhat, T.N.; Weissig, H.; Shindyalov, I.N.; Bourne, P.E. The Protein Data Bank. *Nucleic Acids Res* **2000**, *28*, 235-242. https://www.rcsb.org/ (Accessed Oct 15, **2017**).

77. Burley, S.K.; Berman, H.M.; Bhikadiya, C.; Bi, C.; Chen, L.; Costanzo, L.D.; Christie, C.; Dalenberg, K.; Duarte, J.M.; Dutta, S.; Feng, Z.; Ghosh, S.; Goodsell, D.S.; Green, R.K.; Guranović, V.; Guzenko, D.; Hudson, B.P.; Kalro, T.; Liang, Y.; Lowe, R.; Namkoong, H.; Peisach, E.; Periskova, I.; Prlić, A.; Randle, C.; Rose, A.; Rose, P.; Sala, R.; Sekharan, M.; Shao, C.; Tan, L.; Tao, Y.-P.; Valasatava, Y.; Voigt, M.; Westbrook, J.; Woo, J.; Yang, H.; Young, J.; Zhuravleva, M.; Zardecki, C. RCSB Protein Data Bank: biological macromolecular structures enabling research and education in fundamental biology, biomedicine, biotechnology and energy. *Nucleic Acids Res.* **2019**, *47*, D464-D474. doi: 10.1093/nar/gky1004. https://www.rcsb.org/ (Accessed July 6, **2020**).

78. *Molecular Operating Environment (MOE)*, 2015.10; Chemical Computing Group Inc., 1010 Sherbooke St. West, Suite #910, Montreal, QC, Canada, H3A 2R7, **2016**.

79. Verma, S.; Mehta, A.; Shaha, C. CYP5122A1, a novel cytochrome P450 is essential for survival of leishmania donovani. *PLoS ONE* **2011**, *6*, e25273.

80. Pandharkar, T.; Zhu, X.; Mathur, R.; Jiang, J.; Schmittgen, T.D.; Shaha, C.; Werbovetza, K. A. Studies on the antileishmanial mechanism of action of the arylimidamide DB766: azole interactions and role of CYP5122A1. *Antimicrob Agents Ch* **2014**, *58*, 4682-4689.

81. LeadIT version 2.3.2; BioSolveIT GmbH, Sankt Augustin, Germany, 2017, www.biosolveit.de/LeadIT

82. Xie, J.; Yang, F.; Zhang, M.; Lam, C.; Qiao, Y.; Xiao, J.; Zhang, D.; Ge, Y.; Fu, L.; Xie, D. Antiproliferative activity and SARs of caffeic acid esters with mono-substituted phenylethanols moiety. *Bioorg. Med. Chem. Lett.* **2017**, *27*, 131-134.

83. Andrews, M.D.; Bagal, S.K.; Gibson, K.R.; Omoto, K.; Ryckmans, T.; Skerratt, S.E.; Stupple, P.A. Pyrrolo[2,3-*d*]pyrimidine derivatives as inhibitors of tropomyosin-related kinases and their preparation and use in the treatment of pain. **2012**, WO 2012137089 A1.

84. Karaluka, V.; Lanigan, R.M.; Murray, P.M.; Badland, M.; Sheppard, T.D. B(OCH₂CF₃)₃-mediated direct amidation of pharmaceutically relevant building blocks in cyclopentyl methyl ether. *Org. Biomol. Chem.* **2015**, *13*, 10888-10894.

85. Marcotullio, M.C.; Campagna, V.; Sternativo, S.; Costantino, F.; Curini, M. A new, simple synthesis of *N*-tosyl pyrrolidines and piperidines. *Synthesis* **2006**, *16*, 2760-2766.

86. Taban, I.M.; Elshihawy, H.E.A.E.; Torun, B.; Zucchini, B.; Williamson, C.J.; Altuwairigi, D.; Ngu, A.S.T.; McLean, K.J.; Levy, C.W.; Sood, S.; Marino, L.B.; Munro, A.W.; de Carvalho, L.P.S.; Simons, C. Novel aryl substituted pyrazoles as small molecule inhibitors of cytochrome P450 CYP121A1: synthesis and antimycobacterial evaluation. *J. Med. Chem.* **2017**, *60*, 10257-10267.

87. Perron, V.; Abbott, S.; Moreau, N.; Lee, D.; Penney, C.; Zacharie, B. A method for the selective protection of aromatic amines in the presence of aliphatic amines. *Synthesis* **2009**, *2*, 283-289.

88. Rich, D.H.; Singh, J. The carbodiimide method, in Gross, E., Meienhofer, J. eds. The Peptides: Analysis, Synthesis, Biology, Academic, New York, **1979**, *1*, 241-261.

89. Pandey, M.D.; Mishra, A.K.; Chandrasekhar, V.; Verma, S. Silver-guided excimer emission in an adenine-pyrene conjugate: fluorescence lifetime and crystal Studies. *Inorg. Chem.* **2010**, *49*, 2020-2022.

90. Lee, J.; Lee, J.; Kang, M.; Shin, M.; Kim, J-M.; Kang, S-U.; Lim, J-O.; Choi, H-K.; Suh, Y-G.; Park, H-G.; Oh, U.; Kim, H-D.; Park, Y-H.; Ha, H-J., Kim, Y-H.; Toth, A.; Wang, Y.; Tran, R.; Pearce, L.V.; Lundberg, D.J.; Blumberg, P. M. *N*-(3-Acyloxy-2-benzylpropyl)-*N′*-[4-(methylsulfonylamino)benzyl]thiourea analogues: novel potent and high affinity antagonists and partial antagonists of the vanilloid receptor. *J. Med. Chem.* **2003**, *46*, 3116-3126.

91. Müller, S.L.; Schreiber, J.A.; Schepmann, D.; Strutz-Seebohm, N.; Seebohm, G.; Wünsch, B. Systematic variation of the benzenesulfonamide part of the GluN2A selective NMDA receptor antagonist TCN-201. *Eur. J. Med. Chem.* **2017**, *129*, 124-134.

92. Komjáti, B.; Urai, Á.; Hosztafi, S.; Kökösi, J.; Kováts, B.; Nagy, J.; Horváth, P. Systematic study on the TD-DFT calculated electronic circular dichroism spectra of chiral aromatic nitro compounds: a comparison of B3LYP and CAM-B3LYP. *Spectrochim. Acta. Part A* **2016**, *155*, 95-102.

93. Ford, R.L.; Mete, A.; Millichap, I.; Teobald, B.J.; Kinchin, E.C. 1-Aza-bicyclo[2.2.2]octane derivatives useful as muscarinic receptor antagonists. **2009**, WO 2009153536 A1.

94. Taban, I.M.; Zhu, J.; DeLuca, H.F.; Simons, C. Synthesis, molecular modelling and CYP24A1 inhibitory activity of novel of (*E*)-*N*-(2-(1*H*-imidazol-1-yl)-2-(phenylethyl)-3/4-styrylbenzamides. *Bioorg. Med. Chem.* **2017**, *25*, 4076–4087.

95. Clinical and Laboratory Standards Institute. Reference method for broth dilution antifungal susceptibility testing of yeasts; fourth informational supplement. CLSI document M27-S4, **2012**, Wayne, PA.

96. Ghose, A.K.; Crippen, G.M. Atomic physicochemical parameters for three dimensional-structure-directed quantitative structure-activity relationships. 2. Modeling dispersive and hydrophobic interactions. *J. Chem. Inf. Comput. Sci.* **1987**, *27*, 21-35.

97. Lepesheva, G.I.; Ott, R.D.; Hargrove, T.Y.; Kleshchenko, Y.Y.; Schuster, I.; Nes, W.D.; Hill, G.C.; Villalta, F.; Waterman, M.R. Sterol 14α-demethylase as a potential target for

antitrypanosomal therapy: enzyme inhibition and parasite cell growth. *Chem Biol.* **2007**, *14*, 1283-1293.

98. Warrilow, A.G.; Parker, J.E.; Kelly, D.E.; Kelly, S.L. Azole affinity of sterol 14α-demethylase (CYP51) enzymes from *Candida albicans and Homo sapiens . Antimicrob. Agents Chemother.* **2013**, *57*, 1352-1360.

99. Lamb, D.C.; Kelly, D.E.; Waterman, M.R.; Stromstedt, M.; Rozman, D.; Kelly ,S.L. Characteristics of the heterologously expressed human lanosterol 14α-demethylase (other names: P45014DM, CYP51, P45051) and inhibition of the purified human and Candida albicans CYP51 with azole anti-fungal agents. *Yeast* **1999**, *15*, 755–763.

100. Lutz, J.D.; Dixit, V.; Yeung, C.K.; Dickmann, L.J.; Zelter, A.; Thatcher, J.A ;.Nelson, W.L.; Isoherranen, N. Expression and functional characterization of cytochrome P450 26A1, a retinoic acid hydroxylase. *Biochem. Pharmacol.* **2009**, *77* ,258-268.

101. Warrilow, A.G.S.; Hull, C.M.; Parker, J.E.; Garvey, E.P.; Hoekstra, W.J.; Moore ,W.R.; Schotzinger, R.J.; Kelly, D.E.; Kelly, S.L. The clinical candidate VT-1161 is a highly potent inhibitor of Candida albicans CYP51 but fails to bind the human enzyme. *Antimicrob. Agents Chemother.* **2014**, *58*, 7121-7127.

102. Schrödinger Release 2019-1: Desmond Molecular Dynamics System, D. E. Shaw Research, New York, NY, 2019. Maestro-Desmond Interoperability Tools ,Schrödinger, New York, NY, **2019**. [https://www.schrodinger.com/Desmond/]

103. Hou, T.; Wang, J.; Li, Y.; Wang, W. Assessing the performance of the MM/PBSA and MM/GBSA methods. 1. The accuracy of binding free energy calculations based on molecular dynamics simulations. *J. Chem. Inf. Mod.* **2001**, *51*, 69-82.

104. Molinspiration Property Calculation Service. http://www.molinspiration.com.

105. Fresno, N.; Macías-González, M.; Torres-Zaguirre, A.; Romero-Cuevas, M.; Sanz-Camacho, P.; Elguero, J.; Pavón, F.J.; Rodríguez de Fonseca, F.; Goya, P.; Pérez-Fernández, R. Novel oxazolidinone-based peroxisome proliferator activated receptor agonists: molecular modeling, synthesis, and biological evaluation. *J. Med. Chem.* **2015**, *58*, 6639-6652.

106. Zhang, K.; Sun, J.; Xu, J.; Li, G.; Xu, F. Asymmetric Cu-catalyzed Henry reaction using chiral camphor Schiff bases immobilized on a macromolecular chain. *Tetrahedron Lett.* **2019**, *60*, 1819-1824.

107. Bosiak, M.J.; Pakulski, M.M. Asymmetric reduction of α-keto aldoxime *O*-ethers. *Synthesis* **2011**, *2*, 0316-0324.

108. Wydysh, E.A.; Medghalchi, S.M.; Vadlamudi, A.; Townsend, C.A. Design and synthesis of small molecule glycerol 3-phosphate acyltransferase inhibitors. *J. Med. Chem.* **2009**, *52*, 3317-3327.

109. Devi, K.; Sarma, R.J. Exploring urea–fluoride interactions in the vicinity of a tryptophan residue. *RSC Adv.* **2014**, *4*, 9551-9555.

110. Lakner, F.J.; Parker, M.A.; Rogovoy, B.; Khvat, A.; Ivachtchenko, A. Synthesis of novel trisubstituted imidazolines. *Synthesis* **2009**, *12*, 1987-1990.

111. Upadhayaya, R.S.; Jain, S.; Sinha, N.; Kishore, N.; Chandra, R.; Arora, S.K. Synthesis of novel substituted tetrazoles having antifungal activity. *Eur. J. Med. Chem.* **2004**, *39*, 579-592.

112. Szostak, M.; Aubé, J. Corey-Chaykovsky epoxidation of twisted amides: synthesis and reactivity of bridged spiro-epoxyamines. *J. Am. Chem. Soc.* **2009**, *131*, 13246-13247.

113. Lebouvier, N.; Pagniez, F.; Na, Y.M.; Shi, D.; Pinson, P.; Marchivie, M.; Guillon, J.; Hakki, T.; Bernhardt, R.; Yee, S.W.; Simons, C.; Lézé, M.-P.; Hartmann, R.W.; Mularoni, A.; Baut, G.L.; Krimm, I.; Abagyan, R.; Pape, P.L.; Borgne, M.L. Synthesis, optimization, antifungal activity, selectivity and CYP51 binding of new 2-aryl-3-azolyl-1-indolyl-propan-2-ols. *Pharmaceuticals*, **2020**, *13*, 186.

114. Zaihui; Z. Aminopyridine derivatives as TAM family kinase inhibitors. **2015**, WO2015081257 A2.

115. Narayan, S.; Ramisetti, S.; Jaiswal, A.S.; Law, B.K.; Singh-Pillay, A.; Singh, P.; Amin, S.; Sharma, A.K. ASR352, A potent anticancer agent: synthesis, preliminary SAR, and biological activities against colorectal cancer bulk, 5-fluorouracil/oxaliplatin resistant and stem cells. *Eur. J. Med. Chem.* **2019**, *161*, 456-467.

116. Markley, J.L.; Morse, T.L.; Rath, N.P.; Wencewicz, T.A. Stream-lined synthesis of 3-hydroxy-b-lactams: Norrish-Yang type II photocyclizations of β-ketoformamides. *Tetrahedron* **2018**, *74*, 2743-2753.

117. Sekimata, K.; Han, S-Y.; Yoneyama, K.; Takeuchi, Y.; Yoshida, S.; Asami, T. A specific and potent inhibitor of brassinosteroid biosynthesis possessing a dioxolane ring. *J. Agric. Food Chem.* **2002**, *50*, 3486-3490.

118. Astleford, B.A.; Goe, G.L.; Keay, J.G.; Scriven, E.F.V. Synthesis of 1-alkyl-1,2,4-triazoles: a new one-pot regiospecific procedure. *J. Org. Chem.* **1989**, *54*, 731-732.

119. Wang, Y.; Damu, G.L.V.; Lv, J-S.; Geng, R-X.; Yang, D-C.; Zhou, C-H. Design, synthesis and evaluation of clinafloxacin triazole hybrids as a new type of antibacterial and antifungal agents. *Bioorg. Med. Chem. Lett.* **2012**, *22*, 5363-5366.

120. Konosu, T.; Tajima, Y.; Takeda, N.; Miyaoka, T.; Kasahara, M.; Yasuda, H.; Oida, S. Triazole antifungals. II.: synthesis and antifungal activities of 3-acyl-4-methyloxazolidine derivatives. *Chem. Pharm. Bull.* **1990**, *38*, 2476-2486.

121. Kifli, N.; Htar, T.T.; De Clercq, E.; Balzarini, J.; Simons, C. Novel bicyclic sugar modified nucleosides: synthesis, conformational analysis and antiviral evaluation. *Bioorg. Med. Chem.* **2004**, *12*, 3247-3257.

122. Bhabak, K.P.; Arenz, C. Novel amide-and sulfonamide-based aromatic ethanolamines: effects of various substituents on the inhibition of acid and neutral ceramidases. *Bioorg. Med. Chem.* **2012**, *20*, 6162-6170.

123. Parker, J.E.; Warrilow, A.G.S.; Cools, H.J.; Fraaije, B.A.; Lucas, J.A.; Rigdova ,K.; Griffiths, W.J.; Kelly, D.E.; Kelly, S.L. Prothioconazole and prothioconazole desthio activity against *Candida albicans* sterol 14α-demethylase (CaCYP51). *Appl. Environ. Microbiol.* **2011**, *79*, 1639-1645.

124. CDC – Centre for Disease Control and Prevention. Available from: http://www.cdc.gov/parasites/leishmaniasis/ (Access April 15, **2020**).

125. Lepesheva, G.I; Hargrove, T.Y.; Rachakonda, G.; Wawrzak, Z.; Pomel, S.; Cojean, S.; Nde, P.N.; Nes, W.D.; Locuson, C.W.; Calcutt, M.W.; Waterman, M.R.; Daniels, J.S.; Loiseau, P.M.; Villalta, F. VFV as a new effective CYP51 structure-derived drug candidate for Chagas disease and visceral leishmaniasis. *JID* **2015**, *212*, 1439-1448.

126. No, J.H. Visceral leishmaniasis: revisiting current treatments and approaches for future discoveries. *Acta Trop* **2016**, *155*, 113-123.

127. Oliveira, M.; Barreira, L.; Gangadhar, K.N.; Rodrigues, M.J.; Santos, T.; Varela, J.; Custódio, L. Natural products from marine invertebrates against leishmania parasites: a comprehensive review. *Phytochem Rev* **2016**, *15*, 663-697.

128. WHO – World Health Organization. https://www.who.int/leishmaniasis/en/ (Access April 16, **2020**).

129. WHO World Health Organization (WHO) Leishmaniasis Fact Sheet; World Health Organization: Geneva, **2020**; https://www.who.int/news-room/fact-sheets/detail/leishmaniasis (Accessed July 8, **2020**).

130. Dawit, G.; Girma Z.; Simenew, K. A review on biology, epidemiology and public health significance of leishmaniasis. *J. Bacteriol. Parasitol.* **2013**, *4*, 166.

131. Tiuman, T.S.; Santos, A.O.; Ueda-Nakamura, T.; Dias-Filho, B.P.; Nakamura, C.V. Recent advances in leishmaniasis treatment. *Int. J. Infect. Dis.* **2011**, *15*, e525-e532.

132. Freitas-Junior, L.H.; Chatelain, E.; Kim, H.A.; Siqueira-Neto, J.L. Visceral leishmaniasis treatment: what do we have, what do we need and how to deliver it? *Int. J. Parasitol. Drugs Drug Resist.* **2012**, *2*, 11–19.

133. Bhardwaj, R.; Kumar, R.; Singh, S.K.; Selvaraj, C.; Dubey, V.K Understanding the importance of conservative hypothetical protein LdBPK_070020 in *Leishmania donovani* and its role in subsistence of the parasite. *Arch. Biochem. Biophys.* **2016**, *596*, 10-21.

134. Thomas, M.G.; Manu De Rycker, M.; Ajakane, M.; Albrecht, S.; Álvarez-Pedraglio, A.I.; Boesche, M.; Brand, S.; Campbell, L.; Cantizani-Perez, J.; Cleghorn, L.A.T.; Copley, R.C.B.; Crouch, S.D.; Daugan, A.; Drewes, G.; Ferrer, S.; Ghidelli-Disse, S.; Gonzalez, S.; Gresham, S.L.; Hill, A.P.; Hindley, S.J.; Lowe, R.M.; MacKenzie, C.J.; MacLean, L.; Manthri, S.; Martin, F.; Miguel-Siles, J.; Nguyen, V.L.; Norval, S.; Osuna-Cabello, M.; Woodland, A.; Patterson, S.; Pena, I.; Quesada-Campos, M.T.; Reid, I.H.; Revill, C.; Riley, J.; Ruiz-Gomez, J.R.; Shishikura, Y.; Simeons, .C.; Smith, A.; Smith, V.C.; Spinks, D.; Stojanovski, L.; Thomas, J.; Thompson, S.; Tim Underwood, T.; Gray, D.W.; Fiandor, J.M.; Gilbert, I.H.; Wyatt, P.G.; Read, K.D.; Miles, T.J. Identification of GSK3186899/DDD853651 as a preclinical development candidate for the treatment of visceral leishmaniasis. *J. Med. Chem.* **2019**, *62*, 1180-1202.

135. Duthie, M.S.; Raman, V.S.; Piazza, F.M.; Reed, S.G. The development and clinical evaluation of second-generation leishmaniasis vaccines. *Vaccine* **2012**, *30*, 134-141.

136. Bezerra-Souza, A.; Yamamoto, E.S.; Laurenti, M.D.; Ribeiro, S.P.; Passero, L.F.D. The antifungal compound butenafine eliminates promastigote and amastigote forms of *Leishmania* (*Leishmania*) *amazonensis* and *Leishmania* (*Viannia*) *braziliensis*. *Parasitol Int* **2016**, *65*, 702-707.

137. Canuto, G.A.B.; Castilho-Martins, E.A.; Tavares, M.F.M.; Rivas, L.; Barbas, C.; López-Gonzálvez, A. Multi-analytical platform metabolomic approach to study miltefosine mechanism of action and resistance in Leishmania. *Anal Bioanal Chem* **2014**, *406*, 3459-3476.

138. Dea-Ayuela, M.A.; Bilbao-Ramos, P.; Bolás-Fernández, F.; González-Cardenete, M.A. Synthesis and antileishmanial activity of C7- and C12-functionalized dehydroabietylamine derivatives. *Eur J Med Chem* **2016**, *121*, 445-450.

139. DND*i* - Drug for Neglected Diseases *initiative* - https://dndi.org/ (Access July 14, **2020**).

140. Keighobadi, M.; Emami, S.; Lagzian, M.; Fakhar, M.; Rafiei, A.; Valadan, R. Molecular modeling and structural stability of wild-type and mutant CYP51 from *Leishmania major*: in vitro and in silico analysis of a laboratory strain. *Molecules* **2018**, *23*, 696-711.

141. The UniProt Consortium UniProt: a worldwide hub of protein knowledge Nucleic acids res. **2019**, *47*, D506-D515. http://www.uniprot.org/ (Access July 12, **2020**).

142. Bawden, D. Computerized chemical structure-handling techniques in structure-activity studies and molecular property prediction. *J. Chem. Inf. Comput. Sci.* **1983**, *23*, 14-22.

143. Chothia, C.; Lesk, A.M. The relation between the divergence of sequence and structure in proteins. *EMBO J.* **1986**, *5*, 823-826.

144. Berman, H.M.; Westbrook, J.; Feng, Z.; Gilliland, G.; Bhat, T.N.; Weissig, H.; Shindyalov, I.N.; Bourne, P.E. The protein data bank. *Nucleic Acids Res.* **2000**, *28*, 235-242.

145. Artimo, P.; Jonnalagedda, M.; Arnold, K.; Baratin, D.; Csardi, G.; de Castro, E.; Duvaud, S.; Flegel, V.; Fortier, A.; Gasteiger, E.; Grosdidier, A.; Hernandez, C.; Ioannidis, V.; Kuznetsov, D.; Liechti, R.; Moretti, S.; Mostaguir, K.; Redaschi, N.; Rossier, G.; Xenarios, I.; Stockinger, H. ExPASy: SIB bioinformatics resource portal. *Nucleic Acids Res.* 2012, *40* (W1): W597-W603, https://www.expasy.org/

146. Altschul, S.F.; Madden, T.L.; Schaffer, A.A.; Zhang, J.; Zhang, Z.; Miller, W.; Lipman, D.J. Gapped BLAST and PSI-BLAST: a new generation of protein database search programs. *Nucleic Acids Res.* **1997**, *25*, 3385-3402.

147. National Center for Biotechnology Information, U.S. National Library of Medicine 8600 Rockville Pike, Bethesda MD, 20894 USA. https://blast.ncbi.nlm.nih.gov/Blast.cgi

148. Li, W.; Cowley, A.; Uludag, M.; Gur, T.; McWilliam, H.; Squizzato, S.; Mi-Park, Y.; Buso, N.; Lopez, R. EMBL-EBI bioinformatics web and programmatic tools framework. *Nucleic Acids Res* **2015**, *43*, 580-584.

149. Sievers, F.; Wilm, A.; Dineen, D.G.; Gibson, T.J.; Karplus, K.; Li, W.; Lopez, R.; McWilliam, H.; Remmert, M.; Söding, J.; Thompson J.D.; Higgins, D.G. Fast, scalable generation of high-quality protein multiple sequence alignments using clustal omega. *Mol. Syst. Biol.* **2011**, *7*, 539.

150. Gotoh, O. Substrate recognition sites in Cytochrome P450 family 2 (CYP2) proteins inferred from comparative analyses of amino acid and coding nucleotide sequences. *J. Biol. Chem.* **1992**, *267*, 83-90.

151. Jones, D.T. Protein secondary structure prediction based on position-specific scoring matrices. *J. Mol. Biol.* **1999**, *292*, 195-202.

152. Waterhouse, A.; Bertoni, M.; Bienert, S.; Studer, G.; Tauriello, G.; Gumienny, R.; Heer, F.T.; de Beer, T.A.P.; Rempfer, C.; Bordoli, L.; Lepore, R.; Schwede, T. SWISS-MODEL: homology modelling of protein structures and complexes. *Nucleic Acids Res.* **2018**, *46*, W296-W303.

153. Lovell, S.C.; Davis, I.W.; Arendall III, W.B.; de Bakker, P.I.W.; Word, J.M.; Prisant, M.G.; Richardson, J.S.; Richardson, D.C. Structure validation by Cα geometry: φ, ψ and Cβ deviation. *Proteins: Struct. Funct. Genet*. **2003**, *50*, 437-450. http://mordred.bioc.cam.ac.uk/~rapper/rampage.php

154. Weiderstein, M.; Sippl, M. J. ProSA-web: interactive web service for the recognition of errors in three dimensional structures of proteins. *Nucleic Acids Res* **2007**, *35*, 407-410.

155. Sippl, M.J. Recognition of errors in three-dimensional structures of proteins. *Proteins* **1993**, *17*, 355-362. https://prosa.services.came.sbg.ac.at/prosa.php

156. Fiser, A. Template-based protein structure modeling. *Methods Mol. Biol.* **2010**, *673*, 73-94.

157. De Rycker, M.; Hallyburton, I.; Thomas, J.; Campbell, L.; Wyllie, L.; Joshi, D.; Cameron, S.; Gilbert, I.H.; Wyatt, P.G.; Frearson, J.A.; Fairlamb, A.H.; Gray, D.W. Comparison of a high-throughput high-content intracellular *Leishmania donovani* assay with an axenic amastigote assay. *Antimicrob. Agents Chemother.* **2013**, *57*, 2913-2922.

158. Sacks, D.; Sher, A. Evasion of innate immunity by parasitic protozoa. *Nat. Immunol.* **2002**, *3*, 1041-1047. www.nature.com/natureimmunology

159. Ponte-Sucre1, A.; Gamarro, F.; Dujardin, J.-C.; Barrett, M.P.; López-Vélez, R.; García-Hernández, R.; Pountain, A.W.; Mwenechanya, R.; Barbara Papadopoulou, B. Drug resistance and treatment failure in leishmaniasis: A 21st century challenge. *PLoS Negl Trop Dis* **2017**, 11, e0006052. https://doi.org/ 10.1371/journal.pntd.0006052

160. Copeland, RA. Evaluation of enzyme inhibitors in drug discovery: a guide for medicinal chemists and pharmacologists. Wiley-Interscience, New York, ISBN:0-471-68696-4. **2005**, 178-213.

161. Dei, S.; Bartolini, A.; Bellucci, C.; Ghelardini, C.; Gualtieri, F.; Manetti, D.; Romanelli, M. N.; Scapecchi, S.; Teodori, E. Differential analgesic activity of the enantiomers of atropine derivatives does not correlate with their muscarinic subtype selectivity. *Eur. J. Med. Chem.* **1997**, *32*, 595-605.

162. Alizadeh, A.; M. Khodaei, M.M.; Abdi, G.; Kordestani, D. The first report on chemoselective biguanide-catalyzed Henry reaction under neat conditions. *Bull. Korean Chem. Soc.* **2012**, *33*, 3640-3644.

163. Blay, G.; Domingo, L.R.; Hernández-Olmos, V.; Pedro, J.R. New highly asymmetric Henry reaction catalyzed by Cu^{II} and a C_1-symmetric aminopyridine ligand, and its application to the synthesis of miconazole. *Chem. Eur. J.* **2008**, *14*, 4725-4730.

164. Gasteiger, E.; Gattiker, A.; Hoogland, C.; Ivanyi, I.; Appel, R.D.; Bairoch, A. ExPASy: the proteomics server for in-depth protein knowledge and analysis. *Nucleic Acids Res* **2003**, *31*, 3784-3788.

165. Schaffer, A.A.; Aravind, L.; Madden, T.L.; Shavirin, S.; Spouge, J.L.; Wolf, Y.I.; Koonin, E.V.; Altschul, S.F. Improving the accuracy of PSI-BLAST protein database searches with composition-based statics and other refinements. *Nucleic Acids Res* **2001**, *29*, 2994-3005.